Theory of Code Division Multiple Access Communication

KAMIL SH. ZIGANGIROV

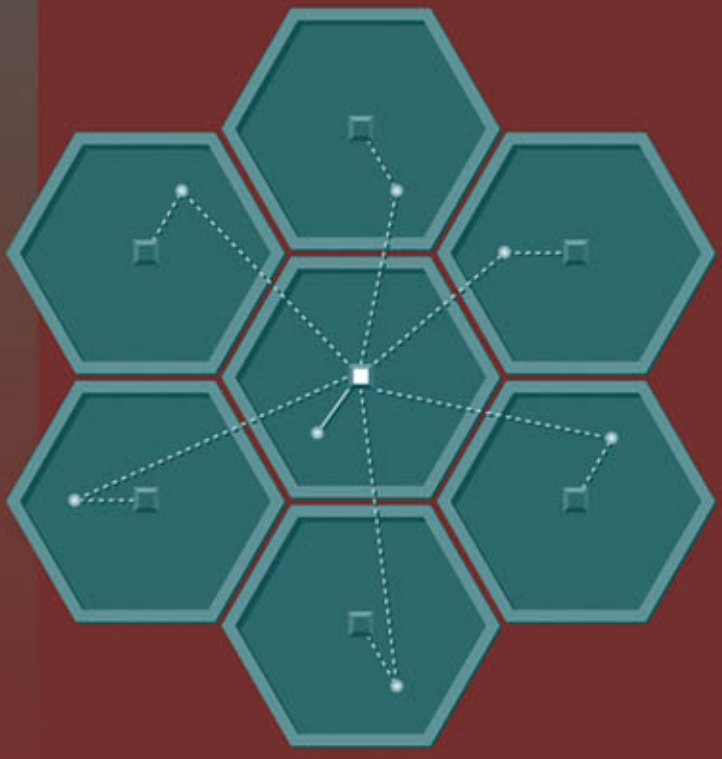

IEEE SERIES ON DIGITAL & MOBILE COMMUNICATION

John B. Anderson, *Series Editor*

THEORY OF CODE DIVISION MULTIPLE ACCESS COMMUNICATION

Kamil Sh. Zigangirov

John B. Anderson, *Series Editor*

A JOHN WILEY & SONS, INC., PUBLICATION

THEORY OF CODE DIVISION MULTIPLE ACCESS COMMUNICATION

IEEE Press Series on Digital & Mobile Communication

The IEEE Press Digital and Mobile Communication Series is written for research and development engineers and graduate students in communication engineering. The burgeoning wireless and personal communication fields receive special emphasis. Books are of two types, graduate texts and the latest monographs about theory and practice.

Books in the IEEE Press Series on Digital & Mobile Communication

John B. Anderson, *Digital Transmission Engineering*

Rolf Johannesson and Kamil Sh. Zigangirov, *Fundamentals of Convolutional Coding*

Raj Pandya, *Mobile and Personal Communication Systems and Services*

Lajos Hanzo, P. J. Cherriman, and J. Streit, *Video Compression & Communications over Wireless Channels: Second to Third Generation Systems and Beyond*

Lajos Hanzo, F. Clare, A. Somerville and Jason P. Woodard, *Voice Compression and Communications: Principles and Applications for Fixed and Wireless Channels*

Mansoor Shafi, Shigeaki Ogose and Takeshi Hartori (Editors), *Wireless Communications in the 21st Century*

IEEE Press
445 Hoes Lane
Piscataway, NJ 08854

THEORY OF CODE DIVISION MULTIPLE ACCESS COMMUNICATION

Kamil Sh. Zigangirov

John B. Anderson, *Series Editor*

A JOHN WILEY & SONS, INC., PUBLICATION

Published simultaneously in Canada.

Library of Congress Cataloging-in-Publication Data is available.

ISBN: 0-471-45712-4

Printed in the United States of America.

10 9 8 7 6 5 4 3 2 1

CONTENTS

PREFACE

The objective of this book is to provide an introduction to code division multiple-access (CDMA) communications. Our motivation for emphasizing CDMA communication is a result of the technological developments that have occurred during the past decade. We are currently witnessing an explosive growth in wireless communication and cellular mobile radio systems, which are based on different multiple-access techniques. We anticipate that, in the near future, we will see a replacement of the current time- and frequency division methods in wireless communication and mobile radio by CDMA.

This textbook originates as an adaptation for undergraduate study of the well-known book *CDMA, Principles of Spread Spectrum Communication* by A.J. Viterbi and is based on courses which I taught several years at Lund University in Sweden. The reader can see an indubitable influence of Viterbi's book on the content of this book. In particular, our treatment of direct-sequence CDMA follows the ideas and methods of Viterbi's book, but for completeness we also include in the book a consideration of frequency hopping CDMA and pulse position hopping ("time hopping") CDMA. We have studied also in more detail forward transmission in the direct-sequence CDMA system. Furthermore, we consider it necessary to include in our textbook information-theoretical analysis of CDMA communication.

My understanding of the field, and hence the content of this text, has been influenced by a number of books on the topic of digital and spread spectrum communications. In addition to the pioneering book by Viterbi I have to mention *Digital Communication* by J.G. Proakis and *Introduction to Spread Spectrum Communication* by R.L. Peterson, R.E. Ziemer, and D.E. Borth. Readers familiar

with these books will recognize their influence here. Numerous other important books and papers are mentioned in the comments to the chapters.

I am grateful for the warm support of the Department of Information Technology of Lund University while this book was being written. I am particularly indebted to my friend Rolf Johannesson, who supported my work on the manuscript of this book. I would like to express appreciation to my colleagues in the department, especially to John Anderson and Göran Lindell, for discussions of related problems of communication theory. Being Series Editor, John Anderson carefully read the original manuscript and made many corrections. Many thanks are also due to the reviewer, Roger Ziemer, for the substantial work he did in improving the text of the book.

I am deeply indebted to Ph.D. students of the department, first of all to Leif Wilhelmsson, Alberto Jimenez, Ola Wintzell, Karin Engdahl, Per Ståhl, Michael Lentmaier, Marc Handlery, and Dmitri Trouhachev, who read the notes and corrected my numerous grammatical (and not only grammatical) errors. I am pleased to acknowledge the patient Swedish undergraduate students who studied from this work over the last few years.

But above all, I am deeply indebted to Doris Holmqvist, who with great patience typed, corrected, retyped, again corrected ... etc. my notes. Without the help and ingenuity of Doris, this text could not have been written.

1

INTRODUCTION TO CELLULAR MOBILE RADIO COMMUNICATION

The subject of this book is code division multiple access (CDMA) communications. A major application of CDMA is wireless communication including mobile radio. In this chapter we introduce the basic concepts of mobile radio systems, including cellular concepts, consider the general structure of a cellular system, and study different principles of multiple-access (time, frequency, and code division) and spread spectrum concepts.

This chapter begins with an overview of the principles of cellular radio systems. Next, given the focus on simultaneous wideband transmission of all users over a common frequency spectrum, we consider direct-sequence CDMA systems, frequency-hopped CDMA systems, and pulse position-hopped CDMA systems. The chapter concludes with a description of this book. The book is devoted to the analysis of different aspects of CDMA communication. Given the rapid and continuing growth of cellular radio systems throughout the world, CDMA digital cellular radio systems will be the widest-deployed form of spread spectrum systems for voice and data communication. It is a major technology of the twenty-first century.

1.1 CELLULAR MOBILE RADIO SYSTEMS

A cellular radio system provides a wireless connection to the public telephone network for any user location within the radio range of the system. The term *mobile* has traditionally been used to classify a radio terminal that can be moved during

Theory of Code Division Multiple Access Communication, by Kamil Sh. Zigangirov
ISBN 0-471-45712-4

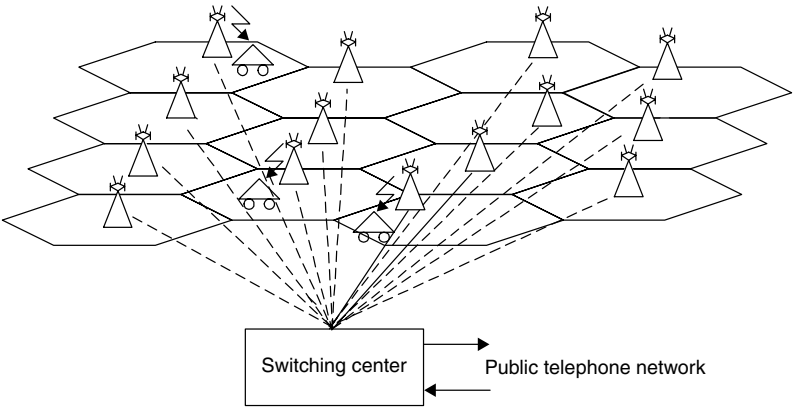

Figure 1.1. An illustration of a cellular system.

communication. Cellular systems accommodate a large number of mobile units over a large area within a limited frequency spectrum. There are several types of radio transmission systems. We consider only *full duplex systems*. These are communication systems that allow simultaneous two-way communication. Transmission and reception for a full duplex system are typically on two different channels, so the user may constantly transmit while receiving signals from another user.

Figure 1.1 shows a basic cellular system that consists of *mobiles*, *base stations*, and a *switching center*. Each mobile communicates via radio with one or more base stations. A call from a user can be transferred from one base station to another during the call. The process of transferring is called *handoff*.

Each mobile contains a *transceiver* (transmitter and receiver), an antenna, and control circuitry. The base stations consist of several transmitters and receivers, which simultaneously handle full duplex communications and generally have towers that support several transmitting and receiving antennas. The base station connects the simultaneous mobile calls via telephone lines, microwave links, or fiber-optic cables to the switching center. The switching center coordinates the activity of all of the base stations and connects the entire cellular system to the public telephone network.

The channels used for transmission from the base station to the mobiles are called *forward* or *downlink channels*, and the channels used for transmission from the mobiles to the base station are called *reverse* or *uplink channels*. The two channels responsible for call initiation and service request are the *forward control channel* and *reverse control channel*.

Once a call is in progress, the switching center adjusts the transmitted power of the mobile (this process is called *power control*[1]) and changes the channel of the mobile and base station (handoff) to maintain call quality as the mobile moves in and out of range of a given base station.

[1]Sometimes the mobile adjusts the transmitted power by measuring the power of the received signal (so-called *open-loop power control*).

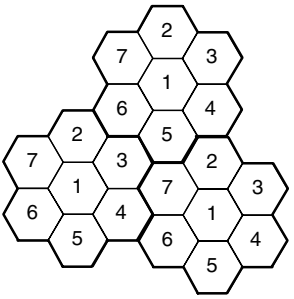

Figure 1.2. An illustration of the cellular frequency reuse concept.

The cellular concept was a major breakthrough in solving the problem of spectral congestion. It offered high system capacity with a limited spectrum allocation. In a modern conventional mobile radio communication system, each base station is allocated a portion of the total number of channels available to the entire system and nearby base stations are assigned different groups of channels so that all the available channels are assigned to a relatively small number of neighboring base stations. Neighboring base stations are assigned different groups of channels so that interference between the users in different cells is small.

The idealized allocation of cellular channels is illustrated in Figure 1.2, in which the cells are shown as contiguous hexagons. Cells labeled with the same number use the same group of channels. The same channels are never reused in contiguous cells but may be reused by noncontiguous cells. The κ cells that collectively use the complete set of available frequencies is called a *cluster*. In Figure 1.2, a cell cluster is outlined in bold and replicated over the coverage area. Two cells that employ the same allocation, and hence can interfere with each other, are separated by more than one cell diameter.

The factor κ is called the *cluster size* and is typically equal to 3, 4, 7, or 12. To maximize the capacity over a given coverage area we have to choose the smallest possible value of κ. The factor $1/\kappa$ is called the *frequency reuse factor* of a cellular system. In Figure 1.2 the cluster size is equal to 7, and the frequency reuse factor is equal to 1/7.

EXAMPLE 1.1

The American analog technology standard, known as Advanced Mobile Phone Service (AMPS), employs frequency modulation and occupies a 30*-kHz frequency slot for each voice channel [47]. Suppose that a total of* 25*-MHz bandwidth is allocated to a particular cellular radio communication system with cluster size* 7*. How many channels per cell does the system provide?*

Solution

Allocation of 12.5 *MHz each for forward and reverse links provides a little more than* 400 *channels in each direction for the total system, and correspondingly a little less than* 60 *per cell.*

The other-cell interference can be reduced by employing sectored antennas at the base station, with each sector using different frequency bands. However, using sectored antennas does not increase the number of slots and consequently the frequency reuse factor is not increased.

A multiple access system that is more tolerant to interference can be designed by using digital modulation techniques at the transmitter (including both source coding and channel error-correcting coding) and the corresponding signal processing techniques at the receiver.

1.2 FREQUENCY DIVISION AND TIME DIVISION MULTIPLE ACCESS

Multiple access schemes are used to allow many mobile users to share simultaneously a common bandwidth. As mentioned above, a full duplex communication system typically provides two distinct bands of frequencies (channels) for every user. The forward band provides traffic from the base station to the mobile, and the reverse band provides traffic from the mobile to the base station. Therefore, any duplex channel actually consists of two simplex channels.

Frequency division multiple access (FDMA) and *time division multiple access (TDMA)* are the two major access techniques used to share the available bandwidth in a conventional mobile radio communication systems.

Frequency division multiple access assigns individual channels (frequency bands) to individual users. It can be seen from Figure 1.3 that each user is allocated a unique frequency band. These bands are assigned on demand to users who request service. During the period of the call, no other user can share the same frequency band. The bandwidths of FDMA channels are relatively narrow (25–30 kHz) as each channel supports only one call per carrier. That is, FDMA is usually implemented in narrowband systems. If an FDMA channel is not in use (for example, during pauses in telephone conversation) it sits idle and cannot be used by other users to increase the system capacity.

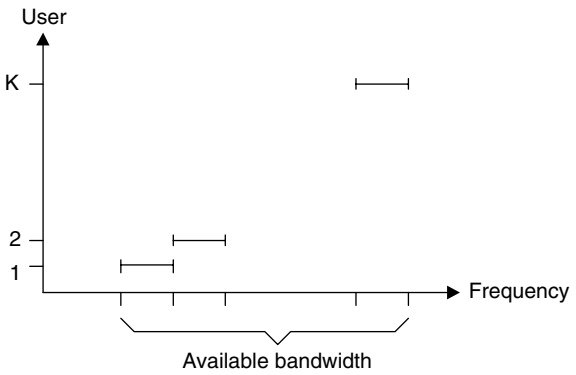

Figure 1.3. FDMA scheme in which different users are assigned different frequency bands.

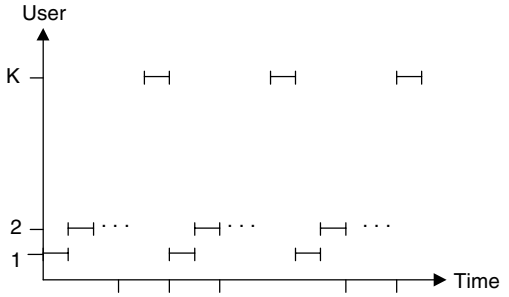

Figure 1.4. TDMA scheme in which each user occupies a cyclically repeating time slot.

Time division multiple access systems divide the transmission time into time slots, and in each slot only one user is allowed to either transmit or receive. It can be seen from Figure 1.4 that each user occupies cyclically repeating wording, so a channel may be thought of as a particular time slot that reoccurs at slot locations in every frame. Unlike in FDMA systems, which can accommodate analog frequency modulation (FM), digital data and digital modulation must be used with TDMA.

TDMA shares a single carrier frequency with several users, where each user makes use of nonoverlapping time slots. Analogously to FDMA, if a channel is not in use, then the corresponding time slots sit idle and cannot be used by other users. Data transmission for users of a TDMA system is not continuous but occurs in bursts. Because of burst transmission, synchronization overhead is required in TDMA systems. In addition, guard slots are necessary to separate users. Generally, the complexity of TDMA mobile systems is higher compared with FDMA systems.

EXAMPLE 1.2

The global system for mobile communications (GSM) utilizes the frequency band 935–960 *MHz for the forward link and frequency range* 890–915 *MHz for the reverse link. Each* 25*-MHz band is broken into radio channels of* 200 *kHz. Each radio channel consists of eight time slots. If no guard band is assumed, find the number of simultaneous users that can be accommodated in GSM. How many users can be accommodated if a guard band of* 100 *kHz is provided at the upper and the lower end of the GSM spectrum?*

Solution

The number of simultaneous users that can be accommodated in GSM in the first case is equal to

$$\frac{25 \cdot 10^6}{(200 \cdot 10^3)/8} = 1000$$

In the second case the number of simultaneous users is equal to 992.

Each user of a conventional multiple access system, based on the FDMA or the TDMA principle, is supplied with certain resources, such as frequency or time slots, or both, which are disjoint from those of any other user. In this system, the multiple access channel reduces to a multiplicity of single point-to-point channels. The transmission rate in each channel is limited only by the bandwidth and time allocated to it, the channel degradation caused by background noise, multipath fading, and shadowing effects.

Viterbi [47] pointed out that this solution suffers from three weaknesses. The first weakness is that it assumes that all users transmit continuously. However, in a two-person conversation, the percentage of time that a speaker is active, that is, talking, ranges from 35% to 50%. In TDMA or FDMA systems, reallocation of the channel for such brief periods requires rapid circuit switching between the two users, which is practically impossible.

The second weakness is the relatively low frequency reuse factor of FDMA and TDMA. As we can see from Example 1.1 the frequency reuse factor 1/7 reduces the number of channels per cell in AMPS from 400 to less than 60.

Using antenna sectorization (Fig. 1.5) for reducing interference does not increase system capacity. As an example, a cell site with a three-sectored antenna has an interference that is approximately one-third of the interference received by an omnidirectional antenna. Even with this technique, the interference power received at a given base station from reused channels in other cells is only about 18 dB below the signal power received from the desired user of the same channel in the given cell. Reuse factors as large as 1/4 and even 1/3 have been considered and even used, but decreasing the distance between interfering cells increases the other-cell interference to the point of unacceptable signal quality.

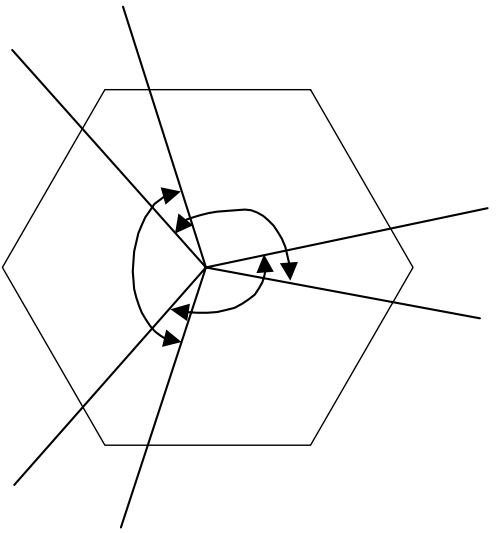

Figure 1.5. A three-sectored antenna in a single isolated cell.

A third source of performance degradation, which is common to all multiple access systems, particularly in terrestrial environments, is fading. Fading is caused by interference between two or more versions of the transmitted signal that arrive at the receiver at slightly different time. This phenomenon is particularly severe when each channel is allocated a narrow bandwidth, as for FDMA systems.

1.3 DIRECT SEQUENCE CDMA

A completely different approach, realized in CDMA systems, does not attempt to allocate disjoint frequency or time resources to each user. Instead the system allocates all resources to all active users.

In *direct sequence* (DS) CDMA systems, the narrowband message signal is multiplied by a very large-bandwidth signal called the *spreading signal*. All users in a DS CDMA system use the same carrier frequency and may transmit simultaneously. Each user has its own spreading signal, which is approximately orthogonal to the spreading signals of all other users. The receiver performs a correlation operation to detect the message addressed to a given user. The signals from other users appear as noise due to decorrelation. For detecting the message signal, the receiver requires the spreading signal used by the transmitter. Each user operates independently with no knowledge of the other users *(uncoordinated transmission)*.

Potentially, CDMA systems provide a larger *radio channel capacity* than FDMA and TDMA systems. The radio channel capacity (not to be confused with *Shannon's channel capacity*, see Chapter 8) can be defined as the maximum number K_0 of simultaneous users that can be provided in a fixed frequency band. Radio channel capacity is a measure of the *spectrum efficiency* of a wireless system. This parameter is determined by the *required signal-to-noise ratio* at the input of the receiver and by the channel bandwidth W.

To explain the principle of DS CDMA let us consider a simple example. Suppose that two users, user 1 and user 2, located the same distance from the base station, wish to send the *information* (or *data*) *sequences*[2] $\boldsymbol{u}^{(1)} = u_0^{(1)}, u_1^{(1)}, u_2^{(1)}, u_3^{(1)} = 1, -1, -1, 1$ and $\boldsymbol{u}^{(2)} = u_0^{(2)}, u_1^{(2)}, u_2^{(2)}, u_3^{(2)} = -1, 1, -1, -1$, respectively, to the base station. First, user 1 maps the data sequence $\boldsymbol{u}^{(1)}$ into the data signal $u^{(1)}(t)$, and user 2 maps $\boldsymbol{u}^{(2)}$ into the data signal $u^{(2)}(t)$, such that the real number 1 corresponds to a positive rectangular pulse of unit amplitude and duration T, and the real number -1 corresponds to a negative rectangular pulse of the same amplitude and same duration (Fig. 1.6a). Then both users synchronously transmit the data signals over the *multiple access adding channel*. Because each pulse corresponds to the transmission of one bit, the transmission rate $R = 1/T$ (bit/s) for each user and the overall rate is $2/T$ (bit/s).

[2]In information-theoretic literature, binary sequences consist of symbols from the binary logical alphabet $\{0, 1\}$. In CDMA applications it is more convenient to use the binary real number alphabet $\{1, -1\}$. The mapping $0 \rightleftarrows 1$, $1 \rightleftarrows -1$ establishes a one-to-one correspondence between sequences of binary logical symbols and sequences of binary real numbers (see also Chapter 4).

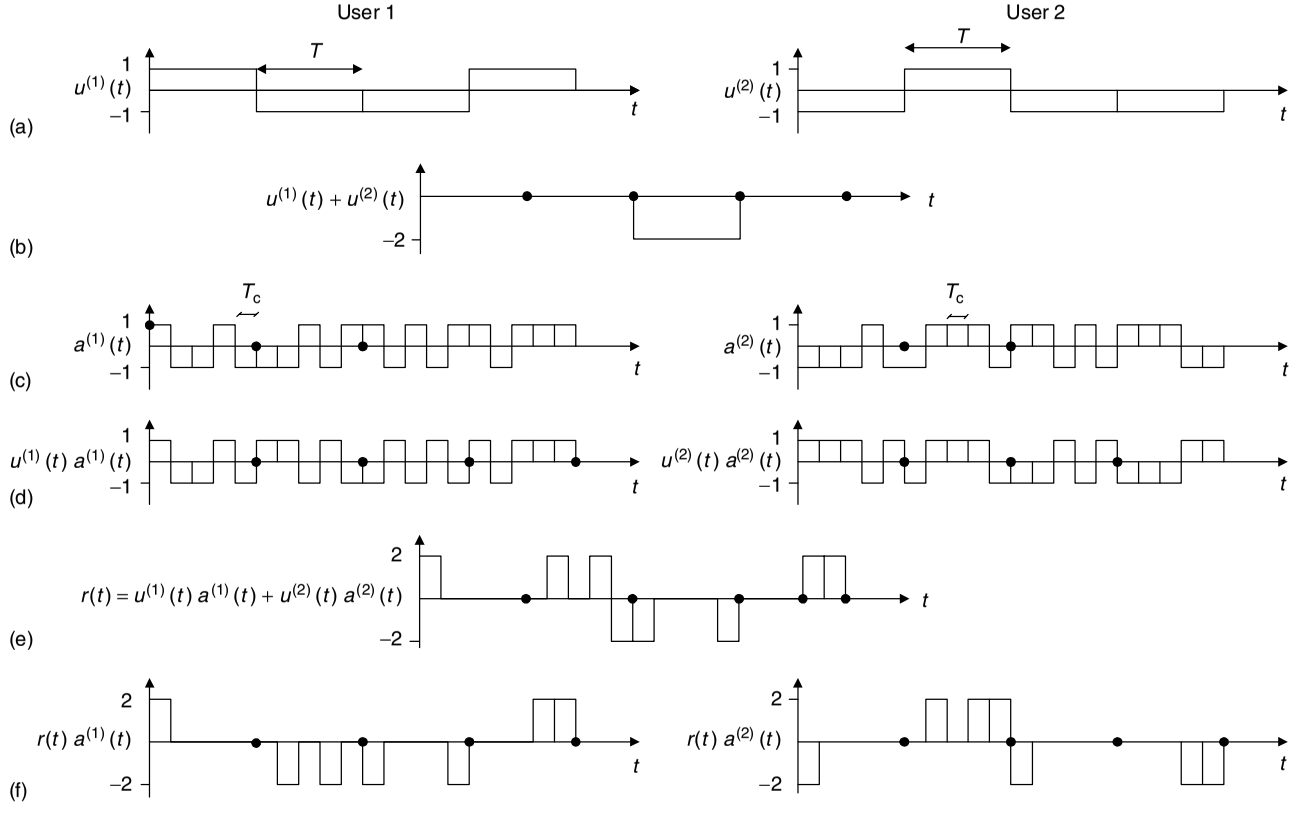

Figure 1.6. Example of the transmission over an adding channel, synchronous case.

If the *propagation delay* and the *attenuation* in the channel for both signals are the same, the output of the adding channel, that is, the input of the base station receiver, is the sum of identically attenuated transmitted signals. In our example the received signal is nonzero only in the third interval (Fig. 1.6b). Then the receiver cannot decide which pulses were sent by the users in the first, second, and fourth intervals, but it knows that in the third interval both of the users have sent negative pulses, and correspondingly $u_2^{(1)} = -1$, $u_2^{(2)} = -1$.

Suppose now that instead of sending the data signals $u^{(1)}(t)$ and $u^{(2)}(t)$ directly over the multiple access adding channel, the users first *spread* them, that is, multiply them by the *spreading signals* $a^{(1)}(t)$ and $a^{(2)}(t)$, respectively. The signals $a^{(1)}(t)$ and $a^{(2)}(t)$, presented in Figure 1.6c, are sequences of positive and negative unit amplitude rectangular pulses of duration T_c, $T_c < T$ (in our example $T_c = T/4$). These pulses are called *chips*, and T_c is called the *chip duration*. We will always consider the case when the ratio $T/T_c = N$ is an integer. The spread signals $u^{(1)}(t) \cdot a^{(1)}(t)$ and $u^{(2)}(t) \cdot a^{(2)}(t)$ (Fig. 1.6d) are sent over the adding channel. The received signal $r(t) = u^{(1)}(t) \cdot a^{(1)}(t) + u^{(2)}(t) \cdot a^{(2)}(t)$ is presented in Figure 1.6e.

As we will see in Chapter 2, the bandwidth of the signal formed by the sequence of positive and negative pulses of duration T is proportional to $1/T$. Therefore, the bandwidth of the signals $u^{(k)}(t)$, $k = 1, 2$, is proportional to the transmission rate R and the bandwidth W of the spread signals is proportional to $1/T_c$. The ratio $T/T_c \approx W/R$ that characterizes the increase of the bandwidth by spreading is called the *spreading factor* or *processing gain*.

The base station receiver *despreads* the received signal $r(t)$, that is, multiplies $r(t)$ by the spreading signals $a^{(1)}(t)$ and $a^{(2)}(t)$. The results of despreading are given in Figure 1.6f. It is obvious that the receiver can correctly decide which data sequences were transmitted by the users in each of the four intervals.

The spreading signal $a^{(k)}(t)$, $k = 1, 2$, can be generated by mapping the *spreading sequences* $\boldsymbol{a}^{(k)} = a_0^{(k)}, a_1^{(k)}, \ldots a_n^{(k)}, \ldots, a_n^{(k)} \in \{1, -1\}$ into sequences of positive and negative pulses, analogous to mapping the data sequence $\boldsymbol{u}^{(k)}$, $k = 1, 2$, into the data signal $u^{(k)}(t)$. Suppose now that we repeat each symbol $u_n^{(k)}$ of the data sequence $\boldsymbol{u}^{(k)}$ N times, $N = T/T_c = W/R$, to get a sequence $\boldsymbol{v}^{(k)} = v_0^{(k)}, v_1^{(k)}, \ldots v_n^{(k)} \ldots$ where $v_n^{(k)} = u_{\lfloor n/N \rfloor}^{(k)}$. Here $\lfloor x \rfloor$ means the largest integer that is less or equal to x. (For example, in Fig. 1.6 we have $N = 4$.) Then we multiply symbols of the sequence $\boldsymbol{v}^{(k)}$ by symbols of the sequence $\boldsymbol{a}^{(k)}$. We get the sequence

$$\boldsymbol{v}^{(k)} * \boldsymbol{a}^{(k)} \stackrel{\text{def}}{=} v_0^{(k)} a_0^{(k)}, v_1^{(k)} a_1^{(k)}, \ldots, v_n^{(k)} a_n^{(k)}, \ldots \tag{1.1}$$

If we map the symbols of the sequence $\boldsymbol{v}^{(k)} * \boldsymbol{a}^{(k)}$ into a sequence of positive and negative pulses, as we did before, we get the spread signals $u^{(k)}(t) \cdot a^{(k)}(t)$, $k = 1, 2$. This is an alternative way of spreading.

The operation of repeating the symbol $u_n^{(k)} N$ times can be considered as *encoding*. The code is called the *repetition code*[3]; it consists of two *codewords*: N is the *block length* and $r = 1/N$ (bit/symbol) is the *code rate*. In the general, we will consider more complicated code constructions. Obviously, for rectangular pulses the operations of mapping sequences into signals and multiplication of signals/sequences are permutable, but for nonrectangular pulses these operations are, generally speaking, not permutable. Below we will consider both ways of generating spread signals.

Figure 1.6 corresponds to the *synchronous model* of the transmission, when the received signals from both transmitters are in the same phase. But the situation would not differ significantly in the *asynchronous case* (Fig. 1.7), when the received signals are in different phases. Using the same procedure of despreading as in the synchronous case, the receiver can even more easily recover both transmitted sequences $\boldsymbol{u}^{(1)}$ and $\boldsymbol{u}^{(2)}$. The necessary condition of the correct despreading is the knowledge of the phases of both transmitted signals $u^{(1)}(t) \cdot a^{(1)}(t)$ and $u^{(2)}(t) \cdot a^{(2)}(t)$. In other words, although the transmitters of the different users can be unsynchronized, the transmitter and the receiver corresponding to a particular user should be *synchronized*.

In general, we do not have two but K simultaneous active users and they operate asynchronously. A realistic model of the received signal should also include additive white Gaussian noise (AWGN) $\xi(t)$. The received (baseband) signal is

$$r(t) = \sum_{k=1}^{K} \sqrt{P^{(k)}} u^{(k)}(t - \delta^{(k)}) a^{(k)}(t - \delta^{(k)}) + \xi(t) \tag{1.2}$$

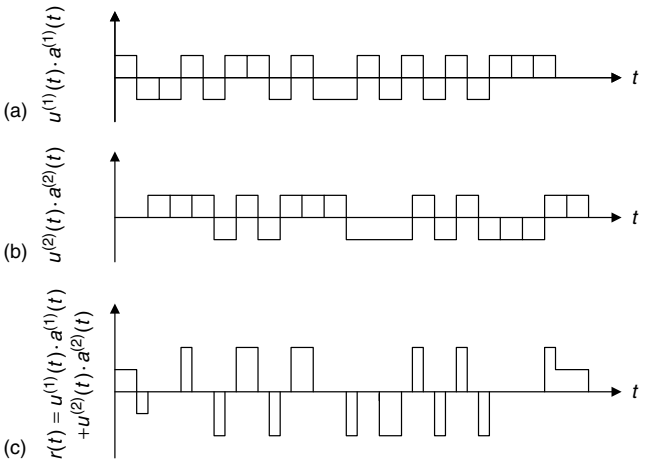

Figure 1.7. Example of the transmission over an adding channel, asynchronous case.

[3]In the literature, repetition coding is sometimes not considered as a coding and the transmission is called *uncoded transmission*.

where $P^{(k)}$ is the power of the signal from the kth user at the base station and $\delta^{(k)}$ is the kth user's *time offset*. The time offset values $\delta^{(k)}$ characterize asynchronism between different users, propagation delay, etc. If we are interested in the reception of the information from the kth user, we will present the received signal (1.2) as

$$r(t) = \sqrt{P^{(k)}}u^{(k)}(t - \delta^{(k)})a^{(k)}(t - \delta^{(k)}) + \xi^{(k)}(t) \tag{1.3}$$

where the total noise

$$\xi^{(k)}(t) = \sum_{k' \neq k} \sqrt{P^{(k')}}u^{(k')}(t - \delta^{(k')})a^{(k')}(t - \delta^{(k')}) + \xi(t) \tag{1.4}$$

includes the interference from the $(K - 1)$ other active users and additive noise. If the receiver is synchronized with the kth user, that is, $\delta^{(k)}$ is known, the despreading of the signal, that is, multiplication by $a^{(k)}(t - \delta^{(k)})$, reduces the problem in the case of repetition coding to detection of the known signal in noise (see Chapter 3) or, in the case of more complicated codes, to the decoding problem (see Chapter 4).

We emphasize that the model of uplink communication in the DS CDMA system considered here is the *information-theoretic* model. The model that is studied in *communication theory* describes processes in the transmitter-receiver, particularly the processes of *modulation-demodulation*, in more detail.

The receiver for binary DS CDMA signaling schemes can have one of two equivalently performing structures, a correlator implementation and a matched-filter implementation (see Chapters 2 and 3). The correlator receiver performs a correlation operation with all possible signals sampling at the end of each T-second signaling interval and comparing the outputs of the correlators. In the matched-filter receiver, correlators are replaced by matched filters.

The model of uplink DS CDMA communication with K users is presented in Figures 1.8 and 1.9. The base station receiver includes K demodulators synchronized with the modulators of the K transmitters. Assuming perfect synchronization, the output of the kth demodulator, $k = 1, 2, \ldots K$, is the sequence $\{v_n^{(k)} a_n^{(k)} + \xi_n^{(k)}\}$, where the noise components $\xi_n^{(k)}$ are contributions of all other active users and AWGN. Despreading consists of multiplication by the spreading sequence $\{a_n^{(k)}\}$. The input of the kth decoder is the sequence

$$\{v_n^{(k)} + \xi_n^{(k)} a_n^{(k)}\} \tag{1.5}$$

The output of the kth decoder is the decoded information sequence $\{\hat{u}_n^{(k)}\}$.

Using power control, the switching center can adjust the powers of transmitted signals such that the powers of the received signals would be approximately the same. If the power control is perfect the power of the received signal equals P independently from the user, that is, $P^{(k)} = P$, $k = 1, 2, \ldots K$. Each receiver at the base station of a single-cell communication system receives a

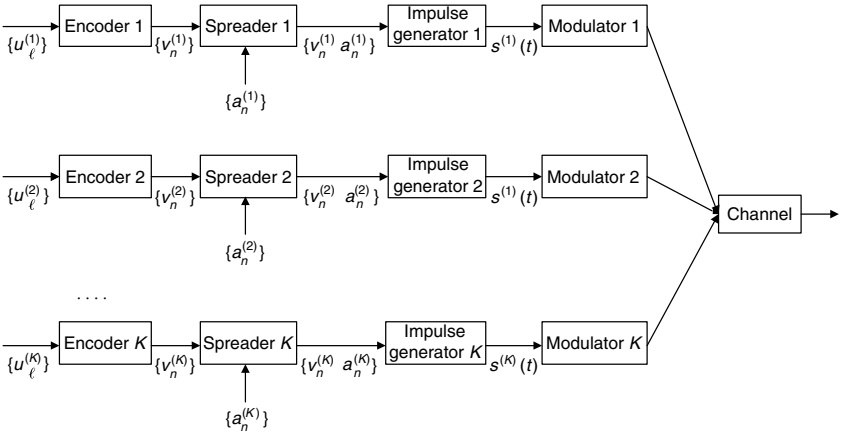

Figure 1.8. The model of uplink transmission in the DS CDMA system.

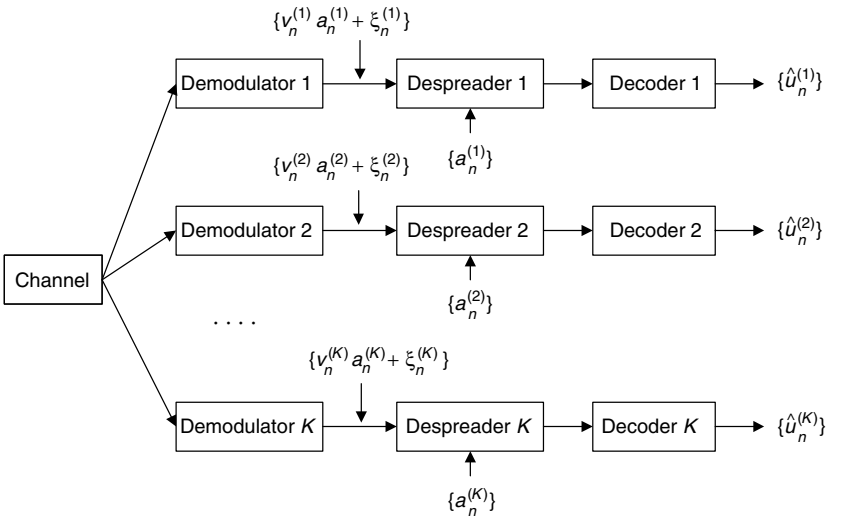

Figure 1.9. The model of the base station receiver of the DS CDMA system.

composite waveform containing the desired signal of power P, the component due to background AWGN $\xi(t)$, and the other-user interference component of power $P(K-1)$. Then the average one-sided total noise power spectral density[4] becomes

$$I_0 = (K-1)\,\frac{P}{W} + N_0 \tag{1.6}$$

[4]In this book we will later use only two-sided power spectral density, which for modulated signals is equal to half of the one-sided power spectral density.

where N_0 is the one-sided power spectral density of the AWGN and W is the signal bandwidth.

As we will see later, the important parameter that is the figure merit of the digital modem is *bit energy-to-noise density ratio* (for brevity we will call this parameter *signal-to-noise ratio, SNR*)

$$\frac{E_b}{I_0} = \frac{P}{I_0 R}, \tag{1.7}$$

where $E_b = P/R$ is the received energy per bit. Combining (1.6) and (1.7) we get

$$\frac{E_b}{I_0} = \frac{P/R}{(K-1)\dfrac{P}{W} + N_0} = \frac{W/R}{(K-1) + \dfrac{N_0 W}{P}} \tag{1.8}$$

From (1.8) follows the next formula for the radio channel capacity K_0 of a single-cell CDMA system:

$$K_0 = 1 + \frac{W/R}{E_b/I_0} - \frac{N_0 W}{P} = 1 + \frac{W/R}{E_b/I_0} - \frac{W/R}{E_b/N_0} \tag{1.9}$$

or, because we usually can neglect the influence of the background AWGN,

$$K_0 \approx 1 + \frac{W/R}{E_b/I_0} \tag{1.10}$$

The ratio W/R (in Hz/bit/s) was defined above as the *spreading factor* or the *processing gain*. Typical values of W/R range from one hundred (20 dB) to one million (60 dB). The required signal-to-noise ratio depends on the type of error-correcting coding used, the type of noise, and the limitations on the output probability of error. Under the condition that the number of active users K is large, we may consider the total noise as Gaussian noise of one-sided power spectral density I_0. Then, if the trivial repetition code is used, the bit error probability is the same as for uncoded transmission, that is,

$$P_b = Q\left(\sqrt{\frac{2E_b}{I_0}}\right) \tag{1.11}$$

where the Q function defined by the integral

$$Q(x) = \frac{1}{\sqrt{2\pi}} \int_x^\infty \exp(-y^2/2)\, dy \tag{1.12}$$

can be upperbounded by the inequality (Problem 1.5)

$$Q(x) \leq \frac{1}{2}\exp(-x^2/2), \quad x \geq 0 \tag{1.13}$$

If the repetition code is used, we get from Formulas (1.10)–(1.13)

$$K_0 \approx 1 - \frac{W/R}{\ln 2 P_b} \tag{1.14}$$

For the voice channel the required bit error rate is in the range 10^{-3}–10^{-4}, and the required signal-to-noise ratio E_b/I_0 is in the interval 4–8 dB, depending on the error correction code.

EXAMPLE 1.3

If the repetition code is used in the communication system and the required bit error rate is 10^{-4}*, what is the required signal-to-noise ratio? What is the required* E_b/I_0 *if* $P_b = 10^{-5}$*?*

Solution

Using Formula (1.11) we get that to $P_b = 10^{-4}$ *corresponds* $E_b/I_0 = 6.92$ *(*8.40 dB*) and to* $P_b = 10^{-5}$ *corresponds* $E_b/I_0 = 9.09$ (9.59 dB). *If we use the upper bound (1.13) we get that if* $E_b/I_0 = 6.12$*, then* $P_b < 4.96 \cdot 10^{-4}$*, and if* $E_b/I_0 = 9.09$*, then* $P_b < 5.6 \cdot 10^{-5}$.

Suppose further that two more processing features are added to the CDMA system to diminish interference. The first involves the monitoring of users' activity such that each transmitter is switched off or reduces its power during the periods of no user activity. In a two-way telephone conversation, the activity of each of the speakers is $1/\gamma_v$, where $\gamma_v \approx 8/3 \approx 2.67$; therefore, we can, in principle, reduce the interference noise in Formulas (1.6)–(1.10) by the factor γ_v. The parameter γ_v is called the *voice activity gain*.

Similarly, if we assume that the population of mobiles is uniformly distributed in the area of the single isolated cell, employing a sectored antenna reduces the interference noise by the *antenna gain* γ_a. For a three-sectored antenna, this gain is less than 3 and can be estimated as $\gamma_a \approx 2.4$.

To calculate the capacity of the entire CDMA system, not only of a single isolated cell, we have to include in I_0 the one-sided power spectral density N_{oc} of the other-cell interference noise. Let us suppose that the frequency reuse factor of the CDMA system is equal to 1, that is, all users in all cells employ the common spectral allocation of W Hz. It was shown previously [47] that the total interference from the users in all the other cells equals approximately 0.6 of that caused by all the users in the given cell *(other-cell relative interference factor* f *is* equal to 0.6*)*, that is, $N_{oc} = 0.6(K-1)P/W$. Thus, in consideration of the total system capacity, the interference term of I_0 should be increased by the factor 1.6. Finally, introducing the voice activity and antenna gain factors,

γ_v and γ_a, and the other-cell relative interference factor, f, into the total noise power spectral density expression yields

$$I_0 = (K-1)\frac{P}{W}\ \frac{1+f}{\gamma_v\gamma_a} + N_0 \tag{1.15}$$

Thus, analogously to Formula (1.9), we get the following expression for the total radio channel capacity of the CDMA system [47]:

$$K_0 = 1 + \frac{W/R}{E_b/I_0}\ \frac{\gamma_v\gamma_a}{1+f} - \frac{N_0 W}{P}\ \frac{\gamma_v\gamma_a}{1+f} = 1 + \frac{W/R}{E_b/I_0}\ \frac{\gamma_v\gamma_a}{1+f} - \frac{W/R}{E_b/N_0}\frac{\gamma_v\gamma_a}{1+f} \tag{1.16}$$

or, if the AWGN is negligible,

$$K_0 \approx 1 + \frac{W/R}{E_b/I_0}\ \frac{\gamma_v\gamma_a}{1+f} \tag{1.17}$$

EXAMPLE 1.4 [47]

Consider a cellular system with voice activity gain $\gamma_v = 2.67$*, antenna gain* $\gamma_a = 2.4$*, required signal-to-noise ratio* $E_b/I_0 = 4$ *(6 dB), and other-cell relative interference factor* $f = 0.6$*. What is the radio channel capacity of this system?*

Solution

Using Formula (1.17), we get

$$K_0 \approx W/R$$

The radio channel capacity is approximately equal to the spreading factor.

In Example 1.1 and Example 1.2 we mentioned two standards, AMPS and GSM. They standardize non-CDMA systems. The first DS CDMA system standardized as Interim Standard 95 (IS-95) [44] was adopted in 1993. IS-95 is specified for uplink operation in 824–849 MHz and for downlink in 869–894 MHz.

EXAMPLE 1.5

Each channel of the CDMA system IS-95 occupies 1.25 MHz of the spectrum on each one-way link. Bands of 25 MHz are available in each direction. The maximum user rate is $R = 9.6$ *kb/s. If a minimum acceptable* E_b/I_0 *is 6 dB, determine the capacity of a CDMA system using*

a) *Omnidirectional base station antennas and no voice activity detection and*
b) *Three-sectored antennas at the base station with* $\gamma_a = 2.4$ *and voice activity detection with* $\gamma_v = 2.67$

The received signal power P *is* 10^{-11} *W, the one-sided AWGN power spectral density* $N_0 = 10^{-17}$ *W/Hz, and the other-cell relative interference factor* $f = 0.6$.

Solution

From Formula (1.17) we have for each channel

a) $K_0 = 1 + \dfrac{1.25 \cdot 10^6/9.6 \cdot 10^3}{4 \cdot 1.6} - \dfrac{10^{-17} \cdot 1.25 \cdot 10^6}{1.6 \cdot 10^{-11}} \approx$
$1 + 18.8 - 0.8 = 19$

b) $K_0 \approx 1 + 18.8 \cdot 2.4 \cdot 2.67 - 0.8 \cdot 2.4 \cdot 2.67 =$
$1 + 120.3 - 5.1 \approx 115$

Because the system has $25/1.25 = 20$ *channels in each link, the total capacity is equal to* 380 *in the first case and* 2300 *in the second case.*

Our last example of this section concerns the third-generation (3G) mobile communication systems, based on wideband CDMA (WCDMA) [55]. For WCDMA there are available bands 1920–1980 MHz in reverse direction and 2110–2170 MHz in forward direction, that is, 60 MHz in each direction. The speech codec in WCDMA employs the Adaptive Multi-Rate (AMR) technique standardized in 1999. It has eight source rates, from 4.75 kb/s up to 12.2 kb/s.

EXAMPLE 1.6

Each channel of the WCDMA system occupies 5 *MHz of the spectrum on each link. Assume that the user rate* 12.2 *kb/s. The other parameters are the same as in Example 1.5. Find the capacity of the WCDMA system under the given conditions.*

Solution

From Formula (1.17) we get for each channel

$$K_0 = 1 + \frac{5 \cdot 10^6/12.2 \cdot 10^3}{4 \cdot 1.6} \cdot 2.4 \cdot 2.6 - \frac{10^{-17} \cdot 5 \cdot 10^6}{1.6 \cdot 10^{-11}} \cdot 2.4 \cdot 2.6$$
$$= 1 + 409 - 20 = 390$$

Under the given conditions, the total capacity of the WCDMA system equals $60 \cdot 390/5 = 4680$.

The mathematical model of the CDMA system considered above is a model of many-to-one transmission. Strictly speaking, it describes only reverse link transmission. In Chapter 3 we show that Formula (1.17) for the radio channel capacity is valid also for forward link. The forward link transmission that is one-to-many transmission has some advantages in comparison to many-to-one transmission. First, the signals transmitted to different users can be synchronized and accommodated by a pilot signal, such that the users can use coherent receivers. For the reverse link, a pilot signal is not always used because of power limitations. Second, because the transmitter knows the transmitted information sequences of all the users, it can in principle use this information in the encoding process, and

improve the performance of the overall system. In this case we can talk about *coordinated transmission* or *partially coordinated transmission*. We consider this problem in Chapter 9.

In the DS CDMA system each of the active users occupies in each time instance all wideband channels. In the next section we consider a system in which the wideband channel is divided into narrow frequency bands. Each of the active users occupies in each time instance only one band and periodically changes this band.

1.4 FREQUENCY-HOPPED CDMA

Conventional frequency-hopped (FH) CDMA is a digital multiple access system in which individual users select one of Q frequencies within a wideband channel as carrier frequency. The pseudorandom changes of the carrier frequencies randomize the occupancy of a specific band at any given time, thereby allowing for multiple access over a wide range of frequencies. In a conventional FH CDMA system, the total hopping bandwidth W is divided into Q narrow bands each of bandwidth B, where $B = W/Q$. Each of the Q bands is defined as a spectral region with a central frequency called the *carrier frequency*. The set of possible carrier frequencies is called the *hopset*. The bandwidth B of a band used in a hopset is called the *instantaneous bandwidth*. The bandwidth of the spectrum W over which the hopping occurs is called the *total hopping bandwidth*. Information is sent by hopping the carrier frequency according to the pseudorandom law, which is known to the desired receiver. In each hop, a small set of code symbols is sent with conventional narrowband modulation before the carrier frequency hops again. The time duration between hops is called *hop duration* or *hopping period* and is denoted by T_c. The time duration between transmission of two consecutive symbols is T.

Usually in FH CDMA frequency shift-keying (FSK) is used. If in FH CDMA system q-FSK is used, then each of the Q bands is divided into q subbands and during each hop one or several of the central frequencies of the subbands within the band can be sent. We will also call each frequency subband the *transmission channel*. We denote the total number Qq of transmission channels by M. If binary FSK (BFSK) is used, $M = 2Q$ and the pair of possible instantaneous frequencies changes with each hop.

At the receiver side, after the frequency hopping has been removed from the received signal, the resulting signal is said to be *dehopped*. Before demodulation, the dehopped signal is applied to a conventional receiver. If another user transmits in the same band at the same time in a FH CDMA system, a *collision* can occur.

Frequency hopping can be classified as slow or fast. *Slow frequency hopping* occurs if one or more q-ary symbols are transmitted in the interval between frequency hops. Thus slow frequency hopping implies that the symbol rate $1/T$ exceeds the hopping rate $1/T_c$. *Fast frequency hopping* occurs if there is more than one frequency hop during one symbol transmission time. If other users

occupied the same frequency band in the same time, the probability of incorrect transmission of the corresponding information symbols would become high. Therefore, it is advisable to combine frequency hopping with *interleaving* and *coding*.

Figure 1.10a illustrates slow frequency hopping if FSK is used in the system and $Q = 4$, $q = 4$, and $M = 16$. In this figure the instantaneous frequency subbands (transmission channels) are shown as a function of the time. The 4-ary symbol transmission time T is equal to $T_c/3$, where T_c is the hop duration. Two bits are collected each T second, and one of four frequencies is generated by the modulator. This frequency is translated to one of $Q = 4$ frequency hop bands by the FH modulator. In this example, a frequency hop occurs after each group of 3 symbols or when 6 bits have been transmitted. The dehopped signal is shown in Figure 1.10b.

A representation of a transmitted signal for a fast frequency-hopped system is illustrated in Figure 1.11. The output of the data modulator is one of the tones as before, but now time T of the transmission of one group of 2 bits is subdivided into $T/T_c = 4$ chips (hops). In this example, each pair of bits is transmitted during 4 carrier frequency hops.

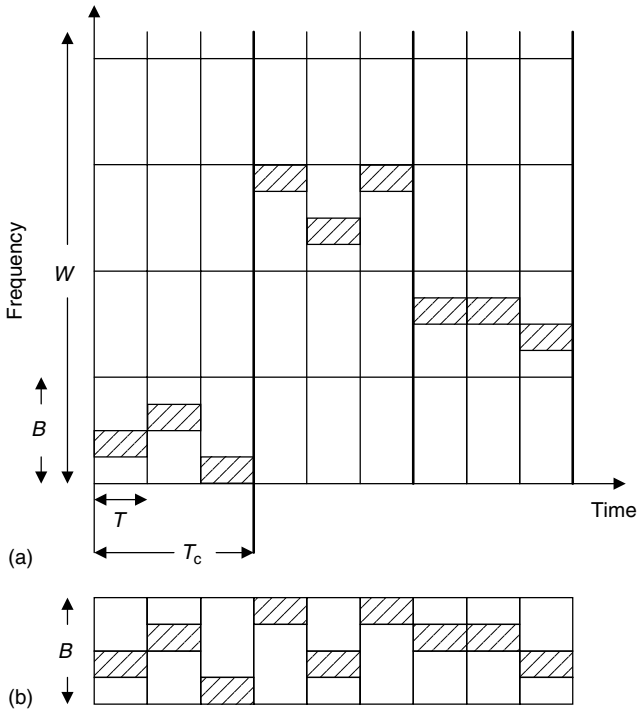

Figure 1.10. Illustration of FSK slow-frequency-hopped spread spectrum system. (a) transmitted signal; (b) dehopped signal. (4-FSK modulation)

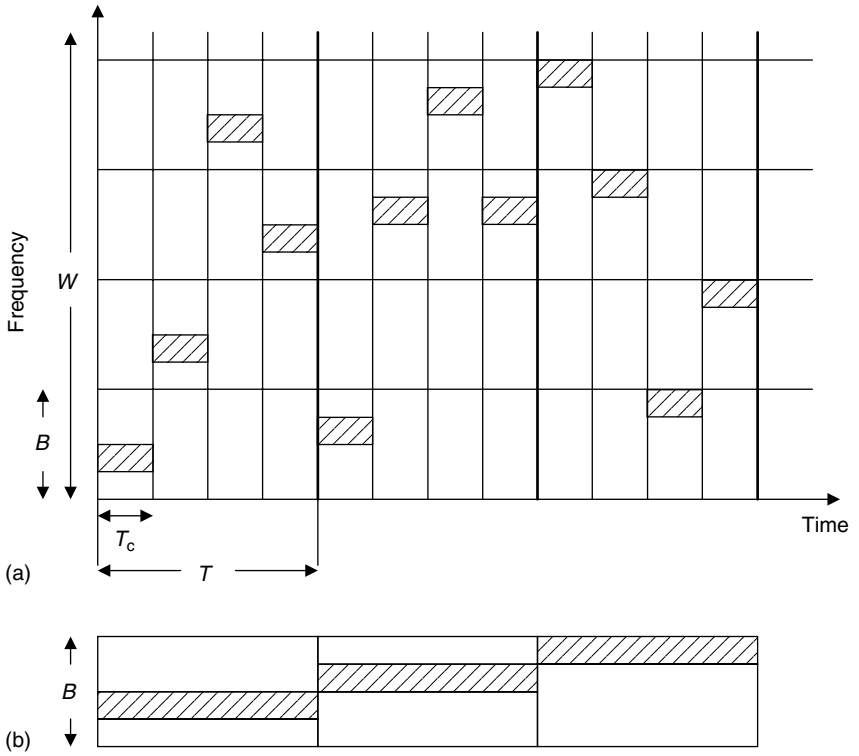

Figure 1.11. Illustration of FSK fast-frequency-hopped spread spectrum system (a) transmitted signal; (b) receiver down-converter output.

In this book, we will consider a scheme slightly different from the conventional scheme of FH CDMA. We will not distinguish between frequency hopping caused by changing of the carrier frequency and frequency hopping caused by transmission of a new symbol. In other words, we will consider any instantaneous frequency (transmission channel) change to be a *hop*. Correspondently, we modify the terminology and call the set of all M possible instantaneous frequencies as a *hopset*. The value M, the ratio of the total hopping bandwidth to the instantaneous bandwidth, is called the *hopset size*. The *hop duration* T_c is defined as the time interval between two consecutive instantaneous frequency changes. Then for the slow frequency hopping scheme in Figure 1.10, the hop duration is equal to one symbol transmission time T and will be labeled as T_c. The time interval between two consecutive carrier frequency changes should be omitted. For both frequency hopping schemes in Figures 1.10 and 1.11, the instantaneous bandwidth should be decreased four times. This modification of the FH CDMA scheme is quite natural, because a modern digital FH CDMA system uses coding and the information bit rate is, as a rule, lower than the hopping rate.

In contrast to a DS CDMA signaling scheme, which uses matched-filter or correlator receivers, we assume that a FH CDMA system uses a *radiometer* as the receiver. A radiometer detects energy received in an instantaneous frequency band by filtering to this bandwidth, squaring the output of the filter, integrating the output of the squarer for time T_c, and comparing the output of the integrator with a threshold. If the integrator output is above a present threshold, the signal is declared present in this instantaneous frequency band; otherwise, the signal is declared absent. Let us assume that there is no additive noise in the channel and that the users are chip synchronized, that is, frequency hops of the received signal occur in the moments nT_c, $n = \ldots 0, 1, 2, \ldots$. Then we may choose zero threshold and the radiometer declares the presence of the signal in the instantaneous band if and only if one OR more users occupy this band. Such a receiver is also called an *OR receiver.*

To explain the mechanism of FH CDMA we consider a simple example. Suppose that the number of users is $K = 2$ and BFSK with an OR receiver is used. The total bandwidth W is divided into two subbands (transmission channels), left and right, $M = q = 2$, and the transmission time is divided into time slots of duration T_c. Each of the users occupies the left channel if it would like to transmit 1 in a given time slot and the right channel if it would like to transmit -1 (Fig. 1.12a). The users are chip synchronized (synchronous reception). If we apply the TDMA principle (see Section 1.2), we assign, for example, even time slots to user 1 and odd time slots to user 2. This gives the overall transmission rate 1 (bits/time slot) conditioned that both of the users are active all the time and the information symbols are equiprobable. But if both users are active only 40% of the time, the average overall transmission rate is only 0.4 (bits/time slot).

Now suppose that both of the users may occupy all time slots (Fig. 1.12b). If either the first user or the second one or both of them transmit in the given subband the radiometer detects this event. If both of the users transmit the

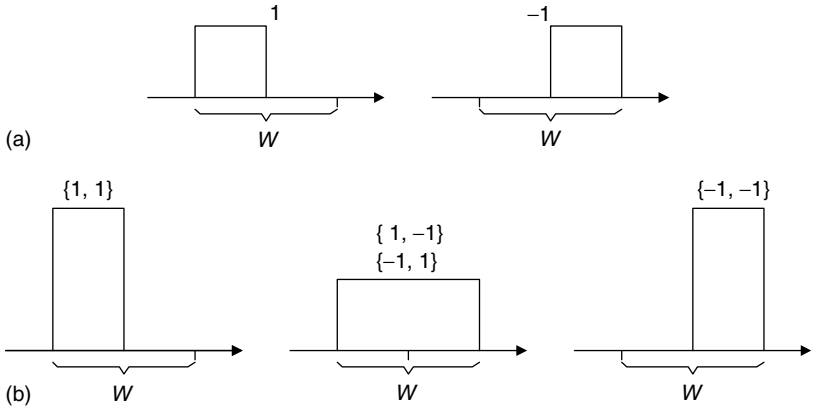

Figure 1.12. Illustration of FH: (a) binary FSK transmission; (b) FH CDMA transmission with two users.

same symbol, energy would be detected only in one of the subbands and the receiver determines which symbol was transmitted by the users. If the symbols are equiprobable we can say that the receiver gets 2 bits of information. If the users transmit different symbols, the radiometer detects energy in both subbands and can not decide which symbol was transmitted. The receiver gets no information. Conditioned that at least one of the users is active, the average transmission rate is still 1 (bits/time slot). If both of the users are active 40% of the time, the average transmission rate is 0.64 (bits/time slot), which is essentially higher than when the TDMA system is used.

Although the average transmission rate in this case is higher than in the time division case, parts of the transmitted symbols vanish. These symbols can be reconstructed if the system uses coding. The following, more complicated example shows how we can do this.

EXAMPLE 1.7

Consider the synchronous FH CDMA system using BFSK with K users, which are active all the time. The hopset size is M, $q = 2$, $Q = M/2$, and the probability that a user chooses a particular band is equal to $1/Q$. Each user transmits one bit of information in N time slots using rate $r = 1/N$ block length N repetition code and an OR receiver. If the user transmits a 1 it occupies the left subband of the band, and if it transmits a -1 it occupies the right subband. Assume that the symbols 1 and -1 are equiprobable. Consider the case $K = 100$, $N = 98$, $M = 36$. What is the overall transmission rate r_{overall} (in bits per time slot)? What is the bit error probability P_{b}?

Solution

Because each active user transmits one bit in N time slots, the individual user transmission rate is $1/N$ (bits/time slot), and the overall transmission rate is $r_{\text{overall}} = K/N$ (bits/time slot). In our case $r_{\text{overall}} = 1.02$.

Now we estimate the error probability. Let the first user be the reference user and the other users be jammers. Suppose that the first user transmits the symbol 1. Then the radiometer always detects energy in the left subband of the band in which the first user transmits in the nth time slot. The receiver makes a correct decision, if at least for one n, $n = 0, 1, \ldots, N-1$, the right subband of this band would not be occupied by one of the $(K-1)$ jammers. The probability of this event for the nth subband, $n = 0, 1, \ldots, N-1$, is

$$\pi = \left(1 - \frac{1}{M}\right)^{K-1}$$

and the probability of the complementary event is

$$1 - \pi = 1 - \left(1 - \frac{1}{M}\right)^{K-1}$$

Then the probability that the receiver cannot make a single decision on the information bit sent by the first user is $(1-\pi)^N$. *Assuming that in the case of a tie the receiver makes a random decision, we have*

$$P_b = \frac{1}{2}\left[1 - \left(1 - \frac{1}{M}\right)^{K-1}\right]^N$$

This probability does not depend on which user is the reference user and on which information symbol was sent. For $N = 98$, $K = 100$, *and* $M = 36$ *we have* $P_b = 10^{-3}$.

For $M \gg 1$,

$$P_b \approx \frac{1}{2}\left[1 - \left(1 - \frac{1}{M}\right)^{M\cdot\frac{K-1}{M}}\right]^N \approx \frac{1}{2}\left(1 - e^{-\frac{K-1}{M}}\right)^N \tag{1.18}$$

In Section 1.3 we defined the processing gain of a DS CDMA system as the bandwidth expansion factor, or equivalently, the number of chips per information bit. In the general case the processing gain represents the advantage gained over the jammer that is obtained by expanding the bandwidth of the transmitted signal. The users' transmission rate R of the FH CDMA system of Example 1.7 is equal to $1/NT_c$. If the system did not use the spread spectrum technique, it would occupy a bandwidth of order $1/NT_c$. Because the FH CDMA system occupies a bandwidth W of order M/T_c, we can estimate the FH CDMA system processing gain as $W/R = MN$.

EXAMPLE 1.8

Under the same condition as in Example 1.7, find the maximal number of active users in the FH CDMA system if the number of active users $K = \lambda M + 1$, *where* λ *is a positive factor,* $M \gg 1$, *and* P_b *is given. Assume that* $T_c = 2/B = M/W$. *Find* λ *that maximizes* K.

Solution

From Formula (1.18) it follows that for $M \gg 1$

$$(1 - e^{-\lambda})^N = 2P_b$$

or

$$N \ln(1 - e^{-\lambda}) = \ln(2P_b) \tag{1.19}$$

But

$$N = \frac{T}{T_c} = \frac{W}{MR} = \frac{W\lambda}{(K-1)R} \tag{1.20}$$

From Formulas (1.19) and (1.20) we have

$$K = 1 + \frac{W/R}{\ln(2P_b)}\,\lambda \ln(1 - e^{-\lambda}) \tag{1.21}$$

The maximum of the right side is at $\lambda = \ln 2$*, and for this* λ *we get the number of active users (radio channel capacity)*

$$K_0 = 1 - \frac{W/R}{\ln(2P_b)}\,(\ln 2)^2 \approx 1 - \frac{W/R}{\ln(2P_b)}\,0.48 \tag{1.22}$$

Analogously to the DS CDMA case the radio channel capacity of the FH CDMA system is proportional to the spreading factor W/R*.*

The number of active users in the FH CDMA system given by (1.22) is about two times less than the radio channel capacity in the DS CDMA system given by (1.14), that is, the efficiency of the FH CDMA is about half of that of DS CDMA. We note that Formula (1.22) is derived under very idealized assumptions (absence of additive noise), and the real capacity of FH CDMA system with the OR receiver is even less. Even if we used in FH a noncoherent receiver (see Chapter 3) instead of the OR receiver, the capacity of the FH CDMA system would be still less than the capacity of the analogous DS CDMA system.

However, FH CDMA systems have an important advantage in comparison with DS CDMA systems. In the DS CDMA system, the signals have a large instantaneous bandwidth. The complexity and cost of the transmitter increases as the instantaneous bandwidth of the signal grows. In an FH CDMA system this bandwidth is much smaller and the complexity of the equipment can be smaller. Thus, although the efficiency of DS CDMA is higher than that of FH CDMA, this advantage is overshadowed by the greater band spreading achievable with FH technology.

FH CDMA can be considered as a counterpart to FDMA. In the next section we consider a counterpart to TDMA, "time-hopped" or *pulse position-hopped CDMA*.

1.5 PULSE POSITION-HOPPED CDMA

Digital radio transmission has traditionally been based on the concept that the carrier frequency is much larger than the bandwidth of the transmitted signal. When the required bandwidth is of the order of 100 MHz this approach encounters many obstacles. Typically, the transmitter would operate at a carrier frequency above 10 GHz, and thus would suffer from absorption by rain and fog. A different technique is the *impulse radio*, multiple access modulated by a pulse position hopping (PPH). The impulse radio technique is also denoted *ultrawideband* transmission. Impulse radio communicates with pulses of very short duration, typically on the order of a nanosecond, thereby spreading the energy of the radio signal

very thinly up to a few gigahertz. It is a promising technique for short-range and indoor communication.

The main advantages of impulse radio are as follows. In an impulse radio system, the transmitted signal is a dithered pulse train without a sinusoidal carrier and, hence, carrier recovery at the receiver is not required. As we mentioned above, in an ultrawideband system, such as impulse radio, fading is not nearly as serious a problem as it is for narrowband systems. Impulse radio systems can operate at variable bit rates by changing the number of pulses used to transmit one bit of information. We note that DS CDMA and FH CDMA use more complex bit rate variation techniques.

In a typical PPH format used by impulse radio the output signal of the kth, $k = 1, 2, \ldots, K$, transmitter is a sequence of monocycle waveforms $h_{T_c}(t - \tau_n^{(k)})$, $n = 0, 1, \ldots$, where t is the clock time of the transmitter, T_c is the pulse duration, and $\tau_n^{(k)}$ is the time delay. Because the pulses have electromagnetic origin, the average pulse amplitude is equal to zero.

In Figure 1.13, we present two examples of $h_{T_c}(t)$, which will be considered in a theoretical treatment. These are:

a) Manchester pulse:

$$h_{T_c}(t) = \begin{cases} -1, & -T_c/2 < t < 0 \\ 1, & 0 < t < T_c/2 \\ 0, & \text{otherwise} \end{cases} \tag{1.23}$$

b) differentiated Gaussian pulse:

$$h_{T_c}(t) = A_{dg} t \exp\left(-\frac{t^2}{4\gamma T_c^2}\right) \tag{1.24}$$

where A_{dg} and γ are normalizing constants (see Chapter 2), and T_c is pulse duration. In PPH CDMA applications we will only study Manchester pulses.

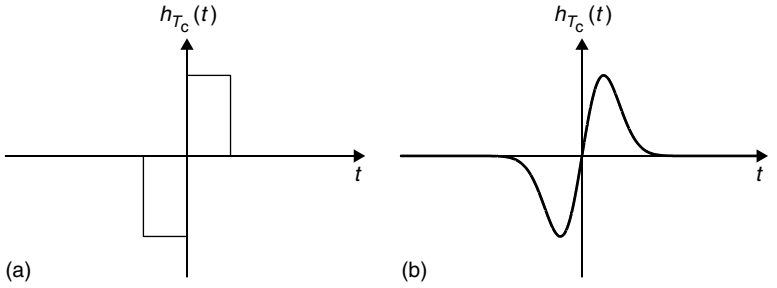

Figure 1.13. Examples of monocycle waveforms that model pulses in impulse radio: (a) Manchester pulse; (b) differentiated Gaussian pulse.

Consider again the uplink transmission. Suppose that the transmission time is divided into frames of duration T_f, $T_f = MT_c$, $M \gg 1$, M is even. The kth user, $k = 1, 2, \ldots, K$, transmits the nth bit $v_n^{(k)}$ of the code sequence $\boldsymbol{v}^{(k)} = v_0^{(k)}, v_1^{(k)}, \ldots, v_{N-1}^{(k)}$, where $v_n^{(k)} \in \{+1, -1\}$, in the nth frame. The users are synchronized such that signals that were sent by the users in the nth frame will be received by the receiver in the same time interval $(t, t + T_f)$.

Each frame is divided into Q time slots, $Q = M/2$, of length $2T_c$, and each slot is divided into two subslots of length T_c (Fig. 1.14).

An individual user selects one of Q time slots within a frame to transmit the code symbol. Each slot can be choosen with probability $1/Q$. If the code symbol is 1, then the user transmits a pulse in the left subslot, if the code symbol is -1, then the user transmits a pulse in the right subslot.

The signal waveform transmitted by the kth user in the nth frame is

$$\tilde{s}_n^{(k)}(t) = h_{T_c}\left(t - nT_f - \tau_n^{(k)} + v_n^{(k)}\frac{T_c}{2}\right) \tag{1.25}$$

where $v_n^{(k)} \in \{+1, -1\}$ is the nth code symbol of the kth user, $\tau_n^{(k)} = 2a_n^{(k)}T_c$ is the *addressable pulse position shift*, and $a_n^{(k)}$ is an integer-valued random variable uniformly distributed on the set $\{0, 1, \ldots, Q-1\}$. The ratio $T_f/T_c = M$ is the *hopset size*.

This is the time-domain analog of the FH CDMA transmission model considered in the previous section. As receiver we can use both the correlator receiver and the OR receiver. If the users are synchronized and use rate $R = 1/N$ block length N repetition codes with OR receivers then the bit error probability is [compare with Formula (1.18)]

$$P_b = \frac{1}{2}\left[1 - \left(1 - \frac{1}{M}\right)^{K-1}\right]^N \approx \frac{1}{2}\,(1 - e^{-\lambda})^N \tag{1.26}$$

where $\lambda = (K-1)/M$. The radio channel capacity reaches its maximum for $\lambda = \ln 2$. The transmission rate R of this PPH CDMA system is equal to $1/NT_f = 1/NMT_c$. Because the transmission rate of the corresponding system not using

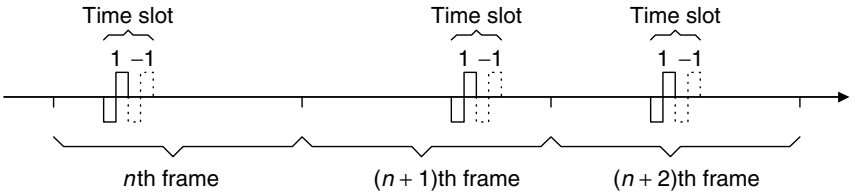

Figure 1.14. Illustration of PPH CDMA transmission.

the spread spectrum technique is $1/T_c$, we define the processing gain as NM, which equals $NT_f/T_c = W/2R$, where we defined the bandwidth[5] $W = 2/T_c$. Analogously to (1.22) we get the radio channel capacity of the PPH CDMA system with OR receiver

$$K_0 \approx 1 - 0.48\frac{W/2R}{\ln(2P_b)} \tag{1.27}$$

Note that if it were possible to use unimodal pulses of duration $T_c = 1/W$ in the PPH transmission, the radio channel capacity would be approximately two times larger.

As we mentioned above, the PPH CDMA signals can be processed by the correlator receiver. Consider again the same model of the PPH CDMA system, but now assuming that the users are not required to be synchronized and may use an arbitrary code rate r length N block code. For simplicity we suppose that the system has perfect power control, that is, the power $P^{(k)}$ of the received signal from the kth user equals P independently of the user. Then the received signal from the kth user is

$$\sum_{n=0}^{N-1} \sqrt{P}\; h_{T_c}\left[t - nT_f - \tau_n^{(k)} + v_n^{(k)}\frac{T_c}{2} - \delta^{(k)}\right] \tag{1.28}$$

where $\delta^{(k)}$ is the kth user's time offset, including propagation delay, asynchronism between the users, etc. The total received signal is

$$r(t) = \sum_{k=1}^{K}\sum_{n=0}^{N-1} \sqrt{P}\; h_{T_c}\left(t - nT_f - \tau_n^{(k)} + v_n\;\frac{T_c}{2} - \delta^{(k)}\right) \tag{1.29}$$

Each receiver at the base station receives a composite waveform containing the desired signal of power P, the component due to background AWGN of one-sided spectral density N_0, and the other user interference component. All the energy PT_c of the desired signal in the nth frame is concentrated in the time window of size $2T_c$,

$$nT_f + \tau_n^{(k)} - T_c + \delta^{(k)} \le t < nT_f + \tau_n^{(k)} + T_c + \delta^{(k)} \tag{1.30}$$

which is only $2T_c/T_f$ part of the frame. Therefore, the average contribution of each of the $(K-1)$ interfering users to the total noise energy is equal to $2PT_c^2/T_f$. The average signal-to-interference ratio per chip is then equal to

$$\frac{PT_c}{2(K-1)PT_c^2/T_f} \tag{1.31}$$

[5]In general, we use the definition $W = 1/T_c$, but for bimodal Manchester and differentiated Gaussian pulses we make an exception.

and the average signal-to-interference ratio per bit is

$$\frac{E_b}{I_0} = \frac{PT_c Nr}{2(K-1)PT_c^2/T_f} \tag{1.32}$$

Because the receiver operates in the window of size $2T_c$, the AWGN contribution to the total noise power spectral density is $2N_0$. Then Equality (1.32) can be modified and we obtain

$$\frac{E_b}{I_0} = \frac{PT_c Nr}{2(K-1)PT_c^2/T_f + 2N_0} \tag{1.33}$$

Because $W = 2/T_c$, $R = r/NT_f$, we get from Formula (1.33)

$$\frac{E_b}{I_0} = \frac{W/4R}{(K-1) + N_0 T_f/PT_c^2}. \tag{1.34}$$

From (1.34) follows the next formula for the radio channel capacity of the PPH CDMA system:

$$K_0 = 1 + \frac{W/4R}{E_b/I_0} - \frac{N_0 T_f}{PT_c^2} \tag{1.35}$$

For the repetition code $P_b \approx \frac{1}{2}\exp(-E_b/I_0)$ and if we neglect AWGN we finally have

$$K_0 \approx 1 - \frac{W/4R}{\ln(2P_b)} \tag{1.36}$$

A comparison of (1.27) and (1.36) shows that PPH CDMA systems with OR and correlator receivers have approximately equal capacities. However, we must note that Formulas (1.22) and (1.27) for the radio channel capacity of the FH CDMA system and the PPH CDMA system with OR receivers are derived under very idealized assumptions. First, we assumed that the users of the systems are synchronized. Asynchronism of the users decreases the capacity about two times. At the same time, asynchronism of the users does not affect the capacity of the PPH CDMA system with correlator receivers. Second, and more important, even small additive noise essentially decreases the capacities of FH CDMA and PPH CDMA systems with OR receivers but practically does not affect the capacity of the PPH CDMA system with correlator receivers. On the other hand, FH CDMA and PPH CDMA systems with OR receivers are robust to imperfection of the power control.

The PPH CDMA system described above uses *pulse position modulation* (PPM) format. It is also in principle possible to use the *pulse amplitude on-off modulation* (PAM) format. Then the signal waveform transmitted by the kth

user in the nth frame is

$$\tilde{s}_n^{(k)}(t) = \frac{[v_n^{(k)} + 1]}{\sqrt{2}} \, h_{T_c}[t - nT_f - \tau_n^{(k)}] \tag{1.37}$$

where $\tau_n^{(k)}$ is the addressable pulse position shift and $1/\sqrt{2}$ is a normalizing factor.

The PPH CDMA system with on-off PAM is analyzed analogously to the system with PPM.

EXAMPLE 1.9

Consider a single cell PPH CDMA system using impulse radio with pulses of duration $T_c = 10^{-9}$s. The user transmission rate is $R = 10$ kb/s. If a minimum acceptable E_b/I_0 is 7 dB, determine the capacity of the system. Estimate the influence of the system on the existing radio transmission systems.

Solution

From Formula (1.36) we have

$$K_0 \approx 2 \, \frac{10^9/4 \cdot 10^4}{5} = 10^4 \tag{1.38}$$

This capacity is much higher than the capacity of existing mobile radio systems. This is good news. The bad news is that the system occupies the full frequency range up to gigahertz, where all existing radio systems operate.

The PPH CDMA system can be used not only in cellular and conventional packet radio architectures, but also in *peer-to-peer* architectures. In peer-to-peer networks, connections between two users are not routed through a base station but are established directly. In peer-to-peer systems the synchronization overhead is minimal, especially for long message holding times.

Impulse radio has some other advantages in comparison with traditional carrier frequency-based radio, but, because it operates over the highly populated frequency range below a few gigahertz, it interferes with narrowband radio systems operating in dedicated bands. Potentially there must be a real payoff in the use of PPH CDMA protocol to undertake the difficult problem of coexistence with existing radio systems.

1.6 ORGANIZATION OF THE TEXT

In the previous three sections we described three different CDMA systems, direct-sequence, frequency-hopped, and pulse position-hopped CDMA systems. All three systems use the spread spectrum communication principle. Chapter 2 is an introduction to spread spectrum communication. It is devoted to the description and the generation of spreading signals in different CDMA systems.

Although spread spectrum systems can use both analog and digital modulation, modern spread spectrum communication systems mostly use digital modulation techniques. Digital modulation offers many advantages over analog transmission systems, including greater noise immunity and robustness to channel impairments. DS CDMA most often employs binary-phase shift keying (BPSK) or quadrature-phase shift keying (QPSK). FH CDMA most often employs, as we mentioned above, frequency shift keying (FSK). Corresponding modulation schemes are considered in Chapter 2. The PPH CDMA system does not use a sinusoidal carrier for the transmission of information but uses pulse position or pulse amplitude modulation. These modulation formats are also considered in Chapter 2.

A DS CDMA system spreads a PSK-modulated carrier by a wideband spreading signal. *Coherent* or *noncoherent demodulation* may be employed in the receiver. The spreading sequence in the case of FH CDMA does not directly modulate the FSK signal but is instead used to control the sequence of hopping frequencies. The demodulation of the received signal is in most cases *noncoherent*. The PPH CDMA system uses both a correlator receiver and an OR receiver. Reception of spread spectrum signals is studied in Chapter 3.

Interference is the major limiting factor in the performance of a cellular CDMA system. Sources of interference include other mobiles in the same or neighboring cells, other base stations operating in the same frequency band, or any radio system that inadvertently leaks energy into the cellular frequency band. Because the number of interference sources is usually large, the resulting interference noise on the receiver input can be considered as additive Gaussian noise and conventional methods of signal detection in additive Gaussian noise can be applied. An overview of these methods is given in Chapter 3.

Spread spectrum CDMA provides a considerably higher dimensionality of signals than needed to transmit information by any single user. This is reflected by the high processing gain. A universally effective method of exploiting redundancy to improve performance is forward error-correcting (or error control) coding. Although most known error-correcting methods can be used in CDMA communication, two of them have an advantage in this application. The first, first-order Reed–Muller code (Hadamard sequences), provides high reliability in low rate transmission, which is the case here. The second, convolutional coding with Viterbi decoding, permits exploitation of soft inputs to decrease the required signal-to-noise ratio at the receiver input. Application of coding to CDMA communication is studied in Chapter 4.

The mobile radio channel places fundamental limitations on the performance of cellular communication systems. The transmission path between the transmitter and the receiver can be obstructed by buildings and mountains. Unlike the one-path AWGN channel that is stationary and predictable, the mobile radio channel is a nonstationary multipath channel. Therefore, the analysis of spread spectrum communication in multipath *fading* channels is an essential part of the theory of CDMA communications. Analysis of spread spectrum CDMA communication in fading channels is carried out in Chapter 5.

In time-varying multipath fading channels, diversity can improve performance markedly. Such diversity can be attained by spatial separation such as multipath antennas or by natural multiple-path propagation with a *Rake receiver* or by temporal separation through an *interleaving* process. Interleaving has become an extremely useful technique in modern digital cellular systems and is also studied in Chapter 5.

The important issue to be dealt with in developing a spread-spectrum system is the generation of pseudorandom signals. This can be achieved in a variety of ways, but the generating process must be easily implemented and reproducible, because the same process must be generated at the transmitter for spreading (or hopping) and at the receiver for despreading (or dehopping). It is shown in Chapter 6 that generation of pseudorandom spreading or hopping process is most easily implemented by linear binary sequence generators, followed by linear filters. The largest part of the chapter is devoted to comprehensive discussion of maximum-length sequences, which are by far the most widely used spreading codes. The chapter concludes with a short discussion of orthogonal spreading sequences, Gold sequences, and Kasami sequences, which are used in the third-generation wireless networks.

Spread spectrum communication requires that the spreading (hopping) process in the transmitter and the despreading (dehopping) process in the receiver should be *synchronized*. If they are out of synchronization, insufficient signal energy will reach the receiver data demodulator. The task of achieving and maintaining synchronization is always delegated to the receiver. There are two components of the synchronization problem. The first component is the determination of the initial phase of the spreading (hopping) sequence. This part of the problem is called the *acquisition process*. The second component is the problem of maintaining synchronization of the spreading sequence after initial acquisition. This part of the problem is called the *tracking process*. The acquisition and tracking of the signal phase and frequency are performed in the same way as for any digital communication system. We consider the synchronization problems in Chapter 7.

Information-theoretical aspects of multiuser communication are considered in Chapter 8. In particular, we analyze such fundamental performance measures as Shannon capacity of CDMA systems and reliability of the transmission in the system.

In a CDMA system, it is possible for the strongest transmitter to successfully capture the intended receiver, even when many other users are also transmitting. Often, the closest transmitter is able to capture a receiver because of the small propagation path loss. This is called the *near-far effect*. A strong transmitter may make it impossible for the receiver to detect a much weaker transmitter that is attempting to communicate to the same receiver.

In practical cellular communication systems the power levels transmitted by every mobile are under constant control by the serving base stations. This is done to ensure that each mobile transmits the smallest power necessary to maintain a good quality link on the reverse channel. *Power control* not only helps prolong

battery life for the user but also reduces reverse channel signal-to-noise ratio in the system.

When a mobile moves into a different cell while a conversation is in progress, the switching center automatically transfers the call to a new channel belonging to the new station. This handoff operation requires that the voice and control signals can be allocated to channels associated with the new base station. The CDMA system provides a handoff capability that cannot be provided by other multiple access systems. Unlike the FDMA and TDMA systems that assign different radio channels during a handoff (called a *hard handoff*), spread spectrum mobiles share the same channel (bandwidth) in every cell. By simultaneously evaluating the received signals from a single user at several neighboring base stations, the switching center may actually decide which version of the user's signal is most probable at a certain time instance. The ability to select between the instantaneous received signals from a variety of base stations is called *soft handoff*. Power control, handoff, and other problems of organizing the spread spectrum multiple access network, such as queueing analysis, are considered in Chapter 9. We also analyze in Chapter 9 two advanced methods of increasing capacity of the CDMA system—successive interference cancellation in the reverse link and user coordination in the forward link. The last section of Chapter 9 gives a short review of the third-generation wireless networks.

1.7 COMMENTS

Spread spectrum communication grew out of research efforts during World War II to provide secure and antijam communication in hostile environment. Starting in 1948 with Shannon's landmark paper "A Mathematical Theory of Communication" [42], information theory became the theoretical base of spread spectrum communication. The idea of the time-hopped CDMA system was expressed in 1949 in a technical memorandum of Bell Telephone Laboratories [35]. The concept of direct sequence spread spectrum was probably first published in 1950 [12]. The Interim Standard 95, adopted in 1993, specifies the spread spectrum communication format and protocols for communication between the base station of a cell and a mobile. It was developed by Qualcomm Inc., a company headed by Jacobs and Viterbi. The theory of CDMA communication was developed by Viterbi, in a number of papers and the classical book [47]. Specification of WCDMA technology has been created in the 3rd Generation Partnership Project (3GPP) started in 1992 [1]–[6]. Application of impulse radio to time-hopped CDMA (PPH CDMA) was described by Scholtz [40]. A general introduction into wireless communication systems is given by Rappaport [39].

PROBLEMS

1.1. If a total of 30 MHz of bandwidth is allocated to a particular cellular radio system that uses 30-kHz simplex channels to provide voice and control

channels, compute the number of channels available per cell if a system uses:

a) 4-cell reuse

b) 7-cell reuse

c) 12-cell reuse

If 1 MHz of the allocated spectrum is dedicated to control channels, determine an equitable distribution of control channels and voice channels in each cell for each of the three systems.

1.2. GSM uses a frame structure in which each frame consists of 8 time slots, each time slot contains 156.25 bits, and data are transmitted at 270.833 kb/s over the channel. Find

a) The time duration of a bit

b) The time duration of a slot

c) The time duration of a frame

d) How long must a user occupying a single time slot wait between two consecutive transmissions?

1.3. Let $\xi(t)$ be a zero mean white Gaussian noise process with one-sided power spectral density N_0. Assume that the process $\xi(t)$ is the input signal to a running integrator and let $y(t)$ be the corresponding output, that is,

$$y(t) = \int_{t-T}^{t} \xi(\tau)\, d\tau$$

a) Find the mean and variance of $y(t)$. Can you say anything about the probability density function?

b) Find the autocorrelation function and the power spectral density for the process $y(t)$.

1.4. Consider a BPSK system in which the signals are given by

$$s(t) = \pm\sqrt{2}\cos(2\pi f_c t),\ \ 0 \le t \le T$$

Assume that the received signal is corrupted by AWGN with one-sided power spectral density N_0. Show that the probability of error for the

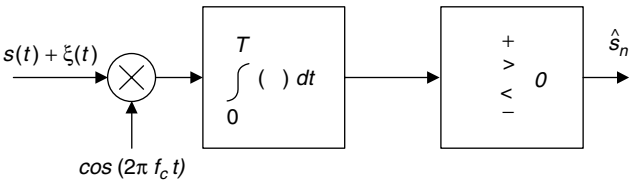

Problem 1.4. Receiver structure for BPSK.

receiver in the figure below is

$$P_{\mathrm{b}} = Q\left(\sqrt{2\,\frac{E_{\mathrm{b}}}{N_0}}\right)$$

where $E_{\mathrm{b}} = T$ is the energy per bit and $Q(x)$ is defined by Formula (1.12).

1.5. Prove the formula

$$Q(x) < \frac{1}{2}e^{-\frac{x^2}{2}},\ x \geq 0$$

Hint: The function

$$F(x) \stackrel{\mathrm{def}}{=} \frac{1}{2}\,e^{-\frac{x^2}{2}} - Q(x)$$

is equal to 0 for $x = 0$, increases in the interval $\left(0, \sqrt{\frac{2}{\pi}}\right)$ strictly decreases in the interval $\left(\sqrt{\frac{2}{\pi}}, \infty\right)$ and goes to 0 if x goes to ∞.

1.6. Find the radio channel capacity of the single-cell DS CDMA system if the total bandwidth of the duplex channel is 25 MHz, the individual transmission rate of the user is $R = 10^4$ bits/s and the required bit error probability is $P_{\mathrm{b}} = 10^{-5}$. The repetition code is used. Neglect the influence of background noise. Consider the next cases: a) no voice activity detection, omni-directional antennas; b) voice activity detection with $\gamma_{\mathrm{v}} = 8/3$, 3-sector antennas.

1.7. Find the processing gain W/R if the radio channel capacity is $K_0 = 100$ and the required signal-to-noise ratio at the demodulator input is equal:

a) 3 dB

b) 5 dB

c) 10 dB

d) 20 dB

Neglect the influence of background noise.

1.8. A total of 30 equal-power users are to share a common communication channel by DS CDMA. Each user transmits information at a rate of 10 kbits/s. Determine the minimum chip rate to obtain a bit error probability of 10^{-5} if

a) Additive noise in the receiver can be ignored

b) $E_{\mathrm{b}}/N_0 = 12$ dB

1.9. If $W = 1.25$ MHz, $R = 9600$ bits/s, and the required E_{b}/I_0 is 10 dB, determine the maximum number of users that can be supported in a single-cell DS CDMA system using

a) Omnidirectional base station antennas and no voice activity detection

b) Three-sectored antennas at the base station and voice activity detection with $\gamma_v = 8/3$

Assume that the background noise can be neglected.

1.10. Suppose that you are a communication engineer and you have to construct a mobile telephone network with bandwidth $W = 4.2$ MHz in each link. The data rate is $R = 10$ kb/s. You have the following alternatives:

a) A system based on TDMA with parameters
- Frequency reuse factor 1/7
- Each link divided into radio channels of 200 kHz
- Ten users per channel

b) A system based on DS CDMA with parameters
- Frequency reuse factor 1
- Voice activity gain $\gamma_v = 2.5$
- No antenna sectorization
- The required signal-to-noise ratio $E_b/I_0 = 6$ dB
- Other-cell relative interference factor $f = 0.6$

What alternative would you choose?

1.11. In an omnidirectional (single cell, single sector) DS CDMA cellular system, let the required SNR be 10 dB. If 100 users, each with a data rate of 13 kb/s, are to be accommodated, determine the minimum channel bit rate of the spread spectrum chip sequence if

a) Voice activity monitoring is absent, and omni-directional antenna is used,

b) Voice activity is equal to 40%, and omni-directional antenna is used,

c) Voice activity is equal to 40%, and a three-sectored antenna is used.

1.12. Two signals $s_0(t)$ and $s_1(t)$ are said to be *orthogonal* (over the time interval T) if

$$\int_0^T s_0(t)s_1(t)\,\mathrm{d}t = 0$$

Let $s_0(t) = \sqrt{2}\,\cos(2\pi f_0 t)$ and $s_1(t) = \sqrt{2}\,\cos(2\pi f_1 t + \varphi_1)$.

a) If $f_0 T = k_0/2$, and $f_1 T = k_1/2$ where k_0, k_1 are integers, show that the smallest value of $|f_1 - f_0|$ that makes the signals orthogonal is $1/T$.

b) If $\varphi_1 = 0$, what is the smallest value of $|f_1 - f_0|$ that makes the signals orthogonal?

c) If $|f_1 - f_0|T \gg 1$, show that the signals can be assumed to be orthogonal.

1.13. Suppose that the FH CDMA system with $K = 30$ synchronized active users uses the same transmission method as in Example 1.7. Let $M = 100$, $q = 2$. What number N of the time slots should be used, if the required bit error probability is $P_b = 10^{-4}$?

1.14. Under the same conditions as in Problem 1.6, find the radio channel capacity, K_0, of the synchronous FH CDMA system. Assume that the system does not use voice activity detection and antenna sectorization.

1.15. Find the radio channel capacity of the PPH CDMA system if the system uses impulse radio with pulses of duration $T_c = 10^{-8}$ s. The user transmission rate is $R = 10$ kb/s, and the required bit error probability is $P_b = 10^{-5}$. The repetition code is used. Neglect the other-cell interference and background noise.

2

INTRODUCTION TO SPREAD SPECTRUM COMMUNICATION SYSTEMS

Spread spectrum (SS) communication technology is used in military communication primary for two purposes: first, to provide resistance to strong intentional interference (jamming) and, second, to hide the signal from an eavesdropper. Both of the goals can be achieved by spreading the signal's spectrum to make it indistinguishable from background noise. The third SS application, both military and civilian, is position location, with accuracy increasing proportionally to the spreading bandwidth. This is realized in the Global Positioning System [17]. Another application of SS, cellular mobile radio, exploits the fourth and fifth SS benefits. These are resistance to signal interference from multiple transmission paths and potentially higher bandwidth efficiency in multiple access communication than in other technologies.

In the beginning of this chapter we describe several modulation techniques that are used in SS communication. Because digital modulation offers numerous benefits and has already replaced conventional analog systems, we limit our consideration to digital modulation schemes.

In the analysis of digital modulation, we treat the signals as stationary stochastic processes. We start with a short mathematical introduction to the theory of stochastic processes and then study correlation and spectral characteristics of DS SS, FH SS, and PPH SS signals. Finally, we discuss orthogonal and quasi-orthogonal expansions of SS signals.

Modulation is a topic that is covered in great detail in various communication textbooks (see, for example, [28], [37], [38], [57]). We focus on modulation as it applies to DS CDMA, FH CDMA, and PPH CDMA.

Theory of Code Division Multiple Access Communication, by Kamil Sh. Zigangirov
ISBN 0-471-45712-4

2.1 MODULATION FORMATS FOR SS COMMUNICATION

A modulated SS signal $s(t)$ carrying digital information can be represented as a sequence of signal waveforms $\tilde{s}_n(t-\tau_n)$, where $\ldots \tau_{-1} < \tau_0 < \tau_1 < \ldots < \tau_n < \ldots$, and

$$s(t) = \sum_{n=-\infty}^{\infty} \tilde{s}_n(t-\tau_n) \tag{2.1}$$

The signal waveforms depend on which modulation format was used. The transmitted signal is $\sqrt{P}s(t)$, where P is a scale factor having dimensionality of power (watt, W). In this chapter we assume that $P = 1$ W and will omit factor $\sqrt{P}$ in front of the transmitted signal.

We start with *pulse amplitude on-off modulation*, which is a partial case of M-ary pulse amplitude modulation (M-PAM) with $M = 2$. This modulation technique can be used in PPH CDMA. Given the input modulator symbol v_n, $n = \ldots -1, 0, 1, 2, \ldots$, $v_n \in \{1, -1\}$, the signal waveform in the nth time instant $\tau_n, \ldots < \tau_{-1} < \tau_0 < \tau_1 < \tau_2 < \ldots < \tau_n < \ldots$, is

$$\tilde{s}_n(t-\tau_n) = \frac{(v_n+1)}{\sqrt{2}}\, h_{T_\mathrm{p}}(t-\tau_n) \tag{2.2}$$

where $h_{T_\mathrm{p}}(t)$ is a pulse of duration T_p. Examples of pulse shapes $h_{T_\mathrm{p}}(t)$ for PPH CDMA are given in Figure 1.13.

In DS and FH CDMA applications other pulses can also be considered:

a) Unit amplitude rectangular pulse (Fig. 2.1a)

$$h_{T_\mathrm{p}}(t) = \begin{cases} 1, & -T_\mathrm{p}/2 < t < T_\mathrm{p}/2, \\ 0, & \text{otherwise} \end{cases} \tag{2.3}$$

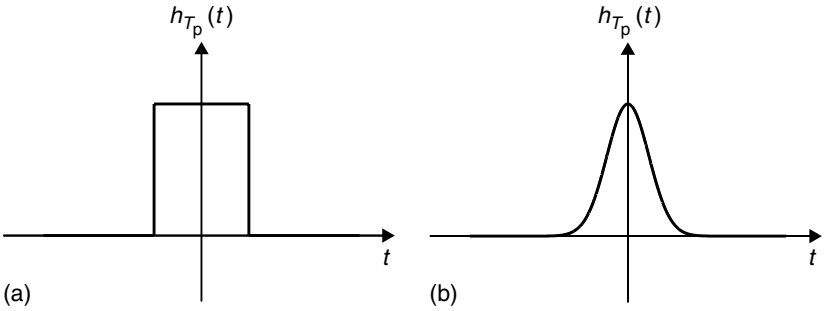

Figure 2.1. Examples of monocycle waveforms: (a) rectangular pulse; (b) Gaussian pulse.

b) Gaussian pulse (Fig. 2.1b)

$$h_{T_p}(t) = A_g \exp\left(-\frac{t^2}{4\gamma T_p^2}\right) \tag{2.4}$$

where A_g and γ are normalizing constants, and

c) Bandlimited pulse (see Example 2.5 below).

The pulse $h_{T_p}(t)$ is characterized by two parameters, the *pulse energy*

$$E \stackrel{\text{def}}{=} \int_{-\infty}^{\infty} h_{T_p}^2(t)\,dt \tag{2.5}$$

and the *pulse duration* T_p, which is defined below. For a unit amplitude rectangular pulse (Fig. 2.1a) the duration is defined as the length of the time interval where $h_{T_p}(t) \neq 0$, but in the general case this definition is not applicable. We will define the pulse duration as the width of the time interval in which the ηth ($\eta \leq 1$) part of the total pulse energy is located, that is,

$$\int_{-T_p/2}^{T_p/2} h_{T_p}^2(t)\,dt = \eta E \tag{2.6}$$

For the rectangular pulse $\eta = 1$, and in the general case $\eta \leq 1$. Usually, η is chosen to be equal to 0.99 or 0.9.

The ratio E/T_p is called the *average power* of the pulse. It is convenient to normalize the average power of the *transmitted* pulse to 1, that is, we suppose that

$$\frac{1}{T_p}\int_{-\infty}^{\infty} h_{T_p}^2(t)\,dt = 1 \tag{2.7}$$

In this chapter we only consider pulses of average power 1. The average power of the *received pulse* depends on the propagation conditions and generally is not equal to 1.

EXAMPLE 2.1

Find the normalizing constants A_g and γ for the Gaussian pulse (2.4) if $\eta = 0.99$.

Solution

From Formula (2.7) we have

$$\begin{aligned} 1 &= \frac{1}{T_p}\int_{-\infty}^{\infty}\left[A_g \exp\left(-\frac{t^2}{4\gamma T_p^2}\right)\right]^2 dt \\ &= \frac{A_g^2}{T_p}\cdot\sqrt{2\pi\gamma T_p^2} \end{aligned} \tag{2.8}$$

then

$$A_{\mathrm{g}} = \frac{1}{\sqrt[4]{2\pi\gamma}} \tag{2.9}$$

From (2.6) we get, using the substitution $x = t/\sqrt{\gamma}\, T_{\mathrm{p}}$,

$$\eta = \int_{-T_{\mathrm{p}}/2}^{T_{\mathrm{p}}/2} \left[\frac{1}{\sqrt[4]{2\pi\gamma T_{\mathrm{p}}^2}} \exp\left(-\frac{t^2}{4\gamma T_{\mathrm{p}}^2}\right) \right]^2 \mathrm{d}t = \frac{1}{\sqrt{2\pi}} \int_{-1/2\sqrt{\gamma}}^{1/2\sqrt{\gamma}} \exp\left(-\frac{x^2}{2}\right) \mathrm{d}x$$

$$= 1 - 2Q\left(\frac{1}{2\sqrt{\gamma}}\right) \tag{2.10}$$

where the Q function is defined by Formula (1.12). To $\eta = 0.99$ *corresponds* $\gamma \approx 1/9\pi \approx 0.0354$. *Finally, we have for the Gaussian pulse*

$$h_{T_{\mathrm{p}}}(t) = \sqrt[4]{\frac{9}{2}} \exp\left(-\frac{9\pi t^2}{4T_{\mathrm{p}}^2}\right), \quad -\infty < t < \infty \tag{2.11}$$

It can be shown (Problem 2.1) that for a differentiated Gaussian pulse (1.24)

$$h_{T_{\mathrm{p}}}(t) = \frac{t}{\sqrt[4]{2\pi\gamma'^3 T_{\mathrm{p}}^4}} \exp\left(-\frac{t^2}{4\gamma' T_{\mathrm{p}}^2}\right) \tag{2.12}$$

where $\gamma' = 0.0205$ when $\eta = 0.99$.

The *Fourier transform* $\mathcal{F}\{h_{T_{\mathrm{p}}}(t)\}$ of a pulse $h_{T_{\mathrm{p}}}(t)$ is defined as

$$H(f) \stackrel{\mathrm{def}}{=} \mathcal{F}\{h_{T_{\mathrm{p}}}(t)\} = \int_{-\infty}^{\infty} h_{T_{\mathrm{p}}}(t) \exp(-2\pi j f t)\, \mathrm{d}t \tag{2.13}$$

and the *inverse Fourier transform* as

$$h_{T_{\mathrm{p}}}(t) = \mathcal{F}^{-1}\{H(f)\} = \int_{-\infty}^{\infty} H(f) \exp(2\pi j f t)\, \mathrm{d}f \tag{2.14}$$

The *normalized autocorrelation function* of the pulse $h_{T_{\mathrm{p}}}(t)$ is

$$R_h(\tau) \stackrel{\mathrm{def}}{=} \frac{1}{T_{\mathrm{p}}} \int_{-\infty}^{\infty} h_{T_{\mathrm{p}}}(t) h_{T_{\mathrm{p}}}(t+\tau)\, \mathrm{d}t \tag{2.15}$$

The distribution of the pulse power with the frequency is given by the Fourier transform of $R_h(\tau)$,

$$\mathcal{H}(f) \stackrel{\mathrm{def}}{=} \mathcal{F}\{R_h(\tau)\} = \int_{-\infty}^{\infty} R_h(\tau) \exp(-2\pi f j \tau)\, \mathrm{d}\tau \tag{2.16}$$

The inverse Fourier transform relationship is

$$R_h(\tau) = \mathcal{F}^{-1}\{\mathcal{H}(f)\} = \int_{-\infty}^{\infty} \mathcal{H}(f) \exp(2\pi f j\tau)\, \mathrm{d}f \tag{2.17}$$

We observe that

$$R_h(0) = \int_{-\infty}^{\infty} \mathcal{H}(f)\, \mathrm{d}f \tag{2.18}$$

Because $R_h(0)$ represents the average pulse power, $\mathcal{H}(f)$ is the distribution of power as a function of frequency. Therefore $\mathcal{H}(f)$ is called the *two-sided power spectral density* (or *spectrum*) of the pulse $h_T(t)$. Although the power spectral density has a physical sense only for positive frequencies $f \geq 0$, it is mathematically more convenient to operate with the spectral density in the whole frequency domain.

From Formulas (2.13), (2.15), and (2.16) it follows that

$$\mathcal{H}(f) = \frac{1}{T_\mathrm{p}} |H(f)|^2, \quad -\infty < f < \infty \tag{2.19}$$

EXAMPLE 2.2

Calculate the two-sided power spectral density of the unit amplitude rectangular pulse (2.3).

Solution

The Fourier transform of the pulse is

$$\begin{aligned} H(f) &= \int_{-T_\mathrm{p}/2}^{T_\mathrm{p}/2} \exp(-2\pi j f t)\, \mathrm{d}t \\ &= -\frac{1}{2\pi j f}\left[\exp\left(-2\pi j f \frac{T_\mathrm{p}}{2}\right) - \exp\left(2\pi j f \frac{T_\mathrm{p}}{2}\right)\right] \\ &= \frac{\sin(\pi f T_\mathrm{p})}{\pi f} = T_\mathrm{p}\,\mathrm{sinc}(f T_\mathrm{p}) \end{aligned} \tag{2.20}$$

In the rightmost expression above, the sinc function is introduced,

$$\mathrm{sinc}\ x = \frac{\sin \pi x}{\pi x} \tag{2.21}$$

The two-sided power spectral density is

$$\mathcal{H}(f) = T_\mathrm{p}\,\mathrm{sinc}^2(f T_\mathrm{p}), \quad -\infty < f < \infty \tag{2.22}$$

The sketch of $\mathcal{H}(f)$ is given in Figure 2.2. The mainlobe has width $2/T_\mathrm{p}$.

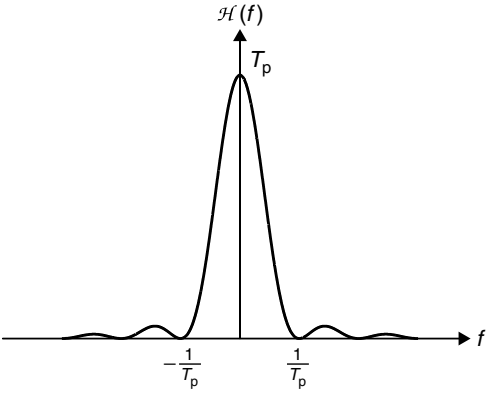

Figure 2.2. The two-sided power spectral density of the rectangular pulse.

Parseval's theorem states that the total pulse energy in the frequency domain is equal to the total pulse energy in the time domain,

$$T_p \int_{-\infty}^{\infty} \mathcal{H}(f)\,\mathrm{d}f = \int_{-\infty}^{\infty} |H(f)|^2\,\mathrm{d}f = \int_{-\infty}^{\infty} h_{T_p}^2(t)\,\mathrm{d}t \tag{2.23}$$

Analogously to our analysis of the pulse power in the time domain we define the pulse bandwidth W as the width of the frequency interval where the ηth, $\eta \leq 1$, part of the total pulse energy is located. Particularly, for the rectangular pulse about 90% of the energy is located within the mainlobe, that is, $W \simeq 2/T_p$ if $\eta = 0.9$

$$\int_{-1/T_p}^{1/T_p} T_p^2\ \mathrm{sinc}^2(fT_p)\,\mathrm{d}f \simeq 0.9 \int_{-\infty}^{\infty} T_p^2\ \mathrm{sinc}^2(fT_p)\,\mathrm{d}f \tag{2.24}$$

For all pulses considered in DS CDMA and FH CDMA, we will use the definition $W = 1/T_p$. Then for the rectangular pulse only 77% of the total pulse energy is located in the frequency band $(-1/2T_c, 1/2T_c)$. Note that according to our (mathematical) definition of the bandwidth it includes both positive and negative frequencies. The conventional (physical) definition of the bandwidth includes only positive frequencies. Then the bandwidth is half as much as our definition, that is, it equals $1/2T_c$.

EXAMPLE 2.3

The carrier spacing in the WCDMA system is 5 MHz, that is, each channel occupies a $W = 5$ MHz band. The chip rate is $R_{\text{chip}} = 3.84 \cdot 10^6$ chips/s. Assuming that chip is a rectangular pulse of duration $T_c = 1/R_c = 0.26 \cdot 10^{-6}$s, find which part η of the pulse energy is located in the bandwidth (-2.5 MHz, 2.5 MHz).

Solution

The total pulse energy is

$$E = T_c^2 \int_{-\infty}^{\infty} \operatorname{sinc}^2(fT_c)\,\mathrm{d}f = T_c \int_{-\infty}^{\infty} \operatorname{sinc}^2(x)\,\mathrm{d}x = T_c$$

In the bandwidth (−2.5 MHz, 2.5 MHz) located in the energy ηE, where

$$\eta = T_c \int_{-2.5\cdot 10^6}^{2.5\cdot 10^6} \operatorname{sinc}^2(fT_c)\,\mathrm{d}f = \int_{-0.65}^{0.65} \operatorname{sinc}^2(x)\,\mathrm{d}x = 0.86$$

EXAMPLE 2.4

Calculate the two-sided power spectral density of the Gaussian pulse (2.4).

Solution

$$\begin{aligned} H(f) &= \int_{-\infty}^{\infty} \sqrt[4]{\frac{9}{2}} \exp\left(-\frac{9\pi t^2}{4T_p^2}\right) \exp(-2\pi j f t)\,\mathrm{d}t \\ &= \sqrt[4]{\frac{9}{2}} \exp\left(-\frac{4\pi f^2 T_p^2}{9}\right) \\ &\quad \times \int_{-\infty}^{\infty} \exp\left[-\frac{9\pi}{4T_p^2}\left(t^2 + 2\,\frac{4}{9}\,jftT_p^2 + \frac{16}{81}\,j^2 f^2 T_p^4\right)\right]\mathrm{d}t \\ &= \sqrt[4]{\frac{9}{2}} \cdot \sqrt{\frac{4}{9}}\,T_p^2 \exp\left(-\frac{4\pi f^2 T_p^2}{9}\right) \\ &= \sqrt[4]{\frac{8}{9}}\,T_p \exp\left(-\frac{4}{9}\,\pi f^2 T_p^2\right) \end{aligned} \tag{2.25}$$

From Formula (2.25) we get

$$\mathcal{H}(f) = \frac{1}{T_p}\,|H(f)|^2 = \frac{2}{3}\,\sqrt{2}\,T_p \exp\left(-\frac{8}{9}\,\pi f^2 T_p^2\right). \tag{2.26}$$

The sketch of the two-sided power spectral density is given in Figure 2.3.

Let us find which part of the energy is located in the frequency interval $(-1/T_p, 1/T_p)$. We have from (2.26)

$$\begin{aligned} &\int_{-1/T_p}^{1/T_p} |H(f)|^2\,\mathrm{d}f = \int_{-1/T_p}^{1/T_p} \frac{2}{3}\,\sqrt{2}\,T_p^2 \exp\left(-\frac{8}{9}\,\pi f^2 T_p^2\right)\mathrm{d}f \\ &= \frac{T_p}{\sqrt{2\pi}} \int_{-\sqrt{16\pi/9}}^{\sqrt{16\pi/9}} \exp\left(-\frac{x^2}{2}\right)\mathrm{d}x = T_p\left[1 - 2Q\left(\frac{4}{3}\,\sqrt{\pi}\right)\right] = T_p\eta \end{aligned} \tag{2.27}$$

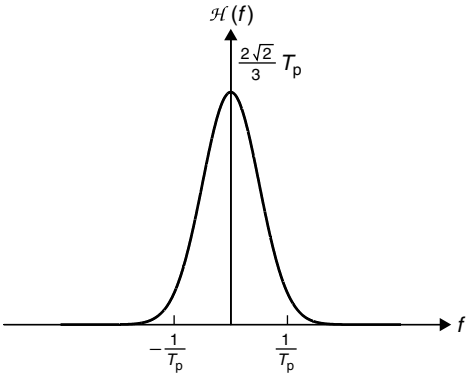

Figure 2.3. The two-sided power spectral density of the Gaussian pulse.

Here we used the substitution $x = \frac{4\sqrt{\pi}}{3}T_p f$. *From (2.27) we get* $\eta = 1 - 2Q\left(\frac{4}{3}\sqrt{\pi}\right) = 0.98$.

For the differentiated Gaussian pulse (2.12) we have (Problem 2.2)

$$\mathcal{H}(f) = \frac{1}{T_p}|H(f)|^2 = 32\sqrt{2\pi^5\gamma'^3}\ T_p^3 \exp(-8\pi^2\gamma' f^2 T_p^2) \tag{2.28}$$

In the frequency interval $\left(-1/T_p,\ 1/T_p\right)$ 94% of the total energy of the differentiated Gaussian pulse is located. In fact from (2.12) and (2.28) we get

$$\int_{-\infty}^{\infty}|H(f)|^2\,\mathrm{d}f = 16\pi^2\gamma' T_p \approx 3.482T_p, \tag{2.29}$$

$$\int_{-1/T_p}^{1/T_p}|H(f)|^2\,\mathrm{d}f = 16\pi^2\gamma' T_p[1 - 2Q(4\pi\sqrt{\gamma'})] \approx 3.266T_p$$

$$\approx 0.94\int_{-\infty}^{\infty}|H(f)|^2\,\mathrm{d}f$$

As a counterpart to the time-limited rectangular pulse we consider the *bandlimited pulse*. By definition, the Fourier transform of the bandlimited pulse is

$$H(f) = \begin{cases} \dfrac{1}{W}, & -\dfrac{W}{2} \le f \le \dfrac{W}{2}, \\ 0, & \text{otherwise} \end{cases} \tag{2.30}$$

(Our choice of the normalizing constant $1/W$ will be explained later.)

EXAMPLE 2.5

Find the representation of the bandlimited pulse in the time domain.

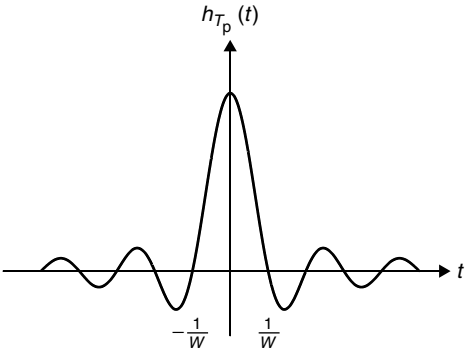

Figure 2.4. Bandlimited pulse (time domain).

Solution

Using the inverse Fourier transform (2.14) we get

$$h_{T_p}(t) = \frac{1}{W}\int_{-W/2}^{W/2} \exp(2\pi jft)\,\mathrm{d}f = \frac{1}{2\pi jWt}\left[\exp\left(2\pi j\,\frac{W}{2}\,t\right) - \right.$$
$$\left. - \exp\left(-2\pi j\,\frac{W}{2}\,t\right)\right] = \frac{\sin(\pi Wt)}{\pi Wt} = \mathrm{sinc}(Wt) \tag{2.31}$$

where the sinc function is defined by Formula (2.21). The sketch of $h_{T_p}(t)$ is presented in Figure 2.4.

We define the bandlimited pulse duration T_p as $1/W$ (half of the mainlobe width). Then two pulses $h_{T_p}(t)$ and $h_{T_p}(t - T_p)$ are orthogonal and the value $T_p = 1/W$ is the minimal pulse duration for which such pulses are orthogonal. Only 77% of the total pulse energy is located in the time interval $\left(-T_p/2,\ T_p/2\right)$. In fact, analogously to (2.24), we have

$$\int_{-T_p/2}^{T_p/2} h_{T_p}^2(t)\,\mathrm{d}t = \int_{-1/2W}^{1/2W} \mathrm{sinc}^2(Wt)\,\mathrm{d}t \approx 0.77\int_{-\infty}^{\infty} \mathrm{sinc}^2(Wt)\,\mathrm{d}t \tag{2.32}$$

Using Parseval's equality (2.23) we calculate the average power of the bandlimited pulse to be

$$\frac{1}{T_p}\int_{-\infty}^{\infty} h^2(t)\,\mathrm{d}t = \frac{1}{T_p}\int_{-\infty}^{\infty} |H(f)|^2\,\mathrm{d}f = W\int_{-W/2}^{W/2}\left(\frac{1}{W}\right)^2\,\mathrm{d}f = 1 \tag{2.33}$$

This explains our choice of the normalizing constant $1/W$ in the definition of the Fourier transform (2.30) of the bandlimited pulse. We chose it such that the average pulse power is equal to 1.

For PPH CDMA application, we have begun with pulse amplitude on-off modulation. Another modulation format that is used in PPH CDMA is (binary) *pulse position modulation* (PPM). Then

$$\tilde{s}_n(t-\tau_n) = h_{T_\mathrm{p}}\left(t-\tau_n+v_n\frac{T_\mathrm{p}}{2}\right) \tag{2.34}$$

where $\tau_n - \tau_{n-1} \geq 2T_\mathrm{p},\ n = \ldots -1, 0, 1, \ldots$

As we mentioned above, in PPH CDMA applications we will also study Manchester pulses (1.23) and differentiated Gaussian pulses (1.24).

EXAMPLE 2.6

Find the normalized autocorrelation function and power spectral density of the Manchester pulse.

Solution

The normalized autocorrelation function of the Manchester pulse is a decreasing function of $|\tau|$ *in the interval* $(0, T_\mathrm{p}/2)$ *and an increasing function in the interval* $(T_\mathrm{p}/2,\ T_\mathrm{p})$. *This function is an affine function*[1] *of* $|\tau|$ *in each of these intervals. Because*

$$R_h(\tau) = \begin{cases} 1, & \tau = 0, \\ -1/2, & |\tau| = T_\mathrm{p}/2, \\ 0, & |\tau| \geq T_\mathrm{p} \end{cases}$$

we have

$$R_h(\tau) = \begin{cases} 1 - 3|\tau|/T_\mathrm{p}, & |\tau| \leq T_\mathrm{p}/2, \\ -1 + |\tau|/T_\mathrm{p}, & T_\mathrm{p}/2 < |\tau| \leq T_\mathrm{p}, \\ 0, & \textit{otherwise} \end{cases} \tag{2.35}$$

The function $R_h(\tau)$ *is presented in Figure 2.5.*
The Fourier transform $H(f)$ *of the Manchester pulse is*

$$\begin{aligned} H(f) &= \int_{-\infty}^{\infty} h_{T_\mathrm{p}}(t)\exp(-2\pi jft)\,\mathrm{d}t \\ &= -\int_{-T_\mathrm{p}/2}^{0}\exp(-2\pi jft)\,\mathrm{d}t + \int_{0}^{T_\mathrm{p}/2}\exp(-2\pi jft)\,\mathrm{d}t \\ &= \frac{1}{2\pi jf}\left[2-\exp(\pi jfT_\mathrm{p})-\exp(-\pi jfT_\mathrm{p})\right] = \frac{2}{\pi jf}\sin^2\left(\frac{\pi fT_\mathrm{p}}{2}\right) \end{aligned} \tag{2.36}$$

[1]Function $f(x) = ax + b$, where $a \neq 0$, $b \neq 0$, is called an affine function.

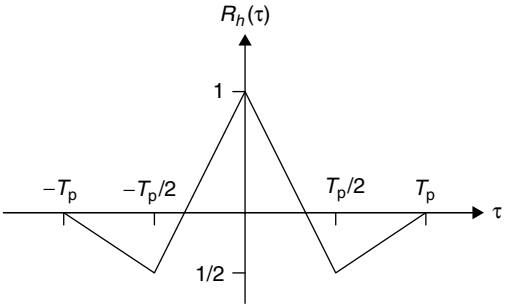

Figure 2.5. The normalized autocorrelation function of the Manchester pulse.

The two-sided power spectral density of the Manchester pulse is

$$\mathcal{H}(f) = \frac{1}{T_p}|H(f)|^2 = \frac{4}{\pi^2 f^2 T_p} \cdot \sin^4\left(\frac{\pi f T_p}{2}\right) \tag{2.37}$$

For further convenience we introduce the *lowpass signal waveform*

$$\tilde{v}_n(t - \tau_n) = v_n h_{T_p}(t - \tau_n) \tag{2.38}$$

where $v_n \in \{1, -1\}$. Obviously, the autocorrelation function $R_{\tilde{v}}(\tau)$ of the waveform $\tilde{v}(t)$ coincides with the autocorrelation function $R_h(\tau)$ of the pulse $h_{T_p}(t)$; the spectrum $\tilde{\mathcal{V}}(f)$ of $\tilde{v}(t)$ coincides with the spectrum $\mathcal{H}(f)$ of $h_{T_p}(t)$, that is,

$$\tilde{\mathcal{V}}(f) \stackrel{\text{def}}{=} \mathcal{F}\{R_{\tilde{v}}(\tau)\} = \mathcal{H}(f) = \frac{1}{T_p}|H(f)|^2 \tag{2.39}$$

Consider now the modulation formats for DS CDMA. DS CDMA most often employs *binary phase shift-keying* (BPSK) or *quadrature phase shift-keying* (QPSK). Given the input modulator symbol v_n, $v_n \in \{1, -1\}$, $n = \ldots -1, 0, 1, \ldots$, the BPSK signal waveform in the nth time instant τ_n, $\ldots \tau_{-1} < \tau_0 < \tau_1 < \ldots < \tau_n < \ldots$ is

$$\begin{aligned} \tilde{s}_n(t - \tau_n) &= \sqrt{2}\tilde{v}_n(t - \tau_n)\cos(2\pi f_c t + \phi) \\ &= \sqrt{2}v_n \cdot h_{T_p}(t - \tau_n) \cdot \cos(2\pi f_c t + \phi) \end{aligned} \tag{2.40}$$

where $h_{T_p}(t - \tau_n)$ is a pulse of duration T_p starting at τ_n, f_c is a *carrier frequency*, and ϕ is a phase. Although it is in principle possible to consider any pulse shaping we will study only time-limited unit amplitude rectangular pulses (2.3) and bandlimited pulses (2.31) in DS CDMA applications.

We suppose that the bandwidth W of the signal waveform (2.40) is much smaller than the carrier frequency f_c, that is, $W \ll f_c$. Such a signal is called a *narrowband bandpass signal waveform*.

The normalized autocorrelation function of the BPSK waveform is

$$\begin{aligned} R_{\tilde{s}}(\tau) &\stackrel{\text{def}}{=} \frac{1}{T_\text{p}} \int_{-\infty}^{\infty} \tilde{s}_n(t)\tilde{s}_n(t+\tau)\,\mathrm{d}t \qquad (2.41)\\ &= \frac{1}{T_\text{c}} \int_{-\infty}^{\infty} h_{T_\text{p}}(t-\tau_n)h_{T_\text{p}}(t+\tau-\tau_n)\cos[2\pi f_\text{c}(2t+\tau)+2\phi]\,\mathrm{d}t \\ &\quad + \frac{1}{T_\text{c}} \int_{-\infty}^{\infty} h_{T_\text{p}}(t-\tau_n)h_{T_\text{p}}(t+\tau-\tau_n)\cos[2\pi f_\text{c}\tau+\phi]\,\mathrm{d}t \\ &= \frac{1}{T_\text{p}} \int_{-\infty}^{\infty} h_{T_\text{p}}(t)h_{T_\text{p}}(t+\tau)\,\mathrm{d}t\cos(2\pi f_\text{c}\tau) = R_h(\tau)\cos(2\pi f_\text{c}\tau) \end{aligned}$$

where the identity

$$\cos\alpha\cos\beta = \frac{\cos(\alpha-\beta)+\cos(\alpha+\beta)}{2}$$

has been used. In the last equality in (2.41) it is assumed that the double carrier frequency term integrates to zero.

The *two-sided power spectral density* of the BPSK signal waveform (2.40), using (2.37), is

$$\tilde{S}(f) \stackrel{\text{def}}{=} \mathcal{F}\{R_{\tilde{s}}(\tau)\} = \frac{1}{2T_\text{c}}|H(f-f_\text{c})|^2 + \frac{1}{2T_\text{c}}|H(f+f_\text{c})|^2,\ -\infty < f < \infty \qquad (2.42)$$

where $H(f)$ is the Fourier transform of the pulse $h_{T_\text{p}}(t)$. The *power spectral density* of the BPSK signal waveform is concentrated near the carrier frequency f_c and near $-f_\text{c}$.

The QPSK signal waveform in the nth time instant is

$$\tilde{s}_n(t-\tau_n) = \tilde{s}_{\text{I}n}(t-\tau_n)\cos(2\pi f_\text{c}t+\phi) - \tilde{s}_{\text{Q}n}(t-\tau_n)\sin(2\pi f_\text{c}t+\phi) \qquad (2.43)$$

where the *lowpass* components $\tilde{s}_{\text{I}n}(t)$ and $\tilde{s}_{\text{Q}n}(t)$ are called the *in-phase* and *quadrature* components, respectively.

The in-phase and quadrature components of the QPSK signal waveform can bear different information. For example, when the signal has the form

$$\tilde{s}_n(t-\tau_n) = [v'_n h_{T_\text{p}}(t-\tau_n)]\cos(2\pi f_\text{c}t+\phi) - [v''_n h_{T_\text{p}}(t-\tau_n)]\sin(2\pi f_\text{c}t+\phi) \qquad (2.44)$$

where $v'_n, v''_n \in \{1, -1\}$, the power spectral density of the QPSK signal waveform is the same as the power spectral density of the BPSK signal waveform, but the data rate is twice that of BPSK. Conversely, for the same data rate, QPSK has half the bandwidth of BPSK.

A common data modulation for FH CDMA systems is frequency shift-keying (FSK). The q-FSK signal waveform is

$$\tilde{s}_n(t-\tau_n) = \sqrt{2}\, h_{T_p}(t-\tau_n)\cos(2\pi f_c t + 2\pi i_n \Delta f t + \phi_n) \tag{2.45}$$

Here $h_{T_p}(t-\tau_n)$ is a pulse of duration T_p starting at τ_n, f_c is a carrier frequency, ϕ_n is a phase, and Δf is the *frequency separation interval*. The *information-bearing parameter* i_n takes values from the set $\{-(q-1)/2, \ldots, -1/2, 1/2, \ldots, (q-1)/2\}$ if q is even and from the set $\{-(q-1)/2, \ldots, -1, 0, 1, \ldots, (q-1)/2\}$ if q is odd. The *instantaneous two-sided power spectral density* of the FSK signal waveform (2.45) is

$$\tilde{S}(f) = \tfrac{1}{2}|H(f - f_c - i_n\Delta f)|^2 + \tfrac{1}{2}|H(f + f_c + i_n\Delta f)|^2 \tag{2.46}$$

where $H(f)$ is the Fourier transform of the pulse $h_{T_p}(t)$. We suppose that $T_p = 1/\Delta f$.

This concludes our discussion of modulation formats for CDMA applications.

Up to now we have treated signal waveforms as *deterministic signals*. In the following sections we treat transmitted signals as *random processes*. In Section 2.2, which can be omitted in the first reading, we will study correlation and spectral properties of these signals. Now we give some definitions, which are necessary for understanding Section 2.3.

A modulated signal carrying digital information is given by Formula (2.1), where the signal waveforms $\tilde{s}_n(t-\tau_n)$ are defined by (2.2), (2.34), (2.40), (2.43), (2.44), and (2.45), depending on which modulation format was used, and $\tau_n = nT_p$. The random information-bearing sequence

$$\boldsymbol{v} = \ldots, v_{-1}, v_0, v_1, \ldots v_n, \ldots, v_n \in \{1, -1\} \tag{2.47}$$

defines a *stationary stochastic process* $s(t)$. The binary symbols v_n can be information or code symbols, but the performance of the random process $s(t)$ depends only on the probabilistic distribution of $\boldsymbol{v}$. We suppose that $\boldsymbol{v}$ is a sequence of equiprobable independent and identically distributed (IID) binary random variables, such that

$$P(v_n = 1) = P(v_n = -1) = 1/2 \tag{2.48}$$

In the DS CDMA and PPH CDMA cases, the symbols v_n directly modulate $s(t)$. In the FH CDMA case, the information-bearing parameter i_n depends on one or several symbols of the sequence $\boldsymbol{v}$. If $q = 2^m$, $m = 1, 2, \ldots$, the sequence $\boldsymbol{v}$ is first divided into m-tuples, and each m-tuple is then mapped into one of the q possible values of i_n.

The stationary stochastic process $s(t)$ is characterized by its (time-invariant) mathematical expectation $E[s(t)] = \mu$, which also is called its *ensemble average*. The mathematical expectation

$$R_s(\tau) = E[s(t)\cdot s(t+\tau)] \tag{2.49}$$

is called the *autocorrelation function* of the process. If $s_1(t)$ and $s_2(t)$ are two stationary stochastic processes,

$$R_{s_1,s_2}(\tau) = E[s_1(t)s_2(t+\tau)] \tag{2.50}$$

is called the *cross-correlation function* of these two processes.

A central problem in the theory of stochastic processes is the estimation of their various statistics. For this purpose, we can observe a large set $\{s(t)\}$ of the samples $s(t)$ and estimate the ensemble average for a particular time instant t. We can also observe only a single sample $s(t)$ function and calculate its *time average*

$$\overline{s(t)} = \lim_{T\to\infty} \frac{1}{2T} \int_{-T}^{T} s(t)\,\mathrm{d}t \tag{2.51}$$

For each sample $s(t)$ function, the limit in Equation (2.51) is a random variable. Equation (2.51) asserts not only that a limit exists for all samples except a set of zero probability, but also asserts that the limit is equal to $\overline{s(t)}$ with probability 1. A stationary stochastic process $s(t)$ is called *ergodic* if all of its ensemble averages are equal to the corresponding time averages. All modulated signal processes that we will consider are ergodic, and we will use the ergodicity property for the calculation of the correlation functions. For the ergodic process we have the mean $\mu = \overline{s(t)}$ and the autocorrelation function

$$R_s(\tau) = \overline{s(t)\cdot s(t+\tau)} = \lim_{T\to\infty} \frac{1}{2T} \int_{-T}^{T} s(t)s(t+\tau)\,\mathrm{d}t \tag{2.52}$$

The spectral characteristics of the stochastic processes are obtained by computing the Fourier transform $S(f)$ of $R_s(\tau)$, that is,

$$S(f) = \int_{-\infty}^{\infty} R_s(\tau)\cdot\exp(-2\pi jf\tau)\,\mathrm{d}\tau \tag{2.53}$$

The inverse Fourier transform relationship is

$$R_s(\tau) = \int_{-\infty}^{\infty} S(f)\exp(2\pi jf\tau)\,\mathrm{d}f \tag{2.54}$$

Because

$$R_s(0) = E[s^2(t)] = \int_{-\infty}^{\infty} S(f)\,\mathrm{d}f \tag{2.55}$$

is equal to the average power of the signal $s(t)$, $S(f)$ is called the *two-sided power spectral density* of the process. We must emphasize that although the expressions of the correlation functions and the spectra for deterministic signals and stochastic processes often coincide, they have different meanings.

In the next section we study the correlation and spectral properties of some modulated signals. In the Sections 2.3–2.5 we recapitulate these properties.

2.2 CORRELATION AND SPECTRAL PROPERTIES OF MODULATED SIGNALS*

Consider a stationary lowpass stochastic process $s(t) \stackrel{\text{def}}{=} v(t)$, where

$$v(t) = \sum_{n=-\infty}^{\infty} v_n h_{T_p}(t - nT_p) \tag{2.56}$$

Here $\boldsymbol{v}$ is the sequence (2.47) of equiprobable IID binary random variables and $h_{T_p}(t)$ is a pulse of duration T_p. The autocorrelation function of the process is defined by Formula (2.49), and the spectrum is defined by (2.53).

To calculate the autocorrelation function $R_s(\tau)$ of process (2.56) in the general case we use both ensemble and time averaging

$$\begin{aligned} R_s(\tau) \stackrel{\text{def}}{=} R_v(\tau) &= \lim_{T\to\infty} \left\{ \frac{1}{2T} E\left[\int_{-T}^{T} s(t)\cdot s(t+\tau)\,\mathrm{d}t \right] \right\} \\ &= \lim_{N\to\infty} \left\{ \frac{1}{2NT_p} E\left[\int_{-NT_p}^{NT_p} \sum_{n=-N}^{N} v_n h_{T_p}(t-nT_p) \right.\right. \\ &\qquad \left.\left. \cdot \sum_{n'=-N}^{N} v_{n'} h_{T_p}(t-n'T_p+\tau)\,\mathrm{d}t \right] \right\} \\ &= \lim_{N\to\infty} \left\{ \frac{1}{2N} \sum_{n=-N}^{N} \sum_{n'=-N}^{N} E(v_n v_{n'}) \frac{1}{T_p} \int_{-NT_p}^{NT_p} h_{T_p}(t-nT_p) \right. \\ &\qquad \left. \cdot\, h_{T_p}(t-n'T_p+\tau)\,\mathrm{d}t \right\} \end{aligned} \tag{2.57}$$

But $E(v_n v_{n'})$ is equal to 1 if $n = n'$ and equals 0 otherwise. Then

$$\begin{aligned} R_s(\tau) &= \lim_{N\to\infty} \left\{ \frac{1}{2N} \sum_{n=-N}^{N} \frac{1}{T_p} \int_{-NT_p}^{NT_p} h_{T_p}(t-nT_p)\cdot h_{T_p}(t-nT_p+\tau)\,\mathrm{d}t \right\} \\ &= \frac{1}{T_p} \int_{-\infty}^{\infty} h_{T_p}(t) h_{T_p}(t+\tau)\,\mathrm{d}t \end{aligned} \tag{2.58}$$

The Fourier transform of $R_s(\tau)$, the two-sided power spectral density, is

$$\mathcal{F}\{R_s(\tau)\} = \mathcal{S}(f) \stackrel{\text{def}}{=} \mathcal{V}(f) = \int_{-\infty}^{\infty} R_s(\tau)\cdot \exp(-2\pi j f\tau)\,\mathrm{d}\tau$$

*This section may be omitted on a first reading

$$= \frac{1}{T_p}\int_{-\infty}^{\infty}\int_{-\infty}^{\infty} h_{T_p}(t)\cdot h_{T_p}(t+\tau)\exp(-2\pi jt\tau)\,\mathrm{d}t\,\mathrm{d}\tau \tag{2.59}$$

$$= \frac{1}{T_p}\int_{-\infty}^{\infty} h_{T_p}(t)\exp(2\pi jft)\left\{\int_{-\infty}^{\infty} h_{T_p}(t+\tau)\exp[-2\pi jf(t+\tau)]\,\mathrm{d}\tau\right\}\mathrm{d}t$$

The integral in the brackets is equal to the Fourier transform $H(f)$ of $h_{T_p}(t)$.

Finally, we have

$$S(f) = \frac{1}{T_p}H(f)\int_{-\infty}^{\infty} h_{T_p}(t)\exp(2\pi jft)\,\mathrm{d}t$$

$$= \frac{1}{T_p}\,H(f)H^*(f) = \frac{1}{T_p}|H(f)|^2, \quad -\infty < f < \infty \tag{2.60}$$

Here $H^*(f)$ is the complex conjugate of $H(f)$. Using the inverse Fourier transform we get

$$R_s(\tau) = \int_{-\infty}^{\infty} S(f)\exp(2\pi jf\tau)\,\mathrm{d}t$$

$$= \frac{1}{T_p}\int_{-\infty}^{\infty}|H(f)|^2\exp(2\pi jf\tau)\,\mathrm{d}f \tag{2.61}$$

From Formulas (2.1) and (2.40) it follows that the BPSK signal is defined as

$$s(t) = \sqrt{2}\sum_{n=-\infty}^{\infty} v_n h_{T_p}(t-nT_p)\cos(2\pi f_c t+\phi) = \sqrt{2}\,v(t)\cos(2\pi f_c t+\phi) \tag{2.62}$$

It can be considered as a product of the lowpass stochastic process (2.56) and $\sqrt{2}\cos(2\pi f_c t+\phi)$.

The autocorrelation function of the BPSK signal is (Problem 2.6)

$$R_s(\tau) = R_v(\tau)\cos(2\pi f_c\tau) \tag{2.63}$$

where $R_v(\tau)$ is the autocorrelation function of the lowpass process (2.56). The two-sided power spectral density (the Fourier transform) of the BPSK signal (2.62) is [compare with Formula (2.42)]

$$S(f) = \frac{1}{2}\mathcal{V}(f-f_c) + \frac{1}{2}\mathcal{V}(f+f_c)$$

$$= \frac{1}{2T_p}|H(f-f_c)|^2 + \frac{1}{2T_p}|H(f+f_c)|^2, \quad -\infty < f < \infty \tag{2.64}$$

where $\mathcal{V}(f) = \frac{1}{T_p}|H(f)|^2$ is the Fourier transform of the lowpass process (2.56).

Let $\boldsymbol{v}' = \ldots v'_{-1}, v'_0, v'_1, \ldots, v'_n$ and $\boldsymbol{v}'' = \ldots v''_{-1}, v''_0, v''_1, \ldots, v''_n$ be independent sequences of equiprobable IID binary random variables in the real number alphabet $\{1, -1\}$ and let

$$s_{\mathrm{I}}(t) \stackrel{\mathrm{def}}{=} v_{\mathrm{I}}(t) = \sum_{n=-\infty}^{\infty} v'_n h_{T_{\mathrm{p}}}(t - nT_{\mathrm{p}}) \tag{2.65}$$

$$s_{\mathrm{Q}}(t) \stackrel{\mathrm{def}}{=} v_{\mathrm{Q}}(t) = \sum_{n=-\infty}^{\infty} v''_n h_{T_{\mathrm{p}}}(t - nT_{\mathrm{p}}) \tag{2.66}$$

be in-phase and quadrature lowpass stochastic processes, respectively; $h_{T_{\mathrm{p}}}(t)$ is a pulse of duration T_{p}. Then the QPSK signal is defined as [compare with Formula (2.43)]

$$s(t) = s_{\mathrm{I}}(t)\cos(2\pi f_{\mathrm{c}} t + \phi) - s_{\mathrm{Q}}(t)\sin(2\pi f_{\mathrm{c}} t + \phi) \tag{2.67}$$

The autocorrelation function of $s(t)$ is

$$\begin{aligned} R_s(\tau) &= E[s(t)s(t+\tau)] \qquad (2.68)\\ &= \tfrac{1}{2}\{E[s_{\mathrm{I}}(t)s_{\mathrm{I}}(t+\tau)] + E[s_{\mathrm{Q}}(t)s_{\mathrm{Q}}(t+\tau)]\}\cos(2\pi f_{\mathrm{c}}\tau)\\ &\quad -\tfrac{1}{2}\{E[s_{\mathrm{I}}(t)s_{\mathrm{Q}}(t+\tau)] + E[s_{\mathrm{Q}}(t)s_{\mathrm{I}}(t+\tau)]\}\sin(2\pi f_{\mathrm{c}}\tau)\\ &= \tfrac{1}{2}\,[R_{s_{\mathrm{I}}}(\tau) + R_{s_{\mathrm{Q}}}(\tau)]\,\cos(2\pi f_{\mathrm{c}}\tau) - \tfrac{1}{2}[R_{s_{\mathrm{I}}s_{\mathrm{Q}}}(\tau) + R_{s_{\mathrm{I}}s_{\mathrm{Q}}}(-\tau)]\sin(2\pi f_{\mathrm{c}}\tau) \end{aligned}$$

where $R_{s_{\mathrm{I}}}(\tau)$ and $R_{s_{\mathrm{Q}}}(\tau)$ are the autocorrelation functions of processes (2.65) and (2.66), respectively, and $R_{s_{\mathrm{I}}s_{\mathrm{Q}}}(\tau)$ is the cross-correlation function of these two processes. Because the processes $s_{\mathrm{I}}(t)$ and $s_{\mathrm{Q}}(t)$ are independent and have the same statistical properties and zero mean, $R_{s_{\mathrm{I}}}(\tau) = R_{s_{\mathrm{Q}}}(\tau)$, $R_{s_{\mathrm{I}}s_{\mathrm{Q}}}(\tau) = R_{s_{\mathrm{Q}}s_{\mathrm{I}}}(\tau) = 0$. Then we get for $R_s(\tau)$ the same expression (2.63) as for the BPSK signal. Correspondingly, the power spectral density of the QPSK signal coincides with the power spectral density (2.64) of the BPSK signal for equal symbol rates.

Consider now the FSK signal

$$s(t) = \sum_{n=-\infty}^{\infty} \tilde{s}_n(t - nT_{\mathrm{p}})$$

where $\tilde{s}_n(t)$ is defined by Formula (2.45). Then

$$s(t) = \sum_{n=-\infty}^{\infty} \sqrt{2}\, h_{T_{\mathrm{p}}}(t - nT_{\mathrm{p}})\cos(2\pi f_{\mathrm{c}} t + 2\pi i_n \Delta f t + \phi_n) \tag{2.69}$$

We suppose that ϕ_n are IID random variables with uniform distribution in the interval $[0, 2\pi]$; i_n are q-ary IID random variables, uniformly distributed on

the set $(-(q-1)/2, \ldots, -1/2,\ 1/2, \ldots, (q-1)/2)$ if q is even and on the set $(-(q-1)/2, \ldots, -1, 0, 1, \ldots, (q-1)/2)$ if q is odd. The autocorrelation function of process (2.69) is

$$R_s(\tau) = \lim_{T\to\infty} \frac{1}{2T} E\left[\int_{-T}^{T} s(t)s(t+\tau)\,\mathrm{d}t\right] \tag{2.70}$$

$$= \lim_{N\to\infty} \frac{1}{NT_\mathrm{p}} E\left\{\int_{-NT_\mathrm{p}}^{NT_\mathrm{p}} \sum_{n=-N}^{N} h_{T_\mathrm{p}}(t-nT_\mathrm{p}) \cos(2\pi f_\mathrm{c} t + 2\pi i_n \Delta f t + \phi_n)\right.$$

$$\left. \times \sum_{n'=-N}^{N} h_{T_\mathrm{p}}(t+\tau-n'T_\mathrm{p}) \cdot \cos[2\pi f_\mathrm{c}(t+\tau) + 2\pi i_{n'} \Delta f (t+\tau) + \phi_{n'}]\,\mathrm{d}t\right\}$$

Because $\phi_n, n = \ldots -1, 0, 1, \ldots$, are independent,

$$R_s(\tau) = \lim_{N\to\infty} \frac{1}{N} \sum_{n=-N}^{N} \frac{1}{T_\mathrm{p}} \int_{-NT_\mathrm{p}}^{NT_\mathrm{p}} h_{T_\mathrm{p}}(t-nT_\mathrm{p}) \cdot h_{T_\mathrm{p}}(t+\tau-nT_\mathrm{p})\,\mathrm{d}t \tag{2.71}$$

$$\times E[\cos(2\pi f_\mathrm{c}\tau + 2\pi i_n \Delta f \tau)]$$

$$= \frac{1}{qT_\mathrm{p}} \int_{-\infty}^{\infty} h_{T_\mathrm{p}}(t) h_{T_\mathrm{p}}(t+\tau)\,\mathrm{d}t \sum_{j=0}^{q-1} \cos\left[2\pi f_\mathrm{c}\tau + 2\pi\left(j - \frac{q-1}{2}\right)\Delta f \tau\right]$$

The two-sided power spectral density of the FSK signal is

$$S(f) = \int_{-\infty}^{\infty} R_s(\tau) \exp(-2\pi j f \tau)\,\mathrm{d}\tau \tag{2.72}$$

$$= \frac{1}{2qT_\mathrm{p}} \sum_{j=0}^{q-1} \left| H\left(f - f_\mathrm{c} - j\Delta f + \frac{q-1}{2}\,\Delta f\right)\right|^2$$

$$+ \frac{1}{2qT_\mathrm{p}} \sum_{j=0}^{q-1} \left| H\left(f + f_\mathrm{c} + j\Delta f - \frac{q-1}{2}\Delta f\right)\right|^2, \quad -\infty < f < \infty$$

where $H(f)$ is the Fourier transform of the pulse $h_{T_\mathrm{p}}(t)$.

Consider now the pulse amplitude on-off modulated signal

$$s(t) = \sum_{n=-\infty}^{\infty} \tilde{s}_n(t-nT_\mathrm{p}) = \sum_{n=-\infty}^{\infty} \frac{(v_n+1)}{\sqrt{2}} h_{T_\mathrm{p}}(t-nT_\mathrm{p}) \tag{2.73}$$

where $\tilde{s}_n(t)$ is defined by (2.2). We represent $s(t)$ as a sum of two independent processes, one stochastic

$$s'(t) = \frac{1}{\sqrt{2}} \sum_{n=-\infty}^{\infty} v_n h_{T_p}(t - nT_p) \tag{2.74}$$

and one deterministic

$$s''(t) = \frac{1}{\sqrt{2}} \sum_{n=-\infty}^{\infty} h_{T_p}(t - nT_p) \tag{2.75}$$

The stochastic process (2.74) has the autocorrelation function [compare with (2.58)]

$$R_{s'}(\tau) = \frac{1}{2T_p} \int_{-\infty}^{\infty} h_{T_p}(t) h_{T_p}(t + \tau)\, dt \tag{2.76}$$

and the two-sided power spectral density [compare with (2.60)]

$$S'(f) = \frac{1}{2T_p} |H(f)|^2, \quad -\infty < f < \infty \tag{2.77}$$

where $H(f)$ is the Fourier transform of the pulse $h_{T_p}(t)$.

The deterministic process (2.75) is periodic with period T_p. It can be expanded as a Fourier series [see Formulas (2.133) and (2.134) below]. The spectrum of this process consists of discrete spectral lines at all harmonics of $1/T_p$. The power spectral density of the process (2.73) is equal to the sum of the power spectral densities of the processes (2.74) and (2.75). A sketch of the spectrum of the process (2.73) is given in Figure 2.17 below.

Finally, consider the pulse position modulated signal

$$s(t) = \sum_{n=-\infty}^{\infty} \tilde{s}(t - 2nT_p) = \sum_{n=-\infty}^{\infty} h_{T_p}\left(t - 2nT_p + v_n \frac{T_p}{2}\right) \tag{2.78}$$

where $\tilde{s}_n(t)$ is defined by (2.34). Then

$$\begin{aligned} R_s(\tau) &= \lim_{T\to\infty} \left\{ \frac{1}{2T} E\left[\int_{-T}^{T} s(t) \cdot s(t + \tau)\, dt \right] \right\} \\ &= \lim_{N\to\infty} \left\{ \frac{1}{4NT_p} E\left[\int_{-2NT_p}^{2NT_p} \sum_{n=-N}^{N} h_{T_p}\left(t - 2nT_p + v_n \frac{T_p}{2}\right) \right.\right. \\ &\quad \left.\left. \times \sum_{n'=N}^{N} h_{T_p}\left(t + \tau - 2n'T_p + v_{n'} \frac{T_p}{2}\right) dt \right] \right\} \end{aligned}$$

$$= \frac{1}{T_p}\int_{-\infty}^{\infty} h_{T_p}(t)\cdot h_{T_p}(t+\tau)\,dt + $$

$$+\frac{1}{2T_p}\sum_{\substack{n=-\infty\\ n\neq 0}}^{\infty}\int_{-\infty}^{\infty} h_{T_p}(t)\cdot h_{T_p}(t+\tau+nT_p)\,dt$$

$$= R_h(\tau) + \frac{1}{2}\sum_{\substack{n=-\infty\\ n\neq 0}}^{\infty} R_h(\tau+nT_p) \tag{2.79}$$

where $R_h(\tau)$ is the normalized autocorrelation function of the pulse $h_{T_p}(t)$.

The function $R_s(\tau)$ is periodic with period T_p. The power spectral density of the process consists of discrete spectral lines at all harmonics of $1/T_p$.

2.3 GENERATION OF DS SS SIGNALS

In the uncoded transmission of digital information over a communication channel, the modulator is the interface device that maps the digital information into an analog waveform that matches the characteristics of the channel. It is convenient to represent the mapping of the information sequence

$$\boldsymbol{u} = \ldots u_{-1}, u_0, u_1, \ldots, u_n, \ldots \qquad u_n \in \{1, -1\}$$

into the narrowband modulated signal $s(t)$ in two steps. In the first step, the sequence $\boldsymbol{u}$ is mapped into the lowpass data signal

$$u(t) = \sum_{n=-\infty}^{\infty} u_n h_T(t-nT) \tag{2.80}$$

where $h_T(t)$ is a pulse of duration T. We will only consider the case of time-limited pulses (2.3) and bandlimited (2.31) pulses. The data signal occupies a bandwidth W, which is equal to the data rate $R = 1/T$ (bits/s). In the second step the lowpass data signal $u(t)$ is mapped into the narrowband modulated signal $s(t)$ with carrier frequency f_c. In the encoded transmission of digital information, the information sequence $\boldsymbol{u}$ is first encoded into a code sequence

$$\boldsymbol{v} = \ldots v_{-1}, v_0, v_1, \ldots, v_n, \ldots \qquad v_n \in \{1, -1\} \tag{2.81}$$

which is mapped into the lowpass code signal

$$v(t) = \sum_{n=-\infty}^{\infty} v_n h_T(t-nT) \tag{2.82}$$

Then the lowpass code signal $v(t)$ is mapped into the modulated signal $s(t)$. The code signal $v(t)$ defines the lowpass process. We assume that the sequences $\boldsymbol{u}$ and $\boldsymbol{v}$ are sequences of equiprobable IID binary random variables.

EXAMPLE 2.7

Calculate the autocorrelation function and the power spectral density of the random process (2.82) if $h_T(t)$ is an unit amplitude rectangular pulse (2.3).

Solution

For the calculation of the autocorrelation function $R_s(\tau)$ we use Formula (2.52). When $|\tau| \geq T$, the integral on the right-hand side of (2.52) is zero, because the sequence $\boldsymbol{v}$ has been modeled as an infinite sequence of independent zero-mean random binary digits. For $|\tau| < T$ the integral is equal to the fraction of the chip time for which $s(t) = s(t + \tau)$, as illustrated in Figure 2.6. Therefore

$$R_s(\tau) = \begin{cases} 1 - \dfrac{|\tau|}{T}, & |\tau| < T, \\ 0, & |\tau| \geq T \end{cases}$$

as shown in Figure 2.7.

The power spectral density of the stochastic process $s(t)$ is the Fourier transform (2.53) of the autocorrelation function $R_s(\tau)$:

$$\begin{aligned} S(f) &= \int_{-\infty}^{\infty} R_s(\tau) \exp\{-2\pi j f \tau\} \, d\tau \\ &= 2 \int_0^T \left(1 - \frac{\tau}{T}\right) \cos(2\pi f \tau) \, d\tau = T \operatorname{sinc}^2[fT] \end{aligned} \tag{2.83}$$

where the sinc function is defined by Formula (2.21). A sketch of $S(f)$ is given in Figure 2.2.

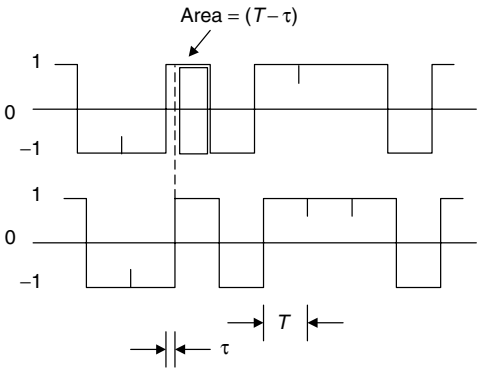

Figure 2.6. Calculation of the autocorrelation function of Example 2.7.

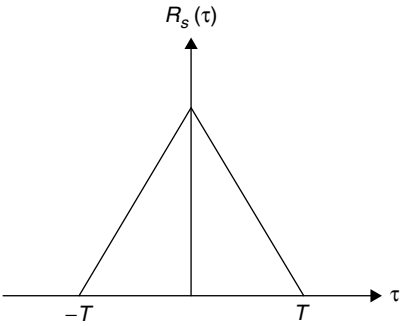

Figure 2.7. Autocorrelation function of Example 2.7.

Note that the autocorrelation function and the power spectral density of the random process (2.82), formed by sequences of unit amplitude rectangular pulses, coincide with the normalized autocorrelation function and power spectral density, respectively, of the unit amplitude rectangular pulse (2.3). This follows from Formulas (2.58) and (2.60) proved in the previous section. This phenomenon takes place in the general case.

EXAMPLE 2.8

Calculate the autocorrelation function and the power spectral density of the random process (2.82) if $h_T(t)$ is the constant bandlimited pulse (2.31).

Solution

From Formulas (2.30) and (2.60) it follows that the spectrum of $R_s(\tau)$ is equal to $|H(f)|^2/T = W|H(f)|^2$, that is,

$$S(f) = \begin{cases} \dfrac{1}{W}, & -\dfrac{W}{2} \le f \le \dfrac{W}{2} \\ 0, & \textit{otherwise} \end{cases}, \tag{2.84}$$

The autocorrelation function $R_s(\tau)$ is the inverse Fourier transform of $S(f)$, that is,

$$\begin{aligned} R_s(\tau) &= \int_{-\infty}^{\infty} S(f)\ \exp(2\pi j f\tau)\,\mathrm{d}f \\ &= \int_{-W/2}^{W/2} \frac{1}{W}\ \exp(2\pi j f\tau)\,\mathrm{d}f = \operatorname{sinc}(W\tau) \end{aligned} \tag{2.85}$$

A sketch of $R_s(\tau)$ is given in Figure 2.4.

If the code rate (number of information symbols divided by number of code symbols) is equal to r, $r \le 1$, then the data rate is equal to $R = r/T$ (bits/s)

and the code signal occupies a bandwidth that is $1/r$ times larger than in the uncoded case.

Without loss of generality we can consider the uncoded transmission as a partial case of the encoded transmission with code rate $r = 1$.

The simplest form of DS spreading modulation is binary phase shift-keying (BPSK). Ideal BPSK modulation results in instantaneous phase changes of the carrier by 180 degrees. The modulated signal can be mathematically represented as a multiplication of the carrier by the function $v(t)$ such that

$$s(t) = \sqrt{2}\, v(t) \cos(2\pi f_c t + \phi) \tag{2.86}$$

where $v(t)$ is defined by Formula (2.82), f_c is the carrier frequency, ϕ is the phase, and the transmitted signal is $\sqrt{P}s(t)$.[2] If we assume that $\boldsymbol{v}$ is a sequence of the equiprobable IID binary symbols and that $h_T(t)$ is the unit amplitude rectangular pulse, then the signal bandwidth is $W = 1/T = R/r$. The autocorrelation function of the BPSK signal is (Problem 2.6)

$$R_s(\tau) = R_v(\tau) \cos(2\pi f_c \tau) \tag{2.87}$$

where $R_v(\tau)$ is the autocorrelation function of the lowpass signal (2.82). The two-sided power spectral density of the BPSK signal is

$$S(f) = \frac{1}{2T}|H(f - f_c)|^2 + \frac{1}{2T}|H(f + f_c)|^2, \quad -\infty < f < \infty, \tag{2.88}$$

where $H(f)$ is the Fourier transform of $h_T(t)$. The BPSK modulator is illustrated in Figure 2.8.

Consider the reverse (uplink) transmission in the DS CDMA system. The *information sequence* of the kth user, $k = 1, 2, \ldots, K$,

$$\boldsymbol{u}^{(k)} = \ldots, u_{-1}^{(k)}, u_0^{(k)}, u_1^{(k)}, u_2^{(k)}, \ldots, u_n^{(k)}, \ldots \qquad u_n^{(k)} \in \{1, -1\} \tag{2.89}$$

is encoded by a rate r encoder into a *code sequence*

$$\boldsymbol{v}^{(k)} = \ldots, v_{-1}^{(k)}, v_0^{(k)}, v_1^{(k)}, v_2^{(k)}, \ldots, v_n^{(k)}, \ldots \qquad v_n^{(k)} \in \{1, -1\} \tag{2.90}$$

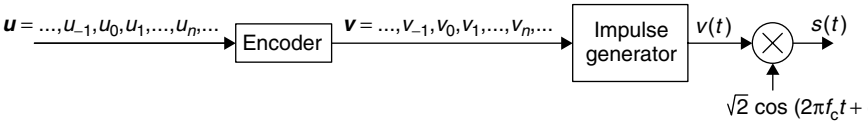

Figure 2.8. The BPSK modulator.

[2]Because for the system analysis the power of the *received signal* is important, we do not specify the power P of the *transmitted signal*, assuming that it can be adjusted by a power control mechanism, such that the received signal has appropriate power.

Then the code symbols $v_n^{(k)}$ are multiplied by the symbols of a *spreading sequence*

$$\boldsymbol{a}^{(k)} = \ldots a_{-1}^{(k)}, a_0^{(k)}, a_1^{(k)}, a_2^{(k)}, \ldots, a_n^{(k)}, \ldots \tag{2.91}$$

which in our model is a sequence of equiprobable IID binary symbols. The sequence $\boldsymbol{v}^{(k)} * \boldsymbol{a}^{(k)} \stackrel{\text{def}}{=} \{v_n^{(k)} a_n^{(k)}\}$, which still is a sequence of equiprobable IID binary symbols, enters into an *impulse generator*, which generates a sequence of pulses (chips) $\{v_n^{(k)} a_n^{(k)} h_{T_c}(t - nT_c)\}$, $n = \ldots -1, 0, 1, 2, \ldots$, of duration T_c. The output signal of the kth transmitter is

$$s^{(k)}(t) = \sqrt{2}\, v_a^{(k)}(t) \cos(2\pi f_c t + \phi^{(k)}) \tag{2.92}$$

where

$$v_a^{(k)}(t) = \sum_{n=-\infty}^{\infty} v_n^{(k)} a_n^{(k)} h_{T_c}(t - nT_c) \tag{2.93}$$

EXAMPLE 2.9

Construct the transmitted signal $s^{(k)}(t)$ for a system using Gaussian-shaped pulses (2.4). Assume that $\gamma = 1/9\pi$, that the pulse duration T_p is equal to the chip time T_c, that $\phi^{(k)} = 0$, and that the carrier frequency is given by $f_c = 10/T_c$.

Solution

From Formula (2.92) it follows that the transmitted signal is given by

$$s^{(k)}(t) = \sum_{n=-\infty}^{\infty} \sqrt[4]{18}\, v_n^{(k)} a_n^{(k)} \exp\left\{-\frac{9\pi[t - (n + 1/2)T_c]^2}{4T_c^2}\right\} \cos\left(\frac{2\pi 10t}{T_c}\right) \tag{2.94}$$

A sketch of the signal is presented in Figure 2.9.

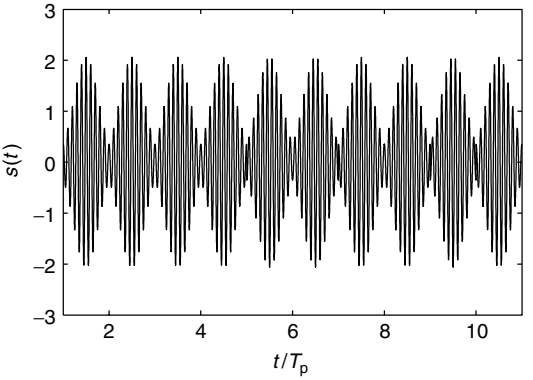

Figure 2.9. The transmitted signal $s^{(k)}(t)$ for Example 2.9.

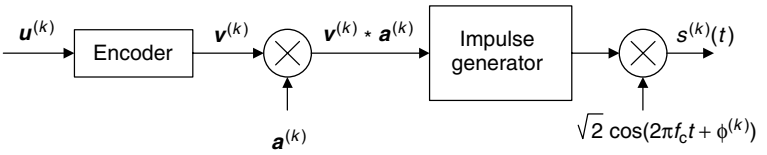

Figure 2.10. The BPSK modulator for the kth user of the DS CDMA system.

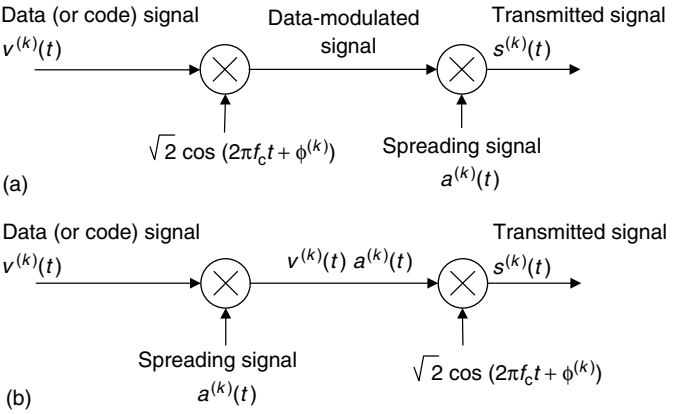

Figure 2.11. Analog forms of the BPSK modulator for the kth user in the DS CDMA system.

The BPSK DS SS modulator for the kth user in the uplink direction is illustrated in Figure 2.10.

The alternative analog forms of BPSK SS modulators, *in the case when* $h_{T_c}(t)$ *is the unit amplitude rectangular pulse*, are presented in Figure 2.11. Here

$$v^{(k)}(t) = \sum_{n=-\infty}^{\infty} v_n^{(k)} h_{T_c}(t - nT_c) \tag{2.95}$$

is a code signal

$$a^{(k)}(t) = \sum_{n=-\infty}^{\infty} a_n^{(k)} h_{T_c}(t - nT_c) \tag{2.96}$$

is a spreading signal. The transmitted signal is

$$s^{(k)}(t) = \sqrt{2}\, v^{(k)}(t) a^{(k)}(t) \cos(2\pi f_c t + \phi^{(k)}) \tag{2.97}$$

With the assumption that $\boldsymbol{a}^{(k)}$ is a sequence of equiprobable IID binary symbols and that $h_{T_c}(t)$ is the unit amplitude rectangular pulse, we have the spread signal

bandwidth $W = 1/T_c$ and the autocorrelation function of the signal

$$R_s(\tau) = R_a(\tau)\cos(2\pi f_c \tau) \tag{2.98}$$

where $R_a(\tau)$ is the autocorrelation function of the lowpass signal $v_a^{(k)}(t)$. (It coincides with the autocorrelation function of $a^{(k)}(t)$.) The two-sided power spectral density of the signal is

$$S(f) = \frac{1}{2T_c}|H(f - f_c)|^2 + \frac{1}{2T_c}|H(f + f_c)|^2, \ -\infty < f < \infty \tag{2.99}$$

The bandwidth of the spread signal (2.97) increases T/T_c times in comparison to the nonspread signal (2.86). The ratio T/T_c is the spreading factor (processing gain).

Consider now the forward (downlink) transmission of the BPSK SS signals. The modulated signal is the sum of the signals (2.92) from the individual users. Because mobiles are at different distances from the base station, the amplitudes of the different users' signals are also different. Therefore the signals (2.92) should be summarized with different weight coefficients $\gamma^{(k)}$, $\gamma^{(k)} > 0$, such that more powerful signals will be sent to distant mobiles. A spread spectrum system will be much more effective if the base station transmits an unmodulated pilot signal $s^{(0)}(t)$ for phase evaluation and time tracking, that is,

$$s^{(0)}(t) = \sqrt{2} \sum_{n=-\infty}^{\infty} a_n^{(0)} h_{T_c}(t - nT_c)\cos(2\pi f_c t + \phi^{(0)}) \tag{2.100}$$

where $\{a_n^{(0)}\}$ is a spreading sequence of a given cell/base station. Then the downlink transmitted signal is $\sqrt{P}\, s(t)$, with

$$s(t) = \sum_{k=0}^{K} \gamma^{(k)} s^{(k)}(t) \tag{2.101}$$

where $s^{(k)}(t)$ are defined by Formulas (2.92) and (2.100). It is convenient to choose the symbol $a_n^{(k)}$, $k = 1, 2, \ldots, K$, of the user spreading sequence as a product of the symbol of the pilot spreading sequence $a_n^{(0)}$ and the symbol of the user-specific sequence $\tilde{a}_n^{(k)}$, that is, $a_n^{(k)} = a_n^{(0)}\tilde{a}_n^{(k)}$, $k = 1, 2, \ldots, K$. We will assume that $\phi^{(0)} = 0$ and that $\{\phi^{(k)}, k \neq 0\}$ is a set of uniformly distributed on $[0, 2\pi)$ independent random variables.

Assuming that the pilot spreading sequence $\{a_n^{(0)}\}$ and the user-specific spreading sequences $\{\tilde{a}_n^{(k)}\}$, $k = 1, \ldots, K$, are sequences of equiprobable IID binary symbols, we get that the autocorrelation function of the signal (2.101) is

$$R_s(\tau) = \left[\sum_{k=0}^{K} (\gamma^{(k)})^2\right] R_a(\tau)\cos(2\pi f_c \tau) \tag{2.102}$$

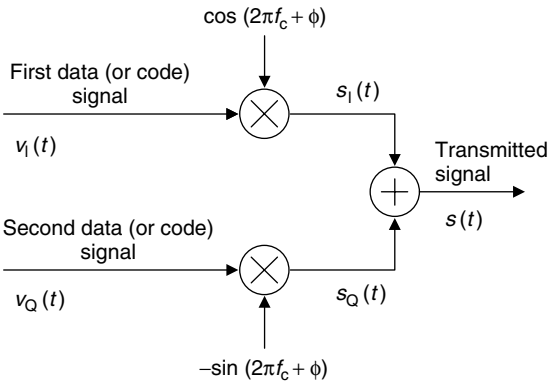

Figure 2.12. The QPSK modulator (in analog form).

where $R_a(\tau)$ is the autocorrelation function of the spreading signal (2.96). The power spectral density of the signal (2.101) is equal to the power spectral density (2.99) of the signal (2.92) times $\left[\sum_{k=0}^{K}(\gamma^{(k)})^2\right]$.

Consider now the QPSK modulation. The conventional QPSK modulator (in analog form) is shown in Figure 2.12. The in-phase and quadrature QPSK channels use different BPSK data modulators. This modulation is called *dual-channel QPSK*. The transmitted signal is

$$s(t) = s_{\mathrm{I}}(t) + s_{\mathrm{Q}}(t) = v_{\mathrm{I}}(t)\cos(2\pi f_{\mathrm{c}}t + \phi) - v_{\mathrm{Q}}(t)\sin(2\pi f_{\mathrm{c}}t + \phi) \quad (2.103)$$

where $v_{\mathrm{I}}(t)$ and $v_{\mathrm{Q}}(t)$ are data (or code) signals analogous to (2.95),

$$\begin{aligned} v_{\mathrm{I}}(t) &= \sum_{n=-\infty}^{\infty} v_{\mathrm{I}n} h_{T_{\mathrm{c}}}(t - nT_{\mathrm{c}}) \\ v_{\mathrm{Q}}(t) &= \sum_{n=-\infty}^{\infty} v_{\mathrm{Q}n} h_{T_{\mathrm{c}}}(t - nT_{\mathrm{c}}) \end{aligned} \quad (2.104)$$

$v_{\mathrm{I}n} \in \{1, -1\}$ and $v_{\mathrm{Q}n} \in \{1, -1\}$. If the data rate for each of the signals is equal to R, the overall data rate is $2R$, that is, two times larger than for BPSK signals. Analogous to the BPSK case, the signal bandwidth is $W = 1/T_{\mathrm{c}}$, the autocorrelation function $R_s(\tau)$ is defined by Formula (2.87), and the two-sided power spectral density is $S(f) = |H(f - f_{\mathrm{c}})|^2/2T_{\mathrm{c}} + |H(f + f_{\mathrm{c}})|^2/2T_{\mathrm{c}}$, where $H(f)$ is the Fourier transform of $h_{T_{\mathrm{c}}}(t)$.

Let us suppose that QPSK is used in a DS CDMA system. Consider reverse (uplink) transmission. The dual-channel QPSK DS SS modulator for the kth user (in analog form) in the case when $h_{T_{\mathrm{c}}}(t)$ is a rectangular pulse is shown in

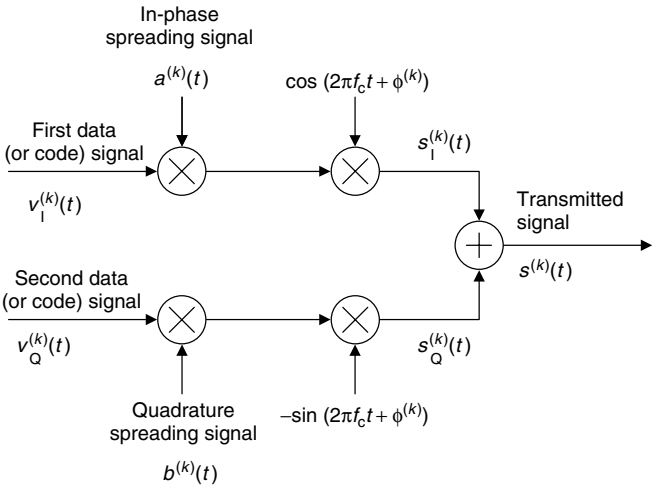

Figure 2.13. Dual-channel QPSK DS SS modulator for the kth user.

Figure 2.13. The transmitted uplink signal is

$$s^{(k)}(t) = v_{\mathrm{I}}^{(k)}(t)a^{(k)}(t)\cos(2\pi f_{\mathrm{c}}t + \phi^{(k)}) - v_{\mathrm{Q}}^{(k)}(t)b^{(k)}(t)\sin(2\pi f_{\mathrm{c}}t + \phi^{(k)}) \tag{2.105}$$

where $v_{\mathrm{I}}^{(k)}(t)$ and $v_{\mathrm{Q}}^{(k)}(t)$ are the biphase modulated data (or code) signals and $a^{(k)}(t)$ and $b^{(k)}(t)$ are the in-phase and the quadrature spreading signals

$$a^{(k)}(t) = \sum_{n=-\infty}^{\infty} a_n^{(k)} h_{T_{\mathrm{c}}}(t - nT_{\mathrm{c}}) \tag{2.106}$$

$$b^{(k)}(t) = \sum_{n=-\infty}^{\infty} b_n^{(k)} h_{T_{\mathrm{c}}}(t - nT_{\mathrm{c}}) \tag{2.107}$$

We suppose that the in-phase and the quadrature spreading sequences

$$\boldsymbol{a}^{(k)} = \ldots, a_{-1}^{(k)}, a_0^{(k)}, a_1^{(k)}, \ldots, a_n^{(k)}, \ldots \qquad a_n^{(k)} \in \{1, -1\} \tag{2.108}$$

$$\boldsymbol{b}^{(k)} = \ldots, b_{-1}^{(k)}, b_0^{(k)}, b_1^{(k)}, \ldots, b_n^{(k)}, \ldots \qquad b_n^{(k)} \in \{1, -1\} \tag{2.109}$$

are independent sequences of equiprobable IID binary random variables and that $h_{T_{\mathrm{c}}}(t)$ is the unit amplitude rectangular pulse (2.3).

Analogous to BPSK SS modulation, the bandwidth W of the QPSK SS modulated signal is equal to $1/T_{\mathrm{c}}$, the autocorrelation function $R_s(\tau)$ is defined by Formula (2.98), and the two-sided power spectral density is equal to $S(f) = |H(f - f_{\mathrm{c}})|^2/2T_{\mathrm{c}} + |H(f + f_{\mathrm{c}})|^2/2T_{\mathrm{c}}$, where $H(f)$ is the Fourier transform of $h_{T_{\mathrm{c}}}(t)$. The spreading factor is equal to T/T_{c}.

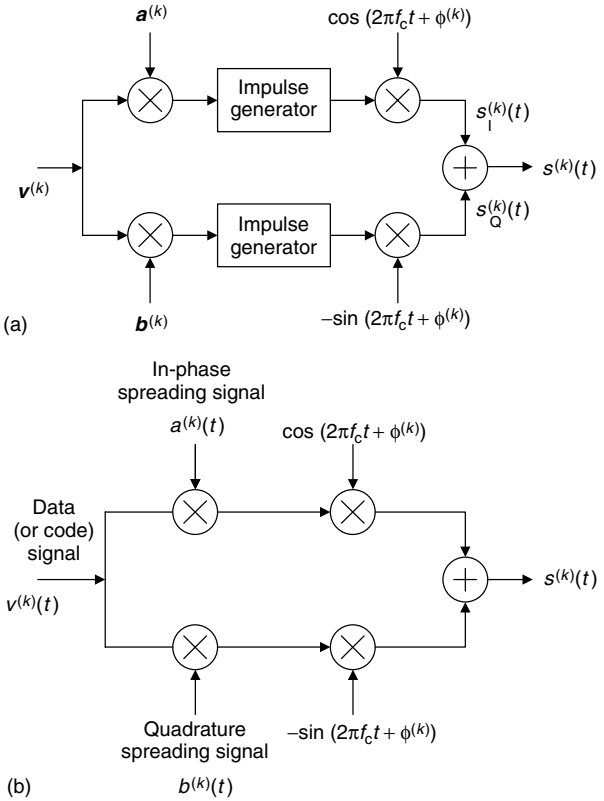

Figure 2.14. The balanced QPSK DS SS modulator for the kth user: (a) discrete form; (b) analog form (for rectangular pulses).

In this book, we will consider and analyze another type of QPSK modulation. It is called *balanced QPSK modulation* [34], because the data modulation is balanced between the in-phase and quadrature phase spreading channels. The balanced QPSK DS SS modulator for the kth user is shown in Figure 2.14.

The modulated QPSK DS SS uplink signal (see Fig. 2.14a) is

$$s^{(k)}(t) = \sum_{n=-\infty}^{\infty} v_n^{(k)} a_n^{(k)} h_{T_c}(t - nT_c) \cos(2\pi f_c t + \phi^{(k)}) - \sum_{n=-\infty}^{\infty} v_n^{(k)} b_n^{(k)} h_{T_c}(t - nT_c) \sin(2\pi f_c t + \phi^{(k)}) \qquad (2.110)$$

where $\{v_n^{(k)}\}$ is the code sequence, $\{a_n^{(k)}\}$ and $\{b_n^{(k)}\}$ are in-phase and quadrature spreading sequences (2.108) and (2.109), and $h_{T_c}(t)$ is a pulse of duration T_c.

The analog form of the QPSK DS SS modulator in Figure 2.14b is valid when $h_T(t)$ is the rectangular pulse (2.3). Note that the input data (or code) signal $v(t)$ is still biphase modulated. The output of the QPSK modulator of the kth user (see Fig. 2.14b) is

$$s^{(k)}(t) = v^{(k)}(t)[a^{(k)}(t)\cos(2\pi f_c t + \phi^{(k)}) - b^{(k)}(t)\sin(2\pi f_c t + \phi^{(k)})] \quad (2.111)$$

where the spreading signals $a^{(k)}(t)$ and $b^{(k)}(t)$ are defined by (2.106) and (2.107).

The modulated QPSK DS SS downlink signal is given by Formula (2.101), where $s^{(k)}(t)$, $k = 1, 2, \ldots, K$, are defined by (2.110) and

$$\begin{aligned} s^{(0)}(t) = &\sum_{n=-\infty}^{\infty} a_n^{(0)} h_{T_c}(t - nT_c)\cos(2\pi f_c t) \\ &- \sum_{n=-\infty}^{\infty} b_n^{(0)} h_{T_c}(t - nT_c)\sin(2\pi f_c t) \end{aligned} \quad (2.112)$$

Here $\{a_n^{(0)}\}$ and $\{b_n^{(0)}\}$ are the in-phase and the quadrature spreading sequences of the given cell/base station. The symbols $a_n^{(k)}$ and $b_n^{(k)}$, $k = 1, 2, \ldots, K$, of the user's in-phase and quadrature spreading sequences are products of the symbols $a_n^{(0)}$, $b_n^{(0)}$ of the pilot spreading sequences and the symbols $\tilde{a}_n^{(k)}$, $\tilde{b}_n^{(k)}$ of the user-specific sequences, that is,

$$\begin{aligned} a_n^{(k)} &= a_n^{(0)}\ \tilde{a}_n^{(k)}, \\ b_n^{(k)} &= b_n^{(0)}\ \tilde{b}_n^{(k)}, \end{aligned} \quad k = 1, 2, \ldots, K \quad (2.113)$$

The signal bandwidth, the signal autocorrelation function, and the power spectral density of QPSK SS signals are the same as for BPSK DS SS downlink signals.

2.4 FREQUENCY-HOPPED SS SIGNALS

A second method for spreading the spectrum of a data-modulated signal is to change the carrier frequency periodically. The spreading sequence in this case does not directly modulate the data-modulated signal but is instead used to control the carrier frequencies. Because the transmitted signal appears as a data-modulated signal that is hopping from one carrier frequency to another, this type of spread spectrum is called *frequency-hopped spread spectrum* (FH SS).

As we mentioned before, the FH SS system most often uses FSK. The FSK signal is a sequence of tones of duration T,

$$s(t) = \sqrt{2}\sum_{n=-\infty}^{\infty} h_T(t - nT)\cos(2\pi f_c t + 2\pi i_n \Delta f t + \phi_n) \quad (2.114)$$

Here $h_T(t)$ is a pulse of duration T, f_c is the carrier frequency, Δf is the frequency separation interval, i_n is the information-bearing parameter, and ϕ_n is a phase. We suppose that $\{i_n,\ n = \ldots -1, 0, 1, \ldots,\}$ is a sequence of IID random variables uniformly distributed on the set $\{-(q-1)/2, \ldots, (q-1)/2\}$ and $\{\phi_n,\ n = \ldots -1, 0, 1, \ldots\}$ is a sequence of IID random variables uniformly distributed in the interval $[0, 2\pi)$.

In Section 2.2 we proved that the autocorrelation function of the process $s(t)$ is [see Formula (2.71)]

$$R_s(\tau) = \frac{1}{qT}\int_{-\infty}^{\infty} h_T(t)h_T(t+\tau)\,dt \sum_{j=0}^{q-1}\cos\left[2\pi f_c\tau + 2\pi\left(j - \frac{q-1}{2}\right)\Delta f\tau\right] \tag{2.115}$$

and the two-sided power spectral density is [see (2.72)]

$$S(f) = \frac{1}{2qT}\sum_{j=0}^{q-1}\left[\left|H\left(f - f_c - j\Delta f + \frac{q-1}{2}\Delta f\right)\right|^2 + \left|H\left(f + f_c + j\Delta f - \frac{q-1}{2}\Delta f\right)\right|^2\right], \quad -\infty < f < \infty \tag{2.116}$$

where $H(f)$ is the Fourier transform of the pulse $h_T(t)$.

EXAMPLE 2.10

Calculate the autocorrelation function and the power spectral density of the FSK signal (2.114) if $h_T(t)$ is a unit amplitude rectangular pulse of duration $T = 1/\Delta f$.

Solution

From Formulas (2.115) and (2.116) follows

$$R_s(\tau) = \begin{cases} \dfrac{1}{q}\left(1 - \dfrac{|\tau|}{T}\right)\displaystyle\sum_{j=0}^{q-1} \\ \quad \times \cos\left[2\pi f_c\tau + 2\pi\left(j - \dfrac{q-1}{2}\right)\Delta f\tau\right], & \text{for } |\tau| \le T, \\ 0, & \text{otherwise} \end{cases} \tag{2.117}$$

$$S(f) = \frac{T}{2q}\sum_{j=0}^{q-1}\left\{\operatorname{sinc}^2\left[\left(f - f_c - j\Delta f + \frac{q-1}{2}\,\Delta f\right)T\right] + \operatorname{sinc}^2\left[\left(f + f_c + j\Delta f - \frac{q-1}{2}\,\Delta f\right)T\right]\right\}, \quad -\infty < f < \infty \tag{2.118}$$

A sketch of function (2.118) for $q = 8$ is plotted in Figure 2.15.

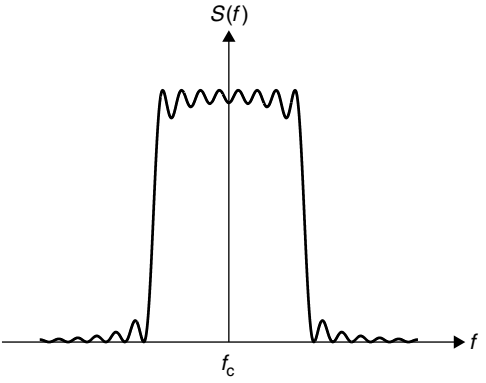

Figure 2.15. The power spectral density of the 8-FSK signal.

If the transmitter does not use coding, the transmission rate is $R = (\log_2 q)/T$; if it uses rate r coding, then $R = r(\log_2 q)/T$. The total signal bandwidth is $W = q\Delta f$.

EXAMPLE 2.11

Calculate the autocorrelation function and the two-sided power spectral density of the FSK signal (2.114) if $h_T(t)$ is a bandlimited pulse with spectrum

$$H(f) = \begin{cases} \dfrac{1}{\Delta f}, & -\dfrac{\Delta f}{2} \le f \le \dfrac{\Delta f}{2}, \\ 0, & \textit{otherwise} \end{cases} \tag{2.119}$$

Solution

From Formula (2.116) we get, because $T = 1/\Delta f$, that the two-sided power spectral density is

$$S(f) = \begin{cases} \dfrac{1}{2q\Delta f}, & \textit{if} \quad f_c - \dfrac{q}{2}\Delta f \le f \le f_c + \dfrac{q}{2}\Delta f, \\ & \textit{or} \ -f_c - \dfrac{q}{2}\Delta f \le f \le -f_c + \dfrac{q}{2}\Delta f, \\ 0, & \textit{otherwise} \end{cases} \tag{2.120}$$

Using the inverse Fourier transform (2.54) we get

$$\begin{aligned} R_s(\tau) &= \int_{-\infty}^{\infty} S(f)\exp(2\pi f t\tau)\,\mathrm{d}f \\ &= \frac{1}{2q\Delta f}\int_{-f_c-\frac{q}{2}\Delta f}^{-f_c+\frac{q}{2}\Delta f} \exp(2\pi j f\tau)\,\mathrm{d}f + \frac{1}{2q\Delta f}\int_{f_c-\frac{q}{2}\Delta f}^{f_c+\frac{q}{2}\Delta f} \exp(2\pi j f\tau)\,\mathrm{d}f \\ &= \operatorname{sinc}(q\Delta f\tau)\cos(2\pi f_c\tau) = \operatorname{sinc}(W\tau)\cos(2\pi f_c\tau) \end{aligned} \tag{2.121}$$

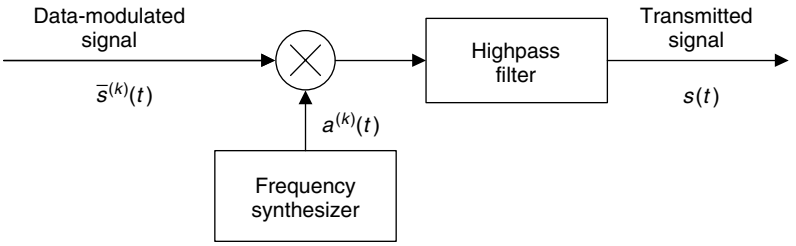

Figure 2.16. FH SS modulator for the kth user.

Consider the FH CDMA uplink transmission system. The modulator for the kth user, $k = 1, 2, \ldots K$, is shown in Figure 2.16. Here the kth user's data modulated signal is [compare with (2.114)] the sequence of tones of duration T_c, that is,

$$\overline{s}^{(k)}(t) = \sqrt{2} \sum_{n=-\infty}^{\infty} h_{T_c}(t - nT_c) \cos(2\pi f_c t + 2\pi i_n^{(k)} \Delta f t + \phi_n^{(k)}) \qquad (2.122)$$

where $h_{T_c}(t)$ is the unit amplitude rectangular pulse and the parameters f_c, $i_n^{(k)}$, Δf, and $\phi_n^{(k)}$ are defined below Formula (2.114), with $\Delta f = 1/T_c$. The frequency synthesizer output is also the sequence of tones of duration T_c,

$$a^{(k)}(t) = 2 \sum_{n=-\infty}^{\infty} h_{T_c}(t - nT_c) \cos[2\pi a_n^{(k)} \Delta F t] \qquad (2.123)$$

where $h_{T_c}(t)$ is the unit amplitude rectangular pulse (2.3) of duration T_c, ΔF is the *carrier frequency separation interval*, and $\Delta F = q\Delta f$. We assume that the hopping sequence

$$\boldsymbol{a}^{(k)} = \ldots a_{-1}^{(k)}, a_0^{(k)}, a_1^{(k)}, \ldots a_n^{(k)}, \ldots, \; a_n^{(k)} \in \left\{ -\frac{Q-1}{2}, -\frac{Q-3}{2}, \ldots, \frac{Q-1}{2} \right\} \qquad (2.124)$$

is the sequence of the IID Q-ary random variables uniformly distributed on the set $\{-(Q-1)/2, -(Q-3)/2, \ldots, (Q-1)/2\}$. The transmitted signal is the data-modulated carrier upconverted to a new frequency $f_c + a_n^{(k)} \Delta F$ for each FH chip, that is, the new signal is

$$s^{(k)}(t) = \sqrt{2} \sum_{n=-\infty}^{\infty} h_{T_c}(t - nT_c) \cos\left[2\pi \left(f_c + i_n^{(k)} \Delta f + a_n^{(k)} \Delta F \right) t + \phi_n^{(k)} \right] \qquad (2.125)$$

The cosine argument in Formula (2.125) can be presented as

$$2\pi[f_c + (i_n^{(k)} + a_n^{(k)} q)\Delta f]t + \phi_n^{(k)}$$

where $i_n^{(k)} + a_n^{(k)} q$ is the random variable uniformly distributed on the set $\{-(M-1)/2, \ldots, (M-1)/2\}$, where $M = qQ$ (Problem 2.7). The sequence $\{i_n^{(k)} + a_n^{(k)} q,\ n = \ldots -1, 0, 1, \ldots\}$ is a sequence of IID random variables, and the hopset is $\{f_c - (M-1)\Delta f/2, \ldots, f_c + (M-1)\Delta f/2\}$. The signal (2.125) can be treated as a frequency shift-keyed signal.

Because $h_T(t)$ is a rectangular pulse, the autocorrelation function of the signal (2.125) is [compare with (2.117)]

$$R_s(\tau) = \frac{1}{M}\left(1 - \frac{|\tau|}{T_c}\right) \sum_{j=0}^{M-1} \cos\left[2\pi f_c \tau + 2\pi\left(j - \frac{M-1}{2}\right)\Delta f \tau\right] \tag{2.126}$$

The two-sided power spectral density is [compare with (2.118)]

$$S(f) = \frac{T_c}{2M} \sum_{j=0}^{M-1} \left\{ \operatorname{sinc}^2\left[\left(f - f_c - j\Delta f + \frac{M-1}{2}\Delta f\right) T_c\right] \right. \tag{2.127}$$
$$\left. + \operatorname{sinc}^2\left[\left(f + f_c + j\Delta f - \frac{M-1}{2}\Delta f\right) T_c\right]\right\}, \quad -\infty < f < \infty$$

The *total hopping bandwidth* W equals $M\Delta f$, the *instantaneous bandwidth* is Δf, and the hop duration is T_c. If the transmitter does not use coding, the transmission rate is $R = (\log_2 q)/T_c$; if it uses rate r coding, the transmission rate is $R = r(\log_2 q)/T_c$. The hopset size is $W/\Delta f = M$. Formulas (2.126) and (2.127) describe the autocorrelation and spectral properties of FH CDMA signals.

The transmitted downlink FH SS signal is the weighted sum of the signals (2.125).

2.5 PULSE POSITION-HOPPED SS SIGNALS

A pulse amplitude on-off modulated signal has the form

$$s(t) = \sum_{n=-\infty}^{\infty} \tilde{s}_n(t - nT) = \sum_{n=-\infty}^{\infty} \frac{(v_n + 1)}{\sqrt{2}}\, h_T(t - nT) \tag{2.128}$$

Here $\tilde{s}_n(t - \tau_n)$ is defined by Formula (2.2), $\tau_n = nT$, $h_T(t)$ is a pulse of duration T, and $\{v_n\}$ is a code sequence (2.81). If the code rate is r, the data rate is $R = r/T$. The theory in this section will consider different models of pulses, in practice having a duration of the order of a nanosecond, but the average pulse amplitude should be equal to zero, that is, $\int_{-\infty}^{\infty} h_T(t)\, dt = 0$. It is convenient to present the process $s(t)$ as a sum of two processes, one stochastic

$$s'(t) = \frac{1}{\sqrt{2}} \sum_{n=-\infty}^{\infty} v_n h_T(t - nT) \tag{2.129}$$

and one deterministic

$$s''(t) = \frac{1}{\sqrt{2}} \sum_{n=-\infty}^{\infty} h_T(t - nT). \tag{2.130}$$

The autocorrelation function of the process (2.129) is [see Formula (2.76)]

$$R_{s'}(\tau) = \frac{1}{2T} \int_{-\infty}^{\infty} h_T(t) h_T(t + \tau)\, \mathrm{d}t = \frac{1}{2} R_h(\tau) \tag{2.131}$$

and the two-sided power spectral density is [see (2.77)]

$$S'(f) = \frac{1}{2T} |H(f)|^2, \quad -\infty < f < \infty \tag{2.132}$$

where $R_h(\tau)$ and $H(f)$ are the normalized autocorrelation function and the Fourier transform of the pulse $h_T(t)$, respectively.

The deterministic process (2.130) is periodic with period T. It can be expanded as a Fourier series, that is,

$$s''(t) = \sum_{n=-\infty}^{\infty} c_n \exp\left(\frac{2\pi n j}{T} t\right) \tag{2.133}$$

where the complex coefficients c_n are defined as

$$c_n = \frac{1}{T} \int_{-T/2}^{T/2} s''(t) \exp\left(-\frac{2\pi n j}{T} t\right) \mathrm{d}t \tag{2.134}$$

The spectrum of this process consists of discrete spectral lines at all harmonics of $1/T$. Parseval's theorem for Fourier series is [37]

$$\int_{-T/2}^{T/2} [s''(t)]^2 \, \mathrm{d}t = T \sum_{n=-\infty}^{\infty} |c_n|^2 \tag{2.135}$$

EXAMPLE 2.12

Calculate the autocorrelation function and power spectral density of the random process (2.129) and the power spectral density of the deterministic process (2.130) if $h_T(t)$ is a Manchester pulse of duration T.

Solution

From Formulas (2.35) and (2.131) we have

$$R_{s'}(\tau) = \begin{cases} \dfrac{1}{2} - \dfrac{3|\tau|}{2T}, & |\tau| \le T/2 \\ -\dfrac{1}{2} + \dfrac{|\tau|}{2T}, & T/2 < |\tau| \le T \\ 0, & \textit{otherwise} \end{cases} \tag{2.136}$$

The two-sided power spectral density of the process $s'(t)$ we get from (2.36) and (2.132),

$$S'(f) = \frac{2}{\pi^2 f^2 T} \sin^4\left(\frac{\pi f T}{2}\right) \tag{2.137}$$

From Formulas (1.23), (2.130) and (2.134) we have, analogously to (2.36),

$$c_n = \frac{1}{\sqrt{2}T} \int_{-T/2}^{T/2} h_{T_p}(t) \exp\left(-\frac{2\pi n}{T}\, jt\right) \mathrm{d}t = \frac{\sqrt{2}}{\pi jn} \sin^2\left(\frac{\pi n}{2}\right) \tag{2.138}$$

The power of the nth harmonic of the process $s''(t)$ is (2.135)

$$T|c_n|^2 = \frac{2T}{\pi^2 n^2} \sin^4\left(\frac{\pi n}{2}\right) \tag{2.139}$$

The process $s''(t)$ has only odd harmonics. The two-sided power spectral density of the process $s(t)$ is equal to the sum of the spectral density (2.137) of the process $s'(t)$ and of the (discrete) spectrum of the process $s''(t)$. The sketch of the spectrum given in Figure 2.17 shows that the spectral density has a null at zero frequency.

We recall that, in the case of Manchester pulses (not modulated by a sinusoidal carrier), it is natural to define the bandwidth W of the signal as $2/T$. Because T is of the order of nanoseconds, W is of the order of gigahertz.

Consider the pulse position hopping format based on pulse amplitude on-off modulation. Because transmitted down- and uplink PPH CDMA signals have the same structure, we study only the reverse (uplink) transmission. The kth transmitter's output signal $s^{(k)}(t)$ is given by

$$s^{(k)}(t) = \sum_{n=-\infty}^{\infty} \frac{(v_n^{(k)} + 1)}{\sqrt{2}} h_{T_c}(t - nT_f - a_n^{(k)}\Delta) \tag{2.140}$$

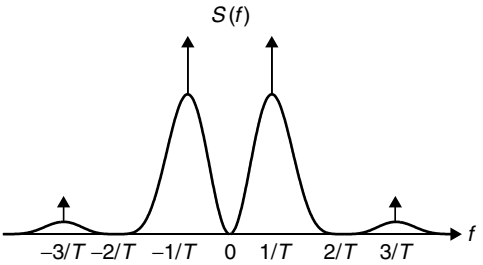

Figure 2.17. The sketch of the two-sided spectral density of the process for Example 2.12. (Local maxima are at points $\pm(2k+1)/T$, $k = 0, 1, \ldots$; nulls are at $2k/T$, $k = 0, 1, \ldots$.)

where the symbols $v_n^{(k)}$ are symbols of the kth user's code sequence [Formula (2.90)], Δ is the *duration of the addressable time delay bin* (in particular, Δ can be equal to T_c), and $h_{T_c}(t)$ is the pulse of duration T_c. The *frame time* $T_f \stackrel{\text{def}}{=} Q\Delta$ may typically be a hundred to a thousand times the pulse duration T_c, that is, $T_f \gg T_c$. Each user is assigned a *time-shift pattern* $\tau_n^{(k)} = a_n^{(k)}\Delta$ $\{a_n^{(k)},\ n = \ldots -1, 0, 1, \ldots\}$ called the *addressable pulse position shift*, which provides an additional time shift to each pulse in the pulse train. The nth pulse undergoes an additional shift of $a_n^{(k)}\Delta$ seconds. The elements $a_n^{(k)}$ of the sequence are choosen from a finite set $\{-(Q-1)/2, (Q-3)/2, \ldots, (Q-1)/2\}$, where $Q = T_f/\Delta$, and hence time shifts from $(-T_f + \Delta)/2$ to $(T_f - \Delta)/2$ are possible. We assume that $\boldsymbol{a}^{(k)} = \ldots a_{-1}^{(k)}, a_0^{(k)}, a_1^{(k)}, \ldots, a_n^{(k)}, \ldots$ is a sequence of IID random variables uniformly distributed on the set $\{-(Q-1)/2, (Q-3)/2, \ldots, (Q-1)/2\}$ and that $Q \gg 1$.

The autocorrelation function of the process $s^{(k)}(t)$ is

$$R_{s^{(k)}}(\tau) = \lim_{T\to\infty}\left\{\frac{1}{4T}\int_{-T}^{T} E\left[\sum_{n=-\infty}^{\infty}(v_n^{(k)}+1)h_{T_c}(t-nT_f-a_n^{(k)}\Delta)\right.\right.$$
$$\left.\left.\times\sum_{n'=-\infty}^{\infty}(v_{n'}^{(k)}+1)\,h_{T_c}(t+\tau-n'T_f-a_{n'}^{(k)}\Delta)\right]\mathrm{d}t\right\} \qquad (2.141)$$

where $E(\cdot)$ means ensemble averaging. Then

$$R_{s^{(k)}}(\tau) = \lim_{N\to\infty}\left\{\frac{1}{4NT_f}\sum_{n=-N}^{N}\sum_{n'=-N}^{N} E\left[(v_n^{(k)}+1)(v_{n'}^{(k)}+1)\right]\right. \qquad (2.142)$$
$$\left.\times\, E\left[\int_{-NT_f}^{NT_f} h_{T_c}(t-nT_f-a_n^{(k)}\Delta)\cdot h_{T_c}(t+\tau-n'T_f-a_{n'}^{(k)}\Delta)\,\mathrm{d}t\right]\right\}$$

If $|\tau| \geq T_c$, the integral $\int_{-\infty}^{\infty} h_{T_c}(t)h_{T_c}(t+\tau)\,\mathrm{d}t$ is equal to zero for the Manchester pulse and close to zero for the differentiated Gaussian pulse. Then for $T_f \gg T_c$, the integral on the right-hand side of (2.142) vanishes for $n \neq n'$, and we finally get

$$R_{s^{(k)}}(\tau) \approx \frac{1}{T_f}\int_{-\infty}^{\infty} h_{T_c}(t)h_{T_c}(t+\tau)\,\mathrm{d}t = T_c\frac{R_h(\tau)}{T_f} \qquad (2.143)$$

The two-sided power spectral density of the signal $s^{(k)}(t)$ is [compare with (2.132)]

$$S^{(k)}(f) \approx \frac{1}{T_f}|H(f)|^2, \quad -\infty < f < \infty \qquad (2.144)$$

where $H(f)$ is the Fourier transform of the pulse $h_{T_c}(t)$.

Consider now pulse position modulation (PPM). The transmitted signal is

$$s(t) = \sum_{n=-\infty}^{\infty} h_T\left(t - 2nT + \frac{v_n}{2}T\right) \tag{2.145}$$

where $\{v_n\}$ is a code sequence. The autocorrelation function of the signal, as was proved in Section 2.2, is

$$R_s(\tau) = R_h(\tau) + \frac{1}{2}\sum_{n=-\infty}^{\infty} R_h(\tau + nT) \tag{2.146}$$

where $R_h(\tau)$ is the normalized autocorrelation function of the pulse $h_T(t)$. Because $R_s(\tau)$ includes a periodical function with the period T, the power spectral density of the process includes discrete spectral lines at all harmonics of $1/T$.

In the PPH CDMA system employing PPM, the signal transmitted by the kth user is

$$s^{(k)}(t) = \sum_{n=-\infty}^{\infty} h_{T_c}\left(t - nT_f - a_n^{(k)}\Delta + \frac{v_n^{(k)}}{2}T_c\right) \tag{2.147}$$

where the notations coincide with the notations in Formula (2.140). The autocorrelation function and the power spectral density of the process (2.147) coincide with the autocorrelation function and the power spectral density of the process (2.140) and are given by (2.143) and (2.144), respectively (Problem 2.17).

2.6 ORTHOGONAL AND QUASI-ORTHOGONAL EXPANSIONS OF SS SIGNALS

In the study of signal theory, orthogonal series expansions have played a prominent role in the analysis. A set $\{\phi_n(t), n = 1, 2, \dots\}$ of functions is called *orthogonal* if

$$\int_{-\infty}^{\infty} \phi_n(t)\phi_{n'}(t)\,dt = 0, \quad n \neq n' \tag{2.148}$$

If, additionally,

$$\int_{-\infty}^{\infty} \phi_n^2(t)\,dt = 1, \tag{2.149}$$

the set $\{\phi_n(t)\}$ is called *orthonormal*. Examples of orthogonal sets include nonoverlapping unit amplitude rectangular pulses and bandlimited pulses (see Example 2.13).

The infinite set $\{\phi_n(t), n = 1, 2, \dots\}$ is called *complete* if every deterministic finite energy signal $s(t)$ can be represented by a series expansion

$$s(t) = \sum_{n=1}^{\infty} v_n\phi_n(t) \tag{2.150}$$

In particular, the set of trigonometric functions $\{\sqrt{2/T}\cos(2\pi nt/T), \sqrt{2/T}\sin(2\pi nt/T)\}$ is complete. Every deterministic, finite-energy, *time-limited* signal can be represented as a Fourier series.

In SS applications, it is more convenient to use a noncomplete set of functions $\{\phi_n(t)\}$, or even sometimes a nonorthogonal (but quasi-orthogonal) set, as a basis. In fact, consider the baseband signal

$$s(t) = v(t) = \sum_{n=-\infty}^{\infty} v_n h_{T_c}(t - nT_c) \tag{2.151}$$

where $v_n \in \{1, -1\}$ and $h_{T_c}(t)$ is a pulse of duration T_c. Formula (2.151) can be treated as an expansion of a signal over a set $\{h_{T_c}(t - nT_c)\}$. The (infinite dimensional) vector of the coefficients $\{v_n\}$ bears all information about the signal $s(t)$.

Let $R_h(\tau)$ be the normalized autocorrelation function (2.15) of the pulse $h_{T_c}(t)$. In particular, if $h_{T_c}(t)$ is the rectangular pulse,

$$R_h[(n-n')T_c] = \frac{1}{T_c}\int_{-\infty}^{\infty} h_{T_c}(t - nT_c)h_{T_c}(t - n'T_c)\,dt = \begin{cases} 1, & \text{if } n = n' \\ 0, & \text{otherwise} \end{cases} \tag{2.152}$$

and $\{h_{T_c}(t - nT_c), n = \ldots -1, 0, 1, \ldots\}$ is a set of orthogonal functions.

EXAMPLE 2.13

Prove that the set $\{h_{T_c}(t - nT_c)\}$ of the bandlimited pulses (2.31) is a set of orthogonal functions.

Solution

From Formulas (2.19) and (2.30) we have for the bandlimited pulse

$$\mathcal{H}(f) = \begin{cases} \dfrac{1}{W}, & -\dfrac{W}{2} \le f \le \dfrac{W}{2} \\ 0, & \textit{otherwise} \end{cases} \tag{2.153}$$

The inverse Fourier transform of (2.153) gives

$$R_h(\tau) = \operatorname{sinc}(W\tau). \tag{2.154}$$

From (2.154) follows (2.152).

For the baseband signal (2.151) and the orthogonal sets of rectangular or bandlimited pulses we have[3]

$$v_n = \frac{1}{T_c}\int_{-\infty}^{\infty} s(t)h_{T_c}(t - nT_c)\,dt \tag{2.155}$$

[3]Actually, the estimation of the coefficients $\{v_n\}$ is processed in the receiver, where the power of the received signal P is, generally speaking, not equal to 1. In this section, we assume for simplicity that $P = 1$.

that is, v_n is the normalized *cross-correlation* between $s(t)$ and $h_{T_c}(t - nT_c)$. In the *correlation-type estimator*, the baseband signal $s(t)$ is passed through a parallel bank of cross-correlators, which basically compute the cross-correlation between $s(t)$ and the basis functions $\{h_{T_c}(t - nT_c)\}$. If $\{h_{T_c}(t - nT_c)\}$ is not an orthogonal set, then the integral on the right-hand side of (2.155) is equal to

$$\hat{v}_n \stackrel{\text{def}}{=} v_n + \sum_{n' \neq n} v_{n'} I_{nn'} \tag{2.156}$$

where $I_{nn'}$ is the *interchip interference*,

$$I_{nn'} = \frac{1}{T_c} \int_{-\infty}^{\infty} h_{T_c}(t - nT_c) h_{T_c}(t - n'T_c)\, dt, \;\; n' \neq n \tag{2.157}$$

If the interchip interference $I_{nn'}$, $n' \neq n$, is small, the set $\{h_{T_c}(t - nT_c)\}$ is called *quasi-orthogonal* and we will consider $\hat{v}_n$ as an estimate of v_n. If $\{v_n\}$ is a set of equiprobable IID binary random variables 1 or -1, then

$$\begin{aligned} E(\hat{v}_n) &= v_n \\ \text{var}(\hat{v}_n) &= \sum_{n' \neq n} I_{nn'}^2 \end{aligned} \tag{2.158}$$

EXAMPLE 2.14

Find the interchip interference for a set of Gaussian pulses (2.11).

Solution

The normalized autocorrelation function of the Gaussian pulse is

$$R_h(\tau) = \frac{1}{T_c} \int_{-\infty}^{\infty} h_{T_c}(t) h_{T_c}(t + \tau)\, dt = \exp\left(-\frac{9\pi}{8} \frac{\tau^2}{T_c^2}\right). \tag{2.159}$$

Then $R_h(0) = 1$, $I_{n,n-1} = I_{n,n+1} = R_h(\pm T_c) = \exp\left(-\frac{9\pi}{8}\right) = 0.0292$, $I_{n,n-2} = I_{n,n+2} = R_h(\pm 2T_c) = \exp\left(-\frac{9\pi}{2}\right) = 7.25 \cdot 10^{-7}$.

Instead of using the correlator to generate the estimates $\{\hat{v}_n\}$ we may use a *matched filter*. To be specific, let us suppose that the impulse response of the filter is

$$g(t) = \frac{1}{T_c} h_{T_c}(-t), \quad -\infty < t < \infty \tag{2.160}$$

The output of this filter is

$$z(t) = \frac{1}{T_c} \int_{-\infty}^{\infty} s(\tau) h_{T_c}(\tau - t)\, d\tau \tag{2.161}$$

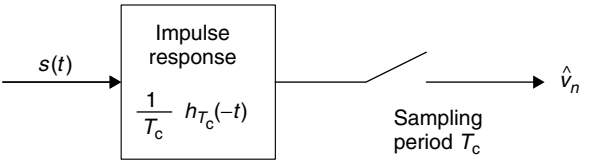

Figure 2.18. Matched-filter estimator.

Then the output of the matched filter at $t = nT_c$,

$$z(nT_c) = \frac{1}{T_c}\int_{-\infty}^{\infty} s(\tau)h_{T_c}(\tau - nT_c)\,d\tau \tag{2.162}$$

coincides with the output of the correlator (2.155). Hence, the sampled outputs of the filter $\{z(nT_c)\}$ are exactly the set of $\{\hat{v}_n\}$ obtained from the infinite bank of linear correlators (Fig. 2.18). Sampling of the filter output at $t = nT_c$ assumes that the timing of the baseband signal (2.151) is precisely known to the estimator.

The estimation $\hat{v}_n$ of v_n can be made on the base of the noisy version of $s(t)$,

$$r(t) = s(t) + \xi(t) \tag{2.163}$$

where $\xi(t)$ is AWGN of two-sided spectral density $N_0/2$. Then

$$\begin{aligned}\hat{v}_n &= \frac{1}{T_c}\int_{-\infty}^{\infty} r(t)h_{T_c}(t - nT_c)\,dt \\ &= v_n + \sum_{n' \neq n} v_{n'} I_{nn'} + \xi_n\end{aligned} \tag{2.164}$$

that is, the estimation $\hat{v}_n$ contains additionally the noise component

$$\xi_n = \frac{1}{T_c}\int_{-\infty}^{\infty} \xi(t)h_{T_c}(t - nT_c)\,dt \tag{2.165}$$

EXAMPLE 2.15

Under the assumption that $\{h_{T_c}(t - nT_c)\}$ is an orthogonal set, show that the set $\{\hat{v}_n\}$ defined by (2.164) is the set of IID Gaussian random variables. Find the first two moments of $\hat{v}_n$.

Solution

Because the set $\{h_{T_c}(t - nT_c)\}$ is orthogonal,

$$E(\hat{v}_n) = \frac{1}{T_c}\int_{-\infty}^{\infty} E[r(t)]h_{T_c}(t - nT_c)\,dt = v_n$$

The covariance between $\hat{v}_n$ and $\hat{v}_{n'}$ is

$$\begin{aligned}\operatorname{cov}[\hat{v}_n \hat{v}_{n'}] &= \frac{1}{T_c^2}\int_{-\infty}^{\infty}\int_{-\infty}^{\infty} E[\xi(t)\xi(t')]h_{T_c}(t-nT_c)h_{T_c}(t'-n'T_c)\,dt\,dt' \\ &= \frac{1}{T_c^2}\int_{-\infty}^{\infty}\frac{N_0}{2}\delta(t-t')h_{T_c}(t-nT_c)h_{T_c}(t'-n'T_c)\,dt\,dt' \\ &= \frac{N_0}{2T_c^2}\int_{-\infty}^{\infty} h_{T_c}(t-nT_c)h_{T_c}(t-n'T_c)\,dt = \begin{cases} N_0/2T_c, & \text{if } n=n' \\ 0, & \text{otherwise}\end{cases}\end{aligned}$$

Because $\xi(t)$ is a Gaussian process and $h_{T_c}(t)$ is a deterministic function, it follows from (2.165) that $\{\xi_n\}$ are Gaussian random variables; so are $\{\hat{v}_n\}$. Because the covariance between $\hat{v}_n$ and $\hat{v}_{n'}$, $n' \neq n$, is zero, $\{\hat{v}_n\}$ are independent Gaussian random variables.

It is worth while to recall that the set of time-limited or bandlimited pulses is not a *complete orthogonal set*. In other words, not any function $f(t)$ can be represented in the basis that forms this set. But we can always add additional functions to the set $\{h_{T_c}(t-nT_c)\}$ to get a complete orthogonal basis. Obviously, the coefficients obtained by projecting the transmitted baseband signal $s(t)$ onto each of the additional functions are zeros [because the expansion of $s(t)$ in the complete basis is unique]. Therefore, the coefficients obtained by projecting the noisy version at the baseband signal $s(t)$ onto each of the additional functions has no information about the signal $s(t)$ and can be omitted from the estimation process.

Suppose now that the input of the linear time-invariant system (filter) that is characterized by its impulse response (2.160) or, equivalently, by its frequency response $H^*(f)/T_c$, is the stationary zero-mean random process $s(t)$. The output of the filter is [compare with (2.161)]

$$z(t) = \frac{1}{T_c}\int_{-\infty}^{\infty} s(t')h_{T_c}(t'-t)\,dt' \tag{2.166}$$

Because $E[s(t)] = 0$, we have $E[z(t)] = 0$. The autocorrelation function of the output is

$$\begin{aligned}R_z(\tau) &= E[z(t)z(t+\tau)] \\ &= \frac{1}{T_c^2}\int_{-\infty}^{\infty}\int_{-\infty}^{\infty} E[s(t')\cdot s(t'')]h_{T_c}(t'-t)h_{T_c}(t''-t-\tau)\,dt'\,dt'' \\ &= \frac{1}{T_c^2}\int_{-\infty}^{\infty}\int_{-\infty}^{\infty} R_s(t'-t'')h_{T_c}(t'-t)h_{T_c}(t''-t-\tau)\,dt'\,dt''\end{aligned}$$

$$= \frac{1}{T_c^2}\int_{-\infty}^{\infty}\int_{-\infty}^{\infty} R_s(\tau')h_{T_c}(t)h_{T_c}(t-\tau'-\tau)\,d\tau'\,dt$$

$$= \frac{1}{T_c}\int_{-\infty}^{\infty} R_s(\tau')R_h(\tau'+\tau)\,d\tau' \tag{2.167}$$

Taking the Fourier transform of both sides of (2.167), we obtain the power spectral density $Z(f)$ of the output random process in the form

$$Z(f) = \frac{1}{T_c^2}S(f)|H(f)|^2 \tag{2.168}$$

In particular, if the input process is (2.151), where v_n is the set of IID equiprobable random variables and $v_n \in \{1, -1\}$, then

$$Z(f) = \frac{1}{T_c^3}|H(f)|^4 \tag{2.169}$$

We emphasize the difference between the two considered cases (2.161) and (2.166). In the first case, the input of the filter is a deterministic signal $s(t)$ and the filter is matched (synchronized) with the signal. In the second case, the input is a stationary random process $s(t)$ and the filter is not matched with the input signal.

The variance of the zero-mean stochastic process $z(t)$ is

$$\text{var}[z(t)] = E[z^2(t)] = R_z(0) = \int_{-\infty}^{\infty} Z(f)\,df = \frac{1}{T_c^3}\int_{-\infty}^{\infty}|H(f)|^4\,df \tag{2.170}$$

But $|H(f)|^2/T_c$ is the power spectral density of the input process $s(t)$. Using Parseval's theorem, which is valid also for random processes, we get

$$\int_{-\infty}^{\infty}\frac{1}{T_c^2}|H(f)|^4\,df = \int_{-\infty}^{\infty} R_s^2(\tau)\,d\tau \tag{2.171}$$

or

$$\text{var}[z(t)] = R_z(0) = \frac{1}{T_c}\int_{-\infty}^{\infty} R_s^2(\tau)\,d\tau \tag{2.172}$$

EXAMPLE 2.16

Find the variance of the output process (2.166) for bandlimited pulses (2.31) of duration $T_c = 1/W$ if the filter is bandlimited with frequency response $H^*(f)$ where $H(f)$ is defined by (2.30).

Solution

From Formulas (2.30) and (2.170) we get, because $T_c = 1/W$

$$\text{var}[z(t)] = R_z(0) = W^3\int_{-W/2}^{W/2}\frac{1}{W^4}\,df = 1 \tag{2.173}$$

EXAMPLE 2.17

Find the variance of the output process (2.166) with unit amplitude rectangular pulses $h_{T_c}(t)$, defined by (2.3), if the filter's impulse response is equal to $h_{T_c}(-t)/T_c$.

Solution

From Example 2.7 it follows that

$$R_s(\tau) = \begin{cases} 1 - \dfrac{|\tau|}{T_c}, & |\tau| < T_c \\ 0, & |\tau| \geq T_c \end{cases} \tag{2.174}$$

Application of (2.172) gives

$$R_z(0) = \frac{2}{T_c} \int_0^{T_c} \left(1 - \frac{\tau}{T_c}\right)^2 d\tau = \frac{2}{3} \tag{2.175}$$

Up to now we have considered expansions of baseband signals. Consider now the BPSK signal

$$s(t) = \sqrt{2}\, v(t - \delta) \cos[2\pi f_c (t - \delta) + \varphi] \tag{2.176}$$

where the baseband signal $v(t)$ is defined by (2.82), f_c is a carrier frequency, δ is a time-offset, and φ is a phase. Generally speaking, δ and φ can be unknown to the estimator.

To estimate the set $\{v_n\}$ we must demodulate the signal (2.176). Consider the case when δ and φ are known. Without loss of generality we will assume that $\delta = 0$ and $\varphi = 0$. The signal $s(t)$ should be multiplied by $\sqrt{2}\cos(2\pi f_c t)$ and then passed through the matched filter with impulse response $h_{T_c}(-t)/T_c$. The filter output process is

$$\begin{aligned} z(t) &= \frac{1}{T_c} \int_{-\infty}^{\infty} s(\tau) \sqrt{2} \cos(2\pi f_c \tau) h_{T_c}(\tau - t)\, d\tau \\ &= \frac{2}{T_c} \int_{-\infty}^{\infty} v(\tau) \cos^2(2\pi f_c \tau) h_{T_c}(\tau - t)\, d\tau \\ &\approx \frac{1}{T_c} \int_{-\infty}^{\infty} v(\tau) h_{T_c}(\tau - t)\, d\tau \end{aligned} \tag{2.177}$$

where we use the equality $\cos^2 \alpha = (1 + \cos 2\alpha)/2$ and the condition $f_c \gg 1/T_c$. The output $z(nT_c)$ of the matched filter at $t = nT_c$ is an estimation $\hat{v}_n$ of the coefficient v_n analogous to (2.156).

Consider now the case when the signal on the input of the estimator is a sum of independent signals sent by different users,

$$s^{(k)}(t) = \sqrt{2}\, v^{(k)}\left(t - \delta^{(k)}\right) \cos\left[2\pi f_c \left(t - \delta^{(k)}\right) + \varphi^{(k)}\right], \quad k = 1, 2, \ldots, K \tag{2.178}$$

which have different values of time offset $\delta^{(k)}$ and phase $\varphi^{(k)}$. This is a typical situation in the acquisition process of the DS CDMA system. We assume that $\varphi^{(k)}$ are independent random variables uniformly distributed on $[0, 2\pi)$. The output of the filter is a sum of random processes, corresponding to input signals $s^{(k)}(t)$. To the input process $s^{(k)}(t)$ corresponds the output process

$$\begin{aligned} z^{(k)}(t) &= \frac{1}{T_c} \int_{-\infty}^{\infty} s^{(k)}(\tau)\sqrt{2}\cos(2\pi f_c \tau) h_{T_c}(\tau - t)\, d\tau \\ &\approx \frac{\cos\varphi^{(k)}}{T_c} \int_{-\infty}^{\infty} v^{(k)}(\tau) h_{T_c}(\tau - t)\, d\tau \end{aligned} \tag{2.179}$$

The mathematical expectation of the output process is $E\left[z^{(k)}(t)\right] = 0$, and the autocorrelation function of the random process $z^{(k)}$ is [compare with Formula (2.167)]

$$R_z(\tau) = \frac{E\left(\cos^2\varphi^{(k)}\right)}{T_c^2} \int_{-\infty}^{\infty}\int_{-\infty}^{\infty} R_v(\tau') h_{T_c}(t) h_{T_c}(t - \tau' - \tau)\, d\tau'\, dt \tag{2.180}$$

where $R_v(\tau)$ is the autocorrelation function of the baseband signal $v^{(k)}(t)$ (it does not depend on k). Because the phase $\varphi^{(k)}$ is distributed uniformly on $[0, 2\pi]$, we have

$$R_z(\tau) = \frac{1}{2T_c^2} \int_{-\infty}^{\infty}\int_{-\infty}^{\infty} R_v(\tau') h_{T_c}(t) h_{T_c}(t - \tau' - \tau)\, d\tau'\, dt \tag{2.181}$$

Then, analogously to (2.170) and (2.172), we get

$$\operatorname{var}\left[z^{(k)}(t)\right] = \frac{1}{2T_c^3} \int_{-\infty}^{\infty} |H(f)|^4\, df = \frac{1}{2T_c} \int_{-\infty}^{\infty} R_v^2(\tau)\, d\tau \tag{2.182}$$

If $K \gg 1$, the random process on the output of the matched filter can be considered as Gaussian with zero mean and variance that is the sum of the variances of processes $z^{(k)}(t)$, $k = 1, 2, \ldots, K$.

During the acquisition process, one of the users, say the first, sends the periodical acquisition signal $s^{(1)}(t)$, the baseband component of which is known to the receiver. If $\delta^{(1)}$ and $\varphi^{(1)}$ were known to the receiver, it could reconstruct the filter output process corresponding to the input signal $s^{(1)}(t)$. Even if $\varphi^{(1)}$ is unknown, the receiver can do it using noncoherent reception. The output signals

corresponding to input signals from other users can be considered as interference noise processes. In practice, the acquisition receiver does not know $\delta^{(1)}$. A widely used technique for acquisition is to search serially through all potential time offset shifts $\delta^{(1)}$ until the correct shift is identified.

When synchronization is established, the receiver starts to operate in the regime of digital communication. The coherent reception of the DS CDMA signal assumes that the time offset $\delta^{(1)}$ and the phase $\varphi^{(1)}$ of the desired signal are known. The sum of the filter output processes corresponding to interfering signals from other users can be considered as zero-mean Gaussian noise with variance equal to the sum of the variances of interfering processes. We consider in more detail the acquisition and digital reception of DS signals in Chapters 3–7.

The PAM signals (2.128) and PPM signals (2.145) can be expanded analogously to the baseband BPSK signals. In fact, the matched filter for the PAM signal (2.128) has impulse response $g(t) = \sqrt{2}\ h_{T_c}(-t)/T_c$, and the estimate $\hat{v}_n$ is equal to the output of the matched filter at $t = nT_c - 1$. The matched filter for the PPM signal (2.145) has impulse response $g(t) = [h_{T_c}(-t + T_c/2) - h_{T_c}(-t - T_c/2)]/T_c$ (see Chapter 3), and the estimate $\hat{v}_n$ is equal to output of the matched filter at $t = nT_p$.

The FSK signals used in the FH SS systems bear information in their frequencies. Analogously to the DS CDMA case, the expansion of FSK signals should be combined with their demodulation. The demodulator/estimator for FSK signals also will be considered in the next chapters.

The results of this section will be used in Chapter 3 in the analysis of the optimal receivers of SS systems.

2.7 COMMENTS

In this chapter we have provided a review of basic concepts in SS theory. The characteristics of SS signals are very useful in the design of optimum modulation/demodulation and coding/decoding techniques for a variety of CDMA systems. In particular, the digital modulation methods introduced in this chapter are widely used in CDMA communication. The next chapter is concerned with optimal reception techniques for these signals and their performances in the AWGN channel.

Of particular importance in the design of CDMA systems are correlation and spectral characteristics of digitally modulated SS signals, which are presented in this chapter. There are a large number of references dealing with correlation and spectral characteristics of SS signals. As references, we should mention the pioneering book by Viterbi [47] and the textbook by Peterson, Ziemer, and Borth [34]. A tutorial treatment of PPH CDMA systems that were developed recently, is given in [41]. The text books by Lindell [28], Proakis [38], and Proakis and Salehi [37] provide comprehensive analysis and design of signals and digital communication systems.

PROBLEMS

2.1. The carrier spacing in the IS-95 standard is $W = 1.25$ MHz. The chip rate is $R_c = 1.2288 \cdot 10^6$ chips/s. Assuming that chips are rectangular pulses of duration $T_c = 1/R_c$, find which part of the pulse energy is located in the bandwidth $(-W/2, W/2)$.

2.2. Find the normalizing constants A_{dg} and γ' for the differentiated Gaussian pulse

$$h_{T_p}(t) = A_{dg} t \exp\left(-\frac{t^2}{4\gamma' T_p^2}\right)$$

if $\eta = 0.99$.

2.3. Calculate the two-sided power spectral density for the differentiated Gaussian pulse. What part of the total pulse energy is located in the frequency interval $\left(-1/T_p,\ 1/T_p\right)$?

2.4. Find the pulse $h_{T_p}(t)$ if its Fourier transform $H(f)$ is defined by

$$H(f) = \frac{1}{1 + (2\pi f \alpha)^2}$$

where $\alpha > 0$.

2.5. Find the Fourier transform of the pulses $h_{T_p}(t)$ if:

a) $h_{T_p}(t) = \delta(t)$

b) $h_{T_p}(t) = \begin{cases} \cos 2\pi f_c t, & 0 < t \le T \\ 0, & \text{otherwise} \end{cases}$

2.6. Prove Formula (2.63).

2.7. Let q be an integer, $i_n^{(k)}$ is uniformly distributed on the set $\{-(q-1)/2, \ldots, q-1/2\}$, $a_n^{(k)}$ is uniformly distributed on the set $\{-(Q-1)/2, \ldots, (Q-1)/2\}$. Show that the random variable $i_n^{(k)} + a_n^{(k)} q$ is uniformly distributed on the set $\{-(M-1)/2, \ -(M-3)/2, \ldots, (M-1)/2\}$, $M = qQ$.

2.8. Find the normalizing constants and calculate the two-sided power spectral density for the harmonic Gaussian pulse

$$h_{T_c}(t) = A_{h_g} \cos\frac{\pi t}{T_c} \exp\left(-\frac{t^2}{4\gamma T_c^2}\right), \quad -T_c/2 \le t \le T_c/2$$

2.9. The autocorrelation function of a white noise stochastic process is

$$R_s(\tau) = \tfrac{1}{2} N_0 \delta(\tau)$$

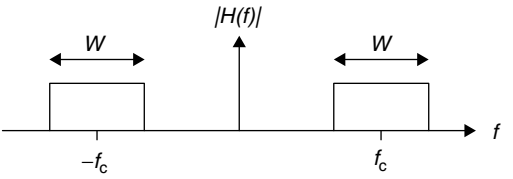

Problem 2.9. Bandpass filter.

a) Find the two-sided power spectral density of the process.

b) Suppose that the white noise stochastic process $s(t)$ is the input to a bandpass filter having the frequency response shown below. Find the filter output process.

2.10. Determine the autocorrelation function of the stochastic process

$$s(t) = \cos(2\pi f_c t + \varphi)$$

where f_c is the carrier frequency and φ is uniformly distributed on the interval $[0, 2\pi)$.

2.11. Consider the three waveforms $\tilde{s}_i(t)$, $i = 1, 2, 3$, shown below.

a) Are these waveforms orthogonal?

b) If

$$\tilde{s}(t) = \begin{cases} 2, & 0 \le t < 1, \\ -2, & 1 \le t < 3, \\ 2, & 3 \le t < 4 \end{cases}$$

can $\tilde{s}(t)$ be represented as a weighted linear combination of the $\tilde{s}_i(t)$ that follow?

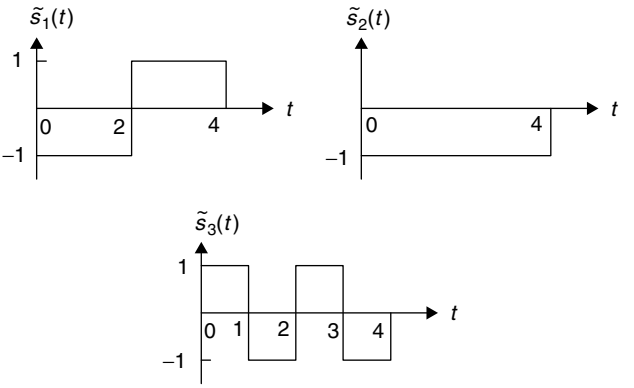

Problem 2.11.

2.12. Determine the correlation coefficients $\lambda_{ij} = \int_0^4 \tilde{s}_i(t)\tilde{s}_j(t)\,dt$, $i, j = 1, 2, 3, 4$, among the four waveforms shown below.

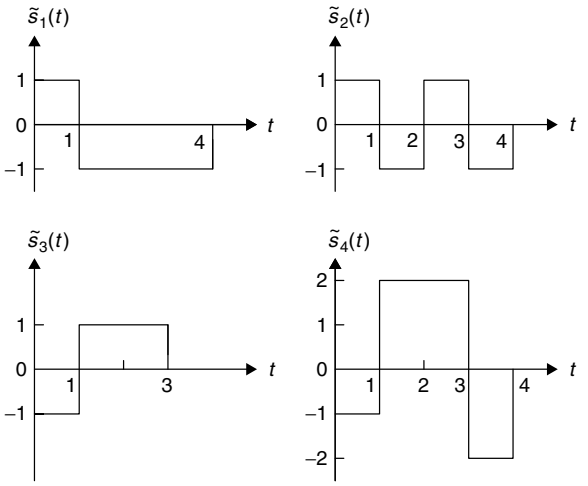

Problem 2.12.

2.13. Find the orthonormal basis for the four signals shown below.

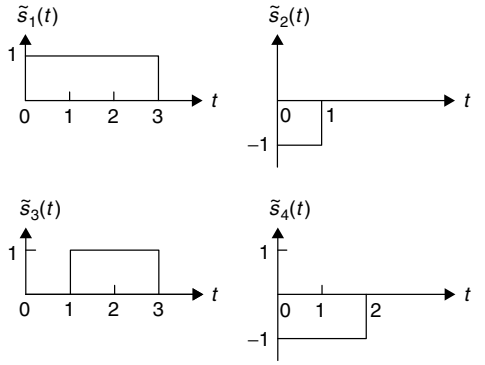

Problem 2.13.

2.14. Determine the power spectral density of the binary FSK signals in which the waveforms are

$$s(t) = \sum_{n=-\infty}^{\infty} h_{T_c}(t - nT_c)\cos 2\pi f_n t$$

where $h_{T_c}(t)$ is a unit amplitude rectangular pulse, f_n is $k/2T_c$ or $m/2T_c$, $k \neq m$, and m and k are arbitrary positive integers. Assume that the frequencies $k/2T_c$ and $m/2T_c$ are equiprobable. Sketch the spectrum.

2.15. Determine the power density spectrum of the FSK signal for which the signal waveforms are

$$\tilde{s}_n(t - nT_c) = h_{T_c}(t - nT_c) \cos \frac{2\pi i_n t}{T_c}, \quad i_n = 1, 2, \ldots, M$$

where $h_{T_c}(t)$ is a unit amplitude rectangular pulse. Assume that the waveforms are equiprobable.

2.16. Find the power spectral density of the signal

$$s(t) = \sum_{n=-\infty}^{\infty} u_n h_{T_c}(t - nT_c)$$

where $h_{T_c}(\cdot)$ is the Manchester pulse shown below and $\{u_n\}$ is a sequence of IID random variables, each taking values $+1$ and -1 with equal probability.

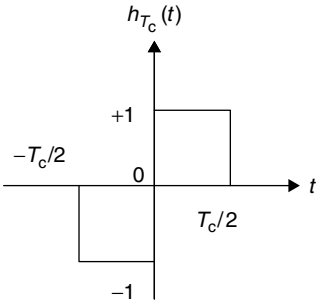

Problem 2.16.

2.17. Show that the autocorrelation function of the process (2.147) is given by Formula (2.143) and the two-sided power spectral density of the process is given by (2.144).

3

RECEPTION OF SPREAD SPECTRUM SIGNALS IN AWGN CHANNELS

In Chapter 2 we described the modulation processes in a spread spectrum communication system. An essential part of this system is the digital modulator. A digital modulator is a device for converting a sequence of symbols, whether precoded or not, into continuous-time signals suitable for transmission by the physical channel provided. In this chapter we consider the reception of SS signals, particularly the demodulation, which we started to study at the end of Chapter 2. Demodulation is the inverse process to modulation, and a demodulator is a device for processing a noisy, perhaps distorted, version of the transmitted signal and producing numerical outputs.

The demodulation process includes statistical detection of signals in noise. By "statistical detection" we mean the application of probability and statistical tools to design a receiver that can discriminate noise-corrupted signals from noise or that can distinguish between different signals in the presence of noise.

Our intent is to design the optimum receiver and to analyze it. This chapter is concerned with the design and performance characteristics of receivers for the AWGN channel. The design and performance of receivers for fading channels are treated in Chapter 5.

3.1 PROBLEM FORMULATION

In the next section we develop the basic ideas of the binary hypothesis testing theory. The classic application of this theory is synthesis and analysis of radar

Theory of Code Division Multiple Access Communication, by Kamil Sh. Zigangirov
ISBN 0-471-45712-4

systems. In a radar system we look at a particular range and azimuth and try to decide whether a target is present; hypothesis H_1 corresponds to the presence of a target, and H_0 corresponds to no target.

Acquiring synchronization and digital communication in CDMA system both involve testing binary hypotheses: whether the synchronization is achieved or not in the first case and whether $+1$ or -1 was transmitted in the second case. The model we consider assumes that the process $r(t)$ is observed in some time interval. It also assumes that the conditional probability distributions of the process $r(t)$ are known for the observations under the two hypotheses. In the case of the acquisition problem we denote these hypotheses H_1 (synchronization is achieved) and H_0 (synchronization is absent). In the case of binary digital data reception we denote the hypothesis that $+1$ was transmitted as H_1 and the hypothesis that -1 was transmitted as H_{-1}.

We consider the following model of the CDMA system. We assume that K active users simultaneously send digital information by using one of the modulation formats described in Chapter 2. The transmitted signals are $s^{(k)}(t)$, $k = 1, 2, \ldots, K$, and the received signal is

$$r(t) = \sum_{k=1}^{K} \sqrt{P^{(k)}} s^{(k)}(t - \delta^{(k)}) + \xi(t) \tag{3.1}$$

where $P^{(k)}$ is the power of the received signal from the kth user, $\xi(t)$ is AWGN of the two-sided power spectral density $N_0/2$, and $\delta^{(k)}$ is the kth user time offset. The time offset includes asynchronism between users, propagation delay, etc. We represent the received signal (3.1) as the sum of the desired (relative to the kth user) signal $\sqrt{P^{(k)}} s^{(k)}(t - \delta^{(k)})$ and the total noise including other-user interference components and additive noise. That is,

$$r(t) = \sqrt{P^{(k)}} s^{(k)}(t - \delta^{(k)}) + \xi^{(k)}(t) \tag{3.2}$$

where

$$\xi^{(k)}(t) = \sum_{k' \neq k} \sqrt{P^{(k')}} s^{(k')}(t - \delta^{(k')}) + \xi(t) \tag{3.3}$$

We suppose that each of the K active users uses the block transmission method; that is, the information sequence $\boldsymbol{u}$ is divided into blocks $\boldsymbol{u}_m = u_{mL}, u_{mL+1}, \ldots, u_{(m+1)L-1}$, $m = \ldots -1, 0, 1 \ldots$, of length L. Then a block $\boldsymbol{u}_m$ of L information symbols is encoded into a block $\boldsymbol{v}_m = v_{mN}, v_{mN+1}, \ldots v_{(m+1)N-1}$ of N code symbols. The code rate is $r = L/N$. In particular, in the repetition coding case r is $1/N$. Because the chip duration is T_c, the block transmission time T is NT_c. The spreading sequence directly modulates the data-modulated carrier (in the DS CDMA case), controls the sequence of the carrier frequencies (in the FH CDMA case), or controls the pulse position shift (in the PPH CDMA case).

In this chapter we will mainly study the reception problem when repetition coding is used. Chapter 4 is devoted to the decoding problem in the general

encoded transmission case. In Chapter 7 we study the acquisition problem. It is convenient to subdivide the receiver/acquisition process into two parts—the signal *demodulator* and the *decision making device*. The function of the demodulator is to convert the received signal into a sequence of N-dimensional vectors, corresponding to the transmitted codewords, and remodulate them with the spreading sequence. The output of the demodulator is a sequence of N-dimensional vectors $\boldsymbol{z}_m = z_{mN}, z_{mN+1}, \ldots, z_{(m+1)N-1}$, $m = \ldots -1, 0, 1, \ldots$. The function of the decision device of the receiver is to decide which codeword was transmitted. The function of the decision device of the acquisition receiver is to decide whether or not synchronization is achieved.

To simplify the notation, we will skip index m of the vector $\boldsymbol{z}_m$, denoted $\boldsymbol{z} = z_0, z_1, \ldots, z_{N-1}$. We will start with the analysis of two problems that we call the *simple reception problem* and the *simple acquisition problem*.

Simple Reception Problem

H_1: The components of the vector $\boldsymbol{z}$ are IID Gaussian random variables with a mean value $E(z_n) = \mu$, $\mu > 0$, and a variance $\text{var}(z_n) = \sigma^2$, $n = 0, 1, \ldots, N-1$. The probability density function for $\boldsymbol{z}$ is

$$p_1(\boldsymbol{z}) = \left(\frac{1}{\sqrt{2\pi\sigma^2}}\right)^N \exp\left[-\sum_{n=0}^{N-1}(z_n - \mu)^2/2\sigma^2\right] \tag{3.4}$$

H_{-1}: The components of $\boldsymbol{z}$ are IID Gaussian random variables with a mean value $E(z_n) = -\mu$, and a variance $\text{var}(z_n) = \sigma^2$, $n = 0, 1, \ldots, N-1$. The probability density function for $\boldsymbol{z}$ is

$$p_{-1}(\boldsymbol{z}) = \left(\frac{1}{\sqrt{2\pi\sigma^2}}\right)^N \exp\left[-\sum_{n=0}^{N-1}(z_n + \mu)^2/2\sigma^2\right] \tag{3.5}$$

Simple Acquisition Problem

H_1: The components of the vector $\boldsymbol{z}$ are IID Gaussian random variables with a mean value $E(z_n) = \mu$, $\mu > 0$, and a variance $\text{var}(z_n) = \sigma^2$, $n = 0, 1, \ldots, N-1$. The probability density function for $\boldsymbol{z}$ is defined by Formula (3.4).
H_0: The components of $\boldsymbol{z}$ are IID Gaussian random variables with zero mean and variance σ^2. The probability density function is

$$p_0(\boldsymbol{z}) = \left(\frac{1}{\sqrt{2\pi\sigma^2}}\right)^N \exp\left(-\sum_{n=0}^{N-1} z_n^2/2\sigma^2\right) \tag{3.6}$$

The simple reception problem originates in DS CDMA communication under the following assumptions. The system uses repetition coding and BPSK modulation. The receiver is coherent and perfectly synchronized with the received

signal. If symbol $+1$ was sent (hypothesis H_1) the expectation $E(z_n)$ is equal to $\sqrt{P^{(k)}}$, the square root of the power of the signal received from the desired user, and if symbol -1 was sent (hypothesis H_{-1}) $E(z_n)$ is equal to $-\sqrt{P^{(k)}}$. The variance $\text{var}(z_n)$ is determined by the background noise and the other-user and other-cell interference signals.

The simple acquisition problem arises from "genie-aided" acquisition in the DS CDMA system. We assume that the desired user sends a known periodic BPSK signal to the acquisition receiver. A kind genie helps the receiver by imparting the phase $\varphi^{(k)}$ of the received signal but does not inform it about the time offset shift $\delta^{(k)}$. The receiver searches serially through all potential time offset shifts $\delta^{(k)}$. If synchronization is not established (hypothesis H_0), $E(z_n) = 0$; otherwise, (hypothesis H_1) $E(z_n) \neq 0$. Analogously to the first problem, the variance $\text{var}(z_n)$ is in both cases determined by background noise and the other-user and other-cell interference signals.

The Neyman–Pearson criterion gives the optimal solution for these two problems.

3.2 NEYMAN–PEARSON HYPOTHESIS TESTING CONCEPT

In the binary hypothesis problem we know that either one or the other hypothesis is true. The probabilities of the decision errors depend on the decision criterion we select. For example, in the acquisition problem there is the probability to accept the hypothesis H_1 when H_0 is true and to accept the hypothesis H_0 when H_1 is true. The first probability P_F is called the *false alarm probability*. The second probability P_M is called the *probability of a miss*. The terminology is chosen from the radar problem in which the hypothesis H_1 corresponds to the presence of a target and the hypothesis H_0 corresponds to its absence. The probability $P_D = 1 - P_M$ is the probability of detection (i.e., we say that the target is present when it really is). In general, we should like to make P_F as small as possible and P_D as large as possible (P_M as small as possible). For most problems of practical importance these are conflicting objectives. An obvious criterion is to constrain one of the probabilities and maximize (or minimize) the other. *The Neyman–Pearson criterion maximizes P_D (or minimizes P_M) under the constraint $P_F \leq \alpha$, where α is a prechosen constant.*

The solution is obtained easily by using Lagrange multipliers. We construct the function Φ

$$\Phi = P_M + \lambda[P_F - \alpha] \tag{3.7}$$

or

$$\Phi = \int_{Z_0} p_1(z)\,dz + \lambda\left[\int_{Z_1} p_0(z)\,dz - \alpha\right] \tag{3.8}$$

Here the total observation space Z is divided into two parts, Z_0 and Z_1. Whenever an observation falls into Z_0 we say H_0; whenever an observation falls into Z_1

we say H_1. Clearly, if $P_F = \alpha$, then minimizing Φ minimizes P_M and

$$\Phi = \lambda(1 - \alpha) + \int_{Z_0} [p_1(z) - \lambda p_0(z)]\, dz \tag{3.9}$$

Now we show that the Neyman–Pearson criterion leads us to the *likelihood ratio test*

$$\Lambda(z) \stackrel{\text{def}}{=} \frac{p_1(z)}{p_0(z)} \underset{H_0}{\overset{H_1}{\gtrless}} \psi \tag{3.10}$$

where ψ is a numerical threshold that depends on the constraint on P_F. If the ratio exceeds ψ, the hypothesis H_1 is chosen, whereas if it does not, the hypothesis H_0 is chosen. In fact, for any positive λ the likelihood ratio test will minimize Φ. This follows directly because to minimize Φ we assign a point z to Z_0 only when the term in the bracket of Formula (3.9) is negative. This is equivalent to the test (3.10) with $\psi = \lambda$. To satisfy the constraint we choose λ such that $P_F = \alpha$.

It is more convenient to operate with the log-likelihood ratio $\ln \Lambda(z)$ rather than the likelihood ratio. Then the test reduces to

$$\ln \Lambda(z) \underset{H_0}{\overset{H_1}{\gtrless}} \ln \psi \stackrel{\text{def}}{=} \theta. \tag{3.11}$$

EXAMPLE 3.1

Construct the likelihood ratio test for the simple acquisition problem.

Solution

From Formulas (3.4), (3.6), and (3.10)–(3.11) we have

$$\ln \Lambda(z) = \frac{-\sum_{n=0}^{N-1}(z_n - \mu)^2 + \sum_{n=0}^{N-1} z_n^2}{2\sigma^2} \underset{H_0}{\overset{H_1}{\gtrless}} \theta$$

or

$$\frac{\mu}{\sigma^2} \sum_{n=0}^{N} z_n - N\frac{\mu^2}{2\sigma^2} \underset{H_0}{\overset{H_1}{\gtrless}} \theta$$

or

$$y \stackrel{\text{def}}{=} \frac{\mu}{\sigma^2} \sum_{n=0}^{N} z_n \underset{H_0}{\overset{H_1}{\gtrless}} \theta + N\frac{\mu^2}{2\sigma^2} \stackrel{\text{def}}{=} \theta' \tag{3.12}$$

where θ' is a new threshold.

The decision statistic y in Example 3.1 has the Gaussian distribution with expectation

$$E(y) = \begin{cases} 2N\rho_c, & \text{if } H_1 \text{ is true,} \\ 0, & \text{otherwise} \end{cases} \tag{3.13}$$

and with variance

$$\text{var}(y) = 2N\rho_c \tag{3.14}$$

in either case, where

$$\rho_c \stackrel{\text{def}}{=} \frac{\mu^2}{2\sigma^2} \tag{3.15}$$

The parameter ρ_c defines the SNR per sample (chip). The parameter $\rho_B \stackrel{\text{def}}{=} N\rho_c$ defines the SNR per block of N samples (chips). When the repetition code is used ρ_B is equal to the SNR per bit, ρ_b.

For the AWGN channel ρ_b coincides with the bit energy-to-noise density ratio E_b/I_0 that was introduced in Section 1.3. The ratio E_b/I_0 traditionally characterizes communication systems and, following the tradition, we will use this notation.

From Formulas (3.13) and (3.14) follows

$$P_D = \int_{\theta'}^{\infty} \frac{1}{\sqrt{4\pi\rho_b}} \exp\left[-\frac{(y-2\rho_b)^2}{4\rho_b}\right] dy = Q\left(\frac{\theta' - 2\rho_b}{\sqrt{2\rho_b}}\right) \tag{3.16}$$

$$P_F = \int_{\theta'}^{\infty} \frac{1}{\sqrt{4\pi\rho_b}} \exp\left(-\frac{y^2}{4\rho_b}\right) dy = Q\left(\frac{\theta'}{\sqrt{2\rho_b}}\right) \tag{3.17}$$

where the Q function is defined by (1.12).

From (3.16) and (3.17) it follows that P_D and P_F are functions of the threshold θ' and the SNR ρ_b. In Figure 3.1 we have plotted P_D versus P_F for various values of ρ_b, with θ' as the varying parameter. As we would expect, the performance increases monotonically with ρ_b. The result in Figure 3.1 is referred to as the *receiver operating characteristic (ROC)*. It completely describes the performance of the test as a function of the parameter of interest.

A special case that is important when we look at a binary digital communication system is the symmetrical case in which the probability to accept the hypothesis H_1 when H_{-1} is true is equal to the probability to accept H_{-1} when H_1 is true. This probability is called the *bit error probability*, $P_b = P_F = P_M$. For this special case the threshold ψ in Formula (3.10) equals 1.

EXAMPLE 3.2

Construct the symmetrical likelihood ratio test for the simple reception problem.

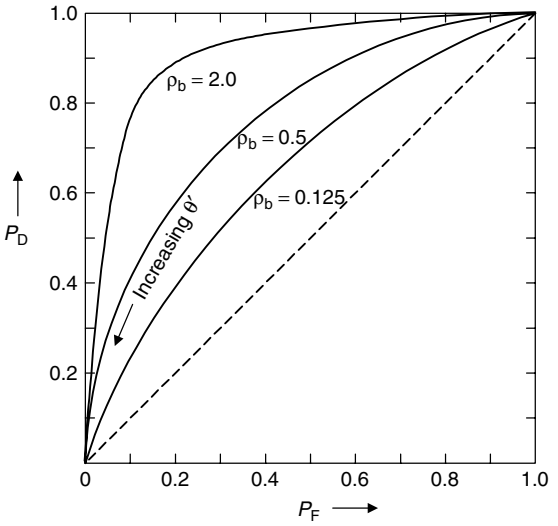

Figure 3.1. The receiver operating characteristic, simple acquisition problem.

Solution

From Formulas (3.4) and (3.5) and Formulas (3.10) and (3.11) we have

$$\ln \Lambda(z) = \frac{-\sum_{n=0}^{N-1}(z_n - \mu)^2 + \sum_{n=0}^{N-1}(z_n + \mu)^2}{2\sigma^2} \underset{H_{-1}}{\overset{H_1}{\gtrless}} 0$$

or

$$y \overset{\text{def}}{=} \frac{2\mu}{\sigma^2} \sum_{n=0}^{N-1} z_n \underset{H_{-1}}{\overset{H_1}{\gtrless}} 0 \tag{3.18}$$

The decision statistic y in Example 3.2 has a Gaussian distribution with expectation

$$E(y) = \begin{cases} 4\rho_b, & \text{if } H_1 \text{ is true,} \\ -4\rho_b, & \text{if } H_{-1} \text{ is true} \end{cases} \tag{3.19}$$

and variance

$$\text{var}(y) = 8\rho_b \tag{3.20}$$

in either case, where ρ_b is the SNR per bit. Then

$$P_F = P_M = \int_0^\infty \frac{1}{\sqrt{16\pi\rho_b}} \exp\left[-(y + 4\rho_b)^2/16\rho_b\right] dy = Q\left(\sqrt{2\rho_b}\right) \tag{3.21}$$

where the Q function is defined by (1.12).

It is obvious that we can also obtain P_F/P_M from the ROC. However, it is generally easier to calculate P_F/P_M directly.

EXAMPLE 3.3

Several different situations, for example, communication over a Rayleigh channel (Chapter 5), lead to the mathematical model of interest in this example. The observation vector $\mathbf{z}$ *is a set of N IID zero-mean Gaussian variables. Under* H_1 *each* z_n *has a variance* σ_1^2*, and under* H_0 *each* z_n*,* $n = 0, 1, \ldots, N-1$*, has a variance* σ_0^2*,* $\sigma_1^2 > \sigma_0^2$*. Construct the likelihood ratio test for this example.*

Solution

Because the variables z_n *are zero-mean IID Gaussian random variables,*

$$p_1(\mathbf{z}) = \left(\frac{1}{\sqrt{2\pi\sigma_1^2}}\right)^N \exp\left(-\sum_{n=0}^{N-1} z_n^2/2\sigma_1^2\right) \tag{3.22}$$

$$p_0(\mathbf{z}) = \left(\frac{1}{\sqrt{2\pi\sigma_0^2}}\right)^N \exp\left(-\sum_{n=0}^{N-1} z_n^2/2\sigma_0^2\right) \tag{3.23}$$

Substituting (3.22) and (3.23) into (3.11), we have

$$\frac{1}{2}\left(\frac{1}{\sigma_0^2} - \frac{1}{\sigma_1^2}\right)\sum_{n=0}^{N-1} z_n^2 + N \ln\frac{\sigma_0}{\sigma_1} \underset{H_0}{\overset{H_1}{\gtrless}} \theta \tag{3.24}$$

or

$$y \overset{\text{def}}{=} \sum_{n=0}^{N-1} z_n^2 \underset{H_0}{\overset{H_1}{\gtrless}} \frac{2\sigma_0^2\sigma_1^2}{\sigma_1^2 - \sigma_0^2}\left(\theta - N \ln\frac{\sigma_0}{\sigma_1}\right) \overset{\text{def}}{=} \theta' \tag{3.25}$$

The decision statistic y in Example 3.3 is said to be a χ^2*-random variable with N degrees of freedom*. Its probability density function is [32]

$$f_{\sigma^2}(y) = \frac{1}{2^{N/2}\sigma^N \Gamma\left(\frac{N}{2}\right)} y^{\frac{N}{2}-1} \exp\left(-\frac{y}{2\sigma^2}\right), \; y \geq 0 \tag{3.26}$$

where σ^2 is the variance of z_n and $\Gamma(\cdot)$ is the gamma function, evaluated for an integer x by

$$\Gamma(x) = (x-1)! \tag{3.27}$$

or by

$$\Gamma\left(x+\frac{1}{2}\right)=\frac{1\cdot 3\cdot 5\cdots(2x-1)}{2^x}\sqrt{\pi} \tag{3.28}$$

Under H_1 the probability density function of y is $f_{\sigma_1^2}(y)$, and under H_0 the probability density function of y is $f_{\sigma_0^2}(y)$. Then

$$P_{\mathrm{D}}=1-P_{\mathrm{M}}=\int_{\theta'}^{\infty} f_{\sigma_1^2}(y)\,\mathrm{d}y \tag{3.29}$$

$$P_{\mathrm{F}}=\int_{\theta'}^{\infty} f_{\sigma_0^2}(y)\,\mathrm{d}y \tag{3.30}$$

The receiver operating characteristic $P_{\mathrm{D}}=P_{\mathrm{D}}(P_{\mathrm{F}})$ calculation for arbitrary N is somewhat tedious. So we consider a simple case when $N=2$ that appears frequently in practice. From (3.26)–(3.30) we have

$$P_{\mathrm{D}}=\int_{\theta'}^{\infty}\frac{1}{2\sigma_1^2}\exp\left(-\frac{y}{2\sigma_1^2}\right)\mathrm{d}y=\exp\left(-\frac{\theta'}{2\sigma_1^2}\right) \tag{3.31}$$

$$P_{\mathrm{F}}=\int_{\theta'}^{\infty}\frac{1}{2\sigma_0^2}\exp\left(-\frac{y}{2\sigma_0^2}\right)\mathrm{d}y=\exp\left(-\frac{\theta'}{2\sigma_0^2}\right) \tag{3.32}$$

To construct the ROC we can combine (3.31) and (3.32) to eliminate the threshold θ'. This gives

$$P_{\mathrm{D}}=(P_{\mathrm{F}})^{\sigma_0^2/\sigma_1^2} \tag{3.33}$$

The random variable $x=\sqrt{y}$, where y is a χ^2-random variable with 2 degrees of freedom, is called the *Rayleigh random variable*. The Rayleigh probability density function is

$$f_{\sigma^2}(x)=\frac{x}{\sigma^2}\exp\left(-\frac{x^2}{2\sigma^2}\right),\quad x\geq 0. \tag{3.34}$$

Suppose now that under hypothesis H_1 the probability density function depends on an unknown parameter. Particularly, we consider the case when we have two observable vectors (in-phase and quadrature outputs),

$$\boldsymbol{z}_{\mathrm{I}}=(z_{\mathrm{I}0},z_{\mathrm{I}1},\ldots,z_{\mathrm{I}N-1})\text{ and }\boldsymbol{z}_{\mathrm{Q}}=(\boldsymbol{z}_{\mathrm{Q}0},z_{\mathrm{Q}1},\ldots,z_{\mathrm{Q}N-1})$$

where

$$E(z_{\mathrm{I}n})=\mu\cos\varphi\qquad E(z_{\mathrm{Q}n})=\mu\sin\varphi$$

and

$$\mathrm{var}(z_{\mathrm{I}n})=\mathrm{var}(z_{\mathrm{Q}n})=\sigma^2,\ n=0,1,\ldots N-1$$

Here φ can be interpreted as the phase of the received signal, which according to our assumptions is not available to the receiver. We model the variable φ as uniformly distributed on $[0, 2\pi)$, which, in the absence of prior information, is certainly a reasonable assumption. Assuming independent and Gaussian distributed components, we get that under H_1 the conditional probability density function of $(z_{\mathrm{I}}, z_{\mathrm{Q}})$ given φ satisfies the formula

$$p_1(z_{\mathrm{I}}, z_{\mathrm{Q}}|\varphi) = \left(\frac{1}{2\sigma^2}\right)^N \exp\left\{-\sum_{n=0}^{N-1}(z_{\mathrm{I}n} - \mu\cos\varphi)^2/2\sigma^2\right\} \times \exp\left\{-\sum_{n=0}^{N-1}(z_{\mathrm{Q}n} - \mu\sin\varphi)^2/2\sigma^2\right\} \tag{3.35}$$

Under hypothesis H_0 the vectors z_{I} and z_{Q} are independent sets of IID zero-mean Gaussian random variables,

$$p_0(z_{\mathrm{I}}, z_{\mathrm{Q}}) = \left(\frac{1}{2\pi\sigma^2}\right)^N \exp\left[-\left(\sum_{n=0}^{N-1} z_{\mathrm{I}n}^2 + \sum_{n=0}^{N-1} z_{\mathrm{Q}N}^2\right)/2\sigma^2\right] \tag{3.36}$$

The two-hypothesis testing problem when the phase of the received signal is not available to the receiver is called the *problem of noncoherent detection*.

Because the ratio of the two probability density functions depends only on the sums

$$x_{\mathrm{I}} = \sum_{n=0}^{N-1} z_{\mathrm{I}n}, \quad x_{\mathrm{Q}} = \sum_{n=0}^{N-1} z_{\mathrm{Q}n} \tag{3.37}$$

we may choose them as decision statistics. The means and variances of x_{I} and x_{Q} are

$$E(x_{\mathrm{I}}) = \begin{cases} N\mu\cos\varphi, & \text{if } H_1 \text{ is true,} \\ 0, & \text{if } H_0 \text{ is true} \end{cases} \tag{3.38}$$

$$E(x_{\mathrm{Q}}) = \begin{cases} N\mu\sin\varphi, & \text{if } H_1 \text{ is true,} \\ 0, & \text{if } H_0 \text{ is true} \end{cases} \tag{3.39}$$

$$\mathrm{var}(x_{\mathrm{I}}) = \mathrm{var}(x_{\mathrm{Q}}) = N\sigma^2, \text{ in either case} \tag{3.40}$$

We may express the probability density functions of x_{I} and x_{Q} as

$$p_1(x_{\mathrm{I}}, x_{\mathrm{Q}}|\varphi) = \frac{1}{2\pi N\sigma^2}\exp\{-[(x_{\mathrm{I}} - N\mu\cos\varphi)^2 + (x_{\mathrm{Q}} - N\mu\sin\varphi)^2]/2N\sigma^2\} \tag{3.41}$$

$$p_0(x_{\mathrm{I}}, x_{\mathrm{Q}}) = \frac{1}{2\pi N\sigma^2}\exp\{-(x_{\mathrm{I}}^2 + x_{\mathrm{Q}}^2)/2N\sigma^2\} \tag{3.42}$$

Because the phase φ is a uniform random variable, we may obtain the unconditional probability density function

$$\begin{aligned} p_1(x_\mathrm{I}, x_\mathrm{Q}) &= \int_0^{2\pi} p_1(x_\mathrm{I}, x_\mathrm{Q}|\varphi)\,\mathrm{d}\varphi/2\pi \\ &= \frac{1}{2\pi N\sigma^2}\exp[-(x_\mathrm{I}^2 + x_\mathrm{Q}^2 + N^2\mu^2)/2N\sigma^2] \\ &\quad \times \int_0^{2\pi} \exp[\mu(x_\mathrm{I}\cos\varphi + x_\mathrm{Q}\sin\varphi)/\sigma^2]\frac{\mathrm{d}\varphi}{2\pi} \\ &= \frac{1}{2\pi N\sigma^2}\exp[-(x_\mathrm{I}^2 + x_\mathrm{Q}^2 + N^2\mu^2)/2N\sigma^2] \times I_0\left(\frac{\mu\sqrt{x_\mathrm{I}^2 + x_\mathrm{Q}^2}}{\sigma^2}\right) \\ &= \frac{1}{2\pi N\sigma^2}\exp\left(-\frac{y + N^2\mu^2}{2N\sigma^2}\right) I_0\left(\frac{\mu\sqrt{y}}{\sigma^2}\right) \end{aligned} \tag{3.43}$$

where

$$y = x_\mathrm{I}^2 + x_\mathrm{Q}^2 \tag{3.44}$$

and

$$I_0(v) \stackrel{\mathrm{def}}{=} \int_0^{2\pi} \exp(v\cos\varphi)\,\mathrm{d}\varphi/2\pi \tag{3.45}$$

is the *zeroth-order modified Bessel function of the first kind.*

EXAMPLE 3.4

Construct the likelihood ratio test for the problem of noncoherent detection.

Solution

From Formulas (3.11), (3.43), and (3.42) follows

$$\ln\Lambda(z_\mathrm{I}, z_\mathrm{Q}) = \ln I_0\left(\frac{\mu\sqrt{y}}{\sigma^2}\right) - \frac{N\mu^2}{2\sigma^2} \underset{H_0}{\overset{H_1}{\gtrless}} \theta \tag{3.46}$$

However, because $I_0(v)$ is a monotone-increasing function of its argument, the test may be simplified to

$$y \underset{H_0}{\overset{H_1}{\gtrless}} \hat{\theta}\,, \tag{3.47}$$

where $\hat{\theta}$ is obtained from the Neyman–Pearson constraint that the false alarm probability will be kept at the value P_F.

Under H_0 the decision statistic y has *central* χ^2*-distribution* with two degrees of freedom. The probability density function is [compare with (3.26)]

$$f_{N\sigma^2}(y) = \frac{1}{2N\sigma^2} \exp(-y/2N\sigma^2) \tag{3.48}$$

In the case of H_1, the random variable y is the sum of the squares of two independent Gaussian variables with variances $N\sigma^2$ and means $N\mu \cos\varphi$ and $N\mu \sin\varphi$. It has *(noncentral)* χ^2*-distribution* with two degrees of freedom, whose two-parametric probability density function is given by [32]

$$f_{N\mu,N\sigma^2}(y) = \frac{1}{2N\sigma^2} \exp[-(y + N^2\mu^2)/2N\sigma^2] I_0\left(\frac{\mu\sqrt{y}}{\sigma^2}\right), \quad y \geq 0 \tag{3.49}$$

The random variable $x = \sqrt{y}$ is called a *Rician random variable*. Its probability density function is

$$f_{N\mu,N\sigma^2}(x) = \frac{x}{N\sigma^2} \exp[-(x^2 + N^2\mu^2)/2N\sigma^2] I_0\left(\frac{\mu x}{\sigma^2}\right), \quad x \geq 0 \tag{3.50}$$

From the probability density functions (3.48) and (3.49), the false alarm probability and the probability of detection are obtained as

$$P_{\mathrm{F}} = \int_{\theta'}^{\infty} \frac{1}{2N\sigma^2} \exp(-y/2N\sigma^2)\, \mathrm{d}y = \exp(-\theta'/2N\sigma^2) \tag{3.51}$$

$$P_{\mathrm{D}} = \int_{\theta'}^{\infty} \frac{1}{2N\sigma^2} \exp[-(y + N^2\mu^2)/2N\sigma^2] I_0\left(\frac{\mu\sqrt{y}}{\sigma^2}\right) \mathrm{d}y \tag{3.52}$$

or

$$P_{\mathrm{D}} = \int_{-\ln P_{\mathrm{F}}}^{\infty} \exp(-z - \rho_{\mathrm{b}}) I_0(2\sqrt{\rho_{\mathrm{b}} z})\, \mathrm{d}z \tag{3.53}$$

where $\rho_{\mathrm{b}} = N\mu^2/2\sigma^2$ is the SNR per bit. The noncoherent detection operating characteristic is presented in Figure 3.2.

Consider now a more complicated problem. Suppose that we make N pairs of independent observations

$$(z_{\mathrm{I}0}, z_{\mathrm{Q}0}), (z_{\mathrm{I}1}, z_{\mathrm{Q}1}), \ldots, (z_{\mathrm{I}N-1}, z_{\mathrm{Q}N-1})$$

where $z_{\mathrm{I}n}, z_{\mathrm{Q}n}$, $n = 0, 1, \ldots, N-1$, are IID Gaussian random variables with variance σ^2. Under H_0

$$E(z_{\mathrm{I}n}) = E(z_{\mathrm{Q}n}) = 0, \quad n = 0, 1, \ldots, N-1$$

and under H_1

$$E(z_{\mathrm{I}n}) = \mu \cos\varphi_n,$$

$$E(z_{\mathrm{Q}n}) = \mu \sin\varphi_n, \quad n = 0, 1, \ldots, N-1$$

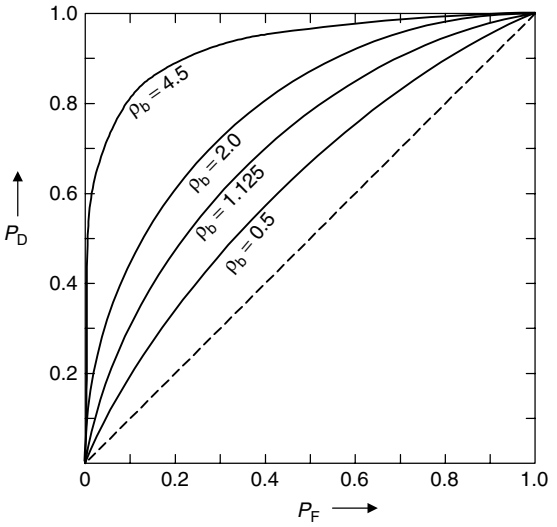

Figure 3.2. The noncoherent detector operating characteristic.

where $\mu > 0$ and φ_n are IID random variables uniformly distributed on $[0, 2\pi)$. This is a typical situation if the phase of the received signal is not only unknown, but also unstable. Then, analogously to (3.43), we have under H_1

$$p_1(z_{In}, z_{Qn}) = \frac{1}{2\pi\sigma^2} \exp\left[-(z_{In}^2 + z_{Qn}^2 + \mu^2)/2\sigma^2\right] I_0\left(\frac{\mu\sqrt{z_{In}^2 + z_{Qn}^2}}{\sigma^2}\right), \quad (3.54)$$

$$n = 0, 1, \ldots, N-1$$

and, analogously to (3.36), we have under H_0

$$p_0(z_{In}, z_{Qn}) = \frac{1}{2\pi\sigma^2} \exp[-(z_{In}^2 + z_{Qn}^2)/2\sigma^2], n = 0, 1, \ldots, N-1 \quad (3.55)$$

EXAMPLE 3.5

Construct the likelihood ratio test for the case when the probability density functions of the independent pairs of the observations are defined by Formulas (3.54) and (3.55) under hypotheses H_1 and H_0, respectively.

Solution

Because z_{In}, z_{Qn}, $n = 0, 1, \ldots, N-1$, are independent, it follows from (3.11), (3.54), and (3.55) that

$$\ln \Lambda(\mathbf{z}_I, \mathbf{z}_Q) = \ln \prod_{n=0}^{N-1} \frac{p_1(z_{In}, z_{Qn})}{p_0(z_{In}, z_{Qn})}$$

$$= \sum_{n=0}^{N-1} \left[\ln\ I_0\left(\frac{\mu\sqrt{z_{In}^2 + z_{Qn}^2}}{\sigma^2} \right) - \frac{\mu^2}{2\sigma^2} \right] \underset{H_0}{\overset{H_1}{\gtrless}} \theta \tag{3.56}$$

For small x the function $\ln I_0(x)$ can be approximated by $x^2/4$. In fact,

$$\begin{aligned} \ln\ I_0(x) &= \ln\left[\int_0^{2\pi} \exp(x \cdot \cos\varphi)\, \mathrm{d}\varphi/2\pi \right] \\ &\approx \ln\left[\int_0^{2\pi} \left[1 + x\cos\varphi + \frac{x^2\cos^2\varphi}{2} \right] \mathrm{d}\varphi \right] \\ &= \ln\left(1 + \frac{x^2}{4} \right) \approx \frac{x^2}{4} \end{aligned} \tag{3.57}$$

Then the likelihood ratio test (3.56) is reduced to

$$\frac{\mu^2}{4\sigma^2} \sum_{n=0}^{N-1} (z_{In}^2 + z_{Qn}^2) - \frac{N\mu^2}{2\sigma^2} \underset{H_0}{\overset{H_1}{\gtrless}} \theta \tag{3.58}$$

or

$$y \overset{\text{def}}{=} \sum_{n=0}^{N-1} (z_{In}^2 + z_{Qn}^2) \underset{H_0}{\overset{H_1}{\gtrless}} \frac{4\theta\sigma^2}{\mu^2} + 2N \overset{\text{def}}{=} \theta' \tag{3.59}$$

The statistic y is the sum of the squares of $2N$ IID Gaussian random variables. Under H_0 it has a central χ^2-distribution with $2N$ degrees of freedom. Then [compare with (3.26)]

$$p_0(y) = f_{\sigma^2}(y) = \frac{1}{2^N\sigma^{2N}(N-1)!}\ y^{N-1} \exp\left(-\frac{y}{2\sigma^2} \right),\ y \geq 0 \tag{3.60}$$

Under H_1 the statistic y has a noncentral χ^2-distribution with $2N$ degrees of freedom [38, 57],

$$\begin{aligned} p_1(y) = f_{\mu,\sigma^2}(y) &\overset{\text{def}}{=} \frac{1}{2\sigma^2} \left(\frac{y}{N\mu^2} \right)^{\frac{N-1}{2}} \exp\left[-(y + N\mu^2)/2\sigma^2 \right] \\ &\times I_{N-1}\left(\frac{\sqrt{N\mu^2 y}}{\sigma^2} \right),\ y \geq 0 \end{aligned} \tag{3.61}$$

where $I_{N-1}(\cdot)$ is the $(N-1)$*th-order modified Bessel function of the first kind*. The false alarm and the detection probabilities are

$$\begin{aligned} P_{\mathrm{F}} &= \int_{\theta'}^{\infty} p_0(y)\,\mathrm{d}y = \int_{\theta'}^{\infty} \frac{y^{N-1}}{2^N\sigma^{2N}(N-1)!}\,\exp\left(-\frac{y}{2\sigma^2}\right)\mathrm{d}y \\ &= \int_{\theta'/\sigma^2}^{\infty} \frac{x^{N-1}}{2^N(N-1)!}\,\exp\left(-\frac{x}{2}\right)\mathrm{d}x \\ &= \exp\left(-\frac{\theta'}{2\sigma^2}\right)\sum_{n=0}^{N-1}\frac{\theta'^n}{2^n\sigma^{2n}n!} \end{aligned} \tag{3.62}$$

$$\begin{aligned} P_{\mathrm{D}} &= \int_{\theta'}^{\infty} p_1(y)\,\mathrm{d}y \\ &= \int_{\theta'}^{\infty} \frac{1}{2\sigma^2}\left(\frac{y}{N\mu^2}\right)^{\frac{N-1}{2}}\exp[-(y+N\mu^2)/2\sigma^2]I_{N-1}\left(\frac{\sqrt{N\mu^2 y}}{\sigma^2}\right)\mathrm{d}y \\ &= \int_{\frac{\theta'}{2\sigma^2}}^{\infty}\left(\frac{x}{\rho_{\mathrm{b}}}\right)^{\frac{N-1}{2}}\exp\left(-x-\rho_{\mathrm{b}}\right)I_{N-1}(2\sqrt{\rho_{\mathrm{b}}x})\,\mathrm{d}x \end{aligned} \tag{3.63}$$

The latter integral is the Nth-order Marcum Q function [47].

In the following sections we will use results of this section for analysis of the receivers. In this chapter, we suppose that transmission is over the AWGN channel. The application of binary hypothesis testing theory to communication over fading channels is considered in Chapter 5. In Chapter 7 we apply the results of this section to the analysis of the acquisition receivers.

3.3 COHERENT RECEPTION OF DS CDMA SIGNALS (UPLINK TRANSMISSION)

Consider transmission over the AWGN channel. As a first application of the likelihood ratio test, let us analyze the BPSK direct-sequence spread spectrum receiver given in Figure 3.3. This is the coherent receiver of both uplink and downlink transmitted signals in a DS CDMA system. We suppose that the system uses a rate $1/N$ repetition code and that the receiver is perfectly synchronized with the transmitter; that is, the receiver knows exactly the phase $\varphi^{(k)}$ of the received signal and time offset $\delta^{(k)}$, $\hat{\varphi}^{(k)} = \varphi^{(k)}$, $\hat{\delta}^{(k)} = \delta^{(k)}$. To avoid cumbersome notation we introduce the kth receiver's clock time $t^{(k)} \stackrel{\text{def}}{=} t - \delta^{(k)}$. As we mentioned in Section 3.1 we only consider the reception of the 0th block.

Let us first study the uplink transmission. Consider first the case where all K users are active all the time. The received signal at the input of the kth user

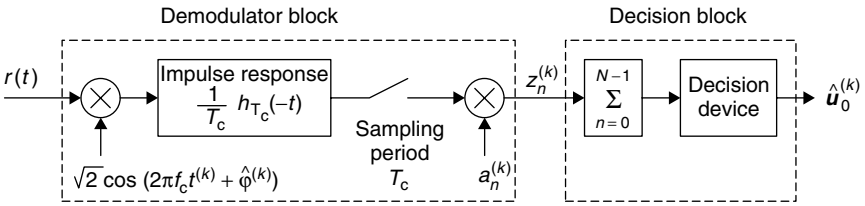

Figure 3.3. BPSK direct-sequence SS receiver for the kth user.

receiver is [compare with Formulas (2.92) and (3.1)]

$$r(t) = \sqrt{2P^{(k)}} \sum_{n=-\infty}^{\infty} v_n^{(k)} a_n^{(k)} h_{T_c}(t^{(k)} - nT_c) \cos(2\pi f_c t^{(k)} + \varphi^{(k)}) + \xi^{(k)}(t),$$
$$k = 1, 2, \ldots, K \tag{3.64}$$

where

$$\xi^{(k)}(t) = \sum_{k' \neq k} \sqrt{2P^{(k')}} \sum_{n=-\infty}^{\infty} v_n^{(k')} a_n^{(k')} h(t^{(k')} - nT_c) \cos(2\pi f_c t^{(k')} + \varphi^{(k')}) + \xi(t)$$

is the total noise. Here $P^{(k)}$ is the power of the received signal from the kth user and $\varphi^{(k)}$ is the phase of the received signal. The noise process $\xi(t)$ includes AWGN with two-sided power spectral density $N_0/2$ and the other-cell interference noise of the two-sided power spectral density $N_{oc}/2 \stackrel{\text{def}}{=} P_{oc} T_c$, where P_{oc} is the power of the other-cell interference noise.

The bandpass signal at the input of the matched filter is

$$\tilde{r}^{(k)}(t) = \sqrt{P^{(k)}} \sum_{n=-\infty}^{\infty} v_n^{(k)} a_n^{(k)} h_{T_c}(t^{(k)} - nT_c) + \tilde{\xi}^{(k)}(t) \tag{3.65}$$

where $\tilde{\xi}^{(k)}(t)$ is a modified noise. The output of the matched filter at time $t^{(k)} = nT_c$ is the sum of five terms [compare with (2.164)]

$$\sqrt{P^{(k)}} v_n^{(k)} a_n^{(k)} + \sqrt{P^{(k)}} \sum_{n' \neq n} v_{n'}^{(k)} a_{n'}^{(k)} I_{nn'} + \tilde{\xi}_n^{(k)} + \hat{\xi}_n^{(k)} + \check{\xi}_n^{(k)} \tag{3.66}$$

The first term is the desired component due to the signal received from the kth user. The other four terms are noise components. The second term is the sum of the interchip interference components. It is a zero-mean random variable with variance $P^{(k)} \sum_{n' \neq n} I_{nn'}^2$, where $I_{nn'}$ is defined by Formula (2.157). If the pulses $h_{T_p}(t)$ are orthogonal, this term vanishes. The third term is the sum of the other-user interference components. We consider this term below. The fourth

component, $\hat{\xi}_n^{(k)}$, is due to the background noise. It is a zero-mean Gaussian random variable with variance $N_0/2T_c$ (see Example 2.15). If the pulses $h_{T_c}(t - nT_c)$, $n = \ldots -1, 0, 1, \ldots$, are not orthogonal, then the $\{\hat{\xi}_n^{(k)}\}$ are dependent and

$$\operatorname{cov}(\hat{\xi}_n^{(k)}, \hat{\xi}_{n'}^{(k)}) = \frac{N_0}{2T_c} I_{nn'} \tag{3.67}$$

The fifth term, $\check{\xi}_n^{(k)}$, is due to the other-cell interference. It can be considered to be a zero-mean Gaussian random variable with variance $N_{oc}/2T_c = P_{oc}$. Analogously to (3.67) we have

$$\operatorname{cov}(\check{\xi}_n^{(k)}, \check{\xi}_{n'}^{(k)}) = \frac{N_{oc}}{2T_c} I_{nn'}$$

As we know, for orthogonal pulses $I_{nn'} = 0$, $n' \neq n$, and $\hat{\xi}_n^{(k)}$ (correspondingly $\check{\xi}_n^{(k)}$) are independent random variables.

The other-user interference component $\tilde{\xi}_n^{(k)}$ is a sum of $(K-1)$ terms $\tilde{\xi}_n^{(k,k')}$, $k' \neq k$. Here $\tilde{\xi}_n^{(k,k')}$ is the response of the matched filter at time $t^{(k)} = nT_c$ to the received signal from the k'th user. Considering this signal as a random process on the input of the filter, we can calculate the expectation and the variance of the corresponding interference component. Because the expectation of the input process is zero, the expectation of the output process is also zero. The variance is [compare with Formula (2.182)]

$$\operatorname{var}(\tilde{\xi}_n^{(k,k')}) = R_z(0) = \frac{P^{(k')}}{2T_c^3} \int_{-\infty}^{\infty} |H(f)|^4 \, \mathrm{d}f = \frac{P^{(k')}}{2T_c} \int_{-\infty}^{\infty} R_s^2(\tau) \, \mathrm{d}\tau \tag{3.68}$$

where $H(f)$ is the Fourier transform of $h_{T_c}(t)$, $R_z(\tau)$ is the autocorrelation function of the process at the output of the filter, and $R_s(\tau)$ is the autocorrelation function of the process at the input of the filter. From (3.68) and the equation

$$\operatorname{var}(\tilde{\xi}_n^{(k)}) = \sum_{k' \neq k} \operatorname{var}(\tilde{\xi}_n^{(k,k')})$$

we get

$$\operatorname{var}(\tilde{\xi}_n^{(k)}) = \frac{1}{2T_c^3} \sum_{k' \neq k} P^{(k')} \int_{-\infty}^{\infty} |H(f)|^4 \, \mathrm{d}f = \frac{1}{2T_c} \sum_{k' \neq k} P^{(k')} \int_{-\infty}^{\infty} R_s^2(\tau) \, \mathrm{d}\tau \tag{3.69}$$

For the repetition code $v_n^{(k)} = u_0^{(k)}$, $n = 0, 1, \ldots, N-1$. Thus, after despreading, we have at the input of the summation the sequence $\{z_n^{(k)}\}$, where

$$z_n^{(k)} = \sqrt{P^{(k)}} u_0^{(k)} + \sqrt{P^{(k)}} \sum_{n' \neq n} v_{n'}^{(k)} a_{n'}^{(k)} a_n^{(k)} I_{nn'} + \tilde{\xi}_n^{(k)} a_n^{(k)} + \hat{\xi}_n^{(k)} a_n^{(k)} + \check{\xi}_n^{(k)} a_n^{(k)},$$

$$n = 0, 1, \ldots, N-1 \tag{3.70}$$

Because $a_n^{(k)} = \pm 1$, multiplication by $a_n^{(k)}$ does not change the statistical behavior of the last four terms. Therefore, we will not distinguish the noise components in Formula (3.70) from the corresponding noise components in Formula (3.66).

On the input of the decision device we have the statistic $y^{(k)} = \sum_{n=0}^{N-1} z_n^{(k)}$, and the receiver must decide whether $+1$ or -1 was transmitted (accept hypothesis H_1 or H_{-1}, respectively).

Assuming that all signals have constant power throughout the transmission period and that the number of users K is large, we get that the random variables are approximately Gaussian and independent with the following expectation and variance:

$$E(z_n^{(k)}) = \begin{cases} \mu \stackrel{\text{def}}{=} \sqrt{P^{(k)}}, & \text{if } H_1 \text{ is true,} \\ -\mu, & \text{if } H_{-1} \text{ is true} \end{cases} \tag{3.71}$$

$$\begin{aligned} \sigma^2 &\stackrel{\text{def}}{=} \operatorname{var}(z_n^{(k)}) \\ &= P^{(k)} \sum_{n' \neq n} I_{nn'}^2 + \frac{1}{2T_c^3} \sum_{k' \neq k} P^{(k')} \int_{-\infty}^{\infty} |H(f)|^4 \, \mathrm{d}f + \frac{N_0}{2T_c} + \frac{N_{oc}}{2T_c} \stackrel{\text{def}}{=} \frac{I_0}{2T_c} \end{aligned} \tag{3.72}$$

We recall that the SNR per chip ρ_c was defined in Section 3.2 as equal to $\mu^2/2\sigma^2 = P^{(k)}T_c/I_0$. The SNR per block ρ_B, which in the case of the repetition code coincides with the SNR per bit $\rho_b = E_b/I_0$, is equal to $N\rho_c$.

The application of the symmetrical likelihood ratio test of Example 3.2 gives the following decision rule for the transmitted information symbol u_0:

$$y^{(k)} \underset{H_{-1}}{\overset{H_1}{\gtrless}} 0 \tag{3.73}$$

From Formulas (3.21) and (3.73) it follows that the bit error probability is given by

$$P_b = Q(\sqrt{2N\rho_c}) = Q\left(\sqrt{\frac{2E_b}{I_0}}\right) \tag{3.74}$$

where

$$\begin{aligned} \frac{E_b}{I_0} &= \frac{\mu^2}{2\sigma^2} N = \frac{P^{(k)}T_c N}{I_0} \\ &= \frac{P^{(k)}N}{2P^{(k)} \sum_{n' \neq n} I_{nn'}^2 + \sum_{k' \neq k} P^{(k')} \displaystyle\int_{-\infty}^{\infty} |H(f)|^4 \, \mathrm{d}f / T_c^3 + N_0/T_c + N_{oc}/T_c} \end{aligned} \tag{3.75}$$

Equation (3.74) is the classic expression for the bit error probability of coherent BPSK reception of an uncoded information bit transmitted over an AWGN channel with two-sided power spectral density $I_0/2$. It coincides with the expression for the bit error probability in the case when the repetition code is used.

We have considered the case when each of the $(K-1)$ other users continuously transmits a signal to the base station. In the case of perfect power control, $P^{(k)} = P$, $k = 1, 2, \ldots, K$. Assume sectored antennas and voice activity monitoring to reduce the other-user interference by a factor $1/\gamma_v\gamma_a$ (here γ_v is voice activity gain and γ_a is antenna gain). Then the second term in the denominator of the right-hand side of Formula (3.75) is

$$\sum_{k' \neq k} P^{(k')} \int_{-\infty}^{\infty} |H(f)|^4 \, \mathrm{d}f/\gamma_v\gamma_a T_c^3 = (K-1)P \int_{-\infty}^{\infty} |H(f)|^4 \, \mathrm{d}f/\gamma_v\gamma_a T_c^3 \tag{3.76}$$

Geometric and statistical arguments based on the propagation model and the terrestrial transmission model lead to the conclusion that for a uniformly distributed population of users in all cells, where each user is power-controlled by the base station in its respective cell, the total interference from users in all other cells equals a fraction f of that caused by all users in the given cell. The other-cell relative interference factor f depends on the propagation model (see Section 9.1). Thus the last term in the denominator of the right-hand side of Formula (3.75) $N_{oc}/T_c = 2P_{oc}$ equals $f(K-1)\int_{-\infty}^{\infty} |H(f)|^4 \, \mathrm{d}f/\gamma_v\gamma_a T_c^3$.

There is one more factor that reduces the signal-to-noise ratio on the input of the coherent DS SS receiver. For coherent reception we must know the phase shift $\varphi^{(k)}$ and the time offset $\delta^{(k)}$ of the received signal. In a SS system estimation of the received signal parameters is performed on a special unmodulated pilot signal (in downlink transmission; see Section 3.4) or on a special pilot chip (in uplink transmission; see Section 5.3). In the latter case, the uplink transmitted code sequence is punctured infrequently. Every gth symbol/chip in the uplink transmitted code sequence is replaced by a pilot chip, which is used to estimate $\varphi^{(k)}$ and $\delta^{(k)}$. We call $1/g$ the puncturing rate or the pilot chip rate. The puncturing reduces the signal-to-noise ratio by factor $(1 - 1/g)$.

Taking into account power control, the other-cell relative interference, antenna sectorization, voice activity monitoring, and pilot chip transmission and neglecting the interchip interference, we get from (3.75) and (3.76)

$$\begin{aligned} \frac{E_b}{I_0} &= \frac{N(1-1/g)}{(1+f)(K-1)\displaystyle\int_{-\infty}^{\infty} |H(f)|^4 \, \mathrm{d}f/\gamma_v\gamma_a T_c^3 + N_0/PT_c} \\ &= \frac{(1-1/g)}{R(1+f)(K-1)\displaystyle\int_{-\infty}^{\infty} |H(f)|^4 \, \mathrm{d}f/\gamma_v\gamma_a T_c^2 + RN_0/P} \end{aligned} \tag{3.77}$$

where $R = 1/NT_c$ is the transmission rate.

In the case of bandlimited pulses, $\int_{-\infty}^{\infty} |H(f)|^4 \, \mathrm{d}f / T_c^3 = 1$ [see (2.173)] and we get the following formula for the radio channel capacity:

$$K_0 = 1 + \frac{W/R}{E_b/I_0} \frac{\gamma_v \gamma_a (1 - 1/g)}{1 + f} - \frac{N_0}{PT_c} \frac{\gamma_v \gamma_a}{1 + f} \tag{3.78}$$

In the case of unit-amplitude rectangular pulses, $\int_{-\infty}^{\infty} |H(f)|^4 \, \mathrm{d}f / T_c^3 = 2/3$ [see Formulas (2.170) and (2.175)] and we get

$$K_0 = 1 + \frac{3}{2} \frac{W/R}{E_b/I_0} \frac{\gamma_v \gamma_a (1 - 1/g)}{1 + f} - \frac{3}{2} \frac{N_0}{PT_c} \frac{\gamma_v \gamma_a}{1 + f} \tag{3.79}$$

Because the definition of the bandwidth in Section 2.1 includes some arbitrariness, in which only part η of the pulse energy is in the bandwidth W, we will not take (3.79) as a perfect estimate. In the general case, independently from the pulse shaping, we will use Formula (3.78) for the uplink radio channel capacity.

EXAMPLE 3.6

The uplink channel of a DS CDMA system occupies 10 *MHz of the spectrum. The user rate is* $R = 10$ *kb/s. If the maximal acceptable* P_b *is* 10^{-3}*, determine the capacity of a single-cell CDMA system using sectored base station antennas and voice activity detection. Antenna gain* $\gamma_a = 2.4$*, and voice activity gain* $\gamma_v = 2.67$*. Assume that the other-cell relative interference factor* f *is equal to zero* ($f = 0$) *and the pilot chip rate* $1/g = 0.2$*. The system has perfect power control and uses a repetition code. Neglect the influence of the background AWGN. Repeat the problem with the maximal acceptable* P_b 10^{-4}*. Consider also analogous multicell CDMA systems if the other-cell relative interference factor* $f = 0.6$*.*

Solution

If $P_b = 10^{-3}$*, we get from Formula (3.74)* $E_b/I_0 = 4.77$*. Because the spreading factor is* $W/R = 1000$*, from (3.78) we have* $K_0 = 1075$ *in the single-cell case and* $K_0 = 672$ *in the multicell case. If* $P_b = 10^{-4}$ *we have* $E_b/I_0 = 6.92$ *and* $K_0 = 741$ *in the single-cell case and* $K_0 = 464$ *in the multicell case.*

Because the performances of uncoded transmission and transmission using a repetition code coincide, we will refer to the performances of the system in Example 3.6 as uncoded transmission performances.

In the case of rectangular pulses, the BPSK SS receiver in analog form is presented in Figure 3.4. We have

$$y^{(k)} = \int_0^T \tilde{r}(t) a^{(k)}(t) \, \mathrm{d}t \tag{3.80}$$

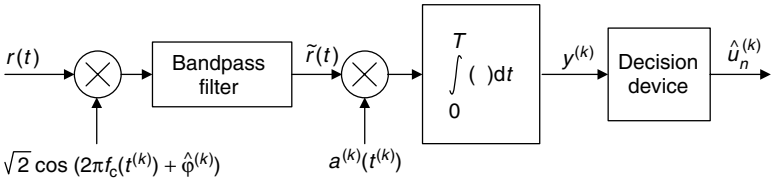

Figure 3.4. BPSK direct-sequence SS receiver for the kth user (in analog form).

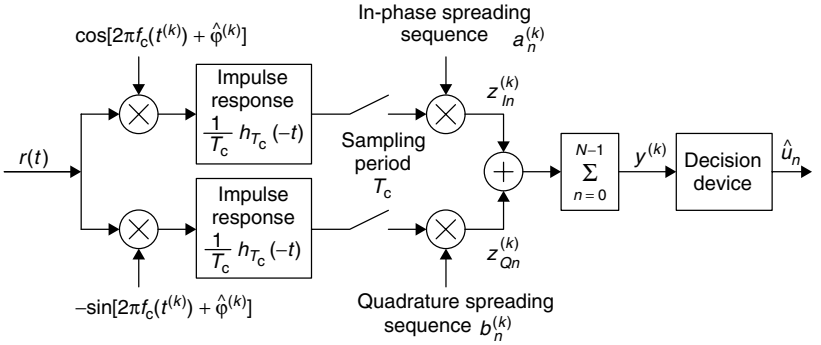

Figure 3.5. QPSK direct-sequence SS receiver for the kth user.

where $T = NT_c$, $\tilde{r}^{(k)}(t)$ is the signal at the output of the bandpass filter, and $a^{(k)}(t)$ is the spreading signal (2.96). The performance of the receiver is analogous to the performance of the receiver in Figure 3.3.

Figure 3.5 shows the QPSK DS SS receiver for the kth user. We will analyze the receiver under the same assumptions as in the BPSK case. The received signal is [compare with Formulas (2.110) and (3.64)]

$$r(t) = \sqrt{P^{(k)}} \sum_{n=-\infty}^{\infty} v_n^{(k)} a_n^{(k)} h_{T_c}(t^{(k)} - nT_c) \cos(2\pi f_c t^{(k)} + \varphi^{(k)}) \tag{3.81}$$

$$-\sqrt{P^{(k)}} \sum_{n=-\infty}^{\infty} v_n^{(k)} b_n^{(k)} h_{T_c}(t^{(k)} - nT_c) \cdot \sin(2\pi f_c t^{(k)} + \varphi^{(k)}) + \xi^{(k)}(t)$$

where

$$\xi^{(k)}(t) = \sum_{k' \neq k} \left[\sqrt{P^{(k')}} \sum_{n=-\infty}^{\infty} v_n^{(k')} a_n^{(k')} h_{T_c}(t^{(k')} - nT_c) \cos(2\pi f_c t^{(k')} + \varphi^{(k')}) \right.$$

$$\left. - \sqrt{P^{(k')}} \sum_{n=-\infty}^{\infty} v_n^{(k')} b_n^{(k')} h_{T_c}(t - nT_c) \sin(2\pi f_c t^{(k')} + \varphi^{(k')}) \right] + \xi(t) \tag{3.82}$$

The analysis of the QPSK demodulator is analogous to that of the BPSK case. At the summation input we have the sum of two sequences $\{z_{\mathrm{I}n}^{(k)}\}$ and $\{z_{\mathrm{Q}n}^{(k)}\}$ [compare with (3.70)]

$$z_{\mathrm{I}n}^{(k)} = \sqrt{P^{(k)}}u_0^{(k)}/2 + \frac{\sqrt{P^{(k)}}}{2}\sum_{n'\neq n} v_{n'}^{(k)} a_{n'}^{(k)} a_n^{(k)} I_{nn'} + \tilde{\xi}_{\mathrm{I}n}^{(k)} a_n^{(k)} + \hat{\xi}_{\mathrm{I}n}^{(k)} a_n^{(k)} + \check{\xi}_{\mathrm{Q}n}^{(k)} a_n^{(k)} \tag{3.83}$$

$$z_{\mathrm{Q}n}^{(k)} = \sqrt{P^{(k)}}u_0^{(k)}/2 + \frac{\sqrt{P^{(k)}}}{2}\sum_{n'\neq n} v_{n'}^{(k)} b_{n'}^{(k)} b_n^{(k)} I_{nn'} + \tilde{\xi}_{\mathrm{Q}n}^{(k)} b_n^{(k)} + \hat{\xi}_{\mathrm{Q}n}^{(k)} b_n^{(k)} + \check{\xi}_{\mathrm{Q}n}^{(k)} b_n^{(k)}, \tag{3.84}$$

$$n = 0, 1, \ldots, N-1$$

where the first terms of the right-hand sides of (3.83) and (3.84) are the desired components, the second terms are due to interchip interference, the third terms are due to other-user interference, the fourth terms are due to background AWGN, and the fifth terms are results of the other-cell interference.

Then

$$E(z_{\mathrm{I}n}^{(k)}) = E(z_{\mathrm{Q}n}^{(k)}) = \begin{cases} \sqrt{P^{(k)}}/2, & \text{if } H_1 \text{ is true,} \\ -\sqrt{P^{(k)}}/2, & \text{if } H_{-1} \text{ is true} \end{cases} \tag{3.85}$$

$$\begin{aligned} \operatorname{var}(z_{\mathrm{I}n}^{(k)}) &= \operatorname{var}(z_{\mathrm{Q}n}^{(k)}) \\ &= \frac{P^{(k)}}{4}\sum_{n'\neq n} I_{nn'}^2 + \frac{1}{4T_{\mathrm{c}}^3}\sum_{k'\neq k} P^{(k')}\int_{-\infty}^{\infty} |H(f)|^4 \,\mathrm{d}f + \frac{N_0}{4T_{\mathrm{c}}} + \frac{N_{\mathrm{oc}}}{4T_{\mathrm{c}}} \end{aligned} \tag{3.86}$$

and

$$\operatorname{cov}(z_{\mathrm{I}n}^{(k)}, z_{\mathrm{Q}n}^{(k)}) = 0 \tag{3.87}$$

We conclude from Formulas (3.85)–(3.87) that the first- and second-order statistics of $z_n^{(k)} \stackrel{\mathrm{def}}{=} z_{\mathrm{I}n}^{(k)} + z_{\mathrm{Q}n}^{(k)}$ for QPSK modulation by a random spreading sequence are exactly the same as those for BPSK modulation, except that the interchip interference is reduced by half (through the use of independent spreading sequences $\boldsymbol{a}^{(k)}$ and $\boldsymbol{b}^{(k)}$ on the in-phase and quadrature channels). The variance of $z_n^{(k)}$ is [compare with (3.72)]

$$\sigma^2 \stackrel{\mathrm{def}}{=} \operatorname{var}(z_n^{(k)}) = \frac{P^{(k)}}{2}\sum_{n'\neq n} I_{nn'}^2 + \frac{1}{2T_{\mathrm{c}}^3}\sum_{k'\neq k} P^{(k')}\int_{-\infty}^{\infty} |H(f)|^4 \,\mathrm{d}f + \frac{N_0}{2T_{\mathrm{c}}} + \frac{N_{\mathrm{oc}}}{2T_{\mathrm{c}}} \tag{3.88}$$

Then Formulas (3.77) and (3.78) are applicable also for the QPSK DS SS case.

Nonperfect synchronization causes a degradation of the receiver performance. In particular, if there are errors $\Delta\delta^{(k)} = \hat{\delta}^{(k)} - \delta^{(k)}$ and $\Delta\varphi^{(k)} = \hat{\varphi}^{(k)} - \varphi^{(k)}$ in the estimation of the time offset and the phase of the received signal, the parameter μ in Formula (3.75) should be replaced by $\sqrt{P^{(k)}} R_{s^{(k)}}(\Delta\delta^{(k)}) \cos(\Delta\varphi^{(k)})$, where $R_{s^{(k)}}(\cdot)$ is the autocorrelation function of the signal $s^{(k)}(t)$. This degrades the SNR by the factor $R^2_{s^{(k)}}(\Delta\delta^{(k)}) \cos^2(\Delta\varphi^{(k)})$.

EXAMPLE 3.7

How does the capacity of the DS CDMA system, considered in Example 3.6, decrease if the timing error $\Delta\delta^{(k)} = T_c/4$ *and the phase error* $\Delta\varphi^{(k)} = \pi/6$*? Assume unit-amplitude rectangular pulse shaping.*

Solution

For unit-amplitude rectangular pulses $R_{s^{(k)}}(T_c/5) = 4/5$. *Because* $\cos(\pi/6) = \sqrt{3}/2$, *the SNR degradation is equal to* $(4/5)^2(\sqrt{3}/2)^2 = 12/25$, *that is, the channel capacity decreases more than two times.*

In this section, we have analyzed reception under known-signal conditions, which means that the demodulator is provided with all parameters required to perform optimal processing. This assumption presumes that a phase-synchronized reference is also available. An important practical case arises when this reference phase is not known, and we have modeled this situation in Section 3.2 by assuming that the unknown phase is a random variable uniformly distributed on $[0, 2\pi)$. We have referred to this regime as noncoherent detection (see also Section 4.3). In Section 3.5 we analyze *differential phase shift-keying (DPSK)* with *partially coherent (or differentially coherent) demodulation*, when the transmitter does not send the reference phase signal and the receiver uses the previous symbol carrier phase.

3.4 COHERENT RECEPTION OF DS CDMA SIGNALS (DOWNLINK TRANSMISSION)

If a base station does not use voice activity monitoring and a sectored antenna, the downlink transmitted BPSK SS signal is $\sqrt{P}s(t)$, where $s(t)$ is given by Formula (2.101). The downlink transmitted signal in the case when the system uses voice activity monitoring and antenna sectorization is $\sqrt{P}s(t)$, where P is the power of the transmitted signal given by

$$s(t) = \sqrt{2} \sum_{k=0}^{K} \gamma^{(k)} \theta^{(k)} \sum_{n=-\infty}^{\infty} v_n^{(k)} a_n^{(k)} h_{T_c}(t - nT_c) \cos(2\pi f_c t + \phi^{(k)}) \qquad (3.89)$$

Here $v_n^{(0)} = 1$, $\theta^{(0)} = 1$; for $k \neq 0$ we have

$$\theta^{(k)} = \theta^{(k)}(t) = \begin{cases} 1, & \text{if } k\text{th user is active at } t \\ & \text{and in this sector;} \\ 0, & \text{otherwise} \end{cases}$$

The weighting coefficients $\gamma^{(k)}$ are defined in the description of downlink transmission given in Section 2.3. We can treat $\theta^{(k)}$, $k \neq 0$, as a random variable with expectation $E(\theta^{(k)}) = 1/\gamma_v\gamma_a$, where γ_v is the voice activity gain and γ_a is the antenna gain. The average power of the transmitted signal is $P\psi$, where ψ is given by

$$\psi = (\gamma^{(0)})^2 + \sum_{k=1}^{K} (\gamma^{(k)})^2/\gamma_v\gamma_a \tag{3.90}$$

The ratio $1/g \stackrel{\text{def}}{=} (\gamma^{(0)})^2/\psi$ shows which part of the total transmitted power is alloted to the pilot component. We call this ratio the *pilot signal rate*.

The phase shifts $\phi^{(k)}$ are independent random variables uniformly distributed on $[0, 2\pi)$. We assume that they are chosen in advance and known both to the transmitter and to the receiver.

The statistical properties of the received signal depend on propagation losses of terrestrial transmission. The propagation models used in the theory of CDMA communication have traditionally focused on predicting the average received signal strength at a given distance from the base station. Propagation models that predict the mean signal strength for an arbitrary {base station—mobile} separation distance d are useful in estimating the radio channel capacity as well as the radio coverage area.

The path loss κ is generally modeled as the product of the mth power of distance d and a log-normal component representing shadowing losses. We study this model in Section 9.1. Here we only note that the kth user path loss, $\kappa^{(k)}$, and the other-cell interference power, $P_{oc}^{(k)}$, on the input of the kth receiver are functions of the geometric location of the kth mobile. The spectral density N_0 of the AWGN on the input of the kth receiver does not depend on k.

The signal received at the kth mobile is

$$\begin{aligned} r^{(k)}(t) = \sqrt{\frac{2P}{\kappa^{(k)}}} \sum_{k'=0}^{K} \gamma^{(k')}\theta^{(k')} \sum_{n=-\infty}^{\infty} v_n^{(k')} a_n^{(k')} h_{T_c}(t - nT_c) \\ \times \cos(2\pi f_c t^{(k')} + \varphi^{(k')}) + \xi(t), \\ k = 1, 2, \ldots, K \end{aligned} \tag{3.91}$$

where $\kappa^{(k)}$ is the kth user path loss and $\gamma^{(k)}$ is the weighting coefficient defined above. The other notations coincide with the notations in Formula (3.64). The pilot signal ($k = 0$) is known to all users in the cell and can be deleted from the received signal. From now on we exclude the pilot signal from consideration and in the sequel the summation will be over $k = 1, 2, \ldots, K$. We may assume also that $\theta^{(k)} = 1$, because information to the kth user is transmitted only if $\theta^{(k)} = 1$.

The noise component $\xi^{(k)}(t)$ includes the interchip interference component, the AWGN $\hat{\xi}^{(k)}(t)$ with two-sided power spectral density $N_0/2$ and the other-cell interference process $\check{\xi}^{(k)}(t)$. The process $\check{\xi}^{(k)}(t)$ can be modeled as AWGN with

two-sided spectral density $N_{\mathrm{oc}}^{(k)}/2 = P_{\mathrm{oc}}^{(k)} T_{\mathrm{c}}$. Here $P_{\mathrm{oc}}^{(k)}$ is equal to the sum of the powers of the signals from all base stations, except the base station of the cell where the kth user is located.

Multiplying both sides of (3.91) by $\sqrt{\kappa^{(k)}}$ we have

$$\overline{r}^{(k)}(t) = \sqrt{\kappa^{(k)}} r^{(k)}(t) \tag{3.92}$$

$$= \sqrt{2P}\ \gamma^{(k)} \sum_{n=-\infty}^{\infty} v_n^{(k)} a^{(k)} h_{T_{\mathrm{c}}}(t - nT_{\mathrm{c}}) \cos(2\pi f_{\mathrm{c}} t^{(k)} + \varphi^{(k)}) + \overline{\xi}^{(k)}(t)$$

where

$$\overline{\xi}^{(k)}(t) = \sqrt{2P} \sum_{\substack{k' \neq k \\ k' \neq 0}} \gamma^{(k')} \theta^{(k')} \sum_{n=-\infty}^{\infty} v_n^{(k')} a_n^{(k')} h_{T_{\mathrm{c}}}(t - nT_{\mathrm{c}}) \tag{3.93}$$

$$\times \cos(2\pi f_{\mathrm{c}} t^{(k')} + \varphi^{(k')}) + \sqrt{\kappa^{(k)}}\ \xi^{(k)}(t)$$

Obviously, the performance of a receiver operating with $r^{(k)}(t)$ is equal to the performance of a receiver operating with $\overline{r}^{(k)}(t)$. In the sequel we analyze the receiver block in Figure 3.3, where $r(t)$ is replaced by $\overline{r}^{(k)}(t)$.

The output of the matched filter at time $t = nT_{\mathrm{c}}$ is

$$\sqrt{P}\gamma^{(k)} v_n^{(k)} a_n^{(k)} + \sqrt{P}\gamma^{(k)} \sum_{n' \neq n} v_{n'}^{(k)} a_{n'}^{(k)} I_{n'n} + \tilde{\xi}_n^{(k)} + \hat{\xi}_n^{(k)} + \check{\xi}_n^{(k)}$$

where the five terms are analogous to the terms in Formula (3.66). Further analysis of the receiver is analogous to (3.67)–(3.75), except that (3.68) should be replaced by the equation

$$\mathrm{var}(\tilde{\xi}^{(k,k')}) = \frac{P(\gamma^{(k')})^2}{2T_{\mathrm{c}}\gamma_{\mathrm{v}}\gamma_{\mathrm{a}}} \int_{-\infty}^{\infty} h_{T_{\mathrm{c}}}^2(t)\, \mathrm{d}t = \frac{P(\gamma^{(k')})^2}{2\gamma_{\mathrm{v}}\gamma_{\mathrm{a}}} \tag{3.94}$$

This is because the lowpass filters are matched not only to the desired signal but also to the interfering other-user signals. The factor $1/2$ in the right-hand side of (3.94) is there because of the random phase shift of the interfering signal carrier with respect to the desired signal carrier.

Analogously to (3.75)–(3.77) we get the following formula for the signal-to-noise ratio in the kth receiver:

$$\frac{(\gamma^{(k)})^2 N}{2(\gamma^{(k)})^2 \sum_{n' \neq n} I_{n,n'} + \sum_{\substack{k' \neq k \\ k' \neq 0}} (\gamma^{(k')})^2 / \gamma_{\mathrm{v}}\gamma_{\mathrm{a}} T_{\mathrm{c}} + \kappa^{(k)} N_0 / P T_{\mathrm{c}} + \kappa^{(k)} P_{\mathrm{oc}}^{(k)} / P} \tag{3.95}$$

It is natural to choose weight coefficients $\{\gamma^{(k)}\}$ such that the signal-to-noise ratio for all receivers would be the same. Then, in the case of orthogonal pulses, we have

$$\frac{E_b}{I_0} = \frac{(\gamma^{(k)})^2 W/R}{\sum_{\substack{k' \neq k \\ k' \neq 0}} (\gamma^{(k')})^2 / \gamma_v \gamma_a T_c + \kappa^{(k)} N_0 / P T_c + \kappa^{(k)} P_{oc}^{(k)} / P}, \tag{3.96}$$

$$k = 1, 2, \ldots, K$$

For given required signal-to-noise ratio E_b/I_0, processing gain W/R, set of path loss coefficients $\{\kappa^{(k)}\}$, two-sided spectral density AWGN $N_0/2$, and set of other-cell interference powers $\{P_{oc}^{(k)}\}$ we can from Formula (3.96) calculate the weighting coefficients $\{\gamma^{(k)}\}$, $k = 1, 2, \ldots, K$. From (3.96) it follows that

$$(\gamma^{(k)})^2 = \frac{E_b/I_0}{W/R} \left[\frac{\psi - (\gamma^{(0)})^2 - (\gamma^{(k)})^2}{\gamma_v \gamma_a} + \frac{\kappa^{(k)} N_0}{P T_c} + \kappa^{(k)} \frac{P_{oc}^{(k)}}{P} \right], \tag{3.97}$$

$$k = 1, 2, \ldots, K$$

where ψ is defined by Formula (3.90). Summation of (3.97) over $k = 1, 2, \ldots, K$ gives

$$[\psi - (\gamma^{(0)})^2] \gamma_v \gamma_a = \frac{E_b/I_0}{W/R} \left\{ (K-1)[\psi - (\gamma^{(0)})^2] + K \overline{\kappa} \frac{N_0}{P T_c} + f K \psi \right\} \tag{3.98}$$

where

$$\overline{\kappa} = \frac{1}{K} \sum_{k=1}^{K} \kappa^{(k)} \tag{3.99}$$

and

$$f = \frac{1}{K P \psi} \sum_{k=1}^{K} \kappa^{(k)} P_{oc}^{(k)} \tag{3.100}$$

The first parameter $\overline{\kappa}$ is the average (over all users in the cell) *path loss* in the cell. The second parameter f is the *forward link other-cell relative interference factor*.

We will estimate the parameter f in Section 9.2 and we will show that it coincides with the other-cell relative interference factor in the uplink transmission.

Because $(\gamma^{(0)})^2 = \psi/g$, where $1/g$ is the pilot signal rate, we get from (3.98) that

$$\psi(1 - 1/g) \gamma_v \gamma_a = \frac{E_b/I_0}{W/R} \left\{ (K-1)\psi(1 - 1/g) + K \overline{\kappa} \frac{N_0}{P T_c} + f K \psi \right\} \tag{3.101}$$

From Formula (3.101) follows the formula for the downlink DS BPSK CDMA radio channel capacity,

$$K_0 = 1 + \frac{\dfrac{W/R}{E_b/I_0}\,\gamma_v\gamma_a\left(1-\dfrac{1}{g}\right) - \overline{\kappa}N_0/P\psi T_c - f}{1 - 1/g + \overline{\kappa}N_0/P\psi T_c + f} \tag{3.102}$$

Because usually $N_0/P \ll 1$ and $1/g \ll f$, the main term of the right-hand side of (3.102) has order

$$\frac{W/R}{E_b/I_0}\,\frac{\gamma_v\gamma_a}{1+f}\,\left(1-\frac{1}{g}\right) \tag{3.103}$$

This is the same order as the main term in the formula for the uplink radio channel capacity (3.78). The pilot signal rate $1/g$ in the downlink case is less than the pilot chip's rate $1/g$ in the uplink case. Therefore, the downlink radio channel capacity is larger than the uplink radio channel capacity.

If the phases $\phi^{(k)}$ of the component signals in Formula (3.87) are the same, that is, $\phi^{(k)} = 0$, $k = 0, 1, \ldots, K$, the capacity of the downlink DS CDMA system is half the capacity (3.103) (Problem 3.4). We can also get the capacity (3.103) if for half of the users $\phi^{(k)} = 0$ and for half of the users $\phi^{(k)} = -\pi/2$. The transmitted signal is $\sqrt{P}s(t)$, where

$$s(t) = \sqrt{2}\sum_{k=0}^{\lfloor K/2\rfloor}\gamma^{(k)}\theta^{(k)}\sum_{n=-\infty}^{\infty}v_n^{(k)}a_n^{(k)}h_{T_c}(t-nT_c)\cos(2\pi f_c t)$$

$$-\sqrt{2}\sum_{k=\lfloor K/2\rfloor+1}^{K}\gamma^{(k)}\theta^{(k)}\sum_{n=\infty}^{\infty}v_n^{(k)}a_n^{(k)}h_{T_c}(t-nT_c)\sin(2\pi f_c t) \tag{3.104}$$

In Chapter 9 we consider a method for further increasing the downlink capacity called *user coordination*.

EXAMPLE 3.8

Find the downlink radio channel capacity of the multicell DS CDMA system with parameters of Example 3.6, assuming that the system occupies the same bandwidth on each one-way link. The pilot signal rate is $1/g = 0.05$. *The other-cell relative interference factor is* $f = 0.6$.

Solution

If $P_b = 10^{-3}$ *we get from (3.102)* $K_0 = 798$ *and if* $P_b = 10^{-4}$ *then* $K_0 = 550$. *The capacity of the forward channel is larger than the capacity of the reverse channel because the pilot signal rate is less.*

The forward transmission in the DS QPSK CDMA system is analyzed by using the same scenario as the DS BPSK CDMA system. The radio channel capacity is defined by Formula (3.102).

3.5 RECEPTION OF DS DPSK SS SIGNALS

Transmission of a pilot is very valuable for obtaining a good phase estimation, making coherent reception possible. Unfortunately, it may not always be affordable, especially on the reverse link. Without phase estimation, noncoherent or differentially coherent reception is required. In the present section we study differential phase shift-keying with partially coherent demodulation in the uplink channel.

The receiver of DPSK signals exploits the reference-phase idea in a clever fashion to transmit a binary sequence of signals over a channel whose phase is unknown but changes very slowly. To transmit the first binary symbol a signal is preceded by a reference signal. For the second bit, the signal portion of the first bit is used as a reference and only the new signal is sent. This scheme is continued, with each signal serving as reference for the next. The key is to encode information in phase differences and then use phase differencing at the receiver to demodulate.

In the DPSK DS system the information sequence of the kth user $\boldsymbol{u}^{(k)} = \ldots u_{-1}^{(k)}, u_0^{(k)}, u_1^{(k)}, \ldots, u_n^{(k)}, \ldots$ is first differentially encoded into the sequence $\tilde{\boldsymbol{v}}^{(k)} = \ldots \tilde{v}_{-1}^{(k)}, \tilde{v}_0^{(k)}, \tilde{v}_1^{(k)}, \ldots, \tilde{v}_n^{(k)} \ldots$, where

$$\tilde{v}_n^{(k)} = \begin{cases} \tilde{v}_{n-1}^{(k)}, & \text{if } u_n^{(k)} = 1 \\ -\tilde{v}_{n-1}^{(k)}, & \text{if } u_n^{(k)} = -1 \end{cases} \tag{3.105}$$

Then each of the symbols $\tilde{v}_n^{(k)}$ is repeated N times such that $v_n^{(k)} = \tilde{v}_{\lfloor n/N \rfloor}^{(k)}$, that is, $\{v_{mN+n}^{(k)} = \tilde{v}_m^{(k)}\}, n = 0, 1, \ldots, N-1, m = \ldots -1, 0, 1, \ldots$, are codewords of the repetition code. The transmitted sequence is $\boldsymbol{v}^{(k)} = \ldots v_{-1}^{(k)}, v_0^{(k)}, v_1^{(k)}, \ldots, v_n^{(k)}, \ldots$, the BPSK modulated signal is given by Formula (2.92), and the received signal is given by (3.64).

A differentially encoded PSK signal allows demodulation that does not require the estimation of the carrier phase. Instead, the received signal in the given interval $[mNT_c, (m+1)NT_c)$ is compared to the phase of the received signal from the preceding signal interval $[(m-1)NT_c, mNT_c)$. But we assume that the receiver knows the time offset, $\hat{\delta}^{(k)} = \delta^{(k)}$. The receiver for $u_0^{(k)}$ is presented in Figure 3.6.

Neglecting the interchip interference terms we have, analogously to (3.83) and (3.84),

$$z_{\mathrm{I}n}^{(k)} = \sqrt{P^{(k)}} v_n^{(k)} \cos\varphi^{(k)} + \tilde{\xi}_{\mathrm{I}n}^{(k)} a_n^{(k)} + \hat{\xi}_{\mathrm{I}n}^{(k)} a_n^{(k)} + \check{\xi}_{\mathrm{I}n}^{(k)} a_n^{(k)} \tag{3.106}$$

$$z_{\mathrm{Q}n}^{(k)} = \sqrt{P^{(k)}} v_n^{(k)} \sin\varphi^{(k)} + \tilde{\xi}_{\mathrm{Q}n}^{(k)} a_n^{(k)} + \check{\xi}_{\mathrm{Q}n}^{(k)} a_n^{(k)} + \check{\xi}_{\mathrm{Q}n}^{(k)} a_n^{(k)}, \tag{3.107}$$

$$n = 0, 2, \ldots, N-1$$

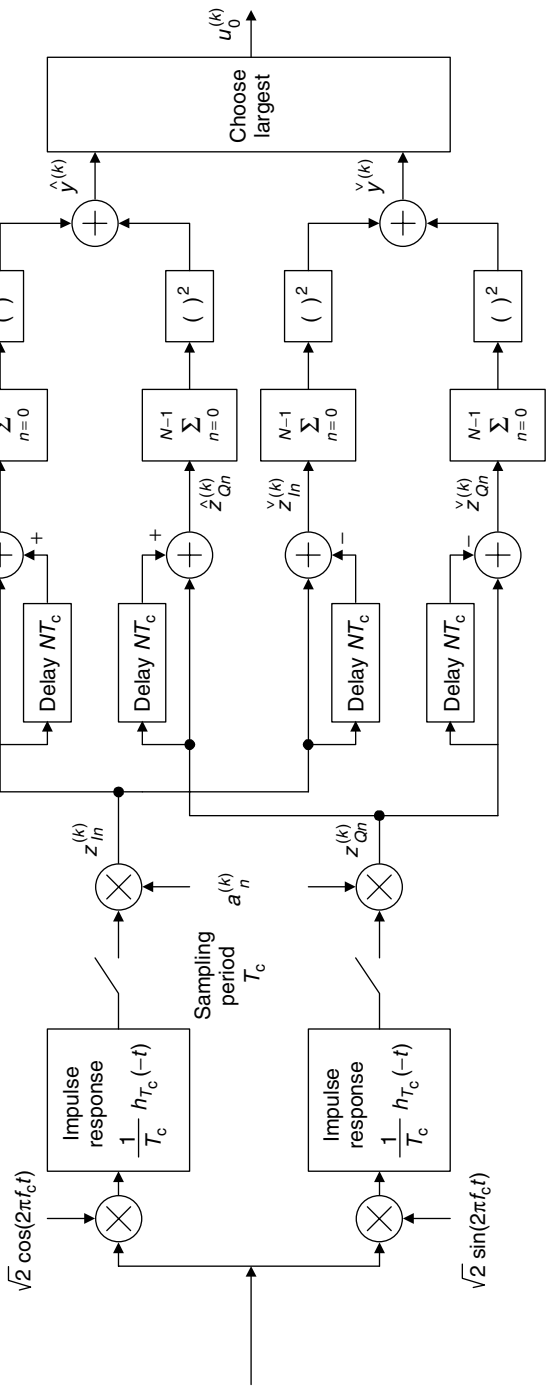

Figure 3.6. Differentially coherent receiver for the kth user.

The first terms on the right-hand side of (3.106) and (3.107) are the desired components, the second terms are the other-user interference components, the third terms are due to background AWGN, and the fourth terms are due to the other-cell interference.

Analogously to Formulas (3.85)–(3.87) we have from (3.106) and (3.107)

$$E(z_{\mathrm{I}n}^{(k)}) = \sqrt{P^{(k)}} v_n^{(k)} \cos\varphi^{(k)} = \sqrt{P^{(k)}} u_0^{(k)} \tilde{v}_{-1}^{(k)} \cos\varphi^{(k)} \tag{3.108}$$

$$E(z_{\mathrm{Q}n}^{(k)}) = \sqrt{P^{(k)}} v_n^{(k)} \sin\varphi^{(k)} = \sqrt{P^{(k)}} u_0^{(k)} \tilde{v}_{-1}^{(k)} \sin\varphi^{(k)}$$

$$\mathrm{var}(z_{\mathrm{I}n}^{(k)}) = \mathrm{var}(z_{\mathrm{Q}n}^{(k)}) = \frac{1}{2T_{\mathrm{c}}^3} \sum_{k' \neq k} P^{(k')} \int_{-\infty}^{\infty} |H(f)|^4 \, \mathrm{d}f + \frac{N_0}{2T_{\mathrm{c}}} + \frac{N_{\mathrm{oc}}}{2T_{\mathrm{c}}} \stackrel{\mathrm{def}}{=} \frac{I_0}{2T_{\mathrm{c}}} \tag{3.109}$$

and

$$\mathrm{cov}(z_{\mathrm{I}n}, z_{\mathrm{Q}n}) = 0 \tag{3.110}$$

Consider now the following statistics on the inputs of the summing functions

$$\begin{aligned} \hat{z}_{\mathrm{I}n}^{(k)} &= z_{\mathrm{I}n}^{(k)} + z_{\mathrm{I},n-N}^{(k)} \\ \hat{z}_{\mathrm{Q}n}^{(k)} &= z_{\mathrm{Q}n}^{(k)} + z_{\mathrm{Q},n-N}^{(k)} \\ \check{z}_{\mathrm{I}n}^{(k)} &= z_{\mathrm{I}n}^{(k)} - z_{\mathrm{I},n-N}^{(k)} \\ \check{z}_{\mathrm{Q}n}^{(k)} &= z_{\mathrm{Q}n}^{(k)} - z_{\mathrm{Q},n-N}^{(k)} \end{aligned} \tag{3.111}$$

These statistics are independent and have the following conditional mean values

$$\begin{aligned} E(\hat{z}_{\mathrm{I}n}^{(k)} | u_0^{(k)} = 1) &= E(\check{z}_{\mathrm{I}n}^{(k)} | u_0^{(k)} = -1) \\ &= 2\sqrt{P^{(k)}} \tilde{v}_{-1}^{(k)} \cos\varphi^{(k)} = \mu \cos\varphi^{(k)} \end{aligned} \tag{3.112}$$

$$E(\hat{z}_{\mathrm{I}n}^{(k)} | u_0^{(k)} = -1) = E(\check{z}_{\mathrm{I}n}^{(k)} | u_0^{(k)} = 1) = 0 \tag{3.113}$$

$$\begin{aligned} E(\hat{z}_{\mathrm{Q}n}^{(k)} | u_0^{(k)} = 1) &= E(\check{z}_{\mathrm{Q}n}^{(k)} | u_0^{(k)} = -1) \\ &= 2\sqrt{P^{(k)}} \tilde{v}_{-1}^{(k)} \sin\varphi^{(k)} = \mu \sin\varphi^{(k)} \end{aligned} \tag{3.114}$$

$$E(\hat{z}_{\mathrm{Q}n}^{(k)} | u_0^{(k)} = -1) = E(\check{z}_{\mathrm{I}n}^{(k)} | u_0^{(k)} = 1) = 0 \tag{3.115}$$

where $\mu \stackrel{\mathrm{def}}{=} 2\sqrt{P^{(k)}} \tilde{v}_{-1}^{(k)}$,

$$\mathrm{var}(\hat{z}_{\mathrm{I}n}^{(k)}) = \mathrm{var}(\hat{z}_{\mathrm{Q}n}^{(k)}) = \mathrm{var}(\check{z}_{\mathrm{I}n}^{(k)}) = \mathrm{var}(\check{z}_{\mathrm{Q}n}^{(k)}) = \frac{I_0}{T_{\mathrm{c}}} \stackrel{\mathrm{def}}{=} \sigma^2 \tag{3.116}$$

We reduced the reception problem to a problem of testing two hypothesis, H_1 (that $u_0^{(k)} = 1$) and H_{-1} (that $u_0^{(k)} = -1$). If hypothesis H_1 is true, then (see Examples 3.3 and 3.4) the statistic

$$\hat{y}^{(k)} = \left(\sum_{n=0}^{N-1} \hat{z}_{\mathrm{I}n}^{(k)} \right)^2 + \left(\sum_{n=0}^{N-1} \hat{z}_{\mathrm{Q}n}^{(k)} \right)^2$$

has *noncentral* χ^2*-distribution* with two degrees of freedom and the statistic

$$\check{y}^{(k)} = \left(\sum_{n=0}^{N-1} \check{z}_{\mathrm{I}n}^{(k)} \right)^2 + \left(\sum_{n=0}^{N-1} \check{z}_{\mathrm{Q}n}^{(k)} \right)^2$$

has *central* χ^2*-distribution* with two degrees of freedom. If hypothesis H_{-1} is true, then the statistic $\hat{y}^{(k)}$ has *central* χ^2*-distribution* with two degrees of freedom and the statistic $\check{y}^{(k)}$ has *noncentral* χ^2*-distribution* with two degrees of freedom. The probability density functions are [compare with Formulas (3.26) and (3.49)]: if H_1 is true,

$$p_1(\hat{y}^{(k)}) = \frac{1}{2N\sigma^2} \exp[-(\hat{y}^{(k)} + N^2\mu^2)/2N\sigma^2] I_0\left(\frac{\mu\sqrt{\hat{y}^{(k)}}}{\sigma^2} \right), \hat{y}^{(k)} \geq 0, \quad (3.117)$$

$$p_1(\check{y}^{(k)}) = \frac{1}{2N\sigma^2} \exp\left(-\frac{\check{y}^{(k)}}{2N\sigma^2} \right), \check{y}^{(k)} \geq 0$$

and if H_{-1} is true,

$$\begin{aligned} p_{-1}(\hat{y}^{(k)}) &= \frac{1}{2N\sigma^2} \exp\left(-\frac{\hat{y}^{(k)}}{2N\sigma^2} \right), \hat{y}^{(k)} \geq 0, \\ p_{-1}(\check{y}^{(k)}) &= \frac{1}{2N\sigma^2} \exp[-(\check{y}^{(k)} + N^2\mu^2)/2N\sigma^2] \, I_0\left(\frac{\mu\sqrt{\check{y}^{(k)}}}{\sigma^2} \right), \check{y}^{(k)} \geq 0 \end{aligned} \quad (3.118)$$

To analyze the bit error probability P_{b}, we may assume without loss of generality that $u_0^{(k)} = 1$. The probability of bit error, given that $u_0^{(k)} = 1$ is sent, is

$$\begin{aligned} P_{\mathrm{b}} &= \int_0^\infty \int_{\hat{y}}^\infty p_1(\hat{y}) p_1(\check{y}) \, \mathrm{d}\check{y} \, \mathrm{d}\hat{y} \\ &= \int_0^\infty \frac{1}{2N\sigma^2} \exp\left(-\frac{\hat{y}}{2N\sigma^2} \right) \exp[-(\hat{y} + N^2\mu^2)/2N\sigma^2] \, I_0\left(\frac{\mu\sqrt{\hat{y}}}{\sigma^2} \right) \mathrm{d}\hat{y} \end{aligned}$$

$$= \frac{1}{2}\exp\left(-\frac{\mu^2}{4\sigma^2}N\right)\int_0^\infty \frac{1}{N\sigma^2}\exp[-(\hat{y}+N^2\mu^2/4)/N\sigma^2]\, I_0\left(\frac{\mu\sqrt{\hat{y}}}{\sigma^2}\right)\mathrm{d}\hat{y}$$

$$= \frac{1}{2}\exp\left(-\frac{\mu^2}{4\sigma^2}N\right) \tag{3.119}$$

because the integrand is the probability density function of the noncentral χ^2-random variable with two degrees of freedom, with parameters $\mu' = \mu/\sqrt{2}$, $\sigma' = \sigma/\sqrt{2}$. It is remarkable that the rather complex integral in (3.119) is reduced to such a simple form. From Formula (3.119) we have [compare with (1.13)]

$$P_\mathrm{b} = \frac{1}{2}\ \exp\left(-\frac{P^{(k)}T_\mathrm{c}N}{I_0}\right) = \frac{1}{2}\ \exp\left(-\frac{E_\mathrm{b}}{I_0}\right) \tag{3.120}$$

A comparison with Formula (3.74) shows that DPSK has only a slight loss in energy efficiency relative to coherent PSK, even if we did not take into account the pilot chip gain.

A plot of P_b versus E_b/I_0 is shown in Figure 3.7. Also shown in that illustration is the bit error probability (3.74) for coherent BPSK. We observe that at an error probability of $P_\mathrm{b} \leq 10^{-5}$, the difference in the SNR between binary PSK and binary DPSK is less than 1 dB.

Consider uplink transmission in a DS CDMA system using binary DPSK. Analogously to (3.77) we get from Formulas (3.108)–(3.116), when assuming perfect power control that $P^{(k)} = P$ and neglecting interchip inteference, the

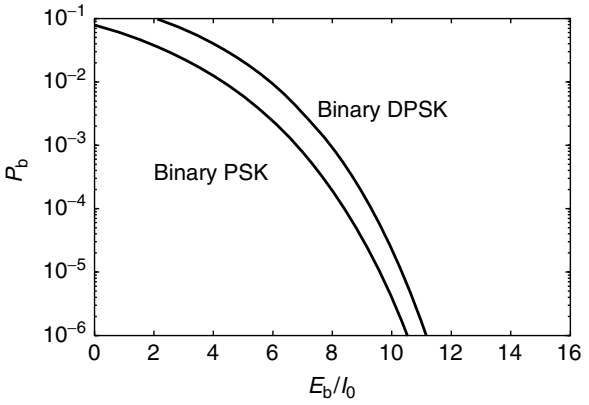

Figure 3.7. Probability of error for DS CDMA systems using coherent BPSK and binary DPSK.

following expression for the signal-to-noise ratio:

$$\frac{E_b}{I_0} = \frac{\mu^2}{2\sigma^2} N = \frac{N}{(K-1)\int_{-\infty}^{\infty} |H(f)|^4 \, df/\gamma_v\gamma_a T_c^3 + N_0/PT_c + N_{oc}/PT_c}$$

$$= \frac{W/R}{(K-1)/\gamma_v\gamma_a + N_0/PT_c + N_{oc}/PT_c}$$

$$= \frac{W/R}{(K-1)(1+f)/\gamma_v\gamma_a + N_0/PT_c} \tag{3.121}$$

In the second equality we assumed $\int_{-\infty}^{\infty} |H(f)|^4 \, df/T_c^3 = 1$, that is, bandlimited pulse shaping. Then the radio channel capacity of a DS DPSK CDMA system is

$$K_0 = 1 + \frac{W/R}{E_b/I_0} \frac{\gamma_v\gamma_a}{1+f} - \frac{N_0}{PT_c} \frac{\gamma_v\gamma_a}{1+f} \approx 1 + \frac{W/R}{E_b/I_0} \frac{\gamma_v\gamma_a}{1+f} \tag{3.122}$$

where $E_b/I_0 = -\ln 2P_b$.

EXAMPLE 3.9

Consider a multicell CDMA system with the same parameter as in Example 3.6. Determine the radio channel capacity of the CDMA system if it uses differentially coherent binary PSK and maximal acceptable bit error rate $P_b = 10^{-3}$ *and* 10^{-4}.

Solution

From (3.122) we have

$$K_0 = 1 + \frac{W/R}{-\ln 2P_b} \frac{\gamma_v\gamma_a}{1+f} \tag{3.123}$$

If $P_b = 10^{-3}$ *then* $K_0 = 645$, *and if* $P_b = 10^{-4}$ *then* $K_0 = 471$. *This is slightly less than the radio channel capacity of the system in Example 3.6, using coherent BPSK with pilot (chip) signaling.*

In the next section we study noncoherent reception of FSK signals in a FH CDMA system.

3.6 RECEPTION OF FH SS SIGNALS

Although a fully coherent frequency-hopping system is theoretically possible, the frequency hopping is done noncoherently in most cases. Consider a FH CDMA system with total hopping bandwidth W. Let the system use BFSK with the hopset consisting of Q carrier frequencies, such that the M-parameter (see

Section 1.4) is equal to $2Q$. The frequency separation interval is $\Delta f = W/M$, and the pulse duration is $T_c = 1/\Delta f$. Suppose that the transmission rate is $R = 1/T$ for each of the K users, the hopping rate is $R_h = 1/T_c$, the ratio $N = T/T_c$ is an integer, and the system uses a rate $r = 1/N$ repetition code, that is, $v_n^{(k)} = u_{\lfloor n/N \rfloor}^{(k)}$. Analysis of downlink transmission and analysis of uplink transmission are analogous, and we analyze only uplink transmission. We model the other-cell interference as Gaussian noise. The kth user's modulated signal is [compare with (2.125)]

$$s^{(k)}(t) = \sqrt{2} \sum_{n=-\infty}^{\infty} h_{T_c}(t - nT_c) \cos \left\{ 2\pi \left[f_c + \frac{v_n^{(k)}}{2} \Delta f + 2a_n^{(k)} \Delta f \right] t + \phi_n^{(k)} \right\} \tag{3.124}$$

Here $h_{T_c}(t)$ is the rectangular unit amplitude pulse of duration T_c, f_c is a central carrier frequency, Δf is the frequency separation interval, $2\Delta f$ is the carrier frequency separation interval, $a_n^{(k)} \in \{-(Q-1)/2, -(Q-3)/2, \ldots, (Q-1)/2\}$ is the spreading/hopping sequence, and $\phi_n^{(k)}$ is a phase. The received signal at the base station is

$$r(t) = \sum_{k=1}^{K} \sqrt{P^{(k)}} s^{(k)}(t^{(k)}) + \xi(t) \tag{3.125}$$

where $P^{(k)}$ is the power of the received signal from the kth user, $t^{(k)} = t - \delta^{(k)}$, $\delta^{(k)}$ is the kth user time offset, and $\xi(t)$ is background AWGN. Then, analogously to (3.2) and (3.3), the received signal (3.125) can be represented as the sum of the desired (relative to the kth user) signal component $\sqrt{P^{(k)}} s^{(k)}(t^{(k)})$ and the total noise $\xi^{(k)}(t)$. The noncoherent BFSK FH SS receiver for the 0th block of symbols is represented in Figure 3.8. We assume that the system has perfect power control, that is, $P^{(k)} = P$, $k = 1, 2, \ldots, K$.

The frequency synthesizer output $a^{(k)}(t)$ is the signal (2.123) with $\Delta F = 2\Delta f$. We suppose that the time offset $\delta^{(k)}$ is known to the receiver. The down-converted signal on the output of the bandpass filter is

$$\tilde{r}^{(k)}(t) = \sqrt{2P} \sum_{n=-\infty}^{\infty} h_{T_c}(t^{(k)} - nT_c) \times \cos \left[2\pi \left(f_c + v_n^{(k)} \frac{\Delta f}{2} \right) t^{(k)} + \varphi_n^{(k)} \right] + \tilde{\xi}^{(k)}(t) \tag{3.126}$$

where $\varphi_n^{(k)}$ is a phase shift and $\tilde{\xi}^{(k)}(t)$ is the modified noise including the background AWGN and the other-user interference.

Without loss of generality we will study reception of the signal from the first user, assuming that $u_0^{(1)} = 1$. To simplify the analysis, we consider first the case when all users are chip synchronized, that is, $t^{(k)}/T_c = \text{integer}$, $k = 1, 2, \ldots, K$.

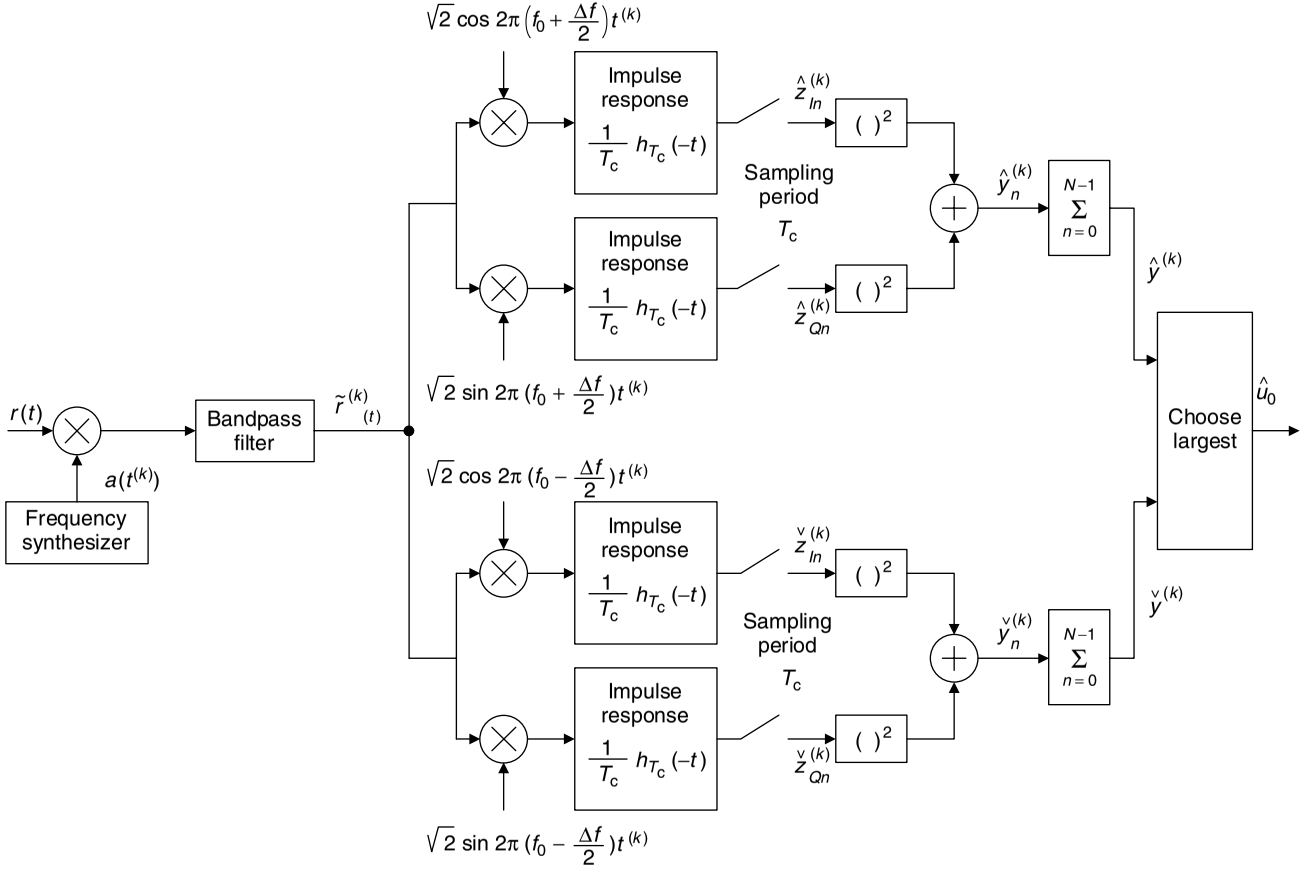

Figure 3.8. BFSK FH spread spectrum noncoherent receiver.

The output statistics of the matched filters are

$$\begin{aligned}
\hat{z}_{\mathrm{I}n}^{(1)} &= \sqrt{P}\cos\varphi_n^{(1)} + \sqrt{P}\sum_{k=2}^{K}\hat{\theta}_n^{(k)}\cos\varphi_n^{(k)} + \hat{\xi}_{\mathrm{I}n}^{(1)} \\
\hat{z}_{\mathrm{Q}n}^{(1)} &= \sqrt{P}\sin\varphi_n^{(1)} + \sqrt{P}\sum_{k=1}^{K}\hat{\theta}_n^{(k)}\sin\varphi_n^{(k)} + \hat{\xi}_{\mathrm{Q}n}^{(1)} \\
\check{z}_{\mathrm{I}n}^{(1)} &= \sqrt{P}\sum_{k=2}^{K}\check{\theta}_n^{(k)}\cos\varphi_n^{(k)} + \check{\xi}_{\mathrm{I}n}^{(1)} \\
\check{z}_{\mathrm{Q}n}^{(1)} &= \sqrt{P}\sum_{k=2}^{K}\check{\theta}_n^{(k)}\sin\varphi_n^{(k)} + \check{\xi}_{\mathrm{Q}n}^{(1)}
\end{aligned} \tag{3.127}$$

Here

$$\hat{\theta}_n^{(k)} = \begin{cases} 1, & \text{if in the } n\text{th moment the } k\text{th user occupies} \\ & \text{the same subband as the first user,} \\ 0, & \text{otherwise} \end{cases} \tag{3.128}$$

$$\check{\theta}_n^{(k)} = \begin{cases} 1, & \text{if in the } n\text{th moment the } k\text{th user occupies} \\ & \text{the opposed subband to the subband} \\ & \text{occupied by the first user,} \\ 0, & \text{otherwise} \end{cases} \tag{3.129}$$

Also, $\hat{\xi}_{\mathrm{I}n}^{(1)}$, $\hat{\xi}_{\mathrm{Q}n}^{(1)}$, $\check{\xi}_{\mathrm{I}n}^{(1)}$, and $\check{\xi}_{\mathrm{Q}n}^{(1)}$ are zero-mean Gaussian noise components with variance σ_0^2 due to background noise and other-cell interference. We assume that $\sigma_0^2 = N_0/2T_{\mathrm{c}} + N_{\mathrm{oc}}/2T_{\mathrm{c}}$, where $N_0/2$ is two-sided power spectral density of the background AWGN and $N_{\mathrm{oc}}/2$ is two-sided power spectral density of the other-cell interference noise. Analogously to the DS CDMA case we estimate the power of the other-cell interference in all bandwidths as $f(K-1)P$, where f is the other-cell interference factor. Then the power of the other-cell interference noise within the bandwidth $\Delta f = W/M$ is equal to $f(K-1)P/M = N_{\mathrm{oc}}/2T_{\mathrm{c}}$. Finally, we estimate the variance of the noise components as $\sigma_0^2 = N_0/2T_{\mathrm{c}} + f(K-1)P/M$. The sets $\hat{\theta}_n^{(k)}$ and $\check{\theta}_n^{(k)}$ are sets of IID random variables such that

$$\begin{aligned}
&P(\hat{\theta}_n^{(k)} = 1) = P(\check{\theta}_n^{(k)} = 1) = 1/M \\
&P(\hat{\theta}_n^{(k)} = 1,\ \check{\theta}_n^{(k)} = 1) = 0, \qquad k = 1, 2, \ldots, K, \quad n = 0, 1, \ldots, N-1
\end{aligned} \tag{3.130}$$

The random variables $\varphi_n^{(k)}$ are independent and uniformly distributed on $[0, 2\pi)$.

The statistics $\hat{y}_n^{(1)}$ and $\check{y}_n^{(1)}$ are

$$\begin{aligned}\hat{y}_n^{(1)} &= (\hat{z}_{\mathrm{I}n}^{(1)})^2 + (\hat{z}_{\mathrm{Q}n}^{(1)})^2 \\ &= P\left[1 + \sum_{k=2}^{K} \hat{\theta}_n^{(k)}\right] + 2P \sum_{k=2}^{K} \hat{\theta}_n^{(k)} \cos(\varphi_n^{(1)} - \varphi_n^{(k)}) \\ &\quad + 2P \sum_{k=2}^{K} \sum_{k'=k+1}^{K} \hat{\theta}_n^{(k)} \hat{\theta}_n^{(k')} \cos(\varphi_n^{(k)} - \varphi_n^{(k')}) \\ &\quad + 2\sqrt{P}\left(\cos\varphi_n^{(1)} + \sum_{k=2}^{K} \hat{\theta}_n^{(k)} \cos\varphi_n^{(k)}\right) \hat{\xi}_{\mathrm{I}n}^{(k)} \\ &\quad + 2\sqrt{P}\left(\sin\varphi_n^{(1)} + \sum_{k=2}^{K} \hat{\theta}_n^{(k)} \sin\varphi_n^{(k)}\right) \hat{\xi}_{\mathrm{Q}n}^{(1)} + (\hat{\xi}_{\mathrm{I}n}^{(1)})^2 + (\hat{\xi}_{\mathrm{Q}n}^{(1)})^2 \end{aligned} \tag{3.131}$$

$$\begin{aligned}\check{y}_n^{(1)} &= (\check{z}_{\mathrm{I}n}^{(1)})^2 + (\check{z}_{\mathrm{Q}n}^{(1)})^2 \\ &= P \sum_{k=2}^{K} \check{\theta}_n^{(k)} + 2P \sum_{k=2}^{K} \sum_{k'=k+1}^{K} \check{\theta}_n^{(k)} \check{\theta}_n^{(k')} \cos(\varphi_n^{(k)} - \varphi_n^{(k')}) \\ &\quad + 2\sqrt{P}\left(\sum_{k=2}^{K} \check{\theta}_n^{(k)} \cos\varphi_n^{(k)}\right) \check{\xi}_{\mathrm{I}n}^{(1)} + 2\sqrt{P}\left(\sum_{k=2}^{K} \check{\theta}_n^{(k)} \sin\varphi_n^{(k)}\right) \check{\xi}_{\mathrm{Q}n}^{(k)} \\ &\quad + (\check{\xi}_{\mathrm{I}n}^{(1)})^2 + (\check{\xi}_{\mathrm{Q}n}^{(1)})^2 \end{aligned} \tag{3.132}$$

In **APPENDIX A** (see (A.15)–(A.18)), we analyze the moments of decision statistics $\hat{y}^{(1)} = \sum_{n=0}^{N-1} \hat{y}_n^{(1)}$ and $\check{y}^{(1)} = \sum_{n=0}^{N-1} \check{y}_n^{(1)}$. For the means we get

$$E(\hat{y}^{(1)}) = N\left[P\left(1 + \frac{K-1}{M}\right) + 2\sigma_0^2\right] \tag{3.133}$$

$$E(\check{y}^{(1)}) = N\left[P\,\frac{K-1}{M} + 2\sigma_0^2\right] \tag{3.134}$$

and for the variances we get

$$\begin{aligned}\mathrm{var}(\hat{y}^{(1)}) = N\Bigg\{ & P^2\left[3\,\frac{K-1}{M} + \left(\frac{K-1}{M}\right)^2\right] \\ & + 4P\left(1 + \frac{K-1}{M}\right)\sigma_0^2 + 4\sigma_0^4\Bigg\}\end{aligned} \tag{3.135}$$

$$\mathrm{var}(\check{y}^{(1)}) = N\left\{P^2\left[\frac{K-1}{M}+\left(\frac{K-1}{M}\right)^2\right]+4P\frac{K-1}{M}\,\sigma_0^2+4\sigma_0^4\right\} \tag{3.136}$$

If $K \gg 1$, the decision statistics $\hat{y}^{(1)}$, $\check{y}^{(1)}$ and the statistic

$$y^{(1)} \stackrel{\text{def}}{=} \hat{y}^{(1)} - \check{y}^{(1)}$$

are approximately Gaussian random variables. From Figure 3.8 it follows that if $y^{(1)} > 0$, we accept the hypothesis H_1; otherwise, we accept H_{-1}. The first two moments of $y^{(1)}$ are

$$E(y^{(1)}) = E(\hat{y}^{(1)}) - E(\check{y}^{(1)}) = NP \tag{3.137}$$

$$\begin{aligned}\mathrm{var}(y^{(1)}) &= \mathrm{var}(\hat{y}^{(1)}) + \mathrm{var}(\check{y}^{(1)}) \\ &= N\left\{P^2\left[4\,\frac{K-1}{M}+2\left(\frac{K-1}{M}\right)^2\right]\right. \\ &\qquad \left.+4P\left(1+2\,\frac{K-1}{M}\right)\sigma_0^2+8\sigma_0^4\right\}\end{aligned} \tag{3.138}$$

The signal-to-noise ratio is

$$\begin{aligned}\frac{E_\mathrm{b}}{I_0} &= \frac{[E(y^{(1)})]^2}{2\mathrm{var}(y^{(1)})} \\ &= \frac{P^2N}{4P^2\left[2\,\frac{K-1}{M}+\left(\frac{K-1}{M}\right)^2\right]+8P\sigma_0^2\left(1+2\,\frac{K-1}{M}\right)+16\sigma_0^4} \\ &= \frac{W\lambda/R(K-1)}{4(A+A^2)+8\lambda(1+A)+4\lambda^2}\end{aligned} \tag{3.139}$$

where $\lambda = (K-1)/M$, $R = 1/NT_\mathrm{c}$, $T_\mathrm{c} = M/W$, and $A = 2\sigma_0^2/P$.

From Formula (3.139) it follows that

$$K-1 = \frac{W/R}{E_\mathrm{b}/I_0}\,\frac{1}{4\lambda^{-1}(A+A^2)+8(1+A)+4\lambda} \tag{3.140}$$

If background AWGN is negligible, we have $\sigma_0^2 \approx N_\mathrm{oc}/2T_\mathrm{c} = f(K-1)P/M = f\lambda P$ and $A \approx 2f\lambda$. Then we have from (3.140)

$$K-1 \approx \frac{W/R}{E_\mathrm{b}/I_0}\,\frac{1}{8(1+f)+4\lambda(1+4f+4f^2)} \tag{3.141}$$

The maximum of the right-hand side of (3.141) occurs at $\lambda = 0$. Then we get the following formula for the uplink radio channel capacity of the synchronized multicell FH CDMA system:

$$K_0 \approx 1 + \frac{W/R}{8E_b/I_0} \frac{1}{1+f}$$

Voice activity monitoring and antenna sectorization increase the second term by a factor of $\gamma_v\gamma_a$. Finally, we get the following formula for the radio channel capacity of the multicell synchronized FH CDMA system:

$$K_0 \approx 1 + \frac{W/R}{8E_b/I_0} \frac{\gamma_v\gamma_a}{1+f} \tag{3.142}$$

Note that capacity of the synchronized FH CDMA system with a noncoherent receiver is less than the capacity of the idealized synchronized FH CDMA system with an OR receiver considered in Section 1.4 [see (1.22)].

EXAMPLE 3.10

Consider a synchronous FH CDMA system with the same bandwidth W and user rate R as in Example 3.6, with maximal acceptable $P_b = 10^{-3}$ *and* 10^{-4}. *The other-cell relative interference factor is* $f = 0.6$, *the voice activity gain is* $\gamma_v = 2.67$, *and the antenna gain is* $\gamma_a = 2.4$. *Determine the uplink radio channel capacity of the system. Neglect the background AWGN.*

Solution

The radio channel capacity of the synchronous multicell FH CDMA system is given by Formula (3.142). Then for $P_b = 10^{-3}$ *we have* $K_0 = 105$, *and for* $P_b = 10^{-4}$ *we have* $K_0 = 73$.

We have considered the case when the users are chip synchronized. In the realistic, asynchronous case each of the $(K-1)$ other users can give two contributions in components of (3.127). This is because a received pulse of the first user can overlap with two received pulses of the kth user, $k \neq 1$. The length of an overlapping with each of the pulses of kth user is on average half of the pulse duration. To avoid cumbersome calculations we consider the single-cell system when the background AWGN is negligible. The output statistics of the matched filters are

$$\hat{z}_{In}^{(1)} = \sqrt{P}\cos\varphi_n^{(1)} + \sqrt{P}\sum_{k=2}^{K}[\hat{\theta}_n^{(k)}\eta_n^{(k)}\cos\varphi_n^{(k)} + \hat{\theta}_{n+1}^{(k)}(1-\eta_n^{(k)})\cos\varphi_{n+1}^{(k)}] + \hat{\xi}_{In}^{(1)}$$

$$\hat{z}_{Qn}^{(1)} = \sqrt{P}\sin\varphi_n^{(1)} + \sqrt{P}\sum_{k=2}^{K}[\hat{\theta}_n^{(k)}\eta_n^{(k)}\sin\varphi_n^{(k)} + \hat{\theta}_{n+1}^{(k)}(1-\eta_n^{(k)})\sin\varphi_{n+1}^{(k)}] + \hat{\xi}_{Qn}^{(1)}$$

$$\check{z}_{\mathrm{I}n} = \sqrt{P}\sum_{k=2}^{K}[\check{\theta}_n^{(k)}\eta_n^{(k)}\cos\varphi_n^{(k)} + \check{\theta}_{n+1}^{(k)}(1-\eta_n^{(k)})\cos\varphi_{n+1}^{(k)}] + \check{\xi}_{\mathrm{I}n}^{(1)}$$

$$\check{z}_{\mathrm{Q}n} = \sqrt{P}\sum_{k=1}^{K}[\check{\theta}_n^{(k)}\eta_n^{(k)}\sin\varphi_n^{(k)} + \check{\theta}_{n+1}^{(k)}(1-\eta_n^{(k)}\sin\varphi_{n+1}^{(k)}] + \check{\xi}_{\mathrm{Q}n}^{(1)} \tag{3.143}$$

The asynchronous FH CDMA system is analyzed in the second part of **APPENDIX A**. Then [see (A.22)–(A.25)]

$$E(\hat{y}_n^{(1)}) = P\left(1 + \frac{2}{3}\,\lambda\right) \tag{3.144}$$

$$E(\check{y}_n^{(1)}) = P\,\frac{2}{3}\,\lambda \tag{3.145}$$

$$\mathrm{var}(\hat{y}_n^{(1)}) \approx P^2\left(\frac{26}{15}\,\lambda + \frac{4}{9}\,\lambda^2\right) \tag{3.146}$$

$$\mathrm{var}(\check{y}_n^{(1)}) \approx P^2\left(\frac{2}{5}\,\lambda + \frac{4}{9}\,\lambda^2\right) \tag{3.147}$$

where $\lambda = (K-1)/M$.

Combining Formulas (3.144)–(3.147) gives the signal-to-noise ratio [compare with (3.139)]

$$\frac{E_\mathrm{b}}{I_0} \approx \frac{P^2N}{2P^2(32\lambda/15 + 8\lambda^2/9)} = \frac{W/R(K-1)}{64/15 + 16\lambda/9} \tag{3.148}$$

The maximum of E_b/I_0 occurs when $\lambda = 0$. Then the radio channel capacity of an asynchronous single-cell FH CDMA system is

$$K_0 \approx 1 + \frac{W/R}{4.25E_\mathrm{b}/I_0} \tag{3.149}$$

Taking into account voice activity monitoring, antenna sectorization, and other-cell interference we estimate the capacity of asynchronous multicell FH CDMA system as

$$K_0 \approx 1 + \frac{W/R}{4.25E_\mathrm{b}/I_0}\,\frac{\gamma_\mathrm{v}\gamma_\mathrm{a}}{1+f} \tag{3.150}$$

EXAMPLE 3.11

Determine the radio channel capacity of the asynchronous multicell FH CDMA system with same parameters (W, R, P_b, γ_v, γ_a and f) as in Example 3.6–3.10. No pilot signaling. The background AWGN is negligible.

Solution

Formula (3.150) gives the following data: The radio channel capacity is equal to 199 *if* $P_b = 10^{-3}$ *and equals* 137 *if* $P_b = 10^{-4}$.

From Example 3.11 we can see that even if we took into account asynchronism, the radio channel capacity of the FH CDMA system is more than four times less than the radio channel capacity of the DS CDMA system. This is partly because of noncoherence, since the receiver in Figure 3.8 is a noncoherent receiver and the receiver in Figure 3.3 is a coherent receiver.

3.7 RECEPTION OF PPH SS SIGNALS

In Section 2.5 we introduced two typical PPH formats employed by an impulse radio system, amplitude on-off modulation and pulse position modulation. In this section we study reception of these signals for the case of uplink transmission in a single-cell system.

The uplink signal $s^{(k)}(t)$ transmitted by the kth user in the PPH CDMA system using amplitude on-off modulation is given by Formula (2.140); that is,

$$s^{(k)}(t) = \sum_{n=-\infty}^{\infty} \frac{v_n^{(k)} + 1}{\sqrt{2}} h_{T_c}(t - nT_f - a_n^{(k)}\Delta) \tag{3.151}$$

Consider the case when a repetition code of length N is used, that is, $v_n^{(k)} = u_{\lfloor n/N \rfloor}^{(k)}$. The received signal is

$$r(t) = \sum_{k=1}^{K} \sqrt{P^{(k)}} s^{(k)}(t - \delta^{(k)}) + \xi(t) \tag{3.152}$$

where $P^{(k)}$ is the power of the received signal from the kth user, $\delta^{(k)}$ is the kth user's time offset, and $\xi(t)$ is the AWGN with two-sided power spectral density $N_0/2$. We assume that $\delta^{(k)}$ is known to the receiver.

Consider the matched filter receiver for the kth user as given in Figure 3.9. As usual, we only study the reception of the 0th block.

The output of the matched filter at time $t^{(k)} = \delta^{(k)} + nT_f + a_n^{(k)}\Delta$ is

$$\begin{aligned} z_n^{(k)} &= \frac{1}{T_c} \int_{-\infty}^{\infty} r(t) h_{T_c}(t - nT_f - a_n^{(k)}\Delta - \delta^{(k)})\, dt \\ &= \sqrt{P^{(k)}} \frac{u_0^{(k)} + 1}{\sqrt{2}} + \sum_{n' \neq n} \sqrt{P^{(k)}} \frac{u_0^{(k)} + 1}{\sqrt{2}} I_{nn'}^{(k)} + \tilde{\xi}_n^{(k)} + \hat{\xi}_n^{(k)} \end{aligned} \tag{3.153}$$

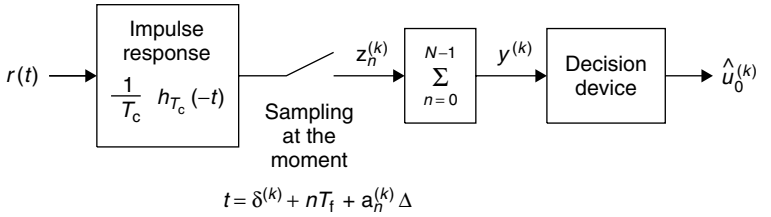

Figure 3.9. PPH CDMA receiver for the kth user.

where

$$I_{nn'}^{(k)} = \frac{1}{T_c} \int_{-\infty}^{\infty} h_{T_c}(t - nT_f - a_n^{(k)}\Delta) h_{T_c}(t - n'T_f - a_{n'}^{(k)}\Delta)\, dt \tag{3.154}$$

is the interframe interference component, $\hat{\xi}_n^{(k)}$ is the component due to the background AWGN noise, and $\tilde{\xi}_n^{(k)}$ is the other-user interference component. If $T_f \gg T_c$ we have $I_{nn'}^{(k)} \approx 0$ for $n' \neq n$, that is, interframe interference is negligible. From (3.153) we have directly

$$E(\hat{\xi}_n^{(k)}) = 0, \ \text{var}(\hat{\xi}_n^{(k)}) = \frac{N_0}{2T_c} \tag{3.155}$$

The other-user interference component $\tilde{\xi}^{(k)}$ is a sum of $(K-1)$ terms $\tilde{\xi}^{(k,k')}$, $k' \neq k$. Here $\tilde{\xi}^{(k,k')}$ is the response of the kth matched filter at time $t^{(k)}$ from the received signal $r^{(k')} = \sqrt{2P^{(k')}}\, s^{(k')}(t - \delta^{(k')})$ from the k'th user. The signal $r^{(k')}(t)$ is the train of pulses uniformly distributed on the frame intervals of length T_f. The probability that a pulse of this train starts in an interval $[t^{(k')}, t^{(k')} + dt)$ is equal to dt/T_f. With probability 1/2 the amplitude of the pulse is equal to zero, and with probability 1/2 it is equal to $\sqrt{2P^{(k')}}$. In the second case the contribution of this pulse to the output of the match filter at time $t^{(k)} = \delta^{(k)} + nT_f + a_n^{(k)}\Delta$ is equal to

$$\sqrt{2P^{(k')}}\, \frac{1}{T_c} \int_{-\infty}^{\infty} h_{T_c}(t - t^{(k)}) \cdot h_{T_c}(t - t^{(k')})\, dt = \sqrt{2P^{(k')}} \cdot R_h(t^{(k')} - t^{(k)}) \tag{3.156}$$

where $R_h(\tau)$ is the normalized autocorrelation function (2.15) of the pulse $h_{T_c}(t)$.

Correspondingly, the average contribution of the k'th user to $z_n^{(k)}$ is

$$E\left(\tilde{\xi}_n^{(k,k')}\right) = \frac{\sqrt{P^{(k')}}}{\sqrt{2}T_f} \int_{-\infty}^{\infty} R_h(\tau)\, d\tau \tag{3.157}$$

For Manchester and differentiated Gaussian pulses the integral on the right-hand side of Formula (3.157) is equal to zero. To find the second moment of the

contribution of the k'th user to the statistics z_n we use a method similar to the one used in Section 3.3 to estimate the other-user interference component.

The autocorrelation function of the signal $r^{(k')}(t) = \sqrt{2P^{(k)}}\, s^{(k)}(t - \delta^{(k)})$ is [compare with (2.143)]

$$R_{r^{(k')}}(\tau) \approx \frac{P^{(k')}}{T_\mathrm{f}} \int_{-\infty}^{\infty} h_{T_\mathrm{c}}(t) h_{T_\mathrm{c}}(t+\tau)\,\mathrm{d}t = T_\mathrm{c} \frac{P^{(k')}}{T_\mathrm{f}} R_h(\tau) \tag{3.158}$$

The two-sided power spectral density of the signal $r^{(k')}(t)$ is [compare with (2.144)]

$$S^{(k')}(f) \approx \frac{P^{(k')}}{T_\mathrm{f}} |H(f)|^2, \quad -\infty < f < \infty \tag{3.159}$$

where $H(f)$ is the Fourier transform of $h_{T_\mathrm{c}}(t)$.

The random process $r^{(k')}(t)$ is the input process of the filter with impulse response $g(t) = h_{T_\mathrm{c}}(-t)/T_\mathrm{c}$ [compare with (2.166)]. Using the same arguments as in Section 2.6, we get the autocorrelation function $R_{z^{(k')}}(\tau)$ of the filter output process $z^{(k')}(t)$:

$$\begin{aligned} R_{z^{(k')}}(\tau) &\approx \frac{1}{T_\mathrm{c}^2} \int_{-\infty}^{\infty} \int_{-\infty}^{\infty} R_{r^{(k')}}(\tau') h_{T_\mathrm{c}}(t) \cdot h_{T_\mathrm{c}}(t - \tau' - \tau)\,\mathrm{d}\tau'\,\mathrm{d}t \\ &= \frac{P^{(k')}}{T_\mathrm{f}} \int_{-\infty}^{\infty} R_h(\tau') R_h(\tau' + \tau)\,\mathrm{d}\tau' \end{aligned} \tag{3.160}$$

From Formula (3.159) it follows analogously to (2.168) that the power spectral density $Z^{(k')}(f)$ of the output random process is

$$Z^{(k')}(f) \approx \frac{P^{(k')}}{T_\mathrm{f} T_\mathrm{c}^2} \cdot |H(f)|^4, \quad -\infty < f < \infty \tag{3.161}$$

The second moment of the filtered output process $z^{(k')}(t)$ is

$$R_{z^{(k')}}(0) \approx \frac{P^{(k')}}{T_\mathrm{f} T_\mathrm{c}^2} \int_{-\infty}^{\infty} |H(f)|^4\,\mathrm{d}f = \frac{P^{(k')}}{T_\mathrm{f}} \int_{-\infty}^{\infty} R_h^2(\tau)\,\mathrm{d}\tau \tag{3.162}$$

Because the first moment of the process $z^{(k')}(t)$ is equal to zero, the variance of the process is equal to the second moment. The variance of $\tilde{\xi}_n^{(k)}$ is equal to the sum of the variances of the components $\tilde{\xi}_n^{(k,k')}$:

$$\begin{aligned} \mathrm{var}(\tilde{\xi}_n^{(k)}) &\approx \frac{1}{T_\mathrm{f} T_\mathrm{c}^2} \int_{-\infty}^{\infty} |H(f)|^4\,\mathrm{d}f \sum_{k' \neq k} P^{(k')} \\ &= \frac{1}{T_\mathrm{f}} \int_{-\infty}^{\infty} R_h^2(\tau)\,\mathrm{d}\tau \sum_{k' \neq k} P^{(k')} \end{aligned} \tag{3.163}$$

Finally, from, Formulas (3.153), (3.155), and (3.163) we get

$$E(z_n^{(k)}) = \begin{cases} \sqrt{2P^{(k)}}, & \text{if } u_0^{(k)} = 1, \\ 0, & \text{otherwise} \end{cases} \tag{3.164}$$

$$\text{var}(z_n^{(k)}) \approx \frac{N_0}{2T_c} + \frac{1}{T_f} \int_{-\infty}^{\infty} R_h^2(\tau)\, d\tau \sum_{k' \neq k} P^{(k')} \tag{3.165}$$

Assuming that the system has perfect power control and that all signals have constant power P throughout the transmission period, we get the following expressions for the moments of the decision statistic $y^{(k)} = \sum_{n=0}^{N-1} z_n^{(k)}$:

$$E(y^{(k)}) = \begin{cases} \mu_1 \stackrel{\text{def}}{=} \sqrt{2P}\, N, & \text{if } u_0 = 1, \\ \mu_{-1} \stackrel{\text{def}}{=} 0, & \text{otherwise} \end{cases} \tag{3.166}$$

$$\sigma^2 \stackrel{\text{def}}{=} \text{var}(y^{(k)}) = \frac{N_0}{2T_c} N + \frac{N(K-1)P}{T_f} \int_{-\infty}^{\infty} R_h^2(\tau)\, d\tau \tag{3.167}$$

Our goal is to construct a symmetrical decision rule such that the error probability conditioned on $u_0 = 1$ should be equal to the error probability conditioned on $u_0 = -1$. This is the decision rule

$$y^{(k)} \begin{array}{c} H_1 \\ > \\ < \\ H_{-1} \end{array} \frac{\mu_1 + \mu_{-1}}{2} = \sqrt{P}\, N/\sqrt{2} \tag{3.168}$$

The following parameter, on SNR per bit, defines the performances of the receiver:

$$\begin{aligned} \frac{E_b}{I_0} \stackrel{\text{def}}{=} \frac{[(\mu_1 - \mu_{-1})/2]^2}{2\sigma^2} &= \frac{PT_c N}{2\left[N_0 + \dfrac{2P(K-1)T_c}{T_f} \displaystyle\int_{-\infty}^{\infty} R_h^2(\tau)\, dt\right]} \\ &= \frac{PT_c N}{2\left[N_0 + \dfrac{2P(K-1)}{T_f T_c} \displaystyle\int_{-\infty}^{\infty} |H(f)|^4\, df\right]} \end{aligned} \tag{3.169}$$

Using the Gaussian approximation, we get from (3.21) and (3.168) the following expression for the bit error probability:

$$P_b = Q\left(\sqrt{\frac{2E_b}{I_0}}\right) \tag{3.170}$$

From (3.170) we can find the radio channel capacity of the PPH CDMA system. Particularly, if we ignore the background noise, we get for Manchester pulse shaping

$$K_0 = 1 + \frac{T_f N}{4\dfrac{E_b}{I_0}\displaystyle\int_{-\infty}^{\infty} R_h^2(\tau)\,d\tau}$$

$$= 1 + \frac{W/R}{E_b/I_0}\frac{T_c}{8\displaystyle\int_{-\infty}^{\infty} R_h^2(\tau)\,d\tau} = 1 + \frac{W/R}{E_b/I_0}\frac{T_c^3}{8\displaystyle\int_{-\infty}^{\infty} |H(f)|^4\,df} \tag{3.171}$$

where $W = 2/T_c$ is the Manchester pulse bandwidth and $R = 1/NT_f$ is the transmission rate.

Because for Manchester pulses $\int_{-\infty}^{\infty} R_h^2(\tau)\,d\tau = T_c/3$ (Problem 3.17), we get from (3.171) the following expression for the radio channel capacity of a PPH CDMA system using amplitude on-off modulation with Manchester pulses:

$$K_0 = 1 + \frac{3}{8}\,\frac{W/R}{E_b/I_0} \tag{3.172}$$

The expression for the radio channel capacity of a PPH CDMA system is similar to the expression for the radio channel capacity of a DS CDMA system (1.10), but because the signal bandwidth in the second case is much less than in the first case, the PPH CDMA system potentially provides much larger capacity.

EXAMPLE 3.12

Find the radio channel capacity of a single-cell PPH CDMA system using Manchester pulses of duration 1 *ns, if the maximal acceptable* $P_b = 10^{-3}$ *or* 10^{-4} *and the transmission rate* $R = 10$ *kb/s. Neglect background noise.*

Solution

To $P_b = 10^{-3}$ *corresponds* $E_b/I_0 = 4.77$. *Then from Formula (3.172) we get* $K_0 = 15724$. *If* $P_b = 10^{-4}$, *then* $E_b/I_0 = 6.92$ *and* $K_0 = 10839$.

Consider now a PPH CDMA system using another modulation format, pulse position modulation. The signal transmitted by the kth user is defined by Formula (2.147),

$$s^{(k)}(t) = \sum_{n=-\infty}^{\infty} h_{T_c}\left(t - nT_f - a_n^{(k)}\Delta + \frac{v_n^{(k)}}{2}T_c\right) \tag{3.173}$$

The received signal is given by (3.152). The correlation (matched filter) receiver is analogous to the one presented in Figure 3.9, where the matched filter with

impulse response $h_{T_c}(-t)/T_c$ should be replaced by a filter with impulse response

$$g(t) = \frac{1}{T_c}\left[h_{T_c}\left(-t + \frac{T_c}{2}\right) - h_{T_c}\left(-t - \frac{T_c}{2}\right)\right] \tag{3.174}$$

The output of the matched filter at the moment $t = \delta^{(k)} + nT_f + a_n^{(k)}\Delta$ is [compare with (3.153)]

$$z_n^{(k)} = \frac{1}{T_c}\int_{-\infty}^{\infty} r(t)\left[h_{T_c}\left(t - nT_f - a_n^{(k)}\Delta + \frac{T_c}{2} - \delta^{(k)}\right)\right.$$
$$\left. - h_{T_c}\left(t - nT_f - a_n^{(k)}\Delta - \frac{T_c}{2} - \delta^{(k)}\right)\right] dt = \sqrt{P^{(k)}}u_0^{(k)} + \tilde{\xi}_n^{(k)} + \hat{\xi}_n^{(k)} \tag{3.175}$$

where we ignore interframe interference components. Here $\tilde{\xi}_n^{(k)}$ and $\hat{\xi}_n^{(k)}$ are components due to the other-user interference and the background noise.

The decision rule is

$$y^{(k)} \overset{\text{def}}{=} \sum_{n=0}^{N-1} z_n^{(k)} \underset{H_{-1}}{\overset{H_1}{\gtrless}} 0 \tag{3.176}$$

The autocorrelation function of the impulse response function $g(t)$ is

$$R_g(\tau) = \frac{1}{T_c}\int_{-\infty}^{\infty}\left[h_{T_c}\left(-t + \frac{T_c}{2}\right) - h_{T_c}\left(-t - \frac{T_c}{2}\right)\right]$$
$$\times\left[h_{T_c}\left(-t + \frac{T_c}{2} + \tau\right) - h_{T_c}\left(-t - \frac{T_c}{2} + \tau\right)\right] dt$$
$$= 2R_h(\tau) - R_h(\tau - T_c) - R_h(\tau + T_c) \tag{3.177}$$

and the Fourier transform of $R_g(\tau)$ is

$$\mathcal{F}\{R_g(\tau)\} = \frac{2}{T_c}|H(f)|^2 - \frac{2}{T_c}|H(f)|^2\cos(2\pi f T_c)$$
$$= \frac{2}{T_c}|H(f)|^2[1 - \cos(2\pi f T_c)] \tag{3.178}$$

The background noise component $\hat{\xi}^{(k)}$ is a zero-mean Gaussian variable with variance N_0/T_c. The other-user interference component is analyzed analogously to (3.156)–(3.165).

Let $r^{(k')}(t)$, $k' \neq k$, which is the received signal from the k'th user, the input process of the filter. The autocorrelation function of the signal $r^{(k')}(t)$ is given by (3.158). The autocorrelation function of the output process $z^{(k')}(t)$ is

$$\begin{aligned} R_{z^{(k')}}(\tau) &= \frac{P^{(k')}}{T_{\mathrm{f}}} \int_{-\infty}^{\infty} R_h(\tau') R_g(\tau' + \tau)\, \mathrm{d}\tau' \\ &= \frac{2P^{(k')}}{T_{\mathrm{f}}} \int_{-\infty}^{\infty} R_h(\tau') R_h(\tau' + \tau)\, \mathrm{d}\tau' \\ &\quad - \frac{P^{(k')}}{T_{\mathrm{f}}} \int_{-\infty}^{\infty} R_h(\tau') R_h(\tau' + \tau - T_{\mathrm{c}})\, \mathrm{d}\tau' \\ &\quad - \frac{P^{(k')}}{T_{\mathrm{f}}} \int_{-\infty}^{\infty} R_h(\tau') R_h(\tau' + \tau + T_{\mathrm{c}})\, \mathrm{d}\tau' \end{aligned} \tag{3.179}$$

Because the second and third integrals in (3.179) coincide, we have

$$R_{z^{(k')}}(0) = \frac{2P^{(k')}}{T_{\mathrm{f}}} \int_{-\infty}^{\infty} R_h^2(\tau)\, \mathrm{d}\tau - \frac{2P^{(k')}}{T_{\mathrm{f}}} \int_{-\infty}^{\infty} R_h(\tau) R_h(\tau + T_{\mathrm{c}})\, \mathrm{d}\tau \tag{3.180}$$

For the Manchester pulse $\int_{-\infty}^{\infty} R_h^2(\tau)\, \mathrm{d}\tau = T_{\mathrm{c}}/3$, $\int_{-\infty}^{\infty} R_h(\tau) R_h(\tau + T_{\mathrm{c}})\, \mathrm{d}\tau = 0$ (Problem 3.17).

Then for the Manchester pulse, the first two moments of the decision statistic $y^{(k)}$ are

$$E(y^{(k)}) = \sqrt{P^{(k)}}\, u_0^{(k)} N \tag{3.181}$$

$$\sigma^2 \stackrel{\mathrm{def}}{=} \mathrm{var}(y^{(k)}) = N \left[\frac{N_0}{T_{\mathrm{c}}} + \frac{2T_{\mathrm{c}}}{3T_{\mathrm{f}}} \sum_{k' \neq k} P^{(k')} \right] \tag{3.182}$$

The SNR per bit for the PPH CDMA system with perfect power control is

$$\frac{E_{\mathrm{b}}}{I_0} = \frac{N}{\dfrac{4T_{\mathrm{c}}}{3T_{\mathrm{f}}}(K-1) + \dfrac{2N_0}{PT_{\mathrm{c}}}} \tag{3.183}$$

If AWGN is negligible, the radio channel capacity of a PPH CDMA system with pulse position modulation is

$$K_0 = 1 + \frac{3}{8} \frac{W/R}{E_{\mathrm{b}}/I_0} \tag{3.184}$$

The radio channel capacity of the PPH CDMA system using pulse position modulation with Manchester pulses is the same as for the system using amplitude on-off modulation [compare Formulas (3.172) and (3.184)].

The PPH CDMA system using pulse position modulation with differentiated Gaussian pulses has a slightly different capacity than the PPH CDMA system using amplitude on-off modulation (see Problems 3.18 and 3.19).

3.8 COMMENTS

In the derivation of the optimum receivers for signals corrupted by AWGN and other-user interference we applied a mathematical technique that was originally used in deriving optimum detector structures for radar. The detection methods are based on hypothesis testing as developed by the statisticians Neyman and Pearson. For further reading we can recommend classic books by Davenport and Root [11], Helstrom [20], and Van Trees [45]. A number of books have been published on the topic of reception of modulated signals ([28], [38], [37], [57]). In our treatment of the reception of uplink transmitted DS CDMA signals we follow the book of Viterbi [47]. The downlink transmission was studied in more detail by Wintzell [58]. The analysis of FH CDMA given in Section 3.6 is original. In Section 3.7 our theory of reception of PPH signals follows [40, 41].

PROBLEMS

3.1. A choice is made between hypotheses H_0 and H_1 on the basis of a single measurement of a positive quantity r

$$H_0 : \ r = \eta$$
$$H_1 : \ r = s + \eta$$

Here s and η are independent positive random variables with the probability density functions

$$p(\eta) = be^{-b\eta}, \quad \eta \geq 0,$$
$$p(s) = ce^{-cs}, \quad s \geq 0$$

where $c > b > 0$.

a) Calculate the probability density function of r under H_0 and H_1.

b) Prove that the likelihood ratio test reduces to

$$r \underset{H_0}{\overset{H_1}{\gtrless}} \theta$$

c) Find θ as the function of P_F, where

$$P_F \overset{\text{def}}{=} P(\text{accept } H_1 | H_0 \text{ is true}).$$

3.2. Consider a ternary communication system with equally likely signals

$$s_0(t) = 0,$$
$$s_1(t) = A \sin \omega_0 t,$$
$$s_2(t) = -A \sin \omega_0 t$$

a) Design a likelihood ratio test to minimize the error probability.

b) Show that the probability of a correct decision is

$$P_c = \frac{2}{3}\left[2\int_0^{\sqrt{E/2N_0}} \frac{1}{\sqrt{2\pi}} \exp\left(-\frac{u^2}{2}\right) du + \frac{1}{2}\right]$$

c) Compare this system with coherent BFSK. Which one is best in terms of error probability?

3.3. A decision problem requires us to decide among two signal hypothesis. Under H_0 the observation is normal with zero mean and unit variance, whereas under H_1 the observation is normal with zero mean and variance 16. Ten independent observations are made.

Assuming that the false alarm probability is equal to the probability of a miss, find the threshold for the likelihood test ratio of Example 3.3 and the probability of error.

3.4. Consider the downlink transmission in a DS CDMA system, where the transmitted signal is given by Formula (3.89) with $\phi^{(k)} = 0, k = 0, 1, \ldots K$. Show that the radio channel capacity of the system is about two times less than the capacity of the system considered in Section 3.4, where the phase shifts $\phi^{(k)}$ are independent random variables uniformly distributed on $[0.2\pi)$.

3.5. Suppose that binary PSK is used for transmitting information over an AWGN channel with two-sided power spectral density $N_0/2 = 10^{-10}$ W/Hz. The transmitted signal energy is $E = PT_c$, where T_c is the pulse duration and P is the signal power. Determine the signal power required to achieve an error probability of 10^{-6} when the data rate is

a) 10 kb/s

b) 100 kb/s

c) 1 Mb/s

3.6. Differentially encode the following binary sequences:

a) $1\ -1\ -1\ \ 1\ -1 \qquad -1\ \ 1\ \ 1\ -1\ \ 1 \qquad 1\ \ 1 \qquad 1\ -1\ -1$

b) $1\ \ 1\ -1\ -1\ -1 \qquad 1\ -1\ -1\ -1\ \ 1 \qquad -1\ -1 \qquad 1\ \ 1\ -1$

c) $-1\ -1\ -1\ \ 1\ -1 \qquad 1\ -1\ -1\ -1\ -1 \qquad 1\ -1 \qquad 1\ \ 1\ \ 1$

3.7. Suppose we wish to transmit the data sequence

$$-1,\ -1,\ 1,\ -1,\ -1,\ 1,\ 1,\ -1,\ 1,\ -1,\ -1,\ 1$$

using differential BPSK. Let $\tilde{s}(t) = \sqrt{2}\, h_{T_c}(t - nT_c)\ \cos(2\pi f_c t + \phi)$ represent the signal waveform in the nth signaling interval of duration T_c. Give the phase of the transmitted signal for the data sequence. Use $\phi_0 = 0$ for the phase of the first (reference) signal waveform. Determine and sketch the power density spectrum of the signal transmitted by differential BPSK.

3.8. In differential BPSK, the receiver measures the following sequence of phases: 50°, 51°, 228°, 235°, 49°, 226°. Decode the sequence using the first phase measurement as a reference.

3.9. A total of 50 equal-power users are to share a common communication channel by DS CDMA. Each user transmits information at a rate of 10 kb/s using coherent BPSK. Determine the minimum chip rate to obtain a bit error probability of 10^{-4}. Neglect the background AWGN. Assume that there is no voice activity monitoring and that the antenna is omnidirectional.

3.10. Consider a DS CDMA system with a processing gain of 1000 and BPSK modulation. Determine the number of users if the system has perfect power control and the desired level of error probability is 10^{-5}. Assume that there is no voice activity monitoring and that antenna is omnidirectional. The pilot signal puncturing rate $1/g \ll 1$. Repeat the computation with the processing gain changed to 500 and the error probability changed to 10^{-6}.

3.11. Consider a DS BPSK CDMA system communicating over an uplink AWGN channel of bandwidth 5 MHz. The user rate is $R = 10$ kb/s. The two-sided power spectral density of the AWGN is $N_0/2 = 10^{-10}$ W/Hz. The maximal acceptable P_b is 10^{-4}. Other parameters are voice activity gain $\gamma_v = 2.67$, antenna gain $\gamma_a = 2.4$, pilot chip rate $1/g = 0.2$, and other-cell relative interference factor $f = 0.6$. The system uses a repetition code and has perfect power control. The power of the received signal is $P = 0.1$ mW. Find the radio channel capacity of the system.

3.12. Consider a coherent DS BPSK CDMA system of bandwidth $W = 20$ MHz with K users. Assuming that the system has perfect power control, that all users transmit information at rate $R = 9.6$ kb/s, that delays and phases of the received signals are known exactly, and that the maximal acceptable bit error probability P_b is 10^{-5}, calculate the capacity of the single-cell system. Transmitted signals are sequences of ideal nonoverlapping rectangular pulses. Neglect the influence of the background noise. The voice activity factor is $\gamma_v = 8/3$, and the antenna is omnidirectional.

3.13. Consider uplink transmission in a DS CDMA system consisting of 150 users that transmit information at a rate of 10000 b/s, each using a DS spread spectrum signal operating at a chip rate of 10 MHz. The modulation is binary PSK, the system has perfect power control, and the background AWGN is negligible. There is no voice activity monitoring and antenna sectorization. The pilot signal puncturing rate $1/g \ll 1$.

a) Determine the signal-to-noise ratio on the input of the receiver of the base station.

b) What is the processing gain?

c) How much should the processing gain be increased to allow for doubling the number of users without affecting the input SNR?

3.14. For the IS-95 proposal for DS CDMA, it has been found that a signal-to-interference ratio of 6 dB suffices for voice communication in the uplink direction. In IS-95 the bandwidth of a channel is 1.25 MHz and the bit rate is 9.6 kb/s. Assume that the voice activity factor is 8/3, that three sectored antennas are used, and that the interference from the users in the other cells is 60% of the interference from the users in the home cell. Note that uplink transmission does not use pilot signaling. If the background noise can be neglected, what is the maximum number of users per channel?

3.15. Prove that the downlink system that transmits the signal (3.104) has the same capacity as the system that transmits the signal (3.89).

3.16. Repeat Problem 3.10 assuming that the DS CDMA system uses differential PSK.

3.17. Prove that for Manchester pulses

$$\int_{-\infty}^{\infty} R_h^2(\tau)\,\mathrm{d}t = T_c/3, \int_{-\infty}^{\infty} R_h(\tau)R_h(\tau' + T_c)\,\mathrm{d}\tau = 0$$

3.18. Find the capacity of a PPH CDMA system using amplitude on-off modulation with differentiated Gaussian pulse shaping.

3.19. Find the capacity of a PPH CDMA system using pulse position modulation with differentiated Gaussian pulse shaping.

4

FORWARD ERROR CONTROL CODING IN SPREAD SPECTRUM SYSTEMS

Spectrum spreading by itself produces large communication system performance improvements, especially in multipath channels and in an interference environment. Further improvements can be reached by using a universally effective method of exploiting redundancy, *forward error control* or *forward error-correcting (FEC) coding*.

A FEC encoder can be viewed as an additional level of digital linear filtering (over the binary field) that introduces redundancy in the original digital data sequence. Such redundancy is already present in a spread spectrum system and available for exploitation.

Error-correcting coding is a topic to which entire books are dedicated. In this chapter only a few basic concepts of FEC are discussed, emphasizing low-rate codes, suitable for wideband communication. We study two major types of codes, block codes and convolutional codes. We consider especially low-rate first-order Reed–Muller (block) codes, orthogonal convolutional codes, and some concatenated code constructions that are already used in CDMA systems.

4.1 INTRODUCTION TO BLOCK CODING

As we mentioned above, with block coding the information sequence is divided into blocks of length L and each block is mapped into blocks of N code symbols. This mapping is independent from the previous blocks, that is, there exists no memory from one block to another block.

Theory of Code Division Multiple Access Communication, by Kamil Sh. Zigangirov
ISBN 0-471-45712-4

Table 4.1 Addition and Multiplication in $GF(2)$

Addition			Multiplication		
$+$	0	1	$\times$	0	1
0	0	1	0	0	0
1	1	0	1	0	1

For the construction and description of binary codes, classic coding theory uses the binary logical alphabet (or, equivalently, operations in the binary *Galois field* $GF(2)$) instead of the real number alphabet $\{1, -1\}$ that we used in the previous chapters. For the description of binary codes, we will use both logical alphabet language and the real number alphabet language. The mapping $0 \leftrightarrow 1$ and $1 \leftrightarrow -1$ establishes one-to-one correspondence between code symbols of a code presented in the binary logical alphabet and a code presented in the real number alphabet.

Consider first linear block codes over $GF(2)$. The addition and multiplication tables for $GF(2)$ are shown in Table 4.1, which are operations mod 2.

A binary block (N, L)-code consists of 2^L binary sequences $\boldsymbol{\alpha}_i$ of length N called codewords,

$$\boldsymbol{\alpha}_i = (\alpha_{i0}, \alpha_{i1}, \ldots \alpha_{i,(N-1)}), \quad i = 0, 1, \ldots, 2^L - 1, \quad \alpha_{in} \in GF \tag{4.1}$$

A block code is linear if it includes the all-zero codeword and if the vector sum of two codewords $\boldsymbol{\alpha}_i = (\alpha_{i0}, \alpha_{i1}, \ldots, \alpha_{i,(N-1)})$ and $\boldsymbol{\alpha}_j = (\alpha_{j0}, \alpha_{j1}, \ldots, \alpha_{j,(N-1)})$ in $GF(2)$,

$$\boldsymbol{\alpha}_i + \boldsymbol{\alpha}_j = (\alpha_{i0} + \alpha_{j0}, \alpha_{i1} + \alpha_{j1}, \ldots, \alpha_{i,(N-1)} + \alpha_{j,(N-1)}) \tag{4.2}$$

is also a codeword. Note that linearity of a code only depends on the codewords and not on the way that the information sequence

$$\boldsymbol{\beta}_i = (\beta_{i0}, \beta_{i1}, \ldots, \beta_{i,(L-1)}), \quad i = 0, 1, \ldots, 2^L - 1, \quad \beta_{i\ell} \in GF(2) \tag{4.3}$$

is mapped into the codeword $\boldsymbol{\alpha}_i$. However, it is natural to assume that if the information sequence $\boldsymbol{\beta}$ is mapped into the codeword $\boldsymbol{\alpha}$ and the information sequence $\boldsymbol{\beta}'$ is mapped into $\boldsymbol{\alpha}'$, then $\boldsymbol{\beta} + \boldsymbol{\beta}'$ is mapped into $\boldsymbol{\alpha} + \boldsymbol{\alpha}'$, where addition is in $GF(2)$.

Suppose that to codewords $\boldsymbol{\alpha}_i$, $\boldsymbol{\alpha}_j$ in the binary logical alphabet $\{0, 1\}$ correspond codewords $\boldsymbol{v}_i = (v_{i0}, v_{i1}, \ldots, v_{i,(N-1)})$ and $\boldsymbol{v}_j = (v_{j0}, v_{j1}, \ldots, v_{j,(N-1)})$ in the real number alphabet $\{1, -1\}$. Then

$$\boldsymbol{v}_i * \boldsymbol{v}_j \stackrel{\text{def}}{=} (v_{i0}v_{j0}, v_{i1}v_{j1}, \ldots, v_{i,(N-1)}v_{j,(N-1)}) \tag{4.4}$$

corresponds to $\boldsymbol{\alpha}_i + \boldsymbol{\alpha}_j$.

Independently from the alphabet, the *Hamming distance* between two words is defined as the number of positions in which the words differ. The *minimum distance* $d_{\min}$ of a code is the minimum Hamming distance between any two different codewords.

An important parameter of a codeword is its *weight*, which is simply the number of nonzero elements in the logical alphabet representation of the code and number of -1s in the real number alphabet representation. By listing the various Hamming weights, w, of the codewords, and the number of codewords, a_w, at each weight, we obtain the *weight spectrum* of the code.

The important result is that for a linear code the set of Hamming distances between distinct codewords is the same as the set of weights of the nonzero (in $GF(2)$) codewords in the code and is invariant to the choice of reference codeword. Then a_w can for a linear code be treated as the number of codewords at distance w from any reference codeword.

Suppose that the symbols of the codeword are transmitted using BPSK in the AWGN channel. Thus each codeword $\boldsymbol{v}_i = (v_{i0}, v_{i1}, \ldots, v_{i,(N-1)})$, $v_{in} \in \{1, -1\}$ results in one of 2^L signals [compare with Formula (2.86)]

$$s_i(t) = \sqrt{2} \sum_{n=0}^{N-1} v_{in} h_{T_p}(t - nT_c) \cos(2\pi f_c t + \phi), \quad i = 0, 1, 2, \ldots, 2^L - 1 \quad (4.5)$$

where $h_{T_c}(t)$ is a pulse of duration T_c, f_c is the carrier frequency, and ϕ is the phase.

The received signal is

$$r(t) = \sqrt{P} \sum_{n=0}^{N-1} v_{in} h_{T_p}(t - nT_p - \delta) \cos[2\pi f_c(t - \delta) + \varphi] + \xi(t) \quad (4.6)$$

where P is the power of the received signal, δ is propagation delay, φ is the phase, and $\xi(t)$ is AWGN with two-sided power spectral density $N_0/2$.

The demodulator part of the receiver is presented in Figure 3.3. The despreading part should be excluded and the index k dropped. If the ith codeword was sent, at the output of the demodulator we have the sequence of the statistics

$$z_n = \sqrt{P} v_{in} + \tilde{\xi}_n \stackrel{\text{def}}{=} \mu v_{in} + \tilde{\xi}_n \quad (4.7)$$

where $\mu = \sqrt{P}$, and $\tilde{\xi}_n$ is a sequence of IID zero-mean Gaussian variables with variances $N_0/2T_c$. The decision block in Figure 3.3 should be replaced by the *decoder block*. Consider the *maximum likelihood* (ML) *decoding*.

Let us treat the problem of the symmetrical binary hypothesis testing of Example 3.2 as decoding of the repetition code that consists of two N-dimensional antipodal codewords

$$\boldsymbol{v}_0 = (v_{00}, v_{01}, \ldots, v_{0,(N-1)}) = (1, 1, \ldots, 1)$$

and

$$\boldsymbol{v}_1 = (v_{10}, v_{11}, \ldots, v_{1,(N-1)}) = (-1, -1, \ldots, -1)$$

Let us replace the operation of calculation decision statistic y in (3.73) by calculation of two decision statistics

$$y_0 = \sum_{n=0}^{N-1} z_n v_{0n}$$

and

$$y_1 = \sum_{n=0}^{N-1} z_n v_{1n}$$

Then the likelihood ratio test (3.73) is equivalent to the ML decision test:

Accept H_1 *if* $y_0 > y_1$,

Accept H_{-1} *if* $y_0 < y_1$

Suppose now that we have not 2 but 2^L different codewords. If the channel is an AWGN channel, then the conditional probability density function to receive the vector $\boldsymbol{z} = (z_0, z_1, \ldots, z_{N-1})$ given the transmitted codeword $\boldsymbol{v}_i$, $i = 0, 1, \ldots, 2^L - 1$, is

$$p(\boldsymbol{z}\,|\boldsymbol{v}_i) = \left(\frac{1}{\sqrt{2\pi\sigma^2}}\right)^N \exp\left[-\sum_{n=0}^{N-1}(z_n - \mu v_{in})^2/2\sigma^2\right] \tag{4.8}$$

where $\mu = \sqrt{P}$, $\sigma^2 = N_0/2T_c$.

The conditional probability density function $p(\boldsymbol{z}\,|\boldsymbol{v}_i)$ or any monotonic function of it is usually called the *likelihood function*. The decision criterion based on the maximum of $p(\boldsymbol{z}\,|\boldsymbol{v}_i)$ over the 2^L hypotheses is called the *ML criterion*. In the case of an AWGN channel, we may work with the natural logarithm of $p(\boldsymbol{z}\,|\boldsymbol{v}_i)$, which is a monotonic function. Thus

$$\ln p(\boldsymbol{z}\,|\boldsymbol{v}_i) = -\frac{N}{2}\ln(2\pi\sigma^2) - \sum_{n=0}^{N-1}(z_n - \mu v_{in})^2/2\sigma^2 \tag{4.9}$$

The maximum of $\ln p(\boldsymbol{z}\,|\boldsymbol{v}_i)$ over $\boldsymbol{v}_i$ is equivalent to finding the vector $\boldsymbol{v}_i$ that minimizes the squared Euclidean distance

$$d_E(\boldsymbol{z}, \boldsymbol{v}_i) = \sum_{n=0}^{N-1}(z_n - \mu v_{in})^2 \tag{4.10}$$

Hence, for the AWGN channel the decoding rule based on the ML criterion reduces to finding the codeword $\boldsymbol{v}_i$ that is closest in distance to the vector $\boldsymbol{z}$. We will refer to this decoding rule as a *minimum-distance decoding*.

Another interpretation of the optimum decision rule based on the ML criterion is obtained by expanding the distance metric in (4.10) as

$$d_E(\boldsymbol{z}, \boldsymbol{v}_i) = \sum_{n=0}^{N-1} z_n^2 - 2\mu \sum_{n=0}^{N-1} z_n v_{in} + \mu^2 \sum_{n=0}^{N-1} v_{in}^2$$
$$= \sum_{n=0}^{N-1} z_n^2 - 2\mu \sum_{n=0}^{N-1} z_n v_{in} + N\mu^2 \tag{4.11}$$

The first and the third terms are common for all decision metrics, and, hence, they may be ignored in the computations of the metrics. The result is a set of metrics

$$y_i = \frac{\mu}{2\sigma^2} \sum_{n=0}^{N-1} z_n v_{in}, \quad i = 0, 1, \ldots, 2^L - 1 \tag{4.12}$$

that are usually called the *correlation metrics*. Here we normalized the correlation by the factor $\mu/2\sigma^2$. Obviously, it can be omitted. So, the ML decoder can be realized as a parallel bank of 2^L correlators matched to the 2^L possible transmitted codewords. The outputs of the 2^L correlators are compared, and the codeword corresponding to the largest correlator output is selected.

From (4.7) and (4.12) follows that if the ith codeword was sent [compare with Formulas (3.19) and (3.20)]

$$E(y_j) = \begin{cases} \rho_B, & \text{if } j = i, \\ \rho_B \left(1 - \dfrac{2d_{ij}}{N}\right), & \text{if } j \neq i, \end{cases} \tag{4.13}$$

$$\text{var}(y_j) = \rho_B/2, \quad j = 0, 1, \ldots, 2^L - 1 \tag{4.14}$$

where d_{ij} is the Hamming distance between $\boldsymbol{v}_i$ and $\boldsymbol{v}_j$, and $\rho_B = \mu^2 N/2\sigma^2 = PT_c N/N_0$ is the SNR per block. Obviously, y_j are Gaussian variables.

In determining the probability of error for a linear block code, note that when such a code is employed on the AWGN channel with ML decoding, the error probability for the transmission of the ith codeword is the same for all i, $i = 0, 1, \ldots, 2^L - 1$. Hence, we assume for simplicity that the all-zero (in logical alphabet) or all-one (in real number alphabet) codeword labeled here by index 0, $\boldsymbol{v}_0$, is transmitted. For correct decoding the correlation metric y_0 must exceed all the other $2^L - 1$ correlation metrics y_j.

The derivation of the exact expression for the probability of erroneous decoding is complicated by the correlation among the 2^L correlation metrics. Instead of attempting to derive the exact error probability, we resort to a *union bound* (Problem 4.1). That is, if $\mathcal{E}_i$ represents the events that $y_i \geq y_0$ for $i \neq 0$, and $\mathcal{E}$

is the union of events $\mathcal{E}_i$, $\mathcal{E} = \bigcup_{i=1}^{2^L-1} \mathcal{E}_i$, then we have

$$P(\mathcal{E}) = P\left(\bigcup_{i=1}^{2^L-1} \mathcal{E}_i\right) \leq \sum_{i=1}^{2^{L-1}} P(\mathcal{E}_i) \tag{4.15}$$

The probability $P_B = P(\mathcal{E})$ is called the *block error probability*. To calculate the probability P_B we consider the following example.

EXAMPLE 4.1

Prove that the probability of confusing two codewords at Hamming distance w, when BPSK is employed over the AWGN channel with two-sided noise spectral density $N_0/2$, is

$$P_w = Q\left(\sqrt{2\rho_c w}\right)$$

where ρ_c is SNR per chip.

Solution

The probability of confusing two codewords depends only on the symbols that differ. Let us suppose that these are the first w symbols. The probability density function to receive $\boldsymbol{z} = (z_0, z_1, \ldots, z_{w-1})$ given that the vector $\boldsymbol{v}_0 = (v_{00}, v_{01}, \ldots v_{0,w-1}) = (1, 1, \ldots, 1)$ was sent is (see Example 3.2)

$$p(\boldsymbol{z}|\boldsymbol{v}_0) = \left(\frac{1}{\sqrt{2\pi\sigma^2}}\right)^w \exp\left[-\sum_{n=1}^{w-1}(z_n - \mu)^2/2\sigma^2\right]$$

where $\mu = \sqrt{P}$, $\sigma^2 = N_0/2T_c$, P is the power of the received signal, and T_c is the chip duration. The probability density function to receive $\boldsymbol{z} = (z_0, z_1, \ldots, z_{w-1})$ given that the vector $\boldsymbol{v}_1 = -\boldsymbol{v}_0$ was sent is

$$p(\boldsymbol{z}|\boldsymbol{v}_1) = \left(\frac{1}{\sqrt{2\pi\sigma^2}}\right)^w \exp\left[-\sum_{n=1}^{w}(z_n + \mu)^2/2\sigma^2\right]$$

Then, analogously to (3.21), we get

$$P_w = Q\left(\sqrt{2\rho_c w}\right) \tag{4.16}$$

where $\rho_c = PT_c/N_0$ and the Q function is defined by Formula (1.12).

From Formulas (4.15) and (4.16) we have

$$P_B \leq \sum_{i=1}^{2^L-1} Q(\sqrt{2\rho_c w_i}) = \sum_{w=d_{\min}}^{N} a_w Q(\sqrt{2\rho_c w}) \tag{4.17}$$

where a_w is the weight spectrum of the code, that is, the number of the codewords having weight w, and $d_{\min}$ is the minimum distance of the code.

Because for rate r codes the SNR per bit E_b/N_0 is equal to ρ_c/r, we can rewrite Formula (4.17) as

$$P_B \leq \sum_{w=d_{\min}}^{N} a_w \; Q(\sqrt{2E_b r w/N_0}) \tag{4.18}$$

A somewhat looser bound is obtained by using the inequality (see Problem 1.5) $Q(x) < (1/2)\exp(-x^2/2)$, $x \geq 0$. Consequently,

$$P_B < \frac{1}{2} \sum_{w=d_{\min}}^{N} a_w \exp(-\rho_c w) = \frac{1}{2} \sum_{w=d_{\min}}^{N} a_w \exp\left(-\frac{E_b}{N_0}\, r w\right) \tag{4.19}$$

The function

$$T(W) = \sum_{w=d_{\min}}^{N} a_w W^w \tag{4.20}$$

is called the *weight enumerator function* of the code. Then

$$P_B < \frac{1}{2}\, T(W)\Big|_{W=\exp\left(-\frac{E_b}{N_0}\, r\right)} \tag{4.21}$$

In the next section we consider in more detail the first-order Reed–Muller codes and their application in DS CDMA communication using coherent BPSK modulation.

4.2 FIRST-ORDER REED–MULLER CODE

The *first-order Reed-Muller codes* are binary linear codes whose lengths N are a power of 2, and whose code rate r is $L/N = (\log_2 N + 1)/N$. We give the description of these codes in terms of a Hadamard matrix using the real number alphabet description.

A Hadamard matrix is an orthogonal $N \times N$ matrix whose elements are real number 1 and -1. An *orthogonal* matrix is a matrix whose rows are orthogonal n-tuples (over the field of real numbers). The 2×2 Hadamard matrix is

$$M_2 = \begin{bmatrix} 1 & 1 \\ 1 & -1 \end{bmatrix} \tag{4.22}$$

The 4×4 Hadamard matrix is

$$M_4 = \begin{bmatrix} 1 & 1 & 1 & 1 \\ 1 & -1 & 1 & -1 \\ 1 & 1 & -1 & -1 \\ 1 & -1 & -1 & 1 \end{bmatrix}$$

Generally, if M is an $N \times N$ Hadamard matrix, then the matrix

$$M' = \begin{bmatrix} M & M \\ M & -M \end{bmatrix}$$

is a $2N \times 2N$ Hadamard matrix.

Let M be an $N \times N$ Hadamard matrix. The first-order Reed–Muller code is constructed as follows: form the set of $2N$ vectors $\boldsymbol{m}_0, \boldsymbol{m}_1, \ldots, \boldsymbol{m}_{N-1}, -\boldsymbol{m}_0, -\boldsymbol{m}_1, \ldots, -\boldsymbol{m}_{N-1}$, where $\boldsymbol{m}_0, \boldsymbol{m}_1, \ldots, \boldsymbol{m}_{N-1}$ are the rows of M. This gives the set of $2N$ vectors of N binary symbols $\{1, -1\}$ each, which is the set of codewords. (In coding theory the additional mapping 1s to 0s and -1s to 1s is often used to get the code over the binary field, but in our consideration it is more convenient to operate with the symbols 1 and -1). The codewords $\boldsymbol{m}_i$ and $-\boldsymbol{m}_i$ are *antipodal*, and other pairs of codewords are *orthogonal*. The only thing left is to establish the mapping of the mth information block $\boldsymbol{u}_m^{(k)} = (u_{(Lm)}^{(k)}, u_{(Lm+1)}^{(k)}, \ldots, u_{(L(m+1)-1)}^{(k)})$ onto block $\boldsymbol{v}_m^{(k)} = (v_{(Nm)}^{(k)}, v_{(Nm+1)}^{(k)}, \ldots, v_{(N(m+1)-1)}^{(k)})$. We will assign the antipodal codewords to complementary information sequences i and $\bar{i}$ and will label them by $\boldsymbol{m}_i$ and $\boldsymbol{m}_{\bar{i}}$. In Figure 4.1 an example of such labeling is given for $L = 3$, $N = 4$.

For the first-order Reed–Muller code of block length N the minimum distance $d_{\min}$ is equal to $N/2$. Actually, the distances between the pairs of codewords in the first-order Reed–Muller code of block length N take two values, N and $N/2$. This distance is equal to N if the corresponding codewords are antipodal; otherwise, it is equal to $N/2$. In the latter case the inner, or dot, product of the two codewords in the real number alphabet is zero. This code is sometimes called a *biorthogonal code*, because the set of codewords can be viewed as the union of an N-ary orthogonal set $\{\boldsymbol{m}_i, i = 0, 1, \ldots, N-1\}$ and complementary set $\{-\boldsymbol{m}_i\}$.

The first-order Reed–Muller code has good distance properties but a relatively low code rate. This is not so critical in SS applications, because of the large spreading factor.

For noncoherent demodulation we cannot employ antipodal signals, because the quadratic operation inherent in noncoherent demodulation destroys signs. If we only used the rows of M (the set $\{\boldsymbol{m}_i\}$) as codewords, we would get the set of orthogonal N vectors, but the code rate would be reduced to $r = (\log_2 N)/N$. The corresponding *reduced* first-order Reed–Muller code is considered in Section 4.3. It is also called an *orthogonal code*.

Consider now the case in which the first-order Reed–Muller code is used for BPSK DS CDMA communication with coherent reception. Let

$$\boldsymbol{m}_i = (m_{i0}, m_{i1}, \ldots, m_{i,(N-1)}), \quad i = 0, 1, \ldots, 2N-1 \tag{4.23}$$

be codewords of the code. The block of L information symbols $\boldsymbol{u}_m^{(k)}$ is mapped according to an encoding rule in one of the $2N$ N-tuples $\boldsymbol{m}_i$, $i = 0, 1, \ldots, 2N-1$. This N-tuple forms a codeword $\boldsymbol{v}_m^{(k)} = (v_{(Nm)}^{(k)}, v_{(Nm+1)}^{(k)}, \ldots,$

Codeword number	Binary labeling	Information block	Codeword
0	0 0 0	1 1 1	1 1 1 1
1	0 0 1	1 1 −1	1 −1 1 −1
2	0 1 0	1 −1 1	1 1 −1 −1
3	0 1 1	1 −1 −1	1 −1 −1 1
4	1 0 0	−1 1 1	−1 1 1 −1
5	1 0 1	−1 1 −1	−1 −1 1 1
6	1 1 0	−1 −1 1	−1 1 −1 1
7	1 1 1	−1 −1 −1	−1 −1 −1 −1

Figure 4.1. An illustration of the first-order Reed–Muller code; $L = 3$, $N = 4$.

$v^{(k)}_{((N+1)m-1)}$). The sequence of the codewords $\boldsymbol{v}^{(k)}_m$, $m = \ldots -1, 0, 1 \ldots$, forms a code sequence $\boldsymbol{v}^{(k)} = \ldots v^{(k)}_{-1}, v^{(k)}_0, v^{(k)}_1, \ldots, v^{(k)}_n, \ldots$. The code symbols $v^{(k)}_n$ are multiplied by symbols of the spreading sequence (2.91). The output signal of the kth transmitter is given by Formula (2.92); the received signal is (3.64).

The modulator part of the BPSK SS transmitter for the kth user is analogous to that considered in Section 2.3 (Fig. 2.10).

The demodulator block of the kth user receiver is presented in Figure 3.3. The decision block should be replaced by the decoder block (Fig. 4.2). The decoder performs ML decoding, which was described in the Section 4.1.

The normalized correlation metrics are [compare with (4.12)],

$$\frac{\mu}{2\sigma^2}\sum_{n=0}^{N-1} z^{(k)}_n m_{in} = \frac{\sqrt{P^{(k)}}T_c}{I_0}\sum_{n=0}^{N-1} z^{(k)}_n m_{in} \stackrel{\text{def}}{=} \frac{\sqrt{P^{(k)}}T_c}{I_0}\; y^{(k)}_i,$$
$$i = 0, 1, \ldots, 2N-1 \tag{4.24}$$

where $P^{(k)}$ is the power of the received signal from the kth user, $I_0/2$ is the two-sided total noise power spectral density, and $y^{(k)}_i = \sum_{n=0}^{N-1} z^{(k)}_n m_{in}$. The decoder does not change the performance if we use as metrics $y^{(k)}_i$.

Because in the case of the first-order Reed–Muller code $y^{(k)}_i = -y^{(k)}_{\bar{i}}$, we may calculate metrics $y^{(k)}_i$ only for $i = 0, 1, \ldots, N-1$. The decoder in Figure 4.2 implements the ML decoding rule for the 0th transmitted block $\boldsymbol{v}_0$.

The decoding complexity of the receiver in Figure 4.2 can be significantly reduced if we use the fast Hadamard transform (FHT) in the calculation of the statistics $y^{(k)}_n$, $n = 1, 2, \ldots, N$. Straightforward computation of these statistics in the receiver of Figure 4.2 requires $N \times N$ real multiplications and $N \times N$ real additions for processing of one block. By taking advantage of the symmetries of the elements of the Hadamard matrix the number of computations required in performing the N correlation statistics may be reduced by application of the FHT from the order N^2 computations to $N \log_2 N$ operations. The FHT has a structure very similar to that of the fast Fourier transform. Figure 4.3 shows the FHT structure for the decoding of the block length $N = 8$ first-order Reed–Muller code.

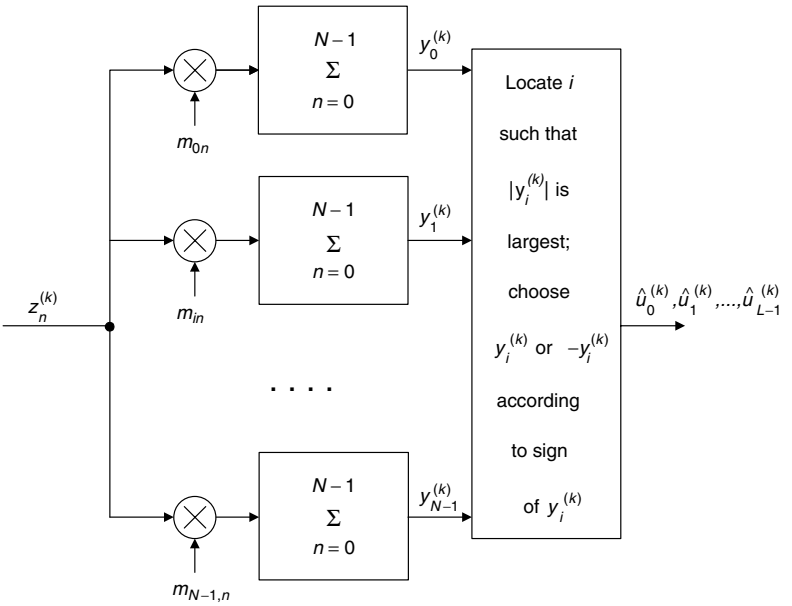

Figure 4.2. The decoder block of the BPSK DS SS receiver.

In contrast to the receiver in Figure 4.2 the statistics $z_n \stackrel{\text{def}}{=} z_n^{(k)}$ in Figure 4.3 are ordered not serially but in parallel. The butterfly operation calculates the sum $z_n^{(+)}$ and difference $z_n^{(-)}$ of the input symbols $\hat{z}_n$ and $\check{z}_n$. The final statistics z_n''' coincide with statistics $y_n^{(k)}$, $n = 0, 1, \ldots, N-1$.

Let us analyze the decoding error probability. For the first-order Reed–Muller codes we can calculate this probability exactly and do not need to use the union bound as in Section 4.1. The decoding error probability for linear codes does not depend on which codeword was sent because of the invariance of distance spectrum to the choice of reference vector. Therefore, we suppose that the zeroth codeword $\boldsymbol{m}_0$ was sent by the kth user, that is, $(v_0, v_1, \ldots, v_{N-1}) = \boldsymbol{m}_0$. Then the mathematical expectation of the statistic $y_i^{(k)}$ is [compare with Formula (4.13)]

$$E(y_i^{(k)}) = \begin{cases} \sqrt{P^{(k)}}\, N \stackrel{\text{def}}{=} \mu N, & \text{if } i = 0, \\ 0, & \text{otherwise} \end{cases} \tag{4.25}$$

The statistics $y_i^{(k)}$, $i = 0, 1, \ldots, N-1$, are uncorrelated, and the variance of the statistic $y_i^{(k)}$ is

$$\operatorname{var}(y_i^{(k)}) = \frac{I_0}{2T_c}\, N = \sigma^2 N, \;\; i = 0, 1, \ldots, N-1 \tag{4.26}$$

Assuming that the number of users K is large, we get that the statistics $y_i^{(k)}$ are approximately Gaussian and independent.

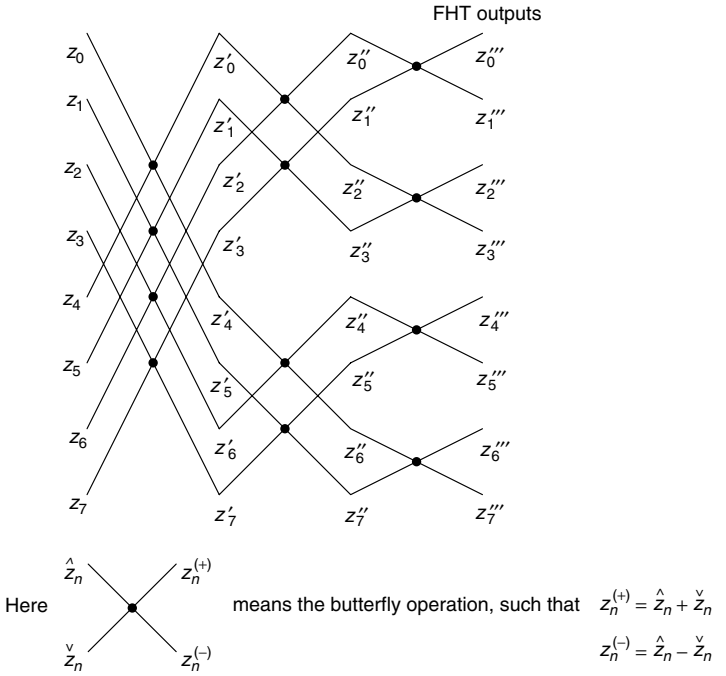

Figure 4.3. FHT diagram for the decoder of the length $N = 8$ first-order Reed–Muller code.

Let us assume that signals from all of the users are received by the base station at the same power level P, because of the perfect power control.

The decoding is correct if $y_0^{(k)} > 0$ and $|y_i^{(k)}| < y_0^{(k)}$ for all $i = 1, 2, \ldots, N-1$. So we have, from (4.25) and (4.26), that the probability of the correct decision $P(\mathcal{C})$ is

$$P(\mathcal{C}) = \int_0^{\infty} \frac{1}{\sqrt{2\pi\sigma^2 N}} \exp\left[-\frac{(x-\mu N)^2}{2\sigma^2 N}\right] \left[\int_{-x}^{x} \frac{1}{\sqrt{2\pi\sigma^2 N}} \times \exp\left(-\frac{y^2}{2\sigma^2 N}\right) \mathrm{d}y\right]^{N-1} \mathrm{d}x$$

$$= \frac{1}{\sqrt{\pi\rho_c N}} \int_0^{\infty} \exp\left[-\frac{(x-\rho_c N)^2}{\rho_c N}\right] \left[1 - 2Q\left(\frac{\sqrt{2}x}{\sqrt{\rho_c N}}\right)\right]^{N-1} \mathrm{d}x \quad (4.27)$$

where $\rho_c = PT_c/I_0$. We must resort to the numerical integration to evaluate the probability $P_B = P(\mathcal{E}) = 1 - P(\mathcal{C})$ that the block would be decoded erroneously.

Because the messages to be communicated are actually just binary data, the bit error probability P_b may be of more interest than the block error probability. Concerning the bit error probability, we note that there are two types of error events,

conditioned on the transmission of the zeroth codeword. These are choosing $-\boldsymbol{m}_0$ instead of $\boldsymbol{m}_0$ or choosing one of the $2N-2$ signals orthogonal to $\boldsymbol{m}_0$.

In the beginning of this section we assigned the antipodal signal pairs with complementary bit labels (see Fig. 4.1). If the first type of error event occurs all bits are decoded incorrectly, but because the Hamming distance between two antipodal codewords is large (equal to N), it should be clear that this case is relatively rare. For the second type of error events, there are $2N-2$ equally likely alternatives and half of these, $N-1$, have bit discrepancies with the transmitted information block in any given position. At all reasonable signal-to-noise ratios, the second type of events are far more probable. Thus, for N large, we have that P_b approaches $P_B/2$.

The probability of error P_B is a function of the parameter $\rho_B = \rho_c N = PT_cN/I_0$, which is the *signal-to-noise ratio per block*. It is more convenient to present P_B as the function of the *signal-to-noise ratio per bit* $\rho_b = E_b/I_0$, which in our case is equal to $\rho_B/(\log_2 N + 1)$. The block error probability $P_B = P(\mathcal{E}) = 1 - P(\mathcal{C})$ is shown in Figure 4.4 as the function of E_b/I_0 for varying N. Tables are found in [30] as well.

EXAMPLE 4.2

Consider uplink transmission in the CDMA system of Example 3.6 with maximal acceptable $P_b = 10^{-4}$. *Determine the capacity of the multicell CDMA system, using the first-order Reed–Muller code of length* $N = 32$, 128, *and* 512.

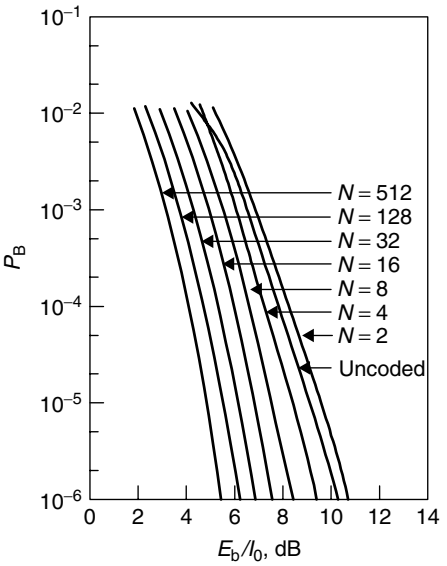

Figure 4.4. The block error probability as a function of E_b/I_0 for the first-order Reed–Muller code of length N.

Solution

From Figure 4.4 we find that to $P_b = 10^{-4}$ $(P(\mathcal{E}) = 2 \cdot 10^{-4})$ *corresponds*

$$E_b/I_0 = 2.88 \text{ (4.6dB) } \textit{if } N = 32$$
$$E_b/I_0 = 2.63 \text{ (4.2dB) } \textit{if } N = 128$$
$$E_b/I_0 = 2.51 \text{ (4.0dB) } \textit{if } N = 512$$

Then $K_0 \approx 1113$, 1219, *and* 1277, *respectively.*

As we mentioned in Section 3.3, the performances of the CDMA system of Example 3.6 coincide with the performances of the uncoded transmission. We refer to the saving in required E_b/I_0 of the encoded transmission over uncoded transmission as the *coding gain*. The coding gain $\gamma_c = [E_b/I_0]_{\text{uncoded}}/[E_b/I_0]_{\text{coded}}$ must always be specified at some operating error probability, say 10^{-4}, and is expressed in decibels. The first-order Reed–Muller code, for example, attains from Figure 4.4 a coding gain of $\gamma_c = 3.8$ dB if $N = 32$, 4.2 dB if $N = 128$, and $= 4.4$ dB if $N = 512$. These data we received by comparison of the uncoded transmission curve with corresponding encoded transmission curves on the ordinate level 10^{-4}. The general formula for the total radio channel capacity of the CDMA system (3.78) reduces in the coded case to the formula

$$K_0 = 1 + \frac{W/R}{E_b/I_0} \frac{\gamma_v \gamma_a \gamma_c (1 - 1/g)}{1 + f} - \frac{N_0}{PT_c} \frac{\gamma_v \gamma_a \gamma_c}{1 + f} \tag{4.28}$$

4.3 NONCOHERENT RECEPTION OF ENCODED DS CDMA SIGNALS

In Section 4.2, we analyzed the reception of the encoded signals under the known-signal condition, which means that the demodulator is provided with all the parameters required to perform optimal processing. In the case of BPSK modulation this assumption presumes that a phase-synchronized reference is also available, for example, by transmission of a pilot signal. Transmission of a pilot, which is studied in Chapter 5, is very valuable for initial acquisition and time tracking. Unfortunately, it is a luxury that may not be affordable, particularly on the many-to-one reverse link from each of the multiple access users to the base station. On the other hand, without phase estimation, noncoherent or differentially coherent reception is required. In the present section we assume that the phase estimate of the received BPSK signal is not available but timing must be acquired and tracked.

As we mentioned in Section 4.2, for noncoherent demodulation we cannot employ antipodal signaling. Therefore, instead of the first-order Reed–Muller code, we will use the *reduced first-order Reed–Muller code* with the code rate $r = (\log_2 N)/N$, that is, a data block of length $L = \log_2 N$ is mapped into one of the N-tuples $\boldsymbol{m}_i$, $i = 0, 1, \ldots, N - 1$, $N = 2^L$, where $\boldsymbol{m}_i$ is the ith row of the

$N \times N$ Hadamard matrix. (In contrast to the encoding considered Section 4.2, the antipodal codewords $-\boldsymbol{m}_i$ are excluded from the code.) Otherwise, the transmitter structure is analogous to the structure of the transmitter considered in Section 4.2.

The modulated signal is given by Formula (2.92), and the received signal is given by (3.64). In Figure 4.5 the noncoherent receiver of the kth user is presented (for the 0th block). We suppose that the delay $\delta^{(k)}$ (but not $\varphi^{(k)}$) of the received signal is known because of time tracking: $\hat{\delta}^{(k)} = \delta^{(k)}$. The processing of the signal in the demodulator and the despreader is analogous to the coherent demodulation/despreading of DPSK signals (see Section 3.5). Then we have, neglecting the interchip interference terms, [compare with Formulas (3.106) and (3.107)]

$$z_{\mathrm{I}n}^{(k)} = \sqrt{P^{(k)}} v_n^{(k)} \cos\varphi^{(k)} + \tilde{\xi}_{\mathrm{I}n}^{(k)} a_n^{(k)} + \hat{\xi}_{\mathrm{I}n}^{(k)} a_n^{(k)} + \check{\xi}_{\mathrm{I}n}^{(k)} a_n^{(k)} \tag{4.29}$$

$$z_{\mathrm{Q}n}^{(k)} = \sqrt{P^{(k)}} v_n^{(k)} \sin\varphi^{(k)} + \tilde{\xi}_{\mathrm{Q}n}^{(k)} a_n^{(k)} + \hat{\xi}_{\mathrm{Q}n}^{(k)} a_n^{(k)} + \check{\xi}_{\mathrm{Q}n}^{(k)} a_n^{(k)} \ , \tag{4.30}$$

$$n = 0, 1, \ldots, N-1$$

The first terms on the right-hand side of (4.29) and (4.30) are the desired components, the second terms are the other-user interference components, the third terms are due to background AWGN, and the fourth terms are due to the other-cell interference.

Analogously to (3.108)–(3.110) we have from (4.29) and (4.30)

$$E(z_{\mathrm{I}n}^{(k)}) = \sqrt{P^{(k)}} v_n^{(k)} \cos\varphi^{(k)} \tag{4.31}$$

$$E(z_{\mathrm{Q}n}^{(k)}) = \sqrt{P^{(k)}} v_n^{(k)} \sin\varphi^{(k)} \tag{4.32}$$

$$\mathrm{var}(z_{\mathrm{I}n}^{(k)}) = \mathrm{var}(z_{\mathrm{Q}n}^{(k)}) = \frac{1}{2T_{\mathrm{c}}^3} \sum_{k' \neq k} P^{(k')} \int_{-\infty}^{\infty} |H(f)|^4 \, \mathrm{d}f + \frac{N_0}{2T_{\mathrm{c}}} + \frac{N_{\mathrm{oc}}}{2T_{\mathrm{c}}} \stackrel{\mathrm{def}}{=} \frac{I_0}{2T_{\mathrm{c}}} \tag{4.33}$$

and

$$\mathrm{cov}(z_{\mathrm{I}n}, z_{\mathrm{Q}n}) = 0 \tag{4.34}$$

The statistics $x_{\mathrm{I}i}^{(k)}$, $x_{\mathrm{Q}i}^{(k)}$, $i = 0, 1, \ldots, N-1$, on outputs of the summers in Figure 4.5 are

$$\begin{aligned} x_{\mathrm{I}i}^{(k)} = \sum_{n=0}^{N-1} z_{\mathrm{I}n}^{(k)} m_{in} &= \sqrt{P^{(k)}} \cos\varphi^{(k)} \sum_{n=0}^{N-1} v_n^{(k)} m_{in} \\ &+ \sum_{n=0}^{N-1} (\tilde{\xi}_{\mathrm{I}n}^{(k)} a_n^{(k)} + \hat{\xi}_{\mathrm{I}n}^{(k)} a_n^{(k)} + \check{\xi}_{\mathrm{I}n}^{(k)} a_n^{(k)}) m_{in} \end{aligned} \tag{4.35}$$

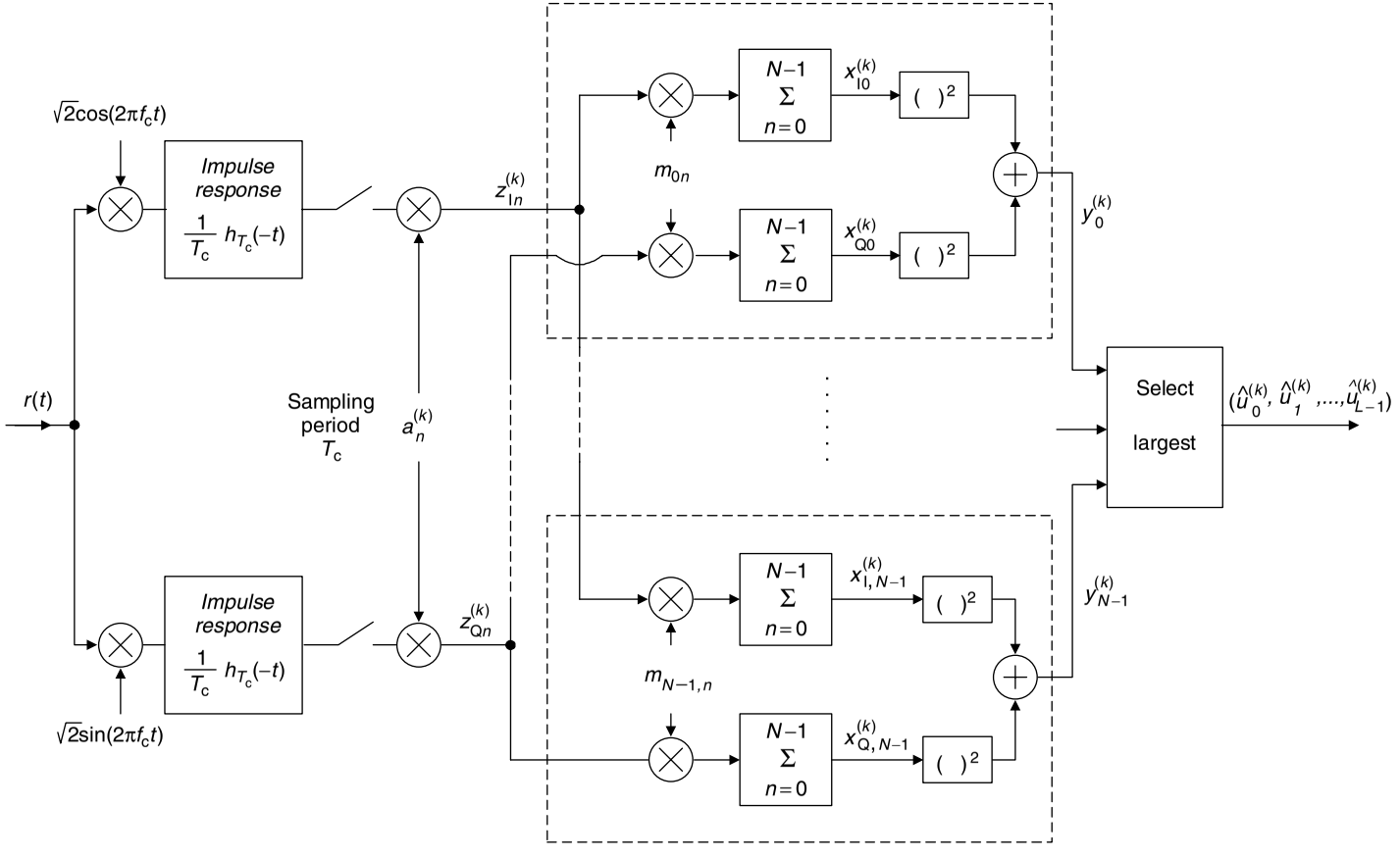

Figure 4.5. The noncoherent receiver of a BPSK DS CDMA system using a reduced first-order Reed–Muller code.

$$x_{\mathrm{Q}i}^{(k)} = \sum_{n=0}^{N-1} z_{\mathrm{Q}n}^{(k)} m_{in} = \sqrt{P^{(k)}}\ \sin\varphi^{(k)} \sum_{n=0}^{N-1} v_{\mathrm{n}}^{(k)} m_{in} + \sum_{n=0}^{N-1} (\tilde{\xi}_{\mathrm{Q}n}^{(k)} a_n^{(k)} + \hat{\xi}_{\mathrm{Q}n}^{(k)} a_n^{(k)} + \check{\xi}_{\mathrm{Q}n}^{(k)} a_n^{(k)}) m_{in} \tag{4.36}$$

Then

$$y_i^{(k)} = \left(x_{\mathrm{I}i}^{(k)}\right)^2 + \left(x_{\mathrm{Q}i}^{(k)}\right)^2,\ i = 0, 1, \ldots, N-1 \tag{4.37}$$

The optimal noncoherent receiver includes N noncoherent correlators acting in parallel, generating statistics $y_0^{(k)}, y_1^{(k)}, \ldots, y_{N-1}^{(k)}$ and a decision device that selects the index of the largest statistics. Note that statistics $y_i^{(k)}$ are similar to statistic y in Example 3.4.

Because the decoding error probability for linear codes does not depend on which codeword was sent, we will analyze the transmission of the zeroth codeword, $i = 0$. Then the mathematical expectations of the statistics $x_{\mathrm{I}i}^{(k)}$ and $x_{\mathrm{Q}i}^{(k)}$ are

$$E(x_{\mathrm{I}i}^{(k)}) = \begin{cases} \sqrt{P^{(k)}}\ N\cos\varphi^{(k)}, & \text{if } i = 0\ , \\ 0, & \text{otherwise} \end{cases}$$

$$E(x_{\mathrm{Q}i}^{(k)}) = \begin{cases} \sqrt{P^{(k)}}\ N\sin\varphi^{(k)}, & \text{if } i = 0\ , \\ 0, & \text{otherwise} \end{cases}$$

The variances of $x_{\mathrm{I}i}^{(k)}$ and $x_{\mathrm{Q}i}^{(k)}$ are

$$\mathrm{var}(x_{\mathrm{I}i}^{(k)}) = \mathrm{var}(x_{\mathrm{Q}i}^{(k)}) = \frac{I_0 N}{2T_{\mathrm{c}}},\ i = 0, 1, \ldots, N-1$$

and $x_{\mathrm{I}i}^{(k)}$ and $x_{\mathrm{Q}i}^{(k)}$ have zero covariance.

Assuming that the system has perfect power control, that is, $P^{(k)} = P$, $k = 1, 2, \ldots, K$, we get

$$E(x_{\mathrm{I}0}^{(k)}) = \sqrt{P}\ N\cos\varphi^{(1)} \stackrel{\mathrm{def}}{=} \mu N\cos\varphi^{(k)} \tag{4.38}$$

$$E(x_{\mathrm{Q}0}^{(k)}) = \sqrt{P}\ N\sin\varphi^{(1)} \stackrel{\mathrm{def}}{=} \mu N\sin\varphi^{(k)} \tag{4.39}$$

$$E(x_{\mathrm{I}i}^{(k)}) = E(x_{\mathrm{Q}i}^{(k)}) = 0,\ i = 1, 2, \ldots, N-1 \tag{4.40}$$

$$\mathrm{var}(x_{\mathrm{I}i}^{(k)}) = \mathrm{var}(x_{\mathrm{Q}i}^{(k)}) = \frac{I_0 N}{2T_{\mathrm{c}}} \stackrel{\mathrm{def}}{=} \sigma^2 N\ ,\ i = 0, 1, \ldots, N-1 \tag{4.41}$$

where $\mu = \sqrt{P}$, $\sigma^2 = I_0/2T_{\mathrm{c}}$. We seek the probability that all $y_i^{(k)}$, $i = 1, 2, \ldots, N-1$, are less than $y_0^{(k)}$, which is the probability $P(\mathcal{C})$ of correct decision. We

attack this by fixing $y_0^{(k)}$, calculating the conditional result, and then averaging over $y_0^{(k)}$.

Because $x_{I0}^{(k)}$ and $x_{Q0}^{(k)}$ are independent Gaussian variables, the statistic $y_0^{(k)}$ has noncentral χ^2-distribution with two degrees of freedom; the statistics $y_i^{(k)}$, $i = 1, 2, \ldots, N-1$, are independent and have central χ^2-distribution with two degrees of freedom [see Formulas (3.48) and (3.49)]. From (4.38)–(4.41) it follows that the conditional probability of correct decision given $y_0^{(k)}$ is

$$P(\mathcal{C}|\ y_0^{(k)}) \le P(y_i^{(k)} < y_0^{(k)},\ i = 1, 2, \ldots, N-1|\ y_0^{(k)})$$

$$= \left[\int_0^{y_0^{(k)}} \frac{1}{2N\sigma^2}\ \exp\left(-\frac{x}{2N\sigma^2}\right) \mathrm{d}x\right]^{N-1} = \left[1 - \exp\left(-\frac{y_0^{(k)}}{2N\sigma^2}\right)\right]^{N-1} \tag{4.42}$$

The averaging $P(\mathcal{C}|y_0^{(k)})$ over $y_0^{(k)}$ gives

$$P(\mathcal{C}) = \int_0^{\infty} P(\mathcal{C}|y_0^{(k)}) f_{N\mu, N\sigma^2}(y_0^{(k)})\, \mathrm{d}y_0^{(k)} \tag{4.43}$$

where $f_{N\mu, N\sigma^2}(y_0^{(k)})$ is the probability density function of $y_0^{(k)}$ given by (3.49). Then

$$\begin{aligned} P(\mathcal{C}) &= \int_0^{\infty} \frac{1}{2N\sigma^2}\ \exp[-(y + N^2\mu^2)/2N\sigma^2]\ I_0\left(\frac{\mu\sqrt{y}}{\sigma^2}\right) \\ &\quad \times \left[1 - \exp\left(-\frac{y}{2N\sigma^2}\right)\right]^{N-1} \mathrm{d}y \\ &= \int_0^{\infty} \exp(-y - \rho_B) I_0(2\sqrt{\rho_B y})[1 - \exp(-y)]^{N-1}\, \mathrm{d}y \end{aligned} \tag{4.44}$$

where $\rho_B = \mu^2 N/2\sigma^2 = PT_c N/I_0$ is SNR per block. The bracketed term raised to the power $(N-1)$ in (4.44) can be expanded by using the binomial expansion. Then, applying the same trick as in (3.119), we obtain the next expression for the probability $P(\mathcal{E})$ of erroneous decoding

$$P_B = P(\mathcal{E}) = 1 - P(\mathcal{C}) = \sum_{i=1}^{N-1} \frac{(-1)^{i+1}}{i+1} \binom{N-1}{i} \exp\left(\frac{i\rho_B}{i+1}\right) \tag{4.45}$$

In particular, for $N = 2$ we have

$$P(\mathcal{E}) = P_b = \frac{1}{2}\ \exp\left(-\frac{P_B}{2}\right) = \frac{1}{2}\ \exp\left(-\frac{PT_c N}{2I_0}\right)$$

Figure 4.6 illustrates the dependence of $P_B = P(\mathcal{E}) = 1 - P(\mathcal{C})$ on N and $E_b/I_0 = PT_c N/I_0 \log_2 N = \rho_B/\log_2 N$. The bit error probability, P_b, can be related to the block error probability P_B in exactly the same way as we did for coherent reception of the signal decoded by the first-order Reed–Muller code: $P_b \approx P_B/2$.

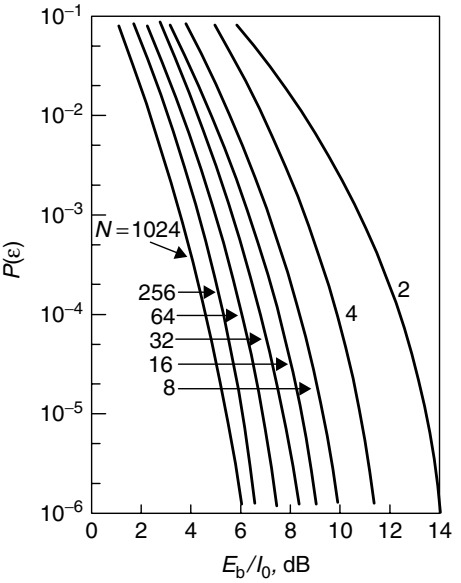

Figure 4.6. The block error probability for the noncoherent reception of the reduced first-order Reed–Muller code of length N.

EXAMPLE 4.3

Consider again uplink transmission in the CDMA system of Example 3.6 with maximal acceptable $P_b = 10^{-4}$. *Determine the capacity of the multicell CDMA system, using the reduced first-order Reed–Muller code of length* $N = 2, 32, 64, 256$ *and noncoherent reception. Note that the system does not use pilot signaling.*

Solution

From Figure 4.6 we find that to $P_b = 10^{-4}$ ($P(\mathcal{E}) = 10^{-4}$ *for* $N = 2$ *and* $P(\mathcal{E}) \approx 2 \cdot 10^{-4}$ *for* $N = 32, 64, 256$) *corresponds*

$$\begin{aligned} E_b/I_0 &= 17.8 \quad (12.5\text{dB}) \quad \textit{if} \quad N = 2 \\ E_b/I_0 &= 4.7 \quad (6.7\text{dB}) \quad \textit{if} \quad N = 32 \\ E_b/I_0 &= 4.0 \quad (6.0\text{dB}) \quad \textit{if} \quad N = 64 \\ E_b/I_0 &= 3.2 \quad (5.1\text{dB}) \quad \textit{if} \quad N = 256 \end{aligned}$$

Then $K_0 = 226, 853, 1002,$ *and* $1252,$ *respectively.*

Comparing Example 4.2 to Examples 3.6 and 4.1 shows that the *coded BPSK DS CDMA* system with *noncoherent receiver* performs better than *uncoded BPSK DS CDMA* with *coherent receiver* but worse than *coded BPSK DS CDMA* with *coherent receiver*.

4.4 INTRODUCTION TO CONVOLUTIONAL CODING

In contrast to a block encoder, a convolutional encoder generates code symbols for transmission utilizing a sequential finite-state machine driven by the information sequence. Decoding these codes then amounts to sequentially observing a corrupted version of the output of this system and attempting to infer the input sequence. From a formal perspective, there is no need to divide the message into segments of some specific length.

The theory of convolutional codes is given in [24]. Here we give a short introduction to the theory. We will describe the generation of code sequences in the logical alphabet {0, 1} language.

Figure 4.7 illustrates one of the simplest nontrivial convolutional encoders. It is implemented by a shift register of memory (number of delay elements) $m = 2$ and three summers $\oplus$ over $GF(2)$. The rate of the code is $r = 1/2$. The information sequence $\ldots \beta_0, \beta_1, \ldots, \beta_n \ldots, \beta_n \in \{0, 1\}$, is the input sequence of the encoder. The encoder is a finite-state machine that can be described in terms of its state transition diagram. This is shown in Figure 4.8, where the nodes refer to the contents of the register just before the next input bit arrives. The encoder inputs $\ldots \beta_0, \beta_1, \ldots, \beta_n, \ldots$, and outputs $\ldots \alpha_0, \alpha_1, \ldots, \alpha_n, \ldots, \beta_n, \alpha_n \in \{0, 1\}$ (2 output symbols per input bit for the rate $r = 1/2$ encoder) are shown as labels on the transition branches.

A trellis diagram (Fig. 4.9) is an infinite replication of the state diagram. It is assumed that the encoder starts in the state 00. The nodes at one level in the trellis are reached from the nodes of the previous level by the transition through one branch, corresponding to one input bit, as determined by the state diagram. Any codeword of a convolutional code corresponds to the symbols along a *path* (consisting of successive branches) in the trellis diagram. The path corresponding to information sequence (1,0,1,1) is indicated with a bold line in Figure 4.9. The convolutional code is a linear code, that is, it includes the all-zero codeword, and the vector sum of two codewords in $GF(2)$ is a codeword (see Section 4.1). The performance of the coded system depends on the relative Hamming distance between the codewords, that is, on the number of symbols in which they differ. The *free distance* d_{free} is defined as the minimum Hamming distance between any two paths over their unmerged span. For the encoder in Figure 4.7 $d_{\text{free}} = 5$.

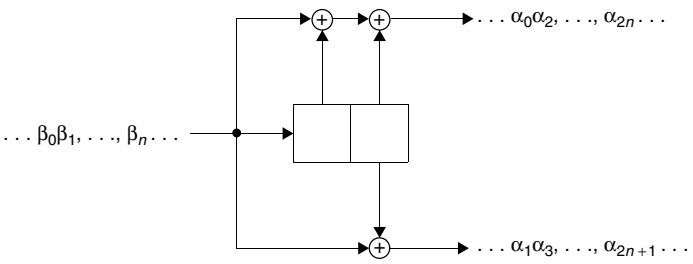

Figure 4.7. A rate $r = 1/2$ memory $m = 2$ convolutional encoder.

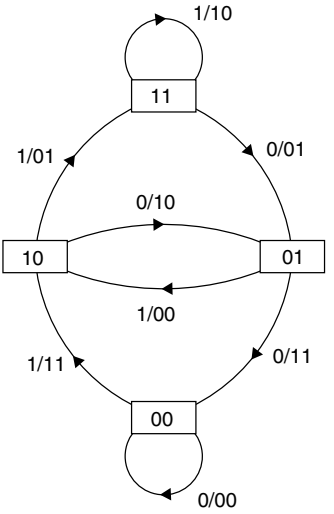

Figure 4.8. The state-transition diagram for the encoder in Figure 4.7.

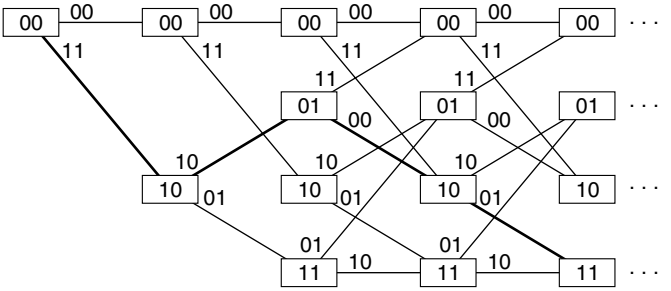

Figure 4.9. The trellis diagram for the encoder in Figure 4.7.

In the BPSK transmitter the code sequence $\ldots \alpha_0, \alpha_1, \ldots \alpha_n, \ldots \alpha_n \in \{0, 1\}$ in the binary logical alphabet maps into the sequence $\ldots v_0, v_1, \ldots v_n \ldots, v_n \in \{1, -1\}$ in the real number alphabet, such that to symbol α_n corresponds symbol v_n. The modulator and demodulator blocks are analogous to the ones presented in Figures 2.8 and 3.3, except that the despreader in the demodulator is absent and the index k is dropped. The transmitted BPSK signal is given by

$$s(t) = \sqrt{2}\, v(t) \cos(2\pi f_c t + \phi) \tag{4.46}$$

where [compare with Formula (2.82)]

$$v(t) = \sum_{n=-\infty}^{\infty} v_n h_{T_c}(t - nT_c) \tag{4.47}$$

Let us suppose that this BPSK signal is transmitted over the AWGN channel. The received signal is [compare with Formula (3.64)]

$$r(t) = \sqrt{2P}\ v(t-\delta)\cos[2\pi f_c(t-\delta)+\varphi] + \xi(t) \tag{4.48}$$

where P is the power of the received signal, δ is the transmission delay, φ is the phase, and the AWGN $\xi(t)$ has two-sided power spectral density $N_0/2$. The output of the demodulator is the sequence

$$z_n = \sqrt{P}v_n + \tilde{\xi}_n,\ \ n = \ldots 0, 1, 2, \ldots \tag{4.49}$$

where $\{\tilde{\xi}_n\}$ is the sequence of IID zero-mean Gaussian variables with variances $N_0/2T_c$.

The maximum likelihood (ML) decoding algorithm for convolutional codes was originally proposed by Viterbi in 1967 [48]. It seeks the maximum likelihood path through the trellis, based on the observation sequence $\boldsymbol{z} = (z_0, z_1, \ldots, z_{n-1})$ and the encoder state at time moment 0. Let at time moment $n = 0$ the encoder be in the zero state and let the input sequence to the channel be $\boldsymbol{v} = (v_0, v_1, \ldots, v_{n-1})$. The conditional probability density function to receive $\boldsymbol{z}$, given $\boldsymbol{v}$, may be expressed as a product [compare with (4.8)]

$$p(\boldsymbol{z}\,|\boldsymbol{v}) = \prod_{i=0}^{n-1} \frac{1}{\sqrt{2\pi\sigma^2}}\ \exp\{-(z_i - \mu v_i)^2/2\sigma^2\} \tag{4.50}$$

where $\mu = \sqrt{P}$ and $\sigma^2 = N_0/2T_c$. Then, given the received sequence $\boldsymbol{z}$, the ML decoder determines the sequence $\boldsymbol{v}$ that maximizes $p(\boldsymbol{z}\,|\boldsymbol{v})$. But, as we showed in Section 4.1, maximization of $p(\boldsymbol{z}\,|\boldsymbol{v})$ is equivalent to maximization of the correlation metric

$$y(\boldsymbol{z}, \boldsymbol{v}) = \sum_{i=0}^{n-1} z_i v_i \tag{4.51}$$

over all $\boldsymbol{v}$. In searching through the trellis for the sequence $\boldsymbol{v}$ that maximizes the metric y, it may appear that we must compute the metric for every possible path. However, this is not the case. We may reduce the number of sequences in the trellis search by using Viterbi's idea to eliminate the sequences as new data are received from the demodulator. This idea follows from the observation that for any two paths that remerge at a given node, we can exclude the one with the smaller metric: Its metric will forever after remain smaller than that of the other path with which it merges. This leads us to define the node metric as the maximum among the metrics of the paths to that node.

To illustrate the decoding process we consider the following

EXAMPLE 4.4

Consider the encoder in Figure 4.7. Suppose that the encoder is initialized to state 00 *and the* 4*-bit message is transmitted, followed by a termination string*

of two zeros. Transmission is over the AWGN channel. The demodulator output sequence is

$$z = (1.0, -0.3, -0.1, 0.9, 0.5, 1.3, 0.5, 0.6, -0.2, -0.5, 1.2, 0.9)$$

Find the ML decoded sequence.

Solution

Figure 4.10 shows the Viterbi decoder progression with the metric (4.51). At the end of the cycle, the information sequence $(0, 0, 0, 0)$ *is released by the decoder.*

Finding the error performance of the convolutional code is different from the method used to find the error performance for the Reed–Muller code, because here we are dealing with very long sequences and, because the free distance of these codes is usually small, some errors will eventually occur.

Convolutional codes are linear codes, making the distance structure invariant to the choice of reference sequence, and the all-zero (in logical alphabet) information sequence can be adopted as the transmitted sequence for error analysis purposes.

We are interested in the probability of two events. The first is the event that in some node, say the nth, the decoded path will diverge from the all-zero path. We say that this constitutes a *burst error* at time n and denote the probability of this event P_B. (This probability does not depend on n; therefore, we omit the

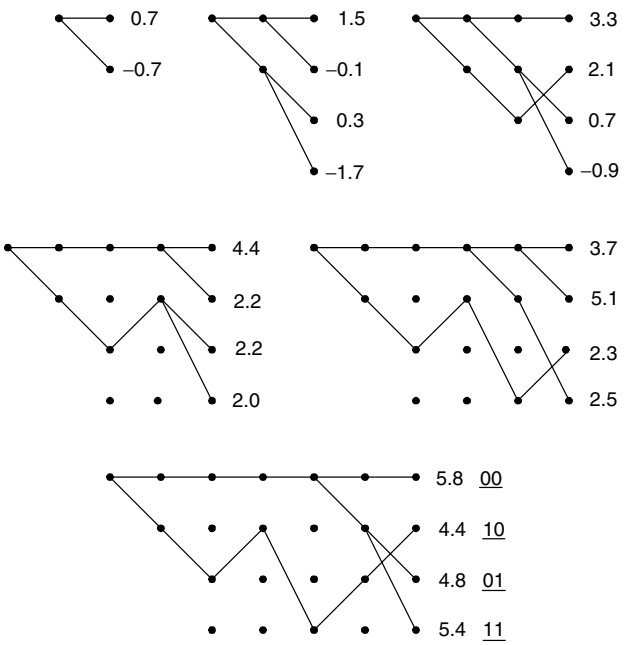

Figure 4.10. Evolution of survivors for Example 4.4.

index n and consider the root node.) Of greater interest is the postdecoding *bit error probability*, denoted P_b. We will get to this by first bounding the *burst error probability*.

To evaluate P_B, consider the *incorrect set*, that is, the set of paths diverging from the all-zero path at the root. The probability that the decoder discards the all-zero path in favor of a path from the incorrect set depends only on the Hamming weight w of this path. Let P_w denote this probability and let a_w denote the number of paths in the incorrect set having Hamming weight w. Then, using union bound arguments, we can, analogously to (4.16), upperbound the burst error probability by

$$P_B \leq \sum_{w=d_{free}}^{\infty} a_w P_w = \sum_{w=d_{free}}^{\infty} a_w Q(\sqrt{2\rho_c w}) \tag{4.52}$$

where $\rho_c = PT_c/N_0$ and the summation starts from d_{free}, because $w \geq d_{free}$. Analogously to (4.18) we can rewrite Formula (4.52) as

$$P_B \leq \sum_{w=d_{free}}^{\infty} a_w Q(\sqrt{2E_b r w/N_0}) \tag{4.53}$$

where E_b/N_0 is the SNR per bit.

Using an upper bound on the Q function (Problem 1.5), we have

$$Q(\sqrt{2\rho_c w}) < \frac{1}{2} e^{-\rho_c w} = \frac{1}{2} W^w \tag{4.54}$$

where $W = e^{-\rho_c}$. Finally, from (4.52) and (4.53) we get

$$P_B < \frac{1}{2} \sum_{w=d_{free}}^{\infty} a_w W^w \Big|_{W=e^{-\rho_c}} = \frac{1}{2} T(W) \Big|_{W=e^{-\rho_c}} \tag{4.55}$$

The function $T(W) = \sum_{w=d_{free}}^{\infty} a_w W^w$ is called the *path weight enumerator* of the convolutional code [24]. It can be found from the encoder state-transition diagram by standard flowchart techniques.

EXAMPLE 4.5

Find the path weight enumerator for the encoder in Figure 4.7.

Solution

Figure 4.11 provides the split state-transition diagram of the encoder. The self-loop at the zero state in the state-transition diagram is removed, and the zero state is split in two—a source and a sink state. Then the branches are labeled by $W^0 = 1$, W, or W^2, where the exponent corresponds to the weight of the particular branch.

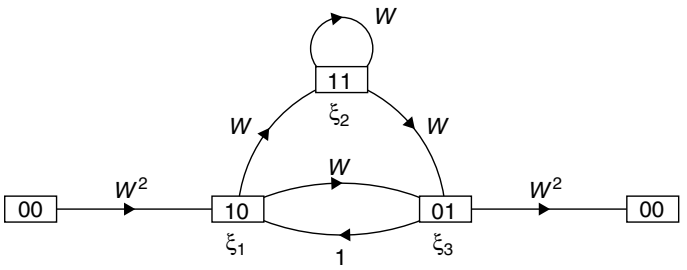

Figure 4.11. The split state-transition diagram for the encoder in Figure 4.7.

Let the input to the source (left zero state) be 1 *and let* ξ_1, ξ_2, *and* ξ_3 *be dummy variables representing the weights of all paths from the left zero state to the intermediate states. Then, from Figure 4.11, we obtain the following system of linear equations*

$$\begin{aligned} \xi_1 &= \xi_3 + W^2 \\ \xi_2 &= W\xi_1 + W\xi_2 \\ \xi_3 &= W\xi_1 + W\xi_2 \end{aligned} \tag{4.56}$$

and the path weight enumerator function is

$$T(W) = W^2\xi_3 \tag{4.57}$$

Solving these equations (by elimination or by the method of determinants) gives

$$T(W) = \frac{W^5}{1-2W} = \sum_{w=5}^{\infty} 2^{w-5} W^w \tag{4.58}$$

The bound (4.55) is a bound on the burst error probability. To find a bound on the bit error probability P_b we note that each path through the trellis causes a certain number of input bits to be decoded erroneously. This means that the average number of input bits in error can be obtained by multiplying the probability of choosing each path by the total number of input errors that would result if that path were chosen. Hence, the average number of bits in error can be bounded by

$$\begin{aligned} P_b &< \sum_{w=d_{\text{free}}}^{\infty} \sum_{i=1}^{\infty} a_{w,i} i P_w = \sum_{w=d_{\text{free}}}^{\infty} a_w i_w P_w \\ &= \sum_{w=d_{\text{free}}}^{\infty} a_w i_w \; Q(\sqrt{2\rho_c w}) = \sum_{w=d_{\text{free}}}^{\infty} a_w i_w Q(\sqrt{2E_b r w/N_0}) \end{aligned} \tag{4.59}$$

Here $a_{w,i}$ is the number of weight w paths introducing i errors in the decoded information sequence, and $i_w = \sum_{i=1}^{\infty} a_{w,i} i / a_w$ is the average number of input errors caused by all paths of weight w. Using Formula (4.54) we get from (4.59) analogously to (4.55)

$$P_b < \frac{1}{2} \sum_{w=d_{free}}^{\infty} a_w i_w W^w$$
$$= \frac{1}{2} \frac{\partial}{\partial I} [T(W, I)] \Big|_{\substack{I=1 \\ W=e^{-\rho_c}}} \tag{4.60}$$

where $T(W, I)$ is the *refined path enumerator*,

$$T(W, I) = \sum_{w=d_{free}}^{\infty} a_{w,i} W^w I^i \tag{4.61}$$

The *refined path enumerator* can be found from the *refined state-transition diagram.*

EXAMPLE 4.6

Find the refined path weight enumerator for the encoder in Figure 4.7 and the upper bound for P_b.

Solution

Figure 4.12 provides the refined state-transition diagram of the encoder. Here we label the branches not only by W^w, *where* w *is the branch weight, but also by* I^i, *where* i *is the number of* 1*s among the information symbols corresponding to the particular branch. From this refined state-transition diagram we obtain the following linear equations*

$$\xi_1 = I\xi_3 + W^2 I$$
$$\xi_2 = WI\xi_1 + WI\xi_2 \tag{4.62}$$
$$\xi_3 = W\xi_1 + W\xi_2$$
$$T(W, I) = W^2 \xi_3$$

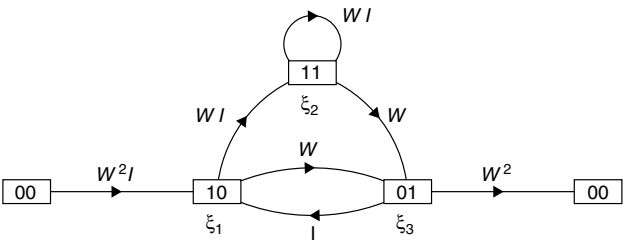

Figure 4.12. The refined split state-transition diagram for the encoder in Figure 4.7.

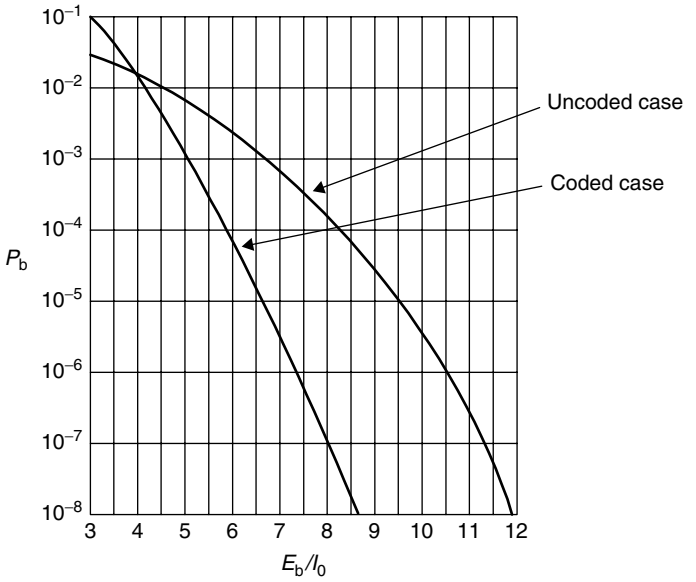

Figure 4.13. The bit error probability bound for the encoder in Figure 4.7.

Solving this equation gives

$$T(W, I) = \frac{W^5 I}{1 - 2WI} = \sum_{w=5}^{\infty} 2^{w-5} W^w I^{w-4} \tag{4.63}$$

By differentiating with respect to I and then setting $I = 1$, we find that

$$\left.\frac{\partial T(W, I)}{\partial I}\right|_{\substack{I=1 \\ W=e^{-\rho c}}} = \sum_{w=d_{\text{free}}}^{\infty} (w-4)2^{w-5} W^w \Big|_{W=e^{-\rho c}} = \left.\frac{W^5}{(1-2W)^2}\right|_{W=e^{-\rho c}} \tag{4.64}$$

Figure 4.13 shows the bound on the bit error probability for the running example in Figure 4.7 as obtained from Formula (4.60). The bit error probability is plotted as a function of the signal-to-noise ratio per bit $E_b/I_0 = 2PT_c/I_0 = PT_c/rI_0$.

4.5 CONVOLUTIONAL CODING IN DS CDMA SYSTEMS

Two parameters of the running example of the convolutional code in Figure 4.7 can be changed: the number of delay elements of the shift register, and the ratio of the number of input symbols to the number of output symbols. The number of delay elements in the shift register is called the *encoder memory*, m. Thus the running example of Figure 4.7 has $m = 2$. The second parameter is the convolutional *code rate* r. The running example code rate is $r = 1/2$. It should

then be obvious that all the algorithms and procedures described so far can be applied more generally.

The most general class of convolutional codes with arbitrary rational rate $r = b/c$ may be generated by using b parallel registers, each connected with c outputs. An example with $b = 2$ and $c = 3$ is shown in Figure 4.14. The state-transition diagram for a memory length m will have 2^{bm} states, and each trellis node has now 2^b branches going out and coming into it. The Viterbi decoder operates as before, except that the path selected is the one with the largest metric among 2^b incoming paths at a node, rather than just two for rate $1/2$ codes.

Most code constructions for the convolutional codes has been done by computer search. A list of convolutional codes with maximal free distance for rate $r = 1/2$ is given in Table 4.2[1] The code generators are given in octal notation. This notation gives the connections between the encoder shift register stages and the modulo-2 adders. Consider, for example, the memory 6 code. The generators are (634,564) in octal or (110 011 100, 101 110 100) in binary form. This means that connections to the first modulo-2 adder are from shift register stage 0,1,4,5,6 and those to the second modulo-2 adder are from shift register stage 0,2,3,4,6. This encoder is illustrated in Figure 4.15.

Consider the transmission of BPSK DS CDMA signals when the system uses a convolutional code. Let

$$\boldsymbol{\beta}^{(k)} = \ldots \beta_0^{(k)}, \beta_1^{(k)}, \ldots, \beta_n^{(k)} \ldots \tag{4.65}$$

be an information sequence (in binary logical alphabet) transmitted by the kth, $k = 1, 2, \ldots, K$, user. This sequence is encoded by a rate $r = b/c$ memory m convolutional encoder. The output sequence of the encoder (in binary logical

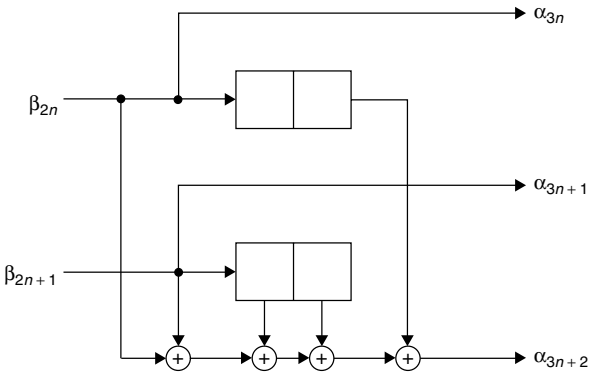

Figure 4.14. The 16-state rate $r = 2/3$, memory $m = 2$ convolutional encoder.

[1]More detailed table of convolutional codes with maximal free distance can be found in [24].

Table 4.2 The Maximum Free Distance Convolutional Codes for $m = 2$–10, $r = 1/2$, and their weight spectra $a_{d_{\text{free}+1}}$ for $0 \le i \le 9$.

m	First generator	Second generator	d_{free}	Weight spectrum $a_{d_{\text{free}+i}}$									
				0	1	2	3	4	5	6	7	8	9
2	7	5	5	1	2	4	8	16	32	64	128	256	512
3	74	54	6	1	3	5	11	25	55	121	267	589	1299
4	62	56	7	2	3	4	16	37	68	176	432	925	2156
5	77	45	8	2	3	8	15	41	90	224	515	1239	2896
6	634	564	10	12	0	53	0	234	0	1517	0	8862	0
7	626	572	10	1	6	13	20	64	123	321	764	1858	4442
8	751	557	12	10	9	30	51	156	340	875	1951	5127	11589
9	7664	5714	12	1	8	8	31	73	150	441	940	2214	5531
10	7512	5562	14	19	0	80	0	450	0	2615	0	15276	0

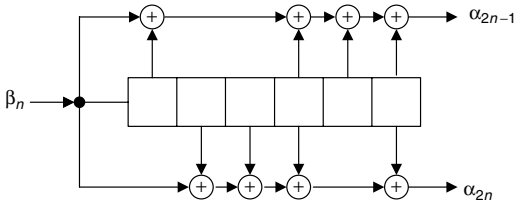

Figure 4.15. The rate $r = 1/2$, memory $m = 6$ (634,564) convolutional encoder.

alphabet) is

$$\boldsymbol{\alpha}^{(k)} = \ldots \alpha_0^{(k)}, \alpha_1^{(k)}, \ldots, \alpha_{c-1}^{(k)}, \alpha_c^{(k)}, \alpha_{c+1}^{(k)}, \ldots, \alpha_{2c-1}^{(k)}, \ldots, \alpha_{cn}^{(k)}, \alpha_{cn+1}^{(k)}, \ldots, \alpha_{c(n+1)-1}^{(k)}, \ldots. \tag{4.66}$$

There are two ways to transform the sequence $\boldsymbol{\alpha}^{(k)}$ into the low-rate code sequence $\boldsymbol{v}^{(k)}$. If $r = b/c$ is small, then the sequence $\boldsymbol{\alpha}^{(k)}$ is transformed directly by the mapping $0 \to 1$, $1 \to -1$ into sequence (in real number form)

$$\boldsymbol{v}^{(k)} = \ldots v_0^{(k)}, v_1^{(k)}, \ldots, v_n^{(k)}, \ldots, v_n \in \{1, -1\} \tag{4.67}$$

such that

$$\alpha_n^{(k)} \longrightarrow v_n^{(k)} \tag{4.68}$$

But if the rate r is not small, for example, $r = 1/2$, to get a low-rate code the sequence $\boldsymbol{\alpha}^{(k)}$ maps into sequence $\boldsymbol{v}$ in two steps. On the first step each symbol $\alpha_n^{(k)}$ of $\alpha^{(k)}$ is mapped into the symbol $\tilde{v}_n^{(k)}$ of the sequence

$$\tilde{\boldsymbol{v}}^{(k)} = \tilde{v}_0^{(k)}, \tilde{v}_1^{(k)}, \ldots, \tilde{v}_n^{(k)}, \ldots, \qquad \tilde{v}_n^{(k)} \in \{1, -1\} \tag{4.69}$$

Then each symbol $\tilde{v}_n^{(k)}$ of the sequence $\tilde{\boldsymbol{v}}^{(k)}$ is repeated N times to get a sequence $\boldsymbol{v}^{(k)}$, such that $v_n^{(k)} = \tilde{v}_{\lfloor n/N \rfloor}^{(k)}$. This way of constructing low-rate codes is treated later, in Section 4.8, as concatenated coding with a rate r outer convolutional code and a rate $1/N$ inner repetition code.

The code symbols $v_n^{(k)}$ of the code sequence $\boldsymbol{v}^{(k)}$ are multiplied by symbols of the spreading sequence (2.91). The output signal of the kth transmitter is given by Formula (2.92), the received signal is (3.64), and the demodulator block of the receiver is analogous to the one presented in Figure 3.3. The Viterbi decoder calculates the metrics (4.51) and searches for the most probable path in the trellis.

Let us analyze the decoding error probability for the concatenated construction. Again consider the transmission of the all-zero codeword. Assuming coherent reception of BPSK DS CDMA signal with perfect power control and a large number of users, $K \gg 1$, we get that the random variables $z_n^{(k)}$ are approximately Gaussian and independent and [compare with Formulas (3.71) and (3.72)]

$$E(z_n^{(k)}) = \begin{cases} \mu \stackrel{\text{def}}{=} \sqrt{P}, & \text{if } v_n^{(k)} = 1\ , \\ -\mu, & \text{otherwise}\ , \end{cases} \qquad n = 0, 1, \ldots \tag{4.70}$$

$$\operatorname{var}(z_n^{(k)}) = \frac{I_0}{2T_c} \stackrel{\text{def}}{=} \sigma^2, \quad n = 0, 1, \ldots \tag{4.71}$$

Here P is the power of the received signal, which does not depend on k because of perfect power control, and $I_0/2$ is the average two-sided power spectral density of the total noise.

It is convenient to divide the sequence z into blocks of length N, corresponding to the transmitted symbols $\tilde{v}_n$, and let

$$\tilde{z}_n^{(k)} = \sum_{i=0}^{N-1} z_{(Nn+i)}^{(k)} \tag{4.72}$$

From (4.70) and (4.71) follows

$$E(\tilde{z}_n^{(k)}) = \begin{cases} N\mu, & \text{if } \tilde{v}_n^{(k)} = 1\ , \\ -N\mu, & \text{otherwise}\ , \end{cases} \qquad n = 0, 1, \ldots \tag{4.73}$$

$$\operatorname{var}(\tilde{z}_n^{(k)}) = \frac{I_0 N}{2T_c} = \sigma^2 N, \quad n = 0, 1, 2 \ldots \tag{4.74}$$

Then we reduce the study to the analysis of soft decoding of a rate $r = b/c$ memory m convolutional code used in the AWGN channel. The SNR per bit is $E_b/I_0 = PT_cN/I_0 = \rho_c N$.

In Figure 4.16 the upper bounds on P_b are plotted versus E_b/I_0 for $r = 1/2$ memory $m = 2, 4, 6$ and 8 codes. We may obtain similar bounds for any convolutional code as a function of signal-to-noise ratio per bit E_b/I_0. Comparison of

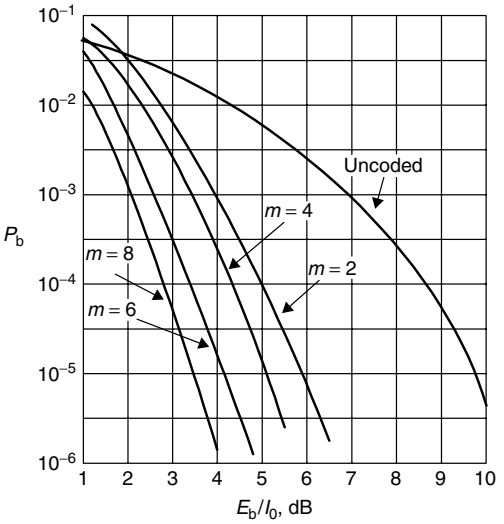

Figure 4.16. The bit error probability bounds of various convolutional codes for the AWGN channel.

the bounds with the required E_b/I_0 in the uncoded case gives us an estimation of the coding gain γ_c for the given codes. Then, applying Formula (4.28), we get the estimation of the radio channel capacity of the CDMA system.

EXAMPLE 4.7

Consider again the CDMA system of Example 3.6 with maximal acceptable $P_b = 10^{-4}$. *Determine the capacity of the multicell CDMA system using rate* $r = 1/2$ *convolutional codes of various memory* $m = 2, 4, 6, 8$. *The pilot signal rate* $1/g = 0.2$. *Neglect the influence of the AWGN.*

Solution

From Figure 4.16 we find that to $P_b = 10^{-4}$ *for* $m = 2, 4, 6, 8$ *corresponds the next coding gains*

$$\gamma_c = 2.24 \text{ (3.5 dB) } \textit{for } m = 2$$

$$\gamma_c = 2.69 \text{ (4.3 dB) } \textit{for } m = 4$$

$$\gamma_c = 3.16 \text{ (5.0 dB) } \textit{for } m = 6$$

$$\gamma_c = 3.47 \text{ (5.4 dB) } \textit{for } m = 8$$

Application of Formula (4.28) for $f = 0.6$, $N_0 = 0$, *gives the following estimations of the numbers of users:* $K_0 = 1038$, 1246, 1464, *and* 1607, *respectively.*

Consider again Formula (4.59), which gives an upper bound for the bit error probability of any rate r convolutional code. If we compare the main term of

(4.59) with the performance of uncoded signaling $P_b = Q\left(\sqrt{2E_b/I_0}\right)$ and ignore the other terms in the upper bound for the bit error probability in the coded case, we see an effective gain in the signal-to-noise ratio of $10\log_{10}(rd_{free})$. This quantity is called *asymptotic coding gain (ACG)*. It represents the savings provided by coding at high signal-to-noise ratio where the main (first) term of (4.59) is dominant. The coding gain represents a potential increase in the system capacity. Thus, for the rate $r = 1/2$, memory $m = 2$ code with $d_{free} = 5$ we project an asymptotical coding gain of $10\log_{10}(5/2) = 4$ dB. The actual gain at $P_b = 10^{-4}$ is, according to Figure 4.16, roughly 3.5 dB. The difference is due to the error multiplier effect and due to the error events caused by paths at a distance greater than d_{free}. Generally, codes with small memory approach their asymptotic gains relatively fast, whereas codes with larger memory are dilatory in achieving the asymptotic gain. For example, the $r = 1/2$ memory $m = 6$ code has an asymptotical coding gain of $10\log_{10}(10/2) = 7$ dB, but at $P_b = 10^{-4}$ the actual gain (according to Fig. 4.16) is only 5 dB.

4.6 ORTHOGONAL CONVOLUTIONAL CODES

In this section we consider a method of constructing very powerful low-rate convolutional (or sliding) codes. These codes are sliding analogs of the first-order Reed–Muller block codes. They were invented by Viterbi in the 1960s and later modified.

As in the description of the first-order Reed–Muller codes we will use the real number alphabet $\{1, -1\}$. Consider the first construction, the memory m, rate 2^{-m} *orthogonal convolutional code*. An example of a memory $m = 2$ rate $r = 2^{-2}$ orthogonal convolutional code is presented in Figure 4.17.

The triple $\{u_{n-2}, u_{n-1}, u_n\}$, $u_n \in \{1, -1\}$, of input symbols maps after each shift into a set of four output decoder symbols $\{v_{4n}, v_{4n+1}, v_{4n+2}, v_{4n+3}\}$, $v_n \in \{1, -1\}$ according to the table in Figure 4.1. In one input bit time the block Reed–Muller encoder outputs one of 2^3 codewords of the Reed–Muller code.

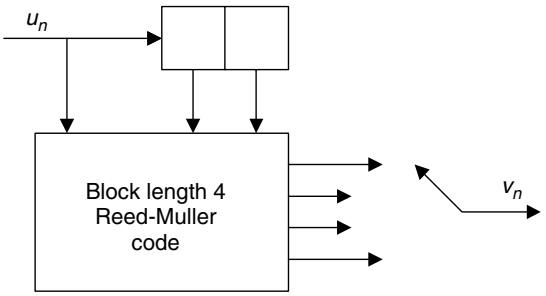

Figure 4.17. A rate $r = 1/4$ memory $m = 2$ orthogonal convolutional encoder (the first construction).

In the general case, a memory m, rate $r = 2^{-m}$ orthogonal convolutional encoder (first construction) has m delay elements and includes the length 2^m first-order Reed–Muller encoder. The branches connecting nodes on the tth level of the trellis with nodes on the $(t + 1)$th level are orthogonal or antipodal.

If we replace the length 2^m first-order Reed–Muller encoder by the reduced block length 2^{m+1} first-order Reed–Muller encoder we get the second construction of the orthogonal convolutional encoder. The memory of the encoder is m, and the code rate $r = 2^{-m-1}$. The branches connecting nodes on the tth level of the trellis with nodes on the $(t + 1)$th level are mutually orthogonal.

Figure 4.18 presents an example of another of Viterbi's encoders, the *superorthogonal convolutional encoder*. The memory of the encoder is $m = 3$; the code rate is $r = 2^{-m+1} = 1/4$. The block length 2^{m-1} first-order Reed–Muller encoder is only connected with m stages of the shift register; the last stage is excluded. The output symbols of the reduced first-order Reed–Muller encoder are multiplied by the content of the last stage of the shift register.

The maximum likelihood decoder for the considered orthogonal convolutional codes is analogous to the Viterbi decoder considered in Section 4.4. The decoder has a copy of the Reed–Muller encoder used in the transmitter that outputs branches of the orthogonal convolutional code. The decoder also includes correlators that output correlations of these branches with the corresponding branches of the received sequence $\{z_n\}$ analogously to the block encoder in Figure 4.2. It gives branch metrics. Summation of branch metrics gives path metrics.

One outstanding feature of the considered class of orthogonal convolutional codes endows it with superior performance and makes its analysis particularly simple. We start with analysis of the second construction.

The refined reduced state-transition diagram of this code is given in Figure 4.19. The block labeled "Start" generates 0s and 1s; the block labeled "Final" absorbs symbols. Suppose we enumerate stages in the shift register from right to left. Let ν be the position of the leftmost 1 in the shift register, $\nu = 1, 2, \ldots, m$, such that the leftmost stage of the shift register corresponds $\nu = m$. We can consider ν as the state of the encoder. Every internal branch of the labeled

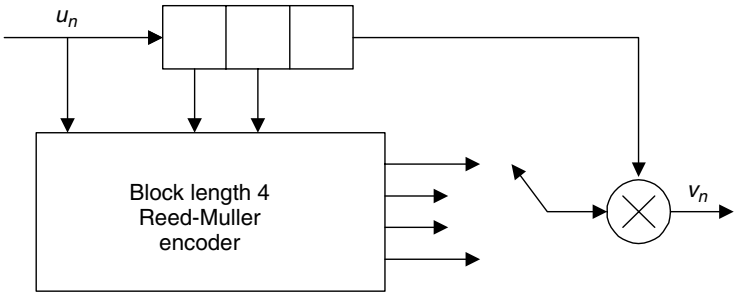

Figure 4.18. A rate $r = 1/4$ memory $m = 3$ superorthogonal convolutional encoder (the third construction).

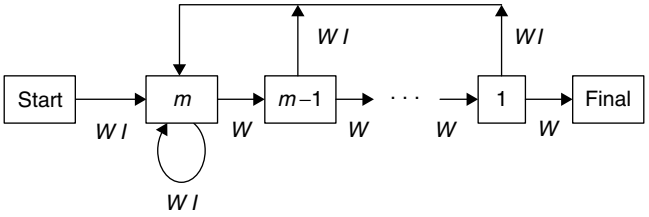

Figure 4.19. The refined reduced state transition diagram for the second construction of the orthogonal sliding encoder.

state diagram has the same weight (distance from the corresponding branch on the all-zero path), $w = 2^m$, that is $W = \exp\{-\rho_c \cdot 2^m\} = \exp\{-E_b/2I_0\}$. From the state ν the encoder can transit to the state $\nu - 1$ (these transitions are labeled by W) or to the state m (these transitions are labelled by WI). Then the path weight enumerator of the second type sliding encoder is

$$T(W, I) = \frac{IW^{m+1}(1 - W)}{1 - W[1 + I(1 - W^m)]} \tag{4.75}$$

Application of Formulas (4.55) and (4.60) with $W = \exp(-\rho_c 2^m)$ gives the upper bounds for the burst and bit error probabilities of the code:

$$P_B < \frac{W^{m+1}(1 - W)}{2(1 - 2W + W^{m+1})} < \frac{W^{m+1}(1 - W)}{2(1 - 2W)} \tag{4.76}$$

$$P_b < \frac{W^{m+1}(1 - W)^2}{2(1 - 2W + W^{m+1})^2} < \frac{W^{m+1}(1 - W)^2}{2(1 - 2W)^2} \tag{4.77}$$

Formulas (4.76) and (4.77) are valid also for the first construction of the orthogonal convolutional codes if we let $W = \exp\{-\rho_c \cdot 2^{m-1}\} = \exp\{-E_b/2I_0\}$ and replace W^{m+1} by W^{m+2} (Problem 4.14).

The refined reduced state-transition diagram of Viterbi's superorthogonal convolutional code is given in Figure 4.20. Every internal branch (except the transition $1 \to m + 1$) has the same weight $w = 2^{m-2}$, that is, $W = \exp\{-\rho_c \cdot 2^{m-2}\}$ $= \exp\{-E_b/2I_0\}$. The first branch on diverging from the start zero state has weight $2w$ and is labeled by W^2I. The last branch before merging to the final zero state also has weight $2w$ and is labeled by W^2. The branch leading from state 1 to state m has zero weight and is labeled by I. The refined path enumerator of this diagram is easily obtained to be

$$T(W, I) = \frac{IW^{m+3}(1 - W)}{1 - W[1 + I(1 + W^{m-2} - 2W^{m-1})]} \tag{4.78}$$

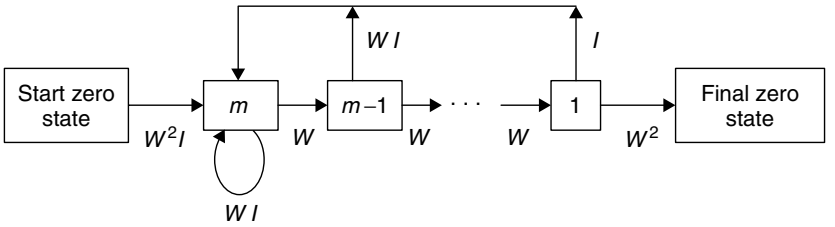

Figure 4.20. The refined reduced state-transition diagram for the third construction of the orthogonal sliding encoder.

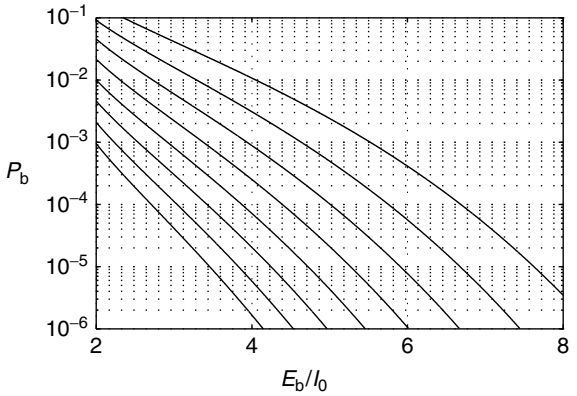

Figure 4.21. Bit error probability bounds for the superorthogonal sliding code of memory $m = 2$–9 (from top to bottom).

Then using Formulas (4.55) and (4.60) we have

$$P_{\mathrm{B}} < \frac{1}{2}\,\frac{W^{m+3}}{(1-2W)}\,\frac{(1-W)}{(1-W^{m-1})} \tag{4.79}$$

$$P_{\mathrm{b}} < \frac{1}{2}\,\frac{W^{m+3}}{(1-2W)^2}\,\frac{(1-W)}{(1-W^{m-1})} \tag{4.80}$$

where $W = \exp\{-\rho_{\mathrm{c}} 2^{m-2}\}$.

Figure 4.21 plots the upper bounds for the bit error probability, obtained from (4.80), for $m = 2$–9 as function of E_{b}/I_0 for the AWGN channel.

EXAMPLE 4.8

Determine the capacity of the multicell uplink DS CDMA system of Example 3.6 using rate $r = 2^{-m+1}$ memory $m = 2, 5, 9$ superorthogonal convolutional codes

with maximal acceptable $P_b = 10^{-4}$. *The pilot signal rate is* $1/g = 0.2$. *Neglect the influence of the background AWGN.*

Solution

From Figure 4.21 we find that to $P_b = 10^{-4}$ *correspond the following values* E_b/I_0*:*

$$E_b/I_0 = 4.79 \text{ (6.8 dB) } \textit{for } m = 2$$
$$E_b/I_0 = 3.02 \text{ (4.8 dB) } \textit{for } m = 5$$
$$E_b/I_0 = 2.19 \text{ (3.4 dB) } \textit{for } m = 9$$

From Formula (3.78) we have $K_0 = 669$, 1061, *and* 1464, *respectively.*

The free distances of the considered codes are

$d_{\text{free}} = (m+2)2^{m-1}$ for the first construction, $\text{ACG} = 10\log_{10}\left(\frac{m+2}{2}\right)$

$d_{\text{free}} = (m+1)2^{m}$ for the second construction, $\text{ACG} = 10\log_{10}\left(\frac{m+1}{2}\right)$

$d_{\text{free}} = (m+3)2^{m-2}$ for the third construction, $\text{ACG} = 10\log_{10}\left(\frac{m+3}{2}\right)$

The considered constructions can be used for DS CDMA communication with coherent reception, but in a DS CDMA system with noncoherent receiver only the second construction can be used. In Section 4.7 we consider application of the orthogonal sliding codes in the FH CDMA system.

4.7 CODING IN FH AND PPH CDMA SYSTEMS

Our focus thus far in this chapter has been on error control aspects of DS CDMA communication. In FH and PPH CDMA systems, the same coding methods as in DS CDMA system can be used. In this section, we consider examples of coding theory in FH CDMA and PPH CDMA communication to demonstrate the potential capability of error control methods.

Consider a FH CDMA system with total hopping bandwidth W using BFSK with Q carrier frequencies, such that the hopset size M is equal to $2Q$. The frequency separation interval $\Delta f = W/M$, and the pulse duration $T_c = 1/\Delta f$ (see Section 3.6). Suppose that the system uses a length N reduced first-order Reed–Muller code. The hopping rate is $R_h = 1/T_c$, and the transmission rate is $R = \log_2 N/(NT_c)$ (bit/s).

The kth user's uplink transmitted signal is given by Formula (3.124). The sets $\{v^{(k)}_{(Nm)}, v^{(k)}_{(Nm+1)}, \ldots, v^{(k)}_{(N(m+1)-1)}\}$ are codewords of the reduced first-order

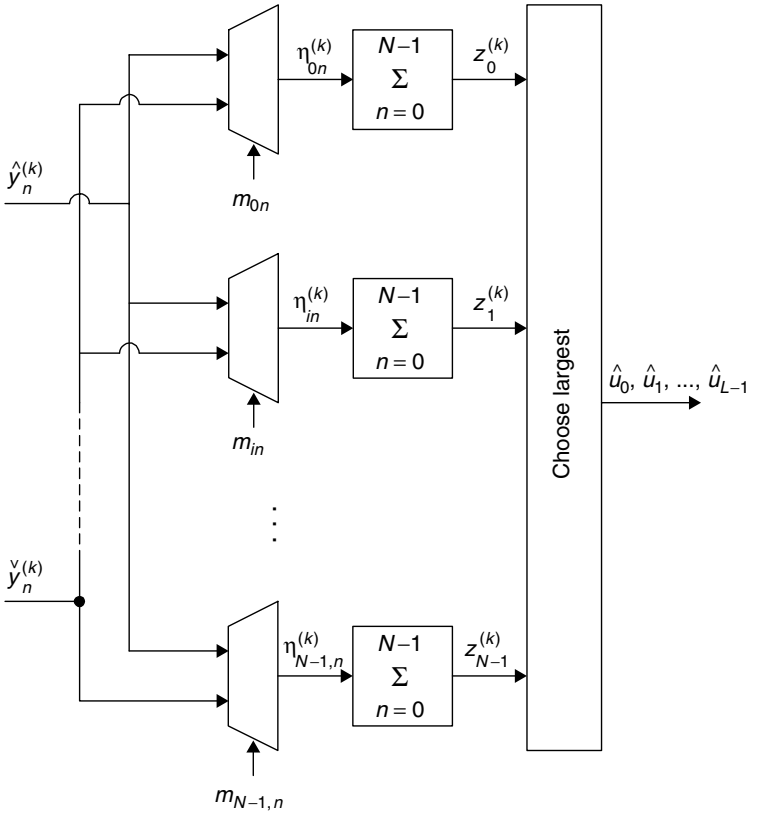

Figure 4.22. The decoder block of the BFSK speed spectrum noncoherent receiver.

Reed–Muller code (orthogonal). The received signal is given by Formula (3.125). The down-converted signal at the input of the demodulator is (3.126). The demodulator part of the receiver coincides with this part of the receiver in Figure 3.8, but the decision making device should be replaced by the decoder given in Figure 4.22.

We assume that the inputs to the decoder are the sequences $\hat{y}_n^{(k)}$ and $\check{y}_n^{(k)}$ from the outputs of the summers in Figure 3.8. The symbols $\hat{y}_n^{(k)}$ and $\check{y}_n^{(k)}$ are inputs to N parallel multiplexers, controlled by variables m_{in}, $n = 0, 1, \ldots, N-1$, where m_{in} is the nth element of the $(i-1)$th row of the Hadamard matrix, such that the output $\eta_{in}^{(k)}$ of the ith multiplexer at the nth moment is $\hat{y}_n^{(k)}$ if $m_{in} = 1$ and $\check{y}_n^{(k)}$ if $m_{in} = -1$.

Without loss of generality we will study decoding of the 0th block of the information symbols transmitted by the first user. We assume also that the zeroth (first row of the Hadamard matrix) codeword was sent. The users are not chip synchronized, but the system has perfect power control. The AWGN is negligible.

Statistics $\hat{y}_n^{(1)}$ and $\check{y}_n^{(1)}$, $n = 0, 1, \ldots, N-1$, are given by (3.131) and (3.132). The moments of $\hat{y}_n^{(1)}$ and $\check{y}_n^{(1)}$ are [see Formulas (3.144)–(3.147)]

$$E(\hat{y}_n^{(1)}) = P\left(1 + \frac{2\lambda}{3}\right) \tag{4.81}$$

$$E(\check{y}_n^{(1)}) = \frac{2}{3}\, P\lambda \tag{4.82}$$

$$\mathrm{var}(\hat{y}_n^{(1)}) = P^2\left[\frac{26}{15}\,\lambda + \frac{4}{9}\,\lambda^2\right] \tag{4.83}$$

$$\mathrm{var}(\check{y}_n^{(1)}) = P^2\left(\frac{2}{5}\,\lambda + \frac{4}{9}\,\lambda^2\right) \tag{4.84}$$

where $\lambda = (K-1)/M$.

Consider statistics

$$x_i^{(1)} \stackrel{\mathrm{def}}{=} z_0^{(1)} - z_i^{(1)} = \sum_{n=0}^{N-1} \eta_{0n}^{(1)} - \sum_{n=0}^{N-1} \eta_{in}^{(1)},\ i = 1, 2, \ldots, N-1 \tag{4.85}$$

The necessary condition of the decoding error $\mathcal{E}$ is that

$$\{x_1^{(1)} \le 0,\ \text{or}\ x_2^{(1)} \le 0, \ldots,\ \text{or}\ x_{N-1}^{(1)} \le 0\} \tag{4.86}$$

The mathematical expectation of $x_i^{(1)}$ is

$$E(x_i^{(1)}) = \frac{NP}{2}\ ,\ i = 1, 2, \ldots, N-1 \tag{4.87}$$

The variance is

$$\mathrm{var}(x_i^{(1)}) = \frac{N}{2}\ P^2\left(\frac{32}{15}\,\lambda + \frac{8}{9}\,\lambda^2\right),\ i = 1, 2, \ldots, N-1 \tag{4.88}$$

The union bound is particularly easy to apply in this case because all signal pairs are equidistant in signal space. Assuming that statistics $x_i^{(1)}$ are normally distributed because of the central limit theorem we get the next union bound for the block error probability

$$P_{\mathrm{B}} < (N-1)Q(\sqrt{2\rho_{\mathrm{B}}}) \tag{4.89}$$

where

$$\rho_{\mathrm{B}} = \frac{[E(x_i^{(1)})]^2}{2\mathrm{var}(x_i^{(1)})} = \frac{W/R(K-1)}{2(4.25 + 1.8\lambda)}\ \log_2 N \tag{4.90}$$

is signal-to-noise ratio per block.

If we take into account voice activity monitoring, antenna sectorization, and other-cell interference, we get for $\lambda = 0$

$$\rho_B = \frac{W/R}{8.5(K-1)} \frac{\gamma_v \gamma_a}{1+f} \log_2 N \tag{4.91}$$

where γ_v and γ_a are voice activity and antenna gain factors and f is the other-cell interference factor.

Combination of Formulas (4.89) and (4.91) gives the following lower bound for radio channel capacity [compare with (3.142)]

$$K_0 \geq 1 + \frac{W/R}{4.25[Q^{-1}(2P_b/N-1)]^2} \frac{\gamma_v \gamma_a}{1+f} \log_2 N \tag{4.92}$$

where $P_b \approx P_B/2$ is the bit error probability and $Q^{-1}(\cdot)$ is the inverse Q function.

EXAMPLE 4.9

Estimate the uplink capacity of the asynchronous multicell FH CDMA system with the same parameters as in Example 3.11. The system uses a reduced first-order Reed–Muller code of length $N = 64$, 256, *and* 1024. *No pilot signaling. Neglect the background AWGN.*

Solution

If $P_b = 10^{-3}$ *we get from Formula* (4.92) *that* $K_0 \approx 354$, 405, 443 *for* $N = 64$, 256, *and* 1024, *respectively. If* $P_b = 10^{-4}$, *then* $K_0 \approx 278$, 328, 367.

Comparisons of Example 4.9 with Example 3.10 and Example 4.3 shows that the *coded BFSK FH CDMA system* with noncoherent receiver performs better than *uncoded BFSK FH CDMA system* with noncoherent receiver, but worse than the *coded BPSK DS CDMA system* with noncoherent receiver.

We have considered only one example of using FEC coding in the FH CDMA systems. In principle, any codes can be used in FH and PPH CDMA, and if we used nonbinary codes the system performance would be better than in the case of binary codes.

As an example of application of the first-order Reed–Muller (biorthogonal) code, consider code transmission in PPH CDMA system using pulse position modulation with Manchester pulse shaping. The signal transmitted by the kth user is defined by (2.147) and (3.173), where $v_n^{(k)}$, $v_n^{(k)} \in \{1, -1\}$, are symbols of the length N rate $r = (\log_2 N + 1)/N$ first-order Reed–Muller (biorthogonal) code. The received signal is given by Formula (3.152), and the receiver (for the zeroth block) is presented in Figure 4.23.

Here the impulse response $g(t)$ of the matched filter is given by (3.174), and m_{in} is the nth symbol of the $(i-1)$th row of the $N \times N$ Hadamard matrix. We assume that the system has perfect power control, that is, $P^{(k)} = P$, $k = 1, 2, \ldots, K$.

Without loss of generality we consider decoding of the zeroth block of information symbols transmitted by the first user, conditioned that the zeroth (first

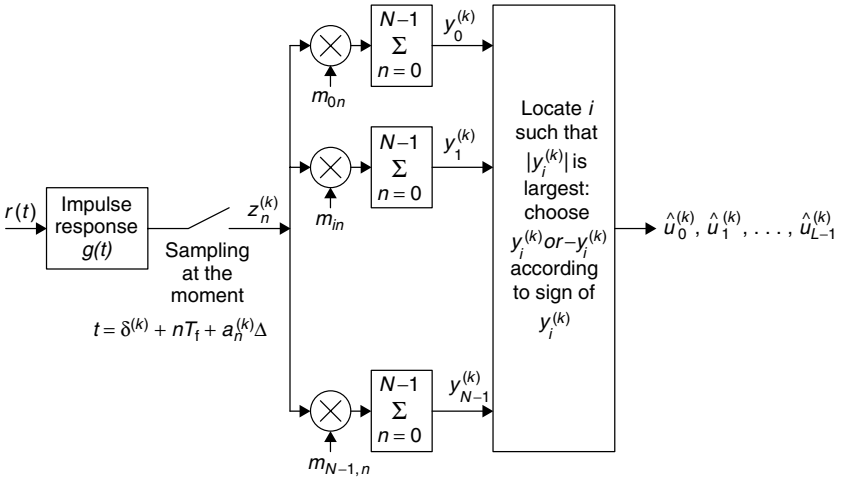

Figure 4.23. The PPH CDMA receiver for the kth user with decoder block.

row of the Hadamard matrix) codeword was sent. The first two moments of the decision statistics $y_i^{(k)}$, $i = 0, 1, \ldots, N-1$, are [compare with Formulas (3.181) and (3.182)]

$$E(y_i^{(k)}) = \begin{cases} \sqrt{P}\,N, & \text{if } i = 0\ , \\ 0, & \text{otherwise} \end{cases} \tag{4.93}$$

$$\operatorname{var}(y_i^{(k)}) = \left[\frac{2T_c}{3T_f}\,(K-1)P + \frac{N_0}{T_c}\right] N \tag{4.94}$$

Then the probability of correct decision $P(\mathcal{C})$ is given by (4.27), where

$$\rho_c = \frac{P}{\frac{4}{3}\frac{T_c}{T_f}(K-1)P + \frac{2N_0}{T_c}} = \frac{1}{\frac{4}{3}\frac{T_c}{T_f}(K-1) + \frac{2N_0}{T_c P}} \tag{4.95}$$

In Figure 4.4, the block error probability $P_B = 1 - P(\mathcal{C})$ is shown as the function of the signal-to-noise ratio per bit $E_b/I_0 = \rho_c N/(\log_2 N + 1)$. If AWGN is negligible, the capacity is [compare with Formula (3.184)]

$$K_0 = 1 + \frac{3}{8}\,\frac{W/R}{E_b/I_0}\,(\log_2 N + 1) \tag{4.96}$$

EXAMPLE 4.10

Consider the PPH CDMA system of Example 3.12 with maximal acceptable $P_b = 10^{-4}$. *Determine the capacity of the system using the first-order Reed–Muller (biorthogonal) code of length* $N = 32, 128, 512$.

Solution

From Figure 4.4 we find that to $P_b = 10^{-4}$ *(*$P(\mathcal{E}) = 2 \cdot 10^{-4}$*) correspond*

$$E_b/I_0 = 2.88 \text{ (4.6 dB) } \textit{if } N = 32$$
$$E_b/I_0 = 2.63 \text{ (4.2 dB) } \textit{if } N = 128$$
$$E_b/I_0 = 2.51 \text{ (4.0 dB) } \textit{if } N = 512$$

Then from Formula (4.96) follows $K_0 \approx 156251,\ 228138,\ 298806.$

We can see that PPH CDMA systems have fantastic theoretical capacity! Unfortunately, as we mentioned, these systems, if they were implemented, would occupy the full spectrum where all existing radio systems operate.

4.8 CONCATENATED CODES IN CDMA SYSTEMS

In this section, we present a technique for combining two codes to produce a more powerful error control technique. This method seeks the power of a long code, without suffering the complexity of the associated decoding, by employing shorter component codes. Figure 4.24 illustrates a general concatenation approach.

The inner encoder and decoder use a block or a convolutional code, called the *inner code*. Usually, the inner code is binary and the interleaver/deinterleaver is absent. The combination of the inner encoder, the digital modulator, the channel, the digital demodulator, and the inner decoder can be thought as forming a new channel (called a *superchannel*), whose input and output are binary blocks of length k, or equivalently, elements of the q-ary Galois field, where $q = 2^k$. Most often, a Reed–Solomon code is used as an *outer code*. In particular, this concatenation is included in the WCDMA proposal for standard IMT-2000 as a coding scheme for packet transmission with rates above 2 Mb/s. The inner code is a rate $r_i = 1/3$ memory 8 convolutional code. The outer code is a (40,32) Reed–Solomon code, where 40 is the block length and 32 is the number of

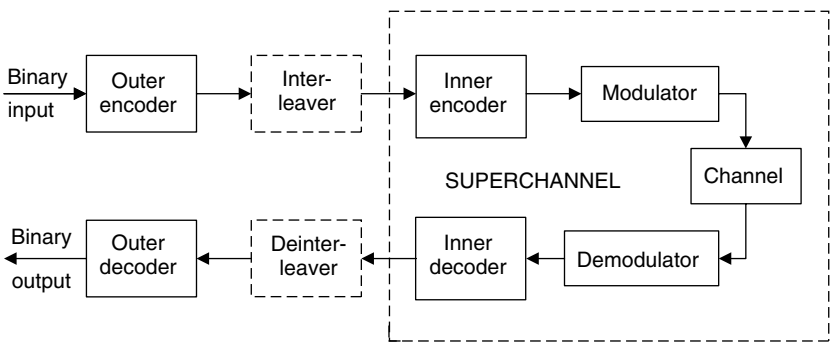

Figure 4.24. Block diagram of a communication system with concatenated coding.

information symbols in the block. It can be seen easily that if the code rate of the inner code is r_i and the code rate of the outer code is r_o, the total code rate r_c of the concatenated code equals

$$r_c = r_i r_o \tag{4.97}$$

In Section 4.5 we considered a concatenated code with an outer rate $r_o = b/c$ convolutional code and an inner rate $1/N$ repetition code. In this section we consider coding schemes used by IS-95 in forward and reverse communication.

EXAMPLE 4.11

Consider the forward (down)link transmission in IS-95. The base station transmits the code sequences $\boldsymbol{v}^{(1)}, \boldsymbol{v}^{(2)}, \ldots, \boldsymbol{v}^{(K)}$ *from K users plus all-ones (in the real number alphabet) sequence* $\boldsymbol{v}^{(0)} = \mathbf{1} = (\ldots 1, 1, \ldots, 1 \ldots)$ *(Fig. 4.25). The last sequence, the pilot sequence, is used for determining multipath component characteristics in the fading environment (see Chapter 5). It is further scaled by* $\gamma^{(0)}$*, the additional gain allotted to the pilot signal. The kth user signal scaled by* $\gamma^{(k)}$ *(see Section 5 and 3.4). The encoder of the kth user is a concatenated encoder. The outer code is the rate* $r_o = 1/2$ *memory* $m = 8$ *convolutional code with generators (*753,561*). The inner code is the rate* $1/64$ *length* $N = 64$ *repetition code. Between the outer and the inner encoder there is a* 24×16 *block interleaver. The modulation method is QPSK.*

The input symbols of the outer encoder are output symbols of the speech coder. The data rates are 9.6, 4.8, 2.4, *or* 1.2 *kb/s.*

Assuming that the highest data rate of 9.6 *kb/s is used, find:*

a) *The bit rate on the output of the outer encoder*
b) *The bit rate on the output in the inner encoder*

Solution

a) *The bit rate on the output of the outer encoder is* 19.2 *kb/s.*
b) *The code symbol rate on the output of the inner encoder is* $64 \times 19.2 =$ 1.2288 *Mb/s.*

In IS-95, the code sequences from the individual users and the pilot sequence $\boldsymbol{v}^{(0)}$ are multiplied by the base station-specific spreading sequences $\{a_n^{(0)}\}$ and $\{b_n^{(0)}\}$, where $\{a_n^{(0)}\}$ is the in-phase spreading sequence and $\{b_n^{(0)}\}$ is the quadrature spreading sequence. They are pseudorandom sequences of period $2^{15} - 1$ chips. So, in IS-95, rather than randomizing the spread signals for each individual user, the pseudorandom spreading signal is assigned only to the individual base station. Now, instead of using individual pseudorandom sequences to separate the users, the separation is achieved by employing orthogonal signals. This, in turn, is done by assigning one of the N Hadamard sequences $\boldsymbol{m}_i$ (rows of the Hadamard

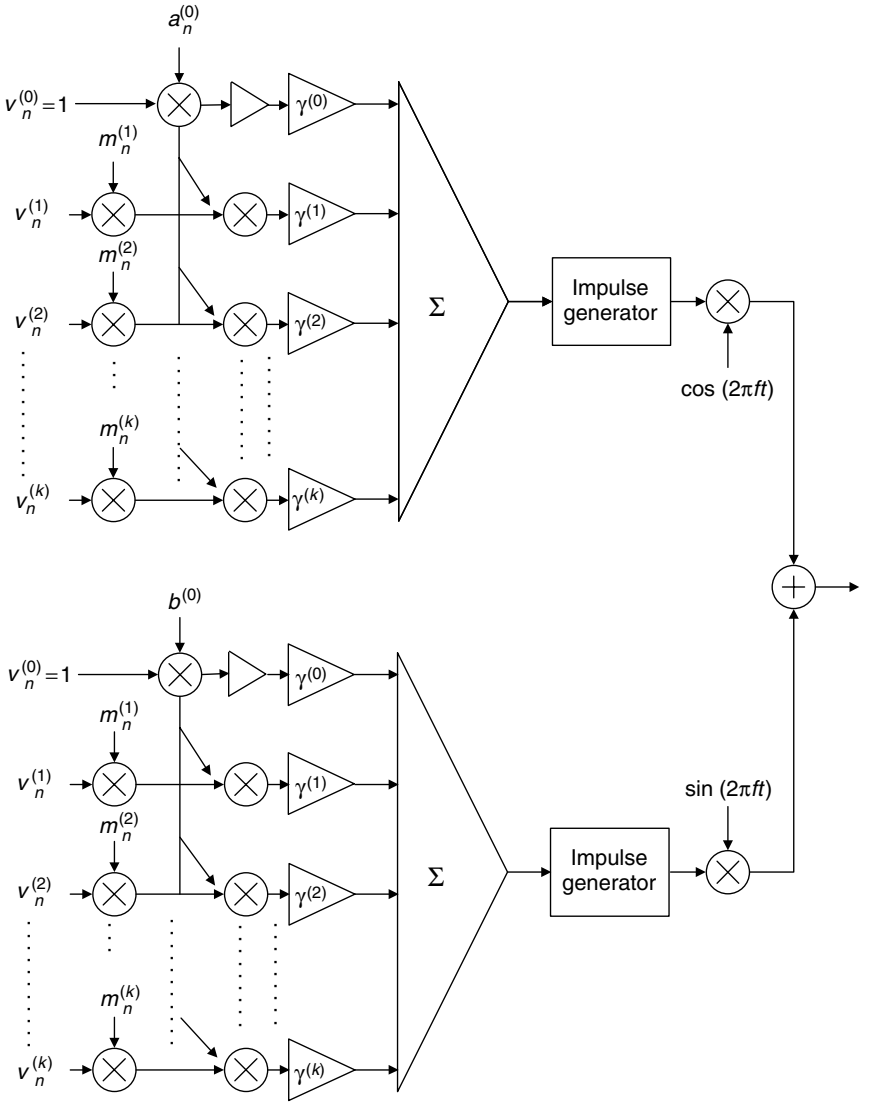

Figure 4.25. Base station modulator employing orthogonal Hadamard multiplexing; $\boldsymbol{m}^{(k)} = (m_0^{(k)}, m_2^{(k)}, \ldots, m_{N-1}^{(k)})$ is a Hadamard sequence for the kth user, $k \leq N-1$.

matrices, which are also codewords of the first-order Reed–Muller code) of duration N to spread each codeword of the inner code, as shown in Figure 4.25. When the base station receives and recognizes a newly accessing user, it must assign it a Hadamard sequence. Then, while the base station transmitter multiplies the code sequence by this sequence to spread and orthogonalize, the receiver must similarly multiply the received sequence by the same Hadamard sequence, as well

as by the cell's pseudorandom sequence, to remove the spreading. Note that in contrast to the system considered in Sections 2.3 and 3.4, the phases $\phi^{(k)}$ of the signals transmitted by different users are the same, that is, $\phi^{(k)} = 0$. It can be done because the lowpass signals of different users are orthogonal.

EXAMPLE 4.12

What is the maximal number of users in IS-95?

Solution

Obviously, the total number of users in the forward link in a cell cannot exceed $N - 1$*, because one Hadamard sequence is assigned to the pilot signal. In the IS-95 system, where* $N = 64$*, only* 61 *Hadamard sequences are available to individual users; the remaining three sequences are reserved for the pilot, the paging, and the synchronization channel, which are common to all the users in the cell.*

The pilot signal allows a mobile receiver to acquire timing and provides a phase reference for the *coherent demodulation*. In the forward link receiver, the operations at the base transmitter are essentially reversed. The received signal is initially despread, with the quadrature period $2^{15} - 1$ pseudorandom sequence. The resulting signal will then consist of the signals intended for all users in the desired cell, the pilot, the paging, and the synchronization signals for the desired cell, and an attenuated version of interference from other cells. The pilot signal is initially recovered from the despreader signal and is used to perform coherent demodulation of the desired user's signal as well to perform multipath searching and tracking (see the following chapters). The despread, coherently demodulated signal is further despread by the desired user's Hadamard sequence. In the absence of multipath the Hadamard-despread signal will contain only the desired user's signal and an attenuated version of the signals from other cells. The Hadamard-despread signal is then convolutionally decoded with a Viterbi decoder.

EXAMPLE 4.13

The reverse (up) link IS-95 communication system employs noncoherent demodulation and a concatenated code. The outer code is a rate $r_o = 1/3$*, memory* $m = 8$ *convolutional code with generators (*557,663,771*). The coded and interleaved (the interleaver size is* 32×18*) symbols are then block coded by the inner encoder. The inner code is the rate* $r_i = 6/64$ *block length* 64 *reduced first-order Reed–Muller code. The output stream from the outer encoder is divided in blocks of* 6 *symbols and encoded by the inner code to codewords of length* 64*. The encoder uses* 6 *successive symbols from the interleaver to form an index of the chosen codeword. As was the case with the forward link, the encoder output signals are spread further by simultaneously spreading the code symbol stream in quadrature with two shortlength (period* $2^{15} - 1$*) sequences.*

Under the same assumptions as in Example 4.11, find the bit rate on the outputs of the outer and the inner encoder.

Solution

The symbol rate after the convolutional encoder is $3 \times 96 = 28.8$ *kb/s; the symbol rate after Reed–Muller encoder is* $28.8 \times 64/6 = 307.2$ *kb/s. Actually, the coded symbol stream is then spread and scrambled by mixing with the* 1.2288 *Mb/s code, so that the modulator input rate becomes* 1.2288 *Mb/s.*

At the reverse link receiver of IS-95, the operations at the mobile transmitter are essentially reversed. The received signal is initially despread with the quadrature period $(2^{15} - 1)$ pseudorandom sequences. The 64-ary noncoherent demodulator/inner code decoder takes as an input the length 64 received signal real-valued vectors $\{z_{\mathrm{I}n}\}$, $\{z_{\mathrm{Q}n}\}$ (see Fig. 4.5). The block decoder computes correlation statistics $\{y_i\}$ and selects the maximum of all the y_i. The binary value of the maximum index is then mapped into a corresponding 6-bit convolutionally coded symbol for application to the deinterleaver/convolutional decoder.

The output of the block decoder is then fed to the deinterleaver and the Viterbi decoder. We did not here describe the search processor used in the Rake receiver for tracking multipath (see Chapter 5). Further details of implementation of the IS-95 system may be found in [44].

A further evolution of the IS-95 system is the CDMA2000 multicarrier (MC) option being standardized by the 3rd Generation Partnership Project [55]. The name for the MC mode comes from the forward transmission link, where instead of a single wideband carrier, multiple (in this case, 3) parallel CDMA carriers are transmitted from each base station. Each carrier's chip rate is equal to the IS-95 chip rate, that is, 1.2288 Mb/s. The total chip rate is $1.2288 \times 3 = 3.6864$ Mb/s. As illustrated in Figure 4.26, three IS-95 signals each with 1.25-MHz bandwidth form a multicarrier signal in the forward link with approximately 3.75-MHz bandwidth. The carriers can be operated independently, or the mobile can demodulate them in common. The channel on each carrier is spread with Hadamard sequences using a constant spreading factor during the connection. The spreading factors for data transmission range from 4 up to 256. The base station/cell pseudorandom spreading sequences and user-specific Hadamard spreading sequences are the same for three carriers.

CDMA2000 uses concatenated convolutional coding, analogous to that implemented in IS-95, and turbo-coding. The last is used for rates above 14.4 kb/s.

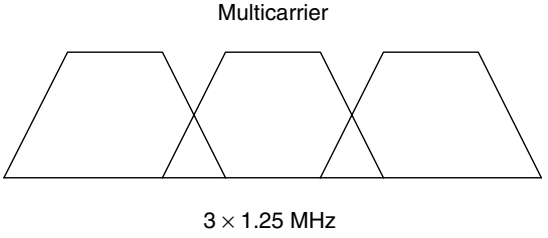

Figure 4.26. Spectrum usage in forward link of CDMA2000 system.

Differences in convolutional coding also exist: In addition to IS-95 1/2 and 1/3 rates, 1/4 and 1/6 convolutional codes have been specified in CDMA2000. The encoder memory $m = 8$ is the same as in IS-95.

4.9 COMMENTS

Coding theory started at the end of the 1940s. During the period 1950–1975, there were a number of significant contributions to the development of coding theory and decoding algorithms. In particular, Reed–Muller codes were invented in 1954, convolutional codes was described by Elias in 1955, and Viterbi published his algorithm in 1967. The interested reader is referred to books on coding theory by Peterson and Weldon [33], Lin and Costello [27], Johannesson and Zigangirov [24] and Wilson [57]. Particularly, in our analysis of the Reed–Muller code decoding we followed the last book. The application of FEC in SS systems is described in books by Peterson, Ziemer, and Borth [34] and Viterbi [47].

In the conventional (i.e., non-spread spectrum) communication systems, the employment of FEC coding requires that either the signal bandwidth must be increased or the transmission rate must be decreased. In contrast, the employment of FEC coding in CDMA systems does not require bandwidth expansion or transmission rate reduction. Furthermore, the processing gain is not decreased by the use of forward error correction (see Viterbi [50]).

Finally, the subjects addressed in this chapter describe only a small portion of the research results regarding coded spread spectrum communications. Additional information and references are available in the book by Simon, Omura, Scholz, and Levitt [43].

PROBLEMS

4.1. Prove the union bound (4.15).

4.2. The weight enumerator function of the length $N = 2^{\kappa} - 1$, where $\kappa \geq 3$ is an integer, binary *Hamming code* is given by the formula

$$T(W) \stackrel{\text{def}}{=} \sum_{w=3}^{N} a_w \; W^w = \frac{1}{(N+1)} \times \left[(1+W)^N + N(1+W)^{\frac{N-1}{2}} (1-W)^{\frac{N+1}{2}} \right] - 1$$

The rate of the code is $r = (N - \kappa)/N$. Find the upper bound for the erroneous decoding probability $P(\mathcal{E})$ if $N = 7$, $E_b/N_0 = 3$ dB, 5 dB, 10 dB.

4.3. Consider a situation where orthogonal signals (reduced first-order Reed–Muller code) are used to improve the performance of the system. Let the

number of orthogonal signals be $M = 2^L$, where L is the number of bits transmitted per signal, and let E_b/I_0 be the signal-to-interference ratio.

a) If $N = 2$ and coherent reception is used, prove that

$$P_B = P_b = Q\left(\sqrt{\frac{E_b}{I_0}}\right)$$

b) For the general case, where $N = 2^L$, prove that

$$Q\left(\sqrt{\frac{E_b}{I_0}\,L}\right) \le P_B \le (M-1)Q\left(\sqrt{\frac{E_b}{I_0}\,L}\right)$$

c) Given that a signal error has occurred, what is the probability that a specific bit is in error?

d) If $N = 2$ and noncoherent reception is used, find the required excess energy in comparison to the coherent case for $P_b = 10^{-3}$ and $P_b = 10^{-5}$, respectively.

e) Consider a DS CDMA system with repetition coding and coherent BPSK where the maximum number of active users that can be supported is 10, if the required bit error probability is 10^{-3}. If instead 64-ary orthogonal signaling was used, estimate how many users could be supported in this case if the bit error probability was the same.

4.4. Consider a system using the first-order Reed–Muller code. A straightforward way of decoding is described in Figure 4.2.

a) Construct a $N = 8$ Hadamard matrix.

b) Determine the complexity of the decoder in Figure 4.2, that is, the number of additions and multiplications per block.

c) Assuming communication over an AWGN channel, decode the sequences

$$\boldsymbol{r} = 2.06,\ -0.94,\ -1.09,\ \ 0.16,\ \ 1.29,\ -2.33,\ -0.28,\ \ 2.62$$
$$\boldsymbol{r} = 0.30,\ \ 1.85,\ \ 0.25,\ -2.59,\ -2.44,\ -0.42,\ \ 0.60,\ 1,68$$

encoded by the length $N = 8$ code.

4.5. Consider a system with the same encoder and transmitter as in Problem 4.4, but with a receiver using the fast Hadamard transform (FHT) (see Fig. 4.3).

a) Determine the complexity of the FHT decoder, that is, the number of additions and multiplications per block.

b) Decode the sequences $\boldsymbol{r}$ of Problem 4.4 using the FHT.

4.6. Suppose that for transmission over the AWGN channel a first-order Reed–Muller code of length $N = 8$ is used. The received sequence is $z_0 = 1.5$,

$z_1 = -1.3,\ z_2 = -1.2,\ z_3 = -1.8,\ z_4 = 0.2,\ z_5 = -0.3,\ z_6 = 1.4,\ z_7 = -0.1$.

Use the FHT to find the decoded sequence.

4.7. Consider the same system as in Problem 3.11, assuming that it uses a first-order Reed–Muller code of length $N = 2^9$. Calculate the radio channel capacity.

4.8. Explain why using the first-order Reed–Muller code of length $N = 2$ is worse than the uncoded transmission (see Fig. 4.4).

4.9. Consider the same system as in Problem 3.11, assuming that it uses the reduced first-order Reed–Muller code of length $N = 2^{10}$ and the noncoherent receiver. Calculate the radio channel capacity.

4.10. For the $r = 1/2$, memory $m = 8$ code listed in Table 4.2,

a) Draw the encoder

b) Find the asymptotic coding gain

c) Using Figure 4.16, find the coding gain at $P_b = 10^{-5}$

4.11. In the figure below is given the (7,6) convolutional encoder.

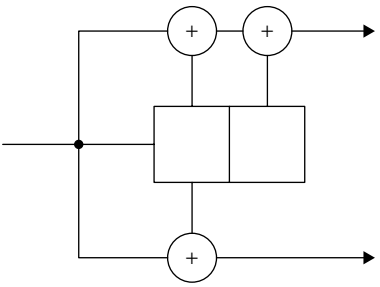

Problem 4.11.

a) Draw the trellis description of the (7,6) convolutional encoder.

b) Make the same assumption as in Example 4.4. Assuming 4-bit all-zero message sequence and 2 dummy zeros tail, decode the received sequence $z = (1.0,\ -0.3,\ -0.1,\ 0.9,\ 0.5,\ 1.3,\ 0.5,\ 0.6,\ -0.2,\ -0.5,\ 1.2,\ 0.9)$ by using the Viterbi algorithm.

c) Find the asymptotic coding gain.

4.12. Estimate P_b for the encoder of Problem 4.11 by using Formula (4.60). Choose

a) $\frac{E_b}{I_0} = 4$ dB

b) $\frac{E_b}{I_0} = 6$ dB

c) $\frac{R_b}{I_0} = 8$ dB

4.13. Find the asymptotic coding gain for the convolutional encoder given below.

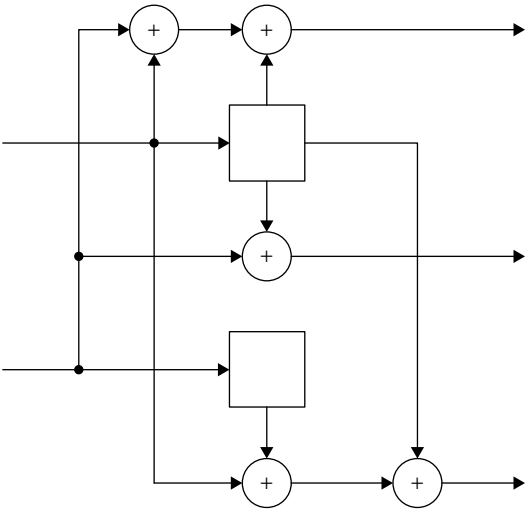

Problem 4.13.

4.14. Prove that for the first construction of the orthogonal convolutional codes, (4.76) and (4.77) are valid formulas with $W = \exp\{-\rho_c 2^{(m-1)}\}$ and W^{m+1} replaced by W^{m+2}.

4.15. Let a memory $m = 5$ orthogonal convolutional code (first construction) be used for communication over AWGN channel with signal-to-noise ratio $E_b/I_0 = 3$ dB. The receiver is coherent. Find upper bounds for burst and bit probabilities of error. Repeat the problem for the second orthogonal convolutional code construction and for the superorthogonal convolutional code.

4.16. Consider the following system using DS CDMA and BPSK modulation.

— $W = 1.25$ kHz

— $R = 9.6$ kb/s

— Required probability of bit error $\leq 10^{-3}$

— No antenna gain

— Voice activity gain = 2

— Other-cell relative interference factor = 1.

a) If the channel is an AWGN channel, what is the maximum number of users if a rate 1/2 memory 4 encoder is used and soft-decision Viterbi decoding is employed? (You may neglect the background noise and model the multiple access interference as Gaussian.)

b) If instead a rate 1/2 memory 6 encoder is used?

4.17. A rate 1/2 convolutional code with $d_{\text{free}} = 10$ is used to encode a data sequence occurring at a rate of 1000 b/s. The modulation is binary PSK. The spread spectrum sequence has a chip rate of 10 MHz.

a) Determine the asymptotic coding gain.

b) Determine the processing gain.

4.18. In the downlink (from the base station to the mobile terminals) of the IS-95 DS CDMA system, Hadamard sequences are used as spreading sequences. Consider a system using Hadamard sequences of length 8, where the base station transmits to five active users with equal power. If a mobile terminal receives the following slightly noisy signal

$$\boldsymbol{r} = (-0.8\ 0.5\ 1.2\ 3.4\ 2.7\ -1.0\ -3.0\ 3.1)$$

what users were active at the moment?

5

CDMA COMMUNICATION ON FADING CHANNELS

The mobile radio channel places fundamental limitations on the performance of CDMA systems. In previous chapters the channel model employed in analyzing CDMA communication systems was the AWGN channel model. In this chapter the concept of fading channels is introduced in connection with mobile radio communication. Fading is caused by interference between two or more versions of the transmitted signal that arrive at the receiver at different times. As will be seen, fading channels, and in particular mobile radio channels, can cause significant degradation in the performance of a CDMA system.

The method commonly employed to overcome the degradation in performance due to fading is the use of *diversity*. The goal of diversity is to reduce the fading effect by supplying the receiver with multiple replicas of the signal that have passed through a multipath channel. If the signal bandwidth is sufficiently wide, as in CDMA communication, a receiver can resolve the multipath components and combine the multipath copies in an advantageous manner. For spread spectrum CDMA, a modern implementation of *multipath diversity* involves the use of a *Rake receiver*.

In this chapter, we consider, together with the Rake receiver, the application of forward error correction (FEC) techniques in communication over fading channels. The problem is that successive chips cannot be regarded as independent in a multipath fading environment. Because the FEC technique performs best when channel errors are independent, interleaving is assumed for FEC schemes.

5.1 STATISTICAL MODELS OF MULTIPATH FADING

In built-up urban areas, the transmitted signal is reflected and refracted by a variety of terrestrial objects, so that it is replicated at the receiver with many

Theory of Code Division Multiple Access Communication, by Kamil Sh. Zigangirov
ISBN 0-471-45712-4

different time delays. Each version of the transmitted signal arrives with its own amplitude and carrier phase. The fading channel model arises from the combination at the receiver of many versions of the transmitted signal. In addition, the channel is usually corrupted by AWGN.

Fading encountered over a mobile radio channel can be of two types: short-duration rapid fading over time spans of less than a few seconds and long-duration slow fading over spans of several minutes to several hours. A more detailed introduction to fading theory is given in [34]. Here, only a brief description of simple models for fading channels is given.

The propagation loss of mobile radio channels is generally modeled as the product of the mth power of the distance and a log-normal component representing shadowing losses. This model represents slowly varying losses, even for users in motion, and applies to both reverse and forward links. We consider the model of slow fading in Chapter 9, when we study CDMA handoff strategies and other-cell interference.

The description of the rapid fluctuation of the amplitude of a radio signal over a short period of time or travel distance uses another model than that considered for the description of slowly varying losses. Several models for the rapid varying amplitude of the received signal have been considered in the literature. The *Rayleigh and*, to a lesser degree, *Rician fading models* are emphasized in our treatment because of their analytical convenience.

The Rayleigh and Rician random variables were introduced in Section 3.2 [see Formulas (3.34) and (3.50)]. By definition, the *Rayleigh random variable* is a nonnegative continuous random variable having the one-parameter probability density function

$$f_a(\alpha) = \begin{cases} \dfrac{\alpha}{a^2} \exp\left(-\dfrac{\alpha^2}{2a^2}\right), & \alpha \geq 0, \\ 0, & \alpha < 0 \end{cases} \tag{5.1}$$

where a is the parameter. It arises as the root-sum square of independent Gaussian variables; that is, $\alpha = \sqrt{x_1^2 + x_2^2}$, where x_1 and x_2 are independent zero-mean Gaussian random variables having the variance a^2.

It is interesting to note that if α is a Rayleigh random variable with probability density function (5.1) and the random variable φ is uniformly distributed on the interval $[0, 2\pi)$, the random variables $x_1 = \alpha \cos \varphi$ and $x_2 = \alpha \sin \varphi$ are independent zero-mean Gaussian variables with variances a^2 (Problem 5.10).

If x_1 and x_2 are independent Gaussian random variables having nonzero means and the same variance a^2, then the random variable $\alpha = \sqrt{x_1^2 + x_2^2}$ has Rician distribution with the probability density function

$$f_{\mu,a}(\alpha) = \begin{cases} \dfrac{\alpha}{a^2} I_0\left(\dfrac{\mu\alpha}{a^2}\right) \exp[-(\alpha^2 + \mu^2)/2a^2], & \alpha \geq 0, \\ 0, & \alpha < 0 \end{cases} \tag{5.2}$$

where $\mu = \sqrt{\mu_1^2 + \mu_2^2}$, μ_1 and μ_2 are the mean values of x_1 and x_2, respectively, and $I_0(x)$ is the zero-order modified Bessel function of the first kind. The Rayleigh random variable is a special case ($\mu = 0$) of the Rician random variable.

Let us give the definition of the *Rayleigh fading channel* if the *carrier transmission* is involved. We will use complex envelope notation for the signal (see Section 2.1), that is,

$$s(t) = \mathrm{Re}\{\hat{s}(t) \exp[j(2\pi f_c t + \phi)]\} \tag{5.3}$$

where $\hat{s}(t)$ is defined as the *complex envelope* of the signal relative to the adopted carrier frequency f_c. Without loss of generality, we can assume here that the relative phase ϕ is 0. The received signal waveform is

$$r(t) = \mathrm{Re}[\beta(t - \delta)\hat{s}(t - \delta) \exp(2\pi j f_c(t - \delta))] + \xi(t) \tag{5.4}$$

where $\beta(t) = \alpha(t) \exp(j\varphi(t))$ is a complex-valued coefficient, $\alpha = \alpha(t)$ is the *fade amplitude*, $\varphi = \varphi(t)$ is the *phase shift*, and $\xi(t)$ is AWGN with two-sided spectral density $N_0/2$. We suppose that φ is uniformly distributed on $[0, 2\pi)$ and that the attenuation factor α is a Rayleigh random variable having probability density function (5.1). If the power of the transmitted signal equals 1, the instantaneous power of the received signal is α^2 and the average power of the received signal is

$$\begin{aligned} E(\alpha^2) &= \int_0^\infty \alpha^2 \frac{\alpha}{a^2} \exp(-\alpha^2/2a^2)\, d\alpha \\ &= \int_0^\infty \frac{\beta}{2a^2} \exp(-\beta/2a^2)\, d\beta = 2a^2 \end{aligned} \tag{5.5}$$

where we have used the substitution $\beta = \alpha^2$. In the case of *noncarrier modulation formats*, which are used, for example, in PPH CDMA, we have $r(t) = \alpha s(t - \delta) + \xi(t)$.

The Rayleigh model arises from the combination of many randomly phased point scatterers at the receiver, each scattering a small fraction of the total received power. In the general case, $\beta(t)$ is a time-varying transmission coefficient due to the scattering medium. The rate of change in β is clearly controlled by the rate of change in the relative delays of the scatterers.

Formulas (5.3) and (5.4) describe the *time-selective fading channel model*, also called the *frequency-flat fading channel model*. Because the transmitted envelope $\hat{s}(t)$ is being multiplied by $\beta(t)$, which is frequency independent, the received envelope $\hat{s}(t)\beta(t)$ is easily seen to undergo fading that is frequency independent. Rapidly changing scattering media or rapidly moving terminals produce short-duration fades *(fast fading)*. For short-duration fades, the error-correcting code can correct the symbols corrupted during the fade.

In this chapter we consider *slow fading*, where the scattering medium changes slowly relative to the symbol rate R. Then both the fade amplitude and phase shift φ may be treated as constants over a given signaling interval.

Because the fade amplitude α is Rayleigh distributed, the signal power α^2 over the signaling interval has a χ^2-distribution with two degrees of freedom. The probability that the received signal power falls κ dB below the average level $2a^2$ is equal to

$$\int_0^{\sqrt{2\eta a^2}} \frac{\alpha}{a^2} \exp\left(-\frac{\alpha^2}{2a^2}\right) d\alpha = 1 - \exp(-\eta) \tag{5.6}$$

where $\eta = 10^{-\kappa/10}$. If $2a^2\eta/N_0$ is the minimal required level of the signal-to-noise ratio at the input of the receiver, the probability $P_{\text{out}} = 1 - \exp(-\eta)$ can be considered as the *outage probability*.

EXAMPLE 5.1

Consider the transmission of a binary PSK signal over a time-selective Rayleigh fading channel. Assume that the fading is sufficiently slow. Let the minimum required level of the signal-to-noise ratio be $\kappa = -3$ dB *from the average level. Find the outage probability. How much should we increase the average power of the transmitted signal, such that for the same required SNR the outage probability does not exceed* 10%*?*

Solution

The outage probability is

$$P_{\text{out}} = 1 - \exp(-10^{-0.3}) \approx 0.39 \tag{5.7}$$

To get the outage probability 10^{-1} *we must increase the power by*

$$\begin{aligned} -10 \log_{10}[-\ln(1 - P_{\text{out}})] + \kappa &= -10 \log_{10}[-\ln 0.9] - 3 \text{ dB} \\ &= 9.8 - 3 \text{ dB} = 6.8 \text{ dB} \end{aligned}$$

Example 5.1 indicates the rather significant degradation in performance that may occur over the Rayleigh-faded channel. The method commonly employed to overcome the degradation in performance due to fading is *diversity*. The goal of diversity is to reduce the depth of fades or fade duration by supplying the receiver with samples of the transmitted signals that were received during different states of the fading channel.

Diversity reception may be achieved by a number of means. In *time diversity*, identical replicas of the transmitted signal are sent within different time intervals whose durations exceed the coherence time of the channel. The most common method of implementing time diversity is through the use of FEC with *interleaving*. We consider interleaving in Section 5.5.

Another diversity approach that is used in CDMA communication is *multipath diversity*. In this case the received signal will consist of multiple copies of the

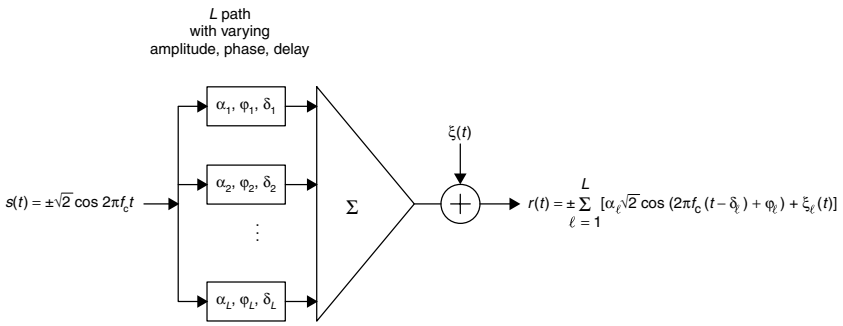

Figure 5.1. The Rayleigh multipath fading channel model for BPSK transmission.

transmitted signal, each experiencing a different path delay, fade amplitude, and phase shift. If the signal bandwidth is sufficiently wide, as in the CDMA case, a receiver can resolve the multipath components. A receiver structure that performs this operation is known as a *Rake receiver*. We consider the Rake receiver in the following sections.

If specular reflection or free space propagation of a signal components takes place, a received signal will appear as the sum of a constant amplitude component plus a Rayleigh-distributed amplitude component. The fade amplitude α is in this case Rician distributed, and the channel model is called a *Rician fading channel*.

As a generalization of the one-path Rayleigh fading channel we consider an *L-path Rayleigh fading channel*. The received signal is

$$r(t) = \sum_{\ell=1}^{L} \{\mathrm{Re}[\alpha_\ell \exp(j\varphi_\ell)\hat{s}(t-\delta_\ell)\exp(2\pi j f_c(t-\delta_\ell))] + \xi_\ell(t)\} \tag{5.8}$$

where $\hat{s}(t)$ is the complex envelope of the transmitted signal, $\xi_\ell(t)$ is AWGN with two-sided spectral density $N_{0\ell}/2$, $\alpha_\ell = \alpha_\ell(t-\delta_\ell)$ is the fade amplitude, $\varphi_\ell = \varphi_\ell(t-\delta_\ell)$ is the phase shift, and δ_ℓ is the propagation delay of path ℓ. The fade amplitudes α_ℓ are IID Rayleigh random variables; the phase shifts are IID random variables uniformly distributed on $[0, 2\pi)$. *The individual paths can be distinguished if they are mutually separated by delays not less than the chip duration* T_c, that is, $|\delta_\ell - \delta_{\ell'}| \geq T_c$, $\ell' \neq \ell$. Actually, each of the distinguishable multipath components will be a linear combination of several indistinguishable paths of varying amplitudes. Because they will add as random vectors, the amplitude of each term will be Rayleigh distributed. The Rayleigh multipath fading channel model for a BPSK-modulated transmitted signal is shown in Figure 5.1.

5.2 COHERENT RECEPTION OF FADED SIGNALS

In this section we study the problem of coherent reception of BPSK signals under the assumption that the transmission is over a Rayleigh channel and the phase of

the received signal is known. We assume that the rate $r = 1/N$ repetition code is used, that is, $v_n = u_{\lfloor n/N \rfloor}$ is a code sequence. The transmitted signal is

$$s(t) = \sqrt{2} \sum_{n=-\infty}^{\infty} v_n h_{T_c}(t - nT_c) \cos(2\pi f_c t + \phi) \tag{5.9}$$

that is, the complex envelope is

$$\hat{s}(t) = \sqrt{2} \sum_{n=-\infty}^{\infty} v_n h_{T_c}(t - nT_c) \tag{5.10}$$

and the received signal is (5.4). The receiver of the 0th block is given in Figure 3.3 (if we exclude despreading and assign $\varphi^{(k)} = \varphi$). On the output of the demodulator we have the sequence $\{z_n\}$,

$$z_n = \alpha u_0 + \tilde{\xi}_n, \quad n = 0, 1, \ldots, N-1 \tag{5.11}$$

where α is the fade amplitude and $u_0 = \pm 1$ and $\{\tilde{\xi}_n\}$ are IID zero-mean Gaussian variables with variances $N_0/2T_c$. If the fade amplitude α is known, the problem is reduced to the simple binary reception problem (see Section 3.1). Application of the Neyman–Pearson criterion (Example 3.2) gives the following decision rule:

$$y \stackrel{\text{def}}{=} \frac{4\alpha T_c}{N_0} \sum_{n=0}^{N-1} z_n \begin{array}{c} H_1 \\ > \\ < \\ H_{-1} \end{array} 0 \tag{5.12}$$

From (5.11) and (5.12) it follows that for given α

$$E(y|\alpha) = \begin{cases} \mu \stackrel{\text{def}}{=} \dfrac{4\alpha^2 T_c N}{N_0}, & \text{if } H_1 \text{ is true,} \\ -\mu, & \text{if } H_{-1} \text{ is true} \end{cases} \tag{5.13}$$

$$\text{var}(y|\alpha) = \frac{8\alpha^2 T_c N}{N_0} \tag{5.14}$$

Because α is nonnegative, the decision does not depend on α and depends only on the sign of y and we may skip the factor $4\alpha T_c/N_0$ in front of the sum of Formula (5.12). From (3.21) it follows that the conditional bit error probability given α is equal to

$$P_b(\alpha) = Q\left(\sqrt{\frac{2\alpha^2 T_c N}{N_0}}\right) \tag{5.15}$$

The unconditional probability of error is then given by

$$P_b = \int_0^\infty P_b(\alpha) f_a(\alpha)\, d\alpha = \int_0^\infty Q\left(\sqrt{\frac{2\alpha^2 T_c N}{N_0}}\right) \frac{\alpha}{a^2} \exp(-\alpha^2/2a^2)\, d\alpha \quad (5.16)$$

Integration by parts (Problem 5.8) gives

$$P_b = \frac{1}{2}\left(1 - \sqrt{\frac{2a^2 T_c N}{N_0 + 2a^2 T_c N}}\right) = \frac{1}{2}\left(1 - \sqrt{\frac{\overline{E}_b/N_0}{1 + \overline{E}_b/N_0}}\right) \quad (5.17)$$

where $\overline{E}_b = 2a^2 T_c N$ is the average received energy per bit, and $\overline{E}_b/N_0 = 2a^2 T_c N/N_0$ is the *average signal-to-noise ratio per bit*.

In Figure 5.2 the probability of bit error P_b is plotted as a function of the average signal-to-noise ratio per bit. For comparison, the probability of bit error for the BPSK signal transmitted over an unfaded AWGN channel is also shown. Observe the significant degradation in performance due to the Rayleigh fading channel. For example, at the value $P_b = 10^{-3}$ the faded signal requires 17.2 dB *excess energy* relative to an unfaded BPSK in an AWGN channel.

The dashed line in Figure 5.2 presents an upper bound on the error probability P_b for the Rayleigh fading channel,

$$P_b < \frac{1}{2(1 + \overline{E}_b/N_0)} \quad (5.18)$$

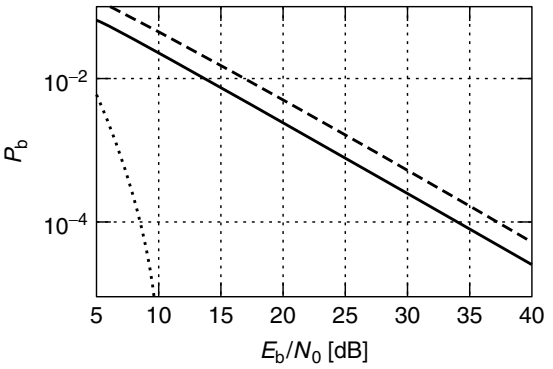

Figure 5.2. Bit error probability P_b as a function of the average signal-to-noise ratio for coherent reception of Rayleigh faded signals: (a) ____ exact (5.17); (b) - - - upper bound (5.18); (c) ..... exact value P_b for unfaded AWGN channel.

To get this bound, we upperbound the Q function in (5.16) by an exponent:

$$Q\left(\sqrt{\frac{2\alpha^2 T_c N}{N_0}}\right) < \frac{1}{2}\ \exp(-\alpha^2 T_c N/N_0) \tag{5.19}$$

Then, from (5.16) and (5.19) it follows that

$$\begin{aligned} P_b &< \frac{1}{2}\int_0^\infty \exp(-\alpha^2 T_c N/N_0)\frac{\alpha}{a^2}\exp(-\alpha^2/2a^2)\,d\alpha \\ &= \frac{1}{4a^2}\int_0^\infty \exp(-\beta T_c N/N_0)\exp(-\beta/2a^2)\,d\beta \\ &= \frac{1}{4a^2}\frac{1}{\dfrac{T_c N}{N_0}+\dfrac{1}{2a^2}} = \frac{1}{2\left(1+\dfrac{\overline{E}_b}{N_0}\right)} \end{aligned} \tag{5.20}$$

where $\overline{E}_b = 2a^2 T_c N$ is the average received energy per bit.

The optimum receiver for the L-path Rayleigh fading channel is the Rake receiver. To describe it, let us represent the received BPSK signal as the sum of L signals [compare with (5.8)]

$$r(t) = \sum_{\ell=1}^{L} r_\ell(t) \tag{5.21}$$

where

$$r_\ell(t) = \alpha_\ell\sqrt{2}\sum_{n=-\infty}^{\infty} v_n h_{T_c}(t - nT_c - \delta_\ell)\cos(2\pi f_c(t-\delta_\ell)+\varphi_\ell) + \xi_\ell(t) \tag{5.22}$$

and the background noise components $\xi_\ell(t)$, $\ell = 1, 2, \ldots L$, are IID Gaussian variables with two-sided power spectral density $N_{0\ell}/2$. We can represent the multipath channel as a set of L parallel Rayleigh channels and the Rake receiver as a combination of L receivers operating with signals $r_\ell(t)$. These receivers are analogous to those given in Figure 3.3 (if we exclude despreading and assign $\varphi^{(k)} = \varphi_\ell$). Each receiver is called a "finger" of the rake. In Section 5.3 we describe the Rake receiver for CDMA applications in more detail. Here we analyze the decision block of the receiver. To simplify notation we assume that all components have equal AWGN levels, that is, $N_{0\ell} = N_0$.

Assuming coherent demodulation in the rake fingers, we get that the decision should be made by considering the set of decision statistics

$$y_\ell = \frac{4\alpha_\ell T_c}{N_0}\sum_{n=0}^{N-1} z_{n\ell}, \quad \ell = 1, 2, \ldots, L \tag{5.23}$$

where $z_{n\ell}$, $n = 0, 1, \ldots, N-1$, is the output sequence of the ℓth demodulator. The statistics y_ℓ are independent and conditionally Gaussian given α_ℓ with expectation

$$E(y_\ell|\alpha_\ell) = \begin{cases} \mu_\ell \stackrel{\text{def}}{=} \dfrac{4\alpha_\ell^2 T_c N}{N_0}, & \text{if } H_1 \text{ is true} \\ -\mu_\ell, & \text{if } H_{-1} \text{ is true} \end{cases}, \qquad \ell = 1, 2, \ldots L \tag{5.24}$$

and variance

$$\sigma_\ell^2 \stackrel{\text{def}}{=} \text{var}(y_\ell|\alpha_\ell) = \frac{8\alpha_\ell^2 T_c N}{N_0}, \qquad \ell = 1, 2, \ldots L \tag{5.25}$$

The joint probability density function of the vector

$$\boldsymbol{y} = (y_1, y_2, \ldots, y_L)$$

is then

$$p_1(\boldsymbol{y}) = \prod_{\ell=1}^{L} \frac{1}{\sqrt{2\pi\sigma_\ell^2}} \exp\{-(y_\ell - \mu_\ell)^2/2\sigma_\ell^2\} \tag{5.26}$$

if H_1 is true and

$$p_{-1}(\boldsymbol{y}) = \prod_{\ell=1}^{L} \frac{1}{\sqrt{2\pi\sigma_\ell^2}} \exp\{-(y_\ell + \mu_\ell)^2/2\sigma_\ell^2\} \tag{5.27}$$

if H_{-1} is true. Applying the Neyman–Pearson criterion gives

$$\ln \Lambda(\boldsymbol{y}) = \ln \frac{p_1(\boldsymbol{y})}{p_{-1}(\boldsymbol{y})} = \sum_{\ell=1}^{L} y_\ell \underset{H_{-1}}{\overset{H_1}{\gtrless}} 0 \tag{5.28}$$

If $\alpha_1, \alpha_2, \ldots, \alpha_L$ are fixed, the statistic

$$\lambda = \sum_{\ell=1}^{L} y_\ell$$

has Gaussian distribution with mean

$$E(\lambda) = \begin{cases} 4\rho_B, & \text{if } H_1 \text{ is true,} \\ -4\rho_B, & \text{if } H_{-1} \text{ is true} \end{cases} \tag{5.29}$$

and variance

$$\text{var}(\lambda) = 8\rho_B \tag{5.30}$$

where

$$\rho_{\mathrm{B}} = T_{\mathrm{c}} N \sum_{\ell=1}^{L} \alpha_\ell^2 / N_0 \tag{5.31}$$

is the SNR per block. From Formulas (5.28)–(5.31) it follows that the conditional bit error probability given $\alpha_1, \alpha_2, \ldots, \alpha_L$ is upperbounded by

$$\begin{aligned} P_{\mathrm{b}}(\alpha_1, \alpha_2, \ldots \alpha_L) &= Q(\sqrt{2\rho_{\mathrm{B}}}) < \frac{1}{2} \exp(-\rho_{\mathrm{B}}) \\ &= \frac{1}{2} \exp\left(-T_{\mathrm{c}} N \sum_{\ell=1}^{L} \alpha_\ell^2 / N_0 \right) \end{aligned} \tag{5.32}$$

The random variables $\alpha_1, \alpha_2, \ldots, \alpha_L$ are independent Rayleigh random variables having the probability density functions [compare with (5.1)]

$$f_a(\alpha_\ell) = \frac{\alpha_\ell}{a^2} \exp\left\{ -\frac{\alpha_\ell^2}{2a^2} \right\}, \quad \alpha_\ell > 0, \quad \ell = 1, 2, \ldots, L \tag{5.33}$$

where we assume that the L multipath components have equal average power strengths $2a^2$.

Then, from (5.29)–(5.33) it follows that an upper bound for the unconditional bit error probability is equal to

$$\begin{aligned} P_{\mathrm{b}} &= \int_0^\infty \cdots \int_0^\infty P_{\mathrm{b}}(\alpha_1, \alpha_2, \ldots, \alpha_L) f_a(\alpha_1) \ldots f_a(\alpha_L) \, \mathrm{d}\alpha_1 \ldots \mathrm{d}\alpha_L \\ &< \frac{1}{2} \int_0^\infty \cdots \int_0^\infty \exp\left(-T_{\mathrm{c}} N \sum_{\ell=1}^{L} \alpha_\ell^2 / N_0 \right) \\ &\quad \times \frac{\alpha_1}{a^2} \exp\left(-\frac{\alpha_1^2}{2a^2} \right) \cdots \frac{\alpha_L}{a^2} \exp\left(-\frac{\alpha_L^2}{2a^2} \right) \mathrm{d}\alpha_1, \ldots, \mathrm{d}\alpha_L \\ &= \frac{1}{2} \frac{1}{\left(1 + \dfrac{2a^2 T_{\mathrm{c}} N}{N_0} \right)^L} = \frac{1}{2} \frac{1}{\left(1 + \dfrac{\overline{E}_{\mathrm{s}}}{N_0} \right)^L} \end{aligned} \tag{5.34}$$

Here $\overline{E}_{\mathrm{s}} = 2a^2 T_{\mathrm{c}} N$ is the average component energy such that

$$\frac{\overline{E}_{\mathrm{s}}}{N_0} = \frac{2a^2 T_{\mathrm{c}} N}{N_0} = \frac{\overline{E}_{\mathrm{b}}}{L N_0} \tag{5.35}$$

where $\overline{E}_{\mathrm{b}}$ is the average total energy of the received signal.

It follows from Formulas (5.34)–(5.35) that

$$P_{\mathrm{b}} < \frac{1}{2}\left(\frac{1}{1+\frac{\overline{E}_{\mathrm{s}}}{N_0}}\right)^{L} = \frac{1}{2}\left(1+\frac{\overline{E}_{\mathrm{b}}}{LN_0}\right)^{-L} \tag{5.36}$$

The bit error probability for an unfaded Gaussian channel is given by (3.74), that is,

$$P_{\mathrm{b}} = Q\left(\sqrt{\frac{2E_{\mathrm{b}}}{N_0}}\right) \leq \frac{1}{2}\exp\left(-\frac{E_{\mathrm{b}}}{N_0}\right) \tag{5.37}$$

By using (5.36) we can calculate the bound on the bit error probability P_{b} as a function of $\overline{E}_{\mathrm{b}}/N_0$ for the multipath faded channel (Fig. 5.3) and compare it with the bit error probability (5.37) of an unfaded AWGN channel for various values of L. This gives us the average excess energy required by the multipath faded channel in comparison with the unfaded AWGN channel.

Note that as $L \to \infty$, the bound P_{b} for the faded channel approaches the upper bound for the unfaded channel,

$$P_{\mathrm{b}} < \tfrac{1}{2}\exp(-E_{\mathrm{b}}/N_0) \tag{5.38}$$

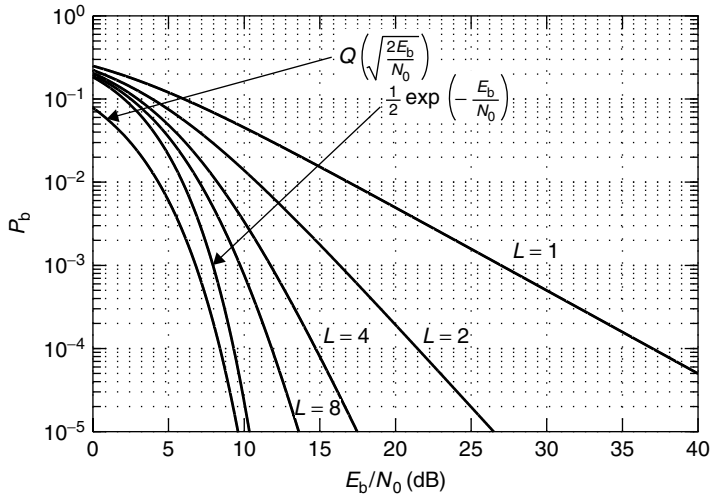

Figure 5.3. The upper bound of the bit error probability P_{b} for the L equal-strength multipath fading channel ($L = 1, 2, 4, 8$) and for the unfaded Gaussian channel, $P_{\mathrm{b}} < (1/2)\exp(-E_{\mathrm{b}}/N_0)$. For comparison the exact value of P_{b} for the unfaded case is also given.

so that the excess energy asymptotically approaches zero. This shows that with an asymptotically large number of independent Rayleigh components, the performance approaches that of unfaded propagation.

EXAMPLE 5.2

Find the average excess energy required for communication over an L-path Rayleigh channel, $L = 1, 2, 4, 8, \infty$, if the required bit error probability is $P_b = 10^{-4}$. Use the upper bound for the bit error probability given by Formulas (5.36) and (5.37).

Solution

From (5.36) we have

$$E_b/N_0 < 10 \log_{10}\{L[(2P_b)^{-\frac{1}{L}} - 1]\}$$

Then, for $L = 1, 2, 4, 8$ we have

$$E_b/N_0(\text{dB}) \approx 37.0,\ 21.8,\ 15.1,\ 13.5,\ 9.3$$

respectively. Because the bit error probability $P_b = 10^{-4}$ corresponds to $E_b/N_0 =$ 8.4 dB in the unfaded AWGN channel, the energy excess is (in dB*)*

$$28.6;\ 13.4;\ 6.7;\ 5.1;\ 0.9$$

5.3 FORWARD TRANSMISSION OVER A MULTIPATH FADED CHANNEL IN A DS CDMA SYSTEM

In Section 4.8 we studied, as an example, the forward transmission in the IS-95 system. In this system, the pseudorandom spreading sequences are assigned only to individual base stations. To separate the users, the system assigns orthogonal (Hadamard) sequences to each of them. In this section, we consider a different scheme for the forward transmission. The difference with this scheme compared with the scheme in Figure 4.25 is that instead of employing orthogonal spreading sequences for individual users, pseudorandom sequences are used. Although it is possible to use both BPSK and QPSK modulation, we only consider the more simple BPSK case. The BPSK modulated signal transmitted by the kth user is [compare with (2.92)]

$$s^{(k)}(t) = \sqrt{2} \sum_{n=-\infty}^{\infty} v_n^{(k)} a_n^{(k)} h_{T_c}(t - nT_c) \cos(2\pi f_c t + \phi^{(k)}), \qquad k = 1, 2, \ldots K \tag{5.39}$$

where $\{v_n^{(k)}\}$ is the code sequence, $\{a_n^{(k)}\}$ is the spreading sequence, and $h_{T_c}(t)$ is a pulse of duration T_c. We suppose that the rate $r = 1/N$ repetition code is used,

that is, $v_n = u_{\lfloor n/N \rfloor}$, and that the phases $\phi^{(k)}$ are IID random variables uniformly distributed on the interval $[0, 2\pi)$ and known to both transmitter and receiver. In contrast to downlink transmission in AWGN channel, considered in Section 3.4, we assume first that the antenna is omnidirectional and the system does not use voice activity monitoring.

To exploit the energy in the multiple components of the multipath propagation, these components must be identified and acquired. It is particularly important to determine the delays and, subsequently when possible, their amplitudes and phases. This can be performed even with fully modulated signals (see Section 7.6), but the estimate is much more precise and the resulting performance is improved if the path identification and parameter estimation are performed on an unmodulated signal. In a spread spectrum system it is effective and easy to separate the unmodulated pilot signal from the data-modulated signal by assigning an individual spreading sequence to it. Without loss of generality we assume that the phase $\phi^{(0)}$ of the pilot signal is equal to zero. The pilot signal is [compare with (2.100)],

$$s^{(0)}(t) = \sqrt{2} \sum_{n=-\infty}^{\infty} a_n^{(0)} h_{T_c}(t - NT_c) \cos(2\pi f_c t) \tag{5.40}$$

Because the same pilot signal is shared among the K users controlled by the base station, the energy devoted to the pilot can be greater than that devoted to the individual user. Also, we assume that the pilot's spreading sequence is shared by all users by multiplying the pilot spreading sequence with all the user-specific sequences. The reason for multiplying the user sequence by the pilot sequence is to identify the user with the particular base station that is handling the call.

Let $a_n^{(0)}$ be the pilot's BPSK spreading sequence. The user's sequences are the product of those of the pilot and of the user-specific sequence $\tilde{a}_n^{(k)}$. That is,

$$a_n^{(k)} = a_n^{(0)} \tilde{a}_n^{(k)}, \qquad k = 1, 2, \ldots K \tag{5.41}$$

The transmitted signal is [compare with (2.101)]

$$s(t) = \gamma^{(0)} s^{(0)}(t) + \sum_{k=1}^{K} \gamma^{(k)} s^{(k)}(t)$$

where $s^{(0)}(t)$ is defined by Formula (5.40) and $s^{(k)}(t)$, $k = 1, 2, \ldots, K$, is defined by (5.39). The weight coefficients $\gamma^{(k)}$ should be chosen such that all users have the same SNR at the receiver input. Because the energy devoted to the pilot should be greater than that devoted to the individual users, $\gamma^{(0)} > \gamma^{(k)}$, $k = 1, 2, \ldots K$.

The received signal containing signals of K users and a pilot signal, all originating from a common base station, is

$$r(t) = r^{(0)}(t) + \sum_{k=1}^{K} r^{(k)}(t) \tag{5.42}$$

Here

$$r^{(0)}(t) = \gamma^{(0)} \sum_{\ell=1}^{L} \alpha_\ell \sum_{n=-\infty}^{\infty} a_n^{(0)} h_{T_c}(t - nT_c - \delta_\ell) \times \cos[2\pi f_c(t - \delta_\ell) + \varphi_\ell] + \sum_{\ell=1}^{L} \xi_\ell(t) \tag{5.43}$$

$$r^{(k)}(t) = \gamma^{(k)} \sum_{\ell=1}^{L} \alpha_\ell \sum_{n=-\infty}^{\infty} v_n^{(k)} a_n^{(k)} h_{T_c}(t - nT_c - \delta_\ell) \times \cos[2\pi f_c(t - \delta_\ell) + \varphi_\ell + \phi^{(k)}], \qquad k = 1, 2, \ldots K \tag{5.44}$$

where $\xi_\ell(t)$ are AWGN processes.

Because the transmission is from one base station, the fade amplitudes α_ℓ, delays δ_ℓ, and phase shifts φ_ℓ do not depend on k. We suppose, as above, that α_ℓ are IID Rayleigh random variables having the probability density functions (5.32).

The pilot-aided coherent Rake receiver for the kth user is shown in Figure 5.4. Analogously to the Rake receiver for the single user considered in Section 5.2, it

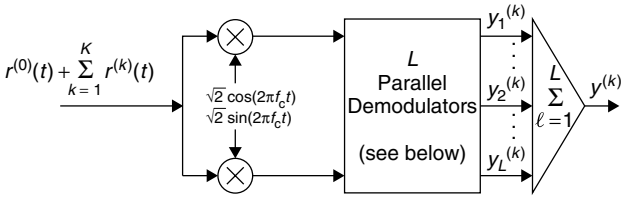

(a) L-Path Demodulator

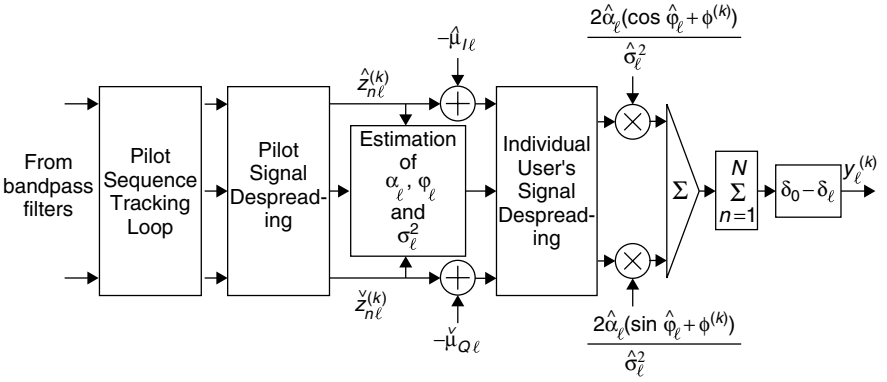

(b) Each of L Parallel Demodulators (Rake Fingers) for the k th User.

Figure 5.4. Pilot-aided coherent Rake demodulator for multipath propagation.

consists of L fingers. The demodulator contains a *pilot sequence tracking loop*, which is considered in Chapter 7. This loop estimates the timing delay of a given path. This is then used to remove the pilot BPSK spreading, giving rise to the quadrature outputs

$$\hat{z}_{n\ell} = \gamma^{(0)}\alpha_\ell \cos\varphi_\ell + \alpha_\ell \sum_{k=1}^{K} \gamma^{(k)} v_n^{(k)} \tilde{a}_n^{(k)} \cos(\varphi_\ell + \phi^{(k)}) + \hat{\xi}_{n\ell} \tag{5.45}$$

$$\check{z}_{n\ell} = \gamma^{(0)}\alpha_\ell \sin\varphi_\ell + \alpha_\ell \sum_{k=1}^{K} \gamma(k) v_n^{(k)} \tilde{a}_n^{(k)} \sin(\varphi_\ell + \varphi^{(k)}) + \check{\xi}_{n\ell} \tag{5.46}$$

The first terms are due to the pilot signal, the second terms are due to given cell user's signals, and $\hat{\xi}_{n\ell}$ and $\check{\xi}_{n\ell}$ are due to the AWGN and the other-cell interference. We neglect in Formulas (5.45) and (5.46) the interchip interference. From (5.45) and (5.46) the relative path values $\alpha_\ell \cos\varphi_\ell$ and $\alpha_\ell \sin\varphi_\ell$ can be estimated if α_ℓ and φ_ℓ remain relatively constant over an estimation interval. Because the second and third terms in the right-hand side of (5.45) and (5.46) are zero-mean random variables,

$$\begin{aligned} \mu_{\mathrm{I}\ell} &\stackrel{\text{def}}{=} E(\hat{z}_{n\ell}) = \gamma^{(0)}\alpha_\ell \cos\varphi_\ell \\ \mu_{\mathrm{Q}\ell} &\stackrel{\text{def}}{=} E(\check{z}_{n\ell}) = \gamma^{(0)}\alpha_\ell \sin\varphi_\ell \end{aligned} \tag{5.47}$$

The expectations $\mu_{\mathrm{I}\ell}$ and $\mu_{\mathrm{Q}\ell}$ can be estimated by simply averaging over an arbitrary number of chips ν.

The value of ν should be as large as possible without exceeding the period over which α_ℓ and φ_ℓ remain relatively constant. We suppose that ν can be chosen equal to the block length N. Then

$$\begin{aligned} \hat{\mu}_{\mathrm{I}\ell} &= \gamma^{(0)}\hat{\alpha}_\ell \cos\hat{\varphi}_\ell \approx \frac{1}{N}\sum_{n=0}^{N-1} \hat{z}_{n\ell}^{(k)} \\ \hat{\mu}_{\mathrm{Q}\ell} &= \gamma^{(0)}\hat{\alpha}_\ell \sin\hat{\varphi}_\ell \approx \frac{1}{N}\sum_{n=0}^{N-1} \check{z}_{n\ell}^{(k)} \end{aligned} \tag{5.48}$$

To remove the kth user spreading from $\hat{z}_{n\ell}$ and $\check{z}_{n\ell}$ we must use not $\hat{\alpha}_\ell \cos\hat{\varphi}_\ell$ and $\hat{\alpha}_\ell \sin\hat{\varphi}_\ell$ but the kth user relative path values

$$\hat{\alpha}_\ell \cos(\hat{\varphi}_\ell + \phi^{(k)}) = (\hat{\alpha}_\ell \cos\hat{\varphi}_\ell)\cos\phi^{(k)} - (\hat{\alpha}_\ell \sin\hat{\varphi}_\ell)\sin\phi^{(k)} \tag{5.49}$$

$$\hat{\alpha}_\ell \sin(\varphi_\ell + \phi^{(k)}) = (\hat{\alpha}_\ell \cos\hat{\varphi}_\ell)\sin\phi^{(k)} + (\alpha_\ell \sin\hat{\varphi}_\ell)\cos\phi^{(k)} \tag{5.50}$$

Because phase shift $\phi^{(k)}$ and weighting coefficients $\gamma^{(0)}$ and $\gamma^{(k)}$ are known to the receiver, the kth user relative path values can be calculated by using estimations

(5.48) and equations

$$\begin{aligned}\hat{\alpha}_\ell \cos\hat{\varphi}_\ell &= \hat{\mu}_{\mathrm{I}\ell}/\gamma^{(0)}\\ \hat{\alpha}_\ell \sin\hat{\varphi}_\ell &= \hat{\mu}_{\mathrm{Q}\ell}/\gamma^{(0)}\end{aligned} \tag{5.51}$$

Our goal is now to get from (5.45) and (5.46) statistics bearing the information of $u_0^{(k)}$. The interference from the pilot signal can be canceled if we subtract from $\hat{z}_{n\ell}$ and $\check{z}_{n\ell}$ $\hat{\mu}_{\mathrm{I}\ell}$ and $\hat{\mu}_{\mathrm{Q}\ell}$, respectively. Then, taking the product of the modulated received in-phase and quadrature components with the kth user spreading sequence $\{\tilde{a}_n^{(k)}\}$ and the relative path values, we get

$$\begin{aligned}z_{n\ell}^{(k)} &= \left[(\hat{z}_{n\ell} - \mu_{\mathrm{I}\ell})\hat{\alpha}_\ell \cos(\hat{\varphi}_\ell + \phi^{(k)}) + (\check{z}_{n\ell} - \mu_{\mathrm{Q}\ell})\check{\alpha}_\ell \sin(\hat{\varphi}_\ell + \phi^{(k)})\right]\tilde{a}_n^{(k)}\\ &= u_0\gamma^{(k)}\alpha_\ell\hat{\alpha}_\ell \cos(\varphi_\ell - \hat{\varphi}_\ell) + \tilde{\xi}_{n\ell}^{(k)}, \qquad n = 0, 1, \ldots, N-1\end{aligned} \tag{5.52}$$

where $\tilde{\xi}_{n\ell}^{(k)}$ is the zero-mean total noise component. The variance of $\tilde{\xi}_{n\ell}$ can be found from Formulas (5.45) and (5.46):

$$\sigma_\ell^2 \stackrel{\text{def}}{=} \mathrm{var}(z_n^{(k)}) = \frac{\alpha_\ell^2\hat{\alpha}_\ell^2}{2}\sum_{\substack{k'=1\\k'\neq k}}^{K}(\gamma^{(k')})^2 + \hat{\alpha}_\ell^2\frac{N_0}{2T_\mathrm{c}} + \hat{\alpha}_\ell^2\frac{N_{\mathrm{oc}}^{(k)}}{2T_\mathrm{c}} \tag{5.53}$$

where $N_0/2$ is the two-sided power spectral density of the background AWGN (we assume that all paths have same AWGN power) and $N_{\mathrm{oc}}^{(k)}/2$ is the two-sided power spectral density of the other-cell interference noise on the input of the ℓth finger of the kth user Rake receiver. The density $N_{\mathrm{oc}}^{(k)}$ depends on the kth user location in the cell. It is smaller for interior users and larger for users near a cell border.

The Neyman–Pearson criterion (5.28) uses σ_ℓ^2, $\ell = 1, 2, \ldots, L$, for calculating the decision statistics y_ℓ. Although, the variances σ_ℓ^2 are not known to the receiver, we can estimate them directly from (5.45) and (5.46):

$$\hat{\sigma}_\ell^2 = \frac{1}{2(N-1)}\sum_{n=0}^{N-1}(\hat{z}_{n\ell} - \hat{\mu}_{\mathrm{I}\ell})^2 + \frac{1}{2(N-1)}\sum_{n=0}^{N-1}(\check{z}_{n\ell} - \hat{\mu}_{\mathrm{Q}\ell}) \tag{5.54}$$

The mathematical expectation of $\hat{\sigma}_\ell^2$ is equal to σ_ℓ^2 [see (5.53)] plus a term $\alpha_\ell^2\hat{\alpha}_\ell^2(\gamma^{(k)})^2/2$. Because $K \gg 1$, $E(\hat{\sigma}_\ell^2) \approx \sigma_\ell^2$.

The decision statistics

$$y_\ell^{(k)} = \frac{2}{\hat{\sigma}_\ell^2}\sum_{n=0}^{N-1} z_{n\ell}^{(k)}, \qquad \ell = 1, 2, \ldots, L \tag{5.55}$$

can be considered as independent and Gaussian because of the central limit theorem. If we neglect the inaccuracy in the fade amplitude, phase, and variance estimates, taking $\hat{\alpha}_\ell = \alpha_\ell$, $\hat{\varphi}_\ell = \varphi_\ell$, $\hat{\sigma}_\ell^2 = \sigma_\ell^2$, we obtain [compare with Formulas (5.24) and (5.25)]

$$E\left(y_\ell^{(k)}\right) = \begin{cases} 4\rho_{c\ell}^{(k)} N, & \text{if } H_1 \text{ is true,} \\ -4\rho_{c\ell}^{(k)} N, & \text{if } H_{-1} \text{ is true} \end{cases} \tag{5.56}$$

$$\operatorname{var}\left(y_\ell^{(k)}\right) = 8\rho_{c\ell}^{(k)} N \tag{5.57}$$

where

$$\begin{aligned} \rho_{c\ell}^{(k)} &= \frac{(\gamma^{(k)})^2 \alpha_\ell^2}{\alpha_\ell^2 \sum_{k=1}^{K} (\gamma^{(k)})^2 + N_0/T_c + N_{oc}^{(k)}/T_c} \\ &= \frac{(\gamma^{(k)})^2 \alpha_\ell^2}{\alpha_\ell^2 [\psi - (\gamma^{(0)})^2] + N_0/T_c + N_{oc}^{(k)}/T_c} \end{aligned} \tag{5.58}$$

is the kth user, ℓth path SNR per chip. Because the antenna is omnidirectional and voice activity monitoring is absent, that is, $\gamma_a = 1$, $\gamma_v = 1$, the normalized average power of the signal (3.90) is $\psi = \sum_{k=0}^{K} (\gamma^{(k)})^2$.

The decision rule is

$$y^{(k)} \stackrel{\text{def}}{=} \sum_{\ell=1}^{L} y_\ell^{(k)} \underset{H_{-1}}{\overset{H_1}{\gtrless}} 0 \tag{5.59}$$

Then, analogously to (5.32), we obtain that the kth user conditional bit error probability is upperbounded by

$$P_b^{(k)}(\alpha_1, \alpha_2, \ldots, \alpha_L) < \frac{1}{2} \exp\left(-N \sum_{\ell=1}^{L} \rho_{c\ell}^{(k)}\right) \tag{5.60}$$

The upper bound for the unconditional bit error probability is [compare with Formula (5.34)]

$$\begin{aligned} P_b^{(k)} &< \int_0^\infty \cdots \int_0^\infty P_b^{(k)}(\alpha_1, \alpha_2, \ldots, \alpha_L) f_a(\alpha_1) \ldots f_a(\alpha_L) d\alpha_1, \ldots, d\alpha_L \\ &< \frac{1}{2} \prod_{\ell=1}^{L} \int_0^\infty \frac{\alpha_\ell}{2a_k^2} \\ &\quad \times \exp\left(-\frac{N\alpha_\ell^2}{[\psi - (\gamma^{(0)})^2]\alpha_\ell^2/(\gamma^{(k)})^2 + N_0/(\gamma^{(k)})^2 T_c + N_{oc}/(\gamma^{(k)})^2 T_c}\right) \\ &\quad \times \exp\left(-\frac{\alpha_\ell^2}{2a_k^2}\right) d\alpha_\ell \end{aligned} \tag{5.61}$$

where we assume that the L multipath components have equal average power strengths, $E(\alpha_\ell^2) = 2a_k^2$, but the strength $2a_k^2$ depends on the kth user location.

The random variable

$$\rho_{b\ell}^{(k)} = N\rho_{c\ell}^{(k)} = \frac{N\alpha_\ell^2}{[\psi - (\gamma^{(0)})^2]\alpha_\ell^2/(\gamma^{(k)})^2 + N_0/(\gamma^{(k)})^2 T_c + N_{oc}^{(k)}/(\gamma^{(k)})^2 T_c} \tag{5.62}$$

is the ℓth path SNR per bit. The mathematical expectation of $\rho_{b\ell}^{(k)}$ is a complicated function (including the exponential integral[1] $\mathrm{Ei}(\cdot)$) of α_ℓ^2 and other parameters. If we replace the random variable α_ℓ^2 by its mathematical expectation and neglect by $(\gamma^{(0)})^2$ in comparison with ψ, we get the approximation of $\mathrm{E}(\rho_{b\ell}^{(k)})$,

$$E(\rho_{b\ell}^{(k)}) \simeq \frac{Na_k^2}{\psi a_k^2/(\gamma^{(k)})^2 + N_0/2(\gamma^{(k)})^2 T_c + N_{oc}^{(k)}/2(\gamma^{(k)})^2 T_c} \tag{5.63}$$

The first term in the denominator of the right-hand side of Formula (5.63) is due to interference from other users of the cell. The second term is due to the background AWGN. The third term is due to the other-cell interference.

Let us assume, as above, that the weighting coefficients $\{\gamma^{(k)}\}$ are chosen such that the average SNR for all users and paths is the same, that is, $E(\rho_{b\ell}^{(k)}) \stackrel{\text{def}}{=} \overline{E}_b/L\overline{I}_0$. Then from (5.63) it follows that

$$(\gamma^{(k)})^2 = \frac{\overline{E}_b}{NLI_0}\left[\psi + \frac{N_0}{2a_k^2 T_c} + \frac{N_{oc}^{(k)}}{2a_k^2 T_c}\right] \tag{5.64}$$

If the background noise is negligible and the ratio of the other-cell interference power $N_{oc}^{(k)}/2T_c$ to the average other-user interference power ψa_k^2 is equal to f, then we get from (5.64)

$$\frac{\overline{E_b}}{\overline{I}_0} \simeq \frac{NL(\gamma^{(k)})^2}{\psi(1+f)} \tag{5.65}$$

Under the assumptions that we made, Formula (5.61) can be rewritten as

$$\begin{aligned} P_b^{(k)} &< \frac{1}{2}\prod_{\ell=1}^{L}\int_0^\infty \frac{\alpha_\ell}{2a_k^2}\exp\left(-\frac{\overline{E_b}}{L\overline{I}_0}(1+f)\frac{\alpha_\ell^2}{\alpha_\ell^2 + 2fa_k^2}\right)\exp\left(-\frac{\alpha_\ell^2}{2a_k^2}\right)\mathrm{d}\alpha_\ell \\ &= \frac{1}{2}\left[\int_0^\infty \exp\left(-\frac{\overline{E}_b}{L\overline{I}_0}(1+f)\frac{x}{x+f}\right)\exp(-x)\,\mathrm{d}x\right]^L \end{aligned} \tag{5.66}$$

where we use the substitution $x = \alpha_\ell^2/2a_k^2$. Note that the bit error probability $P_b^{(k)}$ does not depend on k.

[1]Definition of exponential integral: $\mathrm{Ei}(x) = \int_{-\infty}^{x} \frac{e^t}{t}\,\mathrm{d}t$.

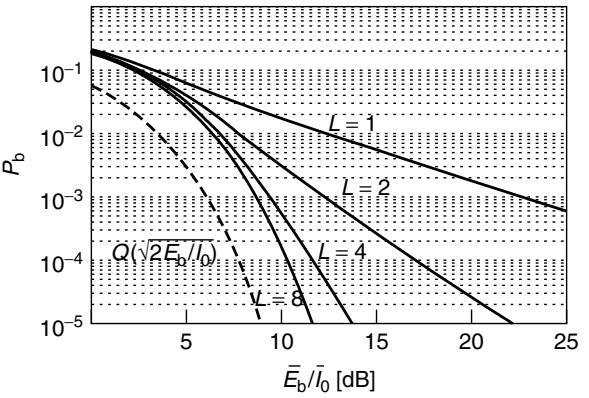

Figure 5.5. Upper bounds on the bit error probability P_b for a downlink DS CDMA system that operates in an L-path Rayleigh channel, $L = 1, 2, 4$, and 8, $f = 0.6$. For comparison, $P_b = Q(\sqrt{2E_b/I_0})$ for an uncoded AWGN channel is given.

We must resort to numerical integration to upper bound the bit error probability P_b for downlink transmission in multipath fading channels. In Figure 5.5 the upper bound on P_b for $L = 1, 2, 4$, and 8 together with the probability P_b for an unfaded AWGN channel are presented. The excess energy is quite large for $L = 1$ but modest for $L = 8$.

The radio channel capacity of a downlink DS CDMA system can be found both by direct calculation of the required SNR and by using the average excess energy. In the last case, we can use the general formula [compare with (4.28)], valid in the case of voice activity monitoring and antenna sectorization,

$$K_0 \approx 1 + \frac{W/R}{\overline{E}_b/\overline{I}_0}(1 - 1/g)\gamma_v\gamma_a\gamma_c\gamma_f \tag{5.67}$$

Here $\overline{E}_b/\overline{I}_0$ is the required average signal-to-noise ratio for an unfaded channel, $1/g$ is the pilot signal rate, γ_v is the voice activity gain, γ_a is the antenna gain, γ_c is the coding gain, and γ_f, $\gamma_f < 1$ are the excess energy loss (or *fading loss*). Because the other-cell user interference is already taken into account, the factor $1/(1 + f)$ in the right-hand side of Formula (5.67) is omitted.

EXAMPLE 5.3

Consider the DS CDMA system of Example 3.6, where the repetition code is used and which operates in a downlink L-path Rayleigh channel. Assuming that the maximal acceptable bit error probability is $P_b = 10^{-4}$, $f = 0.6$, *determine the capacity of the system for* $L = 1, 2, 4, 8$, *and* ∞. *Use the upper bounds (5.66) for* P_b *and neglect the influence of the background noise. The voice activity gain* $\gamma_v = 2.67$, *the antenna gain* $\gamma_a = 2.4$, *the pilot signal rate* $1/g = 0.2$. *Find the average excess energy in each case.*

Solution

Application of the upper bounds (5.66) and Formula (5.67) gives in the following table:

L	*Required* $\overline{E}_b/\overline{I}_0$	*Excess energy* (dB)	K_0
1	7943 (39.0 dB)	30.6	1
2	54.8 (17.4 dB)	9.0	19
4	16.2 (12.1 dB)	3.7	62
8	12.3 (10.9 dB)	2.1	82
∞	10.6 (10.2 dB)	1.8	95
AWGN channel	6.92 (8.4 dB)		

Even though Formula (5.67) was derived for the case of uncoded transmission, we will use it also for the coded case.

EXAMPLE 5.4

Consider the same CDMA system as in Example 5.3 except that instead of the repetition code the first-order Reed–Muller code of length $N = 512$ is used. Estimate the radio channel capacity of the system for $L = 4$.

Solution

Application of Formula (5.67) with $1/g = 0.2$, $\gamma_v = 2.67$, $\gamma_a = 2.4$, $\gamma_c = 2.75$ *(*4.4 dB*) (see the discussion after Example 4.2),* $\gamma_f = 0.43$ (−3.7 dB) *gives*

$$K_0 = 1 + \frac{1000}{6.9}(2.75)(0.43) = 172$$

In Section 5.4 we study uplink multipath communication in a DS CDMA system.

5.4 REVERSE TRANSMISSION OVER A MULTIPATH FADED CHANNEL IN A DS CDMA SYSTEM

Transmission of a special pilot signal in forward channel is very valuable for initial acquisition and time tracking. It is also helpful for good amplitude and phase estimates, making coherent reception and weighted combining of multipath components possible. However, in the reverse link, inserting in each individual user's special pilot signal, whose power is greater than the data-modulated portion of the signal, reduces efficiency to less than 50%. Nevertheless, the pilot signaling in the reverse link was proposed for the Third Generation of cellular mobile communication. In this section, we consider two alternative methods of transmission in the reverse link.

First we consider transmission of special *pilot chips* by the user. The method is to puncture the reverse link code infrequently (e.g., one symbol in g where g is an integer) and dedicate the punctured chips to pilot chips. The punctured code is then reduced in rate by the factor $1 - 1/g$. The pilot chip information can be multiplexed with the uplink transmission from each user and with power control symbols.

The kth user's transmitter punctures every gth symbol of the code sequence (2.81) and replaces it by 1. The transmitted uplink BPSK DS SS signal is given by Formula (2.92), where $\{a_n^{(k)}\}$ is a spreading sequence, and the BPSK modulator for the kth user is presented in Figure 2.10. The L-path demodulator of the kth user is analogous to that presented in Figure 5.4, but the rake fingers in the case of uplink communication should be replaced by the one given in Figure 5.6. In contrast to forward communication the fade amplitudes $\alpha_\ell^{(k)}$, phase shifts $\varphi_\ell^{(k)}$, and delays $\delta_\ell^{(k)}$ depend on k.

The clock period of the switch in Figure 5.6 is T_c, and each gth (pilot) sample goes to the estimator of $\alpha_\ell^{(k)} \cos \varphi_\ell^{(k)}$ and $\alpha_\ell^{(k)} \sin \varphi_\ell^{(k)}$, analogous to the estimator (5.48) of the downlink receiver. The other samples,

$$\begin{aligned} \hat{z}_{n\ell}^{(k)} &= \alpha_\ell^{(k)} v_n^{(k)} \cos \varphi_\ell^{(k)} + \hat{\xi}_{n\ell}^{(k)} \\ \check{z}_{n\ell}^{(k)} &= \alpha_\ell^{(k)} v_n^{(k)} \sin \varphi_\ell^{(k)} + \check{\xi}_{n\ell}^{(k)} \end{aligned} \qquad n(\mathrm{mod}\ g) \neq 0, \tag{5.68}$$

bear information of the code sequence. The zero-mean random variables $\hat{\xi}_{n\ell}^{(k)}$ and $\check{\xi}_{n\ell}^{(k)}$ are total noise components. In contrast to the variables $\hat{\xi}_{n\ell}^{(k)}$ and $\check{\xi}_{n\ell}^{(k)}$ in Formula (5.45) they include the other user of given cell interference components. The variance of the total noise is [compare with ((5.53))]

$$\sigma_\ell^2 \stackrel{\mathrm{def}}{=} \mathrm{var}(\hat{\xi}_{n\ell}^{(k)}) = \mathrm{var}(\check{\xi}_{n\ell}^{(k)}) = \frac{1}{2} \sum_{\substack{k'=1 \\ k' \neq k}}^{K} (\alpha_\ell^{(k')})^2 + \frac{N_0}{2T_c} + \frac{N_{oc}}{2T_c} \tag{5.69}$$

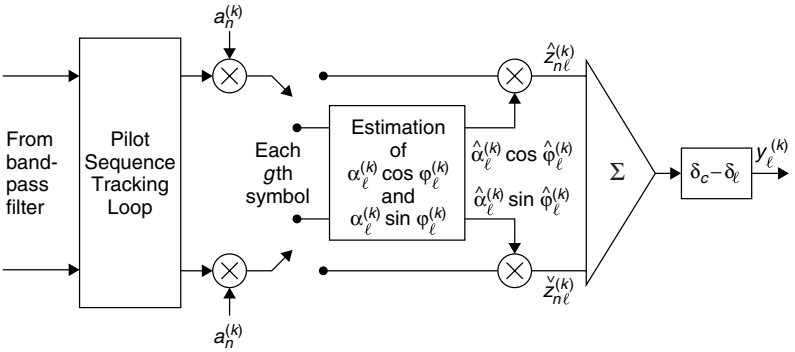

Figure 5.6. Each of the L rake fingers for the kth user receiver of transmitted uplink signals.

where $N_0/2$ is the two-sided power spectral density of the background AWGN (we assume that all paths have same AWGN power) and $N_{oc}/2$ is the two-sided power spectral density of the other-cell interference noise on the ℓth finger of the Rake receiver.

The random variables $\alpha_\ell^{(k')}$, $k' \neq k$, are independent and have Rayleigh distribution. We assume that for all users of the given cell the multipath components are of equal average strength $2a^2$. We can approximate the sum $\sum_{k' \neq k} (\alpha_\ell^{(k')})^2$ on the right-hand side of (5.69) by $2(K-1)a^2$. Then we have

$$\sigma_\ell^2 \approx (K-1)a^2 + \frac{N_0}{2T_c} + \frac{N_{oc}}{2T_c} \tag{5.70}$$

If we estimate the other-cell interference as the fth part of the interference caused by users of the given cell, we can rewrite Formula (5.70) as

$$\sigma_\ell^2 \approx (1+f)(K-1)a^2 + \frac{N_0}{2T_c} \tag{5.71}$$

The decision statistics $y_\ell^{(k)}$ are defined as

$$y_\ell^{(k)} = \sum_{\substack{n=0 \\ n(\mathrm{mod}_g) \neq 0}}^{N-1} \left(\hat{z}_{n\ell}^{(k)} \hat{\alpha}_\ell^{(k)} \cos \hat{\varphi}_\ell^{(k)} + \check{z}_{n\ell}^{(k)} \hat{\alpha}_\ell^{(k)} \sin \hat{\varphi}_\ell^{(k)} \right) \tag{5.72}$$

Because in our model the variances σ_ℓ^2 of the statistics $\hat{z}_{n\ell}^{(k)}$ and $\check{z}_{n\ell}^{(k)}$ do not depend on ℓ, we omitted the factor $2/\hat{\sigma}_\ell^2$ in front of the sum in the right-hand side of (5.72) [compare with Formula (5.55)].

The decision rule is

$$y^{(k)} \overset{\text{def}}{=} \sum_{\ell=1}^{L} y_\ell^{(k)} \begin{array}{c} H \\ > \\ < \\ H_{-1} \end{array} 0$$

Neglecting the inaccuracy in the fade amplitude $\alpha_\ell^{(k)}$ and phase $\varphi_\ell^{(k)}$ estimates and taking $\hat{\alpha}_\ell^{(k)} = \alpha_\ell^{(k)}$ and $\hat{\varphi}_\ell^{(k)} = \varphi_\ell^{(k)}$, we obtain [compare with (5.24) and (5.25)] the following expressions for the conditional expectation and variance of $y_\ell^{(k)}$ given $\alpha_\ell^{(k)}$

$$E\left(y_\ell^{(k)} | \alpha_\ell^{(k)}\right) = \begin{cases} (\alpha_\ell^{(k)})^2 \quad (1-1/g)N, & \text{if } H_1 \text{ is true,} \\ -(\alpha_\ell^{(k)})^2 \quad (1-1/g)N, & \text{if } H_{-1} \text{ is true} \end{cases} \tag{5.73}$$

$$\text{var}\,(y_\ell^{(k)} | \alpha_\ell^{(k)}) = (\alpha_\ell^{(k)})^2 (1-1/g) \left[(1+f)(K-1)a^2 + \frac{N_0}{2T_c} \right] N \tag{5.74}$$

The ℓth path SNR per bit given $\alpha_\ell^{(k)}$ is

$$\frac{[E(y_\ell^{(k)}|\alpha_\ell^{(k)})]^2}{2\text{var}(y_\ell^{(k)}|\alpha_\ell^{(k)})} = \frac{(\alpha_\ell^{(k)})^2(1-1/g)N}{2(1+f)(K-1)a^2 + N_0/T_c} \tag{5.75}$$

Because $E(\alpha_\ell^{(k)}) = 2a^2$, the total average SNR per bit is [compare with (5.35)]

$$\frac{\overline{E}_b}{\overline{I}_0} = \frac{2La^2(1-1/g)N}{2(1+f)(K-1)a^2 + N_0/T_c} \tag{5.76}$$

Then, analogously to (5.32)–(5.36), we get the upper bound for the bit error probability P_b of the L-path equal average strength reverse Rayleigh channel [compare with Formula (5.36)]:

$$P_b < \frac{1}{2}\left(1 + \frac{\overline{E}_b}{L\overline{I}_0}\right)^{-L} \tag{5.77}$$

where $E_b/\overline{I}_0$ is defined by (5.76).

EXAMPLE 5.5

Consider the uplink L-path communication in a DS CDMA system under the same conditions as in Example 5.3. Estimate the radio channel capacity of the system for $L = 1, 2, 4, 8$. *Estimate the average excess energy. Use the upper bound (5.77) for* P_b.

Solution

In the table below we list for $P_b = 10^{-4}$ *the required average SNR per bit estimated from Formula (5.77), the excess energy, and the radio channel capacity* K_0.

L	$\overline{E}_b/\overline{I}_0$	*Average excess energy* (dB)	K_0
1	4999 (37.0 dB)	28.6 dB	1
2	139 (21.4 dB)	13.0 dB	8
4	29.6 (14.7 dB)	6.3 dB	34
8	15.2 (11.8 dB)	3.4 dB	66

Now consider the case when no pilot signal or pilot chips are transmitted. If no pilot signal or pilot chips are transmitted by the user, the estimation of the fade amplitudes and the phases of the multipath components can be performed even with fully modulated signals (see Section 7.6). Other alternatives are noncoherent or differentially coherent reception, which do not require phase and amplitude estimation. Timing, however, must still be acquired and tracked. We return to the acquisition and tracking problem in Chapter 7. Below we will suppose that L independent multipath components are being tracked at a given time and that

neither phase nor attenuation is available. As for the coherent case, we assume that a separate demodulator is provided for each path, but now their outputs are noncoherently combined. This method was implemented in IS-95 [44].

Suppose that all K individual transmitters use a reduced first-order Reed–Muller code of length N. The BPSK signal received by the kth receiver is

$$r^{(k)}(t) = \sum_{\ell=1}^{L} \left\{ \alpha_\ell^{(k)} \sum_{n=-\infty}^{\infty} v_n^{(k)} a_n^{(k)} h_{T_c}(t - nT_c - \delta_\ell^{(k)}) \right.$$
$$\left. \times \cos[2\pi f_c(t - \delta_\ell^{(k)}) + \varphi_\ell^{(k)}] + \xi_\ell^{(k)}(t) \right\} \tag{5.78}$$

where $h_{T_c}(t)$ is a pulse of duration T_c, $\{a_n^{(k)}\}$ is a spreading sequence, and $\xi_\ell^{(k)}(t)$ is AWGN with two-sided power spectral density $N_0/2$. We assume that the L multipath components have equal average power and AWGN level. The code sequence $\{v_n^{(k)}\}$ is a sequence of N-tuples $\boldsymbol{v}_m^{(k)} = (v_{mN}^{(k)}, v_{mN+1}^{(k)}, \ldots, v_{(m+1)N-1}^{(k)})$, where $\boldsymbol{v}_m^{(k)}$ is a codeword of the reduced first-order Reed–Muller code. We suppose that the propagation delay $\delta_\ell^{(k)}$ is known but the fade amplitudes $\alpha_\ell^{(k)}$ and phase shifts $\varphi_\ell^{(k)}$ are unknown. The random variables $\alpha_1^{(k)}, \alpha_2^{(k)}, \ldots, \alpha_L^{(k)}$ are independent Rayleigh random variables characterized by the second moments $E(\alpha_\ell^{(k)})^2 = 2a^2$, and the IID random variables $\varphi_\ell^{(k)}$ are uniformly distributed on the interval $[0, 2\pi)$.

The overall signal received by the base station is

$$r(t) = \sum_{k=1}^{K} r^{(k)}(t) \tag{5.79}$$

The noncoherent receiver (without acquisition and tracking devices) for the kth user is presented in Figure 5.7. The in-phase and quadrature components of the received signal enter after despreading L parallel noncoherent demodulators, analogous to what was presented in Figure 4.5 except that the decision device "select largest" should be omitted. The output of the ℓth demodulator is the N-dimensional vector $\boldsymbol{y}_\ell^{(k)} = (y_{\ell 0}^{(k)}, y_{\ell 1}^{(k)}, \ldots, y_{\ell,N-1}^{(k)})$. (This vector corresponds to the vector $(y_0^{(k)}, y_1^{(k)}, \ldots, y_{N-1}^{(k)})$ in Figure 4.5.) The receiver outputs the vector

$$\boldsymbol{y}^{(k)} = \sum_{\ell=1}^{L} \boldsymbol{y}_\ell^{(k)} \tag{5.80}$$

chooses the largest component of vector $\boldsymbol{y}^{(k)}$, and makes a decision in favor of the corresponding codeword.

As usual, we analyze the reception of the 0th block. We assume that the transmitted 0th block is the zeroth codeword of the reduced first-order Reed–Muller

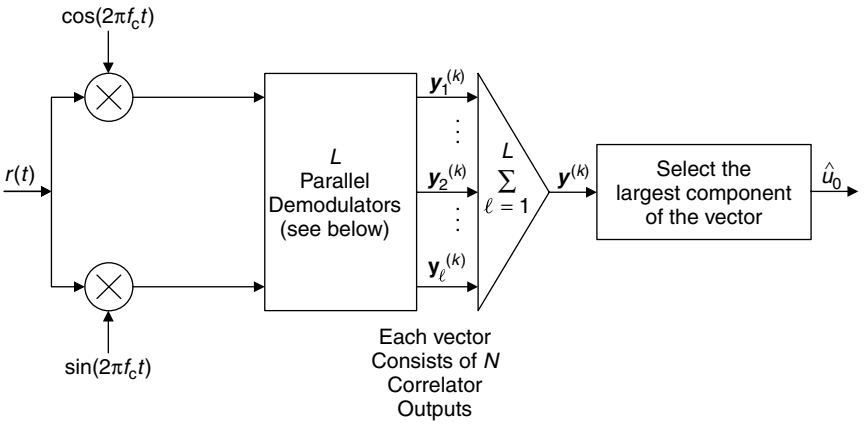

Note: $\boldsymbol{y}^{(k)} = \sum_{\ell=1}^{L} \boldsymbol{y}_{\ell}^{(k)}$, $\boldsymbol{y}_{\ell}^{(k)} = (\boldsymbol{y}_{\ell 0}^{(k)}, \boldsymbol{y}_{\ell 1}^{(k)}, \ldots, \boldsymbol{y}_{\ell, N-1})$

(a) *L*-Path Noncoherent Demodulator.

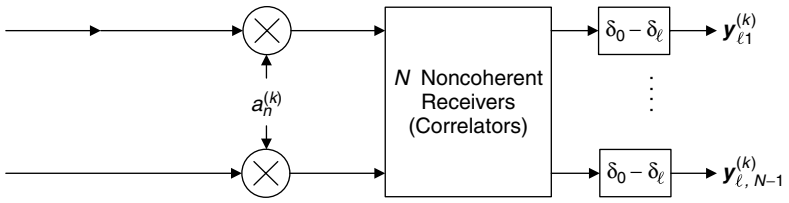

(b) Each of *L* Parallel Demodulators (Fingers of Rake).

Figure 5.7. Noncoherent Rake demodulator for N-ary orthogonal waveforms in L-component multipath.

code, that is, $\boldsymbol{v}_0^{(k)} = (v_0^{(k)}, v_1^{(k)}, \ldots v_{N-1}^{(k)}) = \boldsymbol{m}_0$, where $\boldsymbol{m}_0$ is the first row of the $N \times N$ Hadamard matrix. The component $y_{\ell i}^{(k)}$, $i = 0, 1, \ldots, N-1$, of the vector $\boldsymbol{y}_{\ell}^{(k)}$ is the sum of the squares of the components $\hat{x}_{\ell i}^{(k)}$ and $\check{x}_{\ell i}^{(k)}$, such that

$$y_{\ell i}^{(k)} = (\hat{x}_{\ell i}^{(k)})^2 + (\check{x}_{\ell i}^{(k)})^2 \tag{5.81}$$

where [compare with Formulas (4.35) and (4.36)]

$$\hat{x}_{\ell i}^{(k)} = \begin{cases} N\ \alpha_{\ell}^{(k)} \cos \varphi_{\ell}^{(k)} + \hat{\xi}_{\ell 0}^{(k)}, & \text{if } i = 0, \\ \hat{\xi}_{\ell i}^{(k)}, & \text{otherwise} \end{cases} \tag{5.82}$$

$$\check{x}_{\ell i}^{(k)} = \begin{cases} N\ \alpha_{\ell}^{(k)} \sin \varphi_{\ell}^{(k)} + \check{\xi}_{\ell 0}^{(k)}, & \text{if } i = 0, \\ \check{\xi}_{\ell i}^{(k)}, & \text{otherwise} \end{cases} \tag{5.83}$$

$\hat{\xi}_{\ell i}^{(k)}$, $\check{\xi}_{\ell i}^{(k)}$ are independent zero-mean Gaussian variables with variances [compare with (5.71)]

$$\sigma_0^2 \stackrel{\text{def}}{=} \frac{I_0 N}{2T_c} = N\left[(K-1)(1+f)a^2 + \frac{N_0}{2T_c}\right] \tag{5.84}$$

where $N_0/2$ is the two-sided power spectral density of the AWGN and $(K-1)(1+f)a^2$ is the total contribution of the other users of the given cell and the other-cell interference.

Because the random variables $\alpha_\ell^{(k)} \cos \varphi_\ell^{(k)}$ and $\alpha_\ell^{(k)} \sin \varphi_\ell^{(k)}$ are independent zero-mean Gaussian variables with variances a^2 (Problem 5.10), the random variables $\hat{x}_{\ell i}^{(k)}$ and $\check{x}_{\ell i}^{(k)}$ are independent zero-mean Gaussian variables with variances

$$\operatorname{var}[\hat{x}_{\ell i}^{(k)}] = \operatorname{var}[\check{x}_{\ell i}^{(k)}] = \begin{cases} N^2a^2 + \sigma_0^2 \stackrel{\text{def}}{=} \sigma_1^2, & \text{if } i = 0, \\ \sigma_0^2, & \text{otherwise} \end{cases} \tag{5.85}$$

We introduce the ratio

$$\frac{\sigma_1^2}{\sigma_0^2} = 1 + \frac{2T_c N}{I_0}a^2 = 1 + \rho_B/L \tag{5.86}$$

where $\rho_B = 2T_c a^2 NL/I_0$ is the SNR per block.

The decision statistics

$$y_i^{(k)} = \sum_{\ell=1}^{L} y_{\ell i}^{(k)} = \sum_{\ell=1}^{L}\left[(\hat{x}_{\ell i}^{(k)})^2 + (\check{x}_{\ell i}^{(k)})^2\right], \qquad i = 0, 1, \ldots, N-1 \tag{5.87}$$

have central χ^2-distributions with $2L$ degrees of freedom. The probability density functions of the random variables $y_i^{(k)}$ are

$$P(y_i^{(k)}) = \begin{cases} f_{\sigma_1^2}(y_i^{(k)}), & \text{if } i = 0, \\ f_{\sigma_0^2}(y_i^{(k)}), & \text{otherwise} \end{cases} \tag{5.88}$$

where [compare with Formula (3.60)]

$$f_{\sigma^2}(y) = \frac{1}{2^L \sigma^{2L}(L-1)!}\, y^{L-1} \exp\left(-\frac{y}{2\sigma^2}\right), \quad y \geq 0 \tag{5.89}$$

From (5.87) and (5.88) we get the following expression for the probability of the correct decision

$$P(\mathcal{C}) = \int_0^\infty f_{\sigma_1^2}(y) \left(\int_0^y f_{\sigma_0^2}(x)\, \mathrm{d}x \right)^{N-1} \mathrm{d}y$$

$$= \int_0^\infty \frac{y^{L-1} \exp\left(-\dfrac{y}{2\sigma_1^2}\right)}{2^L \sigma_1^{2L} (L-1)!} \left(\int_0^y \frac{x^{L-1} \exp\left(-\frac{x}{2\sigma_0^2}\right)}{2^L \sigma_0^{2L} (L-1)!} \mathrm{d}x \right)^{N-1} \mathrm{d}y$$

$$= \int_0^\infty \frac{y^{L-1} e^{-y/(1+\rho_\mathrm{B}/L)}}{(L-1)!(1+\frac{\rho_\mathrm{B}}{L})^L} \left[\int_0^y \frac{x^{L-1} e^{-x}}{(L-1)!} \mathrm{d}x \right]^{N-1} \mathrm{d}y \tag{5.90}$$

In general, this probability should be calculated numerically. But for $L = 1$, the term in brackets raised to the power $(N-1)$ in (5.90) may be expanded using binomial expansion:

$$(1 - e^{-y})^{N-1} = \sum_{i=0}^{N-1} \binom{N-1}{i} (-1)^i \; e^{-iy} \tag{5.91}$$

Then, integrating term by term, we obtain for $L = 1$

$$P(\mathcal{C}) = 1 - \sum_{i=1}^{N-1} \frac{(-1)^{i+1}}{i + 1 + i\rho_\mathrm{B}/L} \binom{N-1}{i} \tag{5.92}$$

The block error probability is then

$$P_\mathrm{B} = P(\mathcal{E}) = 1 - P(\mathcal{C}) = \sum_{i=1}^{N-1} \frac{(-1)^{i+1}}{i + 1 + i\rho_\mathrm{B}/L} \binom{N-1}{i} \tag{5.93}$$

For $L \neq 1$, we must resort to the numerical integration of (5.90) to evaluate the probability P_B. The bit error probability versus

$$\frac{E_\mathrm{b}}{I_0} = \frac{\rho_\mathrm{B}}{\log_2 N} = \frac{2T_\mathrm{c} N a^2}{I_0 \log_2 N}$$

is shown in Figure 5.8 for $M = N = 2, 32, 64, 128, 256$ and $L = 1, 2, 4, 8$. (For large N the bit error probability P_b is equal to $P_\mathrm{B}/2$.) We see that a simple energy-increasing strategy to improve the link performance is quite expensive and increasing N is only marginally helpful on the Rayleigh channel, in contrast to the result for the AWGN channel. The study of the noncoherent reception for the L-path Rayleigh channel shows that the performance dramatically improves as L grows (for all but very low signal-to-noise ratios). As Viterbi noted [47], this is because the *diversity gain is greater than the noncoherent combining loss*.

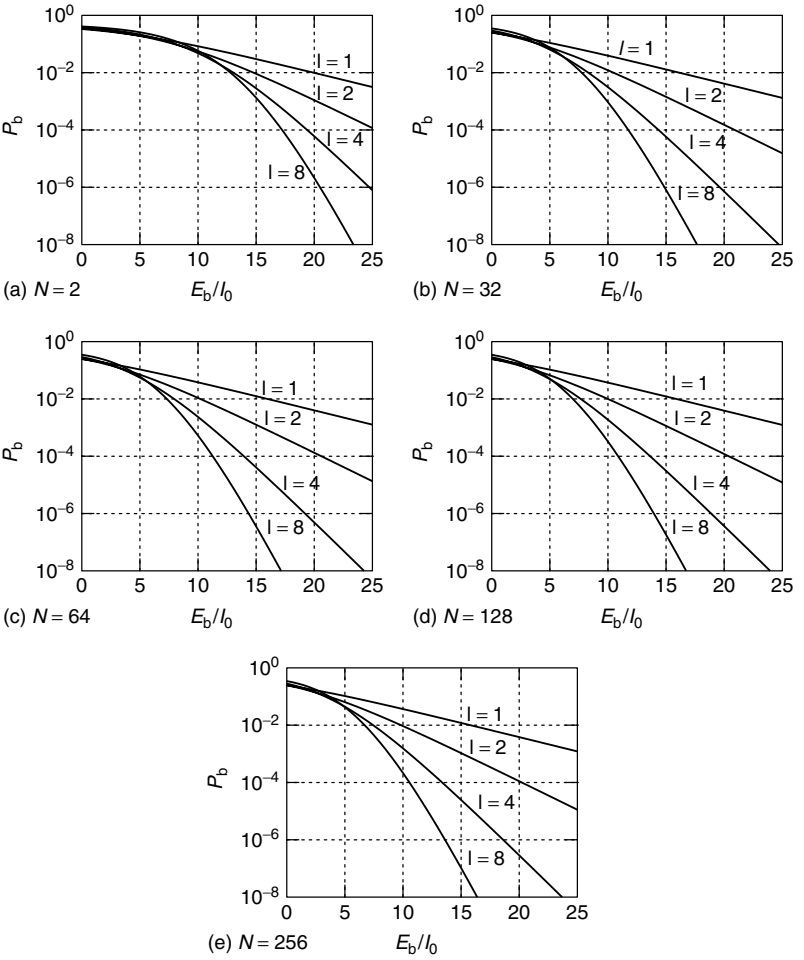

Figure 5.8. Bit error probability for noncoherent demodulation of orthogonal signals, Rayleigh channel.

EXAMPLE 5.6

Consider the DS CDMA system of Example 3.6, which operates on an L multipath Rayleigh channel of equal average strength and uses length N reduced first-order Reed–Muller code with noncoherent reception. Assuming that the maximal acceptable P_b *is* 10^{-4}*, determine the capacity of the single-cell CDMA system for* $N = 256$ *and* $L = 8$.

Solution

If $P_b = 10^{-4}$*, then we get from Figure 5.8(e)* $E_b/I_0 = 10$ *(*10 dB*). Because the spreading factor* $W/R = 1000$*, we get* $K_0 \approx 101$.

5.5 INTERLEAVING FOR A RAYLEIGH CHANNEL

Diversity is a powerful communication technique that provides wireless link improvement at the cost of high excess dimensionality. Diversity exploits the random nature of wireless propagation operating with independent signal paths for communication. In Sections 5.2–5.4, we found that the greater the number L of independent path components available in the presence of Rayleigh fading, the better the performance. This is illustrated in Figures 5.3 and 5.5, which show the total received energy (from all paths combined) required to achieve a given level of performance. These figures show that with more independent paths a factor L less total excess energy is required to achieve a given error probability for the fading channel.

There are a wide range of diversity implementations that are very practical and provide significant channel improvement at relatively low cost. Except L paths, we also have N chips per symbol block. The problem is that successive chips are not symbol/block independent. In fact, in Sections 5.3 and 5.4 we assumed the fade amplitude and phase shift to be constant over N chip intervals. In this section we show that it is possible to reorder the chips before transmission so that N chips depending on the same symbol are no longer transmitted successively. To obtain time diversity in a digital communications system *interleaving* (or *permutation*) is used. Interleaving (permutation) can be performed in a number of ways. We consider "block" and "convolutional" interleaving.

Mathematically, a size Γ block *permutor* can be defined as a $\Gamma \times \Gamma$ squared matrix S having one 1 in each column, one 1 in each row and all other entries zeros. The matrix

$$S = \begin{pmatrix} 01000 \\ 00001 \\ 10000 \\ 00100 \\ 00010 \end{pmatrix}$$

is an example of a size 5 *block permutor*. Multiplication of a Γ-dimensional input block $\boldsymbol{v} = (v_1 v_2, \ldots, v_\Gamma)$ by S changes the order of the symbols. The permutor's output $\boldsymbol{v}' = \boldsymbol{v}S$ is a permutation of the symbols in the input block. In our example $\boldsymbol{v}' = (v_3, v_1, v_4, v_5, v_2)$.

EXAMPLE 5.7

Consider the permutor

$$S = \begin{pmatrix} 10000 \\ 00100 \\ 00010 \\ 01000 \\ 00001 \end{pmatrix}$$

Find the inverse permutor S^{-1}.

Solution

The permutation matrix S permutes the symbol positions such that $\boldsymbol{v}' = (v_1, v_4, v_2, v_3, v_5)$. *The inverse permutation is found by mirror reflection of the symbols with respect to the main diagonal.*

$$S^{-1} = \begin{pmatrix} 10000 \\ 00010 \\ 01000 \\ 00100 \\ 00001 \end{pmatrix}$$

In the transmitter, a permutor usually follows the encoder. The transmitter transmits the code symbols in the order prescribed by the permutor. The receiver performs operations inverse to the operations in the transmitter. The *inverse permutor* S^{-1} is the inverse matrix to the matrix S. The inverse permutor arranges the received symbols $\boldsymbol{r}'$ in the original order, $\boldsymbol{r} = \boldsymbol{r}' S^{-1}$.

A device that permutes input symbols is called an *interleaver*. The *block interleaver* (Fig. 5.9) consists of two I-row by J-column memories, where the interleaver size is $\Gamma = IJ$.

The transmitter writes (before spreading!) the encoder output symbols row-wise into a memory until it is full. Then the memory is read column-wise out to the modulator (with spreading device). While one memory is filling, the other is being emptied, so two memories are needed. The block deinterleaver also consists of two I-row by J-column memories. In the receiver, the inverse operation is effected after despreading by writing the demodulator output column-wise into a memory and reading the decoder input row-wise from the memory. I and J are chosen to be large enough that error bursts will affect different codewords and may be considered as independent.

EXAMPLE 5.8

A 10×10 *block interleaver is presented in Figure 5.10. The interleaver input symbols are numbered consecutively* 1 *through* 100. *These symbols are transmitted over the channel by columns. Bursts of channel errors are assumed to hit the symbols* 14, 24, 34, 44 *and the symbols* 58, 68, 78, 88, 98, *as shown by the shaded blocks. The demodulator output is read row-wise into the memory, resulting in the same array of symbols shown in Figure 5.10.*

Enumerate the error-free intervals.

Solution

The error-free intervals are:

$$[1, 13],\ [15, 23],\ [25, 33],\ [35, 43],\ [45, 57],$$

$$[59, 67],\ [69, 77],\ [79, 87],\ [89, 97],\ [99, 100]$$

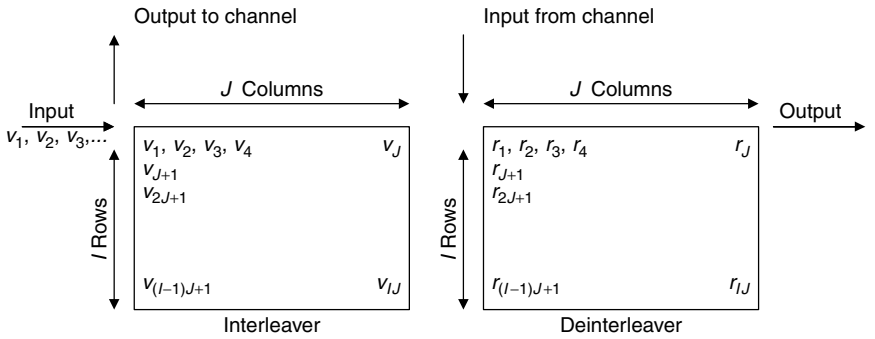

Figure 5.9. Block interleaver-deinterleaver. Interleaved sequence: $v_1, v_{J+1}, v_{2J+1}, \ldots, v_{(I-1)J+1}, v_2, v_{J+2} \ldots$. Any two symbols within less than J of each other are at least I apart.

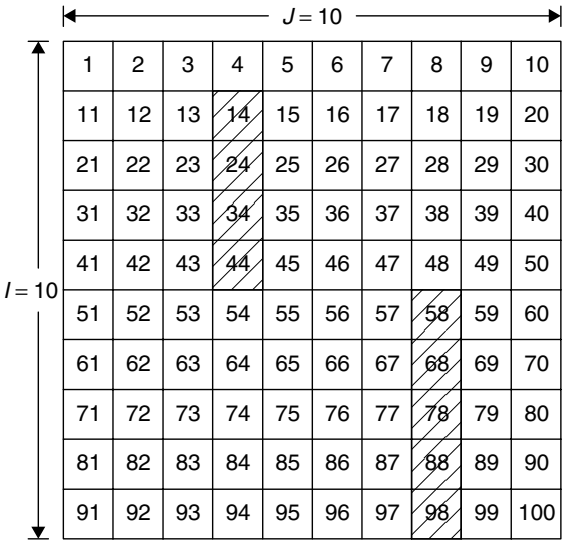

Figure 5.10. A 10×10 block interleaver.

EXAMPLE 5.9

The reverse link of the IS-95 system employs a rate $r = 1/3$, memory $m = 8$ convolutional encoder followed by the 18×32 block interleaver. What is the time delay in the system if the user rate is $R = 9.6$ kb/s?

Solution

Because the code rate is $r = 1/3$, the symbol rate on the input of the interleaver is 28.8 ksym/s. Then the interleaver size of $18 \times 32 = 576$ symbols corresponds to a delay of 20 ms.

Another type of permutor is the convolutional permutor. Convolutional permutors are better matched for use with the convolutional codes. The *convolutional permutor* is a bi-infinite matrix $S = (s_{ij})$ that has one 1 in each row and one 1 in each column and all other entries are zeros, and that satisfies the causality condition

$$s_{ij} = 0, \ i < j$$

A convolutional permutor can be constructed from a block permutor if we unwrap the permutation matrix below the diagonal. The procedure is illustrated in Figure 5.11. The unwrapped matrix is then repeated infinitely, and we obtain a periodical convolutional permutor.

A *convolutional interleaver* is shown in Figure 5.12. The multiplexers in the transmitter and the receiver operate synchronously. The multiplexer switches change positions after each symbol enters the interleaver. The first code symbol entering the first interleaver position is transmitted over the channel immediately. The second code symbol entering the second interleaver position is delayed ν time units before transmission. The following $(I-2)$ code symbols are delayed by progressively increasing time units, such that the Ith symbol is delayed by $(I-1)\nu$ time units. Thus adjacent encoder outputs are transmitted ν symbol times apart and are not affected by the length ν error burst. On reception, the first code symbol is delayed by $(I-1)\nu$ time units, the second code symbol is delayed by $(I-2)\nu$ time units, etc. After passing through both the interleaver and the

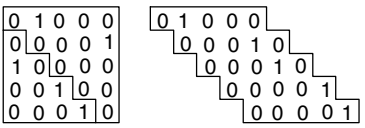

Figure 5.11. Unwrapping a 5×5 matrix.

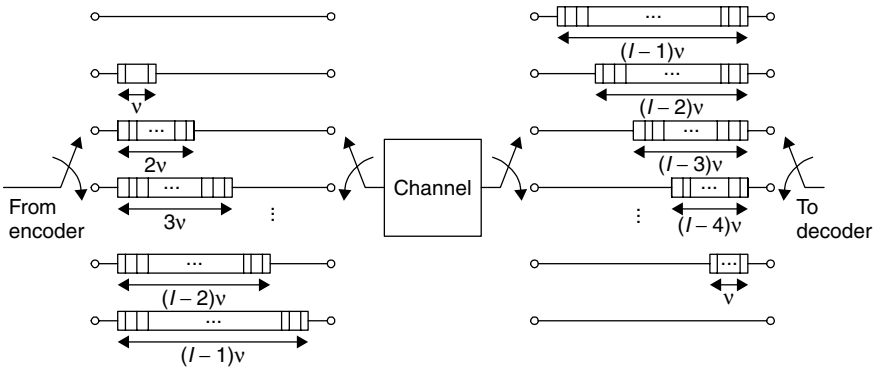

Figure 5.12. Convolutional interleaver-deinterleaver.

deinterleaver, all symbols have the same delay, so that the decoder input symbols are in the same order as the encoder output symbols. As can be seen from the figures, the overall delay produced by the convolutional interleaver-deinterleaver is approximately half of the delay of the block interleaver-deinterleaver.

As an example of an application of interleaving in DS CDMA communication, consider the reverse transmission in a one-path faded channel. Suppose that successive code symbols of the kth user are interleaved to be far enough apart that they encounter the independent fading effect. The interleaved and punctured (as described in the beginning of Section 5.4) code sequence modulates a BPSK DS SS signal (2.92).

The signal, where every gth chip is a pilot chip, is transmitted over a one-path time-selective Rayleigh channel. Then the impact on the performance of a coherent demodulator can be determined by modification of Formulas (5.68)–(5.77). In particular, (5.68) should be modified as

$$\begin{aligned} \hat{z}_{n'}^{(k)} &= \alpha_{n'}^{(k)} \cdot v_{n'}^{(k)} \cdot \cos \varphi_{n'}^{(k)} + \hat{\xi}_{n'}^{(k)}, \\ \check{z}_{n'}^{(k)} &= \alpha_{n'}^{(k)} \cdot v_{n'}^{(k)} \cdot \sin \varphi_{n'}^{(k)} + \check{\xi}_{n'}^{(k)} \end{aligned} \qquad n'(\text{mod } g) \neq 0 \tag{5.94}$$

Here n' are the numbers of the symbols in the interleaved code sequences. Because transmission is over the one-path channel, the index ℓ is omitted, but the fade amplitude $\alpha_{n'}^{(k)}$ and the phase $\varphi_{n'}^{(k)}$ are considered as a function of n'. Statistical properties of $\hat{\xi}_{n'}^{(k)}$ and $\check{\xi}_{n'}^{(k)}$ and $\hat{z}_{n'}^{(k)}$ and $\check{z}_{n'}^{(k)}$ are described by (5.69)–(5.71).

Before summation the statistics $\hat{z}_{n'}^{(k)}$ and $\check{z}_{n'}^{(k)}$ should be deinterleaved, that is, deinterleavers should be added in the receiver in Figure 5.6. Then the decision statistic $y_{\ell}^{(k)}$ [see (5.72)] should be replaced by the statistic

$$y^{(k)} = \sum_{n=0}^{N'-1} z_n^{(k)} \stackrel{\text{def}}{=} \sum_{n=0}^{N'-1} (\hat{z}_n^{(k)} \hat{\alpha}_n^{(k)} \cos \hat{\varphi}_n^{(k)} + \check{z}_n^{(k)} \hat{\alpha}_n^{(k)} \sin \hat{\varphi}_n^{(k)}) \tag{5.95}$$

where n numbers the symbols in the noninterleaved sequence, $N' = N(1 - 1/g)$. [In the sum on the right-hand side of Formula (5.95) the pilot symbols are excluded, i.e., the symbols for which $n'(\text{mod } g) = 0$.] If we neglect the inaccuracy in the amplitude and the phase estimates, we obtain

$$E\left(z_n^{(k)} | \alpha_n^{(k)}\right) = \begin{cases} (\alpha_n^{(k)})^2, & \text{if } H_1 \text{ is true,} \\ -(\alpha_n^{(k)})^2, & \text{if } H_{-1} \text{ is true} \end{cases} \tag{5.96}$$

$$\text{var}(z_n^{(k)} | \alpha_n^{(k)}) = (\alpha_n^{(k)})^2 \frac{\overline{I}_0}{2T_c} \stackrel{\text{def}}{=} (\alpha_n^{(k)})^2 \left((1 + f)(K - 1)a^2 + \frac{N_0}{2T_c} \right) \tag{5.97}$$

Proceeding as in (5.77), we obtain for perfect amplitude and phase estimation

$$P_{\mathrm{b}} < \frac{1}{2}\left(1+\frac{E_{\mathrm{b}}}{N(1-1/g)\overline{I}_0}\right)^{-N(1-1/g)} \approx \frac{1}{2}\exp\left(-\frac{E_{\mathrm{b}}}{\overline{I}_0}\right) \tag{5.98}$$

where $E_{\mathrm{b}} = N(1-1/g)E_{\mathrm{c}}$, $E_{\mathrm{c}} = 2a^2T_{\mathrm{c}}$, are the average energy per bit and chip, respectively. Strictly speaking, the number of code symbols in each block slightly varies because the interleaved stream of transmitted symbols includes pilot symbols, but we neglect this effect.

We have given another proof of the well-known fact that, in time-varying fading channels, diversity can strongly improve performance. Such diversity can be obtained by using base station antennas that are sufficiently separated in space, or by temporal separation through the interleaving process described in this section. The best performance improvement may be achieved by more than one form of diversity. In particular, time diversity via interleaving may be used together with antenna diversity and the Rake receiver.

5.6 FH SS COMMUNICATION OVER RAYLEIGH FADED CHANNELS

Analysis of a FH CDMA system operating in an one-path frequency-flat time-selective Rayleigh channel can be done in the same scenario as the analysis of the uplink DS CDMA system given in Section 5.5. To avoid repetition we first analyze the one-cell uplink communication system and then generalize results on multicell systems, as we did in Section 4.7. The transmitter is almost the same as that considered in Section 4.7. The system uses BFSK with Q carrier frequencies and a length N *reduced first-order Reed–Muller code*. The hopping rate is $R_h = 1/T_{\mathrm{c}}$, and the transmission rate is $R = (\log_2 N)/(NT_{\mathrm{c}})$ bits/s. The kth user's transmitted signal is [compare with Formula (3.124)]

$$s^{(k)}(t) = \sqrt{2}\sum_{n'=-\infty}^{\infty} h_{T_{\mathrm{c}}}(t-T_{\mathrm{c}}) \times \cos\left\{2\pi\left[f_{\mathrm{c}} + \frac{v_{n'}^{(k)}}{2}\Delta f + 2a_{n'}^{(k)}\Delta f\right]t + \varphi_{n'}^{(k)}\right\} \tag{5.99}$$

where $v_{n'}^{(k)}$ is the n'th symbol of the interleaved length N code sequence of the kth user; the other notations are introduced in the comment to Formula (3.126). The received signal is

$$r(t) = \sqrt{2}\sum_{k=1}^{K}\sum_{n'=-\infty}^{\infty} \alpha_{n'}^{(k)} h(t-n'T_{\mathrm{c}}-\delta_{n'}^{(k)}) \times \cos\left\{2\pi\left[f_{\mathrm{c}} + \frac{v_{n'}^{(k)}}{2}\Delta f + 2a_{n'}^{(k)}\Delta f\right]\left(t-\delta_{n'}^{(k)}\right) + \varphi_{n'}^{(k)}\right\} \tag{5.100}$$

where $\alpha_{n'}^{(k)}$, $\varphi_{n'}^{(k)}$, and $\delta_{n'}^{(k)}$ are fade amplitude, phase, and delay of the n'th signal waveform, respectively. The delay $\delta_{n'}^{(k)}$ is assumed to be known by the receiver, but $\alpha_{n'}^{(k)}$ and $\varphi_{n'}^{(k)}$ are unknown, and the receiver is noncoherent. We assume that the fade amplitude $\alpha_{n'}^{(k)}$ is Rayleigh distributed with the parameter a^2, phase $\varphi_{n'}^{(k)}$ is uniformly distributed on $[0, 2\pi)$, the successive chips are interleaved to be far enough apart that they encounter independent fading effects, and the background AWGN is negligible.

The receiver coincides with the receiver of the FH CDMA system considered in Section 4.7, except that the statistics $\hat{y}_{n'}^{(k)}$ and $\check{y}_{n'}^{(k)}$ from the output of the demodulator block of the receiver in Figure 3.8 should be deinterleaved before they enter into the decoder block in Figure 4.22, as shown in Figure 5.13.

As usual, we will study reception of the signal from the first user assuming that the zeroth (first row of the Hadamard matrix) codeword was sent and that AWGN is negligible. Conditioned that all users are not chip synchronized, we have at the output of the matched filter [compare with Formula (3.143)]

$$\hat{z}_{\mathrm{I}n'}^{(1)} = \alpha_{n'}^{(1)} \cos \varphi_{n'}^{(1)} + \sum_{k=2}^{K} \alpha_{n'}^{(k)} \left[\hat{\theta}_{n'}^{(k)} \eta_{n'}^{(k)} \cos \varphi_{n'}^{(k)} + \theta_{n'+1}^{(k)} (1 - \eta_{n'}^{(k)}) \cos \varphi_{n'+1}^{(k)} \right]$$

$$\hat{z}_{\mathrm{Q}n'}^{(1)} = \alpha_{n'}^{(1)} \sin \varphi_{n'}^{(1)} = \sum_{k=2}^{K} \alpha_{n'}^{(k)} \left[\hat{\theta}_{n'}^{(k)} \eta_{n'}^{(k)} \sin \varphi_{n'}^{(k)} + \theta_{n'+1}^{(k)} (1 - \eta_{n'}^{(k)}) \sin \varphi_{n'+1}^{(k)} \right]$$

$$\check{z}_{\mathrm{I}n'}^{(1)} = \sum_{k=2}^{K} \alpha_{n'}^{(k)} \left[\check{\theta}_{n'}^{(k)} \eta_{n'}^{(k)} \cos \varphi_{n'}^{(k)} + \check{\theta}_{n'}^{(k)} (1 - \eta_{n'}^{(k)}) \cos \varphi_{n'+1}^{(k)} \right]$$

$$\check{z}_{\mathrm{Q}n'}^{(1)} = \sum_{k=2}^{K} \alpha_{n'}^{(k)} \left[\check{\theta}_{n'}^{(k)} \eta_{n'}^{(k)} \sin \varphi_{n'}^{(k)} + \check{\theta}_{n'}^{(k)} (1 - \eta_{n'}^{(k)}) \sin \varphi_{n'+1}^{(k)} \right] \tag{5.101}$$

Here [compare with (3.128) and (3.129)]

$$\hat{\theta}_{n'}^{(k)} = \begin{cases} 1, & \text{if the } k\text{th user occupies at the } n'\text{th} \\ & \text{moment the same subband as the first user,} \\ 0, & \text{otherwise} \end{cases} \tag{5.102}$$

Figure 5.13. Deinterleaving in the receiver of FH CDMA system.

$$\breve{\theta}_{n'}^{(k)} = \begin{cases} 1, & \text{if the } k\text{th user occupies at the } n'\text{th} \\ & \text{moment the subband opposed to the} \\ & \text{subband occupied by the first user,} \\ 0, & \text{otherwise} \end{cases} \tag{5.103}$$

$\eta_{n'}^{(k)}$, $0 < \eta_{n'}^{(k)} \leq 1$, is the relative length of overlapping of the n'th chip of the signal received from the first user with the n'th chip of the signal received from the kth user. The random variables $\hat{\theta}_{n'}^{(k)}$ and $\breve{\theta}_{n'}^{(k)}$ satisfy condition (3.130). The random variables $\alpha_n^{(k)} \cos \varphi_n^{(k)}$ and $\alpha_n^{(k)} \sin \varphi_n^{(k)}$ are IID zero-mean Gaussian random variables with variance a^2. The random variables $\eta_n^{(k)}$, $k = 1, 2, \ldots K$, are independent and uniformly distributed on $[0, 1)$.

From Formula (5.101) we get, analogously to (3.144)–(3.147),

$$E(\hat{y}_{n'}^{(1)}) = 2a^2 \left(1 + \frac{2}{3}\lambda\right) \tag{5.104}$$

$$E(\breve{y}_{n'}^{(1)}) = 2a^2 \frac{2}{3}\lambda \tag{5.105}$$

$$\text{var}(\hat{y}_{n'}^{(1)}) = 4a^4 \left[1 + \frac{32}{15}\lambda + \frac{4}{9}\lambda^2\right] \tag{5.106}$$

$$\text{var}(\breve{y}_{n}^{(1)}) = 4a^4 \left[\frac{4}{5}\lambda + \frac{4}{9}\lambda^2\right] \tag{5.107}$$

where $\lambda = (K - 1)/M$. If we assume that interleaving is ideal, producing a memoryless channel, the random variables $\hat{y}_n^{(1)}$ and $\breve{y}_n^{(1)}$ can be considered as independent, and the first two moments of the statistics $x_i^{(1)}$ defined by (4.85) are

$$E(x_i^{(1)}) = Na^2, \ i = 1, 2, \ldots, N - 1 \tag{5.108}$$

$$\text{var}(x_i^{(1)}) = 2Na^4 \left[1 + \frac{44}{15}\lambda + \frac{8}{9}\lambda^2\right] \tag{5.109}$$

The signal-to-noise ratio per block is [compare with (4.90)]

$$\rho_B = \frac{[E(x_i^{(1)})]^2}{2\text{var}\left(x_i^{(1)}\right)} = \frac{N}{4\left(1 + \frac{44}{15}\lambda + \frac{8}{9}\lambda^2\right)}$$

$$= \frac{\lambda W/R}{4\left(1 + \frac{44}{15}\lambda + \frac{8}{9}\lambda^2\right)(K - 1)} \log_2 N \tag{5.110}$$

The maximum of ρ_B occurs at $\lambda = \lambda_0 = 3/2\sqrt{2}$. The maximum is equal to

$$\rho_B = \frac{W/R}{(K-1)\cdot(2+22/5\sqrt{2})}\log_2 N \approx \frac{W/R}{(K-1)20}\log_2 N \tag{5.111}$$

Assuming that statistics $x_i^{(1)}$ are normally distributed because of the central limit theorem, we get the union bound for block error probability [compare with (4.89)]

$$P_B < (N-1)Q(\sqrt{2\rho_B}) \tag{5.112}$$

If we take into account voice activity monitoring, antenna sectorization, and the other-cell interference, we have from (5.111) and (5.112) a lower bound for radio channel capacity of the multicell FH CDMA system [compare with Formula (4.92)]:

$$K_0 > 1 + \frac{W/R}{10[Q^{-1}(2P_b/(N-1))]^2}\frac{\gamma_v\gamma_a}{1+f}\log_2 N \tag{5.113}$$

where γ_1 and γ_v are voice activity and antenna gain factors, f is the other-cell interference factor, $P_b \approx P_B/2$ is the bit error probability, and $Q^{-1}(\cdot)$ is the inverse Q function. In comparison with coded FH CDMA communication over AWGN channel (see Section 4.7) we can see additional degradation of the channel capacity due to fading.

EXAMPLE 5.10

Estimate the uplink capacity of the asynchronous multicell FH CDMA system operating over a Rayleigh channel. The system has the same parameters as in Examples 3.11 and 4.9 and uses reduced first-order Reed–Muller codes of length $N = 64, 256$, *and* 1024. *Neglect background AWGN.*

Solution

If $P_b = 10^{-3}$ *we get from (5.113) that* $K_0 = 149, 171, 185$, *respectively. If* $P_b = 10^{-4}$, *then* $K_0 = 117, 139, 155$.

We have considered only one example of FH CDMA communication over a fading channel. Analysis of other FH CDMA communication schemes, particularly using convolutional coding, can be done analogously.

5.7 COMMENTS

In this chapter, we have considered a number of topics concerning DS and FH CDMA communications over fading multipath channels. We began with a statistical model of the channel and then analyzed the reception of faded signals. We introduced a number of different concepts in this chapter related to downlink and uplink communications in multipath channels of CDMA systems. We

observed that the reliability of the communication system is enhanced by the use of diversity transmission and reception. We concluded by using time interleaving to provide additional diversity so that fading channels perform almost as well as unfaded channels when coherent demodulation is feasible.

The pioneering work on the characterization of fading multipath channels and on signal and receiver design for reliable digital communication over such channels was done by Price [36]. He has also considered diversity transmission and diversity combining techniques under a variety of channel conditions. Our treatment of CDMA communication over fading channels relies on Viterbi [47]. We focused primarily on the Rayleigh fading channel because of the wide acceptance of this model for describing fading effects on CDMA and its mathematical tractability. Although other statistical models, such as the Rician fading model or the Nakagami fading model, may be more appropriate for characterizing fading on some real channels, the general approach in the design of reliable communication presented in this chapter carries over. Much additional information on communication in fading channels is available in [34].

PROBLEMS

5.1. The probability density function of a Rayleigh random variable X is given as

$$f_a(x) = \begin{cases} \dfrac{x}{a^2}\exp(-x^2/2a^2), & x \geq 0 \\ 0, & x < 0 \end{cases}$$

For the random variable X calculate the following:

a) The probability distribution function $F_a(x)$

b) Expectation value $E[X]$

c) The variance var$[X]$

5.2. Consider a DS CDMA system that uses BPSK signalling with coherent reception.

a) Calculate the required E_b/I_0 if we transmit over an AWGN channel and we need $P_b < 10^{-3}$.

b) Suppose that we transmit over a Rayleigh fading channel and use a coherent Rake receiver. Calculate the value of L that is needed to have $P_b < 10^{-3}$, if E_b/I_0 should not exceed the value in a) by more than 3 dB.

c) Repeat a) and b), but use requirement $P_b < 10^{-4}$.

5.3. In CDMA communication theory, the amplitude of the received signal is assumed to be Rayleigh distributed. That is, the signal amplitude is multiplied by a variable α with probability density function

$$f_a(\alpha) = \frac{\alpha}{a^2}\exp\left(\frac{-\alpha^2}{2a^2}\right)$$

This problem is meant to explain why this channel model is used. Assume that the received signal consists of a large number of reflected waves, which are uncorrelated and of approximately the same amplitude. By invoking the central limit theorem it then follows that the received signal can be written as

$$z(t) = x(t)\cos\omega_0 t - y(t)\sin\omega_0 t$$

where $x(t)$ and $y(t)$ are uncorrelated Gaussian processes with zero mean and variance a^2. The envelope of the signal is given by

$$r(t) = \sqrt{x(t)^2 + y(t)^2}$$

For notational simplicity, we drop the explicit time dependence and write x rather than $x(t)$, etc.

a) Show that the joint probability density function of (x, y) is

$$p(x, y) = \frac{1}{2\pi a^2}\exp\left(-\frac{x^2 + y^2}{2a^2}\right)$$

b) Let $x = r\cos\phi$, $y = r\sin\phi$. Show that

$$p(r, \phi) = \frac{r}{2\pi a^2}\exp\left(\frac{-r^2}{2a^2}\right)$$

c) By integrating with respect to ϕ, show that r is Rayleigh distributed.

d) To find the average SNR, $E[r^2]$ is needed. Find this by using the probability density function of r.

e) Find $E[r^2]$ without using the probability density function of r.

5.4. Use Formula (5.36) to find the signal-to-noise ratio E_b/I_0 that is sufficient to achieve $P_b = 10^{-3}$ for $L = 1$, 2, and 4.

5.5. Show that [see Formulas (5.36) and (5.38)]

$$\lim_{L\to\infty}\frac{1}{2}\left[1 + \frac{E_b}{LI_0}\right]^{-L} = \frac{1}{2}\exp(-E_b/I_0)$$

5.6. What average E_b/I_0 is sufficient to reach $P(\mathcal{E}) = 10^{-3}$ for coherent BPSK on the one-path Rayleigh fading channel? On the L-paths Rayleigh fading channel? Repeat for $P(\mathcal{E}) = 10^{-5}$.

5.7. Repeat Problem 5.6 for $L = 1$, the noncoherent receiver, and 8-ary orthogonal waveforms.

5.8. Prove Equation (5.17).

5.9. Repeat Problem 3.11 for the L-path Rayleigh fading channel, $L = 1$, 2, 8, $P_b = 10^{-3}$.

5.10. Prove that the random variables $x = \alpha \cos \varphi$ and $y = \alpha \sin \varphi$, where α has Rayleigh distribution (5.1) and φ is uniformly distributed on $[0, 2\pi)$, are independent zero-mean Gaussian variables with variance a^2.

5.11. A communication system that does not employ diversity and channel coding requires 100 mW of transmitted power to achieve $P_b \leq 10^{-3}$ in the receiver when the system operates over a Rayleigh fading channel. Estimate the order of diversity required to achieve the same probability of error, given that the transmitter can transmit only 10 mW of power.

5.12. When a convolutional code is used for error correction, the probability of a bit error can be upper bounded by using the path weight enumerator function [see Formulas (4.59) and (4.60)]. For a rate 1/2, memory 4 convolutional code with $d_{free} = 7$ the first five coefficients in Formula (4.59) are 4, 12, 20, 72 and 225. Assuming that it is sufficient consider only the first five terms in Formula (4.59), find the required value of E_b/N_0 to guarantee $P_b < 10^{-5}$ for a Rayleigh fading channel with $L = 1$, 2, and 4. Compare with performances of the same system operating in the AWGN channel.

5.13. For the same code as in Problem 5.12 and for the same required error probability, consider a CDMA system with $W = 1.23$ MHz and $R_b = 9.6$ kb/s. Assuming unit amplitude rectangular spreading chips, voice activity 3/8, three sectored antennas, and interference from the other cells corresponding to 0.6 of the interference from the home cell, find the number of users for a Rayleigh fading channel with $L = 1$, 2, and 4. Compare with performances of the system operating over the AWGN channel.

5.14. Consider a DS BPSK CDMA system communicating over an uplink AWGN channel of bandwidth 5 MHz. The user rate is $R = 10$ kb/s. The two-sided power spectral density of the AWGN is $N_0/2 = 10^{-10}$ W/Hz. The maximal acceptable P_b is 10^{-4}. Voice activity gain $\gamma_v = 2.67$, antenna gain $\gamma_a = 2.4$, and pilot chips rate $1/g \ll 1$. The other-cell relative interference factor $f = 0.6$. The system uses a repetition code and has perfect power control, and the power of the received signal is $P = 0.1$ mW.

Find the radio channel capacity of the system. Estimate the capacity for transmission over an L-path equal-strength Rayleigh channel with the same parameters, and $L = 4$.

Hint: Use Figure 5.3 for the analysis of transmission over a Rayleigh channel.

5.15. a) Determine the radio channel capacity of a single-cell DS CDMA system, communicating over an AWGN channel, using a memory $m = 5$, superorthogonal convolutional code, and a coherent receiver, with maximum acceptable bit error probability $P_b < 10^{-5}$. The user rate is 9.6 kb/s, and the system bandwidth is 5 MHz. The voice activity gain is $\gamma_v = 8/3$, and the antenna gain is $\gamma_a = 2.4$.

b) What is the radio channel capacity of the system if the communication is over an $L = 4$ and $L = 8$ path Rayleigh channel?

5.16. Consider the CDMA system of Example 5.6, which operates in an L multipath Rayleigh channel of equal average strength and uses N orthogonal signals with noncoherent reception. Assuming that the maximal acceptable P_b is 10^{-6}, determine the capacity of the single-cell CDMA system for $N = 32, 64, 128, 256$, $L = 4, 8$.
Hint: Use Figure 5.8.

5.17. For an error-correcting code to work appropriately in a fading environment, it is necessary that the code symbols are affected by independent channel conditions, or nearly so. To achieve this an interleaver is used, see the figure below. In the uplink in IS-95, a rate 1/3, memory 8 binary convolutional code is used for error correction. The information rate is 9.6 kb/s, and the delay in the interleaver is 20 ms. How would you choose the dimensions, that is, I and J of the interleaver?
Hint: J should be choosen slightly larger than the length of the most likely error events. (Why?)

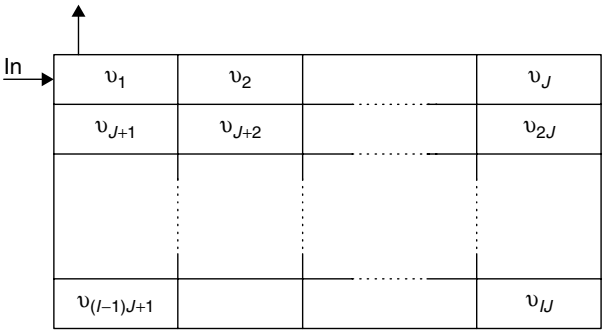

Problem 5.17.

5.18. This problem is meant to give some insight into the problem of transmitting information over a slowly Rayleigh fading channel. To obtain a feeling for what the signal might look like, refer to the figure below.

a) The average power of the received signal is $2a^2$. In the figure the solid line is the ratio of the amplitude of the received signal to the root mean square $\sqrt{2a^2}$ obtained by simulation. The dashed line corresponds to 13 dB below this ratio. Find what percentage of time the amplitude of the received signal is below the dashed line.

b) It can be shown that the average number of drops in signal amplitude below a specific level, α, per second is given by

$$N(\alpha) = f_D\sqrt{2\pi}\ \rho e^{-\rho^2}$$

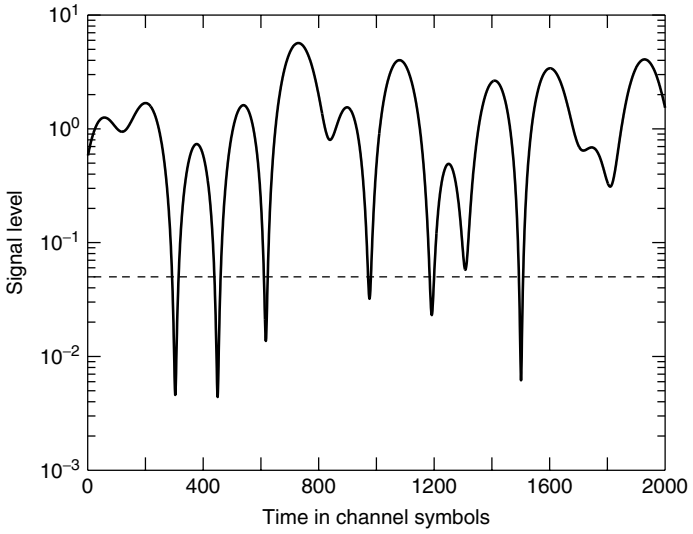

Problem 5.18.

where

$$\rho = \frac{\alpha}{\sqrt{2a^2}}$$

$$f_D = v/\lambda$$

v = speed of the mobile in m/s

λ = wavelength of the transmitted signal

If $v = 30$ km/h and $f_c = 1.8$ GHz, determine $N(\alpha)$ for the data given in a), that is, $\rho = -13$ dB.

c) Using the results in a) and b), find the average duration of a fading dip below the level α.

d) Suppose that the transmission rate R is 10 kb/s and that a code of rate $r = 1/2$ is used for error correction. What is the average number of code symbols received while the relative/amplitude remains below -13 dB?

e) To overcome the problem that many consecutive code symbols are unreliable, an interleaver is used. Estimate the minimum interleaving depth for the interleaver to work properly.

f) Suppose block coding is employed. How should the dimensions of a block interleaver be chosen?

g) If the maximum delay caused by the interleaver is 20 ms, what is the maximum length of a block code if the interleaver should work properly?

5.19. Consider a coded multicell DS CDMA system where the chip rate is equal to 4.096 Mchip/s, $R = 16$ kb/s, and $P_b = 10^{-3}$. The system employs a first-order Reed–Muller code with $N = 32$, three-sectored antennas, and voice activity detection. Calculate the capacity K_0 for the

a) AWGN channel with coherent reception

b) AWGN channel with noncoherent reception

c) Rayleigh fading channel with noncoherent reception, $L = 2$, 4, and 8

d) In which system(s), existing and planned, is this kind of coding used?

e) What are the differences and similarities between the system described above and IS-95 and WCDMA?

6

PSEUDORANDOM SIGNAL GENERATION

In the previous chapters we demonstrated the potential advantages of transmitting signals that appear noiselike. Such signals must be generated by relatively simple devices. Equally important, these signals must be generated at the receiver as well. In this chapter various techniques for generating noiselike (pseudorandom) signals are described and analyzed.

The waveform $a(t)$ used in the systems described in Chapters 2–5 to spread and despread the data-modulated carrier is usually generated by using a shift register whose contents during each time interval are a linear combination of the contents of the register during the preceding time interval. A pseudorandom or PN ("pseudonoise") sequence generated by such a shift register has autocorrelation properties similar to those of white noise.

For the spread spectrum system to operate efficiently, the waveform $a(t)$ is selected to have certain desirable properties. For example, the phase (delay) δ of the received spreading signal $a(t - \delta)$ must be initially determined and then tracked by the receiver. In Chapter 7 we consider the problem of initial detection (acquisition) and tracking of timing of an appropriately chosen spreading signal.

6.1 PSEUDORANDOM SEQUENCES AND SIGNALS

A binary random sequence, or Bernoulli sequence, is known in engineering literature as a coin-flipping sequence. The symbol "0" in the sequence corresponds to a "head" outcome in a succession of independent coin-flip experiments; the

Theory of Code Division Multiple Access Communication, by Kamil Sh. Zigangirov
ISBN 0-471-45712-4

symbol "1" in the sequence corresponds to a "tail" outcome. Even though in principle this random sequence can be stored at both transmitter and receiver, this would require very large memory. This is clearly impossible in a real system, and consequently pseudorandom sequences, described in this chapter, should be employed instead of random sequences. We shall demonstrate that the randomness properties of a coin-flipping sequence can be imitated by a pseudorandom sequence that is generated by a shift register specified by a few parameters.

First of all we should specify what the randomness properties of a coin-flipping (Bernoulli) sequence are. Following Golomb [19], these three properties are classified as follows:

- *Balance Property*: The relative frequencies of "0" and "1" in the coin-flipping sequence are each 1/2.
- *Run Property*: Define a run as a subsequence of identical symbols within the coin-flipping sequence. The length of this subsequence is the length of the run. Then, according to the run property, one-half of all run lengths are unity; one-quarter are of length 2, one-eighth are of length 3,..., a fraction $1/2^n$ of all runs are of length n for all finite n.
- *Delay and Add Property*: If the coin-flipping sequence is shifted, the relative frequencies of agreements and disagreements of the resulting sequence with the original sequence are each 1/2.

As we shall see, a sequence generated by a shift register nearly satisfies these properties. We shall provide a more precise definition after considering the generation process in Section 6.3.

A pseudorandom sequence, $\ldots \alpha_{-2}, \alpha_{-1}, \alpha_0, \alpha_1, \alpha_2 \ldots$, where $\alpha_n \in \{0, 1\}$, generated by shift registers is a periodic sequence of ones and zeros with period N_p. Because the sequence is periodic, $\alpha_n = \alpha_{n+N_\mathrm{p}}$ for any n. The spreading signal $a(t)$ derived from this pseudorandom sequence is also a periodic pseudorandom function of time with period $\mathcal{T} = N_\mathrm{p} T_\mathrm{c}$ and is defined by

$$a(t) = \sum_{n=-\infty}^{\infty} a_n h_{T_\mathrm{c}}(t - nT_\mathrm{c}) \tag{6.1}$$

where $a_n = (-1)^{\alpha_n}$, and $h_{T_\mathrm{c}}(t)$ is a pulse of duration T_c. In this chapter we consider only the unit amplitude rectangular pulse (2.3). The signal $a(t)$ is deterministic, so that its *autocorrelation function* is defined by

$$R_a(\tau) = \frac{1}{\mathcal{T}} \int_0^{\mathcal{T}} a(t) a(t + \tau)\, \mathrm{d}t \tag{6.2}$$

Because $a(t)$ is periodic with period $\mathcal{T}$, it follows that $R_a(\tau)$ is also periodic with period $\mathcal{T}$. The power spectrum $A(f)$ is found by taking the Fourier transform of (6.2). This power spectrum consists of discrete spectral lines at all harmonics

of $1/N_pT_c$

$$A(f) = \sum_{k=-\infty}^{\infty} A_k \delta\left(f - \frac{k}{N_pT_c}\right) \tag{6.3}$$

where $\delta(\cdot)$ is the delta function. Consider two different periodic signals $a(t)$ and $a'(t)$. The *cross-correlation function* of these two deterministic signals is

$$R_{aa'}(\tau) = \frac{1}{\mathcal{T}} \int_0^{\mathcal{T}} a(t)a'(t+\tau)\,dt \tag{6.4}$$

where it has been assumed that $a(t)$ and $a'(t)$ have the same period $\mathcal{T}$. Then the cross-correlation function is also periodic with period $\mathcal{T}$.

The variable τ in Formulas (6.2) and (6.4) can have any value, that is, τ is not constrained to be an integer multiple of T_c. Substituting (6.1) into (6.4) yields

$$R_{aa'}(\tau) = \frac{1}{\mathcal{T}} \sum_m \sum_n a_m a'_n \int_0^{\mathcal{T}} h_{T_c}(t - mT_c) h_{T_c}(t + \tau - nT_c)\,dt \tag{6.5}$$

The integral in (6.5) is nonzero only when the pulses $h_{T_c}(t - mT_c)$ and $h_{T_c}(t + \tau - nT_c)$ overlap. The variable τ can be expressed as $\tau = kT_c + \epsilon$, where $k = \lfloor \tau/T_c \rfloor$, $0 \le \varepsilon < T_c$. Using this substitution, we get from (6.5)

$$\begin{aligned} R_{aa'}(\tau) &= \tilde{R}_{aa'}(k, \varepsilon) \\ &\stackrel{\text{def}}{=} \frac{1}{N_p} \sum_{m=0}^{N-1} a_m a'_{m+k} \frac{1}{T_c} \int_0^{T_c - \varepsilon} h_{T_c}(\delta) h_{T_c}(\delta + \varepsilon)\,d\delta \\ &\quad + \frac{1}{N_p} \sum_{m=0}^{N-1} a_m a'_{m+k+1} \frac{1}{T_c} \int_{T_c - \varepsilon}^{T_c} h_{T_c}(\delta) h_{T_c}(\delta - T_c + \varepsilon)\,d\delta \end{aligned} \tag{6.6}$$

where the additional substitution $\delta = t - mT_c$ has been employed. Because for unit amplitude rectangular pulses

$$\frac{1}{T_c} \int_0^{T_c - \varepsilon} h_{T_c}(\delta) h_{T_c}(\delta + \varepsilon)\,d\delta = 1 - \frac{\varepsilon}{T_c}$$

$$\frac{1}{T_c} \int_{T_c - \varepsilon}^{T_c} h_{T_c}(\delta) h_{T_c}(\delta + \varepsilon)\,d\delta = \frac{\varepsilon}{T_c}$$

we have from (6.6)

$$R_{aa'}(\tau) = \left(1 - \frac{\varepsilon}{T_c}\right) \frac{1}{N_p} \sum_{m=0}^{N-1} a_m a'_{m+k} + \frac{\varepsilon}{T_c} \frac{1}{N_p} \sum_{m=0}^{N-1} a_m a'_{m+k+1}$$

The *discrete periodic cross-correlation function* of two periodical sequences $\{a_n\}$ and $\{a'_n\}$ is defined by

$$\theta_{aa'}(k) = \frac{1}{N_p} \sum_{n=0}^{N-1} a_n a'_{n+k} \tag{6.7}$$

Using this definition, the cross-correlation function (6.5) becomes

$$R_{aa'}(\tau) = \tilde{R}_{aa'}(k, \varepsilon) = \left(1 - \frac{\varepsilon}{T_c}\right) \theta_{aa'}(k) + \frac{\varepsilon}{T_c}\, \theta_{aa'}(k+1) \tag{6.8}$$

This expression is helpful because the theory used to analyze pseudorandom sequences formulates results in terms of unit delays. The discrete periodic cross-correlation function $\theta_{a,a'}(k)$ can be calculated by representing the sequences $\{a_n\}$ and $\{a'_n\}$ as binary vectors $\boldsymbol{a}$ and $\boldsymbol{a}'$ of length N_p. A delay of k positions of the original sequence is represented as a cyclic shift of k time units of the vector representation. The kth cyclic shift of $\boldsymbol{a}$ is represented by $\boldsymbol{a}_k$. With this notation, the function $\theta_{aa'}(k)$ equals $(\nu_0 - \nu_1)/N_p$, where ν_0 is the number of positions in which $\boldsymbol{a}_0$ agrees and ν_1 the number of positions in which $\boldsymbol{a}_0$ disagrees with $\boldsymbol{a}_k$. The *discrete periodic autocorrelation function* $\theta_a(k)$ is defined by Formula (6.7) with $a'_n = a_n$. When the discrete periodic autocorrelation function $\theta_a(k)$ is used instead of the discrete periodic cross-correlation function $\theta_{aa'}(k)$, the result is the autocorrelation function

$$\tilde{R}_a(k, \varepsilon) = \left(1 - \frac{\varepsilon}{T_c}\right) \theta_a(k) + \frac{\varepsilon}{T_c}\, \theta_a(k+1) \tag{6.9}$$

EXAMPLE 6.1

Assume that the spreading sequence is the periodic sequence (period 7):

$$\ldots -1\ -1\ -1 \quad 1\ -1 \quad 1 \quad 1\ -1\ -1\ -1\ -1 \quad 1\ -1 \quad 1 \quad 1 \ldots$$

Find the discrete periodic autocorrelation function $\theta_a(k)$ of this sequence and the autocorrelation function $R_a(\tau)$ of the spreading waveform, specified by this sequence.

Solution

$$\theta_a(k) = \begin{cases} 1, & k = 0, 7, 14 \ldots\ , \\ -\dfrac{1}{7}, & \textit{otherwise} \end{cases} \tag{6.10}$$

The autocorrelation function is presented in Figure 6.1.

The spreading sequence of Example 6.1 is obtained from the periodic pseudorandom sequence

$$\ldots 1\ 1\ 1\ 0\ 1\ 0\ 0\ 1\ 1\ 1\ 0\ 1\ 0\ 0 \ldots \tag{6.11}$$

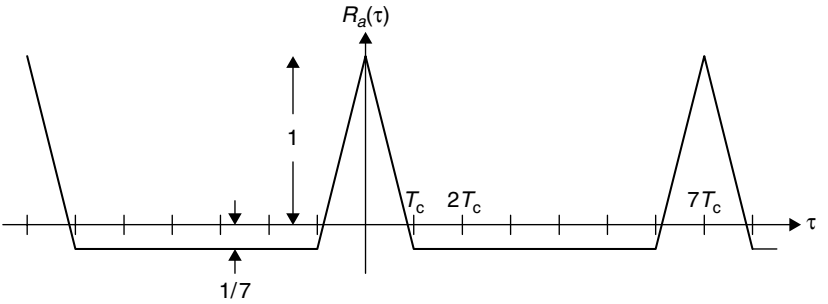

Figure 6.1. The autocorrelation function of the spreading waveform of Example 6.1.

by mapping $0 \rightarrow 1$, $1 \rightarrow -1$. It "almost" satisfies Golomb's randomness properties. Relative frequencies of "0" and "1" are 3/7 and 4/7, respectively (balance property). The sequence contains the following runs: 010, 101, 1001, 01110. Half of the runs have length 1, one-quarter are of length 2, and one-quarter are of length 3. The sequence nearly satisfies the run length property. Finally, from (6.10) it follows that any phase shift of the sequence (6.11) (except shifts multiple to the period 7) gives 3 agreements and 4 disagreements with the original sequence. This is "almost" the delay and add property.

The sequence (6.11) is an example of so-called *maximum-length sequences*. We shall provide a more precise definition after considering the mechanics of finite-field arithmetic.

6.2 FINITE-FIELD ARITHMETIC

Consider the periodic pseudorandom sequence $\ldots \beta_{-2}, \beta_{-1}, \beta_0, \beta_1, \beta_2, \ldots$, where $\beta_n \in \{0, 1\}$. It is convenient to represent this sequence by the polynomial $\beta(D)$. Considering only terms with nonnegative index, we define the generating function of this sequence as

$$\beta(D) \triangleq \beta_0 + \beta_1 D + \beta_2 D^2 + \ldots = \sum_{n=0}^{\infty} \beta_n D^n \tag{6.12}$$

where D is the delay operator. The power of D in each term of this polynomial corresponds to the number of delays of that term.

Let β_n be an element of the binary *Galois field*, $GF(2)$, with addition performed modulo 2 and multiplication according to the logical "and" function. The addition and multiplication tables are shown in Table 4.1.

Consider next the arithmetic of polynomials in the indeterminate D whose coefficients are elements of $GF(2)$. A polynomial of degree m over $GF(2)$ has the form

$$\beta(D) = \beta_0 + \beta_1 D + \cdots + \beta_m D^m \tag{6.13}$$

where β_j is an element of $GF(2)$, $\beta_m = 1$. The operations of addition, subtraction, multiplication, and division are defined for these polynomials in exactly the same way as for polynomials with real coefficients except that binary arithmetic is used.

The division of one polynomial over $GF(2)$ by another yields a quotient $\gamma(D)$ and a remainder $\rho(D)$ just as with ordinary long division of two polynomials.

EXAMPLE 6.2

Divide $\alpha(D) = 1 + D^5$ *by* $\beta(D) = 1 + D + D^3 + D^4$.

Solution

The long division of $\alpha(D)$ *by* $\beta(D)$ *yields*

$$
\begin{array}{r|l}
 & D + 1 \\
\hline
D^4 + D^3 + D^2 + 1 & D^5 + 1 \\
 & D^5 + D^4 + D^3 + D^2 + D \\
\hline
 & D^4 + D^3 + D^2 + D + 1 \\
 & D^4 + D^3 + D^2 + 1 \\
\hline
 & D^2 + D
\end{array}
$$

So $\gamma(D) = 1 + D$ *and* $\rho(D) = D^2 + D^3$. *This result can be verified by calculating* $\alpha(D) = \beta(D)\gamma(D) + \rho(D)$.

A polynomial $\beta(D)$ over a field is said to be *irreducible* if it cannot be factored into products of lower-degree polynomials over the *same* field. The polynomial $1 + D^2$ over $GF(2)$ is not irreducible because $1 + D^2 = (1 + D)^2$ in binary arithmetic but $1 + D + D^4$ is irreducible, as may be verified by testing all binary irreducible polynomials of degree 2 or less as divisors.

To form an *extension field* of size 2^m we take the field elements to be all polynomials over $GF(2)$ of degree $m - 1$ or less, of which there are 2^m. Addition and multiplication of elements are performed by the usual rules for polynomial arithmetic, except we define the results of multiplication (which may produce a polynomial of degree m or larger) as the remainder on division by an irreducible polynomial of degree m. We will indicate this as $\rho(D) = \alpha(D)\beta(D) (\text{mod } \varphi(D))$, where $\varphi(D)$ is irreducible. The polynomial $\varphi(D)$ is called the *generating polynomial* of the field. (Note that the addition of two polynomials of degree $m - 1$ or less produces a polynomial of degree $m - 1$ or less; hence there is no formal need for reduction.) Clearly, the additive identity element of the field is the polynomial $\beta(D) = 0$, and the multiplicative identity element is the polynomial $\beta(D) = 1$.

There is a special class of irreducible polynomials, called *primitive polynomials*. A polynomial $\varphi(D)$ of degree m is called primitive if the smallest integer N for which $\varphi(D)$ divides $D^N + 1$ is $N = 2^m - 1$. Only primitive polynomials can be used as generating polynomials of the extension field. Primitive polynomials over $GF(2)$ are tabulated in [33], and some examples are listed in Table 6.1 for $m = 2$ through 10. These in turn supply fields of size 4, 8, 16, . . . , 1024.

Table 6.1 Primitive Polynomials over *GF*(2)

m	
2	$1 + D + D^2$
3	$1 + D + D^3$
4	$1 + D + D^4$
5	$1 + D^2 + D^5$
6	$1 + D + D^6$
7	$1 + D^3 + D^7$
8	$1 + D^2 + D^3 + D^4 + D^8$
9	$1 + D^4 + D^9$
10	$1 + D^3 + D^{10}$

We now illustrate a construction of $GF(8)$, an extension field of $GF(2)$.

EXAMPLE 6.3

Construct $GF(2^3)$, using the third-degree primitive polynomial $\varphi(D) = 1 + D + D^3$ as a generating polynomial for the field.

Solution

The eight elements of the field can be represented by the binary polynomials $0, 1, D, 1 + D, D^2, 1 + D^2, D + D^2$, *and* $1 + D + D^2$. *We could also label each element with a* 3*-bit vector (the vector of coefficients of each polynomial), or we could label the elements as* 0 *through* 7 *by taking the integer equivalent to each binary representation. Figure 6.2 provides such a listing of these possibilities and gives the complete addition and multiplication table. For example,* $D^2 + 1$ *plus* $D^2 + D + 1$ *equals* D, *and* $D^2 + 1$ *multiplied mod* $\varphi(D)$ *by* $D^2 + D + 1$ *equals* D^2.

Consider the sequence of powers of a nonzero field element β, that is, $\beta^1, \beta^2, \beta^3, \ldots$, which is a sequence of nonzero field elements. This sequence will eventually produce the field element 1 because the field is finite and thereafter be periodic. The *order* of an element β is the smallest nonzero n such that $\beta^n = 1$. It is clear that the largest value for the order of an element is $2^m - 1$, because there are only $2^m - 1$ nonzero elements.

Every finite field with 2^m elements has at least one *primitive element*, an element α whose order is $2^m - 1$. Thus the power sequence $\alpha^1, \alpha^2, \alpha^3, \ldots \alpha^{2^m - 1} = 1 = \alpha^0$ produces all nonzero field elements. Any nonprimitive element has a power sequence that has a shorter period and does not contain every nonzero elements of the field.

It can be shown that a primitive polynomial $\varphi(D)$ of degree m has a primitive element of $GF(2^m)$ as a root. This can be used as an alternative definition of a primitive polynomial.

Polynomial form	Integer form	m-tuple form
0	0	000
1	1	001
D	2	010
$D+1$	3	011
D^2	4	100
D^2+1	5	101
D^2+D	6	110
D^2+D+1	7	111

	0	1	2	3	4	5	6	7
0	0	1	2	3	4	5	6	7
1	1	0	3	2	5	4	7	6
2	2	3	0	1	6	7	4	5
3	3	2	1	0	7	6	5	4
4	4	5	6	7	0	1	2	3
5	5	4	7	6	1	0	3	2
6	6	7	4	5	2	3	0	1
7	7	6	5	4	3	2	1	0

Addition table

	0	1	2	3	4	5	6	7
0	0	0	0	0	0	0	0	0
1	0	1	2	3	4	5	6	7
2	0	2	4	6	3	1	7	5
3	0	3	6	5	7	4	1	2
4	0	4	3	7	6	2	5	1
5	0	5	1	4	2	7	3	6
6	0	6	7	1	5	3	2	4
7	0	7	5	2	1	6	4	3

Multiplication table

Figure 6.2. Construction of $GF(8)$ using the primitive polynomial $\varphi(D) = 1 + D + D^3$.

EXAMPLE 6.4

Construct $GF(2^4)$ using the primitive polynomial from Table 6.1 as generating polynomial.

Solution

Using the primitive polynomial $\varphi(D) = 1 + D + D^4$ for generating the field, we could proceed as before to build arithmetic tables. However, a more convenient construction is provided by letting 0 and 1 be the first two elements (the additive and multiplicative identities, respectively) and letting the next element be α, defined only as a root of the primitive polynomial; thus α is primitive in $GF(16)$. We associate with this element the polynomial D. The remaining field elements are taken to be successive powers of α, because they certainly generate the remaining nonzero elements. Thus α^2 is associated with the polynomial D^2, and α^3 is associated with D^3. Next, we encounter α^4 as a field element and use the fact that $\alpha^4 + \alpha + 1 = 0$, but because α and the element 1 are polynomials over $GF(2)$, where subtraction is the same as addition, $\alpha^4 = \alpha + 1$. Thus α^4 is associated with the polynomial $D + 1$. Continuing this procedure enumerates all the field elements as powers of α, or as polynomials. Table 6.2 provides a listing for the $GF(16)$ elements ordered as increasing powers of α, along with the corresponding polynomial forms. There happened to be eight primitive elements in the field, D being one of them. A complete addition and multiplication table can be constructed analogously to Figure 6.2.

Suppose that we constructed an electronic circuit, which generates the powers of α over $GF(16)$ in inverse order, that is,

$$1, \alpha^{14}, \alpha^{13}, \alpha^{12} \ldots \alpha, 1$$

Table 6.2 Elements of $GF(2^4)$ as powers of α and as polynomials modulo $1 + D + D^4$

As power of α	As polynomials
0	0
1	1
α	D
α^2	D^2
α^3	D^3
α^4	$1 + D$
α^5	$D + D^2$
α^6	$D^2 + D^3$
α^7	$1 + D + D^3$
α^8	$1 + D^2$
α^9	$D + D^3$
α^{10}	$1 + D + D^2$
α^{11}	$D + D^2 + D^3$
α^{12}	$1 + D + D^2 + D^3$
α^{13}	$1 + D^2 + D^3$
α^{14}	$1 + D^3$

Consider the sequence of zero coefficients of the elements in polynomial form of this sequence, that is (compare Table 6.2),

$$1, 1, 1, 1, 0, 1, 0, 1, 1, 0, 0, 1, 0, 0, 0, 1 \tag{6.14}$$

We obtain a periodic "noiselike" (or PN) binary sequence, of period 15, that "almost" satisfies Golomb's randomness properties. Considering $GF(2^m)$ with large m, we can construct pseudorandom sequences of large period. The randomness properties of such sequences are considered in Section 6.4.

6.3 MAXIMUM-LENGTH LINEAR SHIFT REGISTERS

The discussion up to this point has been rather abstract. Now we discuss how the calculation of consecutive powers of the primitive element can be instrumented. The technique for this calculation is illustrated in Figure 6.3, where the coefficients $\varphi_1, \varphi_2, \ldots, \varphi_m$ are elements of $GF(2)$, that is, 0 or 1.

The symbols of the field element over $GF(2^m)$ in polynomial form

$$\beta(D) = \beta_0 + \beta_1 D + \ldots \beta_{m-1} D^{m-1}$$

are initially stored in the stages of a shift register, in the positions shown in Figure 6.3. The first operation is to add (in $GF(2)$) $\beta_0 \varphi_i$ to β_i for $1 \leq i \leq m-1$ and then to shift the register one position to the right, replacing β_{m-1} in the

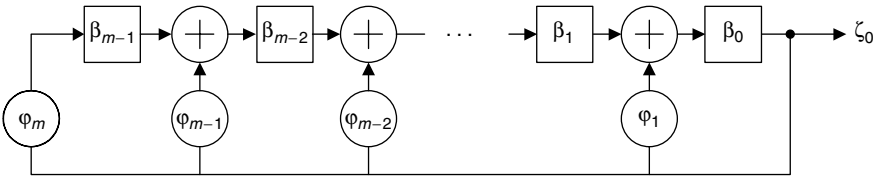

Figure 6.3. An m stage linear shift register (Galois feedback generator).

leftmost position by $\beta_0\varphi_m$. It should be verified that the content of the shift register at this point in polynomial form is

$$\beta^{(1)}(D) = \sum_{i=1}^{m-1} \beta_i D^{i-1} + \beta_0 \sum_{i=1}^{m} \varphi_i D^{i-1} \tag{6.15}$$

From Formula (6.15) it follows that

$$\beta^{(1)}(D)D = \beta(D) + \beta_0\varphi(D) \tag{6.16}$$

where

$$\varphi(D) = 1 + \sum_{i=1}^{m} \varphi_i D^i \tag{6.17}$$

is called the *characteristic polynomial* of the shift register.

Suppose now that $\varphi(D)$ is a primitive polynomial over $GF(2)$, and this polynomial generates $GF(2^m)$. Because a primitive element of the field is a root of $\varphi(D)$ we get from (6.16)

$$\beta^{(1)}(\alpha)\alpha = \beta(\alpha)$$

If $\beta(\alpha) = \alpha^j$, then $\beta^{(1)}(\alpha) = \alpha^{j-1}$.

The circuit in Figure 6.3 generates the powers of α in inverse order. Correspondingly, the output of the shift register, $\zeta(D)$, is the sequence of zero coefficients of the elements of this sequence. The period N_p of this sequence is $(2^m - 1)$, because the number of nonzero elements in $GF(2^m)$ is equal to $(2^m - 1)$. This is the maximal possible period for shift registers of length m. Such a shift register is called a *maximum-length (linear) shift register (MLSR).* The sequence generated by an MLSR is called *MLSR sequence, maximum-length sequence, maximal-length sequence*; or *m-sequence*.

Equation (6.16) can be rewritten in the form

$$\beta^{(t+1)}(D)D^{t+1} = \beta^{(t)}(D)D^t + \zeta_t D^t \varphi(D) \tag{6.18}$$

where $\beta^{(t)}$ is the register content at the tth moment and ζ_t is the register output at the tth moment, $t = 0, 1, 2, \ldots$. Summation of (6.18) over t from $t = 0$ to

$t = \infty$ gives

$$\sum_{t=0}^{\infty} \beta^{(t)}(D) D^t + \beta^{(0)}(D) = \sum_{t=0}^{\infty} \beta^{(t)}(D) D^t + \zeta(D)\varphi(D) \tag{6.19}$$

where

$$\zeta(D) = \sum_{t=0}^{\infty} \zeta_t D^t$$

is the output sequence of the shift register. From (6.19) we have

$$\zeta(D) = \frac{\beta^{(0)}(D)}{\varphi(D)} \tag{6.20}$$

where $\beta^{(0)}(D)$ is the *initial condition polynomial.*

EXAMPLE 6.5

Find the output of the circuit of Figure 6.3 with $\varphi(D) = 1 + D + D^4$ *and initial condition polynomial* $\beta^{(0)}(D) = 1$. *The circuit and the initial condition load are illustrated in Figure 6.4.*

Solution

The shift register output is

$$\zeta(D) = \frac{1}{1 + D + D^4}$$

Performing the polynomial long division yields

$$\begin{array}{r|l}
1 + D + D^4 & 1 + D + D^2 + D^3 + D^5 + D^7 + D^8 + \cdots \\
\hline
1 & \\
1 + D + D^4 & \\
\hline
D + D^4 & \\
D + D^4 & \\
\hline
D^2 + D^5 & \\
D^2 + D^4 + D^5 & \\
\hline
D^3 + D^6 & \\
D^3 + D^4 + D^5 + D^6 & \\
\hline
D^7 & \\
\hline
D^5 + D^6 + D^7 & \\
D^5 + D^6 + D^8 & \\
\hline
D^7 + D^8 & \\
\cdots & \cdots
\end{array}$$

It can be verified that ζ_n *is the sequence (6.14).*

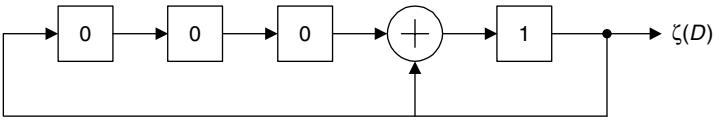

Figure 6.4. The circuit configuration of Example 6.5.

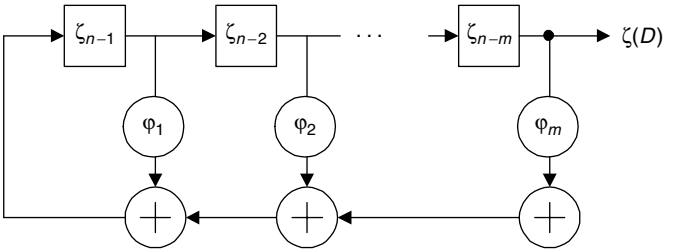

Figure 6.5. The m stage linear shift register sequence generator (Fibonacci feedback generator).

The linear feedback shift register configuration illustrated in Figure 6.3 is often referred to as a *Galois feedback generator*. Another linear feedback shift register configuration illustrated in Figure 6.5 is referred to as a *Fibonacci feedback generator*.

In this generator, the sequence $\zeta(D)$ propagates through with each term generated linearly from the preceding m terms according to the formula

$$\zeta_n = \zeta_{n-m}\varphi_m + \zeta_{n-m+1}\varphi_{m-1} + \cdots + \zeta_{n-1}\varphi_1 \tag{6.21}$$

Multiplying both sides of (6.21) with D^n and summing over $n = 0$ to $n = \infty$ we get

$$\begin{aligned}\zeta(D) &= \sum_{n=0}^{\infty}\zeta_n D^n = \sum_{n=0}^{\infty}\sum_{i=1}^{m}\zeta_{n-m+i-1}\varphi_{m-i+1}D^n \\ &= \sum_{i=1}^{m}\varphi_{m-i+1}D^{m-i+1}\left[\sum_{n=0}^{\infty}\zeta_{n-m+i-1}D^{n-m+i-1}\right] \\ &= \sum_{j=1}^{m}\varphi_j D^j\left[\zeta_{-j}D^{-j} + \cdots + \zeta_{-1}D^{-1} + \sum_{n=0}^{\infty}\zeta_n D^n\right]\end{aligned} \tag{6.22}$$

From this, $\zeta(D)$ can be expressed as the ratio of two polynomials, that is,

$$\zeta(D) = \frac{\beta^{(0)}(D)}{\varphi(D)} \tag{6.23}$$

where the coefficients of the polynomial

$$\beta^{(0)}(D) = \sum_{i=1}^{m} \varphi_i D^i (\zeta_{-i} D^{-i} + \cdots + \zeta_{-1} D^{-1}) \tag{6.24}$$

depend on the initial condition vector $\boldsymbol{\zeta}^{(0)} = (\zeta_{-m}, \zeta_{-m+1}, \ldots, \zeta_{-1})$ and

$$\varphi(D) = 1 + \sum_{i=1}^{m} \varphi_i D^i$$

is the characteristic polynomial of the shift register. Observe that the coefficients of the polynomial

$$\beta^{(0)}(D) = \beta_0 + \beta_1 D + \cdots + \beta_{m-1} D^{m-1}$$

are

$$\begin{aligned}
\beta_0 &= \varphi_1 \zeta_{-1} + \varphi_2 \zeta_{-2} + \cdots + \varphi_m \zeta_{-m} \\
\beta_1 &= \varphi_2 \zeta_{-1} + \varphi_3 \zeta_{-2} + \cdots + \varphi_m \zeta_{-m+1} \\
&\cdots\cdots \\
\beta_{m-1} &= \varphi_m \zeta_{-1}
\end{aligned}$$

Since $\varphi_m \neq 0$, 2^m different values of vector $\zeta^{(0)}$ correspond to 2^m different values of the polynomial $\beta^{(0)}(D)$. Then the properties of the Fibonacci feedback generator are analogous to the properties of the Galois feedback generator.

6.4 RANDOMNESS PROPERTIES OF MAXIMAL-LENGTH SEQUENCES

Now we shall demonstrate that maximal-length sequences almost satisfy the randomness properties of Bernoulli sequences as listed at the beginning of Section 6.1. We must emphasize that the parameters of the generation process (the coefficients φ_i of the generator polynomial $\varphi(D)$) are deterministic but the m terms of the initial vector, or equivalently, the time shift of the MLSR sequence, can be chosen randomly.

Balance Property

Let us examine the first rightmost stage of the register in Figure 6.5 while the entire sequence is shifted through it. The content of this stage coincides with the last (rightmost) bit of the m-dimensional vector $\boldsymbol{\zeta}$ at each clock cycle. Suppose we enumerate the content vectors of the shift register as it generates a maximal-length sequence. This is equivalent to enumerating all possible $2^m - 1$ binary

vectors of length m excluding the all-zero vector. Let us include the all-zero vector. Then among all 2^m vectors exactly one-half have a zero in the rightmost position and one-half have a one there. Because we exclude the all-zero vector, 2^{m-1} of the $N_p = 2^m - 1$ symbols of m-sequence are ones and $2^{m-1} - 1$ are zeros. If we consider the initial vector as random, the probabilities that the shift register output is a zero or a one, respectively, are

$$\begin{aligned} P_0 &= \frac{2^{m-1} - 1}{2^m - 1} = \frac{1}{2}\left(1 - \frac{1}{N_p}\right) \\ P_1 &= \frac{2^{m-1}}{2^m - 1} = \frac{1}{2}\left(1 + \frac{1}{N_p}\right) \end{aligned} \tag{6.25}$$

Thus the imbalance equals $1/N_p$. For instance, for $m = 10$, 20, and 30 the imbalance $1/N_p$ is approximately 10^{-3}, 10^{-6}, and 10^{-9}, respectively.

Run Property

Consider again the shift register in Figure 6.5. There can be no run of ones having length $\ell > m$ because this would require that the all-one shift register state be followed by another all-one state. This cannot occur because then the shift register would stay permanently in the all-one state. Thus there is a single run of m consecutive ones, and this run is preceded and followed by a zero.

Obviously, there is no run of zeros having length $\ell \geq m$. Otherwise, the shift register would permanently stay in the all-zero state. A run of $m - 1$ zeros must be preceded by and followed by ones. Thus the shift register must pass through the state that is a one followed by $m - 1$ zeros. This state occurs only once, so there is a single run of $m - 1$ zeros.

There is no run of ones having length $m - 1$. In fact, a run of $m - 1$ ones must be preceded by and followed by a zero. This requires that the shift register state that is zero followed by $m - 1$ ones be followed immediately by the state that is $m - 1$ ones followed by zero. Then the shift register would never come into the all-one state.

Consider all shift register contents of the forms

$$0\zeta_1\zeta_2 \ldots \zeta_n 0 \text{ and } 1\zeta_1\zeta_2 \ldots \zeta_n 1$$

where $n \leq m - 2$. Of the 2^n possibilities in each case, there is just one that has run length exactly n. This is all-ones in the first case and all-zeros in the second case. Thus, of all the 2^{n+1} possibilities for the two cases, exactly two have run length n. Consequently, a fraction 2^{-n} have run length n for $1 \leq n \leq m - 2$.

We conclude therefore that the relative frequency of run length n (zeros or ones) is $1/2^n$ for all $n \leq m - 1$ and $1/2^{(m-1)}$ for $n = m$, with no run lengths possible for $n > m$.

Delay and Add Property

Consider an output sequence $\zeta_0(D)$ of the shift register in Figure 6.3. According to Formula (6.20) it can be represented as

$$\zeta_0(D) = \frac{\beta^{(0)}(D)}{\varphi(D)}$$

where $\beta^{(0)}$ is the initial condition polynomial and $\varphi(D)$ is the characteristic polynomial of the shift register. If we shift the sequence $\zeta_0(D)$ by an arbitrary number of cycles k, $k < 2^m - 1$, we obtain an output sequence of the shift register $\zeta_k(D)$, for a different initial vector $\beta^{(k)}(D)$

$$\zeta_k(D) = \frac{\beta^{(k)}(D)}{\varphi(D)}$$

If we add the original sequence $\zeta_0(D)$ and the shifted sequence $\zeta_k(D)$, term by term modulo 2, we obtain a new sequence $\zeta_0(D) + \zeta_k(D)$ that itself is an output sequence of the shift register with initial condition vector $\beta^{(0)}(D) + \beta^{(k)}(D)$, that is,

$$\zeta_0(D) + \zeta_k(D) = \frac{\beta^{(0)}(D) + \beta^{(k)}(D)}{\varphi(D)}$$

Hence, the so generated sequence is itself a time shift of the same m sequence. This is the *delay and add property*. The sequence $\zeta_0(D) + \zeta_k(D)$ satisfies the balance property. It follows that two sequences $\zeta_0(D)$ and $\zeta_k(D)$, each of length $2^m - 1$, differ in 2^{m-1} positions and agree in $2^{m-1} - 1$ positions.

We can formulate the first and third properties in terms of the real number alphabet $\{1, -1\}$ instead of the binary logical alphabet $\{0, 1\}$. The first property is reformulated as equality

$$\frac{1}{N_\mathrm{p}} \sum_{n=1}^{N} a_n = -\frac{1}{N_\mathrm{p}} \tag{6.26}$$

where a_n is the equivalent (in the real number alphabet) of the nth term of the MLSR sequence, ζ_n, that is, $a_n = (-1)^{\zeta_n}$. Equation (6.26) follows from the balance property (6.25).

The third property is

$$\theta_a(k) = \frac{1}{N_\mathrm{p}} \sum_{n=1}^{N} a_n a_{n+k} = \begin{cases} 1, & k = 0 \\ -1/N_\mathrm{p}, & k \neq 0 \end{cases} \tag{6.27}$$

that is, the discrete autocorrelation function of the m sequence takes only two values.

If we consider the sequence $\{a_n\}$ as a discrete-time periodical random process, Equation (6.26) implies that the time average of the process is equal to $-1/N_p$; Equation (6.27) implies that the time correlation of the process is equal to 1 or $-1/N_p$. If we treat the initial condition vector as a random vector with IID equiprobable binary components, the m-sequence becomes a stationary ergodic process.

6.5 GENERATING PSEUDORANDOM SIGNALS (PSEUDONOISE) FROM PSEUDORANDOM SEQUENCES

At the end of Section 6.4, we suggested mapping the symbols of the m-sequence $\{\zeta_n\}$ from binary logical symbols, 0 and 1, to real values $a_n = (-1)^{\zeta_n}$. The spreading signal $a(t)$ (6.1) derived from this sequence is periodic with period $\mathcal{T} = N_p T_c$. The autocorrelation function $R_a(\tau)$ of this signal is given by Formula (6.9), which for $0 \le \tau \le T_c$ becomes

$$R_a(\tau) = \left(1 - \frac{\tau}{T_c}\right) - \frac{1}{N_p}\left(\frac{\tau}{T_c}\right) = 1 - \frac{\tau}{T_c}\left(1 + \frac{1}{N_p}\right) \tag{6.28}$$

where (6.27) has been used to evaluate $\theta_a(k)$. For $T_c < \tau < (N_p - 1)T_c$,

$$R_a(\tau) = \left(1 - \frac{\varepsilon}{T_c}\right)\left(-\frac{1}{N_p}\right) + \left(\frac{\varepsilon}{T_c}\right)\left(-\frac{1}{N_p}\right) = -\frac{1}{N_p} \tag{6.29}$$

where $\varepsilon = \tau - \lfloor \tau / T_c \rfloor T_c$. For $(N_p - 1)T_c \le \tau < N_p T_c$, (6.9) becomes

$$R_a(\tau) = \left(1 - \frac{\varepsilon}{T_c}\right)\left(-\frac{1}{N_p}\right) + \frac{\varepsilon}{T_c} = \frac{\varepsilon}{T_c}\left(1 + \frac{1}{N_p}\right) - \frac{1}{N_p} \tag{6.30}$$

where $\varepsilon = \tau - (N_p - 1)T_c$, so that $0 < \varepsilon < T_c$. The autocorrelation function, $R_a(\tau)$, is periodic. The period is $\mathcal{T} = N_p T_c$. It is illustrated in Figure 6.6.

Because the function $R_a(\tau)$ is periodic and even, it can be presented as a Fourier series [34]

$$R_a(\tau) = \sum_{k=-\infty}^{\infty} A_k \cos(2\pi k f_a \tau) \tag{6.31}$$

$A_0 = 1/N_p^2$ (direct current term), $A_k = [(N_p + 1)/N_p^2]\text{sinc}^2(k/N_p)$, $k \neq 0$, and $f_0 = 1/N_p T_c$. The power spectrum is illustrated in Figure 6.7. This spectrum consists of discrete spectral lines at all harmonics of $f_0 = 1/N_p T_c$. The envelope of the spectrum components is given by $[(N_p + 1)/N_p^2]\text{sinc}^2(k/N_p)$ except for the direct current term, which has the amplitude $1/N_p^2$.

The autocorrelation of the m-sequences can be defined by averaging over a complete cycle of the sequence. In practice, synchronization of signals spread by a pseudorandom sequence often requires that an estimate of the correlation

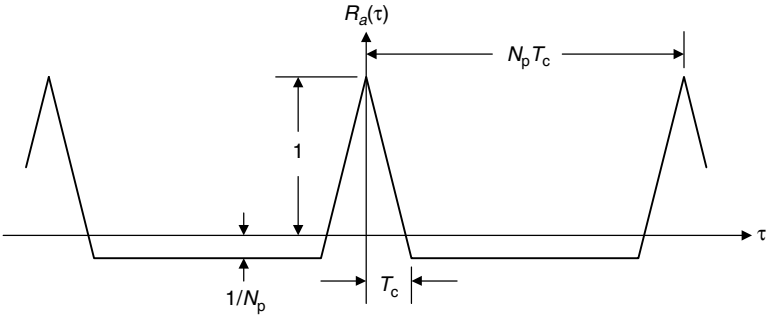

Figure 6.6. Autocorrelation function for a spreading waveform derived from an m-sequence.

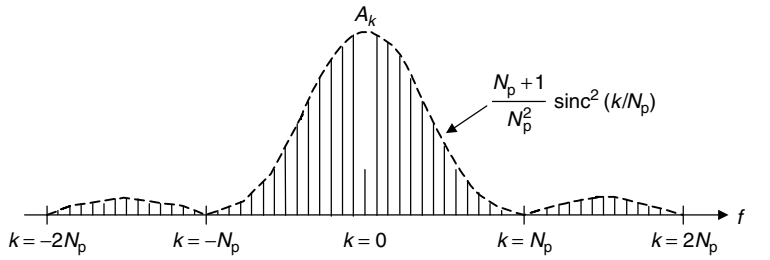

Figure 6.7. Power spectrum of a spreading waveform derived from an m-sequence.

between the received signal and the receiver despreading signal is made in less than a full period. Thus the correlation estimate process is based on the study of the partial autocorrelation function of the spreading signal.

The *partial autocorrelation function* of the spreading signal $a(t)$ is defined by [34]:

$$R_a(\tau, t, T_w) = \frac{1}{T_w} \int_t^{t+T_w} a(\delta)a(\delta + \tau)\, d\delta \tag{6.32}$$

where T_w is the duration (window size) and t is the starting time of the correlation. Analogously to Formulas (6.5)–(6.9) (see [34]) we get from (6.32) that the partial autocorrelation function can be written as

$$R_a(\tau, t, T_w) = \left(1 - \frac{\varepsilon}{T_c}\right) \theta_a(k, \ell, W) + \frac{\varepsilon}{T_c}\, \theta_a(k+1, \ell, W) \tag{6.33}$$

where k and ℓ are integers, $\tau = kT_c + \varepsilon$, $0 \le \varepsilon < T_c$, $t = \ell T_c$, and $T_w = WT_c$. Here

$$\theta_a(k, \ell, W) = \frac{1}{W} \sum_{n=\ell}^{\ell+W-1} a_n a_{n+k} \tag{6.34}$$

is the *discrete partial autocorrelation function* of the sequence $\{a_n\}$. The function $R_a(\tau, t, T_w)$ can easily be calculated from $\theta_a(k, \ell, W)$. The discrete partial autocorrelation function can be calculated in the same manner as the discrete periodic autocorrelation function. The value of $\theta_a(k, \ell, W)$ is the number of agreements ν_0 minus the number of disagreements ν_1 between $\zeta_0(D)$ and $\zeta_k(D)$ over the window beginning at ℓ and ending at $\ell + W$, divided by W. (Here $\zeta_0(D)$ and $\zeta_k(D)$ are the original output m-sequence of the MLSR generator and the sequence shifted by k cycles.) This value is equal to the difference between the number of zeros and the number of ones of the modulo 2 sum of $\zeta_0(D)$ and $\zeta_k(D)$ over the same window.

EXAMPLE 6.6

Find $\theta_a(k, \ell, W)\Big|_{\substack{k=6 \\ W=7}}$ *for the* 15*-bit output m-sequence of the generator of Figure 6.4. The initial condition polynomial is* $\beta^{(0)}(D) = 1 + D + D^2 + D^3$.

Solution

One cycle of $\boldsymbol{\zeta}_0$ *and* $\boldsymbol{\zeta}_6$ *and their modulo* 2 *sum are*

$$\boldsymbol{\zeta}_0 = 1\ 0\ 1\ 0\ 1\ 1\ 0\ 0\ 1\ 0\ 0\ 0\ 1\ 1\ 1$$
$$\boldsymbol{\zeta}_6 = 0\ 0\ 1\ 0\ 0\ 0\ 1\ 1\ 1\ 1\ 0\ 1\ 0\ 1\ 1$$
$$\boldsymbol{\zeta}_0 + \boldsymbol{\zeta}_6 = 1\ 0\ 0\ 0\ 1\ 1\ 1\ 1\ 0\ 1\ 0\ 1\ 1\ 0\ 0$$

Then $\theta_1(6, \ell, 7)$ *is the number of zeros minus the number of ones in* $\boldsymbol{\zeta}_0 + \boldsymbol{\zeta}_6$ *in a seven-unit window beginning at* ℓ. *The value* $\theta_a(6, \ell, 7)$ *is plotted in Figure 6.8 as a function of* ℓ.

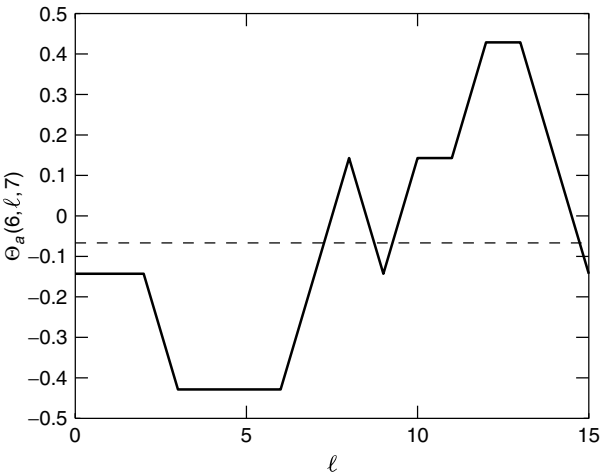

Figure 6.8. Discrete partial autocorrelation function $\theta(6, \ell, 7)$ for the 15-symbol m-sequence generated by $\varphi(D) = 1 + D + D^4$.

In some CDMA applications it is useful to be able to generate m-sequences in different phases. For example, in a DS CDMA system, different phase shifts of a very long spreading sequence may be used to distinguish different users. The DS CDMA receiver selects the desired received signal by choosing the phase of the reference despreading signal. The phase difference may be equivalent to thousands of chips, thus making the use of straightforward phase shift impractical. A practical method is simply to calculate the shift register initial conditions required to generate a sequence delayed by k chips from the sequence generated from another specific initial condition.

From the consideration of the Galois feedback generator in Section 6.3, it follows that these initial contents of the shift register are two elements of $GF(2^m)$ such that $\beta^{(k)} = \beta^{(0)}\alpha^{-k}$.

EXAMPLE 6.7

Consider the generator of Example 6.5 with an initial condition of $\beta^{(0)}(D) = 1$. *What initial condition* $\beta^{(0)}(D)$ *will produce an advance of* 35 *units? What initial condition* $\beta^{(0)}(D)$ *will produce a delay of* 50 *units?*

Solution

The period of the m-sequence is 15 *units, so that an advance of* 35 *units is equivalent to an advance of* 5 *units. But* $1\alpha^{-5} = \alpha^{10}$. *From Example 6.4,* $\alpha^{10} = 1 + D + D^2$, *thus the initial condition* $\beta^{(0)}(D) = 1 + D + D^2$ *corresponds to an advance of* 35 *units. The result can be verified by considering the shift register state (Fig. 6.4) after* 5 *shifts.*

A delay of 50 *units is equivalent to a delay of* 5 *units, so that the initial condition* $\beta^{(0)}(D) = \alpha^5 = D + D^2$ *corresponds to a delay of* 50 *units.*

Binary PN generators are used in practice not only for generating spreading signals in DS CDMA systems but also for selection of the carrier frequencies in FH CDMA systems. The selection of the carrier frequency in each signal interval in the transmitter is made pseudorandomly according to the output from the PN generator. The PN generator outputs ℓ binary digits at a time, implying that the frequency synthesizer generates $Q = 2^\ell$ carrier frequencies. The transmitted signal is the data-modulated carrier upconverted to a new frequency. At the receiver, there is an identical PN sequence generator, synchronized with the received signal, which is used to control the output of the frequency synthesizer. The pseudorandom carrier frequency hopping introduced in the transmitter is removed at the receiver by downconverting of the received signal.

6.6 OTHER SETS OF SPREADING SEQUENCES

A goal of cellular system designers is to find a set of spreading sequences or signals that minimize the mutual interference between users. In addition to pseudorandom maximum-length sequences, other binary sequences can be used in

CDMA systems. Particularly, in IS-95 [44] (see Section 4.8) the separation of the users in the downlink is achieved by employing orthogonal (Hadamard) sequences. Each user uses one Hadamard sequence to spread the transmitted sequence.

Hadamard spreading can be used if the receiver is synchronized with the transmitter by transmission of a pilot signal or pilot chips. In the IS-95 system, a pilot signal is sent in the forward link but not in the reverse link. Therefore, orthogonal spreading is used only in the forward link. In WCDMA the pilot is sent in both directions, so the orthogonal spreading technique is also used in both directions.

WCDMA is designed to support mobile communication with a variety of transmission rates. Because the spread signal bandwidth is the same for all users, multiple-rate communication requires a variable spreading factor. In WCDMA, the spreading factors for data transmission range from 512 down to 4. To maintain orthogonality between different spreading sequences of different lengths, the orthogonal variable spreading factor (OVSF) technique [7] is used. The orthogonal spreading sequences are picked from the code tree, which is illustrated in Figure 6.9.

Let $\boldsymbol{a}$ be a spreading (Hadamard) sequence of length $n = 2^{\kappa}$, $\kappa = 0, 1, 2, \ldots$. This sequence is represented by a branch on the level κ of the tree. Then on the level $\kappa + 1$ it will be followed by branches on which appear $(\boldsymbol{a},\boldsymbol{a})$ and $(\boldsymbol{a}, -\boldsymbol{a})$ of length $2^{\kappa+1}$. It can be understood that the generated sequences of the same level constitute a set of orthogonal Hadamard sequences, although they are not in the same order as in the Hadamard matrix considered in Section 4.2. We can see that two sequences along different levels are also orthogonal except for the case that one of the sequences forms a branch on the path from the root to the branch, labeled by the other sequence. From this observation, we can find that if $\boldsymbol{a} = (a_0, a_1, \ldots, a_{n-1})$ is assigned to a user, all sequences (a_0),

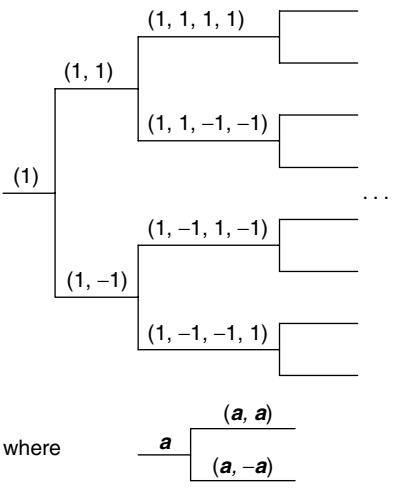

Figure 6.9. Tree for generation of variable-length orthogonal sequences.

$(a_0, a_1), \ldots, (a_0, a_1, \ldots, a_{n/2-1})$ cannot be assigned to other users requesting lower spreading rates.

EXAMPLE 6.8

Four active users in a WCDMA system spread the transmitted sequences by factors 2, 4, 8, 8. Find a set of orthogonal spreading sequences $\boldsymbol{a}^{(1)}, \boldsymbol{a}^{(2)}, \boldsymbol{a}^{(3)}$ *and* $\boldsymbol{a}^{(4)}$ *for these users.*

Solution

One of the possible solutions is:
$\boldsymbol{a}^{(1)} = (1, 1)$, $\boldsymbol{a}^{(2)} = (1, -1, 1, -1)$, $\boldsymbol{a}^{(3)} = (1, -1, -1, 1, 1, -1, -1, 1)$ *and,*
$\boldsymbol{a}^{(4)} = (1, -1, -1, 1, -1, 1, 1, -1)$

Suppose now that we have K active users communicating with spreading factors $g_1, g_2, \ldots g_K$, where g_K is a power of two. Under which conditions does orthogonal variable-length spreading exist? It can be proved (Problem 6.20) that a necessary and sufficient condition for the existence of such spreading is

$$\sum_{k=1}^{K} \frac{1}{g_k} \leq 1 \tag{6.35}$$

Another class of spreading sequences used in WCDMA is *Gold sequences* [18]. The Gold sequences were invented in 1967 at the Magnavox Corporation specially for multiple-access applications of spread sprectrum. We describe how we can generate a set of Gold sequences.

Consider a maximum-length sequence $\boldsymbol{a}$ of period $N_\mathrm{p} = 2^m - 1$ and a second sequence $\boldsymbol{a}'$ obtained by sampling every qth symbol of $\boldsymbol{a}$. The second sequence is said to be the *decimation* of the sequence $\boldsymbol{a}$. The notation $\boldsymbol{a}' = a[q]$ is used for sequence $\boldsymbol{a}'$. Sequence $\boldsymbol{a}'$ has period N_p if and only if $\gcd(N_\mathrm{p}, q) = 1$, where "gcd" means the greatest common divisor. Any pair of maximum-length sequences $\boldsymbol{a}$ and $\boldsymbol{a}'$ having the same period N_p are related as $\boldsymbol{a}' = \boldsymbol{a}[q]$ for some q.

The cross-correlation spectrum of pairs of maximum-length sequences can be three-valued, four-valued, or many-valued. All pairs of maximum-length sequences whose cross-correlation spectrum is three-valued are called *preferred pairs* of m sequences. Those three values are $-t(m)/N_\mathrm{p}$, $-1/N_\mathrm{p}$, $[t(m) - 2]/N_\mathrm{p}$, where $m = \log_2(N_\mathrm{p} + 1)$, N_p is the sequence's period,

$$t(m) = \begin{cases} 1 + 2^{\frac{m+1}{2}}, & \text{for } m \text{ odd}, \\ 1 + 2^{\frac{m+2}{2}}, & \text{for } m \text{ even} \end{cases} \tag{6.36}$$

The following conditions are sufficient to define a preferred pair $\boldsymbol{a}$ and $\boldsymbol{a}'$ of maximum-length sequences with period $N_\mathrm{p} = 2^m - 1$:

- $m \neq 0 (\mathrm{mod}\ 4)$; that is, m is odd or $m = 2 (\mathrm{mod}\ 4)$

- $\boldsymbol{a}' = \boldsymbol{a}[q]$, where either $q = 2^{\kappa} + 1$ or $q = 2^{2\kappa} - 2^{\kappa} + 1$
- $\gcd(m, \kappa) = \begin{cases} 1, & \text{for } m \text{ odd,} \\ 2, & \text{for } m = 2 (\text{mod } 4) \end{cases}$

where gcd means greatest common devisor.

In defining sets of Gold sequences, it is necessary to find *preferred pairs* of maximum-length sequences. Let $\boldsymbol{a}$ and $\boldsymbol{a}'$ represent a preferred pair of maximum-length sequences having period $N_{\mathrm{p}} = 2^m - 1$. Consider the set of $N_{\mathrm{p}} + 2 = 2^m + 1$ sequences $\{\boldsymbol{a}, \boldsymbol{a}', \boldsymbol{a} + \boldsymbol{a}', \boldsymbol{a} + D\boldsymbol{a}', \ldots, \boldsymbol{a} + D^{N-1}\boldsymbol{a}'\}$, where $D^j_{a'}$ means phase shift of $\boldsymbol{a}'$ by j units. This set is called the set of Gold sequences. It can be proved that any pair of sequences in the set has a three-valued cross-correlation spectrum. With the exception of sequences $\boldsymbol{a}$ and $\boldsymbol{a}'$, the set of Gold sequences does not contain maximum-length sequences. Hence, their autocorrelation functions are not two-valued but four-valued and they take the same three values as the cross-correlation plus the value 1.

EXAMPLE 6.9

Construct the set of period $N_{\mathrm{p}} = 31$ *Gold sequences and evaluate the cross-correlation spectrum.*

Solution

Because $N_{\mathrm{p}} = 31$, *then* $m = 5$. *Table 6.1 contains the entry* $\varphi(D) = 1 + D^2 + D^5$, *which may be used to generate a maximum-length sequence* $\boldsymbol{a}$ *of period* 31. *The decimation* $\boldsymbol{a}' = \boldsymbol{a}[3]$ *is proper, because* $m = 1 (mod\, 4)$, $q = 2^{\kappa} + 1$ *for* $\kappa = 1$, *and, finally,* $gcd(5, 1) = 1$. *It can be checked that the sequence* $\boldsymbol{a}'$ *is generated by a shift register with characteristic polynomial* $\varphi'(D) = 1 + D^2 + D^3 + D^4 + D^5$. *The cross-correlation function takes one of three values:* $t(m)/N_{\mathrm{p}} = -9/31$, $1/N_{\mathrm{p}} = -1/31$, $[t(m) - 2]/N_{\mathrm{p}} = 7/31$.

A typical shift register configuration used to generate the family of Gold sequences consists of two parallel shift registers with characteristic polynomials $\varphi(D)$ *and* $\varphi'(D)$ *(Problem 6.21). Gold sequences are generated by adding (modulo 2) the outputs of these two shift registers. The complete family of Gold sequences is obtained by using different initial loads of the shift registers. There are in total* 33 *sequences in the family of length* 31 *Gold sequences.*

Gold sequences form a family of spreading sequences with good cross-correlation properties. These sequences are important, and they have been selected for use in WCDMA standards.

EXAMPLE 6.10

The WCDMA standard proposal recommends using length 38400 *segments of a set of Gold sequences. Let us suppose that these sequences are generated by means of two shift registers with generating polynomials* $\varphi(D) = 1 + D + D^{25}$ *and* $\varphi'(D) = 1 + D + D^2 + D^3 + D^{25}$. *Find the parameters of this set of Gold sequences.*

Solution

The period of the sequences is $N_p = 2^{25} - 1 = 33554431$, *the value of* $t(m)$ *equals* 8193, *the cross-correlation spectrum consists of values* $-t(m)/N_p = -2.4417 \times 10^{-4}$, $1/N_p = 2.9802 \times 10^{-8}$, *and* $[t(m) - 2]/N_p = 2.4411 \times 10^{-4}$.

Another class of spreading sequences that are supposed to be used in the third generation of cellular communication is the *Kasami sequences* [25]. There are two sets of Kasami sequences, the *small set* and the *large set*. A procedure similar to that used for generating Gold sequences will generate the small set of Kasami sequences. The period of the sequences is $N_p = 2^m - 1$, where m is even. The sequence $\boldsymbol{a}$ is a maximum-length sequence; the sequence $\boldsymbol{a}'$ is formed by decimation of $\boldsymbol{a}$ by $2^{m/2} + 1$. The resulting sequence $\boldsymbol{a}'$ is a maximum-length sequence with period $2^{m/2} - 1$. To form a Kasami sequence we add to the sequence $\boldsymbol{a}$ the sequence $\boldsymbol{a}'$ and $2^{m/2} - 2$ consecutive shifts on one bit of sequence $\boldsymbol{a}'$. Then the *small set* consists of $2^{m/2}$ sequences. The cross-correlation spectrum takes values $-1/N_p$, $-(2^{m/2} + 1)/N_p$, and $(2^{m/2} - 1)/N_p$.

The large set of Kasami sequences also consists of sequences of period $N_p = 2^m - 1$, where m is even. It includes both the Gold sequences and the small set of Kasami sequences as subsets. The number of such sequences is $M = 2^{3m/2}$ if $m = 0 \pmod 4$, and $M = 2^{3m/2} + 2^{m/2}$ if $m = 2 \pmod 4$. The cross-correlation spectrum is five-valued. The Kasami sequences are candidates for the spreading code in WCDMA systems.

6.7 COMMENTS

The subject of generating spreading sequences for CDMA communication was taken up in this chapter. In our treatment of the material we mostly follow Peterson, Ziemer, and Borth [34] and Viterbi [47]. After an introduction of finite-field arithmetic, the concept of binary sequence generation with feedback shift register circuits was discussed. After this, the idea of maximum-length sequences, or m-sequences, was introduced. Their properties were discussed, and it was found that an m-sequence has properties similar to a random coin-toss sequence. The autocorrelation function and power spectral density of m-sequences were presented, as well as the correlation function over a part of an m-sequence. Finally, we reviewed the main characteristics of important sets of spreading sequences used in the 3rd Generation Wireless Networks.

A comprehensive treatment of the theory of m-sequences can be found in the book by Golomb [19], and a summary of this material is in Peterson and Weldon [33] or Lin and Costello [27]. The text by Peterson and Weldon also contains a considerable amount of material on basic shift register structures and their use in error correcting coding. Concise summaries of the properties and mathematical structure of maximum-length sequences can be found in the book by MacWilliams and Sloane [31]. An overview of the spreading techniques for use in WCDMA is presented in [13].

PROBLEMS

6.1. Prove that the polynomial $\varphi(D) = 1 + D^2 + D^5$ is primitive.

6.2. Prove that the additive and multiplicative identity elements of a finite field are unique.

6.3. Consider the Galois feedback generator shown below. Determine the output of this circuit with the initial condition $\beta^{(0)}(D) = 1$.

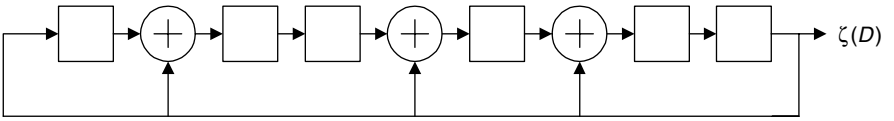

Problem 6.3.

6.4. Consider the Fibonacci feedback generator shown below. Determine the output of this circuit with the initial condition $\beta^{(0)}(D) = 1$ and compare with the result of Problem 6.3.

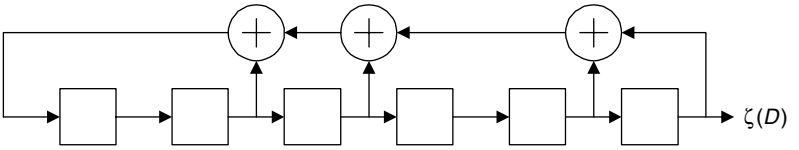

Problem 6.4.

6.5. Find the maximum possible period of the binary sequence generated by the linear feedback shift register shown below. Find all possible output cycles of this circuit.

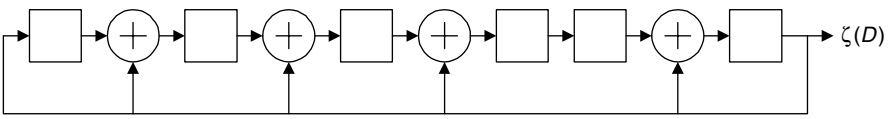

Problem 6.5.

6.6. Consider the maximum-length sequence generated by using the primitive polynomial $\varphi(D) = 1 + D + D^3 + D^4 + D^6$. Demonstrate the balanced property, the run length property, and the delay and add property.

6.7. Plot the autocorrelation function and the power spectrum for the spreading signal specified by the maximal-length sequence defined by the primitive polynomial $\varphi(D) = 1 + D + D^2 + D^4 + D^5$. The generator clock rate is 2.0 kHz.

6.8. The spreading signal of Problem 6.7 is used to BPSK modulate a 2.0-MHz carrier. Plot the power spectrum of the modulated carrier.

6.9. Three maximum-length shift register generators having periods N_1, N_2 and N_3 are run off the same clock. A fourth sequence is generated by modulo 2 adding the outputs of these generators. What is the period of the fourth output sequence?

6.10. Consider the maximum-length sequence generator defined by the primitive polynomial $\varphi(D) = 1 + D + D^2 + D^4 + D^5$. Determine a shift register configuration that will generate this sequence in the forward direction and a shift register configuration that will generate this sequence in the reverse direction.

6.11. From a spread spectrum transmitter the following sequence is received:

$$-1\ 1\ -1\ -1\ -1\ -1\ -1\ 1\ -1\ -1\ 1\ 1\ -1$$

Spectral analysis of the received signal indicates that the power spectrum consists of discrete lines that are spaced at 64.52 kHz and that the spreading rate is 2 MHz. What MLSR is being used in the transmitter?

6.12. Is it possible to generate a maximum-length sequence by using a shift register with an odd number of taps?

6.13. Consider a shift register generator defined by $\varphi(D) = 1 + D + D^4 + D^5$.

a) Does this shift register generate a maximum-length sequence?

b) Find all possible state sequences for the Fibonacci shift register for this generator.

c) Does the delay and add property apply to the sequences generated by this generator?

6.14. Calculate the discrete cross-correlation function for the pair of m-sequences defined by polynomials $\varphi_1(D) = 1 + D^2 + D^3 + D^4 + D^5$ and $\varphi_2(D) = 1 + D + D^2 + D^3 + D^5$.

6.15. Calculate the discrete partial autocorrelation function for an m-sequence defined by $\varphi(D) = 1 + D^2 + D^3 + D^4 + D^5$ using a window size of six chips and a phase difference of two chips.

6.16. Consider the Galois feedback generator defined by $\varphi(D) = 1 + D^2 + D^5$ with an initial load of $\beta(D) = 1$. Using the state machine representation of the shift register, find the load of the shift register five cycles before and five cycles after the initial load.

6.17. Consider the sequence generated by the primitive polynomial $\varphi(D) = 1 + D + D^4$. Now we decimate this sequence by 2, that is, sample every other output bit from the original sequence, and get a new sequence.

a) Is the decimated sequence a MLSR sequence?

b) What is the characteristic polynomial of the decimated sequence?

c) What is the cross-correlation between the original sequence and the decimated one?

6.18. Respond to these statements about m-sequences with True or False.

a) 000100110101111 is a m-sequence of period 15.

b) 000010010110011111100011011101l0 is an m-sequence of period 31.

c) 000010010110011011000110111010l is an m-sequence of period 31.

d) Take two m-sequences generated by $G(D) = 1 + D + D^4$, add them bit by bit (mod 2). The resulting sequence is always an m-sequence.

6.19. Consider a DS CDMA system with K active users. The spreading factors are $g_1, g_2, \ldots, g_K$, where g_k, $k = 1, 2, \ldots, K$, is a power of two. Prove that a necessary and sufficient condition of orthogonal variable-length spreading is given by Formula (6.35).

6.20. Construct a generator of Gold sequences of length 31.

6.21. For separation of users the WCDMA system uses orthogonal variable-length spreading. The spreading factor is varied from 4 up to 256. Suppose that for 1/3 of the users of a cell the spreading factor is 256, for 1/3 of the users the factor is 128, and for 1/3 of the users the factor is 64. What is the maximal number of users in a cell?

6.22. A DS CDMA system using BPSK, rectangular shaping, and bandwidth $W = 1$ MHz utilizes the following shift register to generate the spreading sequence. Because of imperfection in the acquisition process the receiver

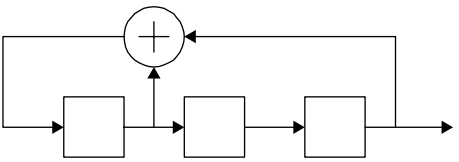

Problem 6.22.

has a timing error of at most 0.2 μs.

a) Is the shift register a MLSR?

b) Calculate the required E_b/I_0 if we need a $P_b < 10^{-3}$ even at maximal timing error.

c) Assume that a MLSR of length 10 is used. Calculate the required E_b/I_0 in this case.

7

SYNCHRONIZATION OF PSEUDORANDOM SIGNALS

The performance analysis of the CDMA systems presented in Chapters 2–5 assumes that the receiver carrier frequency, phase (for coherent reception), and chip timing are perfectly synchronized to those of the transmitted signal, as received with the appropriate propagation delay. In this chapter we consider methods for achieving this synchronization, particularly the timing of the periodic pseudorandom signals.

A widely used technique for initial synchronization (acquisition) is to search through all potential spreading waveform phases (in DS CDMA), carrier frequencies (in FH CDMA), and pulse position-shifted patterns (in PPH CDMA) until the correct phase shift or frequency is identified. Each reference phase/frequency is evaluated by attempting to despread/dehop the received signal. If the estimated phase/frequency is correct, despreading/dehopping will occur and will be sensed. If the estimated phase or frequency is incorrect, the received signal will not be despread/dehopped and the reference waveform will be changed to a new phase/frequency for evaluation. This technique is called *serial search*. A large portion of this chapter is devoted to the analysis of this technique.

When the receiver timing has been synchronized, adjustments of the timing must be made continuously because of the relative motion of the transmitter and the receiver and the instability of clocks. Tracking of timing for spread spectrum is performed by the so-called "early–late gate" device. This is discussed in Section 7.5. We also consider the phase tracking device for coherent reception of uplink transmitted CDMA signals.

Theory of Code Division Multiple Access Communication, by Kamil Sh. Zigangirov
ISBN 0-471-45712-4

7.1 HYPOTHESIS TESTING IN THE ACQUISITION PROCESS

In a DS CDMA system, the PN spreading sequence must be synchronized in time to within a small fraction of the chip interval T_c. The problem of initial synchronization may be viewed as an attempt to synchronize the receiver clock to the transmitter clock. Usually, extremely accurate and stable clocks are used in SS systems to reduce the time uncertainty between the receiver clock and the transmitter clock. Nevertheless, there is always an initial timing uncertainty that is due to propagation delay in the transmission of the signal through the channel. This is especially a problem when the communication is taking place between two mobiles, that is, peer-to-peer.

The usual procedure for establishing initial synchronization is to have the transmitter send a known pseudorandom sequence to the receiver. The receiver is continuously in a search mode looking for this sequence to establish initial synchronization. A similar process may also be used for FH CDMA signals. In this case, the problem is to synchronize the pseudorandom sequence that controls the hopped frequency pattern. To accomplish this initial synchronization, a known FH signal is transmitted to the receiver. The initial acquisition device at the receiver seeks this FH signal pattern.

In the case of PPH CDMA signals the transmitter periodically sends a known pulse train. The receiver is continuously searching for this pulse train to establish initial synchronization.

Consider the acquisition of the uplink DS CDMA system using the BPSK spread signal. The synchronization signal transmitted by the kth user is

$$s^{(k)}(t) = \sqrt{2}a^{(k)}(t)\cos(2\pi f_c t + \phi^{(k)}) \tag{7.1}$$

where $a^{(k)}(t)$ is a periodic pseudorandom spreading signal (6.1) [see also (2.96)] with period $\mathcal{T} = N_p T_c$, f_c is the carrier frequency, $\phi^{(k)}$ is a phase, T_c is a chip duration, and N_p is the period of the spreading sequence. We take the signal to be unmodulated by data [compare with Formula (2.92)], as would be the case for a pilot signal. For the AWGN channel, the received signal is

$$r(t) = \sqrt{2P^{(k)}}a^{(k)}(t - \delta^{(k)})\cos(2\pi f_c(t - \delta^{(k)}) + \varphi^{(k)}) + \xi^{(k)}(t) \tag{7.2}$$

where $P^{(k)}$ is the received signal power, $\varphi^{(k)}$ is the phase of the carrier, $\delta^{(k)}$ is the time offset, and $\xi^{(k)}(t)$ is the total interference and additive noise of two-sided power spectral density $I_0/2$.

For the multipath slow-fading Rayleigh channel, the received signal by the ℓth rake finger is

$$r_\ell(t) = \alpha_\ell^{(k)}\sqrt{2}a^{(k)}(t - \delta_\ell^{(k)})\cos(2\pi f_c(t - \delta_\ell^{(k)}) + \varphi_\ell^{(k)}) + \xi_\ell^{(k)}(t) \tag{7.3}$$

where $\alpha_\ell^{(k)}$, $\varphi_\ell^{(k)}$ and $\delta_\ell^{(k)}$ are the fade amplitude, the phase shift, and the propagation delay of the ℓth path, respectively. The total interference and additive noise

$\xi_\ell^{(k)}(t)$ has the two-sided spectral density $I_0/2$. Because acquisition in the Rake receiver is performed in each finger separately, we will drop the index ℓ.

The receiver must determine the time offset $\delta^{(k)}$ of the spreading sequence and the phase $\varphi^{(k)}$. Usually, the timing of the spreading sequence is determined before any phase measurement is performed (both for the AWGN channel and for a finger of the multipath Rayleigh channel). Hence, the acquisition must be done noncoherently as shown in Figure 7.1. It includes the hypothesis testing device, which tests the binary hypotheses whether the synchronization is achieved or not. In the first case, when the receiver timing has been synchronized to within a fraction of a chip duration, the estimation should be further refined to approach the minimal timing error. This is the function of the tracking device (Section 7.5). In the second case, the receiver changes the timing τ of the despreading signal on Δ and makes a new attempt.

The front part of the receiver in Figure 7.1 is similar to that of the differentially coherent demodulator (Fig. 3.6). The middle part, the noncoherent receiver, is similar to the one in Figure 3.6 and in Figure 4.5. We shall justify the remaining functions of the signal processor in Section 7.2.

If the frequency error Δf is greater than the inverse of the testing (integration) time $T = NT_c$, that is, $\Delta f > 1/T$, the acquisition receiver performance is seriously degraded, such that the hypothesis test becomes unreliable. To avoid this, we can perform "postdetection integration" by accumulating $\nu > 1$ successive decision statistics $y_i^{(k)}$ before making the decision, as shown by the last block of Figure 7.1. If the frequency is stable, we have $\nu = 1$. In Figure 7.1 we considered the case when hypothesis testing is done over the νN chips.

In Figure 7.1 perfect synchronization corresponds to the sampling starting at the moments $t = \delta^{(k)}$, with the following multiplications of the matched filter outputs on the spreading sequence symbols $a_n^{(k)}$. Suppose that the sampling starts at the moment $t = \hat{\delta}^{(k)}$, that is, the timing error is $\tau^{(k)} = \hat{\delta}^{(k)} - \delta^{(k)}$. Then for the

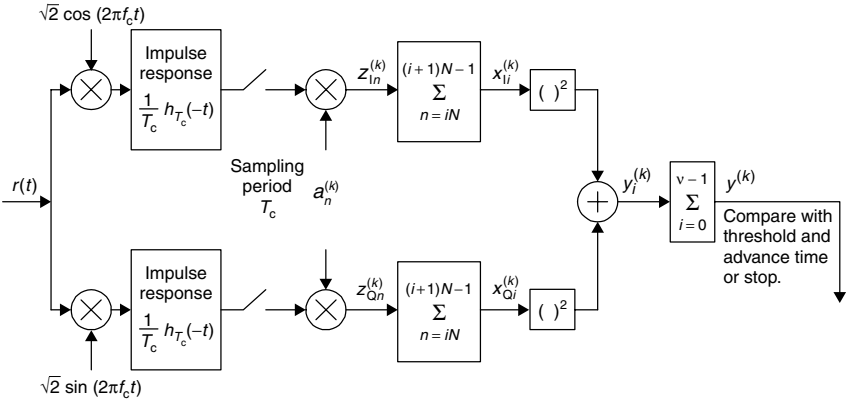

Figure 7.1. Hypothesis testing device in the acquisition process for a BPSK SS system.

AWGN channel we have

$$\begin{aligned} z_{In}^{(k)} &= \sqrt{P^{(k)}} R_a(\tau^{(k)}) \cos \varphi^{(k)} + \tilde{\xi}_{In}^{(k)} \\ z_{Qn}^{(k)} &= \sqrt{P^{(k)}} R_a(\tau^{(k)}) \sin \varphi^{(k)} + \tilde{\xi}_{Qn}^{(k)} \end{aligned} \tag{7.4}$$

where $R_a(\cdot)$ is the autocorrelation function of the spreading signal $a^{(k)}(t)$, and $\tilde{\xi}_{In}^{(k)}$ and $\tilde{\xi}_{Qn}^{(k)}$ are modified zero-mean noise components. The variances of $\tilde{\xi}_{In}^{(k)}$ and $\tilde{\xi}_{Qn}^{(k)}$ are

$$\operatorname{var}(\tilde{\xi}_{In}^{(k)}) = \operatorname{var}(\tilde{\xi}_{Qn}^{(k)}) = \frac{I_0}{2T_c} \tag{7.5}$$

where [compare with (3.72)]

$$\frac{I_0}{2} = \frac{1}{2T_c^2} \sum_{k' \neq k} P^{(k')} \int_{-\infty}^{\infty} |H(f)|^4 \, \mathrm{d}f + \frac{N_0}{2} + \frac{N_{oc}}{2} \tag{7.6}$$

$N_0/2$ is the two-sided power spectral density of the AWGN, and $N_{oc}/2$ is two-sided power spectral density of the other-cell interference. The random variables $\tilde{\xi}_{In}^{(k)}$ and $\tilde{\xi}_{Qn}^{(k)}$ can be considered to be independent Gaussian variables, and $\varphi^{(k)}$ is uniformly distributed on $[0, 2\pi)$. Actually, for $\tau^{(k)} \neq 0$ the density $I_0/2$ should include a term depending on the signal from the desired user. But because $K \gg 1$, we will neglect this term. We suppose that the phase $\varphi^{(k)}$ remains constant over the integration time $T = NT_c$, which implies that the frequency error is negligible.

For the Rayleigh channel

$$\begin{aligned} z_{In}^{(k)} &= \alpha^{(k)} R_a(\tau^{(k)}) \cos \varphi^{(k)} + \tilde{\xi}_{In}^{(k)} \\ z_{Qn}^{(k)} &= \alpha^{(k)} R_a(\tau^{(k)}) \sin \varphi^{(k)} + \tilde{\xi}_{Qn}^{(k)} \end{aligned} \tag{7.7}$$

where $\alpha^{(k)}$ is Rayleigh distributed with the second moment $2a^2$ and the other variables are the same as in the AWGN channel case. The statistics $\alpha^{(k)} \cos \varphi^{(k)}$ and $\alpha^{(k)} \sin \varphi^{(k)}$ are independent zero-mean Gaussian variables with variances a^2.

Consider now the acquisition of the DS CDMA uplink system using the QPSK spreading. The acquisition signal transmitted by the kth user is [compare with (2.110)]

$$s^{(k)}(t) = \sum_{n=-\infty}^{\infty} [a^{(k)}(t) \cos(2\pi f_c t + \phi^{(k)}) - b^{(k)}(t) \sin(2\pi f_c t + \phi^{(k)})] \tag{7.8}$$

where the in-phase and quadrature spreading signals $a^{(k)}(t)$ and $b^{(k)}(t)$ are defined by Formulas (2.106) and (2.107). For the AWGN channel the received signal is

$$\begin{aligned} r(t) = \sqrt{P^{(k)}} [&a^{(k)}(t - \delta^{(k)}) \cos(2\pi f_c (t - \delta^{(k)}) + \varphi^{(k)}) \\ &- b^{(k)}(t - \delta^{(k)}) \sin(2\pi f_c (t - \delta^{(k)}) + \varphi^{(k)})] + \xi^{(k)}(t) \end{aligned} \tag{7.9}$$

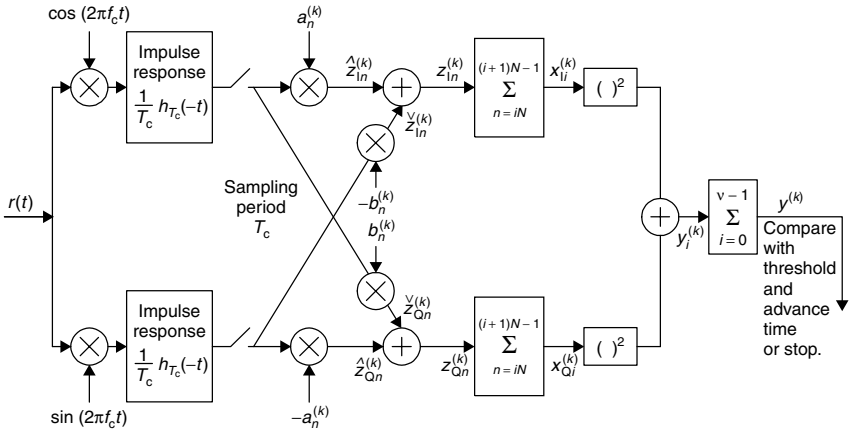

Figure 7.2. Hypothesis testing device in the acquisition process for a QPSK SS system.

where $P^{(k)}$, $\delta^{(k)}$, $\varphi^{(k)}$, and $\xi^{(k)}(t)$ are defined below Formula (7.2). For the Rayleigh channel the received signal is a straightforward modification of the signal (7.9), namely, $\sqrt{P^{(k)}}$ should be replaced by $\alpha^{(k)}$.

The hypothesis testing device for QPSK spreading is shown in Figure 7.2. To accommodate the effect of QPSK spreading it should include the cross-arms. We denote the direct arm terms by $\hat{}$ and the cross-arm terms by $\check{}$, as shown in the figure. Then for the AWGN channel we have [47]

$$\begin{aligned}
\hat{z}_{\mathrm{I}n}^{(k)} &= \tfrac{1}{2}\sqrt{P^{(k)}}R_a(\tau^{(k)})[\cos\varphi^{(k)} + a_n^{(k)}b_n^{(k)}\sin\varphi^{(k)}] + \hat{\xi}_{\mathrm{I}n}\\
\check{z}_{\mathrm{I}n}^{(k)} &= \tfrac{1}{2}\sqrt{P^{(k)}}R_a(\tau^{(k)})[\cos\varphi^{(k)} - a_n^{(k)}b_n^{(k)}\sin\varphi^{(k)}] + \check{\xi}_{\mathrm{I}n}\\
\hat{z}_{\mathrm{Q}n}^{(k)} &= \tfrac{1}{2}\sqrt{P^{(k)}}R_a(\tau^{(k)})[\sin\varphi^{(k)} - a_n^{(k)}b_n^{(k)}\cos\varphi^{(k)}] + \hat{\xi}_{\mathrm{Q}n}\\
\check{z}_{\mathrm{Q}n}^{(k)} &= \tfrac{1}{2}\sqrt{P^{(k)}}R_a(\tau^{(k)})[\sin\varphi^{(k)} + a_n^{(k)}b_n^{(k)}\cos\varphi^{(k)}] + \check{\xi}_{\mathrm{Q}n}
\end{aligned} \tag{7.10}$$

where zero-mean random variables $\hat{\xi}_{\mathrm{I}n}$, $\check{\xi}_{\mathrm{I}n}$, $\check{\xi}_{\mathrm{Q}n}$, and $\hat{\xi}_{\mathrm{Q}n}$ represent the effect of noise and interference. The variances are

$$\mathrm{var}(\hat{\xi}_{\mathrm{I}n}) = \mathrm{var}(\check{\xi}_{\mathrm{I}n}) = \mathrm{var}(\check{\xi}_{\mathrm{Q}n}) = \mathrm{var}(\hat{\xi}_{\mathrm{Q}n}) = \frac{I_0}{4T_{\mathrm{c}}} \tag{7.11}$$

The random variables $\hat{\xi}_{\mathrm{I}n}$, $\check{\xi}_{\mathrm{I}n}$, $\check{\xi}_{\mathrm{Q}n}$, and $\hat{\xi}_{\mathrm{Q}n}$ can be considered as Gaussian distributed and independent.

From Formulas (7.10) and (7.11) it follows that the random variables $z_{\mathrm{I}n}^{(k)} = \hat{z}_{\mathrm{I}n}^{(k)} + \check{z}_{\mathrm{I}n}^{(k)}$ and $z_{\mathrm{Q}n}^{(k)} = \hat{z}_{\mathrm{Q}n}^{(k)} + \check{z}_{\mathrm{Q}n}^{(k)}$ are analogous to the output variables (7.4) and (7.7) of the BPSK DS CDMA matched-filter device and the zero-mean noise components $\xi_{\mathrm{I}n}^{(k)} = \hat{\xi}_{\mathrm{I}n}^{(k)} + \check{\xi}_{\mathrm{I}n}^{(k)}$ and $\xi_{\mathrm{Q}n}^{(k)} = \hat{\xi}_{\mathrm{Q}n}^{(k)} + \check{\xi}_{\mathrm{Q}n}^{(k)}$ have variances given by Equation (7.5).

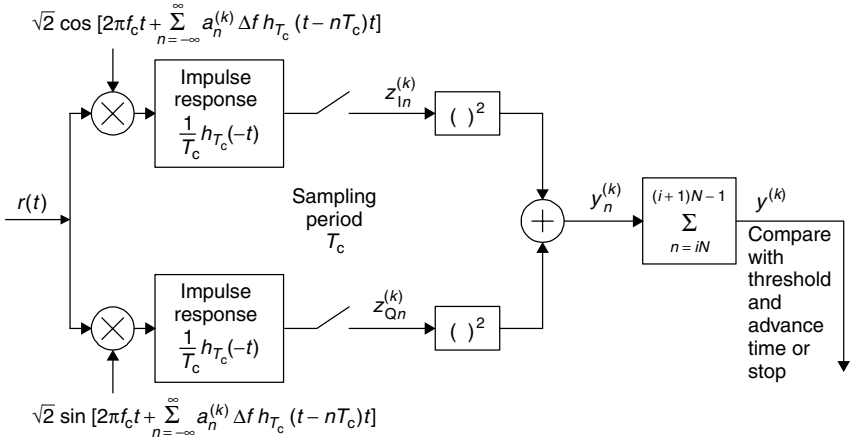

Figure 7.3. Hypothesis testing device in the acquisition process for a FH CDMA system.

In Figure 7.3 the basic hypothesis testing device for acquisition of the FH CDMA system is shown. For simplicity we consider the case when the system uses rectangular pulse shaping and does not utilize postdetection integration. The acquisition signal transmitted by the kth user is [compare with Formula (3.124)]

$$s^{(k)}(t) = \sqrt{2} \sum_{n=-\infty}^{\infty} h_{T_c}(t - nT_c) \cos[2\pi(f_c + a_n^{(k)} \Delta f)t + \phi_n^{(k)}]$$

$$= \sqrt{2} \cos\left[2\pi f_c t + \sum_{n=-\infty}^{\infty} (2\pi a_n^{(k)} \Delta f t + \phi_n^{(k)}) h_{T_c}(t - nT_c)\right] \qquad (7.12)$$

where $h_{T_c}(t)$ is a unit amplitude rectangular pulse of duration T_c, $\phi_n^{(k)}$ is a phase uniformly distributed on $[0, 2\pi)$, and Δf is the frequency separation interval. This signal is unmodulated by data. Consequently the M-ary periodical hopping sequence $\{a_n^{(k)}\}$, $a_n^{(k)} \in \{-(M-1)/2,\ -(M-3)/2, \ldots, (M-1)/2\}$ with period N_p can be used in the acquisition process. Signal (7.12) can be also presented as

$$s^{(k)}(t) = \cos[2\pi(f_c + a_n^{(k)} \Delta f)t + \phi_n^{(k)}],\ t \in \left[nT_c - \frac{T_c}{2}, nT_c + \frac{T_c}{2}\right)$$

We consider the acquisition process only when transmission is over the AWGN channel. The kth user's received signal is

$$r^{(k)}(t) = \sqrt{2P^{(k)}} \sum_{n=-\infty}^{\infty} h_{T_c}(t - nT_c - \delta^{(k)})$$

$$\times \cos[2\pi(f_c + a_n^{(k)} \Delta f)(t - \delta^{(k)}) + \varphi_n^{(k)}] + \xi^{(k)}(t) \qquad (7.13)$$

where $P^{(k)}$ is the received signal power, $\varphi^{(k)}$ is the phase shift, $\delta^{(k)}$ is the time offset, and $\xi^{(k)}(t)$ is the total interference and additive noise with two-sided power spectral density $I_0/2$. The receiver must determine the time offset $\delta^{(k)}$.

To simplify the analysis we consider a single-cell system, but in the case when all users are not chip synchronized. This model was considered already in Section 3.6. Perfect synchronization corresponds to sampling started at $t = \delta^{(k)}$. Then the outputs of the matched filters $z_{\mathrm{I}n}^{(k)}$ and $z_{\mathrm{Q}n}^{(k)}$ are

$$\begin{aligned} z_{\mathrm{I}n}^{(k)} &= \sqrt{P^{(k)}}\ \cos\varphi_n^{(k)} + \tilde{\xi}_{\mathrm{I}n}^{(k)} + \hat{\xi}_{\mathrm{I}n}^{(k)} \\ z_{\mathrm{Q}n}^{(k)} &= \sqrt{P^{(k)}}\sin\varphi_n^{(k)} + \tilde{\xi}_{\mathrm{Q}n}^{(k)} + \hat{\xi}_{\mathrm{Q}n}^{(k)} \end{aligned} \tag{7.14}$$

where $\hat{\xi}_{\mathrm{I}n}^{(k)}$ and $\hat{\xi}_{\mathrm{Q}n}^{(k)}$ are due to the AWGN and $\tilde{\xi}_{\mathrm{I}n}^{(k)}$ and $\tilde{\xi}_{\mathrm{Q}n}^{(k)}$ are the other-user interference components, such that [compare with the first two equations of (3.143)],

$$\begin{aligned} \tilde{\xi}_{\mathrm{I}n}^{(k)} &= \sum_{k'\neq k} \sqrt{P^{(k')}}\ [\theta_n^{(k')}\eta^{(k')}\cos\varphi_n^{(k')} + \theta_{n+1}^{(k')}(1-\eta_n^{(k')})\cos\varphi_{n+1}^{(k')}] \\ \tilde{\xi}_{\mathrm{Q}n}^{(k)} &= \sum_{k'\neq k} \sqrt{P^{(k')}}\ [\theta_n^{(k')}\eta_n^{(k')}\sin\varphi_n^{(k')} + \theta_{n+1}^{(k')}(1-\eta_n^{(k')})\sin\varphi_{n+1}^{(k')}] \end{aligned} \tag{7.15}$$

Here we assume that the nth chip generated by the receiver can overlap with the nth and $(n+1)$th chips of the signal received from the k'th user. The length of the overlapping with the nth chip of the k'th user is $\eta_n^{(k')}T_{\mathrm{c}}$, $0 < \eta_n^{(k)} \leq 1$; the length of the overlapping with the $(n+1)$th chip is $(1-\eta_n^{(k')})T_{\mathrm{c}}$. The binary random variables $\theta_n^{(k')}$, $n = 0, 1, \ldots$, are independent and take the value 1 with probability $1/M$ and the value 0 with probability $(1 - 1/M)$. The random variables $\varphi_n^{(k')}$, $n = 0, 1, \ldots$, are independent and uniformly distributed on $[0, 2\pi)$. If the timing error $|\tau^{(k)}| > T_{\mathrm{c}}$, then the outputs of the matched filter are [compare with the two last equations of (3.143)]

$$\begin{aligned} z_{\mathrm{I}n}^{(k)} &= \tilde{\xi}_{\mathrm{I}n}^{(k)} + \hat{\xi}_{\mathrm{I}n}^{(k)} \\ z_{\mathrm{Q}n}^{(k)} &= \tilde{\xi}_{\mathrm{Q}n}^{(k)} + \hat{\xi}_{\mathrm{Q}n}^{(k)} \end{aligned} \tag{7.16}$$

Here the components $\hat{\xi}_{\mathrm{I}n}^{(k)}$ and $\hat{\xi}_{\mathrm{Q}n}^{(k)}$ are analogous to the corresponding components in (7.14), but in contrast to (7.14) the other-user components $\tilde{\xi}_{\mathrm{I}n}^{(k)}$ and $\tilde{\xi}_{\mathrm{Q}n}^{(k)}$ include terms depending on the signal from the desired user. Since $K \gg 1$, we will neglect this term and will assume that in both cases $\tilde{\xi}_{\mathrm{I}n}^{(k)}$ and $\tilde{\xi}_{\mathrm{Q}n}^{(k)}$ are defined by (7.15). If $|\tau^{(k)}| < T_{\mathrm{c}}$, then

$$\begin{aligned} z_{\mathrm{I}n}^{(k)} &= \sqrt{P^{(k)}}\ R_a(\tau^{(k)})\cos\varphi_n^{(k)} + \tilde{\xi}_{\mathrm{I}n}^{(k)} + \hat{\xi}_{\mathrm{I}n}^{(k)} \\ z_{\mathrm{Q}n}^{(k)} &= \sqrt{P^{(k)}}\ R_a(\tau^{(k)})\sin\varphi_n^{(k)} + \tilde{\xi}_{\mathrm{Q}n}^{(k)} + \hat{\xi}_{\mathrm{Q}n}^{(k)} \end{aligned} \tag{7.17}$$

where $R_a(\tau^{(k)}) = 1 - |\tau^{(k)}|/T_c$ is the autocorrelation function of the unit amplitude rectangular pulse $h_{T_c}(t)$ in the interval $0 \le \tau^{(k)} < T_c$. The other terms in (7.17) coincide with the analogous term for the $|\tau^{(k)}| \ge T_c$ case. Because $R_a(\tau^{(k)}) = 0$ for $|\tau^{(k)}| \ge T_c$, Formula (7.17) passes to (7.16) for $|\tau^{(k)}| \ge T_c$.

In contrast to the statistics (7.4) characterizing the acquisition process in a DS CDMA system, the statistics (7.17) cannot be considered as Gaussian random variables. In Section 7.2 we study the first two moments of the statistics $y_n^{(k)} = (z_{\mathrm{I}n}^{(k)})^2 + (z_{\mathrm{Q}n}^{(k)})^2$ and approximate the distribution of the statistic $y^{(k)} = \sum_{n=iN}^{(i+1)N-1} y_n^{(k)}$ by a Gaussian distribution.

The acquisition receiver for the PPH CDMA system practically coincides with the receiver shown in Figure 3.9. The synchronization signal is [compare with (2.147)]

$$s^{(k)}(t) = \sum_{n=-\infty}^{\infty} h_{T_c}(t - nT_f - a_n^{(k)}\Delta) \tag{7.18}$$

where T_f is the frame duration, $a_n^{(k)}\Delta$ is the addressable pulse-position shift, and Δ is the duration of the addressable time delay bin. The received signal is [compare with (3.152)]

$$r(t) = \sum_{k=1}^{K} \sqrt{P^{(k)}}\, s^{(k)}(t - \delta^{(k)}) + \xi(t)$$

where $P^{(k)}$ is the power of the received signal from the kth user, $\delta^{(k)}$ is the kth user's time offset, and $\xi(t)$ is the AWGN with the two-sided power spectral density $N_0/2$.

The output of the matched filter at the moment $t^{(k)} = nT_f + a_n^{(k)}\Delta + \hat{\delta}^{(k)}$ is [compare with (3.175)]

$$z_n^{(k)} = \sqrt{P^{(k)}} R_h(\tau^{(k)}) + \tilde{\xi}_n^{(k)}$$

where $P^{(k)}$ is the power of the received signal, $R_h(\cdot)$ is the normalized autocorrelation function (2.15) of the pulse $h_{T_c}(\cdot)$, $\tau^{(k)} = \hat{\delta}^{(k)} - \delta^{(k)}$, and $\tilde{\xi}_n^{(k)}$ is the zero-mean total interference and additive noise component with variance

$$\mathrm{var}(\tilde{\xi}_n^{(k)}) \approx \sigma^2 \stackrel{\mathrm{def}}{=} \frac{N_0}{2T_c} + \frac{1}{T_f}\int_{-\infty}^{\infty} R_h^2(\tau)\, d\tau \sum_{k' \ne k} P^{(k')}$$

Here $N_0/2$ is the two-sided power spectral density of the AWGN.

The receiver calculates the decision statistic $y^{(k)} = \sum_{n=iN}^{(i+1)N-1} z_n^{(k)}$ and compares it with the threshold θ. For the Manchester pulse the first two moments of

the statistic $y^{(k)}$ are [compare with Formulas (3.181) and (3.182)]

$$E(y^{(k)}) = \sqrt{P^{(k)}} N R_h(\tau^{(k)}) \tag{7.19}$$

$$\operatorname{var}(y^{(k)}) = N\sigma^2 \stackrel{\text{def}}{=} N \left[\frac{N_0}{T_c} + \frac{2}{3} \frac{T_c}{T_f} \sum_{k' \neq k} P^{(k')} \right] \tag{7.20}$$

The decision rule is (see Example 3.1)

$$y^{(k)} \underset{<}{\overset{H_1}{>}} \theta \underset{N_0}{} \tag{7.21}$$

The sequence of matched filter outputs (7.4), (7.7), (7.10), (7.14), (7.17), and (7.19) defines the decision statistics $y^{(k)}$ for the acquisition of DS CDMA, FH CDMA, and PPH CDMA systems. The receiver performance is optimized if it is perfectly synchronized with the transmitter, that is, if $\hat{\delta}^{(k)} = \delta^{(k)}$.

To find this maximum the decision device uses one of the hypothesis testing algorithms considered in Section 3.2. In the following section we analyze performances of these algorithms when applied to acquisition processes.

7.2 PERFORMANCE OF THE HYPOTHESIS TESTING DEVICE

First we analyze the performance of the hypothesis testing device of the DS CDMA system in the case of an unfaded Gaussian channel. We say that hypothesis H_1 is true, that is, synchronization is reached, if $|\tau^{(k)}| = |\hat{\delta}^{(k)} - \delta^{(k)}| < T_c$; otherwise, we say that hypothesis H_0 is true. From Formulas (7.4), (7.5), (7.10), and (7.11) it follows that the statistics x_{Ii} and x_{Qi} have the following means and variance:

$$\begin{aligned} E(x_{Ii}) &= \sqrt{P^{(k)}}\, N R_a(\tau^{(k)}) \cos \varphi^{(k)}, \quad i = 0, 1, \ldots, \nu - 1, \\ E(x_{Qi}) &= \sqrt{P^{(k)}}\, N R_a(\tau^{(k)}) \sin \varphi^{(k)}, \quad i = 0, 1, \ldots, \nu - 1, \end{aligned} \tag{7.22}$$

and

$$\operatorname{var}(x_{Ii}) = \operatorname{var}(x_{Qi}) \stackrel{\text{def}}{=} \sigma^2 = \frac{I_0 N}{2T_c}, \quad i = 0, 1, \ldots, \nu - 1, \tag{7.23}$$

where $I_0/2$ is defined by (7.6). The random variables x_{Ii} and x_{Qi} are independent and nearly Gaussian for large N because of the central limit theorem.

Consider the case when the pulses $h_{T_c}(t)$ in the spreading signals (2.96), (2.106), and (2.107) are unit amplitude rectangular pulses (2.3). Then for $|\tau| \geq T_c$, $R(\tau) = 0$, $E(x_{Ii}) = E(x_{Qi}) = 0$, and the statistics $y_i^{(k)}$ have a central

χ^2-distribution with two degrees of freedom. If $|\tau^{(k)}| \geq T_c$, hypothesis H_0 is true and the probability density function is [see Formula (3.48)]

$$p_0(y_i^{(k)}) = \frac{1}{2\sigma^2} \exp\left(-\frac{y_i^{(k)}}{2\sigma^2}\right), \quad y_i \geq 0, \quad i = 0, 1, \ldots, \nu - 1 \tag{7.24}$$

If $|\tau^{(k)}| < T_c$, then $R_a(\tau^{(k)}) \neq 0$ and from (7.22) and (7.23) it follows that $y_i^{(k)}$ have a noncentral χ^2-distribution with two degrees of freedom. The probability density function is [see (3.49)]

$$p_1(y_i^{(k)}) = \frac{1}{2\sigma^2} \exp[-(y_i^{(k)} + \mu^2)/2\sigma^2] I_0\left(\frac{\mu\sqrt{y_i^{(k)}}}{\sigma^2}\right) \tag{7.25}$$

$$y_i^{(k)} \geq 0, \quad i = 0, 1, \ldots, \nu - 1$$

where $\mu \stackrel{\text{def}}{=} \sqrt{P^{(k)}} N R_a(\tau^{(k)})$. If $\nu = 1$ and the threshold for the statistic $y^{(k)} = y_0^{(k)}$ is θ, the false alarm and the detection probabilities are [compare with (3.51) and (3.52)]

$$P_F = \int_\theta^\infty \frac{1}{2\sigma^2} \exp\left(-\frac{y}{2\sigma^2}\right) dy = \exp\left(-\frac{\theta}{2\sigma^2}\right) = \exp(-\theta') \tag{7.26}$$

$$\begin{aligned} P_D &= \int_\theta^\infty \frac{1}{2\sigma^2} \exp[-(y + \mu^2)/2\sigma^2] I_0\left(\frac{\mu\sqrt{y}}{\sigma^2}\right) dy \\ &= \int_{\theta'}^\infty \exp(-y - \rho_B)\ I_0(2\sqrt{\rho_B y})\, dy \\ &= \int_{-\ln P_F}^\infty \exp(-y - \rho_B) I_0(2\sqrt{\rho_B y})\, dy \end{aligned} \tag{7.27}$$

where $\rho_B = \mu^2/2\sigma^2 = P^{(k)} N R_a^2(\tau^{(k)})/I_0 T_c$ is the SNR per block and $\theta' = \theta/2\sigma^2$. The receiver operating characteristic is presented in Figure 3.2.

As we mentioned in Section 7.1, if the frequency error is large, it may be necessary to accumulate ν, $\nu > 1$, successive energy measurements as shown by the last block of Figure 7.1. If hypothesis H_0 is true, the decision statistic $y^{(k)}$ has a central χ^2-distribution with 2ν degrees of freedom [compare with (3.60)], that is,

$$p_0(y^{(k)}) = \frac{1}{2^\nu \sigma^{2\nu} (\nu - 1)!} (y^{(k)})^{\nu - 1} \exp\left(-\frac{y^{(k)}}{2\sigma^2}\right), \quad y^{(k)} \geq 0 \tag{7.28}$$

If hypothesis H_1 is true, the decision statistic $y^{(k)}$ has a noncentral χ^2-distribution with 2ν degrees of freedom. The probability density function is [compare

with (3.61)]

$$p_1(y^{(k)}) = \frac{1}{2\sigma^2}\left(\frac{y^{(k)}}{\nu\mu^2}\right)^{\frac{\nu-1}{2}} \exp\left(-\frac{(y^{(k)}+\nu\mu^2)}{2\sigma^2}\right) I_{\nu-1}\left(\frac{\sqrt{\nu\mu^2 y^{(k)}}}{\sigma^2}\right), \quad y^{(k)} \geq 0 \tag{7.29}$$

where $I_{\nu-1}(\cdot)$ is the $(\nu-1)$th-order modified Bessel function. The false alarm and detection probabilities are [compare with (3.62) and (3.63)]

$$\begin{aligned} P_{\mathrm{F}} &= \int_{\theta}^{\infty} \frac{1}{2^{\nu}\sigma^{2\nu}(\nu-1)!} y^{\nu-1} \exp\left(-\frac{y}{2\sigma^2}\right) \mathrm{d}y \\ &= \int_{\theta'}^{\infty} \frac{y^{\nu-1}e^{-y}}{(\nu-1)!}\mathrm{d}y = e^{-\theta'} \sum_{k=0}^{\nu-1} \frac{\theta'^k}{k!} \end{aligned} \tag{7.30}$$

$$\begin{aligned} P_{\mathrm{D}} &= \int_{\theta}^{\infty} \frac{1}{2\sigma^2}\left(\frac{y}{\nu\mu^2}\right)^{\frac{\nu-1}{2}} \exp[-(y+\nu\mu^2)/2\sigma^2] I_{\nu-1}\left(\frac{\sqrt{\nu\mu^2 y}}{\sigma^2}\right) \mathrm{d}y \\ &= \int_{\theta'}^{\infty} \left(\frac{y}{\nu\rho_{\mathrm{B}}}\right)^{\frac{\nu-1}{2}} \exp(-y-\nu\rho_{\mathrm{B}}) I_{\nu-1}\left(2\sqrt{\nu\rho_{\mathrm{B}} y}\right) \mathrm{d}y \end{aligned} \tag{7.31}$$

where $\theta' = \theta/2\sigma^2$, and $\rho_{\mathrm{B}} = \mu^2/2\sigma^2$. The latter integral is the νth order Marcum Q function [20]. The receiver operating characteristics for $\nu = 1, 2$, $\rho_{\mathrm{B}} = 4$ dB and 8 dB are shown in Figure 7.4.

Consider now DS CDMA communication in the Rayleigh fading channel. The components $x_{\mathrm{I}i}^{(k)}$ and $x_{\mathrm{Q}i}^{(k)}$ in Figures 7.1 and 7.2 have zero-mean Gaussian distribution, even if hypothesis H_1 is true. We suppose that the Rayleigh fading is slow enough that the amplitude as well as the phase (and hence the in-phase and quadrature components) remain constant over the integration time T but fast enough that successive integration segments are essentially independent. While the probability density function of $y^{(k)}$ under hypothesis H_0 is the same as for an unfaded AWGN channel, that is, defined by (7.24) and (7.28), the probability density function of $y^{(k)}$ under H_1 is

$$p_1(y^{(k)}) = \frac{(y^{(k)})^{\nu-1}}{2^{\nu}\sigma^{2\nu}(1+\rho_{\mathrm{B}})^{\nu}(\nu-1)!} \exp\left(-\frac{y^{(k)}}{2\sigma^2(1+\rho_{\mathrm{B}})^2}\right), \quad y^{(k)} \geq 0 \tag{7.32}$$

where

$$\rho_{\mathrm{B}} = \frac{2a^2 N T_{\mathrm{c}}}{I_0} R^2(\tau^{(k)})$$

and $2a^2$ is the average power of the Rayleigh-faded signal. In this case, the expression for the detection probability becomes the same as the false alarm

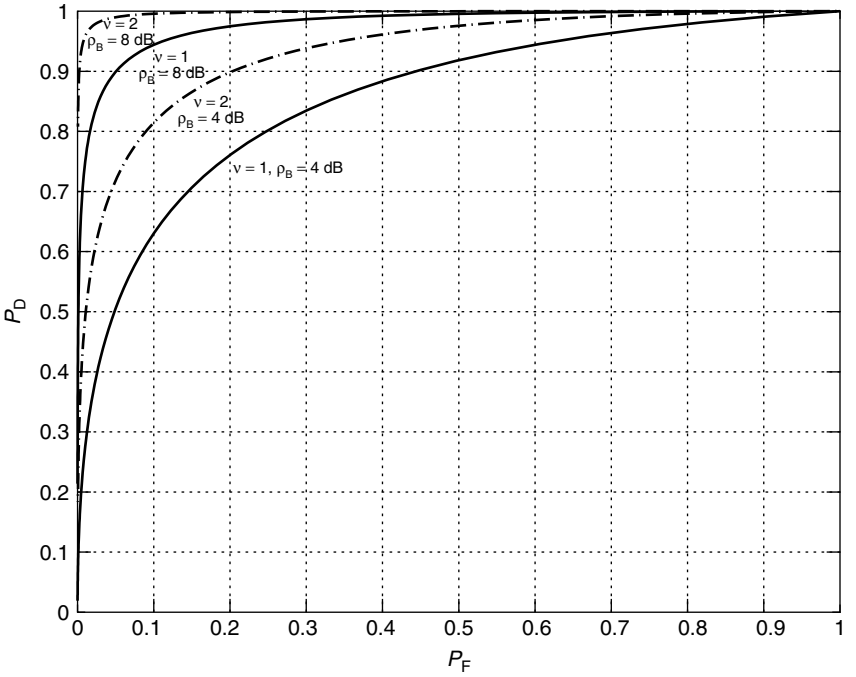

Figure 7.4. The receiver operating characteristic for unfaded AWGN channel, $\nu = 1, 2$.

probability (7.30) but with θ' replaced by $\theta'/(1 + \rho_B)$, that is,

$$P_D = \exp\left(-\frac{\theta'}{(1+\rho_B)}\right) \sum_{k=0}^{\nu-1} \frac{[\theta'/(1+\rho_B)]^k}{k!} \tag{7.33}$$

The receiver operating characteristics for Rayleigh fading signals are shown in Figure 7.5 for $\nu = 1$ and 2. Note that the performance for $\rho_B = 4$ dB with $\nu = 2$ (for total signal-to-noise ratio of 8 dB) is close to the performance for $\rho_B = 8$ dB with $\nu = 1$. This implies that the twofold diversity in this case gains about 1.5 dB.

Consider the acquisition process for a FH CDMA system operating over the AWGN channel. To avoid cumbersome calculations we neglect the background noise components $\hat{\xi}_{In}^{(k)}$ and $\hat{\xi}_{Qn}^{(k)}$ in the output of the matched filter (7.14), (7.16), (7.17). We also assume that $\tau^{(k)}$ can take only the value $\tau^{(k)} = 0$ (perfect synchronization) or $|\tau^{(k)}| \geq T_c$ (no synchronization). This is the so-called "genie-aided" situation (see below, Section 7.3). The following mathematical model will apply. The statistics $y_n^{(k)} \stackrel{\text{def}}{=} (z_{In}^{(k)})^2 + (z_{Qn}^{(k)})^2$ are IID random variables, and the statistics $y^{(k)} = \sum_{n=0}^{N-1} y_n^{(k)}$ (see Fig. 7.3) are nearly Gaussian random variables because of the central limit theorem. As in Sections 3.6 and 4.7 we assume that $P^{(k)} = P$,

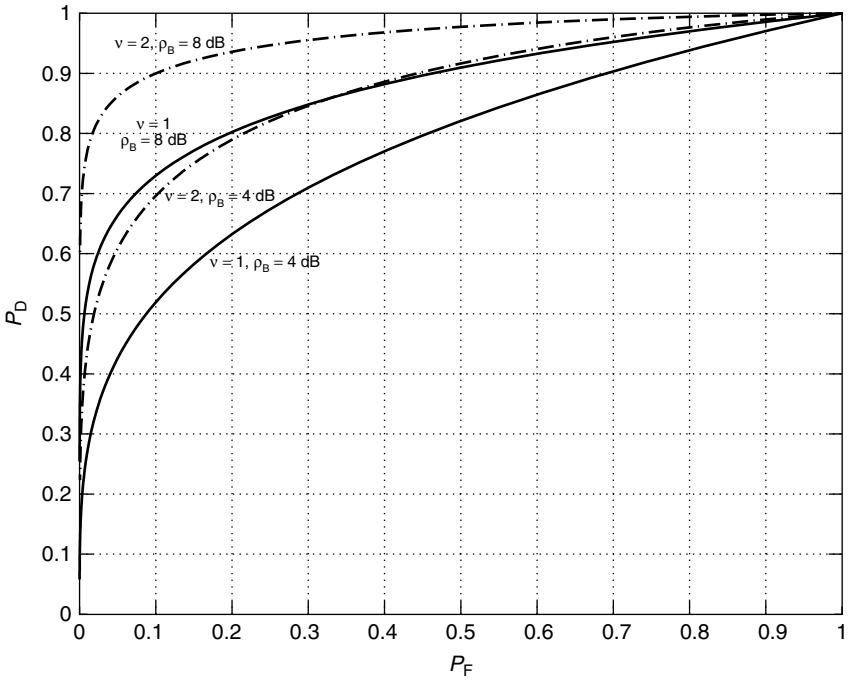

Figure 7.5. The operating characteristic of the decision device of the DS CDMA system for Rayleigh faded channel, $\nu = 1, 2$.

$k = 1, 2, \ldots, K$, because of perfect power control. Then [compare with Formulas (3.144)–(3.147)]

$$E(y_n^{(k)}) = \begin{cases} \mu_1 = P + \dfrac{2}{3} P\ \lambda, & \text{if } \tau^{(k)} = 0, \\ \mu_0 = \dfrac{2}{3} P\ \lambda, & \text{otherwise} \end{cases} \tag{7.34}$$

$$\text{var}(y_n^{(k)}) = \begin{cases} \sigma_1^2 \approx P^2 \left[\dfrac{26}{15}\lambda + \dfrac{4}{9}\lambda^2 \right], & \text{if } \tau^{(k)} = 0, \\ \sigma_0^2 \approx P^2 \left[\dfrac{2}{5}\lambda + \dfrac{4}{9}\lambda^2 \right], & \text{otherwise} \end{cases} \tag{7.35}$$

where $\lambda = (K - 1)/M$. Then the moments of statistic $y^{(k)}$ are

$$E(y^{(k)}) = \begin{cases} N\mu_1, & \text{if } H_1 \text{ is true}, \\ N\mu_0, & \text{if } H_0 \text{ is true} \end{cases} \tag{7.36}$$

$$\text{var}(y^{(k)}) = \begin{cases} N\sigma_1^2, & \text{if } H_1 \text{ is true}, \\ N\sigma_0^2, & \text{if } H_0 \text{ is true} \end{cases} \tag{7.37}$$

If $|\tau^{(k)}| \geq T_c$, hypothesis H_0 is true and the probability density function of $y^{(k)}$ is

$$p_0(y^{(k)}) = \frac{1}{\sqrt{2\pi\sigma_0^2 N}} \exp\left[-\frac{\left(y^{(k)} - N\mu_0\right)^2}{2\sigma_0^2 N}\right] \tag{7.38}$$

If $\tau^{(k)} = 0$, hypothesis H_1 is true and the probability density function of $y^{(k)}$ is

$$p_1(y^{(k)}) = \frac{1}{\sqrt{2\pi\sigma_1^2 N}} \exp\left[-\frac{\left(y^{(k)} - N\mu_1\right)^2}{2\sigma_1^2 N}\right] \tag{7.39}$$

The log-likelihood ratio test is

$$\ln \frac{p_1(y^{(k)})}{p_0(y^{(k)})} = \frac{(y^{(k)})^2}{2N}\left(\frac{1}{\sigma_0^2} - \frac{1}{\sigma_1^2}\right) + y^{(k)}\left(\frac{\mu_1}{\sigma_1^2} - \frac{\mu_0}{\sigma_0^2}\right) + \frac{N}{2}\left(\frac{\mu_0^2}{\sigma_0^2} - \frac{\mu_1^2}{\sigma_1^2}\right) + \ln\frac{\sigma_0}{\sigma_1} \underset{H_0}{\overset{H_1}{\gtrless}} \theta \tag{7.40}$$

Letting $x = y^{(k)}/N$, we rewrite Formula (7.40) as

$$Ax^2 + 2Bx + C \underset{H_0}{\overset{H_1}{\gtrless}} 0 \tag{7.41}$$

where

$$A = \frac{1}{\sigma_0^2} - \frac{1}{\sigma_1^2} \tag{7.42}$$

$$B = \frac{\mu_1}{\sigma_1^2} - \frac{\mu_0}{\sigma_0^2} \tag{7.43}$$

$$C = \frac{\mu_0^2}{\sigma^2} - \frac{\mu_1^2}{\sigma_1} + \frac{2}{N}\ln\frac{\sigma_0}{\sigma_1} - \frac{2\theta}{N} \tag{7.44}$$

Then the log-likelihood ratio test (7.40) reduces to:

Choose H_0, if $\theta_1 \leq x < \theta_2$
Choose H_1, otherwise

Here

$$\begin{aligned} \theta_1 &= -\frac{B}{A} - D \\ \theta_2 &= -\frac{B}{A} + D \end{aligned} \tag{7.45}$$

where

$$D = \sqrt{B^2 - AC}/A \tag{7.46}$$

We can chose θ such that D takes values between 0 and ∞, so we can operate with D instead of θ. The false alarm and the detection probabilities are

$$\begin{aligned} P_{\mathrm{F}} &= 1 - \int_{\theta_1}^{\theta_2} \frac{1}{\sqrt{2\pi\sigma_0^2/N}} \exp\left[-\frac{(x-\mu_0)^2}{2\sigma_0^2}N\right] \mathrm{d}x \\ &= 1 - Q\left(\frac{\theta_1 - \mu_0}{\sqrt{\sigma_0^2/N}}\right) + Q\left(\frac{\theta_2 - \mu_0}{\sqrt{\sigma_0^2/N}}\right) \end{aligned} \tag{7.47}$$

$$\begin{aligned} P_{\mathrm{D}} &= 1 - \int_{\theta_1}^{\theta_2} \frac{1}{\sqrt{2\pi\sigma_1^2/N}} \exp\left[-\frac{(x-\mu_1)^2}{2\sigma_1^2}N\right] \mathrm{d}x \\ &= 1 - Q\left(\frac{\theta_1 - \mu_1}{\sqrt{\sigma_1^2/N}}\right) + Q\left(\frac{\theta_2 - \mu_1}{\sqrt{\sigma_1^2/N}}\right) \end{aligned} \tag{7.48}$$

Note that for the considered model the operating characteristic $P_{\mathrm{D}} = P_{\mathrm{D}}(P_{\mathrm{F}})$ does not depend on the power P, so we can assume that $P = 1$.

The decision algorithm for hypothesis testing device of the PPH CDMA system is given by Formula (7.21). Statistic $y^{(k)}$ can be considered as a Gaussian variable because of the central limit theorem. For the Manchester pulse, the first two moments of $y^{(k)}$ can be calculated from (7.19) and (7.20):

$$\begin{aligned} E(y^{(k)}) &= N\sqrt{P^{(k)}} R_h(\tau^{(k)}) \\ \mathrm{var}(y^{(k)}) &= N\sigma^2 = N\left[\frac{N_0}{T_{\mathrm{c}}} + \frac{2}{3}\frac{T_{\mathrm{c}}}{T_{\mathrm{f}}}\sum_{k' \neq k} P^{(k')}\right] \end{aligned} \tag{7.49}$$

where $P^{(k)}$ is the power of the received signal, $R_h(\cdot)$ is the autocorrelation function of pulse $h_{T_{\mathrm{c}}}(\cdot)$, $\tau^{(k)}$ is the time offset, and $N\sigma^2$ is given by Formula (7.20). From (7.21) it follows that the detection probability P_{D} and false alarm probability P_{F} are given by (3.16) and (3.17), respectively, where

$$\rho_{\mathrm{b}} = \rho_{\mathrm{B}} = N\frac{P^{(k)}}{2\sigma^2} R_h(\tau^{(k)}) \tag{7.50}$$

In particular, perfect synchronization ($\tau^{(k)} = 0$) corresponds to $\rho_{\mathrm{B}} = NP^{(k)}/2\sigma^2$. The receiver operating characteristic is depicted in Figure 3.1.

7.3 THE ACQUISITION PROCEDURE

Time acquisition is the process of determining the time offset $\delta^{(k)}$ of the spreading signal $a^{(k)}(t - \delta^{(k)})$ in the received signal. To do this, the receiver continuously changes its estimate $\hat{\delta}^{(k)}$ in the despreading signal $a^{(k)}(t - \hat{\delta}^{(k)})$. Based on the autocorrelation function of the spreading signals, a timing step size of Δ, $\Delta \leq T_c$, should be chosen. For example, if $\Delta = T_c$, the correct hypothesis H_1 may be tested with a one-half chip timing error. In the case of rectangular pulses, $R_a^2(\tau)$ may be low by a factor of 6 dB, because $R_a(\Delta/2) = 1/2$. Thus every chip hypothesis can be sampled several times per chip. Then to test all hypotheses over the whole period N_p of the spreading/hopping sequence requires a search over $I = N_p T_c/\Delta$ possible hypotheses. Note that to ensure sufficiently high detection probabilities for acceptable false alarm probabilities as determined in Section 7.2, each test requires integration over an interval $T_{tp} = \nu N T_c$, where T_{tp} is the *test period*. Thus the total acquisition time, T_a, is proportional to T_{tp}.

In practical systems, all states of the spreading/hopping sequence do not need to be tested. The base station receiver usually has a reasonable estimate of the correct time offset of all users. The call initiator informs the base station of its intention to communicate by sending its identifying initial vector over an auxiliary channel. In such cases, the parameter I equals the number of chip hypotheses to be tested rather than the multiple of the period of the pseudorandom sequence.

The serial search state diagram is shown in Figure 7.6. The zero-labeled node at the top of the state diagram represents the *correct state*. By definition, this is the

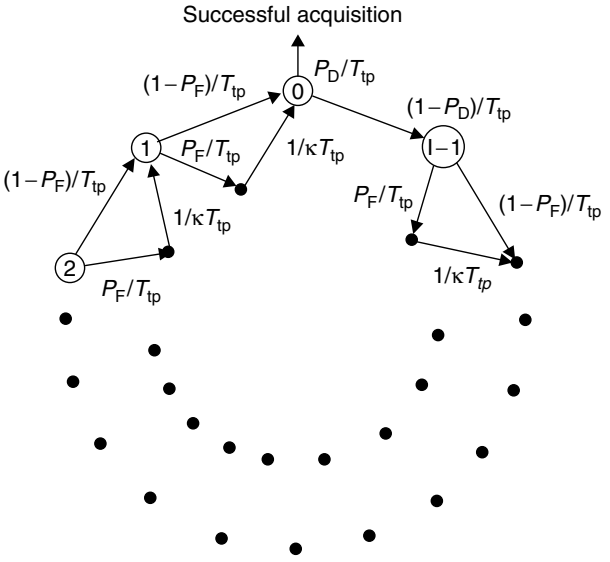

Figure 7.6. The serial search state diagram.

state where $|\hat{\delta}^{(k)} - \delta^{(k)}|$ has a minimum or, equivalently, where $R_a(\hat{\delta}^{(k)} - \delta^{(k)})$ has a maximum. In this point $|\hat{\delta}^{(k)} - \delta^{(k)}| \leq \Delta/2$, where Δ is the timing step size. All other states labeled by $1, 2, \ldots I-1$ on the outer circle represent the $I-1$ *incorrect states*. The states on the inner dotted circle represent *false alarm states* reached as a result of the acceptance of an incorrect hypothesis. We assume that the acquisition device will stay in a false alarm state κ test periods, that is, κT_{tp} seconds *(false alarm penalty)*, during which an auxiliary device recognizes that the timing acquisition is still not reached. Note that the state where the search began can be any of the I states on the outer circle.

The search proceeds until acquisition is reached, that is, hypothesis H_1 is accepted in the correct state. The label on each branch between two nodes indicates the probability of that particular transition and the test period required for making the given transition. (Each test period equals $T_{tp} = \nu N T_c$ seconds.) We suppose that the false alarm probability P_F is the same for all incorrect states. In this section we also assume that there is only one correct state. This gives a slightly pessimistic estimation of the search characteristics.

The acquisition parameter of greatest interest is the total search time required to find the correct timing (within less than T_c). The search (acquisition) time, T_a, is a random variable equal to the sum of the transition times on the path taken in the state diagram, from any of the equally likely initial states to the final correct state. We first find the average search time, $M_a = E[T_a]$.

We start with the consideration of an idealized "genie-aided" situation, where $\Delta = T_c$ and the correct chip sampling occurs at the peak ($R_a(\tau^{(k)}) = 1$, for $\tau^{(k)} = \hat{\delta}^{(k)} - \delta^{(k)} = 0$) and thus only one sample per chip suffices.

The average time of the transition from the ith (incorrect) state to the $(i-1)$th state, $i = 1, 2, \ldots I-1$, is equal

$$m_{in} = (1 - P_F)T_{tp} + P_F(\kappa + 1)T_{tp} = T_{tp}(1 + \kappa P_F) \tag{7.51}$$

The conditional mean time of the first passage to the correct state, given that the initial state is the ith state, $i = 1, \ldots I-1$, is equal to

$$im_{in} = iT_{tp}(1 + \kappa P_F) \tag{7.52}$$

Because all the initial states are equally likely, the unconditional expectation of the first passage time to the correct state $M_{fp} = E(T_{fp})$ equals

$$M_{fp} = \frac{1}{I}\sum_{i=1}^{I-1} iT_{tp}(1 + \kappa P_F) = \frac{I-1}{2}T_{tp}(1 + \kappa P_F) \tag{7.53}$$

Let us designate M_c as the conditional expectation of the search time given that the search starts in the correct (zero) state, $M_c = E[T_a|\text{start in correct state}]$. Then

$$M_c = P_D T_{tp} + (1 - P_D)[T_{tp} + (I-1)m_{in} + M_c] \tag{7.54}$$

From (7.54) we have

$$\begin{aligned} M_c &= \frac{T_{tp} + (1 - P_D)(I - 1)m_{in}}{P_D} \\ &= \frac{1 - P_D}{P_D}(I - 1)m_{in} + \frac{T_{tp}}{P_D} \\ &= \frac{1 - P_D}{P_D}(I - 1)T_{tp}(1 + \kappa P_F) + \frac{T_{tp}}{P_D} \end{aligned} \tag{7.55}$$

Finally, from (7.53) and (7.55) we get that the average time to acquisition, $M_a = E(T_a)$, is equal to

$$M_a = M_c + M_{fp} = (I - 1)\frac{2 - P_D}{2P_D}T_{tp}(1 + P_F\kappa) + \frac{T_{tp}}{P_D} \tag{7.56}$$

This expression for the mean acquisition time is a function of the false alarm probability P_F and the detection probability P_D. They are computed from the expressions given in Section 7.2. Using the receiver operating characteristic of the hypothesis testing device, namely, $P_D(P_F)$, we can minimize the average acquisition time.

EXAMPLE 7.1

Find the minimum acquisition time for the "genie-aided" DS CDMA system operating in the Rayleigh channel. Assume that correct chip sampling occurs at the peak $(R_a(\tau^{(k)}) = 1)$, $\Delta = T_c$, $N_p = 1023$, $T_{tp} = 0.1$ μs, $\nu = 1$, $\kappa = 100$, *and* $\rho_B = 10$ (dB).

Solution

From Formulas (7.30) and (7.33) we have for $\nu = 1$

$$P_F = P_D^{1+\rho_B} = P_D^{11}$$

Then, because $I = N_p$, *we get from (7.56)*

$$\begin{aligned} M_a &= \left[\frac{N_p}{P_D} - \frac{(N_p - 1)}{2}P_F\kappa + (N_p - 1)\frac{P_F}{P_D}\kappa - \frac{N_p - 1}{2}\right]T_{tp} \\ &\approx \left[\frac{1}{P_D} - \frac{P_F}{2}\kappa + \frac{P_F}{P_D}\kappa - \frac{1}{2}\right]N_pT_{tp} \\ &= \left[P_D^{-1} - \frac{P_D^{1+\rho_B}}{2}\kappa + P_D^{\rho_B}\kappa - \frac{1}{2}\right]N_pT_{tp} \end{aligned} \tag{7.57}$$

The minimum of the right-hand side of (7.57) occurs for $P_D = 0.55$ *and is equal to* 0.15 *ms.*

EXAMPLE 7.2

Estimate the acquisition time for the "genie-aided" FH CDMA system with the receiver given in Figure 7.3. The system parameters are $T_c = 0.1$ μs, $N = N_p = 1023$, $\nu = 1$, $\Delta = T_c$, $\kappa = 100$, $K - 1 = M$. *Neglect the background noise. Use the Gaussian approximation for the distribution of the decision statistics.*

Solution

We use Formula (7.57), where $T_{tp} = N_p T_c$; *the false alarm probability* P_F *and detection probability* P_D *are defined by (7.47) and (7.48), respectively. The parameter* $-B/A$ *in (7.45) is equal* 0.2. *Then* M_a *approaches minimum for* $D = 1$ *and the minimum equals* 51.15 *ms.*

Besides the mean of the acquisition time, the probability density function and the moments of this random variable are of interest. Let $P_i(t)$, $i = 0, 1, 2, \ldots, I-1$, be the conditional probability that acquisition time is equal to t, given that the search starts in the ith state. (If κ is an integer, the acquisition time is a multiple of T_{tp}.) Then for an incorrect state we get

$$P_i(t) = (1 - P_F)P_{i-1}(t - T_{tp}) + P_F P_{i-1}(t - (\kappa + 1)T_{tp}), \quad i = 1, 2, \ldots, I-1 \tag{7.58}$$

For the correct state ($i = 0$) we have

$$P_0(t) = \begin{cases} P_D, & \text{if } t = T_{tp} \\ (1 - P_D) \cdot P_{I-1}(t - T_{tp}), & \text{if } t \neq T_{tp} \end{cases} \tag{7.59}$$

Let us introduce the *generating function* of the distribution $P_i(t)$:

$$G_i(z) \stackrel{\text{def}}{=} \sum_{\text{all } t} P_i(t) z^t \tag{7.60}$$

From (7.58) we have

$$\begin{aligned} G_i(z) &= (1 - P_F)z^{T_{tp}} G_{i-1}(z) + P_F z^{(\kappa+1)T_{tp}} G_{i-1}(z) \\ &= H_{in}(z) G_{i-1}(z), \quad i = 1, 2, \ldots, I-1 \end{aligned} \tag{7.61}$$

where

$$H_{in}(z) = (1 - P_F)z^{T_{tp}} + P_F z^{(\kappa+1)T_{tp}} \tag{7.62}$$

is the *transfer function* of an incorrect state. Analogously from (7.59) we get

$$\begin{aligned} G_0(z) &= P_D z^{T_{tp}} + (1 - P_D)z^{T_{tp}} G_{I-1}(z) \\ &= H_c^{(D)}(z) + H_c^{(M)}(z) G_{I-1}(z) \end{aligned} \tag{7.63}$$

where

$$\begin{aligned} H_{\mathrm{c}}^{(\mathrm{D})}(z) &= P_{\mathrm{D}} z^{T_{\mathrm{tp}}} \\ H_{\mathrm{c}}^{(\mathrm{M})} &= (1 - P_{\mathrm{D}}) z^{T_{\mathrm{tp}}} \end{aligned} \tag{7.64}$$

are the *correct-hypothesis-detected and correct-hypothesis-missing transfer functions*, respectively. For the purpose of computing the generating function, only the nodes of the outer circle need to be considered, connected by the branch transfer function $H_{\mathrm{in}}(z)$. This applies to all cases except to the branches coming from the correct state at the top of the circle, which are labeled by $H_{\mathrm{c}}^{(\mathrm{D})}(z)$ and $H_{\mathrm{c}}^{(\mathrm{M})}(z)$ (see Fig. 7.7).

From (7.61) and (7.63) it follows that

$$G_i(z) = [H_{\mathrm{in}}(z)]^i G_0(z), \quad i = 1, 2, \ldots, I-1 \tag{7.65}$$

and

$$G_0(z) = H_{\mathrm{c}}^{(\mathrm{D})}(z) + H_{\mathrm{c}}^{(\mathrm{M})}(z)[H_{\mathrm{in}}(z)]^{I-1} G_0(z) \tag{7.66}$$

The generating function for the correct state is obtained from Formula (7.66)

$$G_0(z) = \frac{H_{\mathrm{c}}^{(\mathrm{D})}(z)}{1 - H_{\mathrm{c}}^{(\mathrm{M})}(z)[H_{\mathrm{in}}(z)]^{I-1}} \tag{7.67}$$

Thus

$$G_i(z) = \frac{H_{\mathrm{c}}^{(\mathrm{D})}(z)[H_{\mathrm{in}}(z)]^i}{1 - H_{\mathrm{c}}^{(\mathrm{M})}(z)[H_{\mathrm{in}}(z)]^{I-1}}, \quad i = 0, 1, \ldots, I-1 \tag{7.68}$$

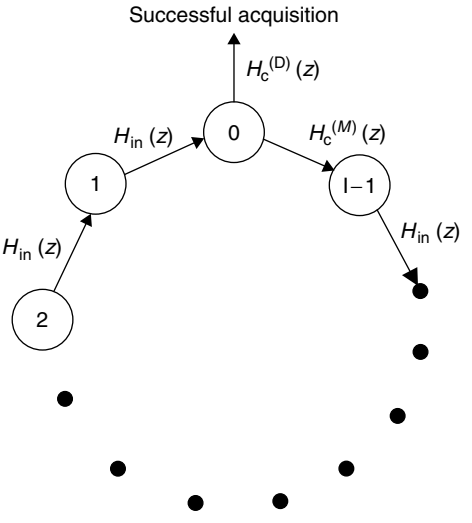

Figure 7.7. The reduced search state diagram.

Now, because all states are a priori equally likely, the generating function for the unconditional probability function of the acquisition time

$$P(t) = \frac{1}{I}\sum_{i=0}^{I-1} P_i(t) \tag{7.69}$$

is obtained by averaging over all I starting states

$$G(z) = \frac{1}{I}\sum_{i=0}^{I-1} G_i(z) = \frac{H_{\mathrm{c}}^{(\mathrm{D})}(t)\{1-[H_{\mathrm{in}}(z)]^I\}}{I[1-H_{\mathrm{in}}(z)]\{1-H_{\mathrm{c}}^{(\mathrm{M})}(z)[H_{\mathrm{in}}(z)]^{I-1}\}} \tag{7.70}$$

The average acquisition time (7.56) can also be obtained from the generating function

$$E[T_{\mathrm{a}}] = M_{\mathrm{a}} = \sum_{\text{all } t} t\,P(t) = \left.\frac{\mathrm{d}G(z)}{\mathrm{d}z}\right|_{z=1} \tag{7.71}$$

Taking the second derivative yields the difference between the second and the first moment,

$$\left.\frac{\mathrm{d}^2G(z)}{\mathrm{d}z^2}\right|_{z=1} = \sum_{\text{all } t} t(t-1)P(t) = E[T_{\mathrm{a}}^2] - E[T_{\mathrm{a}}] \tag{7.72}$$

Hence, it follows that the variance of the acquisition time is

$$\mathrm{var}[T_{\mathrm{a}}] = E[T_{\mathrm{a}}^2] - [E[T_{\mathrm{a}}]]^2 = \left.\left\{\frac{\mathrm{d}^2G(z)}{\mathrm{d}z^2} + \frac{\mathrm{d}G(z)}{\mathrm{d}z}\left[1 - \frac{\mathrm{d}G(z)}{\mathrm{d}z}\right]\right\}\right|_{z=1} \tag{7.73}$$

7.4 MODIFICATIONS OF THE ACQUISITION PROCEDURE

The results up to this point have been derived by assuming that exactly one state corresponds to correct timing, meaning acquisition to within less than T_{c}. Consider now the actual situation in which over each chip duration T_{c} multiple timing hypotheses are serially tested for timing step size Δ, $\Delta < T_{\mathrm{c}}$. For this case, the number of correct states is equal to λ, $2\,T_{\mathrm{c}}/\Delta \le \lambda < 2\,T_{\mathrm{c}}/\Delta + 1$. From the total number $I = N_{\mathrm{p}}T_{\mathrm{c}}/\Delta$ of states, λ states are correct and $I - \lambda$ are incorrect. Each of the λ correct states within one chip of the correct timing appears in the state diagram with its own detection probability $P_{\mathrm{D}i}$, $i = 0, 1, \ldots, \lambda - 1$, depending on the parameter $R_a(\hat{\delta}_i^{(k)} - \delta^{(k)})$, where

$$|\hat{\delta}_i^{(k)} - \delta^{(k)}| < T_{\mathrm{c}}, \quad |\hat{\delta}_{i+1}^{(k)} - \hat{\delta}_i^{(k)}| = \Delta$$

If $2/(2\ell+1) < \Delta/T_{\mathrm{c}} \le 2/(2\ell-1)$, $\ell = 1, 2, \ldots$, the worst case corresponds to $\lambda = 2\ell$ and to sampling times that differ from the peak time by

$$(i - \ell + \tfrac{1}{2})\Delta, \quad i = 0, 1, \ldots, \lambda - 1 \tag{7.74}$$

If $|\hat{\delta}_i^{(k)} - \delta^{(k)}| \geq T_c$, that is, the timing is incorrect, the false alarm probability P_F in our models does not depend on the state. The conditional probability that the search time is equal to t, given that the search starts in the ith (of the λ correct) states, is equal to

$$P_i(t) = \begin{cases} P_{D_i}, & t = T_{tp}, \\ (1 - P_{D_i})P_{i-1}(t - T_{tp}), & t \neq T_{tp} \end{cases} \tag{7.75}$$

for $i = 1, 2, \ldots, \lambda - 1$, and

$$P_0(t) = \begin{cases} P_{D_0}, & t = T_{tp}, \\ (1 - P_{D_0})P_{I-1}(t - T_{tp}), & t \neq T_{tp} \end{cases} \tag{7.76}$$

for $i = 0$. Here P_{D_i}, $i = 0, 1, \ldots, \lambda - 1$, is the detection probability for the ith (correct) state.

The conditional probability that the acquisition time is t, given that the search starts in the ith (incorrect) state, $i = \lambda, \lambda + 1, \ldots, I - 1$, is defined by Formula (7.58). Then the generating function $G_i(z)$ of the distribution $P_i(t)$ for $i = \lambda, \lambda + 1, \ldots, I - 1$ is defined by (7.61).

From (7.75) and (7.76) we have

$$G_i(z) = P_{D_i} z^{T_{tp}} + (1 - P_{D_i}) z^{T_{tp}} G_{i-1}(z) \ , \quad i = 1, 2, \ldots, \lambda - 1 \tag{7.77}$$

$$G_0(z) = P_{D_0} z^{T_{tp}} + (1 - P_{D_0}) z^{T_{tp}} G_{I-1}(z), \tag{7.78}$$

or

$$G_i(z) = H_{c,i}^{(D)}(z) + H_{c,i}^{(M)}(z) G_{I-1}(z), \quad i = 0, 1, \ldots, \lambda - 1 \tag{7.79}$$

where

$$H_{c,i}^{(D)}(z) = \sum_{\ell=0}^{i} P_{D_\ell} z^{T_{tp}} \prod_{j=0}^{\ell-1} [(1 - P_{D_j}) z^{T_{tp}}] \tag{7.80}$$

and

$$H_{c,i}^{(M)}(z) = z^{(i+1)T_{tp}} \prod_{\ell=0}^{i} (1 - P_{D_\ell}), \quad i = 0, 1, \ldots, \lambda - 1 \tag{7.81}$$

The λ states of the correct timing appear in the state diagram as shown in Figure 7.8, together with the transfer functions of branches emanating from these nodes.

Analogously to Formula (7.65) we get

$$G_i(z) = [H_{in}(z)]^{i-\lambda+1} G_{\lambda-1}(z), \ \ i = \lambda, \lambda + 1, \ldots, I - 1 \tag{7.82}$$

where $H_{in}(z)$ is defined by (7.62). Analogously to (7.66) we have from (7.79) and (7.82) that

$$\begin{aligned} G_{\lambda-1}(z) &= H_{c,\lambda-1}^{(D)}(z) + H_{c,\lambda-1}^{(M)}(z) G_{I-1}(z) \\ &= H_{c,\lambda-1}^{(D)}(z) + H_{c,\lambda-1}^{(M)}(z) [H_{in}(z)]^{I-\lambda} G_{\lambda-1}(z) \end{aligned} \tag{7.83}$$

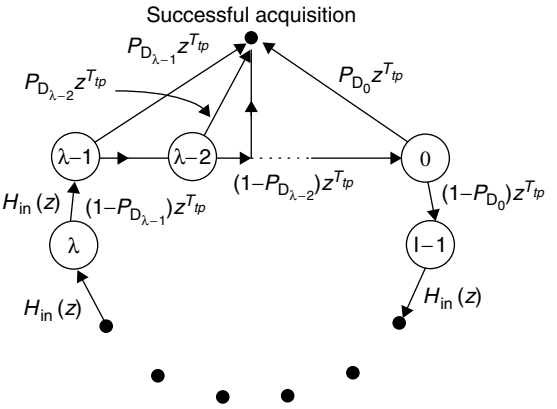

Figure 7.8. The complete serial search state diagram.

or

$$G_{\lambda-1}(z) = \frac{H^{(D)}_{c,\lambda-1}(z)}{1 - H^{(M)}_{c,\lambda-1}(z)[H_{in}(z)]^{I-\lambda}} \tag{7.84}$$

Because all states are a priori equally likely, the generating function for the unconditional probability function (7.69) is

$$\begin{aligned} G(z) &= \frac{1}{I}\sum_{i=0}^{I-1} G_i(z) = \frac{1}{I}\sum_{i=\lambda}^{I-1} G_i(z) + \frac{1}{I}\sum_{i=0}^{\lambda-1} G_i(z) \\ &= \frac{1}{I}\sum_{i=\lambda}^{I-1} [H_{in}(z)]^{i-\lambda+1} G_{\lambda-1}(z) + \frac{1}{I}\sum_{i=0}^{\lambda-1} H^{(D)}_{c,i}(z) \\ &\quad + \frac{1}{I}\sum_{i=0}^{\lambda-1} H^{(M)}_{c,i}(z)[H_{in}(z)]^{I-\lambda} G_{\lambda-1}(z) \\ &= \frac{1}{I}\frac{H_{in}(z)\{1 - [H_{in}(z)]^{I-\lambda}\}}{1 - H_{in}(z)}\, G_{\lambda-1}(z) + \frac{1}{I} H^{(D)}_c(z) \\ &\quad + \frac{1}{I}\, H^{(M)}_c(z)[H_{in}(z)]^{I-\lambda} G_{\lambda-1}(z) \end{aligned} \tag{7.85}$$

where

$$H^{(D)}_c(z) = \sum_{i=0}^{\lambda-1} H^{(D)}_{c,i}(z) = \sum_{i=0}^{\lambda-1}\sum_{\ell=0}^{i} P_{D_\ell} z^{T_{tp}} \prod_{j=0}^{\ell-1} [(1 - P_{D_j}) z^{T_{tp}}] \tag{7.86}$$

$$H^{(M)}_c(z) = \sum_{i=0}^{\lambda-1} z^{(i+1)T_{tp}} \prod_{\ell=0}^{i} (1 - P_{D_\ell}) \tag{7.87}$$

Thus, assuming all nodes are a priori equally likely, the total transfer function averaged over all I starting nodes is

$$G(z) = \frac{1}{I} H_{\mathrm{c}}^{(\mathrm{D})}(z) + \frac{H_{\mathrm{in}}(z)\{1 - [H_{\mathrm{in}}(z)]^{I-\lambda}\} + [1 - H_{\mathrm{in}}(z)] H_{\mathrm{c}}^{(\mathrm{M})}(z)[H_{\mathrm{in}}(z)]^{I-\lambda}}{I[1 - H_{\mathrm{in}}(z)]\{1 - H_{\mathrm{c},\lambda-1}^{(\mathrm{M})}(z)[H_{\mathrm{in}}(z)]^{I-\lambda}\}} H_{\mathrm{c},\lambda-1}^{(\mathrm{D})}(z) \tag{7.88}$$

The mean time to acquisition and the variance of the time to acquisition are obtained as before from Formulas (7.71) and (7.73). It is clear that the mean time to acquisition can be minimized by an appropriate choice of the threshold θ (on which P_{D} and P_{F} depend) and the parameters T_{tp} and ν. The designer has some degree of control over all these variables. It is not correct to assume that minimum mean time to acquisition will always be achieved with $1 - P_{\mathrm{D}} \ll 1$, so that the correct timing is detected on the first sweep. In some cases, the selection of a moderate detection probability P_{D} will result in a much lower T_{tp} than at high P_{D} and will thus result in reduced average T_{a}, even though several sweeps of the uncertainty region may be required.

Another approach to optimizing the serial search is to perform successive tests with multiple dwell times. Figure 7.9 illustrates this concept. Each state is first checked for a time $T_{\mathrm{tp}} = \nu_1 N T_{\mathrm{c}}$ with a moderate detection probability $\hat{P}_{\mathrm{D}}$. If the test hypothesis H_0 (no synchronization) is accepted, the next timing state is checked. If hypothesis H_1 (synchronization is achieved) is accepted, a larger dwell $\nu_2 N T_{\mathrm{c}}$, $\nu_2 = m\nu_1 > \nu_1$, will be checked. The detection probability $\tilde{P}_{\mathrm{D}}$ of the test is larger than $\hat{P}_{\mathrm{D}}$. If hypothesis H_1 is accepted for the second time, the state is deemed correct (although it may be determined as a false alarm κ time periods later). If the test fails the second threshold, the hypothesis H_1 is discarded and the next state is checked. Fast elimination of unlikely states reduces the average acquisition time, because an incorrect state is quickly eliminated in the first pass.

We consider again an idealized "genie-aided" situation in which the correct chip sampling occurs at the peak ($R(\hat{\delta}^{(k)} - \delta^{(k)}) = R(\tau^{(k)}) = 1$) and only one sample per chip suffices. The conditional probability that the search time is equal to t, given that the search is in the ith incorrect state, is equal to

$$\begin{aligned} P_i(t) = {} & (1 - \hat{P}_{\mathrm{F}}) P_{i-1}(t - T_{\mathrm{tp}}) + \hat{P}_{\mathrm{F}}(1 - \tilde{P}_{\mathrm{F}}) P_{i-1}(t - (1+m)T_{\mathrm{tp}}) \\ & + \hat{P}_{\mathrm{F}} \tilde{P}_{\mathrm{F}} P_{i-1}(t - (1 + m + \kappa)T_{\mathrm{tp}}), \quad i = 1, 2, \ldots, I-1 \end{aligned} \tag{7.89}$$

where $\hat{P}_{\mathrm{F}}$ and $\tilde{P}_{\mathrm{F}}$ are false alarm probabilities for the first and second dwells, respectively.

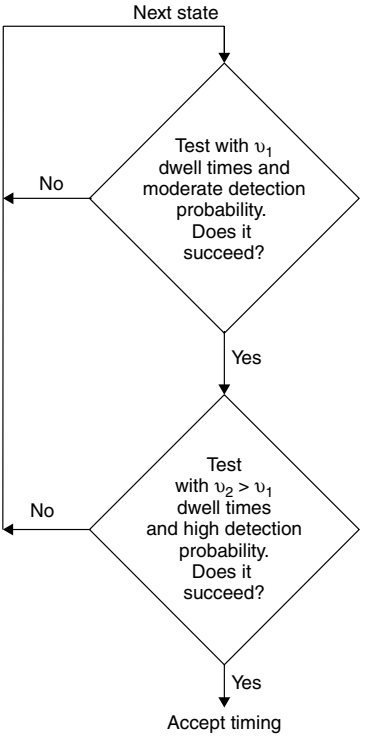

Figure 7.9. Two-dwell serial search.

For the correct state we have

$$P_0(t) = \begin{cases} \hat{P}_{\mathrm{D}}\tilde{P}_{\mathrm{D}}, & t = (1+m)T_{\mathrm{tp}} \\ \hat{P}_{\mathrm{D}}(1-\tilde{P}_{\mathrm{D}})P_{I-1}(t-(1+m)T_{\mathrm{tp}}) & \\ +(1-\hat{P}_{\mathrm{D}})P_{I-1}(t-T_{\mathrm{tp}}), & t \neq (1+m)T_{\mathrm{tp}},\ t > 0 \end{cases} \tag{7.90}$$

where $\hat{P}_{\mathrm{D}}$ and $\tilde{P}_{\mathrm{D}}$ are the detection probabilities for the first and second dwells, respectively.

From Formula (7.90) it follows that the correct-hypothesis-detected and the correct-hypothesis-missing transfer functions are given by

$$H_{\mathrm{c}}^{(\mathrm{D})}(z) = \hat{P}_{\mathrm{D}}\tilde{P}_{\mathrm{D}}z^{T_{\mathrm{tp}}+mT_{\mathrm{tp}}}, \tag{7.91}$$

$$H_{\mathrm{c}}^{(\mathrm{M})}(z) = \hat{P}_{\mathrm{D}}(1-\tilde{P}_{\mathrm{D}})z^{T_{\mathrm{tp}}+mT_{\mathrm{tp}}} + (1-\hat{P}_{\mathrm{D}})z^{T_{\mathrm{tp}}}, \quad i = 0, 1, \ldots, \nu-1 \tag{7.92}$$

respectively. For the incorrect hypothesis branches we have

$$H_{\text{in}}(z) = z^{T_{\text{tp}}}(1 - \hat{P}_{\text{F}}) + z^{T_{\text{tp}}+mT_{\text{tp}}}\hat{P}_{\text{F}}(1 - \tilde{P}_{\text{F}}) + z^{T_{\text{tp}}+mT_{\text{tp}}+\kappa T_{\text{tp}}}\hat{P}_{\text{F}}\tilde{P}_{\text{F}} \qquad (7.93)$$

The state diagram is the same as for the single dwell time in Figure 7.7 but with the branch transfer functions defined as above, with $\hat{}$ and $\tilde{}$ indicating the first and second dwells, respectively.

In all other respects, the procedure for computing the generating function of the acquisition distribution time is the same as for the single-dwell case. Particularly, for the two-dwell case, the generating function $G(z)$ is obtained by replacing the $H(z)$ terms in Formula (7.88) by (7.91)–(7.93). The superiority of the two-dwell search, which may be generalized to multiple dwells, over the one-dwell search depends on the application and on the optimization of parameters [43].

All the results up to this point have been derived by assuming that the received spreading/hopping waveform timing delay τ is uniformly distributed over a particular uncertainty region. Suppose now that the a priori probability density function $f(\tau)$ for the received signal timing delay τ is a unimodal symmetric function such that $f(\tau) = f(-\tau)$ with maximum at $\tau = 0$; it is defined for

$$-\frac{N_{\text{p}}T_{\text{c}}}{2} \le \tau < \frac{N_{\text{p}}T_{\text{c}}}{2}$$

and satisfies the condition

$$\int_{-\frac{N_{\text{p}}T_{\text{c}}}{2}}^{\frac{N_{\text{p}}T_{\text{c}}}{2}} f(\tau)\,\mathrm{d}\tau = 1$$

When $f(\tau)$ is known, a sweep strategy should be used that searches the most likely state first and then the less likely states. Such modified sweep strategies have been used for many years in radar applications. Their usage results in a reduction of the average search time when the distribution of the received signal phase is nonuniform.

Suppose that the interval $[-N_{\text{p}}T_{\text{c}}/2,\ N_{\text{p}}T_{\text{c}}/2)$ is divided into $2I + 1$ (I a positive integer) segments such that $2I + 1 = N_{\text{p}}T_{\text{c}}/\Delta$ and

$$p_i = \int_{\left(i-\frac{1}{2}\right)\Delta}^{\left(i+\frac{1}{2}\right)\Delta} f(\tau)\,\mathrm{d}\tau,\ \ i = 0, \pm 1, \ldots, \pm I \qquad (7.94)$$

We consider again the idealized "genie-aided" situation when the correct chip sampling occurs at the peak ($R(\tau) = 1$) and only one sample per chip suffices. Then the serial search state diagram has $2I + 1$ states, and the probability that the ith state, $i = 0, \pm 1, \ldots, \pm I$, is the correct state is equal to p_i. A reasonable search strategy would be to start with the most likely zero state (zeroth sweep), and then expand the search to the states $-1, 0, 1$ (first sweep), $-2, -1, 0, 1, 2$ (second sweep), and so on. In other words, on the kth sweep, $k = 0, 1, \ldots, I$, we

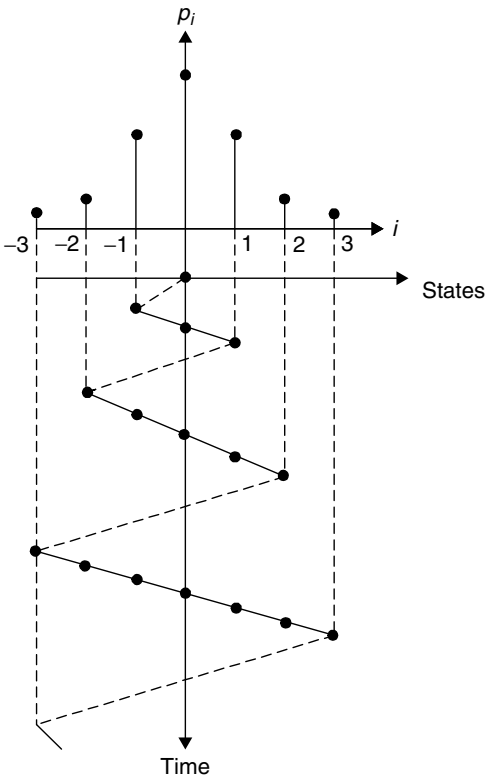

Figure 7.10. The received signal timing probability distribution and a possible sweep strategy.

search the $(2k+1)$ states, $-k, -k+1, \ldots, 0, 1, \ldots k$, if the correct timing has not been reached earlier (Fig. 7.10). Suppose that the ith state is the correct state. This state will be checked for the first time on the $|i|$th sweep. Correspondingly, before coming to this state we have to search i^2 incorrect states if i is negative and $i^2 + 2i$ incorrect states if i is positive. The average time of the first passage to the correct state, given that the ith state is correct, is equal to

$$M_{\text{fp}}(i) = \begin{cases} i^2 m_{\text{in}}, & \text{if } i \text{ is negative} \\ (i^2 + 2i) m_{\text{in}}, & \text{if } i \text{ is positive} \end{cases} \tag{7.95}$$

where m_{in} is given by Formula (7.51).

The unconditional average first passage time, M_{fp}, is

$$M_{\text{fp}} = \sum_{i=-I}^{I} p_i M_{\text{fp}}(i) = m_{\text{in}} \left(\sum_{i=-I}^{I} i^2 p_i + 2 \sum_{i=0}^{I} i p_i \right) = m_{\text{in}} (\sigma_a^2 + \delta) \tag{7.96}$$

where

$$\sigma_a^2 = \sum_{i=-I}^{I} i^2 p_i \tag{7.97}$$

is the variance of the probability distribution $\{p_i\}$ and

$$\delta = 2\sum_{i=0}^{I} i p_i = \sum_{i=-I}^{I} |i| p_i \tag{7.98}$$

Let us designate the conditional expectation of the search time given that the search starts from the correct state on the kth sweep, $k = 0, 1, \ldots, I-1$, as $M_c(k)$. With probability P_D the correct timing will be established after T_{tp} seconds. With probability $1 - P_D$ the system should proceed with the next sweep, that is, to check $(2k+1)$ incorrect states and then repeat the checking of the correct state on the $(k+1)$th sweep. Then we have

$$\begin{aligned} M_c(k) &= P_D T_{tp} + (1 - P_D)[T_{tp} + (2k+1)m_{in} + M_c(k+1)] \\ &= T_{tp} + (1 - P_D)[(2k+1)m_{in} + M_c(k+1)], \quad k = 0, 1, \ldots, I-1 \end{aligned} \tag{7.99}$$

$$M_c(I) = \frac{1 - P_D}{P_D} 2I m_{in} + \frac{T_{tp}}{P_D} \tag{7.100}$$

The last equation is analogous to (7.55). It can be verified that the solution of the system (7.99) and (7.100) is

$$\begin{aligned} M_c(k) = M_c(I)(1 - P_D)^{I-k} + T_{tp}\frac{1 - (1 - P_D)^{I-k}}{P_D} \\ + 2m_{in}\sum_{i=k}^{I-1} i(1 - P_D)^{i-k+1} + m_{in}\frac{(1 - P_D) - (1 - P_D)^{I-k+1}}{P_D} \end{aligned} \tag{7.101}$$

If the ith state is the correct state, then this state will be checked for the first time on the $|i|$th sweep. The expectation of the duration of the search that starts in the correct state is

$$\begin{aligned} M_c = \sum_{i=-I}^{I} p_i M_c(|i|) = \left[M_c(I) - \frac{T_{tp}}{P_D} - m_{in}\frac{1 - P_D}{P_D}\right]\sum_{i=-I}^{I} p_i (1 - P_D)^{I-|i|} \\ + 2m_{in}\sum_{i=-I}^{I} p_i \sum_{j=|i|}^{I-1} j(1 - P_D)^{j-|i|+1} + \frac{T_{tp}}{P_D} + m_{in}\frac{1 - P_D}{P_D} \end{aligned} \tag{7.102}$$

If the probability p_i is decreasing fast enough with $|i|$, such that for large $|i|$

$$p_i \ll (1 - P_D)^{|i|-I} \tag{7.103}$$

we can neglect the first term in (7.102).

To estimate the second term, we note that for $i \geq 0$

$$\sum_{j=i}^{I-1} j(1 - P_D)^{j-i+1} = -I\frac{(1 - P_D)^{I-i}}{P_D} + i\frac{1 - P_D}{P_D} + \left(\frac{1 - P_D}{P_D}\right)^2 \left[1 - (1 - P_D)^{I-i}\right] \tag{7.104}$$

If (7.103) is fulfilled, then we get from Formula (7.104)

$$\begin{aligned} 2m_{in} \sum_{i=-I}^{I} p_i \sum_{j=|i|}^{I-1} j(1 - P_D)^{j-|i|+1} &\approx 2m_{in}\frac{1 - P_D}{P_D} \sum_{i=-I}^{I} p_i|i| + 2m_{in}\left(\frac{1 - P_D}{P_D}\right)^2 \\ &= 2m_{in}\frac{1 - P_D}{P_D}\delta + 2m_{in}\left(\frac{1 - P_D}{P_D}\right)^2 \end{aligned} \tag{7.105}$$

Then

$$M_c \approx \frac{T_{tp}}{P_D} + m_{in}\frac{1 - P_D}{P_D} + 2m_{in}\frac{1 - P_D}{P_D}\delta + 2m_{in}\left(\frac{1 - P_D}{P_D}\right)^2 \tag{7.106}$$

The average time to acquisition $M_a = E[T_a]$ is equal to the sum of the average first passage time and the average search time that starts in the correct state

$$M_a = M_{fp} + M_c \simeq \frac{T_{tp}}{P_D} + m_{in}\left[\sigma_a^2 + \frac{2 - P_D}{P_D}\delta + \frac{1 - P_D}{P_D} + 2\left(\frac{1 - P_D}{P_D}\right)^2\right] \tag{7.107}$$

EXAMPLE 7.3

Consider the same problem as in Example 7.1. Assume that the a priori probability density function of the timing delay τ *can be approximated by the Gaussian probability density function* $f(\tau) = \left(1/\sqrt{2\pi\sigma^2}\right)\exp(-\tau^2/2\sigma^2)$*, where* $\sigma^2 = 25T_c^2$, $-512T_c \leq \tau < 512T_c$. *Find the average acquisition time if the system uses a hypothesis testing device with the same parameters (*P_D *and* P_F*) as in Example 7.1.*

Solution

From (7.94), (7.97), and (7.98) we have

$$\sigma_a^2 = \sum_{i=-512}^{511} i^2 p_i \approx \frac{1}{T_c^2} \int_{-\infty}^{\infty} \frac{\tau^2}{\sqrt{2\pi\sigma^2}} \exp\left(-\frac{\tau^2}{2\sigma^2}\right) d\tau = \frac{\sigma^2}{T_c^2} = 25$$

$$\delta = \sum_{i=-512}^{511} |i| p_i \approx \frac{1}{T_c} \int_{-\infty}^{\infty} \frac{|\tau|}{\sqrt{2\pi\sigma^2}} \exp\left(-\frac{\tau^2}{2\sigma^2}\right) d\tau = \sqrt{\frac{2}{\pi}} \frac{\sigma}{T_c} \approx 3.99$$

Application of (7.107) gives $M_a = 0.042$ *ms. The average acquisition time is more than a factor of three less than for the conventional strategy.*

In this section, we concentrated on the analysis of the DS CDMA system acquisition receiver. The analysis of acquisition process of the FH and PPH CDMA system is analogous. The optimal choice of the parameters of the decision device is determined by the receiver operating characteristic.

7.5 TIME TRACKING OF SS SIGNALS

Time tracking is one of the most critical functions that is performed at the receiver of a CDMA communication system. If the received signal is out of synchronization by a fraction of a chip, insufficient signal energy will reach the receiver demodulator. In this section, we consider the time tracking device called the "early-late" gate. It exploits the symmetry properties of the signal at the output of the matched filter.

To describe this device, let us consider the unit amplitude rectangular pulse $h_{T_c}(t)$ (2.3). The output of the filter matched to $h_{T_c}(t)$ (see Fig. 2.18) is the normalized autocorrelation function of the pulse (2.15). It attains its maximum value at time $t = 0$ as shown in Figure 7.11.

Of course, this statement is valid for any symmetric pulse shaping, not only a rectangular one. Obviously, the best time to sample the output of the matched filter for a maximum output is at the peak of the correlation function.

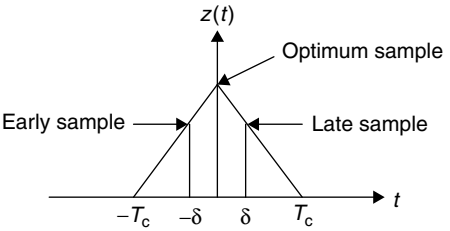

Figure 7.11. The output of the rectangular-matched filter.

In the presence of noise, the determination of the peak value of the signal is difficult. Instead of sampling the signal at $t = 0$, suppose we sample early, at $t = -\delta$ and late, at $t = \delta$ (Fig. 7.11). The outputs of the early sampler $z(-\delta)$ and the late sampler $z(\delta)$ will on the average be smaller than the peak value $z(0)$. Because the autocorrelation function is symmetric with respect to $t = 0$, the samples at $t = -\delta$ and $t = \delta$ are equal. Hence, the proper sampling time is the midpoint between $t = -\delta$ and $t = \delta$.

Figure 7.12 illustrates the block diagram of an early-late gate device for BPSK signals. It is an elaboration of the basic demodulator and acquisition device of the acquisition receiver of Figure 7.1. The early-late gate synchronizer performs the same operation advanced by δ seconds and delayed by δ seconds, where $\delta < T_c$.

The clock timing is maintained by a voltage-controlled oscillator (VCO). The clock frequency of the VCO is controlled by the timing error statistic $y_\delta^{(k)}$, filtered by a digital filter and scaled (see Fig. 7.13). The absolute timing on each chip is equal to the sum of all corrections previously caused by timing errors. Hence, the VCO timing is determined by accumulation over all such previous corrections. The scale factor γ represents the gain introduced in the voltage-to-frequency conversion.

We analyze the early-late gate device in the case of an unfaded AWGN channel and when postdetection integration is absent, that is, $\nu = 1$. Then [compare with Formula (7.4)],

$$\begin{aligned}
\hat{z}_{In}^{(k)} &= \sqrt{P^{(k)}}\, R_a\left(\tau^{(k)} - \delta\right)\cos\varphi^{(k)} + \hat{\xi}_{In}^{(k)} \\
\hat{z}_{Qn}^{(k)} &= \sqrt{P^{(k)}}\, R_a\left(\tau^{(k)} - \delta\right)\sin\varphi^{(k)} + \hat{\xi}_{Qn}^{(k)} \\
\check{z}_{In}^{(k)} &= \sqrt{P^{(k)}}\, R_a\left(\tau^{(k)} + \delta\right)\cos\varphi^{(k)} + \check{\xi}_{In}^{(k)} \\
\check{z}_{Qn}^{(k)} &= \sqrt{P^{(k)}}\, R_a\left(\tau^{(k)} + \delta\right)\sin\varphi^{(k)} + \check{\xi}_{Qn}^{(k)}
\end{aligned} \tag{7.108}$$

where $P^{(k)}$ is the signal power, $R_a(\cdot)$ is the autocorrelation function of the spreading signal, $\hat{\xi}_{In}^{(k)}$, $\hat{\xi}_{Qn}^{(k)}$, $\check{\xi}_{In}^{(k)}$, and $\check{\xi}_{Qn}^{(k)}$ are modified zero-mean noise components with variances $I_0/2T_c$, and I_0 is given by (7.6). Because $\nu = 1$, we can omit the index i of the x statistics. For large N the statistics $\hat{x}_I^{(k)}$, $\hat{x}_Q^{(k)}$, $\check{x}_I^{(k)}$, and $\check{x}_Q^{(k)}$ can be considered as independent Gaussian random variables with expectations [compare with (7.22)]

$$\begin{aligned}
E\left(\hat{x}_I^{(k)}\right) &= N\sqrt{P^{(k)}}R_a\left(\tau^{(k)} - \delta\right)\cos\varphi^{(k)} \\
E\left(\hat{x}_Q^{(k)}\right) &= N\sqrt{P^{(k)}}R_a\left(\tau^{(k)} - \delta\right)\sin\varphi^{(k)} \\
E\left(\check{x}_I^{(k)}\right) &= N\sqrt{P^{(k)}}R_a\left(\tau^{(k)} + \delta\right)\cos\varphi^{(k)} \\
E\left(\check{x}_Q^{(k)}\right) &= N\sqrt{P^{(k)}}R_a\left(\tau^{(k)} + \delta\right)\sin\varphi^{(k)}
\end{aligned} \tag{7.109}$$

respectively, and variances $NI_0/2T_c$.

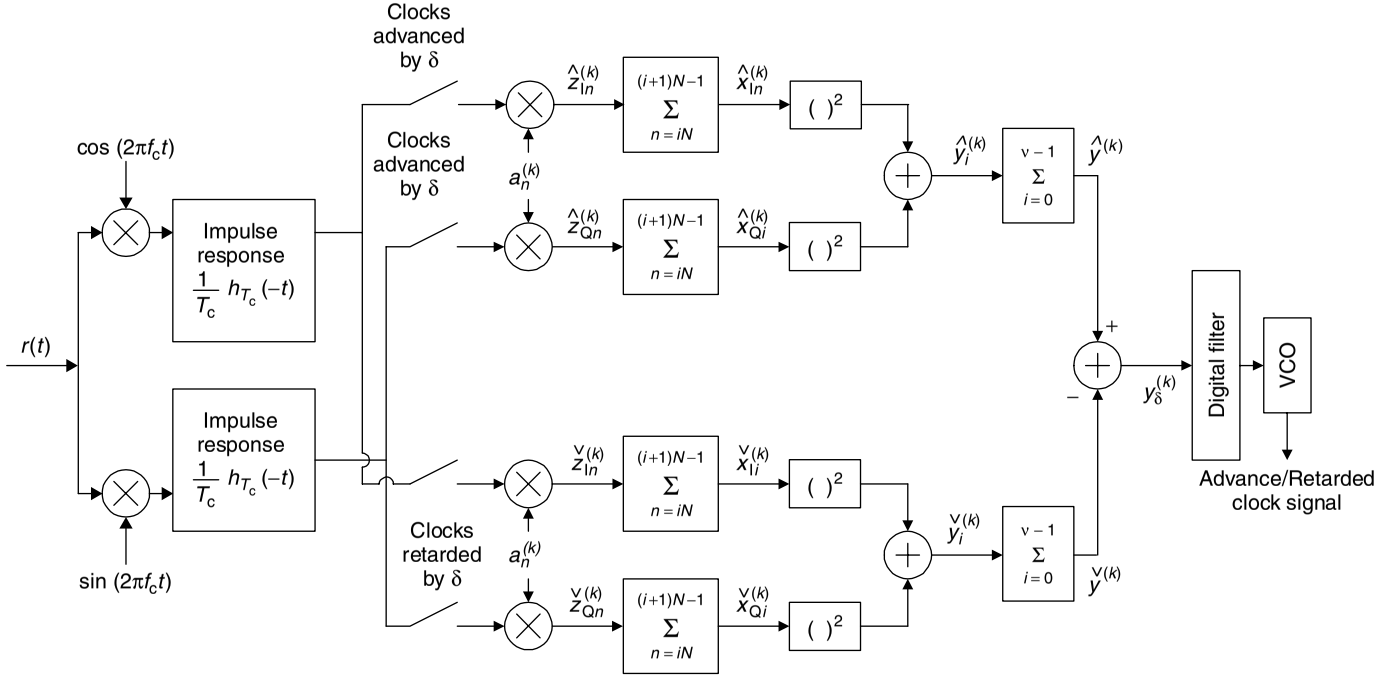

Figure 7.12. Early-late gate device for BPSK signaling.

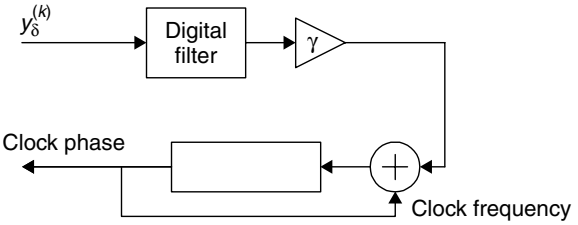

Figure 7.13. The VCO model.

The mean and variance of the advanced measurement statistic $\hat{y}^{(k)}$ can be obtained by a direct but tedious computations as follows:

$$E(\hat{y}^{(k)}) = E[(\hat{x}_{\mathrm{I}}^{(k)})^2] + E[(\hat{x}_{\mathrm{Q}}^{(k)})^2] = N^2 P^{(k)} R_a^2(\tau^{(k)} - \delta) + N I_0 / T_{\mathrm{c}} \quad (7.110)$$

$$E[(\hat{y}^{(k)})^2] = E[(\hat{x}_{\mathrm{I}}^{(k)})^4] + E[(\hat{x}_{\mathrm{Q}}^{(k)})^4] + 2E[(\hat{x}_{\mathrm{I}}^{(k)})^2]E[(\hat{x}_{\mathrm{Q}}^{(k)})^2] \quad (7.111)$$

The squared terms in (7.111) are:

$$\begin{aligned} E[(\hat{x}_{\mathrm{I}}^{(k)})^2] &= N^2 P^{(k)} R_a^2(\tau^{(k)} - \delta)\cos^2\varphi^{(k)} + N I_0 / 2T_{\mathrm{c}} \\ E[(\hat{x}_{\mathrm{Q}}^{(k)})^2] &= N^2 P^{(k)} R_a^2(\tau^{(k)} - \delta)\sin^2\varphi^{(k)} + N I_0 / 2T_{\mathrm{c}} \end{aligned} \quad (7.112)$$

Because the odd moments of the ξ statistics are zero, we have

$$\begin{aligned} E[(\hat{x}_{\mathrm{I}}^{(k)})^4] &= N^4 (P^{(k)})^2 R_a^4(\tau^{(k)} - \delta)\cos^4\varphi^{(k)} \\ &\quad + 2N^3 (I_0/2T_{\mathrm{c}}) P^{(k)} R_a^2(\tau^{(k)} - \delta)\cos^2\varphi^{(k)} + E\left[\left(\sum_{n=0}^{N-1} \hat{\xi}_{\mathrm{I}n}^{(k)}\right)^4\right] \\ E[(\hat{x}_{\mathrm{Q}}^{(k)})^4] &= N^4 (P^{(k)})^2 R_a^4(\tau^{(k)} - \delta)\sin^4\varphi^{(k)} \\ &\quad + 2N^3 (I_0/2T_{\mathrm{c}}) P^{(k)} R_a^2(\tau^{(k)} - \delta)\sin^2\varphi^{(k)} + E\left[\left(\sum_{n=0}^{N-1} \hat{\xi}_{\mathrm{Q}n}^{(k)}\right)^4\right] \end{aligned} \quad (7.113)$$

The fourth moment of the zero-mean Gaussian variable is equal to three times the square of the variance. Consequently, because the $\hat{\xi}_n$ statistics are independent and Gaussian with zero means, we have

$$E\left[\left(\sum_{n=0}^{N-1} \hat{\xi}_{\mathrm{I}n}^{(k)}\right)^4\right] = E\left[\left(\sum_{n=0}^{N-1} \hat{\xi}_{\mathrm{Q}n}^{(k)}\right)^4\right] = 3\left(\frac{N I_0}{2T_{\mathrm{c}}}\right)^2 \quad (7.114)$$

Hence, combining (7.111)–(7.114), we have

$$\begin{aligned} E[(\hat{y}^{(k)})^2] &= N^4 (P^{(k)})^2 R_a^4(\tau^{(k)} - \delta)(\cos^4 \varphi^{(k)} + \sin^4 \varphi^{(k)}) \\ &\quad + N^3 P^{(k)} R_a^2(\tau^{(k)} - \delta) I_0 / 2T_c + 3(N I_0)^2 / 2T_c^2 \\ &\quad + 2N^4 (P^{(k)})^2 R_a^4(\tau^{(k)} - \delta) \cos^2 \varphi^{(k)} \sin^2 \varphi^{(k)} + (N I_0)^2 / 2T_c^2 \\ &\quad + N^3 P^{(k)} R^2(\tau^{(k)} - \delta) I_0 / T_c \\ &= N^4 (P^{(k)})^2 R_a^4(\tau^{(k)} - \delta) + 2N^2 I_0^2 / T_c^2 + 2N^3 P^{(k)} R^2(t^{(k)} - \delta) I_0 / T_c \end{aligned} \tag{7.115}$$

Finally we obtain

$$\begin{aligned} \operatorname{var}(\hat{y}^{(k)}) &= E[(\hat{y}^{(k)})^2] - [E(\hat{y}^{(k)})]^2 \\ &= N^4 (P^{(k)})^2 R_a^4(t^{(k)} - \delta) + 2N^2 I_0^2 / T_c^2 + 2N^3 P^{(k)} R_a^2(t^{(k)} - \delta) I_0 / T_c \\ &\quad - N^4 (P^{(k)})^2 R_a^4(t^{(k)} - \delta) - N^2 I_0^2 / T_c^2 - 2N^3 P^{(k)} I_0 / T_c \\ &\quad - 2N^3 P^{(k)} R_a^2(t^{(k)} - \delta) I_0 / T_c = (N I_0)^2 / T_c^2 \end{aligned} \tag{7.116}$$

The same calculations for $\check{y}^{(k)}$ yield the same results as (7.110) and (7.116), but with $R_a(t^{(k)} - \delta)$ replaced by $R_a(t^{(k)} + \delta)$.

Finally, the mean value and variance of the timing error statistic $y_\delta^{(k)} = \hat{y}^{(k)} - \check{y}^{(k)}$ are

$$E(y_\delta^{(k)}) = N^2 P^{(k)} [R_a^2(t^{(k)} - \delta) - R_a^2(t^{(k)} + \delta)] \tag{7.117}$$

$$\operatorname{var}(y_\delta^{(k)}) \simeq \operatorname{var}(\hat{y}^{(k)}) + \operatorname{var}(\check{y}^{(k)}) = 2 \left(\frac{N I_0}{T_c} \right)^2 \tag{7.118}$$

The reason that the variance of $y_\delta^{(k)}$ only approximately equals the sum of the variances of $\hat{y}^{(k)}$ and $\check{y}^{(k)}$ is that both early and late samplings are based on the same received signal. Thus the correlation of $\hat{y}^{(k)}$ and $\check{y}^{(k)}$ is nonzero.

Given the mean and the variance of the timing error measurement, we can model the effect of applying the measurement as a correction to the clock signal in Figure 7.12. We define the gain function as

$$G(\tau) = R_a^2(\tau - \delta) - R_a^2(\tau + \delta) \tag{7.119}$$

Then, from (7.117) and (7.118) we get

$$\begin{aligned} E(y_\delta^{(k)}) &= N^2 P^{(k)} G(\tau) \\ \operatorname{var}(y_\delta^{(k)}) &\approx 2N^2 I_0^2 / T_c^2 \end{aligned} \tag{7.120}$$

As an example, consider the case when the signal waveforms have rectangular pulse shaping.

EXAMPLE 7.4

Analyze the early-late gate device in Figure 7.12 assuming that the pulses have rectangular shaping.

Solution

For rectangular pulses $R_a(\tau) = 1 - |\tau|/T_c$. *Then, from (7.119) we obtain*

$$\begin{aligned} G(\tau) &= [R_a(\tau-\delta) + R_a(\tau+\delta)][R_a(\tau-\delta) - R_a(\tau+\delta)] \\ &= \left(2 - \frac{|\tau-\delta|}{T_c} - \frac{|\tau+\delta|}{T_c}\right)\left(\frac{|\tau+\delta|}{T_c} - \frac{|\tau-\delta|}{T_c}\right) \\ &= \begin{cases} -4\left(1+\dfrac{\tau}{T_c}\right)\dfrac{\delta}{T_c}, & -T_c \le \tau < -\delta, \\ 4\left(1-\dfrac{\delta}{T_c}\right)\dfrac{\tau}{T_c}, & -\delta < \tau < \delta, \\ 4\left(1-\dfrac{\tau}{T_c}\right)\dfrac{\delta}{T_c}, & \delta < \tau < T_c \end{cases} \end{aligned} \tag{7.121}$$

The gain function is plotted in Figure 7.14 for $\delta = 0.25T_c$.

If the tracking error is less than δ *(see Fig. 7.14), we can use a linear model for the analysis. The gain scale factor is equal to* $4N^2P^{(k)}(1-\delta/T_c)/T_c$. *The analysis of the early-late gate device [47] gives the following estimation for the*

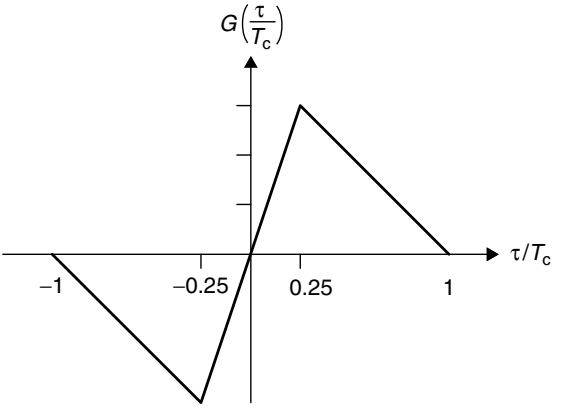

Figure 7.14. The gain function in the rectangular pulse case.

variance of the timing error

$$var(\tau) \approx \frac{2I_0^2\gamma}{P^{(k)} \left.\dfrac{dG(\tau)}{d\tau}\right|_{\tau=0}} = \frac{I_0^2\gamma}{2P^{(k)}(1-\delta/T_c)/T_c} \tag{7.122}$$

where γ is the scale factor in the VCO (see Fig. 7.13).

The early-late gate synchronizer for the QPSK DS CDMA system is analogous to that shown in Figure 7.12 (Problem 7.9). The time tracking for the FH CDMA and PPH systems follows the same scenario as time tracking for the DS CDMA system (Problems 7.10 and 7.11).

7.6 COHERENT RECEPTION OF UPLINK TRANSMITTED SIGNALS IN THE DS CDMA SYSTEM*

One key feature of the cell site transmitter is the inclusion of a pilot signal in the downlink direction. This pilot signal is used by the mobile demodulator to provide a coherent reference, which is effective even in a fading environment because the desired signal and the pilot signal fade together. Although the pilot chips can be used for a coherent reference in the uplink direction (see Section 5.4), a more typical situation is when the uplink transmitted signal does not use a pilot component.

In this section we consider the receivers for reception of a QPSK modulated signal in a DS CDMA system with phase tracking. The receiver, an elaboration of the conventional coherent QPSK receiver (Fig. 3.5), is analyzed when the transmission of data is performed over the AWGN channel. As a reference of coherence, the receivers use the redundancy hidden in these signals. A scheme for extracting the phase information and for the carrier synchronization of the receiver to allow coherent demodulation is presented. Some of the ideas connected with the phase recovering method are well-known in phase-locked loop theory [49], [29], but here they are applied to a specific DS CDMA system.

The uplink transmitted QPSK signal is [compare with (2.111)]

$$s^{(k)}(t) = v^{(k)}(t)[a^{(k)}(t)\cos(2\pi f_c t + \phi^{(k)}) - b^{(k)}(t)\sin(2\pi f_c t + \phi^{(k)})] \tag{7.123}$$

where the code signal $v^{(k)}(t)$ is defined by (2.95) and the spreading signals $a^{(k)}(t)$ and $b^{(k)}(t)$ are defined by (2.106) and (2.107). We assume that the system uses a repetition code of length N and rectangular pulse shaping. The received signal at the base station is given by [compare with (3.81)]

$$\begin{aligned} r(t) = \sqrt{P^{(k)}}\; v^{(k)}(t^{(k)})[a^{(k)}(t^{(k)})\cos(2\pi f_c t^{(k)} + \varphi^{(k)}) \\ - b^{(k)}(t^{(k)})\sin(2\pi f_c t^{(k)} + \varphi^{(k)})] + \xi^{(k)}(t) \end{aligned} \tag{7.124}$$

*This section may be omitted on a first reading.

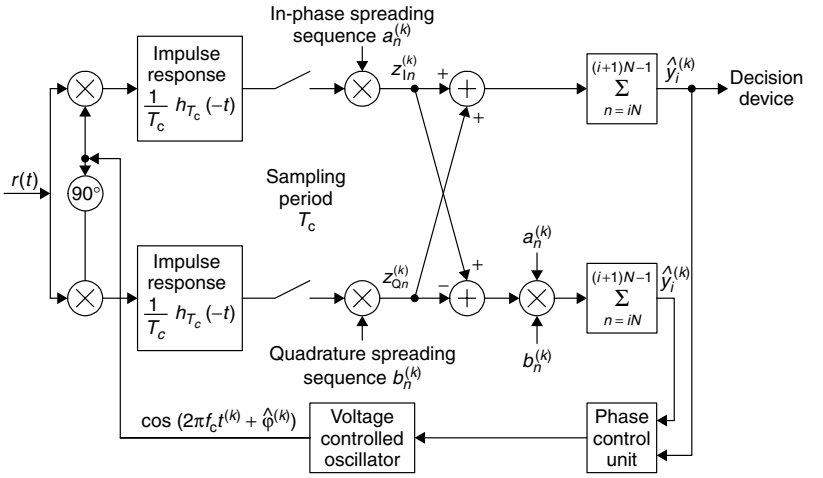

Figure 7.15. The coherent QPSK receiver with phase tracking.

where $\sqrt{P^{(k)}}$ is the power of the received signal, $t^{(k)} = t - \delta^{(k)}$, $\delta^{(k)}$ is the kth user's time offset, $\varphi^{(k)}$ is a phase, and $\xi^{(k)}(t)$ is the total noise.

The receiver that we analyze is depicted in Figure 7.15. This receiver consists of a phase control unit (PCU), a voltage-controlled oscillator (VCO), and a conventional matched-filter demodulator. The outputs from the filters are sampled at the chip rate and postmultiplied by the spreading sequences corresponding to the kth user. The resulting statistics are denoted by $\{z_{In}^{(k)}\}$ and $\{z_{Qn}^{(k)}\}$. In the case of perfect timing and phase synchronization, that is, $\hat{\delta}^{(k)} = \delta^{(k)}$ and $\hat{\varphi}^{(k)} = \varphi^{(k)}$, they are defined by (3.83) and (3.84).

We consider the case when $\hat{\delta}^{(k)} = \delta^{(k)}$ but, generally, $\Delta\varphi^{(k)} \stackrel{\text{def}}{=} \hat{\varphi}^{(k)} - \varphi^{(k)}$ is not equal to 0. We assume that the phase $\varphi^{(k)}$ is not changed in the integration interval $(iN, (i+1)N-1)$ but can be changed in consecutive integration intervals. Then, for $n \in [iN, (i+1)N-1]$ we have [compare with Formulas (3.83) and (3.84)]

$$\begin{aligned} z_{In}^{(k)} &= \sqrt{P^{(k)}}\frac{u_i^{(k)}}{2}[\cos\Delta\varphi_i^{(k)} + a_n^{(k)} b_n^{(k)} \sin\Delta\varphi_i^{(k)}] + \xi_{In}^{(k)} \\ z_{Qn}^{(k)} &= \sqrt{P^{(k)}}\frac{u_i^{(k)}}{2}[\cos\Delta\varphi_i^{(k)} - a_n^{(k)} b_n^{(k)} \sin\Delta\varphi_i^{(k)}] + \xi_{Qn}^{(k)} \end{aligned} \tag{7.125}$$

where $\xi_{In}^{(k)}$ and $\xi_{Qn}^{(k)}$ are IID zero-mean random variables with variances (3.86).

The statistic $\hat{y}_i^{(k)}$ is given by the sum

$$\hat{y}_i^{(k)} = \sum_{n=iN}^{(i+1)N-1} \hat{z}_n^{(k)} \tag{7.126}$$

where $\hat{z}_n^{(k)} = z_{\mathrm{I}n}^{(k)} + z_{\mathrm{Q}n}^{(k)}$ and is used to make the decision

$$\hat{u}_i^{(k)} = \begin{cases} 1, & \text{if } \hat{y}_i^{(k)} > 0, \\ -1, & \text{otherwise} \end{cases} \tag{7.127}$$

Referring to the central limit theorem, $\hat{y}^{(k)}$ can be considered as approximately Gaussian distributed, conditioned on $\Delta\varphi^{(k)}$, such that

$$E(\hat{y}_i^{(k)}) = \sqrt{P^{(k)}} N u_i^{(k)} \cos \Delta\varphi_i^{(k)} \tag{7.128}$$

$$\mathrm{var}(\hat{y}_i^{(k)}) = N\sigma^2 \tag{7.129}$$

where σ^2 is given by Formula (3.88). The bit error probability is given by

$$P_{\mathrm{b}} = \int_{-\pi}^{\pi} Q\left(\sqrt{2\frac{E_{\mathrm{b}}}{I_0}} \cos \Delta\varphi\right) f(\Delta\varphi) \mathrm{d}(\Delta\varphi) \tag{7.130}$$

where $E_{\mathrm{b}}/I_0 = P^{(k)} N/2\sigma^2 = P^{(k)} T_{\mathrm{c}} N/I_0$ is the SNR per bit, and $f(\cdot)$ is the probability density function of the phase error $\Delta\varphi^{(k)}$, which is derived below.

To be able to control the phase, the receiver needs a phase reference signal $x_i^{(k)}$. Referring to Figure 7.15, we introduce the new statistic $\check{y}_i^{(k)}$, which is defined as

$$\check{y}_i^{(k)} = \sum_{n=iN}^{(i+1)N-1} \check{z}_n^{(k)} \tag{7.131}$$

where $\check{z}_n^{(k)} = z_{\mathrm{I}n}^{(k)} - z_{\mathrm{Q}n}^{(k)}$. From Formula (7.125) it follows that

$$\begin{aligned} E(\check{y}_i^{(k)}) &= \sqrt{P^{(k)}}\, N u_i^{(k)} \sin \Delta\varphi_i^{(k)} \\ \mathrm{var}(\check{y}_i^{(k)}) &= N\sigma^2 \end{aligned} \tag{7.132}$$

Because

$$\mathrm{cov}(\hat{z}_n^{(k)}, \check{z}_n^{(k)}) = \mathrm{var}(z_{\mathrm{I}n}^{(k)}) - \mathrm{var}(z_{\mathrm{Q}n}^{(k)}) = 0 \tag{7.133}$$

the Gaussian random variables $\hat{y}_i^{(k)}$ and $\check{y}_i^{(k)}$ are independent. The normalized product of these two statistics $x_i^{(k)} = \frac{1}{P^{(k)} N^2} \hat{y}_i^{(k)} \check{y}_i^{(k)}$ gives the phase reference, which can be expressed as

$$x_i^{(k)} = \tfrac{1}{2} \sin 2\Delta\varphi_i^{(k)} + \zeta_i^{(k)} \tag{7.134}$$

where $\zeta_i^{(k)}$ is a zero-mean random variable with variance

$$\mathrm{var}(x_i^{(k)}) = \left(\frac{I_0}{2T_{\mathrm{c}}}\right)^2 + \frac{I_0}{2T_{\mathrm{c}}} \tag{7.135}$$

The statistic $x_i^{(k)}$ can be expressed as the difference between two independent random variables having noncentral χ^2-distribution with two degrees of freedom.

The PCU controls the carrier phase according to the *up-and-down method*, as it is called in the theory of stochastic approximation [54]. The value $x_i^{(k)}$ is used as an estimate of the phase error $\Delta\varphi_i^{(k)}$. The PCU orders the local oscillator to increase the phase by an amount proportional to this estimate, that is $\gamma x_i^{(k)}$. The gain factor γ is selected such that the changes of the carrier phase are performed fast enough. Then we can write the following difference equation

$$\hat{\varphi}_i^{(k)} = \gamma x_i^{(k)} = \frac{\gamma}{2}\sin(2\Delta\varphi_{i-1}^{(k)}) + \hat{\varphi}_{i-1}^{(k)} + \gamma\zeta_{i-1}^{(k)} \tag{7.136}$$

Here $\varphi_i^{(k)}$ is the received signal phase during the reception of the ith bit and $\hat{\varphi}_i^{(k)}$ is its estimation, $\Delta\varphi_i^{(k)} = \hat{\varphi}_i^{(k)} - \varphi_i^{(k)}$. Equation (7.136) describes a discrete-time phase-locked loop (PLL) of first order. For further details see [49].

For small γ and slow changes in the carrier phase $\varphi^{(k)}$, this discrete-time process can be approximated by a continuous-time process. Then the probability density function of the phase error $p(\Delta\varphi, t)$ at moment t satisfies the Fokker–Planck equation [49], [29],

$$\frac{\partial p(\Delta\varphi, t)}{\partial t} = -\frac{\partial}{\partial(\Delta\varphi)}\left(\frac{\gamma}{2}\sin(2\Delta\varphi)p(\Delta\varphi, t)\right) + \frac{\sigma_\zeta^2}{2}\frac{\partial^2}{\partial(\Delta\varphi)^2}(p\Delta\varphi, t) \tag{7.137}$$

where σ_ζ^2 is the drift variance of the phase process, that is, the variance of $\gamma\zeta_i^{(k)}$. The steady-state probability density function satisfies (7.137) with the initial condition

$$p(\Delta\varphi, t)|_{t=0} = \delta(\Delta\varphi) \tag{7.138}$$

the boundary condition

$$p(-\pi, t) = p(\pi, t) \tag{7.139}$$

and the normalizing condition

$$\int_{-\pi}^{\pi} p(\Delta\varphi, t)\,\mathrm{d}(\Delta\varphi) = 1 \tag{7.140}$$

Therefore, the steady-state probability density function is

$$p(\Delta f) = \frac{1}{2\pi I_0(\beta)}\exp[\beta\cos(2\Delta\varphi)] \tag{7.141}$$

where $I_0(x)$ is the zeroth-order modified Bessel function of the first kind (3.45) and

$$\beta = \frac{2}{\gamma}\left(\frac{E_\mathrm{b}}{I_0}\right)^2\left(1 + 2\frac{E_\mathrm{b}}{I_0}\right)^{-1} \tag{7.142}$$

Note that there is a phase ambiguity. Therefore, the receiver will lock to any phase errors equal to integer multiples of π with the same probability. To avoid this problem, training sequences can be periodically transmitted to detect this ambiguity or differential QPSK should be used. The slip time T_{slip} is defined as the time duration elapsed between the two phase ambiguities $\Delta\varphi^{(k)} = \pm\pi$. The expectation of the slip time $E[T_{\text{slip}}]$ can be used to decide how often training sequences should be transmitted. This expectation is defined as [49], [29]

$$E[T_{\text{slip}}] = \int_0^\infty Pr(T_{\text{slip}} > t)\,\mathrm{d}t = \int_0^\infty \int_{-\pi}^{\pi} p(\Delta\varphi, t)\,\mathrm{d}(\Delta\varphi)\,\mathrm{d}t \tag{7.143}$$

where $p(\Delta\varphi, t)$ is obtained by solving the Fokker–Planck equation (7.137) with absorbing barriers at $\Delta\varphi = \pm\pi$. The initial condition is (7.138), and the boundary conditions are

$$p(\Delta\varphi, t)|_{\Delta\varphi=\pm\pi} = 0 \tag{7.144}$$

After some cumbersome algebraic manipulations, the mean slip time is found to be

$$E[T_{\text{slip}}] = \frac{2\pi^2}{\gamma}\beta I_0(\beta)^2 \tag{7.145}$$

The other performance measure characterizing the synchronization system is the mean time duration to synchronization $E[T_{\text{syn}}]$. As the name connotes, this parameter gives the average time the receiver needs to achieve a zero-phase error. Let $D(\psi)$ denote the expectation of T_{syn} conditioned on the initial phase error $\Delta\varphi = \psi$, that is, $D(\psi) \stackrel{\text{def}}{=} E(T_{\text{syn}}|\Delta\varphi = \psi)$. Although $D(\psi)$ can be found by solving the Fokker–Planck equation (7.137) with the initial condition $p(\Delta\varphi, 0) = \delta(\Delta\varphi - \psi)$, we can use a direct equation [14]:

$$\frac{\mathrm{d}^2 D(\psi)}{\mathrm{d}\psi^2} + \frac{2E[\gamma x_i^{(k)}]}{\text{var}[\gamma x_i^{(k)}]}\frac{\mathrm{d}D(\psi)}{\mathrm{d}\psi} = \frac{2}{\text{var}[\gamma x_i^{(k)}]} \tag{7.146}$$

Because of the phase ambiguity, we restrict the definition of $D(\psi)$ to the phase interval $\psi \in [0, \pi/2]$. Clearly, $D(\psi)$ is a continuous and nonnegative function with one stationary point and global minimum at $\psi = 0$. Therefore, we use the boundary conditions

$$\left.\frac{\mathrm{d}D(\psi)}{\mathrm{d}\psi}\right|_{\psi=0} = D(0) = 0 \tag{7.147}$$

which yield the solution

$$D(\psi) = \frac{4}{\gamma}\beta \int_0^\psi \int_0^y \exp[\beta(\cos(2y) - \cos(2x))]\,\mathrm{d}x\,\mathrm{d}y, \quad 0 \le \psi < \pi/2 \tag{7.148}$$

The mean time duration to synchronization is now given by

$$E[T_{\text{syn}}] = \frac{2}{\pi} \int_0^{\pi/2} D(\psi)\, d\psi \tag{7.149}$$

The results of this section are extended in the paper [23] for the case of a Rake receiver used in L-path slow Rayleigh fading channel. Because we have L independent paths in this channel with independent carrier phases, every finger has a separate phase control unit, operating independently in analogy to the AWGN channel case. The Rake receiver combines the weighted outputs from all the L fingers, analogous to the Rake receiver of Sections 5.3 and 5.4, and makes the decision based on the sign of the combined statistic. The bit error probability depends on the L-phase errors of the Rake fingers. For further details, see [23].

The performance of the receiver in Figure 7.15 has been analyzed numerically for transmission over the AWGN channel using the phase recovery algorithm. In Figure 7.16 (left), the mean slip time is shown for a phase control parameter $\gamma = 0.05, 0.10, 0.20$. The diagram indicates that for the signal-to-noise ratios E_b/I_0 of interest, it is not often that the receiver locks into a phase ambiguity $\pm\pi$. In Figure 7.16 (middle), the mean time duration for synchronization corresponding to the same γ values is shown. We see that $E[T_{\text{syn}}] \ll E[T_{\text{slip}}]$; therefore, we may

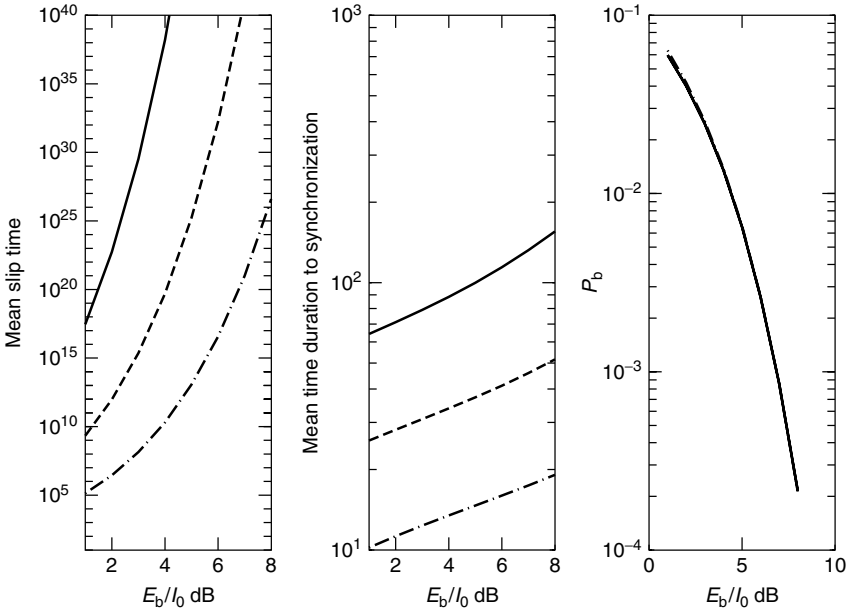

Figure 7.16. The performance of the receiver in Figure 7.15 in the AWGN channel as a function of the E_b/I_0 with $\gamma = 0.05$ (solid line), $\gamma = 0.10$ (dashed line), and $\gamma = 0.20$ (dash-dotted line). Left: mean slip time $E[T_{\text{slip}}]$ in information bit times. Middle: mean time duration to synchronization $E[T_{\text{syn}}]$ measured in information bit time. Right: bit error probability for all three cases.

deduce that the extra energy needed for the transmission of training sequences in relation to the energy used for the transmission of information can be kept very low, especially at higher SNR. The bit error probability for the same system, depicted in Figure 7.16 (right), shows a performance near to the receiver with exact coherence in all three cases. Clearly, the BER decreases with γ but this is done at the expense of a higher $E[T_{\text{syn}}]$ value.

7.7 COMMENTS

Initial spreading signal synchronization and tracking of timing are two extremely important problems in spread spectrum system design. The simplest synchronization scheme is to sweep the receiver spreading/hopping sequence phase until the proper phase is sensed. The most-used time tracking scheme is an early-late gate device. For carrier phase tracking, a Costas loop is used, a variant of which was considered in Section 7.6.

Carrier recovery and timing synchronization are two topics that have been thoroughly investigated over the past few decades. Comprehensive treatments of time tracking loops were first given by Viterbi [49]. We should also mention the book by Gardner [16] and a number of tutorial papers in IEEE journals.

Various aspects concerning the analysis and design of synchronization devices are treated in books by Simon et al. [43], Peterson, Ziemer and Borth [34], and Viterbi [47]. In our presentation of the material of this chapter we mostly follow the last book. The material in Section 7.6 has appeared in the paper by Jimenez and Zigangirov [23].

PROBLEMS

7.1. Consider a DS CDMA system with BPSK. The spreading sequence is generated by a shift register of length 10. Calculate the average time to synchronization if the following data are given:
- All states are equally likely. (Assume "genie-aided" peak sampling.)
- $P_{\text{F}} = 0.01$
- $P_{\text{D}} = 0.85$
- $\kappa = 100$
- $T_{\text{tp}} = 0.1$ ms

7.2. For the same data as in Problem 7.1, find the average time to synchronization by first finding the generating function $G(z)$ and then use that

$$M_{\text{a}} = E[T_{\text{a}}] = \left.\frac{\mathrm{d}G(z)}{\mathrm{d}z}\right|_{z=1}$$

Hint: Use that $\left.\frac{\mathrm{d}G(z)}{\mathrm{d}z}\right|_{z=1} \simeq \frac{G(1+\epsilon)-G(1-\epsilon)}{2\epsilon}$ for small values of ϵ.

7.3. Estimate by the cut-and-try method the minimum acquisition time for a "genie-aided" DS CDMA system operating in the AWGN channel. Assume

that correct chip sampling occurs at the peak ($R_a(\tau) = 1$) and that a kind genie informs not only about the correct sampling but also on the phase of the received signal. Parameters are: $\Delta = T_c$, the number of spreading chips corresponds to a full period, $T_{tp} = 1$ μs, $\nu = 1$, $\kappa = 100$, $\rho_B = 2$ (3 dB), the maximal length shift register has length 12.
Hint: Use Figure 3.1.

7.4. When the channel is undergoing Rayleigh fading, it was shown that the relation between P_F and P_D is

$$P_F = \exp(-\theta)$$

$$P_D = \exp\left(\frac{-\theta}{1+\rho_B}\right)$$

where θ is the threshold and ρ_B is SNR per block. The corresponding receiver operating characteristic (ROC) is shown in the accompanying figure for $\rho_B = 15$ dB. Consider a DS CDMA system operating over a Rayleigh fading channel. Assume that $\rho_B = 15$ dB, spreading sequence generated by a shift register of length 7, $N = N_p$, $T_c = 1$ μs. Presume peak sampling and $\kappa = 50$. Find the average time to synchronization

a) If $P_F = 0.01$

b) If $P_F = 0.04$

c) If $\rho_B \to \infty$, what is the minimum mean time to synchronization?

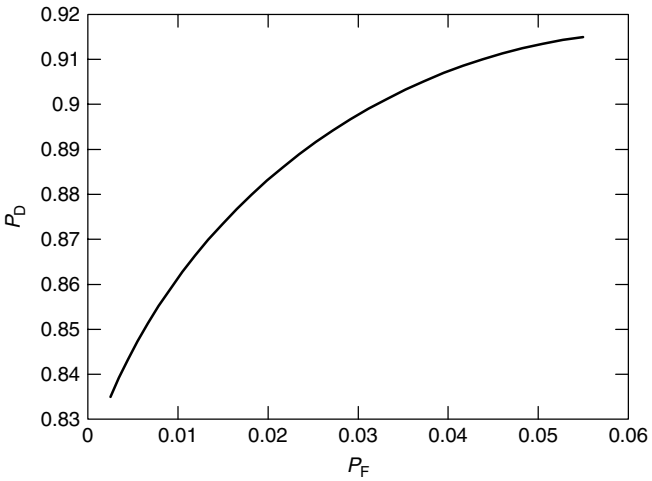

Problem 7.4. Receiver operating characteristic.

7.5. Consider a DS CDMA system operating in a Rayleigh faded channel, where the spreading sequence is generated by a maximum length shift register of length 8 and $\rho_B = 15$ dB, $\nu = 1$, $T_{tp} = 0.15$ ms, $\kappa = 85$.

a) Determine the threshold of θ that minimizes the average time to synchronization.

b) Calculate P_F, P_D, and M_a for the optimum value of θ that was determined in a).

7.6. Consider a DS CDMA system with BPSK, where the spreading sequence is generated by MLSR of length 7. The channel is undergoing Rayleigh fading. Determine the minimum time to acquisition if $\kappa = 100$, $N = N_p$, $T_c = 0.5$ μs, $\nu = 1, 2$, $\rho_B = 8$ dB.

7.7. In Figures 7.4 and 7.5 the ROC is given for the AWGN channel and the Rayleigh fading channel, respectively. Use the figures to find the minimum average time to synchronization if $\rho_B = 4$ dB, a MLSR of length 11 is used, $N = N_p$, $T_c = 0.20$ μs, $\kappa = 100$. Consider two cases:

a) The AWGN channel

b) The Rayleigh fading channel.

7.8. A DS CDMA system transmits over a Rayleigh faded channel. Determine the minimum value of the M_a for $\nu = 1$ and 2.
The following data are given: $T_{tp} = \nu\, 0.1$ ms, $\kappa = 100$, $I = 1023$, $E_b/I_0 = 8$ dB.

7.9. In the accompanying figure the receiver operating characteristics for $\nu = 1$ and $\nu = 2$ are given. The test period time is $T_{tp} = \nu N T_c$. If $\kappa = 100$, determine whether the mean time to acquisition is better or worse for $\nu = 2$. The number of states to search can be assumed to be very large.

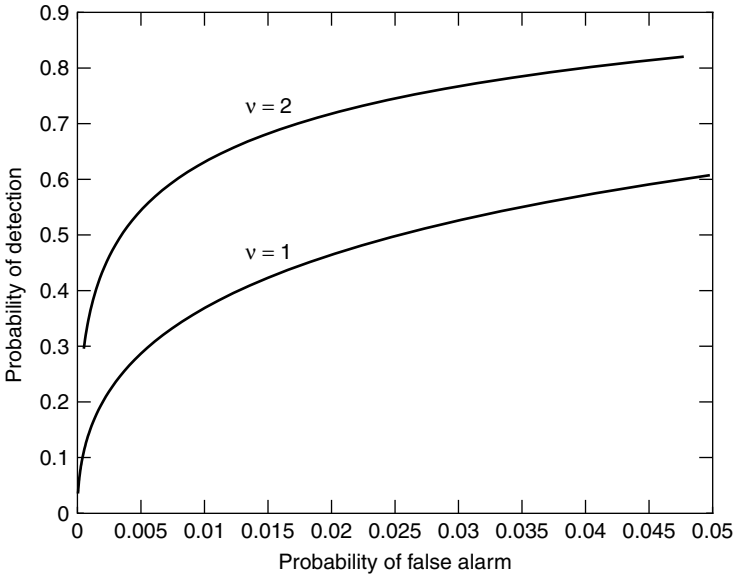

Problem 7.9. Receiver operating characteristic.

7.10. Consider a DS CDMA system that is operating over a Rayleigh fading channel. The modulation is BPSK, and no coding is employed. The following data are given for the system and acquisition receiver: $T_c = 0.1$ μs, $R = 10$ kb/s, $T_{tp} = 1/R$, 1023 equally likely states, $\kappa = 100$.

a) What is the maximum number of users if $P_b \leq 0.01$ and $E_b/N_0 = 20$ dB?

b) For the number of users found in a), what is the average time to synchronization if peak sampling is assumed and $\rho_B = E_b/N_0$?

c) If instead of peak sampling the search for the correct state is performed in half-chip steps, find an upper bound for the average time to synchronization by considering the sampling at the least favourable time. Let P_F be independent of the sampling time, that is, let P_F be the same as in the case of peak sampling. Finally, note that the "effective" SNR when evaluating P_D is

$$\left(\frac{E_b}{I_0}\right)_{\text{eff}} = \left(\frac{E_b}{I_0}\right)_{\text{peak}} \left(1 - \frac{|\tau|}{T_c}\right)^2, \quad \tau \leq T_c$$

d) If in addition there is a phase error $\Delta\varphi = 15^\circ$, how much is the degradation in synchronization time?

7.11. For the system described in Problem 7.7, calculate the generating function, the mean, and the variance.

7.12. For a channel that is undergoing Rayleigh fading, how much is the mean time to synchronization increased if ρ_B is decreased from 9 dB to 6 dB? Assume that the false alarm penalty $T_{fa} = 100T_{tp}$ and that the number of states $I \gg 1$.

7.13. Consider acquisition in a Rayleigh fading channel with $\rho_B = 12$ dB. Assume that a MLSR of memory 8 is used to generate the spreading sequences.

a) Determine the mean time to acquisition. Assume peak sampling, $N = N_p$, $\kappa = 40$, and equally likely states.

b) Is it possible to decrease the mean time by half by increasing the ρ_B?

7.14. Find minimum acquisition time for a "genie-aided" FH CDMA system. The receiver is given in Figure 7.3. The system parameters are $T_c = 0.05$ μs, $N = N_p = 511$, $\nu = 1$, $\Delta = T_c$, $\kappa = 100$, $(K - 1) = M \ln 2$. Neglect background noise. Use the Gaussian approximation for the distribution of the decision statistics.

7.15. Draw and analyze an early-late gate device schematic for a DS CDMA system with QPSK signaling.

7.16. Draw an early-late gate device schematic for a FH CDMA system.

7.17. Draw an early-late gate device schematic for a PPH CDMA system.

8

INFORMATION-THEORETICAL ASPECTS OF CDMA COMMUNICATIONS

The multiple-access potential of wideband signals was noted by Shannon, the father of information theory. Since that time, the Shannon information theory has become the theoretical base of CDMA communication. This chapter is devoted to description of the fundamentals of information theory and in particular to description of the multiuser information theory.

A fundamental result of information theory is that reliable communication (that is, transmission with error probability less than any given value) is possible even over a noisy channel as long as the transmission rate is less than *Shannon capacity*. In this chapter, we consider different aspects of CDMA communication from the point of view of information theory. In particular, we analyze such fundamental characteristics of CDMA systems as Shannon capacity, cut-off rate, reliability function, etc.

We start in Section 8.1 with the introduction of an information-theoretical model of a communication channel and then study lower and upper bounds for the Shannon capacity. The *channel reliability function* is defined as an exponential factor in the function describing the dependence of the decoding error probability from the code length. The upperbounding technique for the decoding error probability uses *random coding arguments*, which we study in Section 8.2. In the same section we introduce the *cut-off rate*, which according to tradition at least, represents an upper limit on transmission rate for practically instrumentable communication. In the following sections we apply our knowledge to analyses of different CDMA systems. In our presentation, we will mostly stress aspects of wideband information theory.

Theory of Code Division Multiple Access Communication, by Kamil Sh. Zigangirov
ISBN 0-471-45712-4

8.1 SHANNON CAPACITY OF DS CDMA SYSTEMS

In the previous chapters we dealt with the *communication channel*. This is the physical medium that is used to send a signal from a transmitter to a receiver. In CDMA applications, this is mostly the atmosphere. The transmitter of the DS CDMA system in Figure 1.8 consists of an encoder, a spreader, an impulse generator, and a modulator. The receiver of the DS CDMA system in Figure 1.9 consists of a demodulator (it includes a matched filter), a despreader, and a decoder. The encoder and the spreader operate with a sequence of discrete variables over the alphabet $\{1, -1\}$. The impulse generator and the modulator map the digital information into an analog signal. The demodulator converts the received signal, corrupted by additive and interference noise, into real-valued statistics. The despreader and the decoder operate with these statistics. In information theory, the cascade of the impulse generator, the modulator, the communication channel, and the demodulator is reduced into an equivalent *discrete-time composite channel*. Such a composite channel is characterized by the set $\{1, -1\}$ of possible inputs, the continuous output, and a set of conditional probability density functions that relate the possible outputs to the possible inputs. This channel model differs from the conventional binary channel model, studied in non-CDMA communications, only by the additional presence of a spreader and a despreader.

A similar situation occurs in FH CDMA communication, where the composite channel consists of an impulse generator, a modulator (excluding frequency synthesizer), a communication channel, and a demodulator [excluding frequency (de)synthesizer]. Because in impulse radio the transmitted signal does not use a sinusoidal carrier, the composite channel in a PPH CDMA system consists only of the impulse generator, the communication channel, and the matched filter.

In this section, we study the mathematical model of the *discrete-time*, *discrete-input* channel. Furthermore, we assume that noise in the communication channel is white Gaussian and that the pulses $h_{T_c}(\cdot)$ on the output of the inpulse generator of the transmitter are orthogonal. Then the channel is a *memoryless* channel with additive Gaussian noise. The channels in DS and PPH CDMA communications can be reduced to this model. The channel model for FH CDMA communication will be studied later.

Consider a general discrete input alphabet $\mathcal{A} = \{a_0, a_1, \ldots, a_{J-1}\}$ including as a special case the binary alphabet $\{1, -1\}$. Without loss of generality, we assume in this chapter that the power of the received signal is equal to the power of the transmitted signal.

We shall restrict our attention in this chapter mainly to block codes. A block (N, L) code is defined by a set of $M = 2^L$ codewords $\boldsymbol{v}_i = (v_{i,0}, v_{i,1}, \ldots, v_{i,N-1})$, $i = 0, 1, \ldots, 2^L - 1$, of length N. Here $v_{i,n}, v_{i,n} \in \mathcal{A}$, $\sum_{n=0}^{N-1} v_{i,n}^2 \leq N$, are code symbols. The transmitted signal is $\boldsymbol{s} = (s_0, s_1, \ldots, s_{N-1})$. If the transmitter sends the ith message, then $\boldsymbol{s} = \sqrt{P}\boldsymbol{v}_i$, where P is some fixed power

constraint. The average power of the signal is upperbounded by the inequality

$$\frac{1}{N}\sum_{n=0}^{N-1} s_n^2 \le P \tag{8.1}$$

The received signal is $\boldsymbol{r} = (r_0, r_1, \ldots, r_{N-1})$, where

$$r_n = s_n + \xi_n \tag{8.2}$$

Here $s_n = \sqrt{P}v_{i,n}$, $\{\xi_n\}$ is a noise sequence. Because the channel is memoryless, $\{\xi_n\}$ is a set of IID zero-mean Gaussian random variables with variances $\sigma^2 = I_0/2T_c$, where $I_0/2$ is the two-sided power spectral density of the additive and interference noise in the communication channel. T_c is the duration of the pulses of the impulse generator of the transmitter. We first consider the case in which the block length $N \to \infty$, the code rate $r = L/N \to 0$, $T_c \to 0$, but $M = 2^L$, the transmission rate $R = r/T_c$, and the block transmission time $T = NT_c$ are fixed.

It follows from (8.1) that the transmitted signal is inside an N-dimensional hypersphere of radius $\sqrt{NP}$. Because of the power constraint (8.1) and independence of the input and noise, we have

$$E(|\boldsymbol{r}|^2) = E\left(\sum_{n=0}^{N-1} r_n^2\right) = \sum_{n=0}^{N-1} s_n^2 + \sum_{n=0}^{N-1} E(\xi_n^2) \le NP + N\sigma^2 \tag{8.3}$$

$$\mathrm{var}(|\boldsymbol{r}|^2) = \sum_{n=0}^{N-1} \mathrm{var}(\xi_n^2) = 2N\sigma^4 \tag{8.4}$$

where $|\cdot|$ means the Euclidean norm.

Using the Chebyshev inequality we get from Formulas (8.3) and (8.4) an upper bound for the probability that $\boldsymbol{r}$ is located outside the N-dimensional hypersphere of radius $\sqrt{N(P+\sigma^2+\varepsilon)}$, where $\varepsilon > 0$, centered at the origin. In fact,

$$\begin{aligned} P(|\boldsymbol{r}| > \sqrt{N(P+\sigma^2+\varepsilon)}) &= P(|\boldsymbol{r}|^2 > N(P+\sigma^2+\varepsilon)) \\ &\le P(||\boldsymbol{r}|^2 - N(P+\sigma^2)| > \varepsilon N) \le \frac{2\sigma^4}{\varepsilon^2 N} \end{aligned} \tag{8.5}$$

This implies that for any given $\varepsilon > 0$, the probability that the received signal point $\boldsymbol{r}$ will be inside the N-dimensional hypersphere of radius $\sqrt{N(P+\sigma^2+\varepsilon)}$ and centered at the origin, goes to 1 if $N \to \infty$.

The optimal decision criterion is the maximum likelihood rule described in Section 4.1. For the AWGN channel this criterion reduces to the minimum distance rule. It divides the N-dimensional space into M decision regions according to the number of messages. The region corresponding to the ith message contains all points $\boldsymbol{r}$ for which the Euclidean distance $|\boldsymbol{r} - \boldsymbol{v}_i|$ does not exceed a distance

of $\boldsymbol{r}$ from any other codeword $\boldsymbol{v}_j$, $j \neq i$. If $\boldsymbol{r}$ falls in the ith region, the decoder says that the ith codeword was transmitted.

The volume of an N-dimensional hypersphere of radius ρ is equal to $\kappa_N \rho^N$, where κ_N is a coefficient (for example, if $N = 2$, then $\kappa_2 = \pi$, if $N = 3$, then $\kappa_3 = 4\pi/3$). Consider the intersections of the decision regions with the hypersphere of radius $\sqrt{N(P + \sigma^2 + \varepsilon)}$. Obviously, at least one of these intersection regions has volume not more than $\kappa_N[N(P + \sigma^2 + \varepsilon)]^{N/2}/M$. Let us estimate the probability that point $\boldsymbol{r}$ will fall outside the "correct" region. This probability is minimal if the region is shaped as a sphere. We will again use the Chebyshev inequality.

Because

$$E(|\boldsymbol{r} - \boldsymbol{s}|^2) = \sum_{n=0}^{N-1} E(\xi_n^2) = N\sigma^2 \tag{8.6}$$

$$\operatorname{var}(|\boldsymbol{r} - \boldsymbol{s}|^2) = \sum_{n=0}^{N-1} \operatorname{var}(\xi_n^2) = 2N\sigma^4 \tag{8.7}$$

we have analogously to (8.5) for $0 < \varepsilon < \sigma^2$

$$P(||\boldsymbol{r} - \boldsymbol{s}| - N\sigma^2| > \varepsilon N) \leq \frac{2\sigma^4}{\varepsilon^2 N} \tag{8.8}$$

This implies that if $N \to \infty$ with probability one the received point will be located in an N-dimensional hypersphere shell (Fig. 8.1). The sphere has radius $\sqrt{N(\sigma^2 + \varepsilon)}$ and is centered at $\boldsymbol{s}$.

In particular, from (8.8) it follows that if $N \to \infty$ with probability one, the received point will be located outside the N-dimensional hypersphere of radius $\sqrt{N(\sigma^2 - \varepsilon)}$ and centered at $\boldsymbol{s}$. This hypersphere has volume $\kappa_N[N(\sigma^2 - \varepsilon)]^{N/2}$. Then a necessary condition for error-free transmission is

$$\kappa_N[N(\sigma^2 - \varepsilon)]^{N/2} \leq \kappa_N[N(P + \sigma^2 + \varepsilon)]^{N/2}/M \tag{8.9}$$

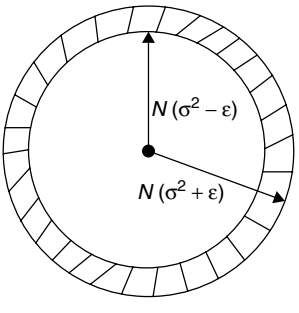

Figure 8.1. A Gaussian channel output space.

or

$$M \leq \left(\frac{P + \sigma^2 + \varepsilon}{\sigma^2 - \varepsilon} \right)^{N/2} \tag{8.10}$$

Because $M = 2^{rN}$ and ε can be chosen arbitrarily small, we get from Formula (8.10)

$$r \leq \frac{1}{2} \log_2 \left(1 + \frac{P}{\sigma^2} \right) \tag{8.11}$$

The transmission rate $R = r/T_c$ and variance $\sigma^2 = I_0/2T_c$. By substituting into the previous relation, we obtain

$$R \leq \frac{1}{2T_c} \log_2 \left(1 + \frac{2PT_c}{I_0} \right) = \frac{1}{2T_c} \log_2(1 + 2\rho_c) \stackrel{\text{def}}{=} C \tag{8.12}$$

where $\rho_c = PT_c/I_0$ is the SNR per chip. C is the *Shannon capacity* of the discrete-time Gaussian memoryless channel. Because according to our definition, given in Section 2.1, $T_c = 1/W$, we have from (8.12)

$$C = \frac{W}{2} \log_2 \left(1 + \frac{2P}{I_0 W} \right) \tag{8.13}$$

Readers familiar with foundations of the information theory can see that conventional expression for the Shannon capacity of the band-limited channel $C = W \log_2(1 + P/I_0 W)$, where W is the channel bandwidth, differs from (8.13). This is because the conventional (physical) definition of the bandwidth includes only positive frequencies of the baseband signal, whereas our (mathematical) definition includes both positive and negative frequencies. If we used a physical definition of the bandwidth, then we should use in Formula (8.12) substitution $T_c = 1/2W$ and get the conventional expression for Shannon capacity. Equality (8.12) defines an upper limit on the maximum transmission rate. For $T_c \to 0$, that is, when the bandwidth is infinite, we have

$$R \leq P/I_0 \ln 2 \text{ b/s} \tag{8.14}$$

which is an upper bound for the transmission rate of reliable communication over an infinite-bandwidth AWGN channel.

The transmission rate $(1/2T_c) \log_2(1 + 2PT_c/I_0)$ is achievable in a band-limited channel if we use Gaussian-like codewords $\{\boldsymbol{v}_i\}$. In this section we limit ourselves to a proof that the rate $C = P/I_0 \ln 2$ is achievable in an infinite-bandwidth channel.

Let us first investigate the effect of an increasing block length N on the probability of error for the first-order Reed–Muller codes, considered in Section 4.2.

The probability of correct decision is given by Formula (4.27), which we present in modified form:

$$P(\mathcal{C}) = \frac{1}{\sqrt{\pi\rho_c N}} \int_0^\infty \exp\left[-\frac{(x-\rho_c N)^2}{\rho_c N}\right] P(\mathcal{C}|x)\,dx$$
$$= \frac{1}{\sqrt{\pi\rho_c N}} \int_0^\infty \exp\left[-\frac{(x-\rho_c N)^2}{\rho_c N}\right] \left[1 - 2Q\left(\frac{\sqrt{2}\,x}{\sqrt{\rho_c N}}\right)\right]^{N-1} dx \quad (8.15)$$

Here $P(\mathcal{C}|x)$ is the conditional probability of correct decision given that the decision statistic corresponding to the transmitted codeword is x and $\rho_c = PT_c/I_0$ is the SNR per chip. We recall that the code rate is $r = (\log_2 N + 1)/N$ and that the transmission rate is $R = r/T_c = (\log_2 N + 1)/T_c N$ b/s.

Consider the case in which $N \to \infty$ such that the block transmission time $NT_c \stackrel{\text{def}}{=} T$ and SNR per bit $E_b/I_0 = PT_c N/I_0(\log_2 N + 1) = \rho_c N/(\log_2 N + 1)$ are fixed.

To simplify the mathematical development, we first derive a lower bound on $P(\mathcal{C})$ that is simpler than the exact form (8.15). Because

$$\left[1 - 2Q\left(\frac{\sqrt{2}\,x}{\sqrt{\rho_c N}}\right)\right]^{N-1} > 1 - 2(N-1)Q\left(\frac{\sqrt{2}\,x}{\sqrt{\rho_c N}}\right)$$
$$\geq 1 - (N-1)\exp\left(-\frac{x^2}{\rho_c N}\right) \quad (8.16)$$

we have from (8.15)

$$P(\mathcal{C}) > \frac{1}{\sqrt{\pi\rho_c N}} \int_0^\infty \exp\left[-\frac{(x-\rho_c N)^2}{\rho_c N}\right] dx$$
$$- \frac{N-1}{\sqrt{\pi\rho_c N}} \int_0^\infty \exp\left[-\frac{(x-\rho_c N)^2 + x^2}{\rho_c N}\right] dx$$
$$= Q(-\sqrt{2\rho_c N}) - (N-1)\exp\left(-\frac{\rho_c N}{2}\right) Q(-\sqrt{\rho_c N}) \quad (8.17)$$

Then from (8.17) it follows that

$$\lim_{N\to\infty} P(\mathcal{C}) \geq \lim_{N\to\infty} Q\left(-\sqrt{\frac{2E_b \cdot \log_2 2N}{I_0}}\right)$$
$$- \lim_{N\to\infty} (N-1)(2N)^{-E_b/2I_0 \ln 2}\, Q\left(-\sqrt{\frac{E_b \cdot \log_2 2N}{I_0}}\right)$$
$$= 1 - \lim_{N\to\infty} (N-1)(2N)^{-E_b/2I_0 \ln 2} \quad (8.18)$$

where we use equality $\rho_c N = E_b(\log_2 N + 1)/I_0 = E_b \ln(2N)/I_0 \ln 2$. If

$$\frac{E_b}{I_0} > 2 \ln 2 = 1.39(1.42 \text{ dB}) \tag{8.19}$$

that is,

$$R < \frac{P}{2I_0 \ln 2} \stackrel{\text{def}}{=} R_0 \tag{8.20}$$

and the second term in the right-hand side of (8.18) and, consequently, the decoding error probability $P(\mathcal{E}) = 1 - P(\mathcal{C})$ go to zero. The value R_0 is called the *computational cut-off rate* for an infinite-bandwidth AWGN channel. It equals half of the Shannon capacity $C = P/I_0 \ln 2$.

The simple lower bound for $P(\mathcal{C})$ given by Formulas (8.17) and (8.18) implies that as long as $E_b/I_0 > 1.42$ dB we can achieve in an infinite-bandwidth AWGN channel arbitrarily low $P(\mathcal{E})$. However, this bound is not a very tight bound at a sufficiently low SNR because the bound (8.16) is loose for small x.

An alternative approach is to use two different bounds for $P(\mathcal{C}|x)$. When x is large, that is, for $x > x_0$, where x_0 depends on N, we use Formula (8.16). When x is small, that is, for $x \le x_0$, we use the trivial bound $P(\mathcal{C}|x) \ge 0$. Thus (8.15) may be lowerbounded as

$$\begin{aligned} P(\mathcal{C}) &> \frac{1}{\sqrt{\pi \rho_c N}} \int_{x_0}^{\infty} \exp\left[-\frac{(x - \rho_c N)^2}{\rho_c N}\right] [1 - (N-1)\exp(-x^2/\rho_c N)]\, dx \\ &> \frac{1}{\sqrt{\pi \rho_c N}} \int_{x_0}^{\infty} \exp\left[-\frac{(x - \rho_c N)^2}{\rho_c N}\right] dx \\ &\quad - \frac{N}{\sqrt{\pi \rho_c N}} \int_{x_0}^{\infty} \exp\left[-\frac{(x - \rho_c N)^2 + x^2}{\rho_c N}\right] dx \end{aligned} \tag{8.21}$$

The value of x_0 that maximizes this lower bound is found by differentiating the right-hand side of (8.21) and setting the derivative equal to zero. It is easily verified that the solution is

$$N = \exp\left(\frac{x_0^2}{\rho_c N}\right) \tag{8.22}$$

or equivalently

$$x_0 = \sqrt{\rho_c N \ln N} \tag{8.23}$$

Having determined x_0, let us compute an exponentially tight bound. For the first integral in (8.21) we have, if $\rho_c N \geq \ln N$,

$$\begin{aligned}
&\frac{1}{\sqrt{\pi\rho_c N}} \int_{x_0}^{\infty} \exp\left[-\frac{(x-\rho_c N)^2}{\rho_c N}\right] \mathrm{d}x \qquad (8.24)\\
&= 1 - \frac{1}{\sqrt{\pi\rho_c N}} \int_{-\infty}^{x_0} \exp\left[-\frac{(x-\rho_c N)^2}{\rho_c N}\right] \mathrm{d}x\\
&= 1 - Q(\sqrt{2\rho_c N} - \sqrt{2\ln N}) \geq 1 - \frac{1}{2}\ \exp\left[-\left(\sqrt{\rho_c N} - \sqrt{\ln N}\right)^2\right]
\end{aligned}$$

The second integral in (8.21) is upperbounded as follows:

$$\begin{aligned}
&\frac{N}{\sqrt{\pi\rho_c N}} \int_{x_0}^{\infty} \exp\left[-\frac{(x-\rho_c N)^2 + x^2}{\rho_c N}\right] \mathrm{d}x\\
&= N \exp\left(-\frac{\rho_c N}{2}\right)\ Q(2\sqrt{\ln N} - \sqrt{\rho_c N})\\
&< \begin{cases} N \exp\left(-\dfrac{\rho_c N}{2}\right), & \text{if } \ln N \leq \dfrac{\rho_c N}{4} \\ \dfrac{1}{2}\exp\left(-(\sqrt{\rho_c N} - \sqrt{\ln N})\right)^2, & \text{if } \ln N > \dfrac{\rho_c N}{4} \end{cases} \qquad (8.25)
\end{aligned}$$

Combining the bounds (8.24) and (8.25) for the two integrals we obtain

$$P(\mathcal{C}) \geq \begin{cases} 1 - \dfrac{1}{2}\exp[-(\sqrt{\rho_c N} - \sqrt{\ln N})^2] - \exp\left[-\dfrac{\rho_c N}{2} + \ln N\right], \\ \qquad\qquad \text{if } \ln N \leq \rho_c N/4, \\ 1 - \dfrac{1}{2}\exp[-(\sqrt{\rho_c N} - \sqrt{\ln N})^2] - \dfrac{1}{2}\exp[-(\sqrt{\rho_c N} - \sqrt{\ln N})^2], \\ \qquad\qquad \text{if } \rho_c N/4 < \ln N \leq \rho_c N \end{cases} \qquad (8.26)$$

The condition $\ln N \leq \rho_c N/4$ is asymptotically (for $N \to \infty$) equivalent to condition $r \approx (\log_2 N)/N \leq \rho_c/4\ln 2$ or to condition

$$R \leq \frac{P}{4I_0 \ln 2} \stackrel{\text{def}}{=} R_{\text{cr}} \qquad (8.27)$$

where the *critical rate* R_{cr} is equal to one quarter of the Shannon capacity of the AWGN channel in the infinite-bandwidth case.

In the range $\ln N \le \rho_c N/4$ the bound may be expressed as

$$P(\mathcal{E}) = 1 - P(\mathcal{C}) \le \exp\left[-\frac{\rho_c N}{2} + \ln N\right]\left\{1 + \exp\left[-\frac{(\sqrt{\rho_c N} - 2\sqrt{\ln N})^2}{2}\right]\right\}$$
$$\le 2\exp\left[-\frac{\rho_c N}{2} + \ln N\right] \tag{8.28}$$

In the range $\rho_c N/4 < \ln N < \rho_c N$, the two exponential terms in (8.26) are identical. Hence, in this range

$$P(\mathcal{E}) \le \exp\left[-\left(\sqrt{\rho_c N} - \sqrt{\ln N}\right)^2\right] \tag{8.29}$$

The first bound (8.28) asymptotically coincides with bound (8.17) in the range $\ln N \le \rho_c N/4$. The second bound is better than (8.17) for $\ln N \ge \rho_c N/4$. We note that $P(\mathcal{E}) \to 0$ as $N \to \infty$ provided that $r \approx \log_2 N/(N) \le \rho_c/\ln 2$ or

$$R < \frac{P}{I_0 \ln 2} = C \tag{8.30}$$

From (8.30) it follows that the Shannon capacity is achievable in an infinite-bandwidth AWGN channel. Because $P/R = E_b$, we can rewrite the necessary condition of reliable communication in the infinite-bandwidth AWGN channel as

$$\rho_b = \frac{E_b}{I_0} \ge \ln 2 = 0.69(-1.6 \text{ dB}) \tag{8.31}$$

It is worth noting that the necessary condition (8.31) is valid not only for an infinite-bandwidth AWGN channel, but also for band-limited AWGN channels.

The radio channel capacity of the DS CDMA system was defined in Chapter 1 by Formula (1.16). Because the SNR per bit cannot be less than -1.6 dB, we have from (1.16) and (8.31) the upper bound for the radio channel capacity

$$K_0 \le 1 + 1.45 \cdot W/R \cdot \frac{\gamma_v \cdot \gamma_a}{1+f} - \frac{N_0 W}{P}\,\frac{\gamma_v \gamma_a}{1+f} \tag{8.32}$$

In the CDMA system, we define the overall transmission rate as the sum of the transmission rates $R^{(k)}$ of all K users, $R_{\text{overall}} = \sum_{k=1}^{K} R^{(k)}$. It is interesting to estimate the maximal achievable overall rate for reliable communication in the CDMA system—the *total Shannon capacity*.

EXAMPLE 8.1

Find the total Shannon capacity of a single-cell DS CDMA system using omnidirectional antennas and no voice activity detection ($\gamma_a = 1, \gamma_v = 1$). Assume that the channel bandwidth goes to infinity and all users transmit with the same rate R.

Solution

From conditions (8.31) and (1.8) we have that the minimal required signal-to-noise ratio is

$$\frac{E_b}{I_0} = \frac{W/R}{(K-1) + \dfrac{N_0 W}{P}} = \ln 2 \tag{8.33}$$

Because $R_{\text{overall}} = K R$, *we obtain from Formula (8.33)*

$$\frac{W/R_{\text{overall}}}{\dfrac{K-1}{K} + \dfrac{N_0 W}{PK}} = \ln 2 \tag{8.34}$$

or, because for $K \gg 1$,

$$R_{\text{overall}} \approx \frac{W}{\ln 2} = 1.45\ W \tag{8.35}$$

As the rate $C_{\text{total}} = 1.45\ W$ *is achievable, we conclude that in each Herz of the DS CDMA single-cell system bandwidth it is in principle possible to send* 1.45 *bit of information.*

8.2 RELIABILITY FUNCTIONS

Consider again bounds (8.28) and (8.29),

$$P(\mathcal{E}) \le \begin{cases} 2\exp\left(-\dfrac{\rho_c N}{2} + \ln N\right), & \text{if } \ln N \le \rho_c N/4, \\ \exp[-(\sqrt{\rho_c N} - \sqrt{\ln N})^2], & \text{if } \rho_c N/4 < \ln N \le \rho_c N \end{cases} \tag{8.36}$$

Using the substitutions $R = \log_2 N/NT_c$, $T = NT_c$, we can rewrite (8.36) as

$$P(\mathcal{E}) \le \begin{cases} 2 \cdot 2^{-T(R_0 - R)}, & \text{if } R \le R_{cr}, \\ 2^{-T(\sqrt{C} - \sqrt{R})^2}, & \text{if } R_{cr} < R \le C \end{cases} \tag{8.37}$$

where the transmission time $T = NT_c$, and R_0, R_{cr}, and C are defined in Section 8.1.

The exponential bounds on the error probability in an infinite-bandwidth AWGN channel given by (8.37) may be expressed as

$$P(\mathcal{E}) < 2 \cdot 2^{-TE(R)} \tag{8.38}$$

The exponential factor

$$E(R) = \begin{cases} R_0 - R, & \text{if } 0 < R \le R_{cr}, \\ \left(\sqrt{C} - \sqrt{R}\right)^2, & \text{if } R_{cr} < R \le C \end{cases} \tag{8.39}$$

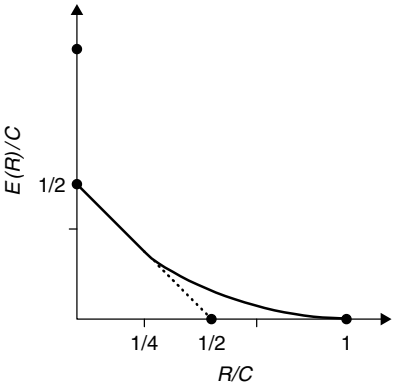

Figure 8.2. The block reliability function for the infinite-bandwidth AWGN channel.

in (8.38) is called the *reliability function* for the infinite-bandwidth AWGN channel. A plot of $E(R)/C$ is shown in Figure 8.2. The bound given by Formulas (8.38) and (8.39) has been shown by Gallager to be exponentially tight. This means that for any coding method

$$\lim_{T\to\infty} \frac{-\log_2 P(\mathcal{E})}{T} \leq E(R) \tag{8.40}$$

where $E(R)$ is given by (8.39).

As we noted above, in the AWGN channel the Shannon capacity is achievable for Gaussian-like coding. In the infinite-bandwidth channel, we can approach Shannon capacity using binary orthogonal signaling in the alphabet $\{1, -1\}$, as was shown in Section 8.1.

There is one very disturbing thing about our analysis of the transmission with orthogonal signals. To make the error probability small at rates close to the Shannon capacity, we must use an enormous number of orthogonal signals and this requires an enormous bandwidth and, correspondingly, infinitesimal chip duration. As we use more and more orthogonal signals in coding, eventually we must exceed the range of frequencies over which a study of the transmission makes sense. Therefore, we must study transmission with nonorthogonal signaling.

We wish to find an upper bound of achievable probability of error as a function of the rate R, the transmission time T, and the bandwidth W. This bound is derived by analyzing a random ensemble of codes rather than just one good code. This peculiar approach is dictated by the fact that for interesting values of R, T, and W, no way is known to find a good particular code and even if such a code could be found, a straightforward calculation of the error probabilities is prohibitive. This, in fact, was Shannon's approach.

We consider an ensemble of code rate r, length N binary codes over the real number alphabet $\{1, -1\}$. The codewords are

$$\boldsymbol{v}_i = (v_{i,0}, v_{i,1}, \ldots, v_{i,N-1}), \ i = 0, 1, \ldots 2^{rN} - 1 \tag{8.41}$$

We assume that $\{v_{i,n}\}$ is a set of IID equiprobable random variables

$$P(v_{i,n} = 1) = P(v_{i,n} = -1) = 1/2, \text{ all } i \text{ and } n \tag{8.42}$$

Consequently, the probability that $\boldsymbol{v}_i$ and $\boldsymbol{v}_j$, $i \neq j$, differ in d positions is simply

$$P(d) = \left(\frac{1}{2}\right)^N \binom{N}{d} \tag{8.43}$$

Without loss of generality let us suppose that the 0th codeword was transmitted. The received sequence is $\boldsymbol{r} = (r_0, r_1, \ldots r_{N-1})$. The ML decoding can be erroneous only if at least for one i, $i = 1, 2, \ldots 2^{rN} - 1$, we have

$$P(\boldsymbol{r}|\boldsymbol{v}_i) \geq P(\boldsymbol{r}|\boldsymbol{v}_0) \tag{8.44}$$

If $\mathcal{E}_i$ represents event (8.44), then for upperbounding of the probability of decoding error $P(\mathcal{E})$ we can use the union bound (4.15). If $\boldsymbol{v}_0$ and $\boldsymbol{v}_i$ differ in d positions, the conditional probability $P(\mathcal{E}_i|d)$ is equal to (see Example 4.1)

$$P(\mathcal{E}_i|d) = Q\left(\sqrt{2\rho_c d}\right) < \frac{1}{2}\exp(-\rho_c d) \tag{8.45}$$

Hence, for the unconditional probability $P(\mathcal{E}_i)$ we have from (8.43) and (8.45)

$$\begin{aligned} P(\mathcal{E}_i) &= \sum_{d=0}^{N} P(\mathcal{E}_i|d) \cdot P(d) < \frac{1}{2}\sum_{d=0}^{N} \exp(-\rho_c d)\left(\frac{1}{2}\right)^N \binom{N}{d} \\ &= \left(\frac{1}{2}\right)^{N+1} [1 + \exp(-\rho_c)]^N \end{aligned} \tag{8.46}$$

We observe that the right-hand side of (8.46) is independent of the index i. Hence, when we substitute the bound (8.46) into (4.15) we obtain

$$\begin{aligned} P(\mathcal{E}) &< \sum_{i=1}^{2^{rN}-1} P(\mathcal{E}_i) < 2^{rN}\left(\frac{1}{2}\right)^{N+1} [1 + \exp(-\rho_c)]^N \\ &= \frac{1}{2}\, 2^{-(r_0 - r)N} \end{aligned} \tag{8.47}$$

where

$$r_0 = 1 - \log_2[1 + \exp(-\rho_c)] \tag{8.48}$$

is the computational cut-off rate (in b/chip).

EXAMPLE 8.2

Find the cut-off rate r_0 of a Gaussian channel with binary input if the chip duration $T_c = 10^{-6}s$, the power of the received signal $P = 2$ W (watt) and the two-sided power spectral density of the AWGN is $N_0/2 = 10^{-6}$ W/Hz.

Solution

The signal-to-noise ratio per chip is

$$\rho_c = \frac{PT_c}{N_0} = 1$$

Then

$$r_0 = 1 - \log_2[1 + \exp(-\rho_c)] = 0.548$$

The capacity of the channel (with arbitrary input) is

$$c = \tfrac{1}{2}\log_2(1 + 2\rho_c) = \tfrac{1}{2}0.792$$

Substitution of $R = r/T_c$, $R_0 = r_0/T_c$, $T = NT_c$ in Formula (8.47) gives the linear part of the *random coding bound* for a band-limited AWGN channel with binary input,

$$P(\mathcal{E}) < \tfrac{1}{2}2^{-(R_0 - R)T} \tag{8.49}$$

The parameter $R_0 = (1/T_c)\{1 - \log_2[1 + \exp(-\rho_c)]\}$ is called the *computational cut-off rate* or *the cut-off rate* (in b/s) of a band-limited channel with binary signaling. Provided that $R < R_0$, $P(\mathcal{E}) \to 0$ as $T \to \infty$. If $T_c \to 0$, that is, the bandwidth $W \to \infty$, we have $R_0 \to P/2I_0 \ln 2$. The computational cut-off rate of a band-limited AWGN channel with binary input goes to the cut-off rate of the infinite-bandwidth AWGN channel [see Formula (8.20)].

Because at least one code in the ensemble has a performance matching or better than the ensemble average, we have demonstrated the existence of good codes as the block length increases, at least for a range of rates less than R_0. Now we develop a stronger result, that the range of rates for which exponentially decreasing error probability holds is $0 \le R < C$, where C is the channel capacity.

First we generalize the discrete memoryless channel model. Suppose that the input discrete channel alphabet is $\mathcal{A} = \{a_0, a_1, \ldots, a_{J-1}\}$ and the output alphabet is $\mathcal{B} = \{b_0, b_1, \ldots, b_{K-1}\}$. The input-output characteristics of the composite channel are described by a set of JK conditional probabilities

$$P(r = b_k | s = a_j) \stackrel{\text{def}}{=} p(j, k) \tag{8.50}$$

where $j = 0, 1, \ldots, J-1$, $k = 0, 1, \ldots, K-1$. Hence, if the input to a discrete memoryless channel is a sequence $\boldsymbol{v} = (v_0, v_1, \ldots, v_{N-1})$ of N symbols selected from the alphabet $\mathcal{A}$ and the corresponding output is the sequence

$\boldsymbol{r} = (r_0, r_1, \ldots, r_{N-1})$ of symbols from the alphabet $\mathcal{B}$, the joint conditional probability is

$$P(r_0 = b_{k_0}, r_1 = b_{k_1}, \ldots, r_{N-1} = b_{k_{N-1}} | s_0 = a_{j_0}, s_1 = a_{j_1}, \ldots, s_{N-1} = a_{j_{N-1}}) = \prod_{n=0}^{N-1} p(j_n | k_n) \tag{8.51}$$

This expression is simply a mathematical statement of the memoryless condition.

Consider again the random ensemble of code rate r, block length N codes over the alphabet $\mathcal{A}$. The codeword $\boldsymbol{v}_i$ corresponding to the ith message, $i = 0, 1, \ldots, 2^{rN} - 1$, is viewed as a sequence of IID random variables. The probability that a symbol $v_{i,n}$ of a codeword $\boldsymbol{v}_i$ is a_j equals

$$P(v_{i,n} = a_j) = p(j) \tag{8.52}$$

The *Gallager function* of the discrete memoryless channel is defined as

$$g(s) = -\log_2 \sum_{k=0}^{K-1} \left[\sum_{j=0}^{J-1} p(j) p(k|j)^{\frac{1}{1+s}} \right]^{1+s}, \quad s > 0 \tag{8.53}$$

The Gallager function $g(s)$ depends on s and the channel input probabilities $\{p(j)\}$. A typical Gallager function is given in Figure 8.3.

In coding theory it is shown that the function

$$e(r) = \max_{\{p(j)\}} \max_{0<s\leq 1} [g(s) - sr] \tag{8.54}$$

defines the random coding bound for a discrete memoryless channel,

$$P(\mathcal{E}) < 2^{-e(r)\cdot N} \tag{8.55}$$

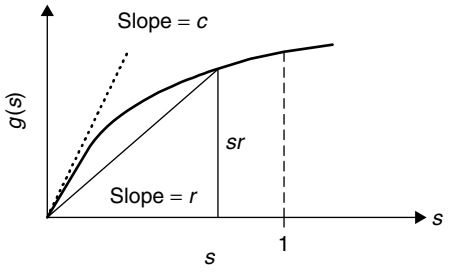

Figure 8.3. A typical Gallager function.

Now, according to (8.54), for any given $\{p(j)\}$ we wish to maximize $g(s) - sr$ for $0 < s \leq 1$. A stationary point, if it exists, will be the solution to equation

$$\frac{\mathrm{d}g(s)}{\mathrm{d}s} = r \tag{8.56}$$

Such a solution exists in the interval $0 < s \leq 1$, if (see Fig. 8.3)

$$r_{\mathrm{cr}} = \left.\frac{\mathrm{d}g(s)}{\mathrm{d}s}\right|_{s=1} \leq r \leq \left.\frac{\mathrm{d}g(s)}{\mathrm{d}s}\right|_{s=0} = c \tag{8.57}$$

where

$$c = \max_{\{p(j)\}} \sum_{j=0}^{J-1} \sum_{k=0}^{K-1} p(j)p(k|j) \log_2 \frac{p(k|j)}{\sum_i p(k|i)p(i)} \tag{8.58}$$

is the discrete channel *capacity rate* (in b/channel use).[1] The rate $g'(s)|_{s=1}$ is the *critical coding rate* (in b/channel use). On the other hand, if $r \leq r_{\mathrm{cr}}$, then the maximizing choice for s is $s = 1$ and the error exponent becomes

$$e(r) = g(1) - r \tag{8.59}$$

This is the linear part of the random coding bound. Here

$$g(1) = \max_{\{p(j)\}} \left\{ -\log_2 \left[\sum_{k=0}^{K-1} \left(\sum_{j=0}^{J-1} p(j) \cdot p(k|j)^{1/2} \right)^2 \right] \right\} = r_0 \tag{8.60}$$

is the computational cut-off rate. For r larger than r_{cr} we have, using Formula (8.56), a parametric form of the solution

$$\begin{aligned} r &= \frac{\partial g(s)}{\partial s}, \\ e(r) &= g(s) - sg'(s) \end{aligned} \qquad 0 < s \leq 1 \tag{8.61}$$

which pertains for $r_{\mathrm{cr}} \leq r < c$.

A typical sketch of the reliability function is shown in Figure 8.2. For all rates $0 \leq r < c$, $e(r)$ remains positive. We observe that, in general, a different input distribution $\{p(j)\}$ optimizes $e(r)$ as the code rate r changes. However, for symmetric channels, as for binary input symmetric channels, the equiprobable input assignment maximizes $e(r)$ for any rate r.

Consider again the model of the AWGN channel with binary input, studied in the beginning of this section. Then $\mathcal{A} = \{1, -1\}$, and the input assignment

[1] We use capital C for notation of the Shannon capacity, which is the maximum achievable *transmission rate* R (in b/s). For notation of the maximal achievable *code rate* (in b/channel use) in a discrete channel we use the small letter c.

$P(v=1)=P(v=-1)=1/2$ maximizes the error exponent $e(r)$. If we replace the finite sum $\sum_k$ in Formula (8.53) over the output channel alphabet $\mathcal{B}$ by the integral over the received signals, we get the next expression for the Gallager function of the AWGN channel with binary input.

$$g(s)=-\log_2\int_{-\infty}^{\infty}\left\{\frac{1}{2}\left[\frac{1}{\sqrt{\pi I_0/T_c}}\exp\left[-\frac{(x-\sqrt{P})^2}{I_0/T_c}\right]\right]^{\frac{1}{1+s}}\right. \tag{8.62}$$
$$\left.+\frac{1}{2}\left[\frac{1}{\sqrt{\pi I_0/T_c}}\exp\left[-\frac{(x+\sqrt{P})^2}{I_0/T_c}\right]\right]^{\frac{1}{1+s}}\right\}^{1+s}\mathrm{d}x,\quad 0<s\le 1$$

where $I_0/2$ is the two-sided power spectral density of the additive and interference noise. The computational cut-off rate is given by the formula

$$r_0=g(1)=1-\log_2\left[1+\exp\left(-\frac{PT_c}{I_0}\right)\right] \tag{8.63}$$

which coincides with expression (8.48). The critical rate is $g'(1)$. The capacity of the binary input AWGN channel (in b/channel use) is [compare with Formula (8.58)]

$$c=\int_{-\infty}^{\infty}\frac{1}{\sqrt{\pi I_0/T_c}}\exp\left[-\frac{(x-\sqrt{P})^2}{I_0/T_c}\right]$$
$$\log_2\frac{2\exp\left[-\frac{(x-\sqrt{P})^2}{I_0/T_c}\right]}{\exp\left[-\frac{(x-\sqrt{P})^2}{I_0/T_c}\right]+\exp\left[-\frac{(x+\sqrt{P})^2}{I_0/T_c}\right]}\mathrm{d}x \tag{8.64}$$
$$=1-\int_{-\infty}^{\infty}\frac{1}{\sqrt{\pi I_0/T_c}}\exp\left[-\frac{(x-\sqrt{P})^2}{I_0/T_c}\right]\cdot\log_2\left[1+\exp\left(-\frac{2x\sqrt{PT_c}}{I_0}\right)\right]\mathrm{d}x$$
$$=1-\int_{-\infty}^{\infty}\frac{1}{\sqrt{\pi\rho_c}}\exp\left[-\frac{(y-\rho_c)^2}{\rho_c}\right]\log_2[1+\exp(-2y)]\,\mathrm{d}y$$

where $\rho_c=PT_c/I_0$ is signal-to-noise ratio per chip.

Formulas (8.61)–(8.64) define the random coding bound for the AWGN channel with binary input, for code rate r (in b/channel use) and block length N. To get the random coding bound in terms of the transmission rate $R=r/T_c$ (in bit/s) and transmission time $T=NT_c$, we introduce the Gallager function $G(s)=g(s)/T_c$, where $g(s)$ is defined by (8.62). Correspondingly, the cut-off rate $R_0=r_0/T_c$, the

critical rate $R_{\mathrm{cr}} = r_{\mathrm{cr}}/T_{\mathrm{c}}$, and the Shannon capacity $C = c/T_{\mathrm{c}}$. Then for $R < R_{\mathrm{cr}}$ we have the following reliability function

$$E(R) = R_0 - R, \qquad 0 < R \leq R_{\mathrm{cr}} \tag{8.65}$$

The parametric form of the reliability function for larger rates is

$$\begin{aligned} R &= \frac{\mathrm{d}G(s)}{\mathrm{d}s}, \\ E(R) &= G(s) - sG'(s) \end{aligned} \qquad 0 < s \leq 1 \tag{8.66}$$

which applies for $R_{\mathrm{cr}} < R < C$.

When $T_{\mathrm{c}} \to 0$, the function $G(s)$ approaches the Gallager function $G_{\mathrm{ib}}(s)$ of the infinite bandwidth AWGN channel

$$G_{\mathrm{ib}}(s) = \frac{P}{I_0 \ln 2} \frac{s}{1+s} \tag{8.67}$$

Application of Formulas (8.65) and (8.66) gives the same expression for the reliability function as (8.39). In the case of the infinite-bandwidth AWGN channel, the random coding bound is exponentially tight. In the general case, the random coding bound is exponentially tight only for $R_{\mathrm{cr}} < R < C$.

So far we have been focusing on block codes. By using random coding arguments we can prove the existence of a memory m and rate $r = b/c$ (in b/channel use) binary convolutional encoder for which the bit error probability is upper-bounded by inequality

$$P_{\mathrm{b}} < 2^{-mc(e_{\mathrm{c}}(r)+o(1))} \tag{8.68}$$

where $o(1) \to 0$ when $m \to \infty$. Here $e_{\mathrm{c}}(r)$ is a random-coding exponent for convolutional codes. The functional form of $e_{\mathrm{c}}(r)$ is given by

$$e_{\mathrm{c}}(r) = \begin{cases} r_0, & \text{if } r \leq r_0, \\ g(s_0), & \text{if } r_0 < r < c \end{cases} \tag{8.69}$$

and s_0 is the solution to equation

$$s_0 r = g(s_0) \tag{8.70}$$

The random-coding bound for convolutional codes in terms of the transmission rate $R = r/T_{\mathrm{c}}$ (in b/s) and the constraint $T = mcT_{\mathrm{c}}$ is

$$P_{\mathrm{b}} < 2^{-T(E_{\mathrm{c}}(R)+o(1))} \tag{8.71}$$

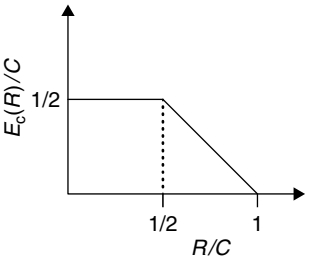

Figure 8.4. The convolutional reliability function for the infinite-bandwidth AWGN channel.

where $o(1) \to 0$ when $mc \to \infty$ and the convolutional random-coding exponent $E_c(R) = e_c(r)/T_c$. In particular, if $T_c \to 0$, $c \to \infty$ such that $r/T_c = R$ and $T = mcT_c$ we have

$$E_c(R) = \begin{cases} R_0 = P/2I_0 \ln 2 = C/2, & \text{if } R \le R_0 = C/2, \\ C - R, & \text{if } R_0 < R < C \end{cases} \tag{8.72}$$

A plot of $E_c(R)/C$ is shown in Figure 8.4.

It is seen that the convolutional random-coding exponent $E_c(R)$ dominates the block coding exponent (reliability function) $E(R)$ sketched in Figure 8.2. This fact, coupled with the practical issue that maximum likelihood decoding is more convenient with convolutional codes than with block codes, has prompted enormous interest in convolutional coding.

8.3 CAPACITY OF FH CDMA SYSTEMS

Formula (8.58) defines the capacity of a discrete memoryless channel with input alphabet $\mathcal{A} = \{a_0, a_1, \ldots, a_{J-1}\}$ and output alphabet $\mathcal{B} = \{b_0, b_1, \ldots, b_{K-1}\}$. The conditional probabilities $p(k|j)$ relate channel outputs to inputs. The probabilities $\{p(j)\}$ determine the input distribution. The output probabilities are

$$p(k) = \sum_{j=0}^{J-1} p(j)p(k|j) \tag{8.73}$$

The double sum in the right-hand side of (8.58) can be rewritten as

$$\begin{aligned} I(v, r) &= \sum_{j=0}^{J-1} \sum_{k=0}^{K-1} p(j)p(k|j) \log_2 \frac{p(k|j)}{\sum_i p(k|i)p(i)} \\ &= -\sum_{k=0}^{K-1} p(k) \log_2 p(k) + \sum_{j=0}^{J-1} \sum_{k=0}^{K-1} p(j)p(k|j) \log_2 p(k|j) \end{aligned} \tag{8.74}$$

where $I(v, r)$ denotes the *(average) mutual information* provided about symbol r by the knowledge of symbol v. The first term of the right-hand side of (8.74),

$$H(r) \stackrel{\text{def}}{=} -\sum_{k=0}^{K-1} p(k) \log_2 p(k) \tag{8.75}$$

is the *entropy* of the channel output r; the term

$$H(r|v) = -\sum_{j=0}^{J-1} \sum_{k=0}^{K-1} p(j)p(k|j) \log_2 p(k|j) \tag{8.76}$$

is the *conditional entropy* of the channel output r conditioned that the channel input v is known. Using definitions (8.75) and (8.76) we can rewrite Formula (8.74) as

$$I(v, r) = H(r) - H(r|v) \tag{8.77}$$

We find that the average mutual information between v and r is the difference between the entropy of the output r and the conditional entropy of r given input v. It can be shown (Problem 8.6) that $I(v, r)$ is equal also to the difference between the entropy of the input v and conditional entropy of v given output r,

$$I(v, r) = H(v) - H(v|r) \tag{8.78}$$

The channel capacity (in b/channel use),

$$c = \max_{\{p(k)\}} I(v, r) \tag{8.79}$$

is found by maximizing the right-hand side of (8.78) over the input distribution. This formula is valid for the wide class of memoryless channels. In the Sections 8.1 and 8.2 we demonstrated this for the AWGN channel with discrete input. In this section, we will find the capacity for the model of the FH CDMA system channel. For simplicity we consider only downlink transmission.

The code sequence $\boldsymbol{x}^{(k)}$ transmitted by the kth user is given by [compare with (2.125)]

$$\boldsymbol{x}^{(k)} = (x_0^{(k)}, x_1^{(k)}, \ldots, x_{N-1}^{(k)}), \quad k = 1, 2, \ldots, K \tag{8.80}$$

where $x_n^{(k)} \in \{0, 1, \ldots, M-1\}$ and M is the input alphabet (hopset) size. The K-dimensional vector

$$\boldsymbol{x}_n = (x_n^{(1)}, x_n^{(2)}, \ldots, x_n^{(K)}) \tag{8.81}$$

where each component takes one of M values, is the channel input at the nth time instant. The channel output at the nth time instant depends on the input $\boldsymbol{x}_n$ and can be represented by the M-ary vector

$$\boldsymbol{y}_n = (y_{n,0}, y_{n,1}, \ldots, y_{n,M-1}) \tag{8.82}$$

whose components take binary values

$$y_{n,j} \stackrel{\text{def}}{=} y_{n,j}(\boldsymbol{x}_n) = \begin{cases} 0, & \text{if } x_n^{(k)} \neq j, k = 1, 2, \ldots, K, \\ 1, & \text{otherwise} \end{cases} \tag{8.83}$$

We assume that none of the users has knowledge of the structure of the codes used by other users, and, hence, other users can be considered as jammers.

We are interested in the total channel capacity c_{total}, which is the sum of the capacities for the individual users. The total capacity c_{total} depends on the alphabet size M and the number of active users K. We must find the ratio of K and M that maximizes the total capacity as $K \to \infty$, $M \to \infty$, when $\lim_{M\to\infty} K/M = \lambda$ exists and is nonzero.

Consider the case where all users use a uniform distribution of the code symbols (frequencies) over the input alphabet (hopset). The average mutual information provided about symbol $x_n^{(k)}$ by the knowledge of vector $\boldsymbol{y}_n$ is

$$I(x_n^{(k)}, \boldsymbol{y}_n) = H(x_n^{(k)}) - H(x_n^{(k)}|\boldsymbol{y}_n), n = 0, 1, \ldots, N-1, \ k = 1, 2, \ldots, K \tag{8.84}$$

Under the condition that all M possible values $x_n^{(k)}$ are equiprobable, $H(x_n^{(k)}) = \log_2 M$. Further, if the Hamming weight of $\boldsymbol{y}_n$ is w, the conditional probability

$$P(x_n^{(k)}|\boldsymbol{y}_n) = \begin{cases} 1/w, & \text{if the } x_n^{(k)}\text{th component of } \boldsymbol{y}_n \text{ is } 1, \\ 0, & \text{otherwise} \end{cases} \tag{8.85}$$

The probability that the received vector $\boldsymbol{y}^{(n)}$ has Hamming weight w depends on the number of users K and hopset size M. We denote this probability $P_{K,M}(w)$. It satisfies the condition $P_{K,M}(w) = 0$, $w > \min(K, M)$. The analytical expression for $P_{K,M}(w)$ is given in [56]

$$P_{K,M}(w) = \frac{\binom{M}{w}}{M^K} \sum_{i=0}^{w} (-1)^i \binom{w}{i} (w-i)^K \tag{8.86}$$

From Formula (8.85) it follows that

$$\begin{aligned} H(x_n^{(k)}|\boldsymbol{y}_n) &= -\sum_{\boldsymbol{y}_n} P(\boldsymbol{y}_n) \left(\sum_{x_n^{(k)}} P(x_n^{(k)}|\boldsymbol{y}_n) \log_2 P(x_n^{(k)}|\boldsymbol{y}_n) \right) \\ &= \sum_{w=1}^{\min(K,M)} P_{K,M}(w) \log_2(w) \end{aligned} \tag{8.87}$$

Therefore,

$$I(x_n^{(k)}, \boldsymbol{y}_n) = \sum_{w=1}^{\min(K,M)} P_{K,M}(w) \log_2 \frac{M}{w} \tag{8.88}$$

This is an expression for the average mutual information $I(x_n^{(k)}, \boldsymbol{y}_n)$ in the case of a uniform distribution over the hopset. We can interpret $I(x_n^{(k)}, \boldsymbol{y}_n)$ as the kth user Shannon capacity $c^{(k)}$ for the uniform distribution of code symbols over the hopset. The total capacity is the sum of capacities of the individual users,

$$c_{\text{total}} = \sum_{k=1}^{K} c^{(k)} = K \sum_{w=1}^{\min(K,M)} P_{K,M}(w) \cdot \log_2 \frac{M}{w} \tag{8.89}$$

Now we will study the case when $K = \lambda M$, $\lambda \neq 0$ is a constant, and $M \to \infty$. The weight of the received vector $\boldsymbol{y}_n$ can be considered as a random variable

$$w_n = \sum_{j=0}^{M-1} y_{n,j} \tag{8.90}$$

It follows from definition (8.83) that

$$P(y_{n,j} = 0) = \left(1 - \frac{1}{M}\right)^K, \quad j = 0, 1, \ldots, M-1 \tag{8.91}$$

and thus

$$\lim_{M\to\infty} P(y_{n,j} = 0) = 1 - \lim_{M\to\infty} E(y_{n,j}) = e^{-\lambda} \tag{8.92}$$

From Formulas (8.91) and (8.92) it follows that the expected value of w_n is given by

$$\begin{aligned} E\{w_n\} &= \sum_{j=0}^{M-1} E(y_{n,j}) = M\left[1 - \left(1 - \frac{1}{M}\right)^K\right] \simeq M(1 - e^{-\lambda}) - e^{-\lambda}\frac{\lambda}{2} + o(1) \\ &= M\beta + o(1) \end{aligned}$$

where $\beta = 1 - e^{-\lambda} - e^{-\lambda}\lambda/2$ and $\simeq$ means equality of the main terms. To find the second moment of w_n we consider the random variable

$$z_{n,j} = 1 - y_{n,j}$$

Obviously,

$$E(z_{n,j}) = \left(1 - \frac{1}{M}\right)^K \simeq e^{-\lambda} - e^{-\lambda}\frac{\lambda}{2M} + o\left(\frac{1}{M}\right)$$

and for $i \neq j$

$$E(z_{n,i}z_{n,j}) = \left(1 - \frac{2}{M}\right)^K \simeq e^{-2\lambda} - e^{-2\lambda}\frac{2\lambda}{M} + o\left(\frac{1}{M}\right)$$

Hence for $i \neq j$

$$\begin{aligned} E(y_{n,i}y_{n,j}) &= E[(1 - z_{n,i})(1 - z_{n,j})] = 1 - E(z_{n,i}) - E(z_{n,j}) + E(z_{n,i}z_{n,j}) \\ &\simeq 1 - 2e^{-\lambda} + e^{-2\lambda} + e^{-\lambda}\frac{\lambda}{M} - e^{-2\lambda}\frac{2\lambda}{M} + o\left(\frac{1}{M}\right) \\ &= (1 - e^{-\lambda})^2 + (e^{-\lambda}\lambda - e^{-2\lambda}2\lambda)\frac{1}{M} + o\left(\frac{1}{M}\right) \end{aligned} \tag{8.93}$$

From Formulas (8.92) and (8.93) we obtain

$$\begin{aligned} E(w_n^2) &= E\left[\left(\sum_{j=0}^{M-1} y_{n,j}\right)^2\right] = M(M-1)E(y_{n,i}y_{n,j}) + ME(y_{n,i}^2) \\ &= M(M-1)(1 - e^{-\lambda})^2 + M(e^{-\lambda}\lambda - e^{-2\lambda}2\lambda) + M(1 - e^{-\lambda}) + o(M) \end{aligned}$$

Consequently, the variance of w_n is given by

$$\sigma_w^2 = E(w_n^2) - [E(w_n)]^2 \simeq M[e^{-\lambda}(1 - e^{-\lambda}) - \lambda e^{-2\lambda}] + o(M)$$

Consider the right-hand side of (8.88). Let us split it into three sums

$$\sum_{w=1}^{\min(K,M)} = \sum_{w=1}^{N_1} + \sum_{w=N_1+1}^{N_2} + \sum_{w=N_2+1}^{\min(K,M)} \tag{8.94}$$

where

$$\begin{aligned} N_1 &= \lfloor M\beta - M^{\frac{1}{2}+\varepsilon} \rfloor \simeq M\beta - M^{\frac{1}{2}+\varepsilon} \\ N_2 &= \lfloor M\beta - M^{\frac{1}{2}+\varepsilon} \rfloor \simeq M\beta + M^{\frac{1}{2}+\varepsilon} \end{aligned} \tag{8.95}$$

Here $\lfloor \cdot \rfloor$ means the integer part and $0 < \varepsilon < 1/2$. If $N_2 + 1 > \min(K, M)$, the third sum in (8.94) vanishes, and in the second sum the upper limit is replaced by $\min(K, M)$. From (8.95) we have

$$\lim_{M\to\infty} \frac{N_1}{M} = \lim \frac{N_2}{M} = \beta$$

Using Chebyshev's inequality, we obtain

$$\sum_{w=1}^{N_1} P_{K,M}(w) + \sum_{w=N_2+1}^{\min(K,M)} P_{K,M}(w)$$

$$\simeq P\{|w - \beta M| \geq M^{\frac{1}{2}+\varepsilon}\} \leq \frac{\sigma_w^2}{M^{1+2\varepsilon}} \approx \frac{e^{-\lambda}(1 - e^{-\lambda}) - \lambda e^{-2\lambda}}{M^{2\varepsilon}} \quad (8.96)$$

Adding the first and third terms in (8.94) and using Formula (8.96), we get

$$\sum_{w=1}^{N_1} P_{K,M}(w) \cdot \log_2 \frac{M}{w} + \sum_{w=N_{2+1}}^{\min(K,M)} P_{K,M}(w) \cdot \log_2 \frac{M}{w}$$

$$\leq \left[\sum_{w=1}^{N_1} P_{K,M}(w) + \sum_{w=N_2+1}^{M} P_{K,M}(w) \right] \log_2 M$$

$$\leq \frac{e^{-\lambda}(1 - e^{-\lambda}) - \lambda e^{-2\lambda}}{M^{2\varepsilon}} \cdot \log_2 M \quad (8.97)$$

Clearly, as $M \to \infty$, the right-hand side of (8.97) goes to zero. Because in the second sum of (8.94) $N_1 < w \leq N_2$,

$$\lim_{M\to\infty} \log_2 \frac{M}{w} = -\log_2 \beta = -\log_2(1 - e^{-\lambda}),\ N_1 < w \leq N_2$$

we can combine Formulas (8.89) and (8.97) to obtain

$$\lim_{M\to\infty} \frac{c_{\text{total}}}{M} = -\lambda \log_2(1 - e^{-\lambda}) \quad (8.98)$$

From (8.98) it follows that the maximum total capacity (in b/channel use) for our model of the FH CDMA system is obtained for $\lambda = \ln 2$ and

$$c_{\text{total}} = M \cdot \ln 2 + O(M) \quad (8.99)$$

In [8] it is shown that a uniform distribution of code symbols (frequencies) of the hopset is optimum, that is, maximizes c_{total}, only if $\lambda = \ln 2$, that is, $K = (\ln 2)M$. In all other cases a uniform distribution is not optimum.

In Table 8.1 the total capacity for the FH CDMA system (in b/channel use) given by Formula (8.89) for different values of K and M is presented. It can be noted that c_{total}/M is approximated by the right-hand side of (8.98) even if K and M are small.

Substitution $C_{\text{total}} = c_{\text{total}}/T_c$, where T_c is the hop duration, gives the maximal total capacity of the FH CDMA system $C_{\text{total}} \simeq M \ln 2/T_c$ (in b/s).

Table 8.1 Total Shannon Capacity (in b/channel use) of the FH CDMA System

	Hopsize					
Number of users	$M = 2$	$M = 4$	$M = 8$	$M = 16$	$M = 32$	$M = 64$
2	1.0000	2.5000	4.2500	6.1250	8.0625	10.0312
3	0.7500	2.5294	4.8952	7.5722	10.4091	13.3272
4	0.5000	2.3713	5.2155	8.6152	12.3094	16.1552
5		2.1339	5.3325	9.3789	13.8890	18.6408
10		0.9450	4.5843	10.8684	18.8714	23.8378
15			3.2945	10.5112	21.1242	33.8033
20				9.4615	21.9274	37.8497
25				8.1861	21.8663	40.5944
30				6.9024	21.2686	42.3936
40					19.2054	43.9729
50					16.6733	44.0417

Because the FH CDMA system occupies bandwidth of order M/T_c,

$$C_{\text{total}} \simeq W(\ln 2) \simeq 0.693\ W \tag{8.100}$$

Comparison of (8.35) and (8.100) shows that the total Shannon capacity of a DS CDMA system is about 2.1 times larger than the total capacity of a FH CDMA system using the same bandwidth W.

EXAMPLE 8.3

Estimate the radio channel capacity of a FH CDMA system operating with a total transmission rate that equals to the total capacity of the system.

Solution

Each user of the system described above operates with the same transmission rate, which equals

$$R = C_{\text{total}}/K = (W \ln 2)/K$$

Then the radio channel capacity $K_0 = (W \ln 2)/R$.

8.4 UPLINK MULTIPLE-ACCESS CHANNELS

Multiple-access channels illustrate important features of CDMA theory. In this section, we consider the Gaussian multiple-access channel, which can be treated as an information-theoretic model of the reverse (uplink) of a DS CDMA system. But first we will study the basic single-user discrete AWGN channel with input power P and noise variance σ^2. The transmitted signal $\boldsymbol{s} = (s_0, s_1, \ldots, s_{N-1})$

has a power constraint

$$\frac{1}{N}\sum_{n=0}^{N-1} s_n^2 \le P \tag{8.101}$$

The output of the channel is modeled as

$$r_n = s_n + \xi_n,\ n = 0, 1, \ldots, N-1 \tag{8.102}$$

where ξ_n are IID zero-mean Gaussian variables with variance σ^2.

Now we generalize the definitions of entropy, conditional entropy, and average mutual information introduced in Section 8.3 for the discrete random variables to continuous random variables.

The entropy of a continuous random variable is called the *differential entropy*. The differential entropy of a continuous random variable x with probability density function $f(x)$ is defined as

$$H(x) = -\int_{-\infty}^{\infty} f(x)\log_2 f(x)\,\mathrm{d}x \tag{8.103}$$

Correspondingly, the *conditional differential entropy* $H(x|y)$ is defined as

$$H(x|y) = -\int_{-\infty}^{\infty}\int_{-\infty}^{\infty} f(x|y)f(y)\log_2 f(x|y)\,\mathrm{d}x\,\mathrm{d}y \tag{8.104}$$

where $f(y)$ is the probability density function of the random variable y and $f(x|y)$ is the conditional probability density function of the random variable x given y.

EXAMPLE 8.4

Calculate the differential entropy of a Gaussian random variable with probability density function

$$f(x) = \frac{1}{\sqrt{2\pi\sigma^2}}\exp\left[-\frac{(x-\mu)^2}{2\sigma^2}\right] \tag{8.105}$$

Solution

From Formulas (8.103)–(8.105), we have

$$\begin{aligned} H(x) &= \int_{-\infty}^{\infty}\frac{1}{\sqrt{2\pi\sigma^2}}\exp\left[-\frac{(x-\mu)^2}{2\sigma^2}\right]\cdot\left[\frac{(x-\mu)^2}{2\sigma^2}\log_2 e + \log_2\sqrt{2\pi\sigma^2}\right]\mathrm{d}x \\ &= \log_2 e\int_{-\infty}^{\infty}\frac{1}{\sqrt{2\pi\sigma^2}}\exp\left[-\frac{(x-\mu)^2}{2\sigma^2}\right]\left[\frac{(x-\mu)^2}{2\sigma^2}\right]\mathrm{d}x + \frac{1}{2}\log_2(2\pi\sigma^2) \\ &= \frac{1}{2}\log_2 e + \frac{1}{2}\log(2\pi\sigma^2) = \frac{1}{2}\log_2(2\pi e\sigma^2) \end{aligned} \tag{8.106}$$

The average mutual information $I(x, y)$ between two continuous random variables x and y is equal to

$$I(x, y) = H(x) - H(x|y) \tag{8.107}$$

where $H(x)$ and $H(x|y)$ are defined by Formulas (8.103) and (8.104).

EXAMPLE 8.5

Let IID Gaussian variables s_n, $n = 0, 1, \ldots, N-1$, with the probability density function

$$f(s) = \frac{1}{\sqrt{2\pi P}} \exp\left(-\frac{s^2}{2P}\right) \tag{8.108}$$

be the input of a discrete-time AWGN channel. By definition, the output of the channel is $r_n = s_n + \xi_n$, where ξ_n, $n = 0, 1, \ldots, N-1$, are zero-mean Gaussian random variables with variance σ^2. Find the average mutual information between input and output of the channel (in b/channel use).

Solution

The average mutual information between the channel input s_n and output r_n is

$$I(s_n, r_n) = H(r_n) - H(r_n|s_n) = H(r_n) - H(\xi_n)$$

But r_n is a zero-mean Gaussian random variable with variance $P + \sigma^2$. From Formula (8.106) we have

$$H(r_n) = \frac{1}{2}\log_2[2\pi e(P + \sigma^2)]$$

$$H(\xi_n) = \frac{1}{2}\log(2\pi e\sigma^2)$$

Finally we have

$$I(s_n, r_n) = \frac{1}{2}\log_2\left(1 + \frac{P}{\sigma^2}\right) \tag{8.109}$$

The right-hand side of (8.109) coincides with the right-hand side of inequality (8.11) and, consequently, defines the channel capacity (in b/channel use). This proves that Gaussian-like signals are optimal in the AWGN channel.

Generally speaking, Gaussian-distributed codewords $\boldsymbol{s} = (s_0, s_1, \ldots, s_{N-1})$, where s_n are zero-mean Gaussian random variables with variance P, do not satisfy the power constraint (8.101). But if N is large, for any $\varepsilon > 0$ almost all codewords satisfy the inequality $\frac{1}{N}\sum_{n=0}^{N-1} s_n^2 \le P + \varepsilon$, that is, satisfy the power constraint $P + \varepsilon$. We define the following event:

$$\mathcal{E}_0 = \left\{\frac{1}{2}\sum_{n=0}^{N-1} s_n^2 > P + \varepsilon\right\}$$

Then if the power constraint $P + \varepsilon$ is violated for the transmitted codeword $\boldsymbol{s}$, we will include the corresponding event $\mathcal{E}_0$ in the decoding error event. Because $P(\mathcal{E}_0) \to 0$ as $N \to \infty$, the probability of decoding error goes to zero if the transmission rate is less than the Shannon capacity of the AWGN channel.

Consider now the model of the Gaussian uplink channel with K users. The received signal is

$$r_n = \sum_{k=1}^{K} s_n^{(k)} + \xi_n, \ n = 0, 1, \ldots, N-1 \tag{8.110}$$

where ξ_n are IID zero-mean Gaussian random variables with variance σ^2. The components of vector $\boldsymbol{s}^{(k)} = (s_0^{(k)}, s_1^{(k)}, \ldots, s_{N-1}^{(k)})$ are IID zero-mean Gaussian random variables with variance $P^{(k)}$. We will assume that the signals $\boldsymbol{s}^{(k)}$ satisfy the power constraint

$$\frac{1}{N} \sum_{n=0}^{N-1} (s_n^{(k)})^2 \le P^{(k)} + \varepsilon, \ k = 1, 2, \ldots, K \tag{8.111}$$

for some $\varepsilon > 0$.

Consider in more detail the case $K = 2$. We assume that the first user uses a (Gaussian) block $(N, Nr^{(1)})$ code, where the codewords are Gaussian random vectors. Analogously, the second user uses a Gaussian $(N, Nr^{(2)})$ code. There are two transmitters (mobiles) and one receiver (base station). The receiver defines which pair $(\boldsymbol{s}^{(1)}, \boldsymbol{s}^{(2)})$ of codewords was sent. If at least one of the sequences $\boldsymbol{s}^{(1)}$ or $\boldsymbol{s}^{(2)}$ are decoded erroneously, we declare an error.

The code rate pair $(r^{(1)}, r^{(2)})$ is said to be achievable if for sufficiently large N there exists a pair $\{(N, Nr^{(1)}), \ (N, Nr^{(2)})\}$ of codes for which the decoding error probability can be made arbitrarily small. The *capacity region* is the closure of the set of achievable $(r^{(1)}, r^{(2)})$ rate pairs.

The achievable *code rate region* $(r^{(1)}, r^{(2)})$ of the Gaussian multiple access channel is given in the following inequalities:

$$\begin{aligned} r^{(1)} &< \frac{1}{2} \log_2 \left(1 + \frac{P^{(1)}}{\sigma^2} \right), \\ r^{(2)} &< \frac{1}{2} \log_2 \left(1 + \frac{P^{(2)}}{\sigma^2} \right), \\ r^{(1)} + r^{(2)} &< \frac{1}{2} \log_2 \left(1 + \frac{P^{(1)} + P^{(2)}}{\sigma^2} \right) \end{aligned} \tag{8.112}$$

This upper bounds are achieved when $s_n^{(1)}$ and $s_n^{(2)}$ are Gaussian-like.

The capacity region of the multiple access channel is convex, that is, if $(r^{(1)}, r^{(2)})$ and $(\hat{r}^{(1)}, \hat{r}^{(2)})$ are achievable, then $\left(\lambda r^{(1)} + (1 - \lambda)\hat{r}^{(1)}, \lambda r^{(2)} + \right.$

$(1-\lambda)\hat{r}^{(2)}\big)$ is achievable for $0 \le \lambda \le 1$. The idea of the proof is time division (time sharing).

Suppose that there exist pairs $\{(\lambda N, \lambda N r^{(1)}), (\lambda N, \lambda N r^{(2)})\}$ and $\{((1-\lambda)N, (1-\lambda)N\hat{r}^{(1)}), ((1-\lambda)N, (1-\lambda)N\hat{r}^{(2)})\}$ of codes for which the decoding error probabilities are less than a given $\varepsilon/2$. Then we can construct a third pair $\{(N, (\lambda r^{(1)} + (1-\lambda)\hat{r}^{(1)})N), (N, (\lambda r^{(2)} + (1-\lambda)\hat{r}^{(2)})N)\}$ of length N codes by using the first code pair for the first λN symbols and the second code pair for the last $(1-\lambda)N$ symbols. The code rate pairs of the new codes are $(\lambda r^{(1)} + (1-\lambda)\hat{r}^{(1)}, \lambda r^{(2)} + (1-\lambda)\hat{r}^{(2)})$. Because the overall probability of the error is less than the sum of the error probabilities for each of the segments, the probability of error of the new codes is less than ε and the rate is achievable.

The surprising fact about inequalities (8.112) is that the sum of the code rate can be as large as $(1/2)\log_2[1 + (P^{(1)} + P^{(2)})/\sigma^2]$, which is that rate achievable by a single transmitter sending with a power equal to the sum of the powers. But we must emphasize that in this case users should be coordinated.

Figure 8.5 presents the achievable region of the Gaussian uplink multiple-access channel. The region has four corner points. The first corner point $((1/2)\log_2(1 + P^{(1)}/\sigma^2), 0)$ corresponds to the maximum code rate achievable from the first user to the receiver when the second user is not sending any information. The second point $((1/2)\log_2(1 + P^{(1)}/\sigma^2), (1/2)\log_2(1 + P^{(2)}/(P^{(1)} + \sigma^2)))$ corresponds to the maximum code rate at which the second user can send as long as the first user sends at his maximum rate. This is the rate that is obtained if the first user is considered as jammer for the channel from the second user to the receiver. In this case the second user can send at code rate $(1/2)\log_2(1 + P^{(2)}/(P^{(1)} + \sigma^2))$. The receiver now knows which codeword was used and can "cancel" its effect (interference) from the channel. We can consider the channel now as a single-user channel. The other two corner points in Figure 8.5 can be explained analogously.

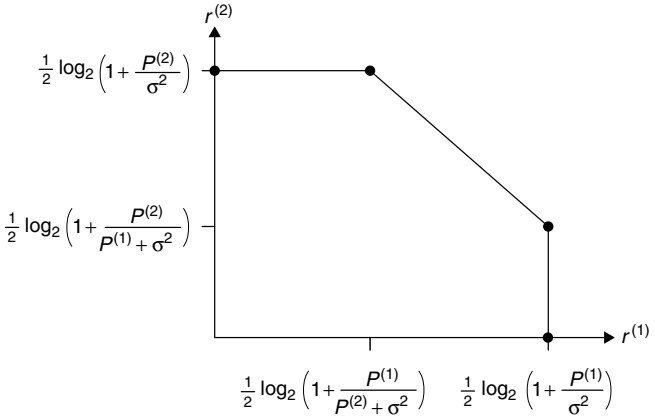

Figure 8.5. Achievable rate region of the Gaussian uplink multiple access channel.

In Chapter 9 we study interference cancellation in more detail. In particular, we generalize results derived in this section for two users to K users.

In many practical situations, simpler schemes like time division of frequency division multiplexing are used. The achievable rate pairs for time division multiplexing are on the line joining points $((1/2)\log_2(1 + P^{(1)}/\sigma^2), 0)$ and $(0, (1/2)\log_2(1 + P^{(2)}/\sigma^2))$.

All results up to now were formulated in terms of code rate (in b/channel use). Substitution $R^{(k)} = r^{(k)}/T_c$, $\sigma^2 = N_0/2T_c$, where T_c is the chip duration and $N_0/2$ is two-sided power spectral density of the AWGN, gives a formulation of the achievable region in terms of transmission rate pairs $(R^{(1)}, R^{(2)})$.

EXAMPLE 8.6

Consider a two-user time division multiplexing system where the transmission rate $R^{(1)}$ of the first user is twice as large as the transmission rate $R^{(2)}$ of the second user, $R^{(1)} = 2R^{(2)}$. The two-sided power spectral density of the AWGN is $N_0/2$, the bandwidth $W = 1/T_c$; the available average signal power is $P^{(1)} = 2P/3$ for the first user and $P^{(2)} = P/3$ for the second user, $\sigma^2 = N_0/2T_c$. Construct signals. Find the total capacity of the system.

Solution

Let $\{\zeta_n,\ n = -1, 0, 1, \dots\}$ be a set of IID zero-mean Gaussian variables with unit variance

$$v_n^{(1)} = \begin{cases} \zeta_n, & n \neq 0 \ (mod\ 3), \\ 0, & otherwise \end{cases}$$

$$v_n^{(2)} = \begin{cases} \zeta_n, & n = 0 \ (mod\ 3), \\ 0, & otherwise \end{cases}$$

The transmitted baseband signals are

$$s^{(1)}(t) = \sqrt{P} \sum_{n=-\infty}^{\infty} v_n^{(1)} h_{T_c}(t - nT_c),$$

$$s^{(2)}(t) = \sqrt{P} \sum_{n=-\infty}^{\infty} v_n^{(2)} h_{T_c}(t - nT_c)$$

where $h_{T_c}(\cdot)$ is the unit amplitude rectangular pulse.

The maximal achievable rates (capacities) are

$$C^{(1)} = \frac{1}{2T_c} \cdot \frac{2}{3} \cdot \log_2\left(1 + \frac{P}{\sigma^2}\right) = \frac{1}{3T_c} \log_2\left(1 + \frac{P}{\sigma^2}\right) \tag{8.113}$$

$$C^{(2)} = \frac{1}{2T_c} \cdot \frac{1}{3} \cdot \log_2\left(1 + \frac{P}{\sigma^2}\right) = \frac{1}{6T_c} \log_2\left(1 + \frac{P}{\sigma^2}\right) \tag{8.114}$$

The total capacity is

$$C = C^{(1)} + C^{(2)} = \frac{1}{2T_c} \log_2 \left(1 + \frac{P}{\sigma^2}\right)$$

With frequency division multiplexing the rates depend on the bandwidth allocated to each user. In the case of two users with powers $P^{(1)}$ and $P^{(2)}$ and nonintersecting frequency bands $W^{(1)}$ and $W^{(2)}$, where $W^{(1)} + W^{(2)} = W$ is the total bandwidth, the following transmission rate pair is achievable:

$$\begin{aligned} R^{(1)} &= \frac{W^{(1)}}{2} \log_2 \left(1 + \frac{2P^{(1)}}{N_0 W^{(1)}}\right) \\ R^{(2)} &= \frac{W^{(2)}}{2} \log_2 \left(1 + \frac{2P^{(2)}}{N_0 W^{(2)}}\right) \end{aligned} \tag{8.115}$$

where $N_0/2$ is two-sided power spectral density of the AWGN.

EXAMPLE 8.7

Consider the two-user frequency multiplexing system where the transmission rates of users and available signal powers are equal: $R^{(1)} = R^{(2)} = R$, $P^{(1)} = P^{(2)} = P$. Construct optimal signals for the users.

Solution

The carrier frequencies for two users are

$$f_c^{(1)} = f_0 - \frac{W}{4}, \quad f_c^{(2)} = f_0 + \frac{W}{4} \tag{8.116}$$

where f_0 is the central frequency of the available frequency band and W is the bandwidth. The transmitted baseband signals are

$$s^{(1)}(t) = \sqrt{P} \sum_{n=-\infty}^{\infty} v_n^{(1)} h_{T_c}(t - nT_c)$$

$$s^{(2)}(t) = \sqrt{P} \sum_{n=-\infty}^{\infty} v_n^{(2)} h_{T_c}(t - nT_c)$$

where $h_{T_c}(\cdot)$ is a bandlimited pulse of duration $T_c = 2/W$ and $\{v_n^{(1)}\}$ and $\{v_n^{(2)}\}$ are two sets of IID zero-mean Gaussian variables with unit variance. The maximal achievable transmission rates (capacities) are

$$C^{(1)} = C^{(2)} = \frac{W}{4} \cdot \log_2 \left(1 + \frac{4P}{N_0 W}\right) \tag{8.117}$$

It is interesting to note, that achievable rates (8.117) define capacity not only of a frequency division multiplexing system but also of a general two-user multiple-access system. In fact, the achievable transmission rates region of the two-user band-limited channel is

$$
\begin{aligned}
R^{(1)} &\le \frac{W^{(1)}}{2}\log\left(1+\frac{2P^{(1)}}{N_0W^{(1)}}\right)\\
R^{(2)} &\le \frac{W^{(2)}}{2}\log\left(1+\frac{2P^{(2)}}{N_0W^{(2)}}\right)\\
R^{(1)}+R^{(2)} &\le \frac{W}{2}\log\left(1+\frac{2(P^{(1)}+P^{(2)})}{N_0W}\right)
\end{aligned}
\tag{8.118}
$$

The region is illustrated in Figure 8.6 (continuous lines). The dashed curve presents achievable rates of a frequency division multiple-access strategy. This curve touches the boundary of the capacity region at one point, which corresponds to allotting bandwidth to each user proportional to the user's available power. In the case $P^{(1)}=P^{(2)}=P$, $W^{(1)}=W^{(2)}=W/2$ and the touch point has coordinates

$$
\left(\frac{W}{4}\log_2\left(1+\frac{4P}{N_0}\right),\ \frac{W}{4}\ \log_2\left(1+\frac{4P}{N_0}\right)\right)
$$

that is, coincides with Formula (8.117).

In Section 8.5 we consider the model of the downlink multiple-access channel.

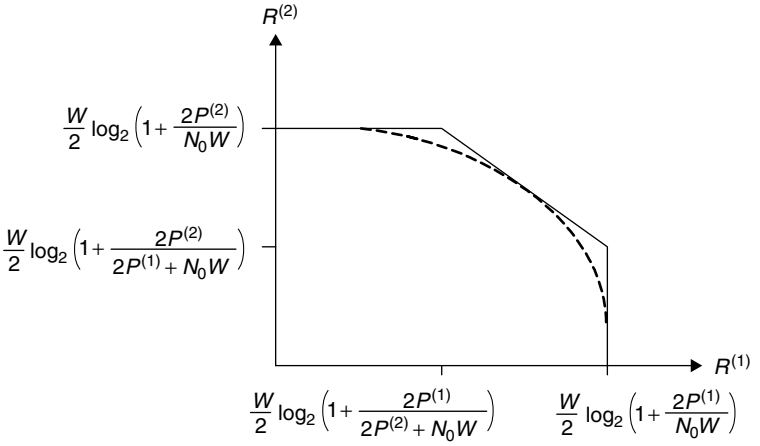

Figure 8.6. Achievable rate region for band-limited Gaussian multiple-access channel.

8.5 DOWNLINK MULTIPLE-ACCESS CHANNELS

Consider the downlink multiple-access channel with K users, which can be treated as a model of the forward (downlink) DS CDMA system. It has one transmitter and K distant receivers. In information theory this channel model is called a *broadcast channel*.

The general downlink multiple-access channel is described by an input alphabet $\mathcal{A}$ and K output alphabets $\mathcal{B}^{(1)}, \mathcal{B}^{(2)}, \ldots, \mathcal{B}^{(K)}$. The continuous memoryless channel is defined by a transition probability density function $p(b^{(1)}, b^{(2)}, \ldots, b^{(K)}|a)$, where $a \in \mathcal{A}, b^{(1)} \in \mathcal{B}^{(1)}, b^{(2)} \in \mathcal{B}^{(2)}, \ldots, b^{(k)} \in \mathcal{B}^{(K)}$. The encoded sequence $\boldsymbol{s} = (s_0, s_1, \ldots, s_{N-1})$ of length N depends on the messages to all K users. The messages can be addressed to an individual user or to a group of users. The code rate of the individual message addressed to the kth user is $r^{(k)}$, the code rate of the common information addressed to k_1th, k_2th, $\ldots$, k_ℓth users is $r^{(k_1,k_2,\ldots,k_\ell)}$.

The simplest downlink multiple-access channel consists of K independent (orthogonal) channels to the receivers. If the transmitter sends only individual messages to the users, it can send information over all the channels and we can achieve code rates $(r^{(1)}, r^{(2)}, \ldots, r^{(k)})$ if $r^{(1)} < c^{(1)}, r^{(2)} < c^{(2)}, \ldots, r^{(k)} < c^{(k)}$, where $c^{(k)}$, $k = 1, 2, \ldots, K$, are capacities of independent channels. This transmission scheme was implemented in IS-95 and some systems of the third generation of cellular mobile radio communication.

Consider now the general model of the Gaussian downlink multiple-access channel. We assume that the transmitter has power P, which is also the power of the received signals at the inputs of the receivers. The power of the AWGN at the input of the kth receiver is σ_k^2, $k = 1, 2, \ldots, K$. (Generally speaking, the power of the received signals $P^{(k)}$ at the inputs of the receivers can also be different, but because receiver performances depend only on the signal-to-noise ratio, we reduce consideration to this model; see Section 3.4.)

Consider in more detail the Gaussian downlink multiple-access channel with two users. The received signals are

$$\begin{matrix} r_n^{(1)} = s_n + \xi_n^{(1)} \\ r_n^{(2)} = s_n + \xi_n^{(2)} \end{matrix}, \quad n = 0, 1, \ldots, N-1, \tag{8.119}$$

where $\{\xi_n^{(1)}\}$ and $\{\xi_n^{(2)}\}$ are sets of IID zero-mean Gaussian random variables with variances σ_1^2 and σ_2^2, respectively. Without loss of generality assume $\sigma_1^2 < \sigma_2^2$. This means that the first receiver is located at a smaller distance from the base station than the second one. The transmitter wishes to send independent messages to the receivers at code rates $r^{(1)}$ and $r^{(2)}$ and a common message at code rate $r^{(1,2)}$.

To encode the messages the transmitter uses two Gaussian codes, one at rate $r^{(1)}$ and another code at rate $\hat{r}^{(2)} = r^{(2)} + r^{(1,2)}$. The powers of the transmitted signals are γP and $(1-\gamma)P$, respectively, where $0 \le \gamma \le 1$. The transmitted signals are $\boldsymbol{s}^{(k)} = (s_0^{(k)}, s_1^{(k)}, \ldots, s_{N-1}^{(k)})$, $k = 1, 2$, where $s_n^{(k)}$ are IID zero-mean

Gaussian random variables with variance γP for $k = 1$ and $(1 - \gamma)P$ for $k = 2$. The transmitter sends the sum $\boldsymbol{s} = \boldsymbol{s}^{(1)} + \boldsymbol{s}^{(2)}$ over the channel.

The receivers must now decode their messages. First consider the "weak" (second) receiver. He merely looks through the list of the codewords of the second code to find the closest codeword to the received vector $\boldsymbol{r}^{(2)} = (r_0^{(2)}, r_1^{(2)}, \ldots, r_{N-1}^{(2)})$. His effective signal-to-noise ratio is $(1 - \gamma)P/(\gamma P + \sigma_2^2)$, because the message $\boldsymbol{s}^{(1)}$ acts as noise to $\boldsymbol{s}^{(2)}$.

The "strong" receiver first decodes the message addressed to the second receiver, which he can accomplish because of his lower noise. He subtracts the decoded signal $\hat{\boldsymbol{s}}^{(2)}$ from $\boldsymbol{r}^{(1)} = (r_0^{(1)}, r_1^{(1)}, \ldots, r_{N-1}^{(1)})$. Then he looks for the codeword in the first code that is closest to $\boldsymbol{r}^{(1)} - \hat{\boldsymbol{s}}^{(2)}$. The resulting probability of error can be made as low as desired if pair $(r^{(1)}, \hat{r}^{(2)})$ is in the capacity region and $N \to \infty$.

The capacity region of the Gaussian downlink multiple-access channel is

$$r^{(1)} < \frac{1}{2}\log_2\left(1 + \frac{\gamma P}{\sigma_1^2}\right)$$

$$r^{(2)} + r^{(1,2)} < \frac{1}{2}\log_2\left(1 + \frac{(1-\gamma)P}{\gamma P + \sigma_2^2}\right)$$

where γ, $0 \le \gamma \le 1$, may be arbitrarily chosen to trade off code rate $r^{(1)}$ for code rate $\hat{r}^{(2)}$.

A dividend of the Gaussian optimal encoding for Gaussian downlink multiple-access channels is that the stronger receiver always knows the message intended for the weak receiver in addition to the message intended for himself. But unfortunately for large K the decoding complexity for strong receivers becomes too large. In Chapter 9 we consider another encoding method, which increases transmission reliability for downlink multiple-access channel without increasing the decoding complexity. We call this method *coordinated transmission*.

8.6 MULTIUSER COMMUNICATION IN THE RAYLEIGH FADING CHANNELS

Although Rayleigh fading demands a large penalty on energy for uncoded transmission, as demonstrated in Chapter 5, coding in combination with space and time diversity can recoup this loss. As an example of multiuser communication in the fading channel consider first the reverse (uplink) transmission in the DS CDMA system over a one-path time-selective Rayleigh channel (see Section 5.5).

The basic model of the kth user uplink communication system without pilot chips inserting device and pilot chip sequence tracking loop is given in Figure 8.7. We assume that users employ a binary block code with code rate $r = L/N$ and block length N. An interleaver (permutor) is inserted between an encoder

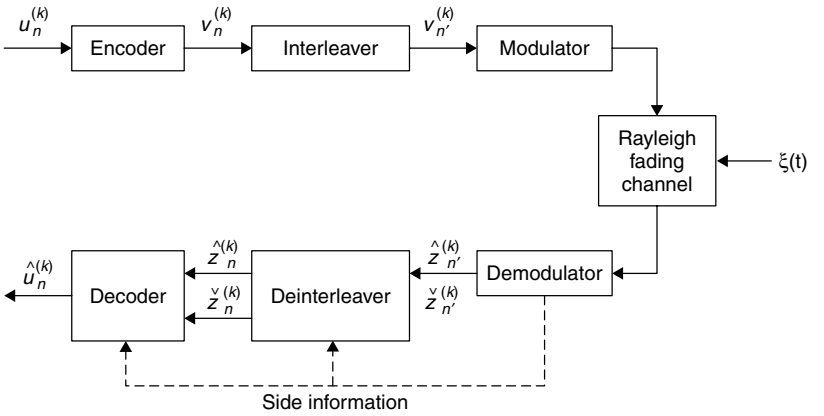

Figure 8.7. The basic model of the kth user reverse communication over a one-path Rayleigh fading channel.

and a modulator, and a deinterleaver (inverse permutor) is inserted between a demodulator and a decoder. Actually, the interleaver does not alter the total information available to the decoder but rearranges it in time. We assume that interleaving is ideal, producing a memoryless channel and that *side information* on the fade amplitude $\alpha^{(k)}$, the phase shift $\varphi^{(k)}$, and the delay $\delta^{(k)}$ is carried along with demodulator outputs in the deinterleaving operation. The modulation format is BPSK.

Let

$$\boldsymbol{v}_i^{(k)} = (v_{i,0}^{(k)}, v_{i,1}^{(k)}, \ldots, v_{i,N-1}^{(k)}), \; v_{i,n}^{(k)} \in \{1, -1\} \tag{8.120}$$

be the ith codeword, $i = 0, 1, \ldots, 2^{rN} - 1$. Given that the zeroth codeword was transmitted, the decision statistics at the deinterleaver output are

$$\begin{aligned} \hat{z}_n^{(k)} &= v_{0,n}^{(k)} \alpha_n^{(k)} \cos \varphi_n^{(k)} + \hat{\xi}_n^{(k)} \\ \check{z}_n^{(k)} &= v_{0,n}^{(k)} \alpha_n^{(k)} \sin \varphi_n^{(k)} + \check{\xi}_n^{(k)} \end{aligned} \tag{8.121}$$

where the noise components $\hat{\xi}_n^{(k)}$ and $\check{\xi}_n^{(k)}$ are due to the other-user interference, the AWGN, and the other-cell interference. We assume that they are IID Gaussian random variables with variance $I_0/2T_c$, where $I_0/2$ is the two-sided power spectral density of the total noise.

Because the Rayleigh fading channel is fully interleaved, the components of the vectors

$$\boldsymbol{\alpha}^{(k)} = (\alpha_0^{(k)}, \alpha_1^{(k)}, \ldots, \alpha_{N-1}^{(k)}) \tag{8.122}$$

$$\boldsymbol{\varphi}^{(k)} = (\varphi_0^{(k)}, \varphi_1^{(k)}, \ldots, \varphi_{N-1}^{(k)}) \tag{8.123}$$

are IID random variables. The probability density function of $\alpha_n^{(k)}$ is given in Formula (5.1); the random variables $\varphi_n^{(k)}$ are uniformly distributed on $[0, 2\pi)$.

Using side information from the demodulator, the decoder first calculates statistics

$$z_n^{(k)} = \hat{z}_n^{(k)} \hat{\alpha}_n^{(k)} \cos \hat{\varphi}_n^{(k)} + \check{z}_n^{(k)} \hat{\alpha}_n^{(k)} \sin \hat{\varphi}_n^{(k)} \tag{8.124}$$

where $\hat{\alpha}_n^{(k)}$ and $\hat{\varphi}_n^{(k)}$ are estimations of the fade amplitudes and phase shifts. If we neglect the inaccuracy in the amplitude and phase estimates, taking $\hat{\alpha}_n^{(k)} = \alpha_n^{(k)}$, $\hat{\varphi}_n^{(k)} = \varphi_n^{(k)}$, we obtain

$$z_n^{(k)} = \upsilon_n^{(k)} (\alpha_n^{(k)})^2 + \xi_n^{(k)} \tag{8.125}$$

where $\xi_n^{(k)} = \hat{\xi}_n^{(k)} \alpha_n^{(k)} \cos \varphi_n^{(k)} + \check{\xi}_n^{(k)} \alpha_n^{(k)} \sin \varphi_n^{(k)}$. Note, that independently on $\varphi_n^{(k)}$, the random variable $\hat{\xi}_n^{(k)} \cos \varphi_n^{(k)} + \check{\xi}_n^{(k)} \sin \varphi_n^{(k)}$ has Gaussian distribution. Given $\alpha_n^{(k)}$, the conditional probability density function of $z_n^{(k)}$ is

$$f(z_n^{(k)} | \alpha_n^{(k)}) = \frac{1}{\sqrt{2\pi\sigma^2}} \exp\left[-\frac{(z_n^{(k)} - \mu)^2}{2\sigma^2} \right] \tag{8.126}$$

where $\mu = \upsilon_n^{(k)} (\alpha_n^{(k)})^2$, $\sigma^2 = (\alpha_n^{(k)})^2 I_0 / 2T_c$.

If $\alpha_n^{(k)} = \alpha$ is fixed, the probability density function (8.126) describes a binary input AWGN channel, as considered in Section 8.2. The input alphabet of the channel is $\mathcal{A} = \{\alpha^2, -\alpha^2\}$, the variance of the AWGN is $\alpha^2 I_0 / 2T_c$. The conditional (given α) capacity of the channel (in b/channel use) is [compare with Formula (8.64)]

$$\begin{aligned} c(\alpha) &= 1 - \int_{-\infty}^{\infty} \frac{1}{\sqrt{\pi \alpha^2 I_0 / T_c}} \exp\left[-\frac{(z - \alpha^2)^2}{\alpha^2 I_0 / T_c} \right] \log_2 \left[1 + \exp\left(-\frac{2z\alpha^2 T_c}{\alpha^2 I_0} \right) \right] dz \\ &= 1 - \int_{-\infty}^{\infty} \frac{1}{\sqrt{\pi I_0 / T_c}} \exp\left[-\frac{(x - \alpha)^2}{I_0 / T_c} \right] \log_2 \left[1 + \exp\left(-\frac{2x\alpha T_c}{I_0} \right) \right] dx \end{aligned} \tag{8.127}$$

where we use substitution $x = z/\alpha$.

The unconditional capacity (in b/channel use) of the fully interleaved binary input Rayleigh channel is

$$\begin{aligned} c &= \int_0^{\infty} c(\alpha) \frac{\alpha}{a^2} \exp\left(-\frac{\alpha^2}{2a^2} \right) d\alpha \\ &= 1 - \int_0^{\infty} \int_{-\infty}^{\infty} \frac{\alpha}{a^2} \exp\left(-\frac{\alpha^2}{2a^2} \right) \frac{1}{\sqrt{\pi I_0 / T_c}} \exp\left[-\frac{(x - \alpha)^2}{I_0 / T_c} \right] \\ &\quad \times \log_2 \left[1 + \exp\left(-\frac{2x\alpha T_c}{I_0} \right) \right] dx \, d\alpha \end{aligned}$$

$$= 1 - \int_0^\infty \beta \exp\left(-\frac{\beta^2}{2}\right) \int_{-\infty}^\infty \sqrt{\frac{\rho_c}{2\pi}} \exp\left[-\frac{(y-\beta)^2}{2}\rho_c\right] \times \log_2\left[1 + \exp(-y\beta\rho_c)\right] dy\, d\beta \tag{8.128}$$

where $\beta = \alpha/a$, $y = x/a$, and $\rho_c = 2a^2 T_c/I_0$ is the average signal-to-noise ratio per chip.

The Shannon capacity (in b/s) of the channel is $C = c/T_c$. The same analysis can be done for the cut-off rate r_0. The conditional (given α) cut-off rate (in b/channel use) is [compare with Formula (8.48)]

$$r_0(\alpha) = 1 - \log_2\left[1 + \exp\left(-\frac{\alpha^2 T_c}{I_0}\right)\right] \tag{8.129}$$

The unconditional cut-off rate (in b/channel use) of the binary input fully interleaved Rayleigh channel is

$$\begin{aligned} r_0 &= \int_0^\infty r_0(\alpha) \frac{\alpha}{a^2} \exp\left(-\frac{\alpha^2}{2a^2}\right) d\alpha \\ &= 1 - \int_0^\infty \frac{\alpha}{a^2} \exp\left(-\frac{\alpha^2}{2a^2}\right) \log_2\left[1 + \exp\left(-\frac{\alpha^2 T_c}{I_0}\right)\right] d\alpha \\ &= 1 - \int_0^1 \log_2[1 + x^{\rho_c}]\, dx \end{aligned} \tag{8.130}$$

where we use substitution $x = \exp(-\alpha^2/2a^2)$, $\rho_c = 2a^2 T_c/I_0 \stackrel{\text{def}}{=} E_s/I_0$. The cut-off rate (in b/s) is $R_0 = r_0/T_c$.

Figure 8.8 presents the capacity c and the cut-off rate r_0 for a fully interleaved Rayleigh channel as a function of the average signal-to-noise ratio E_s/I_0 per chip. For comparison the capacity and the cut-off rate for a binary input Gaussian channel are given as functions of the signal-to-noise ratio. By this comparison we determine the energy penalty attached to the Rayleigh channel. Note that for a throughput approaching one bit per chip the penalties are indeed large, whereas as the code rate decreases, the energy penalty diminishes, as measured by capacity or cut-off rate. For example, to obtain $c = 0.9$ (b/channel use) the Gaussian channel can operate on the SNR level (per chip) of 3.62 dB, whereas a fully interleaved Rayleigh channel should operate on a level of 9.35 dB, that is, 5.73 dB higher. To get $c = 0.5$ (b/channel use), Gaussian and Rayleigh channels should operate on the SNR levels of -1.55 dB and 0 dB, respectively, that is, the fading penalty is 1.55 dB.

In a low-rates region, which is most interesting in CDMA applications, the fading penalty is lower. For $c = 0.1$ (b/channel use), the required levels of SNR are -10 dB and -9.59 dB, that is, the difference is only 0.41 dB.

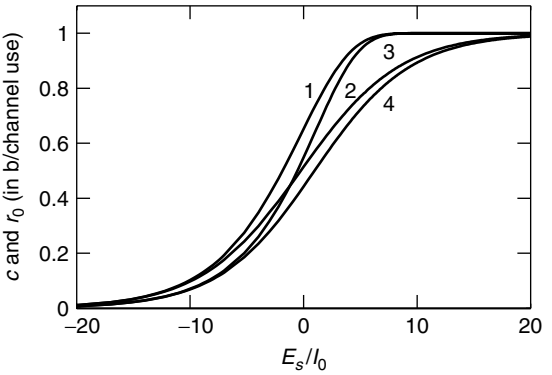

Figure 8.8. Capacity and cut-off rate (in b/channel use) for a Gaussian channel (curves 1 and 2) and for a fully interleaved Rayleigh channel with side information (curves 3 and 4) as functions of signal-to-noise ratio per chip E_s/I_0.

EXAMPLE 8.8

Consider two reverse-link single-cell DS CDMA systems operating in a Gaussian and a fully interleaved Rayleigh channel, respectively. Assume that the code rate in each case is equal to 0.1 *(b/channel use). Find the radio channel capacity of the system. Neglect AWGN.*

Solution

Because AWGN is negligible, the signal-to-noise ratio per chip $\rho_c = E_s/I_0 = P/(K-1)P = 1/(K-1)$. *(Here* P *is average power of the received signal.) For the Gaussian channel* $E_s/I_0 = -10$ dB*; for the Rayleigh channel* $E_s/I_0 = -9.59$ dB. *Then for the Gaussian channel the radio channel capacity* $K_0 = 11$ *and for the Rayleigh channel* $K_0 = 10$.

Now consider reverse transmission over a one-path time-selective Rayleigh channel in a single-cell FH CDMA system. We study the same system as in Section 5.6, except that instead of a Reed–Muller code the system uses random coding. We estimate the capacity and cut-off rate of the system.

We assume that the total hopping bandwidth of the system equals W, and the system employs BFSK with Q carrier frequencies, such that the hopset size $M = 2Q$. The frequency separation interval $\Delta f = W/M$; the pulse duration $T_c = 1/\Delta f$. The hopping rate is $R_h = 1/T_c$. As above, we assume that interleaving in the system is ideal, producing a memoryless channel as seen by the encoder/decoder pair. We consider only the case when all users are chip synchronized.

Without loss of generality, we will study reception of the signal from the first user. Given that all users are synchronized, the output statistics of the first filter are (see Fig. 3.8):

if $v_{n'}^{(1)} = 1$,

$$\hat{z}_{\mathrm{I}n'}^{(1)} = \alpha_{n'}^{(1)} \cos \varphi_{n'}^{(1)} + \sum_{k=2}^{K} \alpha_{n'}^{(k)} \hat{\theta}_{n'}^{(k)} \cos \varphi_{n'}^{(k)} + \hat{\xi}_{\mathrm{I}n'}^{(1)} \tag{8.131}$$

$$\hat{z}_{\mathrm{Q}n'}^{(1)} = \alpha_{n'}^{(1)} \sin \varphi_{n'}^{(1)} + \sum_{k=2}^{K} \alpha_{n'}^{(k)} \hat{\theta}_{n'}^{(k)} \sin \varphi_{n'}^{(k)} + \hat{\xi}_{\mathrm{Q}n'}^{(1)} \tag{8.132}$$

if $v_{n'}^{(1)} = -1$,

$$\hat{z}_{\mathrm{I}n'}^{(1)} = \sum_{k=2}^{K} \alpha_{n'}^{(k)} \check{\theta}_{n'}^{(k)} \cos \varphi_{n'}^{(k)} + \check{\xi}_{\mathrm{I}n'}^{(1)} \tag{8.133}$$

$$\hat{z}_{\mathrm{Q}n'}^{(1)} = \sum_{k=2}^{K} \alpha_{n'}^{(k)} \check{\theta}_{n'}^{(k)} \sin \varphi_{n'}^{(k)} + \check{\xi}_{\mathrm{Q}n'}^{(1)} \tag{8.134}$$

The output statistics $\check{z}_{\mathrm{I}n'}^{(k)}$ and $\check{z}_{\mathrm{Q}n}^{(1)}$ of the second filter equal to the right-hand sides of Equations (8.133) and (8.134), respectively, if $v_{n'}^{(1)} = 1$ and equal to the right-hand sides of Equations (8.131) and (8.132) if $v_{n'}^{(1)} = -1$.

Here [compare with (3.128) and (3.129)]

$$\hat{\theta}_{n'}^{(k)} = \begin{cases} 1, & \text{if the } k\text{th user occupies in the } n'\text{th} \\ & \text{moment the same subband as the first user,} \\ 0, & \text{otherwise} \end{cases} \tag{8.135}$$

$$\check{\theta}_{n'}^{(k)} = \begin{cases} 1, & \text{if the } k\text{th user occupies in the } n'\text{th} \\ & \text{moment the subband opposed to the} \\ & \text{subband occupied by the first user,} \\ 0, & \text{otherwise} \end{cases} \tag{8.136}$$

The noise components $\hat{\xi}_{\mathrm{I}n'}^{(1)}$, $\hat{\xi}_{\mathrm{Q}n'}^{(1)}$, $\check{\xi}_{\mathrm{I}n'}^{(1)}$, and $\check{\xi}_{\mathrm{Q}n'}^{(1)}$ are zero-mean Gaussian random variables with variances $\sigma_0^2 = N_0/2T_{\mathrm{c}}$, where $N_0/2$ is two-sided power spectral density of the background AWGN. The random variables $\hat{\theta}_{n'}^{(k)}$ and $\check{\theta}_{n'}^{(k)}$ satisfy condition (3.130). The random variables $\alpha_n^{(k)} \cos \varphi_n^{(k)}$ and $\alpha_n^{(k)} \sin \varphi_n^{(k)}$ are IID zero-mean Gaussian random variables with variance a^2. $\hat{I}_n$ denotes the number of users that occupy in the n'th moment the same subband as the first user, and $\check{I}_n$ denotes the number of other users that occupy in the nth moment the opposed subband. The conditional probability density function of $\hat{y}_n^{(1)} \stackrel{\text{def}}{=} \hat{y}$, given $\hat{I}_n = i$, is χ^2-distributed with two degrees of freedom; that is,

$$f(\hat{y}|i) = \frac{1}{2(a^2 + ia^2 + N_0/2T_{\mathrm{c}})} \exp\left[-\frac{\hat{y}}{2(a^2 + ia^2 + N_0/2T_{\mathrm{c}})} \right], \hat{y} \geq 0 \tag{8.137}$$

Analogously, the conditional probability density function of $\check{y}_n^{(1)} = \check{y}$, given $\check{I}_n = i$, is

$$f(\check{y}|i) = \frac{1}{2(ia^2 + N_0/2T_c)} \exp\left[-\frac{\check{y}}{2(ia^2 + N_0/2T_c)}\right], \check{y} \geq 0 \tag{8.138}$$

The probability distribution of the random variables $\hat{I}_n = \sum_{k=2}^{K} \hat{\theta}_n^{(k)}$ and $\check{I}_n = \sum_{k=2}^{k} \check{\theta}_n^{(k)}$ is

$$P(\hat{I}_n = i) = P(\check{I}_n = i) = \binom{K-1}{i} \left(\frac{1}{M}\right)^i \left(1 - \frac{1}{M}\right)^{K-1-i} \tag{8.139}$$

Then the unconditional probability density functions of the random variables $\hat{y}$ and $\check{y}$ are

$$f(\hat{y}) = \sum_{i=0}^{K-1} \binom{K-1}{i} \left(\frac{1}{M}\right)^i \left(1 - \frac{1}{M}\right)^{K-1-i} f(\hat{y}|i) \tag{8.140}$$

$$f(\check{y}) = \sum_{i=0}^{K-1} \binom{K-1}{i} \left(\frac{1}{M}\right)^i \left(1 - \frac{1}{M}\right)^{K-1-i} f(\check{y}|i) \tag{8.141}$$

The input of the decoder of the first receiver are two sequences, $\hat{\boldsymbol{y}}^{(k)} = (\hat{y}_0^{(k)}, \hat{y}_1^{(k)}, \ldots, \hat{y}_{N-1}^{(k)})$ and $\check{\boldsymbol{y}}^{(k)} = (\check{y}_0^{(k)}, \check{y}_1^{(k)}, \ldots, \check{y}_{N-1}^{(k)})$. Because the interleaving is ideal, they are sequences of IID random variables. The conditional probability density function of the statistic $\hat{y}_n^{(k)} = \hat{y}$ is [compare with (5.100) and (5.101)]

$$f(\hat{y}|v) = \begin{cases} f_1(\hat{y}) \stackrel{\text{def}}{=} \displaystyle\sum_{i=0}^{K-1} \binom{K-1}{i} \left(\frac{1}{M}\right)^i \left(1 - \frac{1}{M}\right)^{K-1-i} \\ \times \dfrac{1}{2(a^2 + ia^2 + N_0/2T_c)} \\ \times \exp\left[-\dfrac{\hat{y}}{2(a^2 + ia^2 + N_0/2T_c)}\right], & \text{if } v = 1, \ y \geq 0, \\ f_0(\hat{y}) \stackrel{\text{def}}{=} \displaystyle\sum_{i=0}^{K-1} \binom{K-1}{i} \left(\frac{1}{M}\right)^i \left(1 - \frac{1}{M}\right)^{K-1-i} \\ \times \dfrac{1}{2(ia^2 + N_0/2T_c)} \exp\left[-\dfrac{\hat{y}}{2(ia^2 + N_0/2T_c)}\right], & \text{if } v = -1, \ y \geq 0 \end{cases} \tag{8.142}$$

Analogously, the conditional probability density function of the statistic $\check{y}_n^{(k)} = \check{y}$ is

$$f(\check{y}|v) = \begin{cases} f_0(\check{y}), & \text{if } v = 1, \quad \check{y} \geq 0, \\ f_1(\check{y}), & \text{if } v = -1, \quad \check{y} \geq 0 \end{cases} \tag{8.143}$$

Because $K \gg 1$ and $M \gg 1$, we may use the Poisson approximation:

$$f_1(y) = \sum_{i=0}^{\infty} e^{-\lambda} \frac{\lambda!}{i!} \frac{1}{2(a^2 + ia^2 + N_0/2T_c)} \exp\left[-\frac{y}{2(a^2 + ia^2 + N_0/2T_c)}\right] \quad y \geq 0 \tag{8.144}$$

$$f_0(y) = \sum_{i=0}^{\infty} e^{-\lambda} \frac{\lambda!}{i!} \frac{1}{2(ia^2 + N_0/2T_c)} \exp\left[-\frac{y}{2(ia^2 + N_0/2T_c)}\right] y \geq 0 \tag{8.145}$$

where $\lambda = (K-1)/M$.

Thus we can treat the considered FH CDMA system model as a channel with binary input v and two-dimensional continuous output $\{\hat{y}, \check{y}\}$, where $\hat{y}$ and $\check{y}$ are independent random variables with probability density functions (8.142) and (8.143), respectively.

In Figure 8.9 are presented the capacity, c, and cut-off rate, r_0, for a FH CDMA system operating in a fully interleaved Rayleigh channel. To a capacity of $c = 0.9$ (b/channel use) corresponds $E_s/I_0 = 11.80$ dB. This is 8.18 dB larger than for a DS CDMA system operating in a Gaussian nonfading channel and 2.07 dB larger than for a DS CDMA system operating in a fully interleaved Rayleigh channel. To a capacity of $c = 0.5$ and 0.1 correspond $E_s/I_0 = 3.98$ dB and -3.01 dB, respectively. This is 4.53 dB (respectively, 6.99 dB) larger than for a DS CDMA system operating in a Gaussian channel and 3.98 dB (respectively 6.58 dB) larger than for a DS CDMA system operating in a fully interleaved Rayleigh channel.

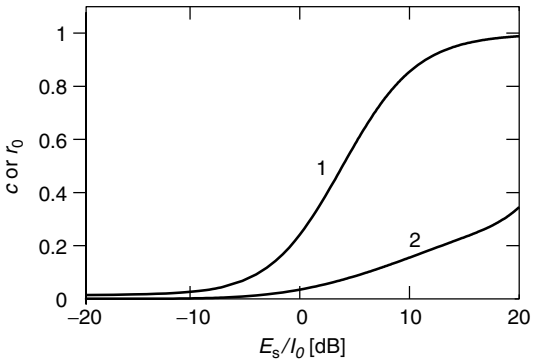

Figure 8.9. Capacity (1) and cut-off rate (2) (in b/channel use) for a FH CDMA system operating in a fully interleaved Rayleigh channel.

8.7 COMMENTS

The modern information theory started with Shannon's landmark paper "A Mathematical Theory of Communication" [42]. In this paper, the concept of channel capacity was introduced. Further development of the theory was done by Fano, Elias, Gallager, etc. For advanced study of information theory, the reader may refer to standard textbooks, such as Gallager [15], Viterbi and Omura [52], and Cover and Thomas [10].

Multiuser information theory deals with basic information-theoretical aspects of multiple-access communication as well as channel coding and modulation for multiple-access channels. A large literature exists on these topics. The reader is referred to the books of Cover and Thomas [10] and Verdu [46], where one can find a large number of references to the original literature.

In our treatment of multiuser information theory we mostly follow Cover and Thomas [10]. Our analysis of FH CDMA system is founded on the original papers by Chang and Wolf [9], Wilhelmsson and Zigangirov [56], and Bassalygo and Pinsker [8].

PROBLEMS

8.1. Find the Shannon capacity of a Gaussian channel with bandwidth $W = 10$ MHz, power $P = 10$ W. The two-sided power spectral density of the AWGN is $N_0/2 = 10^{-8}$ W/Hz.

8.2. Use Formula (8.13) to prove the following lower bound on E_b/I_0 for reliable communication on a band-limited Gaussian channel:

$$\frac{E_b}{I_0} \geq \frac{W}{2R}\left(2^{2R/W} - 1\right)$$

where W is the bandwidth and R is the transmission rate (in b/s). Plot this bound as a function of processing gain W/R and show that this bound does not approach -1.6 dB. Find the processing gain for which the required SNR is 0.5 dB larger than the infinite-bandwidth limit for SNR.

8.3. Prove the following upper bound for the radio channel capacity of a single-cell perfectly power-controlled DS CDMA system:

$$K_0 \leq 1 + \frac{2}{2^{2R/W} - 1}$$

where W/R is the processing gain. Assume that the system does not use activity detection and antenna sectorization. For the multicell DS CDMA system, prove the upper bound

$$K_0 \leq 1 + \frac{2}{(2^{2R/W} - 1)(1 + f)}$$

where f is the other-cell relative interference factor.

8.4. Find the cut-off rate of a Gaussian channel with binary input if the bandwidth $W = 10$ MHz, power $P = 1$ W, and the two-sided power spectral density of the AWGN is $N_0/2 = 10^{-6}$ W/Hz.

8.5. Prove that if the SNR per chip ρ_c in a Gaussian channel with binary input goes to zero, then the ratio of the capacity (8.64) of the channel to ρ_c goes to $1/\ln 2$.

8.6. Prove Equation (8.78), $I(v, r) = H(v) - H(v|r)$.

8.7. Find the differential entropy for the exponential distribution when the probability density function is $f(x) = \lambda e^{-\lambda x}$, $x \geq 0$, and for the Laplace distribution when the probability density function is $f(x) = \lambda/2 \cdot \exp(-\lambda|x|)$.

8.8. (Binary erasure multiple-access channel [10].) Consider an adding channel with two users. The ith user sends the sequence $v_n^{(i)}$, $n = 0, 1, \ldots$, in a real number alphabet, that is, $v_n^{(i)} \in \{1, -1\}$. The received sequence is $r_n = v_n^{(1)} + v_n^{(2)}$, $r_n \in \{-2, 0, 1\}$. Find the capacity region.

8.9. (Binary multiplier channel [10].) Consider a multiple-access channel with binary inputs $v_n^{(1)}, v_n^{(2)}$, $v_n^{(1)}, v_n^{(2)} \in \{0, 1\}$ and binary output $r_n = v_n^{(1)} v_n^{(2)}$. Find the capacity region for this channel.

8.10. (Additive modulo 2 multiple access channel [10].) Consider a two-user multiple-access channel where the ith user sends the sequence $\boldsymbol{v}^{(i)} = (v_0^{(i)}, v_1^{(i)}, \ldots,)$, $i = 1, 2$, in binary logical alphabet, that is, $v_n^{(i)} \in \{0, 1\}$, $n = 0, 1, \ldots$. The received sequence is $r_n = v_n^{(1)} + v_n^{(2)}$, where addition is performed modulo 2. Find the capacity region.

8.11. Consider the frequency division multiple-access system with two users in an AWGN channel. The signal powers are $P^{(1)}$ and $P^{(2)}$, respectively. The frequency bands are $W^{(1)} = \lambda W$, $W^{(2)} = (1 - \lambda)W$, where $0 < \lambda < 1$. Determine the total capacity of the system as function of λ. Plot capacity versus λ. Choose $P^{(1)}$ and $P^{(2)}$ maximizing the total capacity.

8.12. Consider a time division multiple-access system with two users in an AWGN channel. The signal powers are $P^{(1)}$ and $P^{(2)}$, respectively; the channel bandwidth is W. The first user uses the channel λth part of the time; the second user uses the channel $(1 - \lambda)$th part of the time, $0 < \lambda < 1$. Determine the achievable rate region $(C^{(1)}, C^{(2)})$ of the system as a function of λ. Plot the graph of points $(C^{(1)}, C^{(2)})$.

8.13. Find the capacity region for a Gaussian multiple-access channel with $K = 3$ users.

8.14. Consider reverse-link transmission in a perfectly power-controlled single-cell DS CDMA system operating in a fully interleaved Rayleigh channel. Assuming that all users send with code rate $r = 0.01$ (b/channel use), which is equal to the cut-off rate of the channel, find the radio channel capacity. Compare the result with the radio channel capacity of an analogous system operating in the Gaussian channel.

9

CDMA CELLULAR NETWORKS

The study of CDMA systems so far has concentrated almost entirely on the communication aspects of the theory, such as modulation and coding of spread spectrum signals in the transmitter and the inverse operations at the receiver. These functions are common to all wireless digital communication systems regardless of the multiple-access technique used. The real advantages of a CDMA network can be realized through a proper study of the networking concepts in a cellular multiple-access system, which accommodate mobile voice and data users who move throughout cities or countries.

Modern cellular networks are based on digital radio and network technologies in order to maximize system capacity and quality of service. With CDMA, universal frequency reuse applies not only to all users in the same cell but also to those in adjacent cells. In this chapter, cellular network problems specific for CDMA are considered. These are other-cell interference, power control, soft handoff strategies, teletraffic aspects of CDMA, interference cancellation, and user coordination. The importance of these topics is due to the following factors.

Application of the universal frequency reuse principle demands effective power control of each user, in both directions, to reduce other-user interference. Soft handoff makes it possible for a mobile user to receive and send the same call simultaneously from and to several base stations. The designer of the CDMA system should take into account not only voice activity but also date teletraffic variability. As we demonstrated in Chapter 8, the interference from same-cell users can be completely eliminated by a process of successive cancellation

Theory of Code Division Multiple Access Communication, by Kamil Sh. Zigangirov
ISBN 0-471-45712-4

of interfering users. Finally, the introduction of user coordination significantly increases the capacity of CDMA system in the downlink direction.

9.1 GENERAL ASPECTS OF CDMA CELLULAR NETWORKS

To provide wireless communications, an integrated network of base stations must be deployed. The base stations must be connected to the switching center, which provides connectivity between the public telephone network and the base stations, and ultimately between all the users in a system. The public telephone network forms the global telecommunication network that connects conventional telephone switching centers with mobile switching centers.

To connect mobile users to the base station, radio channels are used. Unlike wired channels that are stationary and predictable, radio channels are unpredictable. The mechanisms behind electromagnetic wave propagation are diverse but can be generally attributed to diffraction, reflection, and scattering. Most cellular radio systems operate in urban areas where there is no direct line-of-sight path between the transmitter and the receivers. Because of multiple reflections, the electromagnetic waves travel along different paths of varying lengths. The interaction between these waves causes multipath fading, and the strength of the waves decreases.

Propagation models have traditionally focused on predicting the average received signal strength at a given distance from the transmitter, as well as the random variability of the signal strength. The free space propagation model is used to predict the received signal strength when the transmitter and the receiver have a line-of-sight path between them. In free space it is well known that radio waves propagate with a path loss characteristic proportional to d^2, where d is the distance between the transmitter and the receiver. In the mobile radio environment, propagation is no longer in free space and is often not line-of-sight.

Both theoretical and measurement-based propagation models indicate that the propagation loss κ of mobile radio channels is generally modelled as the product of the mth power of the distance and a log-normal component A representing shadowing losses:

$$\kappa = Ad^m \tag{9.1}$$

This model represents slowly varying losses, even for users in motion, and applies to both reverse and forward links. The more rapidly varying fading losses, such as the Rayleigh fading considered earlier, are not included here. For a user at a distance d from a base station, the path loss factor (in dB) is equal to

$$10\log_{10}\kappa = 10m\log_{10}d + \zeta \tag{9.2}$$

where $\zeta = 10\log_{10}A$ is the decibel path loss due to shadowing. We assume that ζ is normally distributed with zero mean and variance σ^2. Experimental data show that the value of m depends on the specific propagation environment and

ranges from 2 to 4. Jakes [22] and Lee [26] suggest the choice of $m = 4$ and $\sigma = 8$ dB for the standard deviation of ζ. For a system with fast power control ζ is sometimes modeled as a normal random variable with $\sigma = 2$ dB.

EXAMPLE 9.1

Assume that the mean received signal strength at a given point is 0 dB *and that the log-normal standard deviation of the shadowing factor* ζ *in the area is* 8 dB. *Find the probability that the received signal strength at given point is below the threshold* -8 dB.

Solution

$$P(10\log_{10}\kappa > 10m\log d + 8 \text{ dB}) = P(\zeta > +8d) = Q\left(\frac{+8}{8}\right) = Q(1) = 0.16$$

As we know, in a cellular system the interference at a base station will come from the mobile units in the surrounding cells. This is the reverse channel interference. For a particular mobile unit, the closest base station will provide the desired forward channel whereas the surrounding base stations will create the forward channel interference. In Section 9.2 we study the other-cell relative interference factors for both the forward and reverse channels.

One of the major tasks of a cellular system is to monitor the link quality. When a mobile is further away from the base station, the path loss increases and the link quality decreases. When the quality decreases below a certain limit, the switching center should automatically transfer the call to a new base station, thereby providing a higher quality. This handoff operation not only involves identifying a new base station, but also requires that the signal be allocated to channels associated with the new base station. If a handoff algorithm does not detect poor signal quality fast enough, or makes too many handoffs, the system capacity is diminished.

Processing handoff is an important task in any cellular radio system. Handoff can be hard or soft. Hard handoffs release the radio link with the old base station at the same time that the radio link with the new base station is established. Soft handoffs maintain a radio link with at least two base stations in a handoff region, and a link is dropped only when the signal level drops below a certain threshold. In Section 9.3 it will be proved that soft handoff considerably increases both the capacity of a heavily loaded multicellular system and the coverage of each individual cell in a lightly loaded system.

In a CDMA system, the power of multiple users at a receiver determines the noise floor. If the power of each user within a cell is not controlled such that they do not appear equal at the base station receiver, then the near-far effect occurs.

To combat the near-far effect, power control is used in CDMA systems. Power control is provided by each base station in a cellular system and ensures that each mobile within the cell provides the same signal level to the base station receiver. In Section 9.3 we consider the power control problem for the reverse

link. Actually, power control is also necessary in the forward link. We concentrate on power control for the reverse link, because power control is critical for achieving maximum reverse link capacity and much less so for the forward link.

A typical cellular system has far fewer mobile radio channels than subscribers. This is because only a small part of subscribers make call attempts at any time. The network is usually designed such that at the busy hour only a small percentage will have their call attempts blocked because all channels are in use. The Erlang capacity of a multiple-access network is measured by the average number of users receiving service at a given time with a given level of quality. We study the Erlang capacity of CDMA systems in Section 9.5.

Sections 9.6 and 9.7 are devoted to information-theoretical aspects of network theory—to interference cancellation and coordinated transmission in the downlink channel.

9.2 OTHER-CELL RELATIVE INTERFERENCE FACTORS

In CDMA cellular systems that employ separate forward and reverse links, neighboring cells share the same frequency and each base station controls the power of the transmitted signals and the power of the signals transmitted by its own users. However, a particular base station is unable to control the power of neighboring cell base stations and the power of the users in the neighboring cells. These stations and users add to the noise floor and decrease the capacity of the forward and reverse links of the particular cell of interest. The average ratio of the surrounding base station interference power to the power of the signal of the desired base station at a mobile receiver is called the *forward link other-cell relative interference factor*. (Note that if the number of users is large, $K \gg 1$, the total power of signal from desired base station practically coincides with the power of the other-user interference.) We designate this factor f_{f}. Analogously, the ratio of out-of-cell user interference power to the in-cell user interference power at the base station receiver is called the *reverse link other-cell relative interference factor*. We designate it f_{r}. In this section we estimate the relative other-cell interference factors f_{f} and f_{r}.

Let us start with study of f_{f}. We assume that all base stations emit the same power [1] $P\psi$ and that the number of users in each cell is equal to K.

We will label the base stations and the corresponding cells by ℓ, $\ell = 0, 1, \ldots, L-1$, and the users in the ℓth cell by k_ℓ. The desired base station is labeled by $\ell = 0$. Let $\kappa^{(k,\ell)}$ mean the path loss on the link between the kth user and the ℓth station. Then the power of the signal from the desired base station at the k_0th user receiver is equal to $P\psi/\kappa^{(k_0,0)}$. The power of the other-cell interference at the k_0th user receiver equals $\sum_{\ell=1}^{L-1} P\psi/\kappa^{(k_0,\ell)}$. The ratio of $\sum_{\ell=1}^{L-1} P\psi/\kappa^{(k_0,\ell)}$ to $P\psi/\kappa^{(k_0,0)}$ defines the ratio of the other-cell interference to the other-user

[1] In the previous chapters we assumed that the power of the received signal equals P (watt). In this chapter we define that the power of the transmitted signal equals the product of some constant P having dimensionality watt and nondimensional factor ψ depending on the transmitted signal.

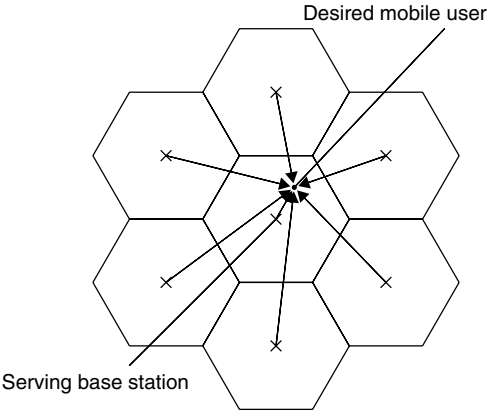

Figure 9.1. Illustration of forward channel interference.

interference at the k_0th user receiver. By definition, the forward link other-cell relative interference factor equals to the *average* ratio of the other-cell interference to the given cell other-user interference, where averaging is over the K users and the shadowing,

$$f_{\mathrm{f}} = \frac{1}{K\psi}\, E\left[\sum_{\text{all } k_0} \kappa^{(k_0,0)} \sum_{\ell=1}^{L-1} \frac{\psi}{\kappa^{(k_0,\ell)}}\right] = \frac{1}{K}\sum_{\ell=1}^{L-1}\sum_{\text{all } k_0} E\left[\frac{\kappa^{(k_0,0)}}{\kappa^{(k_0,\ell)}}\right] \tag{9.3}$$

To estimate f_{f} we will consider an idealized model of a cellular CDMA system. Assume that the system consists of L hexagon-shaped cells with the base stations in the center (Fig. 9.1). Furthermore, assume that the mobile terminals are distributed uniformly in the cells, that is, for a unit radius cell the user density is $2K/(3\sqrt{3})$ per area unit. The goal is to find f_{f} when the number of cells $L \to \infty$.

Let $(x^{(k_\ell)}, y^{(k_\ell)})$ be the coordinates of the k_ℓth mobile in the ℓth cell. The path loss of the signal from the ℓth interfering base station to that mobile terminal in the 0th cell is described by the function $\kappa(x^{(k_\ell)}, y^{(k_\ell)}, \ell)$ and the forward link other-cell relative interference factor is

$$\begin{aligned} f_{\mathrm{f}} &= \lim_{L\to\infty} E\left[\sum_{\ell=1}^{L-1} \frac{2}{3\sqrt{3}} \iint\limits_{S_0} \frac{\kappa(x^{(k_0)}, y^{(k_0)}, 0)}{\kappa(x^{(k_0)}, y^{(k_0)}, \ell)}\right] \mathrm{d}x^{(k_0)}\mathrm{d}y^{(k_0)} \\ &= \lim_{L\to\infty} \sum_{\ell=1}^{L-1} \frac{2}{3\sqrt{3}} \iint\limits_{S_0} E\left[\frac{\kappa(x^{(k_0)}, y^{(k_0)}, 0)}{\kappa(x^{(k_0)}, y^{(k_0)}, \ell)}\right] \mathrm{d}x^{(k_0)}\mathrm{d}y^{(k_0)} \end{aligned} \tag{9.4}$$

where S_0 is the area of the 0th cell.

As previously discussed, the path loss is described by

$$\kappa(x^{(k_0)}, y^{(k_0)}, \ell) = A_\ell \big(d(x^{(k_0)}, y^{(k_0)}, \ell)\big)^m \tag{9.5}$$

where A_ℓ is the shadowing of the signal from the ℓth base station to the mobile terminal and $d(x^{(k_0)}, y^{(k_0)}, \ell)$ is the corresponding distance of the base station to the mobile terminal. Independently of terminal location, for a system with fast power control $\zeta_0 = 10 \log_{10} A_0$ is commonly modeled as a zero-mean normal random variable with standard deviation $\sigma_0 = 2$ dB. The shadowing factors $\zeta_\ell = 10 \log A_\ell$, $\ell \neq 0$, of the signals from the interfering base stations can be modeled as IID normal random variables with standard deviation $\sigma_1 = 8$ dB, because their powers are not controlled by the reference cell. Then from (9.4) we have

$$f_{\mathrm{f}} = E\left[10^{\zeta_0/10} 10^{-\zeta_1/10}\right] \lim_{L\to\infty} \sum_{\ell=1}^{L-1} \frac{2}{3\sqrt{3}} \iint\limits_{S_0} \left[\frac{d(x^{(k_0)}, y^{(k_0)}, 0)}{d(x^{(k_0)}, y^{(k_0)}, \ell)}\right]^m \mathrm{d}x^{(k_0)}, \mathrm{d}y^{(k_0)} \tag{9.6}$$

For $\sigma_0 = 2$ dB and $\sigma_1 = 8$ dB, the coefficient

$$\lambda \stackrel{\mathrm{def}}{=} E\left[10^{\zeta_0/10} 10^{-\zeta_1/10}\right] = E\left[e^{s(\zeta_0 - \zeta_1)}\right] = e^{\frac{s^2(\sigma_0^2 + \sigma_1^2)}{2}}$$

where $s = (\ln 10)/10$, equals 6.06.

Using Monte-Carlo methods the function

$$\overline{f}_{\mathrm{f}} \stackrel{\mathrm{def}}{=} \lambda \sum_{\ell=1}^{L-1} \frac{2}{3\sqrt{3}} \iint\limits_{S_0} \left[\frac{d(x^{(k_0)}, y^{(k_0)}, 0)}{d(x^{(k_0)}, y^{(k_0)}, \ell)}\right]^m \mathrm{d}x^{(k_0)} \mathrm{d}y^{(k_0)} \tag{9.7}$$

was estimated in [58]. In the simulation setup a grid of about 1800 equally sized cells were constructed to generate the other-cell interference. The number of users K per cell was chosen equal to 1000. Note that numerical estimation of the interference factor $\overline{f}_{\mathrm{f}}$ for the propagation model with $m = 3$ leads to the result closest to the hypothetical value of $f_{\mathrm{f}} = 0.6$.

To further investigate the location dependence of the other-cell interference factor, values of $f(x_0^{(k_0)}, y_0^{(k_0)}) = \lambda \sum_{\ell'=1}^{L-1} \frac{2}{3\sqrt{3}} \left[\frac{d(x^{(k_0)}, y^{(k_0)}, 0)}{d(x^{(k_0)}, y^{(k_0)}, \ell)}\right]^m$ at three reference locations were evaluated by the same methods. The reference locations are depicted in Figure 9.2. These are the *interior* locations where the mobile is on halfway between the center and the border, the *border* locations where the mobile is at an equal distance from the reference base station and the closest interfering base station, and *corner* locations where the mobile is at equal distance from the reference base station and the two closest interfering base stations. In Table 9.1 we present the values of $f(x_0^{(k_0)}, y_0^{(k_0)})$ obtained at the reference locations and the average value f_{f}. These values depend only on the geometric configuration of the cell grid.

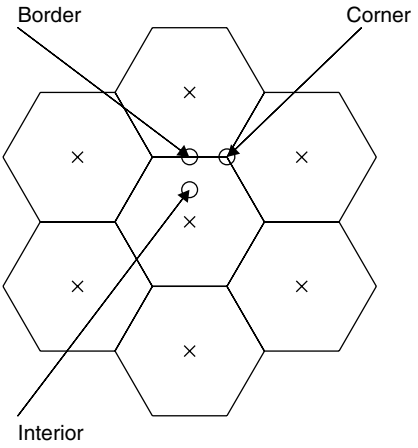

Figure 9.2. Illustration of different mobile terminal locations.

Table 9.1 Interference Factors $f(x_0^{(k_0)}, y_0^{(k_0)})$ at the Reference Locations and Factor $f_{\mathrm{f}}(= f_{\mathrm{r}})$ for $m = 2, 3, 4, 5$ and $\sigma_0 = 2$ dB, $\sigma_1 = 8$ dB

$f(x_0^{(k_0)}, y_0^{(k_0)})$	m			
Location	2	3	4	5
Interior	1.63	0.183	0.0373	0.0095
Border	7.09	2.17	1.41	1.18
Corner	9.54	3.39	2.43	2.16
Average	2.63	0.541	0.232	0.168

The reverse-link interference is illustrated in Figure 9.3, where the central cell is the reference cell and the interference is created by the mobiles located in other cells. We assume that in each cell there are K users and that the system has perfect power control. Then the k_ℓth user's transmitter power is proportional to the propagation path loss, that is, equals $P\kappa^{(k_\ell,\ell)}$, $\ell = 0, 1, \ldots, L$, where P is the required power of the signal from a desired user at base station receiver. The power of the interference caused by the k_ℓth user, $\ell \neq 0$, at the base station receiver of the reference 0th cell is equal to $P\kappa^{(k_\ell,\ell)}/\kappa^{(k_\ell,0)}$. The total average power of the other-cell interference at the reference base station receiver is

$$P \sum_{\ell=1}^{L-1} \sum_{k_\ell} E\left[\frac{\kappa^{(k_\ell,\ell)}}{\kappa^{(k_\ell,0)}}\right]$$

Because the summarized power of the other user of the given cell is approximately equal to PK, we have the following expression for the reverse-link relative

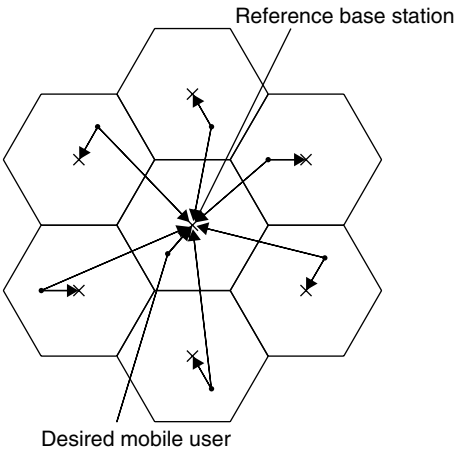

Figure 9.3. Illustration of reverse channel interference.

other-cell interference factor

$$f_{\mathrm{r}} = \frac{1}{K} \sum_{\ell=1}^{L-1} \sum_{k_\ell} E\left[\frac{\kappa^{(k_\ell,\ell)}}{\kappa^{(k_\ell,0)}} \right] \tag{9.8}$$

To estimate f_{r} we consider the same idealized model of a cellular CDMA system as when we estimated f_{f}. Then [compare with (9.4)]

$$f_{\mathrm{r}} = \lim_{L\to\infty} \sum_{\ell=1}^{L-1} \frac{2}{3\sqrt{3}} \iint\limits_{S_\ell} E\left[\frac{\kappa(x^{(k_\ell)}, y^{(k_\ell)}, \ell)}{\kappa(x^{(k_\ell)}, y^{(k_\ell)}, 0)} \right] \mathrm{d}x^{(k_\ell)} \mathrm{d}y^{(k_\ell)} \tag{9.9}$$

where S_ℓ is the area of the ℓth cell.

We will show that for this idealized model $f_{\mathrm{f}} = f_{\mathrm{r}}$. In fact, the forward-link relative interference factor can be expressed as

$$f_{\mathrm{f}} = \lim_{L\to\infty} \frac{1}{L} \sum_{\ell=0}^{L-1} \sum_{\substack{\ell'\neq\ell \\ \ell'=0}}^{L-1} \frac{2}{3\sqrt{3}} \iint\limits_{S_0} E\left[\frac{\kappa(x^{(k_\ell)}, y^{(k_\ell)}, \ell)}{\kappa(x^{(k_\ell)}, y^{(k_\ell)}, \ell')} \right] \mathrm{d}x^{(k_\ell)} \mathrm{d}y^{(k_\ell)} \tag{9.10}$$

and analogously, the reverse-link relative interference factor can be expressed as

$$f_{\mathrm{r}} = \lim_{L\to\infty} \frac{1}{L} \sum_{\ell=0}^{L-1} \sum_{\substack{\ell'\neq\ell \\ \ell'=0}}^{L-1} \frac{2}{3\sqrt{3}} \iint\limits_{S_0} E\left[\frac{\kappa(x^{(k_{\ell'})}, y^{(k_{\ell'})}, \ell')}{\kappa(x^{(k_{\ell'})}, y^{(k_{\ell'})}, \ell)} \right] \mathrm{d}x^{(k_{\ell'})} \mathrm{d}y^{(k_{\ell'})} \tag{9.11}$$

Note that the integrands in Formulas (9.10) and (9.11) are both equal to the expectation of the ratio of the attenuation of the signal between a mobile terminal

and the base station it is connected to and the attenuation of the interfering signals. Thus, by change of the notation, $\ell' \to \ell$ and $\ell \to \ell'$, in the right-hand side of (9.11), we get expression of the right-hand side of (9.10). We note that if the f_{f} and f_{r} are estimated over a finite number of cells L, there will be nonuniform interference at the border of the system and, hence, perhaps f_{f} and f_{r} have slightly differing values.

9.3 HANDOFF STRATEGIES

When the mobile moves into a different cell while a conversation is in progress, the switching center automatically transfers the call to the new base station. This handoff operation not only involves identifying a new base station but also requires that signals can be allocated to the channel associated with the new base station.

Processing handoffs is an important task in any cellular mobile radio system. Handoff must be performed as seldom as possible, to avoid the "ping-pong" effect (see below). When a particular signal level is specified as the minimum acceptable, it is established as a threshold at which handoff is made. Because of the shadowing effect, a margin θ dB must be added to the threshold. Figure 9.4 illustrates a hard handoff situation, when a call is transferred from base station 1 to base station 2 and the handoff is made exactly on the cell boundary. Power levels at points A and B are shown in the case when the mobile communicates with base station 1.

EXAMPLE 9.2

Consider a hard handoff that occurs exactly at the boundary between cells. Without shadowing, the minimum power (in dB*) required from the mobile's transmitter just*

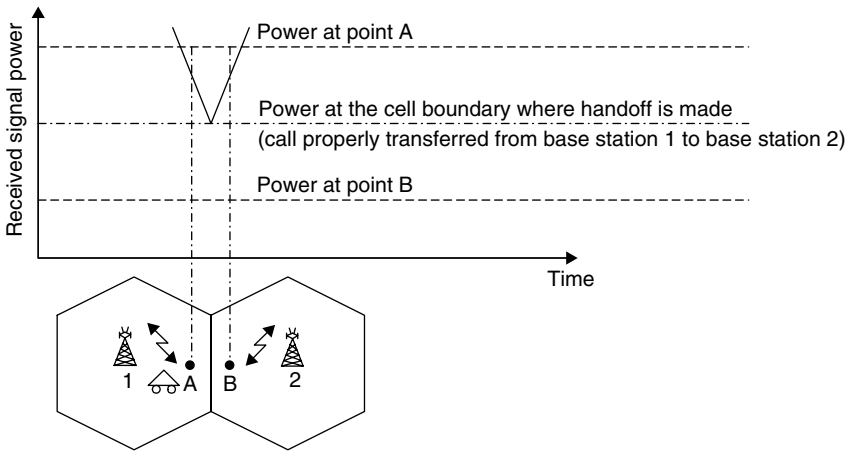

Figure 9.4. Illustration of an ideal handoff at cell boundary.

to overcome background noise on the cell's boundary is equal to $B + 10m \log_{10} d$, *where* d *is the cell's radius and* B *is the desired power level (in* dB*) on the base station receiver. Suppose now that there is shadowing and we require that the link achieve at least the performance of unshadowed propagation all but a fraction* π_{out} *of the time, where* π_{out} *is outage probability. Which margin* θ *should then be added to the transmitter power if* $\pi_{\text{out}} = 0.1$*? Assume that path loss factor is given by Formula (9.2) and* $m = 4$, $\sigma = 8$ dB.

Solution

The desired performance will be achieved whenever the shadowing attenuation $\zeta < \theta$. *Thus the outage probability (or fraction of the time that the performance is not achieved) is*

$$\pi_{\text{out}} = Pr(\zeta > \theta) = \frac{1}{\sqrt{2\pi\sigma^2}} \int_{\theta}^{\infty} e^{-x^2/2\sigma^2} \mathrm{d}x = Q\left(\frac{\theta}{\sigma}\right)$$

For $\sigma = 8$ dB *it follows that the margin* $\theta = 10.3$ dB.

Handoffs must be performed successfully and as infrequently as possible. The ideal hard handoff at the cell boundary is undesirable. This is because it can lead to the *"ping-pong" effect* [47] where a mobile near the boundary is handed back and forth several times from one base station to an other. In practical systems with hard handoffs the handoff occurs only when the mobile has moved some distance d' beyond the boundary such that the first cell's base station power is reduced enough compared with its value at the boundary (Fig. 9.4). Let the ratio of the distance d' to the cell radius d be $\gamma = d'/d$ and the outage probability that the power of the mobile's transmitter is lower than the minimal required power be π_{out}. Then the margin θ (dB), which must be added to the transmitted power on the cell's boundary, should satisfy the equation (compare with Example 9.2)

$$\pi_{\text{out}} = Pr[10m \log_{10} \gamma + \zeta > \theta] = Q\left(\frac{\theta - 10m \log_{10} \gamma}{\sigma}\right) \tag{9.12}$$

where m is the path loss exponent and σ is the standard deviation of the log-normal shadowing

EXAMPLE 9.3

Consider the problem of Example 9.2. Which margin θ *dB must be added to the transmitted power if the hard handoff occurs on the relative distance* γ *from the first base station and* $\gamma = 1.05, 1.15, 1.25$*?*

Solution

In the condition of Example 9.2, $m = 4$, $\sigma = 8$ dB, *and* $\pi_{\text{out}} = 0.1$. *Then from Formula (9.12) it follows that*

$$\theta = 40 \cdot \log_{10} \gamma + 10.3 \text{ dB} \tag{9.13}$$

Thus, for a given range of additional distance beyond cell boundary, that is, for $\gamma = 1.05$, 1.15 *and* 1.25, *the margin must be* 11.1 dB, 12.7 dB, *and* 14.2 dB, *respectively.*

Hard handoffs are used in TDMA and FDMA cellular systems, in which different radio channels are assigned during handoff. CDMA cellular mobile radio systems provide handoff capability that cannot be provided with other wireless systems. In CDMA systems, the term "handoff" does not mean a physical change in the assigned channel but rather that several base stations handle the radio communication task.

For the forward link transmission, while a mobile is tracking the pilot of a particular cell it is also searching for pilots of adjacent cells. When a new pilot is detected and found to have sufficient signal strength, the mobile informs its original base station. This notifies the switching center, which orders the second cell's base station to communicate with the given mobile in parallel with the first cell's base station. When the first cell's signal is too weak relative to the second it will be dropped.

For the reverse link, each base station demodulates and decodes the signals independently. By simultaneously evaluating the received signals from a user at several neighboring base stations, the switching center may decide on the version of the user's signal that is best. This technique exploits macroscopic space diversity provided by the different physical locations of the base stations and allows the switching center to make a soft decision.

The soft handoff strategy has many advantages. It considerably increases the capacity of a multicellular system. We will show that the required margin θ can be reduced by a large amount in the case when two base stations are involved in the process.

Soft handoff for the reverse link occurs throughout a range of distances from the two base stations. At any given time, the best of the receptions from the two base stations is used at the switching center. We assume for simplicity that this depends only on the path loss. Then the strongest, that is, with the lowest path loss, is used. Consequently the path loss is given by

$$\min\{10m \log_{10} d_1 + \zeta_1,\ \ 10m \log_{10} d_2 + \zeta_2\} \tag{9.14}$$

where ζ_i is log-normal shadowing losses in decibels for the ith base station. We may express the random component ζ_i of the decibel loss as the sum of two independent components; one, $\eta_{1,2}$, is the near field of the mobile, which is common to all base stations, and one, η_1/η_2, that pertains to the receiving base station and differs from one base station to another. Then

$$\begin{aligned} \zeta_1 &= \eta_1 + \eta_{1,2} \\ \zeta_2 &= \eta_2 + \eta_{1,2} \end{aligned} \tag{9.15}$$

and we have

$$E(\zeta_1) = E(\zeta_2) = E(\eta_1) = E(\eta_2) = E(\eta_{1,2}) = 0 \tag{9.16}$$

$$E(\zeta_1^2) = E(\eta_1^2) + E(\eta_{1,2}^2) = \sigma^2 \tag{9.17}$$

$$E(\zeta_2^2) = E(\eta_2^2) + E(\eta_{1,2}^2) = \sigma^2 \tag{9.18}$$

$$E(\zeta_1\zeta_2) = E(\eta_{1,2}^2) = \rho\sigma^2 \tag{9.19}$$

where ρ is the correlation coefficient of the losses to two base stations. We assume that the near-field and base station-specific losses have equal standard deviations, that is $\rho = 1/2$. Because the mobile is assumed to be either in the first or in the second cell, it is easily established that $d_1 = d_2$ (the mobile is exactly on the boundary) represents the worst case. Thus the margin θ needed to satisfy the outage probability requirement is

$$\begin{aligned} P_{\text{out}} &= Pr\{\min(\zeta_1, \zeta_2) > \theta\} \\ &= \int_\theta^\infty \int_\theta^\infty \frac{1}{2\pi\sigma^2\sqrt{1-\rho^2}}\, e^{-\frac{x^2-2\rho xy+y^2}{2\sigma^2(1-\rho^2)}}\, dx\, dy \\ &= \int_\theta^\infty \frac{1}{\sqrt{2\pi\sigma^2}}\, e^{-\frac{y^2}{2\sigma^2}}\, Q\left(\frac{\theta-\rho y}{\sigma\sqrt{1-\rho^2}}\right) dy \end{aligned} \tag{9.20}$$

EXAMPLE 9.4

Consider the soft handoff strategy in the conditions of Example 9.1. Let the correlation coefficient of the losses to two base stations be $\rho = 1/2$. *Which margin* θ_{soft} *(in* dB*) must be added to the transmitted power for* $\pi_{\text{out}} = 0.1$*?*

Solution

For $\rho = 1/2$, $\sigma = 8$ dB *we find from (9.20) that* $\theta_{\text{soft}} = 6.2$ dB.

Comparison of Examples 9.2 and 9.4 shows that the required margin for soft handoff is about 4 dB less than for hard handoff. The cell area is proportional to the square of the radius, whereas the propagation loss is proportional to the fourth power. It follows that this reduced margin represents an increased cell area for soft handoff of 3–4 dB, or a reduction in the number of the cells and consequently in the number of base stations by a factor of 2 or 2.5.

9.4 POWER CONTROL

Power control is an important part of any two-way communication system, but it is especially important in DS CDMA systems. To maximize the total user capacity of the system, the power of the signal received from each one of the users over the forward or reverse link must be made nearly equal. If the received

signal is too weak, the user will be dropped. If the received power of the signal is too great, the performance of this receiver will be acceptable but it will add undesired interference to all other users in the cell.

For the reverse link, the transmitted power can be adjusted individually by each user, simply by measuring the forward link power received by the mobile receiver. This would solve the problem if the physical channels were completely symmetric. This ideal situation is not often the case, because, generally, forward and reverse link bandwidths are separated in frequency. Still, the measuring of the received signal power level provides a rough measure of the propagation loss in the link. The higher the received signal power the lower the transmitted power is set, and vice versa. The *open-loop power control* strategy is to keep the sum of the received and transmitted powers (in decibels) constant by the user terminal's choice of transmitted power.

The propagation loss is not symmetric primarily because of Rayleigh fading. Even after adjustment using open-loop power control, the mobile transmitter power may differ markedly from one user to the next. Therefore, a *closed-loop power control* mechanism should be added to control the power transmitted by the mobile. This mechanism is based on measurements made at the base station.

When the base station determines that the received signal from a particular user has too high or too low a power level, a one-bit command is sent by the base station to this user over the forward link, to order the mobile to lower or raise its power by a fixed amount Δ dB. If the power of the mobile is low, a "1" is transmitted over the power control channel; otherwise, a "-1" is transmitted to indicate that the mobile station should decrease its power level.

Before considering the control loop performance, we establish how the decision is made to raise or lower power in a typical DS CDMA system. Consider, for example, communication by DPSK signals in the reverse AWGN channel [2] (see Section 3.5). The decision device is analogous to the differentially coherent receiver presented in Figure 3.6 except that the block "Choose largest" is replaced by the block "Compare the maximum statistic with threshold θ." If the maximum statistic $\max(\hat{y}^{(k)}, \check{y}^{(k)})$ exceeds the threshold, the down-power command is sent; otherwise, the up-power command is sent. The probabilities $\tilde{P}_{\mathrm{d}}$ and $\tilde{P}_{\mathrm{u}}$ that down- and up-commands are sent are functions of the signal-to-noise ratio per bit at the base station α, that is,

$$\begin{aligned} \tilde{P}_{\mathrm{d}}(\alpha) &= P\left[\max(\hat{y}^{(k)}, \check{y}^{(k)}) > \theta | \alpha\right] \\ \tilde{P}_{\mathrm{u}}(\alpha) &= 1 - \tilde{P}_{\mathrm{d}}(\alpha) \end{aligned} \tag{9.21}$$

The desired level α_0 of the signal-to-noise ratio at the base station may be estimated a priori to lie between 3 and 10 dB. Then $\tilde{P}_{\mathrm{d}}(\alpha) > 1/2$ for $\alpha > \alpha_0$ and $\tilde{P}_{\mathrm{d}}(\alpha) < 1/2$ for $\alpha < \alpha_0$.

[2]This example describes only the principle of the power control mechanism. In the Viterbi book [47] is considered a more complicated case when the system uses orthogonal transmission over a Rayleigh fading channel, in a way similar to IS-95.

Analogous decisions are made in DS CDMA systems using noncoherent reception of encoded signals in the reverse AWGN channel (see Section 4.3) and in DS CDMA systems communicating over multipath faded channels (see Section 5.4). In these cases the kth receiver calculates the statistics $y_i^{(k)}$ and compares the maximum statistic $\max y_i^{(k)}$ with the threshold θ. If the maximum statistic exceeds the threshold, the down-power command is sent; otherwise, the up-power command is sent. The probabilities $\tilde{P}_{\mathrm{d}}$ and $\tilde{P}_{\mathrm{u}}$ depend on the channel and the receiver structure.

Because excessive delay in the loop is unacceptable, the commands are sent uncoded, which causes an error probability that is essentially higher than the decoding error probability of the forward link. A simple method used in the reverse transmission (see Section 5.4) is to puncture the forward link code (one symbol out of g) and dedicate the punctured symbols to the uncoded command transmission. (In the IS-95 system, $g = 12$.) The rate of the punctured code is then increased (by the factor $g/(g-1)$ if one in g symbols is punctured), and its performance is slightly degraded.

In the CDMA2000 system, the power control information is multiplexed with the data stream by puncturing of code symbols as it is done in IS-95. The puncturing rate is 800 Hz. Whereas the downlink direction of CDMA2000 has power control information multiplexed with the data channel, the uplink direction has power control information multiplexed with the pilot signal. The pilot channel contains the power control pulses of duration 1.25 ms. This provides downlink closed-loop power control at 800 Hz, the same rate as in uplink direction.

Let us analyze the power control process. The receiver separates power control symbols from data/pilot information and increases or decreases the power of the transmitted signal depending on the received information.

If the power control command is received in error, the wrong action will be taken. Hence, given that a forward link *command error* occurs with probability π, the actual probability that the power will be reduced for a received signal-to-noise ratio α is

$$P_{\mathrm{d}}(\alpha) = (1-\pi)\tilde{P}_{\mathrm{d}}(\alpha) + \pi\tilde{P}_{\mathrm{u}}(\alpha) = (1-2\pi)\tilde{P}_{\mathrm{d}}(\alpha) + \pi \tag{9.22}$$

and that it will be increased is

$$P_{\mathrm{u}}(\alpha) = 1 - P_{\mathrm{d}}(\alpha) = 1 - \pi - (1-2\pi)\tilde{P}_{\mathrm{d}}(\alpha) \tag{9.23}$$

where $\tilde{P}_{\mathrm{d}}(\alpha)$ is given by (9.21).

We consider the following model of power control mechanism. The power control measurement period is Δt. We assume that control device maintains the desired signal-to-noise ratio in an environment where the propagation loss $\gamma(t)$ varies relatively slowly.

Let the signal-to-noise ratio per bit of the signal transmitted by a mobile for the power measurement period $(t-\Delta t, t)$ be $\beta(t)$ dB and let the propagation

loss during this period be $\gamma(t)$ dB. Then the signal-to-noise ratio of the received signal over the measurement period is

$$\alpha(t) = \beta(t) - \gamma(t) \text{ dB} \tag{9.24}$$

Assuming a delay of one measurement period the control device orders an increase or decrease in the transmitted power by Δ dB during the measurement period $(t, t + \Delta t)$, that is,

$$\beta(t + \Delta t) = \beta(t) + \Delta \cdot u[\alpha(t)], \tag{9.25}$$

where

$$u(\alpha) = \begin{cases} -1 & \text{with probability } P_{\text{d}}(\alpha) \\ 1 & \text{with probability } P_{\text{u}}(\alpha) \end{cases} \tag{9.26}$$

Combining Formulas (9.24) and (9.25), we obtain

$$\begin{aligned} \alpha(t + \Delta t) &= \beta(t + \Delta t) - \gamma(t + \Delta t) \\ &= \beta(t) + \Delta \cdot u[\alpha(t)] - \gamma(t + \Delta t) \end{aligned} \tag{9.27}$$

Then

$$\begin{aligned} \Delta\alpha(t) &\stackrel{\text{def}}{=} \alpha(t + \Delta t) - \alpha(t) \\ &= \Delta \cdot u[\alpha(t)] - \Delta\gamma(t) \end{aligned} \tag{9.28}$$

where $\Delta\gamma(t) \stackrel{\text{def}}{=} \gamma(t + \Delta t) - \gamma(t)$.

The propagation loss $\gamma(t)$ depends on the distance from the mobile terminal to the base station and on shadowing. It also includes very rapid variations, shorter than about one millisecond, due to the Rayleigh fading, that cannot be mitigated by the power control. Therefore, we consider only long-term fading and shadowing by objects. They can be mitigated by the power control loop. In our analysis we assume that the propagation loss fluctuation $\Delta\gamma = \Delta\gamma(t)$ is a zero-mean Gaussian random variable with variance $\sigma_\gamma^2 \Delta t$. The probability density function of the random variable $\Delta\gamma$ is

$$\varphi_{\Delta\gamma}(y) = \frac{1}{\sqrt{2\pi\sigma_\gamma^2 \Delta t}} \exp\left[\frac{-y^2}{2\sigma_\gamma^2 \Delta t}\right] \tag{9.29}$$

Let $f_\alpha(x, t)$ be the probability density function of the random variable α at moment t. Then

$$\begin{aligned} f_\alpha(x, t + \Delta t) = &\int_{-\infty}^{\infty} P_{\text{d}}(x - y + \Delta) f_\alpha(x - y + \Delta, t) \varphi_{\Delta\gamma}(y)\, \text{d}y \\ &+ \int_{-\infty}^{\infty} P_{\text{u}}(x - y - \Delta) f_\alpha(x - y - \Delta, t) \varphi_{\Delta\gamma}(y)\, \text{d}y \end{aligned} \tag{9.30}$$

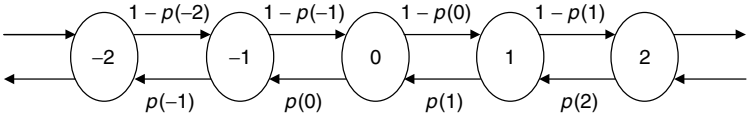

Figure 9.5. A Markov chain with countably infinite state space.

The integral equation (9.30) of the closed-loop power control is not easily solvable in the general case. We analyze the partial case when propagation loss fluctuations $\Delta\gamma$ are very small, that is, $\text{var}(\Delta\gamma) = \sigma_\gamma^2 \Delta t \ll \Delta$, under the assumption that in the beginning $\alpha = \alpha_0$. Then integral equation (9.30) passes into a finite-difference equation relative to the probabilities $\psi_j(i)$, where $\psi_j(i)$ is the probability that at the moment $t = j\Delta t$ the signal-to-noise ratio of the input of the receiver is equal to $\alpha_0 + i\Delta$, $i = \ldots -1, 0, 1, \ldots$. The finite-difference equation is

$$\psi_j(i) = p(i+1)\psi_{j-1}(i+1) + (1 - p(i-1))\psi_{j-1}(i-1) \tag{9.31}$$

where

$$p(i) = \begin{cases} P_{\text{d}}(\alpha_0 + i\Delta), & i \neq 0, \\ 1/2, & i = 0 \end{cases} \tag{9.32}$$

The initial condition is

$$\psi_0(i) = \begin{cases} 1, & i = 0 \\ 0, & \text{otherwise} \end{cases} \tag{9.33}$$

Equation (9.31) describes a Markov chain with countably infinite state space (Fig. 9.5). If $p(i) > 1/2$ for $i > 0$ and $p(i) < 1/2$ for $i < 0$, steady-state probabilities exist.

EXAMPLE 9.5

Find the steady-state probability distribution of the power control system, assuming that the path loss fluctuations $\Delta\gamma$ are negligible in comparison to the power correction step size Δ and that the base station exactly determines the power level of the received signal from a mobile. What is average power of the received signal? What is the standard deviation of the power if $\pi = 0.05$, $\Delta = 0.5$ dB?

Solution

Because the path loss fluctuations are negligible, we may use the finite-difference equations (9.31)–(9.33) to find the steady-state probabilities. Because the base station determines exactly the power level of the received signal we have

$$p(i) = \begin{cases} 1 - \pi, & i > 0, \\ \pi, & i < 0, \\ 1/2, & i = 0 \end{cases} \tag{9.34}$$

where $\pi < 1/2$ is the command error probability.

Then the steady-state probabilities $\psi(i) = \lim_{j\to\infty} \psi_j(i)$ *satisfy the system of equations*

$$\psi(i) = \left\{ \begin{array}{ll} (1-\pi)\psi(i+1) + \pi\psi(i-1), & i > 1, \\ \pi\psi(i+1) + (1-\pi)\psi(i-1), & i < -1, \\ (1-\pi)[\psi(1) + \psi(-1)], & i = 0, \\ (1-\pi)\psi(2) + 1/2\psi(0), & i = 1, \\ 1/2\psi(0) + (1-\pi)\psi(-2), & i = -1 \end{array} \right\} \tag{9.35}$$

$$\sum_{i=-\infty}^{\infty} \psi(i) = 1 \tag{9.36}$$

The solution of Equations (9.35) and (9.36) is

$$\psi(i) = \left\{ \begin{array}{ll} \dfrac{[\pi/(1-\pi)]^{|i|}}{2[1-\pi/(1-\pi)]}, & i \neq 0, \\ \dfrac{1}{1-\pi/(1-\pi)}, & i = 0 \end{array} \right\} \tag{9.37}$$

The average power of the received signal in this example is α_0*, and the standard deviation of the power is*

$$D = \sqrt{var(\alpha)} = \Delta\sqrt{var(i)} = \Delta \sqrt{\sum_{i=0}^{\infty} i^2 \left(\frac{\pi}{1-\pi}\right)^i} = \Delta\sqrt{\frac{\pi(1-\pi)}{(1-2\pi)^3}}$$

In particular, if $\pi = 0.05$*,* $\Delta = 0.5$ dB*, then* $D = 0.255$ dB.

In the general case, instead of solving Equation (9.30), it is more useful to simulate (9.28) and from the simulations generate the histograms of the power of the received signal.

In [53], the power control process was simulated. The transmission of Hadamard sequences of length 64 over unfaded Gaussian channel and over an equal average component Rayleigh fading L-path ($L = 1, 2, 4$) channel was studied. The threshold θ was in each case chosen so that the mean $E_b/I_0 \approx 10$ dB. The path loss increment standard deviation $\sqrt{\text{var}(\Delta\gamma)}$ was chosen equal to 0.5 dB, the power correction step size $\Delta = 0.5$ dB, and $\pi = 0.05$.

The average powers on the input of the receiver were in all cases about 10 dB, the standard deviations D of the power in the Gaussian channel were 1.13 dB, and for the Rayleigh channel they were 1.29 dB ($L = 4$), 1.35 dB ($L = 2$), and 1.47 dB ($L = 1$). We emphasize that the standard deviation of the power in this realistic case was essentially larger than in the idealized case considered in Example 9.5.

Although the desired E_b/I_0 to be received at the base station may be estimated a priori to lie between 3 and 10 dB, conditions will vary according to the multipath

fading environment. Thus it is useful to add a power control mechanism called an *outer loop*, which adjusts the desired E_b/I_0 level according to the individual user's error rate measured at the base station. This guarantees a given error rate per coded voice frame.

We have concentrated on the power control for the reverse link rather than the forward link. This is because the power measurement for reverse link is more complex than for the forward link, where it is possible to measure power on the unmodulated pilot signal.

9.5 ERLANG CAPACITY OF CDMA SYSTEM

The radio channel capacity K_0 defines the maximal number of users that can be provided in a CDMA system at a given grade of service. The grade of service is a criterion used to define the quality of a particular system by specifying a desired likelihood of a user obtaining channel access given a maximum number K_0 of users in the system. It is the network designer's job to estimate the required radio channel capacity and to allocate the appropriate number of users to meet the grade of service. The grade of service is typically given as the probability that a call is blocked or the probability of a call experiencing a delay greater than a certain queuing time.

Typically, for an actual telephone system, the probability that a call arrival is requested by a particular user is small but the total average number of call requests per unit time, λ, is large. The value λ is called the *arrival rate*. The number of arrivals that occur in disjoint intervals is independent, and the number of arrivals $a(t, t+\tau)$ in any time interval of length τ is modeled as Poisson distributed with the parameter λ, that is,

$$P(a(t, t+\tau) = n) = e^{-\lambda\tau} \frac{(\lambda\tau)^n}{n!}, \qquad n = 0, 1, \ldots \tag{9.38}$$

In particular, in an infinitesimal time interval Δt, the probability of a single arrival is $\lambda \Delta t$. If the maximal number of users is K_0, this call will be served as long as the number of served calls $k < K_0$. The call service time per user is assumed to be exponentially distributed with parameter μ, so that the probability distribution function of the service time τ is

$$P(\tau \leq s) = 1 - \exp(-\mu s) \tag{9.39}$$

From Formula (9.39) it follows that the average call duration is $1/\mu$. The parameter μ is called the *service rate*. The probability that a call terminates during an interval of infinitesimal duration Δt is $\mu \Delta t$. If the number of served calls is k, the probability that at least one call will terminate in Δt is on the order of $k\mu\Delta t$. Note that the probability that more than one call terminates is $o(\Delta t)$, $\Delta t \to 0$.

There are two models for determining the occupancy distribution and the probability of lost calls. The first model offers no queuing for call requests. That

is, for every user requesting service, it is assumed there is minimal call setup time and the user is given immediate access to a channel if the number of served users is less than the maximum permitted. If the channel is not available, the requesting user is blocked without access. This type of model is called "lost call cleared" (LCC).

The second kind of teletraffic model is one in which the queue is provided to hold calls that are blocked. If the service is not available immediately, the call request may be delayed until the service become available. This is the "lost call delayed" (LCD) model.

The Markov state diagram of the LCC teletraffic model is given in Figure 9.6. Here k, $k \leq K_0$, is the number of served users. Let P_k be the steady-state probabilities that the number of served users is k. Then

$$P_0 = (1 - \lambda \Delta t) P_0 + \mu \Delta t P_1 \tag{9.40}$$

$$P_k = \lambda \Delta t P_{k-1} + [1 - (\lambda + k\mu)\Delta t] P_k + (k+1)\mu \Delta t P_{k+1}, \qquad k = 1, 2, \ldots, K_0 - 1 \tag{9.41}$$

$$P_{K_0} = \lambda \Delta t P_{K_0 - 1} + [1 - K_0 \mu \Delta t] P_{K_0} \tag{9.42}$$

Hence, in the steady state, we have

$$\lambda P_{k-1} = k\mu P_k, \qquad k \leq K_0 \tag{9.43}$$

Solving the system (9.43) of K_0 equations, we get

$$P_k = \frac{(\lambda/\mu)^k}{k!} P_0, \qquad k \leq K_0 \tag{9.44}$$

Because

$$1 = \sum_{k=0}^{K_0} P_k = P_0 \sum_{k=0}^{K_0} \frac{(\lambda/\mu)^k}{k!} \tag{9.45}$$

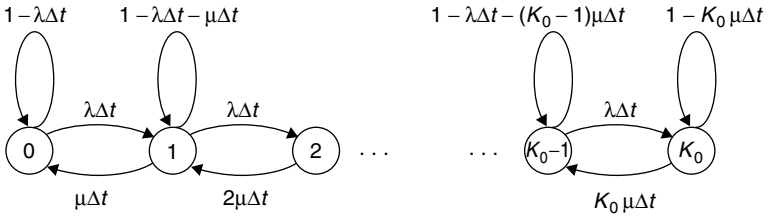

Figure 9.6. Markov state diagram for the LCC model.

we get

$$P_k = \frac{(\lambda/\mu)^k/k!}{\sum_{i=0}^{K_0}(\lambda/\mu)^i/i!} \tag{9.46}$$

The probability that in the LCC model a new user enters the system and will not be served (blocking probability) is

$$P_{\text{block}} = P_{K_0} = \frac{(\lambda/\mu)^{K_0}/K_0!}{\sum_{i=0}^{K_0}(\lambda/\mu)^i/i!} \tag{9.47}$$

The ratio λ/μ is called the *total traffic intensity*. It is measured in Erlangs.

For the LCD model (9.40) still holds, (9.41) holds for all positive integer k, and (9.42) is no longer applicable. Thus

$$1 = \sum_{k=0}^{\infty} P_k = P_0 \sum_{k=0}^{\infty} \frac{(\lambda/\mu)^k}{k!} = P_0 \exp(\lambda/\mu) \tag{9.48}$$

and we have

$$P_k = \frac{(\lambda/\mu)^k}{k!} \exp(-\lambda/\mu), \qquad k = 0, 1, \ldots \tag{9.49}$$

which is the formula of the Poisson distribution. The blocking probability is the probability that when a new call request arrives there are K_0 or more users in the system, either being served or seeking service. Hence, the blocking probability for the LCD model is

$$P_{\text{block}} = \sum_{k=K_0}^{\infty} P_k = \exp(-\lambda/\mu) \sum_{k=K_0}^{\infty} \frac{(\lambda/\mu)^k}{k!} \tag{9.50}$$

For large K_0 the results obtained for the two models are very similar. In both cases λ/μ is slightly increased by lost calls repeating, with λ increased in the LCC model and μ decreased in the LCD model. We shall favor the LCD model because it is more realistic for mobile users.

In spread spectrum systems, the quality of communication is defined by the signal-to-noise ratio on the receiver input. In its own turn, this ratio is a random variable, which depends on the number of served users that are active at the particular moment. Assume that a bandwidth W is occupied by k perfectly power-controlled users of a given cell of a DS CDMA system, so that each of the transmitted signals is received by the base station at the same power level P and that the other-cell interference power is equal to P_{oc}. Moreover, each active user communicates with transmission rate R. Let κ be the number of active users among k served users, and each of served users is active with probability

$\alpha = 1/\gamma_v$ where γ_v is the voice activity gain. Then the number of active users has a binomial distribution; that is, the probability that κ users are active is

$$P(\kappa) = \binom{k}{\kappa} \alpha^{\kappa} \cdot (1-\alpha)^{k-\kappa}, \qquad \kappa = 0, 1, \ldots, k \tag{9.51}$$

If $(E_b/I_0)_{\min}$ is the minimal level of signal-to-noise ratio on the base station receiver, the condition of reliable communication is [compare with (1.8) and (1.15)]

$$(E_b/I_0)_{\min} \le \frac{W/R}{(\kappa - 1) + N_0 W/P + P_{oc}/P} \tag{9.52}$$

where $N_0/2$ is the two-sided power spectral density of the AWGN. From Formula (9.52) it follows

$$\kappa \le \left\lfloor 1 + \frac{W/R}{(E_b/I_0)_{\min}} - \frac{N_0 W}{P} - \frac{P_{oc}}{P} \right\rfloor \stackrel{\text{def}}{=} \kappa_{\max} \tag{9.53}$$

When condition (9.53) is not met, the system will be deemed to be in the outage condition. If the number of users in the cell is equal to the capacity, K_0, the probability of outage is

$$P_{out} = P(\kappa > \kappa_{\max}) = \sum_{i=\kappa_{\max}+1}^{K_0} \binom{K_0}{i} \cdot \alpha^i \cdot (1-\alpha)^{K_0 - i} \tag{9.54}$$

For any given $(E_b/I_0)_{\min}$ and P_{out} we can determine the maximal permissible number of users K_0 (capacity) in the perfectly power-controlled system. In its own turn, Formula (9.50) gives the blocking probability for the LCD system.

EXAMPLE 9.6

Consider a DS CDMA system that occupies 10 *MHz of the spectrum in each one-way link. The user rate* $R = 10$ *kbit/s, the voice activity gain* $\gamma_v = 8/3$*, and the minimum acceptable* $E_b/I_0 = 10$ dB*. The other-cell interference power* $P_{oc} = 0.6P$*. Find the capacity of the system if the outage probability must not exceed* 0.01*. Find the blocking probability for the LCH model if the arrival rate* $\lambda = 1$ *(call/s) and the average call duration* $1/\mu = 100$ *s. Neglect the background noise.*

Solution

From Formula (9.53) we have $\kappa_{\max} = 41$*. Then for* $K_0 = 82$ *the outage probability* $P_{out} \approx 0.01$*. The blocking probability for* $\lambda/\mu = 10^2$ *is equal to* 0.01.

Imperfect power control causes additional degradation of the system capacity [47]. Newly arriving users that are not power-controlled also decrease the number of served users.

We have considered the Erlang capacity of the reverse channel of the DS CDMA system. In the forward link, the dynamic range of the required power level is much less than for the reverse link, because the interference from same-cell users is controlled by the base station. More forward link power must then be provided to users that receive the most interference from other base stations. A more detailed consideration of the forward link teletraffic is given in [47].

9.6 INTERFERENCE CANCELLATION IN THE REVERSE LINK OF THE DS CDMA SYSTEM

In Section 8.4, we used information theory to demonstrate that interference from same-cell users can be eliminated by a process of successive cancellation of interfering users to reach capacity of the multiple-access system. Our approach was based on a simple idea: If a decision has been made about an interfering user's message, then the corresponding interfering signal can be recreated at the base station receiver and subtracted from the received waveform. In this section, we analyze, in more detail, the successive cancellation process in the reverse link of the DS CDMA system with coherent reception of encoded BPSK signals.

The signal received by the base station is [compare with (3.64)]

$$\begin{aligned} r(t) &= \sum_{k=1}^{K} \sqrt{2P^{(k)}} \sum_{n=-\infty}^{\infty} v_n^{(k)} a_n^{(k)} h_{T_c}(t - nT_c) \cos(2\pi f_c + \varphi^{(k)}) + \xi(t) \\ &= \sqrt{2} s_I(t) \cos(2\pi f_c t) - \sqrt{2} s_Q(t) \sin(2\pi f_c t) + \xi(t) \end{aligned} \tag{9.55}$$

where

$$s_I(t) = \sum_{k=1}^{K} \sqrt{P^{(k)}} \cos \varphi^{(k)} \sum_{n=-\infty}^{\infty} v_n^{(k)} a_n^{(k)} h_{T_c}(t - nT_c)$$

and

$$s_Q(t) = \sum_{k=1}^{K} \sqrt{P^{(k)}} \sin \varphi^{(k)} \sum_{n=-\infty}^{\infty} v_n^{(k)} a_n^{(k)} h_{T_c}(t - nT_c)$$

are the in-phase and quadrature lowpass components and $\xi(t)$ is the total noise including the other-cell interference and the background AWGN. The two-sided power spectral density of the total noise is $I_0/2$. The users are ordered according to increasing power on the input of the base station receiver, and the phases $\varphi^{(k)}$ of the signals are known. We assume also that signal-to-noise ratio on the input of the kth user receiver on the base station is small, such that binary transmission gives same effect as transmission by Gaussian-like signaling.

The receiver first demodulates the signal from the strongest, Kth, user. It makes a decision about the sequence sent by this user and subtracts from the total received lowpass signal the lowpass components corresponding to the Kth user.

Then it demodulates the signal from the $(K-1)$th user, makes a decision about the transmitted sequence, subtracts the corresponding lowpass terms, and so on.

We can view this process as transmission over K parallel channels, such that the demodulation of the signal in the kth channel is performed after demodulation of the signal in the $(k+1)$th channel. The Shannon capacity of the kth channel is

$$C^{(k)} \approx \frac{P^{(k)}}{\left(2T_c \sum_{i=0}^{k-1} P^{(i)} + I_0\right) \ln 2} \approx \frac{1}{2T_c} \log_2 \left(1 + \frac{P^{(k)}}{\sum_{i=1}^{k-1} P^{(i)} + I_0/2T_c}\right), \quad k = K, K-1, \ldots, 1 \tag{9.56}$$

EXAMPLE 9.7 (Viterbi [51])

Consider the reception strategy with successive cancellation of interfering users described above. Let the transmission rate $R^{(k)}$ in the kth channel be equal to the Shannon capacity of the channel $C^{(k)}$ given by (9.56) and all transmission rates $R^{(k)}$, $k = 1, 2, \ldots, K$, are equal, that is, $C^{(k)} = R^{(k)} = R$. Find the total power of the signal on the input of the base station receiver.

Solution

From Formula (9.56) we have

$$P^{(1)} = \left(2^{2RT_c} - 1\right) \frac{I_0}{2T_c} \tag{9.57}$$

$$P^{(k)} = \left(2^{2RT_c} - 1\right) \left(\sum_{k'=1}^{k-1} P^{(k')} + \frac{I_0}{2T_c}\right), \qquad k = 2, 3, \ldots, K \tag{9.58}$$

Then from (9.58) we get

$$P^{(k)} - P^{(k-1)} = \left(2^{2RT_c} - 1\right) P^{(k-1)}$$

or

$$P^{(k)} = 2^{2RT_c} P^{(k-1)} = 2^{2RT_c(k-1)} \left(2^{2RT_c} - 1\right) \frac{I_0}{2T_c}, \qquad k = 1, 2, \ldots, K \tag{9.59}$$

The total power on the input of the base station receiver is

$$\begin{aligned} P_{\text{total}} &= \sum_{k=1}^{K} P^{(k)} = \left(2^{2RT_cK} - 1\right) \frac{I_0}{2T_c} \\ &= \left(2^{2R_{\text{total}}T_c} - 1\right) \frac{I_0}{2T_c} \end{aligned} \tag{9.60}$$

where $R_{\text{total}} = KR$ is the total transmission rate of the system.

From (9.60) it follows that the total transmission rate in the reverse link of the DS CDMA system can reach the conventional Shannon capacity (8.12) of the Gaussian channel,

$$C_{\text{total}} = \frac{1}{2T_c} \log_2 \left(1 + \frac{2P_{\text{total}}T_c}{I_0}\right) \tag{9.61}$$

This gives us an expression for the maximal radio channel capacity for the reverse link of the DS CDMA system using interference cancellation. Let us assume that the maximal achievable total transmission rate of the system $R_{\text{total}} = KR$ equals the total capacity of the channel C_{total}. If we can neglect the background AWGN in comparison with the other-cell interference, that is,

$$\frac{I_0}{2T_c} \approx P_{\text{oc}} = f P_{\text{total}}$$

where f is the other-cell relative interference factor, we get from (9.61) the following formula for maximal radio channel capacity of the system not using voice activity monitoring and antenna sectoring:

$$K_0 \approx \frac{W/R}{2} \log_2 \left(1 + \frac{1}{f}\right) \tag{9.62}$$

At first sight, this is a paradoxical result, because the radio channel capacity of the system with interference cancellation can be less than the capacity of the corresponding conventional DS CDMA system, not using interference cancellation. In fact, the maximum radio channel capacity of the latter system for $\gamma_v = 1$, $\gamma_a = 1$ equals [see (8.32)]

$$K_0 \approx 1 + 1.45 \frac{W/R}{1 + f} \tag{9.63}$$

Then, if $f = 0.6$, the radio channel capacities of the system using interference cancellation have an order $0.7\ W/R$ and the conventional system has capacity of an order $0.9\ W/R$.

But in the comparison of the capacities of two DS CDMA systems we must take into account that a system with interference cancellation has essentially lower other-cell relative interference factor than the analogous system not using interference cancellation. In the latter system, the power of the signal radiated by a mobile is proportional to the path loss, that is, it is *increasing* proportionally to d^m, where d is the distance of the mobile from the base station.

In the advanced system with interference cancellation, it is natural to order the users according to decreasing distance from the base station. The power received by the base station from a user increases exponentially with number of the user [see Formula (9.59)], that is, decreases with a user's distance from the base station. The power radiated by a user is proportional to a product of exponentially

decreasing functions of the user's number and the power function d^m of the user's distance d from the base station. Because an exponential function is preponderant over a power function, the power radiated by a user is *decreasing* with its distance from the base station. Then the total power radiated by all mobiles in a cell is much less for the conventional system, and the other-cell relative interference factor is lower. To illustrate this we consider the following example:

EXAMPLE 9.8

Estimate the reverse link other-cell relative interference factor, conditioned that all mobile users radiate signals of equal power P and the users are distributed uniformly over the cells. Assume that the propagation loss is modeled as the mth, $m > 2$, power of the distance and that the minimal distance of a mobile from its base station d_0 is small in comparison with cell radius d_1, that is, $d_0 \ll d_1$.

Solution

We approximate the cell as a circle of radius $d_1 = 1$. The average power of the signals received by the base station from all users of the cell (total power) is

$$P_{\text{total}} \approx \frac{KP}{\pi d_1^2} \int_{d_0}^{d_1} 2\pi x \cdot x^{-m} \mathrm{d}x = -\frac{2KP}{m-2}\, x^{-m+2}\Big|_{d_0}^{d_1=1} \approx \frac{2KP}{m-2}\, d_0^{-m+2} \tag{9.64}$$

Analogously, the overall power of the signals received from the other-cell users is

$$P_{\text{oc}} = \lim_{d\to\infty} \frac{KP}{\pi d_1^2} \int_{d_1}^{d} x^{-m} 2\pi x \mathrm{d}x = KP \lim_{d\to\infty} \left[\frac{-2}{(m-2)}\, x^{-m+2}\Big|_1^d \right] = \frac{2KP}{(m-2)} \tag{9.65}$$

From Formulas (9.64) and (9.65) it follows that the reverse link other-cell interference factor is given by the formula

$$f = \frac{P_{\text{oc}}}{P_{\text{total}}} \approx d_0^{m-2} \ll 1 \tag{9.66}$$

Thus the radio channel capacity of the reverse link of a DS CDMA system with interference cancellation is significantly larger than the radio channel capacity of the system that is not using interference cancellation.

The remarkable result of this section is that the Shannon limit can be achieved in a practical reverse multiple-access system at the cost of transmission delay and higher complexity of the receiver equipment in the base station. A distinguishing feature of the reverse link DS CDMA system with successive cancellation is that the complexity is added only in the base station whereas the battery powered mobile transmitters remain unchanged.

In principle, successive cancellation can be done also in the forward link of a DS CDMA system (see Section 8.5). But in this case the mobile receivers will be of high complexity whereas the base station transmitter structure is not

changed. Because the number of mobile terminals is much higher than the number of base stations, the successive cancellation in the forward link is unpractical. In Section 9.7 we consider a method for increasing the forward link capacity, termed *coordinated transmission*, where the complexity is again concentrated in the base station equipment.

9.7 USER COORDINATION IN THE FORWARD LINK OF THE DS CDMA SYSTEM

The forward link implementation and performance are vastly different from those of the reverse link. This is due primarily to the following factors: access is one-to-many instead of many-to-one; synchronization of signals facilitated by use of pilot signals; knowledge by the transmitter of signals is sent to mobiles. The last factor permits the reduction of mutual interference between signals. In this section, we analyze a special strategy of the transmission, which we call a *coordination strategy*. Using this strategy the downlink capacity of the DS CDMA system significantly increases.

Consider first conventional uncoordinated transmission (see Sections 2.3 and 3.4). For simplicity we confine ourselves to the case when the base station does not use voice activity monitoring or a sectorized antenna. The downlink transmitted BPSK signal (without pilot) is $\sqrt{P}s(t)$ [compare with Formulas (2.101) and (3.89)], where the constant P has the dimension of power; $s(t)$ is

$$s(t) = \sqrt{2}\sum_{k=1}^{K}\gamma^{(k)}\sum_{n=-\infty}^{\infty}v_n^{(k)}a_n^{(k)}h_{T_c}(t-nT_c)\cos(2\pi f_c t+\phi^{(k)}) \tag{9.67}$$

Here $\gamma^{(k)}$, $k=1,2,\dots,K$, are weight coefficients determined by the power control mechanism: $h_{T_c}(\cdot)$ is a unit amplitude rectangular pulse. Because the phases $\phi^{(k)}$, $k=1,2,\dots,K$, are, generally speaking, different, the signal (9.67) corresponds to asynchronous transmission. In principle, it is possible to use synchronous transmission, that is, $\phi^{(k)}=\phi$, $k=1,2,\dots,K$, but in this case the radio channel capacity will be about two times less than in the asynchronous case (Problem 3.4).

The signal (9.67) can be represented as

$$\begin{aligned} s(t) = \sqrt{2}\sum_{n=-\infty}^{\infty}&[s_{\mathrm{I}n}h_{T_c}(t-nT_c)\cos(2\pi f_c t)\\ &-s_{\mathrm{Q}n}h_{T_c}(t-nT_c)\sin(2\pi f_c t)] \end{aligned} \tag{9.68}$$

where

$$s_{\mathrm{I}n}=\sum_{k=1}^{K}\gamma^{(k)}v_n^{(k)}a_n^{(k)}\cos\phi^{(k)} \tag{9.69}$$

and

$$s_{Qn} = \sum_{k=1}^{K} \gamma^{(k)} v_n^{(k)} a_n^{(k)} \sin \phi^{(k)} \tag{9.70}$$

are the in-phase and quadrature components. We assume that $\phi^{(k)}$ are IID random variables uniformly distributed on $[0, 2\pi)$. Then the expected values and variances of the in-phase and the quadrature components are

$$E(s_{In}) = E(s_{Qn}) = 0 \tag{9.71}$$

$$\text{var}(s_{In}) = \text{var}(s_{Qn}) = \psi/2 \tag{9.72}$$

Here $P\psi = P\sum_{k=1}^{K}(\gamma^{(k)})^2$ defines the average transmitted power not including the pilot signal power.

Each of the K active users employs a binary length N block code with $M^{(k)} = 2^{r^{(k)}N}$, $k = 1, 2, \ldots, K$, and equally likely codewords $\boldsymbol{v}_i^{(k)} = (v_{i0}^{(k)}, v_{i1}^{(k)}, \ldots, v_{i,N-1}^{(k)})$, $v_{in}^{(k)} \in \{1, -1\}$, $i = 0, 1, \ldots, 2^{r^{(k)}N} - 1$. We assume that $\{v_{in}^{(k)}\}$ is a set of IID equiprobable random variables,

$$P\left(v_{in}^{(k)} = 1\right) = P\left(v_{in}^{(k)} = -1\right) = 1/2, \text{ all } k, i \text{ and } n \tag{9.73}$$

and that users transmit with the same code rate, that is, $r^{(k)} = r$, $M^{(k)} = M$. Without loss of generality we assume also that 0th codewords are sent by all users, that is, $v_n^{(k)} = v_{0n}^{(k)}$, $n = 0, 1, \ldots, N-1$.

The signal received by the reference kth user is

$$r^{(k)}(t) = \sqrt{P/\kappa^{(k)}}\, s(t - \delta^{(k)}) + \xi^{(k)}(t) \tag{9.74}$$

where $\kappa^{(k)}$ is the path loss from base station to the kth mobile terminal. The process $\xi^{(k)}(t)$ including the other-cell interference and the background noise can be considered as AWGN with two-sided power spectral density $I_0/2$. We assume that noise power is equal for all users and that a propagation delay $\delta^{(k)}$ and a phase $\varphi^{(k)}$ of the received signal from the reference user are known. Then without loss of generality we may assume that $\delta^{(k)} = 0$ and $\varphi^{(k)} = 0$. For mathematical convenience we, as earlier (see Section 3.4), multiply $r^{(k)}(t)$ by $\sqrt{\kappa^{(k)}}$ and operate with $\overline{r}^{(k)}(t) = \sqrt{\kappa^{(k)}} r^{(k)}(t) = \sqrt{P} s(t) + \tilde{\xi}^{(k)}(t)$, where $\tilde{\xi}^{(k)}(t)$ is AWGN of two-sided power spectral density $\kappa^{(k)} I_0/2$, as with received signal. The decoder makes a decision based on the outputs of the matched filters

$$\begin{aligned} \hat{z}_n^{(k)} &= \sqrt{P} s_{In} + \hat{\xi}_n^{(k)} \\ \check{z}_n^{(k)} &= \sqrt{P} s_{Qn} + \check{\xi}_n^{(k)} \end{aligned} \qquad n = 0, 1, \ldots, N-1 \tag{9.75}$$

where $\{\hat{\xi}_n^{(k)}\}$ and $\{\check{\xi}_n^{(k)}\}$ are modeled as sets of IID zero-mean Gaussian random variables with variance $\kappa^{(k)} I_0/2T_c$. The decoder calculates $2^{r^{(k)}N}$ metrics corresponding to all potential codewords of the kth user

$$y_i^{(k)} = \sum_{n=0}^{N-1} (\hat{z}_n^{(k)} v_{in}^{(k)} a_n^{(k)} \cos\phi^{(k)} + \check{z}_n^{(k)} v_{in}^{(k)} a_n^{(k)} \sin\phi^{(k)}), \quad i = 0, 1, \ldots, 2^{r^{(k)}N} - 1 \tag{9.76}$$

and makes a decision in favor of the codeword having maximal metric. We can represent $y_i^{(k)}$ as a sum of three terms

$$\begin{aligned} y_i^{(k)} &= \sqrt{P}\ \gamma^{(k)} \sum_{n=0}^{N-1} v_{0n}^{(k)} v_{in}^{(k)} \\ &\quad + \sqrt{P} \sum_{k' \neq k}^{K} \gamma^{(k')} \sum_{n=0}^{N-1} v_{0n}^{(k')} a_n^{(k')} v_{in}^{(k)} a_n^{(k)} \cos(\phi^{(k')} - \phi^{(k)}) + \xi_i^{(k)} \end{aligned} \tag{9.77}$$

The first term, the desired component, is the cross-correlation between transmitted zeroth codeword of the kth user and the ith codeword. The second term is the other-user interference component. The third term is due to the other-cell interference and the background AWGN. In the ensemble of random codes, AWGN and other-cell interference, we have

$$E(y_i^{(k)}) = \begin{cases} N\sqrt{P}\ \gamma^{(k)} \stackrel{\text{def}}{=} N\mu_0, & \text{if } i = 0, \\ 0, & \text{otherwise} \end{cases} \tag{9.78}$$

and

$$\operatorname{var}(y_i^{(k)}) = \begin{cases} \dfrac{PN}{2} \displaystyle\sum_{k' \neq k} (\gamma^{(k')})^2 + \dfrac{\kappa^{(k)} I_0}{2T_c}\ N \stackrel{\text{def}}{=} N\sigma_0^2, & \text{if } i = 0, \\ \dfrac{PN}{2} \displaystyle\sum_{k'=1}^{K} (\gamma^{(k')})^2 + \dfrac{\kappa^{(k)} I_0}{2T_c}\ N \stackrel{\text{def}}{=} N\sigma_1^2, & \text{otherwise} \end{cases} \tag{9.79}$$

We express σ_0^2 and σ_1^2 as

$$\sigma_0^2 = \frac{P}{2}\ [\psi - (\gamma^{(k)})^2] + \frac{\kappa^{(k)} I_0}{2T_c} \tag{9.80}$$

$$\sigma_1^2 = \frac{P}{2}\ \psi + \frac{\kappa^{(k)} I_0}{2T_c} \tag{9.81}$$

where ψ is the average transmitted power. Particularly, if $K \gg 1$, then $\sigma_0^2 \approx \sigma_1^2$.

For $N \gg 1$, we may use the Gaussian approximation for the distribution of the statistics

$$x_i^{(k)} = y_i^{(k)} - y_0^{(k)}, \qquad i = 1, 2, \ldots, M-1 \tag{9.82}$$

where $M = 2^{rN}$. Because the code is random, the statistics $x_i^{(k)}$ are independent. A decoding error occurs if at least one of the statistics $x_i^{(k)}$ is nonnegative. Using Formulas (9.78)–(9.81) we have for the mean and variance of the statistic $x_i^{(k)}$ the following expressions

$$E(x_i^{(k)}) = -N\mu_0 = -N\sqrt{P}\,\gamma^{(k)} \tag{9.83}$$

$$\begin{aligned} \operatorname{var}(x_i^{(k)}) &= \operatorname{var}(y_i^{(k)}) + \operatorname{var}(y_0^{(k)}) = N(\sigma_0^2 + \sigma_1^2) \\ &\approx NP\psi + \frac{N\kappa^{(k)} I_0}{T_c} \end{aligned} \tag{9.84}$$

The kth user's decoding error probability $P^{(k)}(\mathcal{E})$ of the uncoordinated system is upperbounded by the union bound

$$\begin{aligned} P^{(k)}(\mathcal{E}) &\le (M-1) P(y_1^{(k)} \ge 0) \\ &= (M-1) Q\left(\sqrt{\frac{2N(\gamma^{(k)})^2}{2\psi + 2\kappa^{(k)} I_0 / PT_c}} \right) \\ &< 2^{rN} \exp\left(-\frac{N(\gamma^{(k)})^2}{2\psi + 2\kappa^{(k)} I_0 / PT_c} \right) \end{aligned} \tag{9.85}$$

To minimize $\max_k P^{(k)}(\mathcal{E})$ we have to choose the weight coefficients $\gamma^{(k)}$ such that the signal-to-noise ratios for all users are equal; that is,

$$\frac{(\gamma^{(k)})^2}{2\psi + 2\kappa^{(k)} I_0 / PT_c} = r_0 \ln 2, \quad k = 1, 2, \ldots, K \tag{9.86}$$

where r_0 is a constant. From (9.86) follows

$$(\gamma^{(k)})^2 = 2r_0 \ln 2 \left[\psi + \frac{\kappa^{(k)} I_0}{PT_c} \right] \tag{9.87}$$

Summation of (9.87) over $k = 1, 2, \ldots, K$ gives

$$\psi = 2r_0 K \psi \ln 2 + \frac{2r_0 \overline{\kappa} K I_0 \ln 2}{PT_c} \tag{9.88}$$

where

$$\overline{\kappa} = \frac{1}{K}\sum_{k=1}^{K} \kappa^{(k)} \tag{9.89}$$

is the average path loss in the cell [see Formula (3.99)]. From (9.88) we get

$$r_0 = \frac{1}{2K(1+\overline{\kappa} I_0/\psi P T_c)\ln 2} \tag{9.90}$$

Then (9.85) can be rewritten as

$$P^{(k)}(\mathcal{E}) \stackrel{\text{def}}{=} P(\mathcal{E}) \le \exp[-(r_0 - r)N] \tag{9.91}$$

and r_0 can be treated as the cut-off rate for uncoordinated transmission (in b/channel use).

At low SNR a tighter bound than (9.86) can be obtained by the *few-many approach* described in [24], (see also [58]). We have

$$P^{(k)}(\mathcal{E}) < 2\exp\left[-\ln 2\left(\frac{\gamma^{(k)}}{\sqrt{(\psi - \kappa^{(k)} I_0/PT_c)\ln 2}} - \sqrt{r}\right)^2 N\right] \tag{9.92}$$

when

$$\frac{(\gamma^{(k)})^2}{(4\psi + 4\kappa^{(k)} I_0/PT_c)\ln 2} \le r \le \frac{(\gamma^{(k)})^2}{(\psi + \kappa^{(k)} I_0/PT_c)\ln 2} \tag{9.93}$$

If we chose the weight coefficients $\gamma^{(k)}$, $k = 1, 2, \ldots, K$, analogously to (9.86), then we get

$$P^{(k)}(\mathcal{E}) \stackrel{\text{def}}{=} P(\mathcal{E}) < 2\exp[-\ln 2(\sqrt{c} - \sqrt{r})^2 N] \tag{9.94}$$

where

$$\frac{1}{4K(1+\overline{\kappa} I_0/\psi P T_c)\ln 2} \stackrel{\text{def}}{=} r_{cr} \le r \le c \stackrel{\text{def}}{=} \frac{1}{K(1+\overline{\kappa} I_0/\psi P T_c)\ln 2} \tag{9.95}$$

Because r_{cr} is the point where the union bound passes into the bound (9.94), we treat r_{cr} as the critical rate of an uncoordinated system (in b/channel use). Although we did not prove that the system can not reach code rates larger than c, we will treat c as the "capacity" of an uncoordinated system (in b/channel use).

Now consider coordinated transmission. Just as for uncoordinated transmission, coordinated transmission is based on a rate $r^{(k)} = r$ random block code. The signal is transmitted over an AWGN channel, and the receiver in the coordinated system is identical to the receiver in the uncoordinated system.

For the coordinated transmission strategy, the in-phase and quadrature components s_{In} and s_{Qn} of the transmitted signal are not chosen as a sum of the individual signals (9.69) and (9.70) but are chosen such that

$$\frac{1}{N}\sum_{n=0}^{N-1}(s_{In}v_{0n}^{(k)}a_n^{(k)}\cos\varphi^{(k)} - s_{Qn}v_{0n}^{(k)}a_n^{(k)}\sin\varphi^{(k)}) = \gamma^{(k)},\ \ k = 1, 2, \ldots, K \tag{9.96}$$

where $\gamma^{(k)}$ are determined by the power control mechanism. We will show that this approach decreases the variance of the decision statistics corresponding to the transmitted codeword, $y_0^{(k)}$, which will result in an increased radio channel capacity. We must find s_{In} and s_{Qn} from (9.96). Depending on the length of the codewords and the number of active users, K, there might be infinitely many solutions to (9.96). Because all of these solutions can be expected to provide similar performance in the receiver, the coordinator chooses the signal components that minimize the average power of the transmitted signal, $P\sum_{n=0}^{N-1}(s_{In}^2 + s_{Qn}^2)/N$. We will analyze this signal by the use of Lagrange multipliers. Let us introduce the function

$$\begin{aligned} F&\left(s_{I0}, s_{I1}, \ldots, s_{I,N-1}, s_{Q0}, s_{Q1}, \ldots, s_{Q,N-1}, \lambda^{(1)}, \lambda^{(2)}, \ldots, \lambda^{(K)}\right) \\ &= \sum_{n=0}^{N-1}(s_{In}^2 + s_{Qn}^2) \\ &\quad + \sum_{k=1}^{K}\lambda^{(k)}\left[\sum_{n=0}^{N-1}\left(s_{In}v_{0n}^{(k)}a_n^{(k)}\cos\phi^{(k)} - s_{Qn}v_{0n}^{(k)}a_n^{(k)}\sin\phi^{(k)}\right) - N\gamma^{(k)}\right] \end{aligned} \tag{9.97}$$

The minimum power can be obtained by minimizing (9.97). The condition for the minima are obtained by differentiation of (9.97) with respect to s_{In} and s_{Qn}:

$$\frac{\partial F}{\partial s_{In}} = s_{In} + \sum_{k=1}^{K}\lambda^{(k)}v_{0n}^{(k)}a_n^{(k)}\cos\phi^{(k)} = 0 \tag{9.98}$$

$$\frac{\partial F}{\partial s_{Qn}} = s_{Qn} - \sum_{k=1}^{K}\lambda^{(k)}v_{0n}^{(k)}a_n^{(k)}\sin\phi^{(k)} = 0, \quad n = 0, 1, \ldots, N-1 \tag{9.99}$$

From (9.98) and (9.99) it follows that the transmitted components can be described as

$$s_{In} = -\frac{1}{2}\sum_{k=1}^{K}\lambda^{(k)}v_{0n}^{(k)}a_n^{(k)}\cos\phi^{(k)} \tag{9.100}$$

$$s_{\mathrm{Q}n} = \frac{1}{2}\sum_{k=1}^{K} \lambda^{(k)} v_{0n}^{(k)} a_n^{(k)} \sin\phi^{(k)} \tag{9.101}$$

We multiply the nth equations in (9.98) and (9.99) by $s_{\mathrm{I}n}$ and $s_{\mathrm{Q}n}$, respectively, and summarize the N respective equations. Then we obtain

$$2\sum_{n=0}^{N-1} s_{\mathrm{I}n}^2 + \sum_{k=1}^{K} \lambda^{(k)} \sum_{n=0}^{N-1} s_{\mathrm{I}n} v_{0n}^{(k)} a_n^{(k)} \cos\phi^{(k)} = 0 \tag{9.102}$$

$$2\sum_{n=0}^{N-1} s_{\mathrm{Q}n}^2 - \sum_{k=1}^{K} \lambda^{(k)} \sum_{n=0}^{N-1} s_{\mathrm{Q}n} v_{0n}^{(k)} a_n^{(k)} \sin\phi^{(k)} = 0 \tag{9.103}$$

From (9.96), (9.102), and (9.103) it follows that the average power of the transmitted signal is proportional to

$$\sum_{n=0}^{N-1} (s_{\mathrm{I}n}^2 + s_{\mathrm{Q}n}^2) = -\frac{1}{2}\sum_{k=1}^{K} \lambda^{(k)} \gamma^{(k)} \tag{9.104}$$

By multiplying the nth equations in (9.98) and (9.99) by $v_{0n}^{(k')} a_n^{(k')} \cos\phi^{(k')}$ and $-v_{0n}^{(k')} a_n^{(k')} \sin\phi^{(k')}$, respectively, for $k' = 1, 2, \ldots, K$, and summarizing the results over n we obtain

$$2\sum_{n=0}^{N-1} s_{\mathrm{I}n} v_{0n}^{(k')} a_n^{(k')} \cos\phi^{(k')} + \sum_{k=1}^{K} \lambda^{(k)} \sum_{n=0}^{N-1} v_{0n}^{(k)} a_n^{(k)} v_{0n}^{(k')} a_n^{(k')} \cos\phi^{(k)} \cos\phi^{(k')} = 0 \tag{9.105}$$

$$-2\sum_{n=0}^{N-1} s_{\mathrm{Q}n} v_{0n}^{(k')} a_n^{(k')} \sin\phi^{(k')} + \sum_{k=0}^{K} \lambda^{(k)} \sum_{n=0}^{N-1} v_{0n}^{(k)} a_n^{(k)} v_{0n}^{(k')} a_n^{(k')} \sin\phi^{(k)} \sin\phi^{(k')} = 0 \tag{9.106}$$

By adding (9.105) and (9.106) it follows from Formula (9.96) that

$$-2\gamma^{(k')} = \sum_{k=1}^{k} \lambda^{(k)} \Xi^{(k,k')}, \quad k' = 1, 2, \ldots, K \tag{9.107}$$

where $\Xi^{(k,k')}$ is the cross-correlation coefficient:

$$\Xi^{(k,k')} \stackrel{\mathrm{def}}{=} \frac{1}{N} \cos(\phi^{(k')} - \phi^{(k)}) \sum_{n=0}^{N-1} v_{0n}^{(k)} a_n^{(k)} v_{0n}^{(k')} a_n^{(k')}, \quad k, k' = 1, 2, \ldots, K \tag{9.108}$$

The K equations in (9.107) can be expressed as the linear system of equations

$$\Xi\boldsymbol{\lambda} = -2\boldsymbol{\gamma} \tag{9.109}$$

where Ξ is the $(K \times K)$ cross-correlation matrix with the elements defined by (9.108), $\boldsymbol{\lambda}$ is a K-dimensional column vector containing $\lambda^{(k)}$ in its kth position, and $\boldsymbol{\gamma}$ is a K-dimensional column vector containing $\gamma^{(k)}$ in its kth position. It can be used to find the $\lambda^{(k)}$ that minimizes the transmitted energy. Analysis of the system gives for all $k = 1, 2, \ldots, K$, [58],

$$E[\lambda^{(k)}] = -2\gamma^{(k)} + \overline{\gamma}\ \frac{K-1}{N} + o\left(\frac{1}{N}\right) \tag{9.110}$$

$$\text{var}[\lambda^{(k)}] = 2(\gamma^{(k)})^2\ \frac{K-1}{N} + o\left(\frac{1}{N}\right) \tag{9.111}$$

where $\overline{\gamma} = \sum_{k=1}^{K} \gamma^{(k)}/K$. The expectation and variance of the transmitted power are $P\psi - P(\overline{\gamma})^2\ K(K-1)/2N + o\,(1/N)$ and $P^2\ (K-1)/2N\quad \psi + o\,(1/N)$, respectively.

For large N the average total transmitted power for the coordinated transmission is asymptotically equal to $P\psi$, that is, the same as for noncoordinated transmission. The coordinated transmitted signal is $\sqrt{P}s(t)$, where $s(t)$ is given by the same expression (9.68) as for noncoordinated transmission. But in contrast to the noncoordinated case the in-phase and quadrature components are defined not by Formulas (9.69) and (9.70) but by (9.100) and (9.101).

The correlation receiver performs the same operations as for the uncoordinated transmission. The outputs of matched filter are given by (9.75). The metrics corresponding to each of the codewords are given by (9.76). The mean value of the metric is defined by the same expression (9.78) as for the uncoordinated case, but the expression for the variance of the metric is different from (9.79)–(9.81), namely,

$$\text{var}(y_i^{(k)}) \approx \begin{cases} \dfrac{\kappa^{(k)} I_0}{2T_c}\ N, & \text{if } i = 0 \\ \dfrac{PN}{2}\ \psi + \dfrac{\kappa^{(k)} I_0}{2T_c}\ N, & \text{otherwise} \end{cases} \tag{9.112}$$

Comparison between Formulas (9.112) and (9.79) shows that the other-user interference term in the variance of the metric corresponding to the transmitted codeword in the coordinated case asymptotically vanishes when $N \to \infty$. The statistics $x_i^{(k)}$, defined by (9.82), have the following first two moments [compare

with (9.83) and (9.84)] if we neglect high-order terms:

$$E(x_i^{(k)}) = -N\sqrt{P}\ \gamma^{(k)} \tag{9.113}$$

$$\operatorname{var}(x_i^{(k)}) = \frac{NP}{2}\ \psi + \frac{N\kappa^{(k)} I_0}{T_c}, \quad k = 1, 2, \ldots, M-1 \tag{9.114}$$

The other-user interference term is asymptotically two times less than in the uncoordinated case.

From (9.78), (9.112), and (9.113) we get the following upper bound: for the decoding error probability for the kth user [58] in coordinated transmission case

$$P^{(k)}(\mathcal{E}) < 2\exp[-e^{(k)}(r)N] \tag{9.115}$$

The reliability function $e^{(k)}(r)$ has the following expressions in the "union bound region" and in the "few-many region":

$$e^{(k)}(r) = \begin{cases} \left[\dfrac{(\gamma^{(k)})^2}{(\psi + 2\kappa^{(k)} I_0/PT_c)\ln 2} - r\right]\ln 2, \\ \qquad \text{if } 0 \le r \le \dfrac{(\gamma^{(k)})^2(\psi + \kappa^{(k)} I_0/PT_c)}{(\psi + 2\kappa^{(k)} I_0/PT_c)^2 \ln 2}, \\ \left(1 + \dfrac{P\psi T_c}{\kappa^{(k)} I_0}\right)\left[\sqrt{\dfrac{(\gamma^{(k)})^2}{(\psi + \kappa^{(k)} I_0/PT_c)}} - \sqrt{r}\right]^2, \\ \qquad \text{if } \dfrac{(\gamma^{(k)})^2(\psi + \kappa^{(k)} I_0/PT_c)}{(\psi + 2\kappa^{(k)} I_0/PT_c)^2 \ln 2} \le r \le \dfrac{(\gamma^{(k)})^2}{(\psi + \kappa^{(k)} I_0/PT_c)\ln 2} \end{cases} \tag{9.116}$$

To minimize $\max_k P^{(k)}(\mathcal{E})$ we have to chose the weight coefficients $\gamma^{(k)}$ such that the reliability functions $e^{(k)}(r)$ are equal for all users, that is, $e^{(k)}(r) = e(r)$. Then, analogously to (9.86)–(9.91), we use the union bound on the reliability function and get $e(r) = (r_0 - r)\ln 2$, where the cut-off rate (in b/channel use) is

$$r_0 = \frac{1}{K(1 + 2\overline{\kappa} I_0/\psi PT_c)\ln 2} \tag{9.117}$$

This is significantly larger than cut-off rate (9.90) in the uncoordinated case.

Optimization of the reliability function (9.116) of the coordinated system in the "few-many region" and maximization of the "critical rate" is much more complicated. We have to choose a set of $\gamma^{(k)}$ such that the reliability function (correspondingly the "critical rate") will be the same for all users. The problem

will be reduced to solving systems of K quadratic equations with respect to $\lambda^{(k)}$ and the final expressions for the reliability function (correspondingly the "critical rate") will be complicated. But the "capacity" of the coordinated system is not difficult to get, using the same method as above. It will coincide with the capacity of the uncoordinated system, given by Formula (9.95).

Consider now a general characteristic of a DS CDMA system, the overall code rate r_{overall}. It equals the sum of the code rates of the active users, in this case, Kr (in b/channel use). From (9.90) follows the formula for overall cut-off rate of the downlink *uncoordinated* system

$$r_{0,\text{overall}} = \frac{1}{2(1 + \overline{\kappa} I_0/\psi P T_c)\ln 2} \tag{9.118}$$

Because $\psi P T_c/\overline{\kappa} I_o r = \overline{E}_b/I_0$ is the average signal-to-noise ratio per bit, we get from (9.118)

$$r_{0,\text{overall}} = \frac{1}{2\ln 2} - \frac{1}{\overline{E}_b/I_0} \tag{9.119}$$

Analogously to (9.117), we get the following expression for cut-off rate of the downlink *coordinated* DS CDMA system:

$$r_{0,\text{overall}} = \frac{1}{(1 + 2\overline{\kappa} I_0/\psi P T_c)\ln 2} = \frac{1}{\ln 2} - \frac{2}{\overline{E}_b/I_0} \tag{9.120}$$

The maximum rate (capacity)[3] for both the uncoordinated and the coordinated downlink DS CDMA system is

$$c_{\text{overall}} = \frac{1}{(1 + \overline{\kappa} I_0/\psi P T_c)\ln 2} = \frac{1}{\ln 2} - \frac{1}{\overline{E}_b/I_0} \tag{9.121}$$

The overall cut-off rates for both the uncoordinated and the coordinated transmissions are presented as functions of ratio $\overline{E}_b/I_0 = P T_c/\overline{\kappa} I_0 r_{\text{overall}}$ in Figure 9.7. For comparison, a plot of the capacity is also given. Note that if $\psi P T_c/\overline{\kappa} I_0 r_{\text{overall}} \to \infty$, the cut-off rate of the coordinated system becomes equal to twice the cut-off rate of the uncoordinated system.

More detailed comparison of coordinated and uncoordinated transmission is given in [58]. Simulation shows that coordination significantly improves the performances of the system in comparison to the uncoordinated case. For the AWGN channel, $P_b = 10^{-3}$ and E_b/N_0 in the range 4–6 dB, the number of users can be increased by 50%. For the Rayleigh fading channel the increased capacity is even more significant.

[3]Strictly speaking, the classic definition of the capacity includes the requirement that reliable transmission is impossible for a transmission rate larger than capacity. Although we did not study this aspect of downlink transmission, we retain here the term "capacity" for the maximal guaranteed transmission rate in the system.

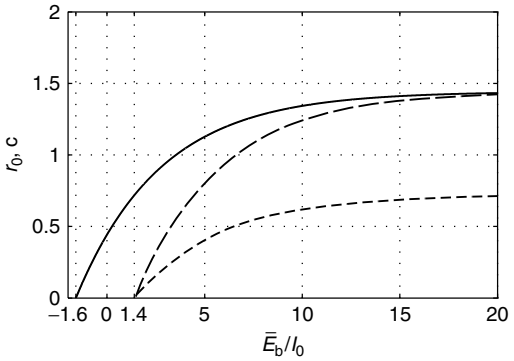

Figure 9.7. The overall computational cut-off rates, $r_{0,\text{overall}}$ (in b/channel use), for the uncoordinated system, lower dashed line, and for the coordinated system, upper dashed line. The overall effective capacities, c_{overall} (in b/channel use), are identical for the systems (solid line).

9.8 THIRD-GENERATION WIRELESS CELLULAR NETWORKS

Since the 1990s, the wireless cellular networks have seen explosive growth. The first digital cellular system based on CDMA was standardized as Interim Standard 95 (IS-95) by US Telecommunication Industry Association in 1993 [44]. This is a second generation (2G) cellular network system. Detailed analysis of the standard is given in [34, 39]. A short review of the standard is presented in Table 9.2 The wideband spread adoption of wireless communications was accelerated when the International Telecommunication Union (ITU) formulated a plan to implement a global frequency band in the 2 GHz range that would support the worldwide wireless communication standard called International Mobile Telecommunication 2000 (IMT-2000). It is leading to the development of new wireless systems and standards for many other types of communications besides mobile telephone service.

The next *3rd generation (3G) cellular networks* are being designed to provide high-speed data communication traffic in addition to conventional mobile telephone service. Similarly, wireless networks will be used as replacements for wires within buildings through the developing of *wireless local area networks* (WLAN). The introduction of the *Bluetooth* standard will provide cordless connections of personal computers with Internet.

In addition to mobile telephone service and data communication, 3G systems will provide multi-megabit Internet access communication using *Voice over Internet Protocol* (VoIP), ubiquitous "always-on" access, simultaneous voice, and data access with multiple parties at the same time, etc. ITU determined new spectrum bands to accommodate 3G networks. They are 806–960 MHz, 1710–1885 MHz, and 2500–2690 MHz.

Up to now, the ITU plan to introduce a single wireless communication standard has not materialized and the mobile radio user community is split between

Table 9.2 IS-95 System Parameters

Parameter	Downlink	Uplink
Frequency band	869–894 MHz	824–849 MHz
Carrier spacing	1.25 MHz	1.25 MHz
Chip rate	1.2288 Mchips/2	1.2288 Mchips/s
Speech coder	Qualcomm Code Excited Linear Predictive (QCELP)	QCELP
Data rates	9.6, 4.8, 2.4, 1.2 kb/s	9.6, 4.8, 2.4, 1.2 kb/s
Power control frequency	Slow power control	800 Hz
	Cell specific QPSK spreading, period $= 2^{15} - 1$	QPSK spreading, period $= 2^{15} - 1$
DS spreading	User specific orthogonal spreading, length 64 Hadamard sequences	
Scrambling for the purpose of privacy	Long PN sequence, period $= 2^{42} - 1$	Long PN sequence, period $= 2^{42} - 1$
FEC	Concatenated code. Outer code is rate 1/2 memory 8 convolutional code. Inner code is length 64 repetition code.	Concatenated code. Outer code is rate 1/3 memory 8 convolutional code. Inner code is rate 6/64 reduced Reed–Muller code.
Frame duration	20 ms	20 ms
Interleaving	Block interleaver, duration = 20 ms	Block interleaver, duration = 20 ms
Receiver structure	Coherent demodulation, three-branch Rake receiver	Noncoherent demodulation, four-branch Rake receiver.

WCDMA and CDMA2000. The WCDMA standard is based on the network fundamentals of GSM, and CDMA2000 is the eventual evolution for IS-95. The ITU IMT-2000 standard organizations are currently split into two parties: *3GPP (3G Partnership Project for Wideband CDMA)* and *3GPP2 (3G Partnership Project for CDMA2000)*.

The WCDMA standard had been designed for packet-based wireless service so that computers and telephones might share the same wireless network and be connected to the Internet. The basic radio frame length is 10 ms, allowing for low-delay speech traffic with rates up to 12.2 kb/s.

Good-quality Internet access requires several hundred kilobits per second rate. Video picture transfer services require bit rates from a few tens of kilobits per second to 2 Mb/s depending on the quality requirement. WCDMA will maintain packet data rates up to 2.049 Mb/s. Future versions of WCDMA will maintain user data rates up to 8 Mb/s.

WCDMA supports highly variable user data rates. Each user allocates 10-ms duration frames during which the data rate is not changed. But the data rate

can be changed from frame to frame. WCDMA employs two basic division principles, frequency division duplex (FDD) and time division duplex (TDD). In the first case two separate 5-MHz bands are used for uplink and downlink communications, whereas in TDD only one 5-MHz band is time-shared between uplink and downlink communications.

As we noted before, WCDMA employs coherent demodulation in the uplink and downlink directions based on pilot signaling, whereas IS-95 uses coherent demodulation only in the downlink.

In WCDMA two channel coding methods have been proposed. Analogously to IS-95, rate 1/2 and 1/3 memory 8 convolutional codes with Viterbi decoding are intended to be used for relatively low data rates. For high data rates, rate 1/3 and 1/2 turbo coding can be applied. To accommodate a higher data rate for better speech quality, WCDMA will employ an Adaptive Multi-Rate (AMR) speech coder. The multi-rate speech coder has 8 source rates: 12.2, 10.2, 7.95, 7.40 (or 6.70), 5.90, 5.15, and 4.75 kb/s.

WCDMA requires a spectrum allocation of 5 MHz with a basic chip rate of 4.096 Mb/s. Data rates range from 8 kb/s to 2 Mb/s. A single 5-MHz channel will be able to support between 100 and 350 simultaneous calls at once, depending on propagation conditions.

The transmitted data sequences in the uplink direction are spread by short or long spreading sequences [55]. The long sequences are 38,400 chips Gold sequences. The actual sequence period is very long with a 41-degree generator, but only 38,400 chips are used. The short sequence length is 256 chips. They belong to the large set of Kasami sequences. The downlink spreading uses the same Gold sequences as for the uplink. For user separation, variable-length orthogonal sequences are implemented.

The CDMA2000 standard uses three adjacent 1.25-MHz radio channels (see Section 4.8) that provide packet data transmission with rates up to 2 Mb/s. Based on the IS-95 standard originally developed by Qualcomm, it allows the introduction of high-data rate equipment compatible with existing IS-95 subscriber equipment. Thus, the current CDMA users may introduce 3G capabilities without changing an entire base station or reallocating spectrum.

Because CDMA2000 is based on IS-95, many blocks and parameters of these two systems coincide. Particularly, in both cases the long cell-specific spreading sequence has period $2^{42} - 1$ chips, which is significantly longer than in WCDMA, where the period is 38,400 chips. The short user-specific spreading sequences in the uplink have period of $2^{15} - 1$ chips, whereas the short spreading sequences of the WCDMA system have period of only 256 chips. Analogously to the IS-95 system, the users are assigned using Hadamard sequences for separation in the downlink. But in contrast to IS-95, the OVSF principle, analogous to implemented in WCDMA, was realized in CDMA2000. The spreading factors for data transmission range from 256 down to 4. The frame duration is 20 ms.

The variable rate speech coder, QCELP13, has been designed to operate with information data rates 14400, 7200, 3600, and 1800 b/s. In addition to using the

higher data rate, QCELP13 has several other improvements over the old QCELP model, including improved voice activity detection.

Analogously to the WCDMA system, the CDMA2000 system uses convolutional coding with Viterbi decoding and turbo coding, but the turbo interleaving and channel interleaving is different because of differences in the number of symbols per frame with different spreading factors. There are differences in coding rates: In addition to the 1/2 and 1/3 rates in WCDMA, 1/4 and 1/6 rate convolutional codes have been specified in the CDMA2000 standard. The convolutional code memory $m = 8$ is the same as in WCDMA and IS-95. In addition, turbo coding with rate 1/4, may be used in CDMA2000.

The basic power control principles are similar in CDMA2000 and WCDMA. Fast closed-loop power control is used in uplink and downlink in both systems. But the power control command rates are different: 1500 Hz in WCDMA and 800 Hz in CDMA2000. The open-loop power control mechanism observes received signal strength in the downlink and adjusts the transmission power.

Because WCDMA and CDMA2000 will require expensive new base station equipment, it may be another 5 to 10 years before installation of the new systems. One major problem is that the multiple 3G standards are incompatible. This makes it difficult to introduce worldwide wireless communication networks.

9.9 COMMENTS

A number of problems were studied in this chapter related to the design and analysis of code division multiple-access digital cellular networks. Among the topics that we have studied, the foremost are other-cell interference; power control for improving the efficiency of two-way communication; soft handoff, which makes it possible for the mobile user to receive and send simultaneously from and to two or more different base stations; Erlang capacity for the CDMA system; user coordination in the forward link, and interference cancellation in the reverse link.

A general principle of organization of wireless communication networks were reviewed by Rappaport [39]. He gave also a description of the Third Generation Wireless Cellular Networks standards. The reader can find more detailed analysis of 3G standards in [55]. In our treatment of wireless networks theory we follow Viterbi [47]. Analysis of the coordinated transmission is given in [58].

In addition to the CDMA digital network concepts covered here, the reader should be aware of the large body of literature that exists and discusses different technical problems of CDMA network implementations.

PROBLEMS

9.1. Suppose that radio propagation loss is given by Formula (9.1), where A is constant (shadowing is absent). $A = 10^{10}$, $m = 4$ and distance d is measured in kilometers. The data rate $R = 10$ kb/s, the receiver bandwidth is

equal to the data rate, and the two-sided power spectral density of the background noise $N_0/2 = 10^{-10}$ W/Hz. Determine the required transmitted power assuming that the receiver can operate at signal-to-noise ratio $E_b/N_0 = 10$ dB and that $d = 3$ km.

9.2. Under the conditions of Problem 9.1 find the required transmitted power if there is shadowing with standard deviation $\sigma = 8$ dB. Assume that the outage probability cannot exceed 0.1.

9.3. Five received power measurements were taken at distances 100 m, 200 m, 500 m, 1000 m, and 2000 m from a transmitter. The transmitted power is 1 W, the received power is 1 mW, 0.125 mW, 0.008 mW, 10^{-3} mW, and $0.25 \cdot 10^{-3}$ mW, respectively. Assuming that propagation loss model is given by Formula (9.1), where A is constant, find parameters of the model.

9.4. Consider the propagation loss model (9.1), where A is the log-normal random variable. Five received power measurements at the same distances as in Problem 9.3 are: 0.5 mW, 0.25 mW, 0.004 mW, $2 \cdot 10^{-3}$ mW, and $0.2 \cdot 10^{-3}$ mW. Estimate the parameters of the model.

9.5. The signal-to-noise ratio E_b/I_0 in a receiver depends on the distance to the base station and the environment, $E_b/I_0 \sim r^{-m}$, where r is the distance to the base station and typical values of m are between 3 and 6. How is the system capacity, in terms of number of users per cell, affected when the attenuation, m, increases?

9.6. Consider the forward transmission of the IS-95 system. Suppose that a cell has a 6-km radius. Assume that two-sided background noise power spectral density is equal to 10^{-10} W/Hz. The shadowing effect is absent and the radio propagation loss is assumed to be given by formula [compare with Formula (9.2)],

$$\log_{10} \kappa = 10m \log_{10} d + 10 \log_{10} A$$

where d is the distance in kilometers, $m = 3.5$, and $A = 10^{10}$. Assume that the bandwidth is equal to 1.25 MHz.

a) Determine the required transmit power assuming that the digital demodulator can operate at a bit-energy-to-noise-density level $E_b/I_0 = 6$ dB. Assume that the mobile receiver is the only user and that it is located on the cell boundary.

b) A second mobile user is added to the system that is also located on the cell boundary. What transmitter power is now required? Assume, as usually, that multiple-access interference may be treated as zero-mean Gaussian noise.

c) Repeat b) for the case of 30 users, all located on the cell boundary.

9.7. As a communication engineer, you are asked to design a system that will provide radio communication within a circular cell area. A cell is being designed that will have 5000-m radius. The radio propagation loss

is assumed to be given by

$$\text{path loss (dB)} = 40 \log_{10} R$$

where R is the distance in meters. The communication system being proposed requires a power level $P = 10^{-13} W$ into the receiver.

a) Determine the required transmitted power needed to achieve a received signal level at the mobile located at the cell boundary. Assume that the mobile receiver is the only receiver and neglect lognormal shadowing effect.

b) Assuming that the lognormal standard deviation of the shadowing factor ζ is 8 dB, find the probability that the received signal strength drops below power level $P/2$.

9.8. This problem deals with soft decision between three cells. Suppose that the user is equidistant from the three base stations. Assume that the shadowing losses in decibels are ζ_1, ζ_2, and ζ_3, respectively, where ζ_1, ζ_2, and ζ_3 are uncorrelated Gaussian random variables with zero mean and variances σ^2, $\sigma = 8$ dB. How much can the margin θ be reduced compared to hard handoff if the outage probability is $\pi_{\text{out}} = 0.1$?

9.9. Consider soft handoff that occurs exactly at the corner point, which is on the boundary of three cells. Let the decibel attenuations due to shadowing be Gaussian variables with zero mean and standard deviation $\sigma = 8$ dB. Let the correlation coefficient of losses to each pair of the three stations be ρ, equal to zero. Which margin θ must be added to the transmitted power to obtain $P_{\text{out}} = 0.05$? Which margin θ must be added if the correlation coefficient of losses to each pair of the stations ρ is equal to one? What happens if ρ is between 0 and 1? To which physical conditions correspond $\rho = 0$, $\rho = 1$?

9.10. Find the uplink channel capacity of the system of Example 3.6 for different models of path loss, that is, different m. Use Table 9.1. Estimate capacity assuming that other-cell interference factor is equal to its average value. How will capacity change if all users of the cell have interior location? Border location?

9.11. Consider a CDMA system employing hard handoff. Give an estimation on the distance d', that is, the distance a mobile terminal must move into a new cell before handoff is executed, for

a) An urban area

b) A rural area

The system requirements are: $P_{\text{out}} = 0.1$, maximum margin $\theta = 11$ dB. Assume that the attenuation is given by Equation (9.2), where $m = 4$, $\sigma = 8$.

Hint:

The radius of an urban cell is 100–5000 m, and a rural cell is about 30 km.

9.12. Formula (9.38) defines the distribution of the number of arrivals in time interval of length τ.

a) Determine the average number of arrivals in τ.

b) Determine the variance of the number of arrivals.

9.13. To get better speech quality, the variable rate speech coder in the IS-95 system QCELP has been modified. The effective information data rates of QCELP are 9600, 4800, 2400, and 1200 b/s. The effective information data rates of the modified version of QCELP, called QCELP13, are given in Section 9.8. To accommodate higher data rates, the convolutional code rates have been changed both in down- and uplink. What are the new code rates?

9.14. Find the uplink channel capacity of the system of Example 3.11 assuming that number of active users κ has binomial distribution (9.51). The blocking probability is 0.001, the traffic intensity $\lambda/\mu = 10$, and the outage probability is 0.01.

9.15. Consider the following system using DS-CDMA and BPSK modulation.

— $W = 1.25$ kHz

— $R = 9.6$ kbit/s

— Frequency reuse factor $= 1$

— Required probability of bit error $\leq 10^{-3}$

— Antenna gain $= 2.4$

— Voice activity gain $= 8/3$

— Other-cell interference factor $= 1$

a) If the channel is not undergoing fading, what is the maximum number of users if a rate 1/2 memory 4 encoder is used and soft Viterbi decoding is employed? (You may neglect the background noise and model the multiple access interference as Gaussian.)

b) What if instead a rate 1/2 memory 8 encoder is used?

c) If the channel is undergoing Rayleigh fading, compare the performance of a rate 1/2 memory 4 and a rate 1/2 memory 8 convolutional codes with soft Viterbi decoding.

Hint 1:

Use Figure 4.16 for estimation of the required signal-to-noise ratio in AWGN channel.

Hint 2:

Use Figure 5.5 for estimation of fading loss in the Rayleigh channel.

9.16. In a DS CDMA the use of a Rake receiver is critical in order to improve the performance of the system. The number of resolvable paths that can be combined depends on the channel and the spreading sequence. More precisely, the number of resolvable paths is proportional to the spreading bandwidth. This was used as an argument in constructing the CDMA2000 system, where a bandwidth of 5 MHz rather than 1.25 MHz was used,

which is the case in IS-95. Assume that a rate 1/2 memory 8 convolutional code is used and soft Viterbi decoding is employed. Compare the spectrum efficiency for a system operating over a bandwidth of 1.25 MHz, where the Rake receiver makes use of only one path ($L = 1$), with a system that is operating over a bandwidth of 5.0 MHz and makes use of four independent paths ($L = 4$). The modulation used is BPSK and P_b should be less than 10^{-3}.

9.17. Compare WCDMA and CDMA2000 standards. What are the merits and demerits of each standard?

9.18. WCDMA standard employs FDD and TDD principles. What advantage has the second method in comparison with the first method?

APPENDIX A

ANALYSIS OF THE MOMENTS OF THE DECISION STATISTICS FOR THE FH CDMA COMMUNICATION SYSTEM

Let us introduce the random variables

$$\begin{aligned} \hat{I}_n &= \sum_{k=2}^{K} \hat{\theta}_n^{(k)} \ , \\ \check{I}_n &= \sum_{k=2}^{K} \check{\theta}_n^{(k)} \end{aligned} \tag{A.1}$$

where $\hat{\theta}_n^{(k)}$ and $\check{\theta}_n^{(k)}$ are defined by Formulas (3.128)–(3.129). Then

$$P(\hat{I}_n = i) = P(\check{I}_n = i) = \left(\begin{array}{c} K-1 \\ i \end{array} \right) \left(\frac{1}{M} \right)^i \left(1 - \frac{1}{M} \right)^{K-1-i} \tag{A.2}$$

The conditional expectation of $\hat{y}_n^{(1)}$ given $\hat{I}_n = i$ is

$$E(\hat{y}_n^{(1)} | \hat{I}_n = i) = P(1+i) + 2\sigma_0^2 \tag{A.3}$$

analogously,

$$E(\check{y}_n^{(1)} | \check{I}_n = i) = Pi + 2\sigma_0^2 \tag{A.4}$$

where σ_0^2 is the variance of the AWGN components $\hat{\xi}_{\mathrm{I}n}^{(1)}$ $\hat{\xi}_{\mathrm{Q}n}^{(1)}$, $\check{\xi}_{\mathrm{I}n}^{(1)}$ and $\check{\xi}_{\mathrm{Q}n}^{(1)}$, $\sigma_0^2 = N_0/2T_{\mathrm{c}}$, $N_0/2$ is two-sided power spectral density of the noise. From (A.2)–(A.4)

Theory of Code Division Multiple Access Communication, by Kamil Sh. Zigangirov
ISBN 0-471-45712-4

it follows

$$E(\hat{y}_n^{(1)}) = P\left(1 + \frac{K-1}{M}\right) + 2\sigma_0^2 \tag{A.5}$$

$$E(\check{y}_n^{(1)}) = P\ \frac{K-1}{M} + 2\sigma_0^2 \tag{A.6}$$

The second conditional moments of $\hat{y}_n^{(1)}$ and $\check{y}_n^{(1)}$ are

$$\begin{aligned} E\left[(\hat{y}_n^{(1)})^2 | \hat{I}_n = i\right] &= P^2(1+i)^2 + 2P^2 i + P^2 i(i-1) \\ &\quad + 4P(1+i)\sigma_0^2 + 6\sigma_0^4 + 4P(1+i)\sigma_0^2 + 2\sigma_0^4 \\ &= P^2(1 + 3i + 2i^2) + 8P(1+i)\sigma_0^2 + 8\sigma_0^4 \end{aligned} \tag{A.7}$$

$$\begin{aligned} E\left[(\check{y}_n^{(1)})^2 | \check{I}_n = i\right] &= P^2 i^2 + P^2 i(i-1) + 4Pi\sigma_0^2 \\ &\quad + 6\sigma_0^4 + 4Pi\sigma_0^2 + 2\sigma_0^4 \\ &= P^2(2i^2 - i) + 8Pi\sigma_0^2 + 8\sigma_0^4 \end{aligned} \tag{A.8}$$

Using the equations

$$\sum_{i=0}^{K-1} i \binom{K-1}{i} \left(\frac{1}{M}\right)^i \left(1 - \frac{1}{M}\right)^{K-1-i} = \frac{K-1}{M} \tag{A.9}$$

$$\begin{aligned} \sum_{i=0}^{K-1} i^2 \binom{K-1}{i} \left(\frac{1}{M}\right)^i \left(1 - \frac{1}{M}\right)^{K-1-i} &= \frac{K-1}{M}\left(1 - \frac{1}{M}\right) + \left(\frac{K-1}{M}\right)^2 \\ &\approx \frac{K-1}{M} + \left(\frac{K-1}{M}\right)^2 \end{aligned} \tag{A.10}$$

we get from (A.7) and (A.8)

$$\begin{aligned} E\left[(\hat{y}_n^{(1)})^2\right] &= P^2\left[1 + 3\ \frac{K-1}{M} + 2\ \frac{K-1}{M} + 2\left(\frac{K-1}{M}\right)^2\right] \\ &\quad + 8P\left(1 + \frac{K-1}{M}\right)\sigma_0^2 + 8\sigma_0^4 \\ &= P^2\left[1 + 5\ \frac{K-1}{M} + 2\left(\frac{K-1}{M}\right)^2\right] \\ &\quad + 8P\left(1 + \frac{K-1}{M}\right)\sigma_0^2 + 8\sigma_0^4 \end{aligned} \tag{A.11}$$

$$E\left[(\check{y}_n^{(1)})^2\right] = P^2\left[2\,\frac{K-1}{M} + 2\left(\frac{K-1}{M}\right)^2 - \frac{K-1}{M}\right] + 8P\,\frac{K-1}{M}\,\sigma_0^2 + 8\sigma_0^4$$

$$= P^2\left[\frac{K-1}{M} + 2\left(\frac{K-1}{M}\right)^2\right] + 8P\,\frac{K-1}{M}\,\sigma_0^2 + 8\sigma_0^4 \qquad \text{(A.12)}$$

Generally speaking, the random variables $\hat{y}_n^{(k)}$ and $\check{y}_n^{(k)}$ are dependent, but because the dependence is very small for $M \gg 1$, we will neglect this dependence.

From (A.5), (A.6), (A.11), and (A.12) we get the variances of $\hat{y}_n^{(1)}$ and $\check{y}_n^{(1)}$:

$$\text{var}(\hat{y}_n^{(1)}) = E\left[(\hat{y}_n^{(1)})^2\right] - \left[E(\hat{y}_n^{(1)})\right]^2 \qquad \text{(A.13)}$$

$$= P^2\left[3\,\frac{K-1}{M} + \left(\frac{K-1}{M}\right)^2\right] + 4P\left(1 + \frac{K-1}{M}\right)\sigma_0^2 + 4\sigma_0^4$$

$$\text{var}(\check{y}_n^{(1)}) = E\left[(\check{y}_n^{(1)})^2\right] - \left[E(\check{y}_n^{(1)})\right]^2 \qquad \text{(A.14)}$$

$$= P^2\left[\frac{K-1}{M} + \left(\frac{K-1}{M}\right)^2\right] + 4P\,\frac{K-1}{M}\,\sigma_0^2 + 4\sigma_0^4$$

Correspondingly,

$$E(\hat{y}^{(1)}) = N\left[P\left(1 + \frac{K-1}{M}\right) + 2\sigma_0^2\right] \qquad \text{(A.15)}$$

$$E(\check{y}^{(1)}) = N\left[P\,\frac{K-1}{M} + 2\sigma_0^2\right] \qquad \text{(A.16)}$$

$$\text{var}(\hat{y}^{(1)}) = N\left\{P^2\left[3\,\frac{K-1}{M} + \left(\frac{K-1}{M}\right)^2\right]\right.$$

$$\left. + 4P\left(1 + \frac{K-1}{M}\right)\sigma_0^2 + 4\sigma_0^4\right\} \qquad \text{(A.17)}$$

$$\text{var}(\check{y}^{(1)}) = N\left\{P^2\left[\frac{K-1}{M} + \left(\frac{K-1}{M}\right)^2\right] + 4P\,\frac{K-1}{M}\,\sigma_0^2 + 4\sigma_0^4\right\} \qquad \text{(A.18)}$$

Consider now the asynchronous case.

In the asynchronous case each of $(K-1)$ interfering users can give two contributions in the output statistics of the matched filters and we have instead

of Formula (3.127)

$$\hat{z}_{\mathrm{I}n}^{(1)} = \sqrt{P}\cos\varphi_n^{(1)} + \sqrt{P}\sum_{k=2}^{K}\left[\hat{\theta}_n^{(k)}\eta_n^{(k)}\cos\varphi_n^{(k)} + \hat{\theta}_{n+1}^{(k)}(1-\eta_n^{(k)})\cos\varphi_{n+1}^{(k)}\right] + \hat{\xi}_{\mathrm{I}n}^{(1)}$$

$$\hat{z}_{\mathrm{Q}n}^{(1)} = \sqrt{P}\sin\varphi_n^{(1)} + \sqrt{P}\sum_{k=2}^{K}\left[\hat{\theta}_n^{(k)}\eta_n^{(k)}\sin\varphi_n^{(k)} + \hat{\theta}_{n+1}^{(k)}(1-\eta_n^{(k)})\sin\varphi_{n+1}^{(k)}\right] + \hat{\xi}_{\mathrm{Q}n}^{(1)}$$

$$\check{z}_{\mathrm{I}n} = \sqrt{P}\sum_{k=2}^{K}\left[\check{\theta}_n^{(k)}\eta_n^{(k)}\cos\varphi_n^{(k)} + \check{\theta}_{n+1}^{(k)}(1-\eta_n^{(k)})\cos\varphi_{n+1}^{(k)}\right] + \check{\xi}_{\mathrm{I}n}^{(1)}$$

$$\check{z}_{\mathrm{Q}n} = \sqrt{P}\sum_{k=1}^{K}\left[\check{\theta}_n^{(k)}\eta_n^{(k)}\sin\varphi_n^{(k)} + \check{\theta}_{n+1}^{(k)}(1-\eta_n^{(k)})\sin\varphi_{n+1}^{(k)}\right] + \check{\xi}_{\mathrm{Q}n}^{(1)} \tag{A.19}$$

Here we assume that the nth chip of the signal received from the first user can overlap with nth and $(n+1)$th chips of the signals received from other users. The length of overlapping with the nth chip of the kth user is $\eta_n^{(k)}T_{\mathrm{c}}$, $0 < \eta_n^{(k)} \le 1$, the length of the overlapping with the $(n+1)$th chip is $(1-\eta_n^{(k)})T_{\mathrm{c}}$. The random variables $\eta_n^{(k)}$, $k = 1, 2, \ldots k$, are independent and uniformly distributed on $[0, 1)$, the other notation coincides with notations in (3.127). To avoid cumbersome calculations, we neglect background noise and the other-cell interference components $\hat{\xi}_{\mathrm{I}n}^{(1)}$, $\hat{\xi}_{\mathrm{Q}n}^{(1)}$, $\check{\xi}_{\mathrm{I}n}^{(1)}$, $\check{\xi}_{\mathrm{Q}n}^{(1)}$ in (A.19). Then the statistics $\hat{y}_n^{(1)}$ and $\check{y}_n^{(1)}$ are

$$\begin{aligned}
\hat{y}_n^{(1)} = {} & P\left\{1 + \sum_{k=2}^{K}\left[\hat{\theta}_n^{(k)}(\eta_n^{(k)})^2 + \hat{\theta}_{n+1}^{(k)}(1-\eta_n^{(k)})^2\right]\right\} \\
& + 2P\sum_{k=2}^{K}\left[\hat{\theta}_n^{(k)}\eta_n^{(k)}\cos(\varphi_n^{(1)} - \varphi_n^{(k)}) + \hat{\theta}_{n+1}^{(k)}(1-\eta_n^{(k)})\cos(\varphi_n^{(1)} - \varphi_{n+1}^{(k)})\right] \\
& + 2P\sum_{k=2}^{K}\sum_{k'=k+1}^{K}\hat{\theta}_n^{(k)}\hat{\theta}_n^{(k')}\eta_n^{(k)}\eta_n^{(k')}\cos(\varphi_n^{(k)} - \varphi_n^{(k')}) \\
& + 2P\sum_{k=2}^{K}\sum_{k'=2}^{K}\hat{\theta}_n^{(k)}\hat{\theta}_{n+1}^{(k')}\eta_n^{(k)}(1-\eta_n^{(k')})\cos(\varphi_n^{(k)} - \varphi_{n+1}^{(k')}) \\
& + 2P\sum_{k=2}^{K}\sum_{k'=k+1}^{K}\hat{\theta}_{n+1}^{(k)}\hat{\theta}_{n+1}^{(k')}(1-\eta_n^{(k)})(1-\eta_n^{(k')})\cos(\varphi_{n+1}^{(k)} - \varphi_{n+1}^{(k')})
\end{aligned} \tag{A.20}$$

$$\begin{aligned}\check{y}_n^{(1)} = P\sum_{k=2}^{K}\left[\check{\theta}_n^{(k)}(\eta_n^{(k)})^2 + \check{\theta}_{n+1}^{(k)}(1-\eta_n^{(k)})^2\right] \\ + 2P\sum_{k=2}^{K}\sum_{k'=k+1}^{K}\check{\theta}_n^{(k)}\check{\theta}_n^{(k')}\eta_n^{(k)}\eta_n^{(k')}\cos(\varphi_n^{(k)}-\varphi_n^{(k')}) \\ + 2P\sum_{k=2}^{K}\sum_{k'=2}^{K}\check{\theta}_n^{(k)}\check{\theta}_{n+1}^{(k')}\eta_n^{(k)}(1-\eta_n^{(k')})\cos(\varphi_n^{(k)}-\varphi_{n+1}^{(k')}) \\ + 2P\sum_{k=2}^{K}\sum_{k'=k+1}^{K}\check{\theta}_{n+1}^{(k)}\check{\theta}_{n+1}^{(k')}(1-\eta_n^{(k)})(1-\eta_n^{(k')})\cos(\varphi_{n+1}^{(k)}-\varphi_{n+1}^{(k')})\end{aligned} \tag{A.21}$$

Finally, from (A.20) and (A.21) we get analogously to Formulas (A.5)–(A.6), (A.11)–(A.12)

$$E(\hat{y}_n^{(1)}) = P\left(1+\frac{2}{3}\,\frac{K-1}{M}\right) \tag{A.22}$$

$$E(\check{y}_n^{(1)}) = P\,\frac{2}{3}\,\frac{K-1}{M} \tag{A.23}$$

$$\begin{aligned}\operatorname{var}(\hat{y}_n^{(1)}) &\approx P^2\,\frac{K-1}{M}\left(\frac{2}{5}+\frac{4}{3}\right) + P^2\left(\frac{K-1}{M}\right)^2\left[\frac{1}{9}+\frac{2}{9}+\frac{1}{9}\right] \\ &= P^2\,\frac{K-1}{M}\,\frac{26}{15} + P^2\left(\frac{K-1}{M}\right)^2\frac{4}{9}\end{aligned} \tag{A.24}$$

$$\operatorname{var}(\check{y}_n^{(1)}) \approx P^2\,\frac{K-1}{M}\,\frac{2}{5} + P^2\left(\frac{K-1}{M}\right)^2\frac{4}{9} \tag{A.25}$$

BIBLIOGRAPHY

1. 3rd Generation Partnership Project; Technical Specification Group Radio Access Network; 25.201: Physical Layer—General Description (Release 5), Version 5.2.0, 2002.
2. 3rd Generation Partnership Project; Technical Specification Group Radio Access Network; 25.211: Physical Channels and Mapping of Transport Channels onto Physical Channels (Release 5), Version 5.2.0, 2002.
3. 3rd Generation Partnership Project; Technical Specification Group Radio Access Network; 25.212: Multiplexing and Channel Coding (Release 5), Version 5.2.0, 2002.
4. 3rd Generation Partnership Project; Technical Specification Group Radio Access Network; 25.213: Spreading and Modulation (Release 5), Version 5.2.0, 2002.
5. 3rd Generation Partnership Project; Technical Specification Group Radio Access Network; 25.214: Physical Layer Procedures (Release 5), Version 5.2.0, 2002.
6. 3rd Generation Partnership Project; Technical Specification Group Radio Access Network; 25.215: Physical Layer—Measurements (Release 5), Version 5.1.0, 2002.
7. Adachi, F., Sawahashi, M. and Okawa, K., "Tree-Structures Generation of Orthogonal Spreading Codes with Different Length for Forward Link of DS-CDMA Mobile," *Electronic Letters*, Vol. 33, No. 1, pp. 27–28, 1997.
8. Bassalygo, L.A. and Pinsker, M.S., "Evaluation of the Asymptotics of the Summarized Capacity of an M-Frequency T-User Multiple-Access Channel," *Problems of Information Transmission*, Vol. 36, N2, pp. 3–9, Apr–June 2000.
9. Chang, S-C. and Wolf, J.K., "On the T-user M-frequency Noiseless Multiple-Access Channel with and without Intensity Information," *IEEE Trans. on Information Theory*, Vol. IT-27, pp. 41–48, January 1981.
10. Cover, T.M. and Thomas, J.A., *Elements of Information Theory.* New York, Wiley, 1991.

Theory of Code Division Multiple Access Communication, by Kamil Sh. Zigangirov
ISBN 0-471-45712-4

11. Davenport, W.B., Jr and Root, W.L., *Random Signals and Noise*, New York, McGraw-Hill, 1958.
12. DeRosa, L.A. and Rogoff, M., Sect. 1 (Communications), *Application of Statistical Methods to Secrecy Communication Systems*, Proposal 946, Fed. Telecommun. Lab., Nutley, NJ, Aug. 28, 1950.
13. Dinan, E.H., and Jabbar, B., "Spreading Codes for Direct Sequence CDMA and Wideband CDMA Cellular Networks," *IEEE Communications*, Vol. 36, No. 9, pp. 48–54, September 1998.
14. Feller, W., *An Introduction to Probability Theory and Its Applications.*, Vol I, New York, Wiley, 1957.
15. Gallager, R.G., *Information Theory and Reliable Communication*. New York, Wiley, 1968.
16. Gardner, F.M., *Phaselock Techniques.* New York, Wiley, 1979.
17. *Global Positioning Systems*, Papers published in *Navigation*, Vol. I–III, Washington, DC; The Institute of Navigation, 1986.
18. Gold, R., "Optimal Binary Sequences for Spread Spectrum Multiplexing," *IEEE Trans. on Information Theory*, Vol. IT-13, pp. 619–621, October 1967.
19. Golomb, S.W., *Shift Register Sequences*. Laguna Hills, Aegeon Park Press, 1982.
20. Helstrom, C.W., *Statistical Theory of Signal Detection*. London, Pergamon, 1968.
21. Holmes, J.K., *Coherent Spread Spectrum Systems*. New York, Wiley, 1982.
22. Jakes, W.C. Jr., *Microwave Mobile Communications*. New York, Wiley, 1974.
23. Jimenez, A.F. and Zigangirov K.Sh., "On Coherent Reception of Uplink Transmitted Signals in the DS CDMA System," *IEEE Trans. on Information Theory*, Vol. IT-45, N7, pp. 2655–2661, November 1999.
24. Johannesson, R. and Zigangirov, K.Sh., *Fundamentals of Convolutional Coding*. IEEE Press, 1999.
25. Kasami, T., "Weight Distribution Formula for Some Class of Cyclic Codes," *Coordinated Science Lab.*, Univ. of Illinois, Urbana, Tech. Rep., R-285, April 1966.
26. Lee, W.C.Y., *Mobile Cellular Telecommunication Systems*. New York, McGraw-Hill, 1989.
27. Lin, S. and Costello D.J., Jr., *Error Control Coding: Fundamentals and Applications*. Englewood Cliffs, NJ, Prentice-Hall, 1983.
28. Lindell, G., *Introduction to Digital Communications* (class notes). Lund University, 2003.
29. Lindsey, W.C. and Chie, C.M., *Phase-Locked Loops.* New York, IEEE Press, 1986.
30. Lindsey W.C. and Simon, M.K., *Telecommunication Systems Engineering*. Englewood Cliffs, NJ, Prentice-Hall, 1973.
31. MacWilliams, F.J. and Sloane, N.J.A., *The Theory of Error Correcting Codes*, Amsterdam, North-Holland, 1977.
32. Papoulis A., *Probability, Random Variables, and Stochastic Processes*. New York, McGraw-Hill, 1984.
33. Peterson, W.W. and Weldon, E.J., Jr., *Error-Correcting Codes*. Cambridge, MA., MIT Press, 1972.
34. Peterson, R.L., Ziemer, R.E., and Borth, D.E., *Introduction to Spread Spectrum Communications*. Englewood Cliffs, NJ, Prentice-Hall, 1995.

35. Pierce, J.R., *Time Division Multiplex System with Erratic Sampling Times*. Technical Memorandum 49-150-15, Bell Telephone Laboratories, June 15, 1949.
36. Price, R., "Optimum Detection of Random Signals in Noise, with Application to Scatter-Multipath Communication," *IRE Trans. on Information Theory*, Vol. IT-2, pp. 125–135, December 1956.
37. Proakis, J.G. and Salehi, M., *Communication Systems Engineering*. Englewood Cliffs, NJ, Prentice-Hall, 1994.
38. Proakis, J.G., *Digital Communication*. New York, McGraw-Hill, 1995.
39. Rappaport, T.S., *Wireless Communications*. Second Edition. Upper Saddle River, NJ, Prentice-Hall PTR, 2002.
40. Scholtz, R.A., "Multiple Access with Time-Hopping Impulse Modulation," in *Proc. Military Comm. Conf.*, October 1993.
41. Scholtz, R.A. and Win, M.Z., "Impulse Radio," IEEE PIMRC'97, Helsinki, Finland, 1997.
42. Shannon, C.E., "A Mathematical Theory of Communication," *Bell System Technical Journal*, 27: 379–423 (Part 1), 625–656 (Part II), 1948.
43. Simon, M.K., Omura, J.K., Scholz, R.A., and Levitt, B.K., *Spread Spectrum Communications*. Vols. I, II, III. Rockville, MD, Computer Science Press, 1985.
44. TIA/EIA/IS-95 Interim Standard, *Mobile Station—Base Station Compatibility Standard for Dual Mode Wideband Spread Spectrum Cellular System*. Washington, DC, Telecommunications Industry Association, 1993.
45. Van Trees, H.L., *Detection, Estimation, and Modulation Theory*, Part I, New York, Wiley, 1968.
46. Verdu, S., *Multiuser Detection.* Cambridge, Cambridge University Press, 1998.
47. Viterbi, A.J., *CDMA Principles of Spread Spectrum Communication*. Reading, MA, Addison-Wesley, 1995.
48. Viterbi, A.J., "Error Bounds for Convolutional Codes and an Asymptotically Optimum Decoding Algorithm," *IEEE Trans. on Information Theory*, Vol. IT-13, pp. 260–269, April 1967.
49. Viterbi, A.J., *Principles of Coherent Communication.* New York, McGraw-Hill, 1966.
50. Viterbi, A.J., "Spread-Spectrum Communications: Myths and Realities," *IEEE Comm. Mag.*, Vol. 12, pp. 11–18, May 1979.
51. Viterbi, A.J., "Very Low Rate Convolutional Codes for Maximum Theoretical performance of Spread-Spectrum Multiple-Access Channels," *IEEE Journal on Selected Areas in Communications*, Vol. 8, N.Y., pp. 641–649, May 1990.
52. Viterbi, A.J. and Omura J.K., *Principles of Digital Communication and Coding.* New York, McGraw-Hill, 1979.
53. Viterbi, A.J., Viterbi, A.M., and Zehavi, E., "Performance of Power-Controlled Wideband Terrestrial Digital Communication," *IEEE Trans. on Communications*, Vol. 41, pp. 559–569, April 1993.
54. Wasan, M.T., *Stochastic Approximation.* Cambridge, The University Press, 1969.
55. *WCDMA for UMTS, Radio Access for Third Generation Mobile Communications*. Second Edition. Edited by Harry Holma and Antti Toskala, New York, Wiley, 2002.

56. Wilhelmsson, L. and Zigangirov, K.Sh., "On the Asymptotic Capacity of a Multiple-Access Channel," *Problems of Information Transmission*, Vol. 33, No. 1, pp. 12–20, January–March 1997.

57. Wilson, S.G., *Digital Modulation and Coding*. Upper Saddle River, NJ, Prentice-Hall, 1996.

58. Wintzell, O., *Coding and Modulation for Wideband CDMA Systems.* PhD thesis, University of Lund, Dept. of Information Technology, February 2002.

INDEX

Theory of Code Division Multiple Access Communication, by Kamil Sh. Zigangirov
ISBN 0-471-45712-4